1-1-2017

Phytochemical Investigation of Psychoactive Medicinal Plants for the Treatment of Neurological Disorders

Vedanjali Gogineni
University of Mississippi

PHYTOCHEMICAL INVESTIGATION OF PSYCHOACTIVE MEDICINAL PLANTS FOR THE TREATMENT OF NEUROLOGICAL DISORDERS

A Dissertation
presented in partial fulfillment of requirements
for the degree of Doctor of Philosophy
in the Department of BioMolecular Sciences
The University of Mississippi

by

Vedanjali Gogineni

December 2017

ABSTRACT

Neurological disorders include disorders such as migraine, tension-type headaches, Parkinson's disease (PD), epilepsy, dementia, and Alzheimer's disease (AD). Globally, PD is the second most common neurodegenerative disorder following AD. In developed countries, PD affects 1% of all population over 60 years of age. The prevalence of PD is increasing over the years and is expected to double by 2030. It is proposed that combination of dopaminergic drugs with monoamine oxidase B (MAO-B) inhibitors, anticholinergics, catechol-*O*-methyl transferase inhibitors, and other non-dopaminergic drugs can better alleviate levodopa-induced motor complications along with better control of motor symptoms. MAO-B inhibitors play a significant role in dopamine (DA) metabolism and can be used as monotherapy in the early stages of PD, or in combination with levodopa. Currently, there are only three MAO-B inhibitors that are approved by Food and Drug Administration (FDA): selegiline, rasagiline, and safinamide. Hence, there is the need to discover potent and selective MAO-B inhibitors for effective treatment of PD.

About 60% of the marketed drugs today are either natural products or derivatives that are inspired from natural products. We studied plants with extensive traditional use in CNS-related disorders, in which the chloroform extract of *C. urticifolia* exhibited potent inhibition of MAO-A and -B. *Calea urticifolia* (Asteraceae) commonly known as "Juanislama" is native to the Central America. Bioassay-guided fractionation has been implemented for the isolation of the secondary metabolites from *C. urticifolia*. From the bioactive fraction, acacetin and a series of sesquiterpenes were isolated; acacetin was found to be the bioactive compound. A series of

acacetin analogs were designed with the aid of computational docking studies, to improve their selectivity towards MAO-B. The structures of the isolated compounds were determined on the basis of HR-MS and 1D- and 2D-NMR studies; configurations were partly established by ECD calculations. Monoamine oxidase assays were performed on the extracts, fractions, and purified compounds. Molecular modeling and molecular dynamic studies were used to predict the binding modes on the active sites of the MAO isoenzymes.

DEDICATION

This dissertation is dedicated with love to my Dad: Dr. Rajagopala Rao Gogineni, Mom: Sarojini Kancharla, Cousin: Ramesh Babu Kota, Brother: Vamsi Kilaru, and Dear Friend: Dr. Prabhakar Polepally. Dr. Polepally encouraged me during the difficult times by extending his helping hand and believing in me towards the completion of my Ph.D. A special dedication goes to Drs. Mark T. Hamann and Stephen J. Cutler, who were responsible in bringing me to the University of Mississippi and getting me enrolled in the Ph.D program.

LIST OF ABBREVIATIONS AND SYMBOLS

1D	One dimensional
2-AG	2-Archidonoylglycerol
2D	Two dimensional
3D	Three dimensional
3-MT	3-methoxytyramine
7TM	Seven transmembrane
A2A	Adenosine 2a receptor
AD	Alzheimer's Disease
AM1-BCC	Semi-empirical (AM1) with bond charge correction (BCC)
AmberFF94	Amber force field 94 charges for standard amino acids
Arg	Arginine
BBr_3	Boron tribromide
BCA	Bicinchoninic Acid Assay
BCl_3	Boron trichloride

BINAP	1,1′-binaphthalene-2,2′-diylbis(diphenylphosphine)
BSA	Bovine Serum Albumin
CB_1	Cannabinoid receptor type 1
CB_2	Cannabinoid receptor type 2
CC	Column Chromatography
CD	Circular Dichroism
$CDCl_3$	Deuterated chloroform
CD_3OD	Deuterated methanol
$CHCl_3$	Chloroform
CH_2Cl_2	Dichloromethane
CNS	Central Nervous System
COMT	Catechol-*O*-methyltransferase
CO_2	Carbondioxide
COSY	COrrelation SpectroscopY
CS	Chemical Shift

DA	Dopamine
DALYs	Daily-Adjusted Life Years
DAMGO	D-Ala^2, *N*-MePhe^4, Gly-ol
DEPT	Distortionless Enhancement by Polarization Transfer
DFT	Density-Functional Theory
DMEM	Dulbecco's Modified Eagle's Medium
DMF	Dimethyl formamide
DMSO	Dimethyl Sulfoxide
DOP	Delta OPiate receptor
DOPAC	3,4-dihydroxyphenylacetic acid
DOR	Delta Opioid Receptor
DPDPE	[D-Pen^2, D-Pen^5]enkephalin
ECD	Electronic Circular Dichroism
EDTA	EthyleneDiamineTetraacetic Acid
ESIMS	Electronspray ionization mass spectrometry

EtOAc	Ethyl acetate
EtOH	Ethanol
FAD	Flavin Adenine Dinucleotide
FDA	Food and Drug Administration
GABA	γ-amino butyric acid
GBD	Global Burden of Disease-study
GIAO	Gauge-Including Atomic Orbitals
GPCRs	G protein-coupled receptors
GSH	Glutathione
GSSG	Oxidized glutathione
HEK293	Human Embryonic Kidney cells 293
Hex	Hexane
H_2O_2	Hydrogen peroxide
HL-60	Human promyelocytic leukemia cells
HMBC	Heteronuclear Multiple Bond Correlation

HMQC	Heteronuclear Multiple Quantum Correlation
HRESIMS	High Resolution Electron Spray Ionization Mass Spectrometry
HRMS	High Resolution Mass Spectroscopy
HSQC	Heteronuclear Single Quantum Coherence/Correlation
HTS	High-throughput Screening
Hz	Hertz
IC_{50}	Half Maximal Inhibitory Concentration
I_2	Iodide
Ile	Isoleucine
IMPS	*Invalid* Metabolic Panaceas
IR	Infrared
K_i	Inhibition/Binding affinity
K_2CO_3	Potassium carbonate
K_M	Michaelis-Menton constant
KOP	Kappa OPiate receptor

KOR	Kappa Opioid Receptor
LC-MS	Liquid chromatography – mass spectrometry
LC-NMR	Liquid chromatography – nuclear magnetic resonance
LID	Levodopa-Induced Dyskinesia
MAO	MonoAmine Oxidase
MCF7	Human breast adenocarcinoma cell-line
MDMA	3,4-methylenedioxymethamphetamine
MeOH	Methanol
mg	milligram
MHz	Megahertz
MMGBSA	Molecular Mechanics/Generalized Born Surface Area
mmol	millimole
MOP	Mu OPiate receptor
MOR	Mu Opioid Receptor
MRI	Magnetic Resonance Imaging

MSA	Multiple Systems Atrophy
m/z	mass-to-charge ratio
NaCl	Sodium Chloride
NaH	Sodium hydride
$NaHCO_3$	Sodium bicarbonate
NaH_2PO_4	Monosodium phosphate
NaOH	Sodium hydroxide
NaO^tBu	Sodium ter-butoxide
NAS	New Active Substances
Na_2SO_4	Sodium sulfate
$Na_2S_2O_3$	Sodium thiosulfate
NCEs	New Chemical Entities
NC-IUPHAR	International Union of Basic and Clinical Pharmacology Committee on Receptor Nomenclature and Drug Classification
NMR	Nuclear Magnetic Resonance
NOESY	Nuclear Overhauser Effect SpectroscopY

N/OFQ	Nociceptin/orphanin FQ
NOP	Nociceptin OPiate receptor
norBNI	nor-Binaltorphimine
NP	Natural product
NPS	New Psychoactive Substances
$O^{2}*^{-}$	Superoxide anion
OH*	Hydroxyl radical
O_2*^{-}	Superoxide radical
OPLS	Optimized Potentials for Liquid Simulations
ORL_1	Opioid Receptor-Like 1
ORNS	Opioid Receptor Nomenclature Subcommittee
PAINS	Pan-assay Interference Compounds
PCM	Polarizable Continuum Model
PD	Parkinson’s Disease
PDB	Protein Data Bank

$Pd_2(dba)_3$	Tris(dibenzylideneacetone)dipalladium
PET	Positron Emission Tomography
pH	potential of hydrogen
Phe	Phenylalanine
PK	Pharmacokinetic
PLD2	Phospholipase D2
ppm	parts per million
PSP	Progressive Supranuclear Palsy
RBF	Round-Bottomed Flask
RCSB	Research Collaboratory for Structural Bioinformatics
R&D	Research and Development
rt	room temperature
SAR	Structure-Activity Relationship
SD	Standard Deviation
SE	Standard Error

SP	Standard Precision
SPE	Solid Phase Extraction
SQ*	Dopamine-quinone species
SZMAP	Solvent-ZAP-Mapping
TDDFT	Time-Dependent Density Functional Theory
TLC	Thin-Layer Chromatography
TMS	Trimethylsilane
TOCSY	TOtal Correlation SpectroscopY
Tris-HCl	Tris-hydrochloride
Tyr	Tyrosine
UCHL1	Ubiquitin Carboxy-terminal Hydrolase L1
UPP	Ubiquitin-Proteasome Pathway
UV	Ultraviolet
V_{max}	Maximum velocity
WHO	World Health Organization

ACKNOWLEDGMENTS

It is well said that “Education is the key to success in life, and teachers make a lasting impact in the lives of their students”. As my Ph.D. journey is coming to an end, I realized how teachers can impact you both scientifically and personally. First and foremost, I would like to thank Drs. Mark T. Hamann, Professor, Medical University of South Carolina, and Stephen J. Cutler, Dean and Professor, University of South Carolina (former Chair of the Department of BioMolecular Sciences), for their guidance and support throughout every aspect of my research. It was Dr. Hamann because of whom I set my foot into the University of Mississipi. Dr. Hamann helped me gain the basic knowledge on instrumentation and in getting my first publication. Dr. Cutler helped me to get into the Ph.D. program in the Department of BioMolecular Sciences, Division of Medicinal Chemistry. His leadership, and constant encouragement and support aided me succeed in the completion of my Ph.D. Both of them helped me advance my skills, along with improving my critical thinking, research, and scientific writing. I was able to evolve from preliminary level to a higher understanding of science. I will forever be grateful to them.

I am very indebted to have known the Late Dr. Ronald F. Borne, Professor Emeritus, University of Mississippi, for being my mentor and making me feel special. He taught me the basic skills and concepts, both in education and life, and motivated me to give my best in everything. He constantly encouraged me saying that “you can be 100% sure about not getting something to which you never applied,” which helped me apply for and win a number of awards during my Ph.D. journey. Dr. Borne’s positive influence will always be reminded and he is a person who will be never forgotten.

I express my sincere thanks to Dr. Christopher R. McCurdy for taking me into his group and supporting me when Dr. Cutler moved to the University of South Carolina as a Dean. I would also like to thank Dr. John M. Rimoldi who supported me in the University of Mississippi when Dr. McCurdy moved to the University of Florida. Both Dr. McCurdy and Dr. Rimoldi helped me focus on my project and complete my Ph.D. Dr. Rimoldi's knowledge in the area of Medicinal Chemistry and his thoughtful scientific questions during our committee meetings gave me a better insight at not only looking into things and understanding the subject, but also in completing my Ph.D.

I would extend my deepest gratitude to my committee members Dr. Robert J. Doerksen, Dr. David A. Colby, and Dr. Samir A. Ross for their constructive comments during committee meetings. Their excellent feedback on my research and constant motivation to make me perform better and enhance my personal skills have been of huge value to me.

A very special thanks to Dr. Francisco León, Assistant Scientist, University of Florida (former Research Scientist and my colleague in the Department of BioMolecular Sciences) for helping me with all my projects. I am also thankful to Mallory Pullman, an intern in our lab, who worked for about two years. She is a great friend of mine and I enjoyed our involvement in fun activities, support, and love whenever needed. The little discussions and fights over the research in the lab with Dr. León and Mallory helped me understand things, and expanded my knowledge.

My deepest gratitude goes to Dr. Prabhakar Polepally who supported me constantly throughout my Ph.D. journey. I am extremely grateful for his support and willingness to help

during extreme times and under constant pressure. It is a true blessing to know him and to have worked closely with him. Thank you for your constant encouragement and blessing.

I extend my thanks to Drs. Manal A. Nael and Khaled Elokely for their constant support and friendship. I am grateful for their willingness to help with anything and everything. I am very happy to have known them, who helped me in every step of my Ph.D. career, in clarifying my doubts and driving me forward during my hard times.

Thanks to all my friends in the Department of BioMolecular Sciences, Dr. Pankaj Pandey, Dr. Rama S. Gadepalli, Dr. Hari R. Khatri, Dr. Imran Hossain, Mohamed Jihan, and Munia Sowaileh for their valuable advice in times of need, their fun talk at times of stress, and their support when needed.

I am thankful to Sara Pettaway for teaching me opioid and cannabinoid assays and to Janet Lambert for her collaboration with my lab and for providing technical knowledge related to the *in vitro* experimental data about opioid and cannabinoid assays. My deepest thanks to the administrative staff Ms. Sherrie Gussow, Ms. Candace G. Lowstuter, and Ms. Danielle Noonan for their continuous support at departmental level, fun talk, and wonderful lunches and dinners. All the department related issues in regards to graduate school, academic holds, purchase orders, or seminar schedules were taken care by them, and none of this would have been possible without their cooperation and involvement.

I would also like to acknowledge the support in part by the grant number P20GM104932 from the National Institute of General Medical Sciences (NIGMS), a component of the National Institutes of Health (NIH), graduate student council (GSC) for the GSC research award, and the

dissertation fellowship from the UM Graduate School for Fall 2017, for the financial support during my Ph.D. study.

Lastly I would like to thank all the members I have met at the University of Mississippi, both in the past and present. Each of them played a significant role in my life and will never be forgotten. Thanks to the Department of BioMolecular Sciences that taught me a lot in life both scientifically and personally, and helped me grow confident. Finally, I am always thankful to my mom, my cousin, my brother, my love, and especially to my dad whose last wish was the completion of my Ph.D. Thank you all for your constant belief, love, support, encouragement, patience, and acceptance during the hard times. Thank you for helping me cross the highest hurdle to reach the pinnacle.

TABLE OF CONTENTS

LIST OF TABLES

LIST OF FIGURES AND ILLUSTRATIONS

LIST OF SCHEMES

CHAPTER 1. INTRODUCTION

1.1. Natural Products in Drug Discovery

Natural products are compounds that are derived from natural sources such as animals, microorganisms, or plants. The medicinal properties of natural products, particularly plants, have been known for more than 60,000 years, based on the evidence of the pollen deposits in one of the graves at a cave site of Shanidar, Iraq. The significance of natural products for health and medicine has been enormous throughout our evolution.[1]

Natural sources play a significant role in healthcare, and their use has been extensively documented in various cultures. In 1985, it was estimated by the World Health Organization (WHO) that approximately 65% of the world's population predominantly depended on plant-derived traditional medicines for primary healthcare.[2] Drugs of natural origin are classified as original natural products, semisynthetic products derived from natural products, or synthetic products based on natural-product cores.[3] Natural products have always been a source for the treatment of injuries and diseases. After the advent of combinatorial chemistry and molecular biology during the earlier decades, natural products took a secondary role in drug discovery and development that made possible the rational design of chemical compounds, to interact with specific biological targets. A renewed interest in the use of natural products, more prominently their role as a basis for drug development, has been documented recently.[1]

1.1.1. Evolution of Natural Products

Natural products and their derivatives have always been a valuable source of therapeutic agents. Nonetheless, during the past decade, natural product research in pharmaceutical industry has greatly deteriorated, owing to the challenges such as lack of affinity of the traditional natural

product extract libraries with high throughput screening (HTS). Natural product structures were long recognized to have biochemical specificity, high chemical diversity, and additional molecular properties that would favor them as lead structures in drug discovery along with separating them from the libraries of synthetic and combinatorial compounds. Natural products differ from the combinatorial libraries and synthetic drugs in the number of solvated hydrogen bond acceptors and donors (higher in natural products), in the ratio of the total heavy atoms to the aromatic ring atoms (lower in natural products), and by larger molecular rigidity, along with better distribution of molecular properties.[4]

The exploration of natural products as unique human therapeutics reached its highest in the pharmaceutical industry during 1970-1980. Among the 877 small-molecule new chemical entities (NCEs) that were introduced during 1981–2002, at least half [49%] were natural products, followed by semi-synthetic natural product analogs, or synthetic compounds based on natural product pharmacophores. The chart below shows the increased patent activity in the 1980s, a flattened or slight drop between 1990 to 1999, and a further escalation between 2000 and 2003.[4] There were 13 natural product related drugs that were approved between 2005 and 2007 (Figure 1.1).[5]

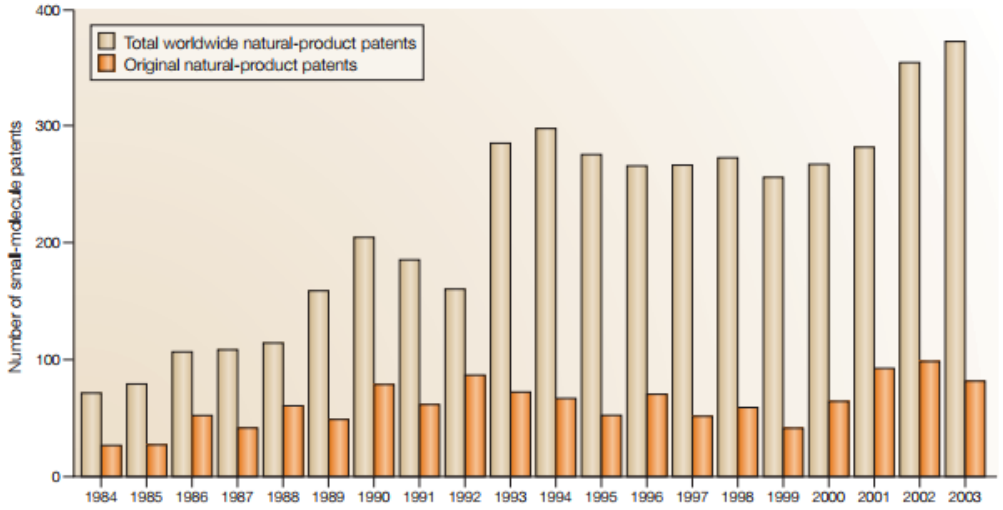

Figure 1.1. Worldwide pharmaceutical natural-product patents. Gold represents the total natural-product patents, including small-molecule natural products as pharmaceuticals. Orange represents original natural product patents. Reprinted with permission from Macmillan Publishers Ltd: Koehn, F. E.; Carter, G. T. *Nat. Rev. Drug Discovery*. **2005**, *4*, 206-220, Copyright © 2005 Nature Publishing Group. [**Permission# 4167820299191**]

There are various reasons for the decreased emphasis on natural product discovery in the pharmaceutical industries which include:

1. The introduction of HTS against definite molecular targets prompting many companies to move to 'screen friendly' synthetic chemical libraries from natural products extract libraries
2. Development of 'combinatorial chemistry' that led to the prospect of simple, drug-like screening libraries with wide chemical diversity
3. Advances in genomics, cellular biology, and molecular biology led to an increase in the number of molecular targets and shortened the drug-discovery timelines
4. A declined emphasis on infectious disease programs in pharmaceutical companies which is a traditional area of strength for natural products and

5. Possible uncertainities in the collection of biomaterials based on the 1991 Rio Convention on Biological Diversity.

Due to the underlying challenges involved in natural product drug discovery for commercial scale production by pharmaceutical industries, there is the need for rapid screening, validated hit identification, and hit-to-lead development. Traditional resource intensive natural product programs which are based on the bioassay-guided isolation, structural elucidation, extract-library screening, and consequent production scale-up face competitive disadvantages when compared to methodologies utilizing well-defined synthetic chemical-libraries. However, the emerging trends combined with the current research and development (R&D) strategies have refocused attention towards natural products as a source of chemical diversity and lead generation.[4]

1.1.2. Chemical Diversity of Natural Products

Natural products, particularly plants, produce a diverse and vast variety of secondary metabolites, the majority of which are not directly involved in growth and development. These novel metabolites have been extensively investigated by organic chemists since the 1850s for various biological effects, thus prompting a reevaluation of the possible roles they play in plants, especially in relation to ecological interactions.[6] Most of the small molecule natural products have chemical properties closely compliant with Lipinski's Rule of Five for orally available compounds,[7] while the remainder have higher molecular weights, and an increased number of stereogenic centers, and rotatable bonds, although with low log *P* values. This makes it evident that natural products are readily absorbed compared to synthetic drugs. Such properties along with the realization that their chemical diversity has been a better match to most of the successful

drugs compared to the diversity in synthetic compounds, enhanced interest in applying the natural chemical diversity to drug-discovery.[5]

Secondary metabolites produced in plants primarily function in defense against pathogens and predators, along with a reproductive advantage as attractants of seed dispensers and pollinators. The study of the biochemistry of natural products involve many practical applications.[6] Natural products have inspired advancements in organic chemistry, leading to developments in synthetic methodologies and to the prospect of making analogs of the original lead compounds with enhanced pharmaceutical or pharmacological properties. Natural product scaffolds have the advantage of being 'privileged' structures based on their ability to be successful drugs. These scaffolds are used as cores of compound libraries which are made by combinatorial techniques. Several such libraries are based on alkaloids, flavonoids, terpenoids, and polyketides. Currently, computational methods are used for the comparison of natural product likeness of the compound libraries, making it more successful for the design of natural product analogs and derivatives. These advancements and technologies could result in novel bioactive compounds that could be patented.[5]

1.1.3. History of Natural Products in Drug Discovery

The practice of medicine dates as far back as 2900 BC by the ancient Egyptians. The first known record of Egyptian pharmaceutical practice is "Ebers Papyrus", that is dated to 1500 BC, with a description of over 700 drugs, of which mostly are from plant origin. The papyrus included details of different drug formulations including pills, ointments, infusions, poultices, snuffs, and gargles mixed with honey, milk, wine, and beer as vehicles. Dioscorides is the first documented source with the medicinal uses of natural substances, that dated back to 78 AD. There are thousands of medicinal plants that are relevant in modern medicine today, that were

described back then. Some hallmark examples of natural product derived drugs in modern pharmaceutical care include penicillin G, quinine, paclitaxel/taxol, vitamin A, digoxin, morphine, vincristine, theophylline, doxorubicin, artemisinin, camptothecin, and cyclosporine (Figure 1.2).[8]

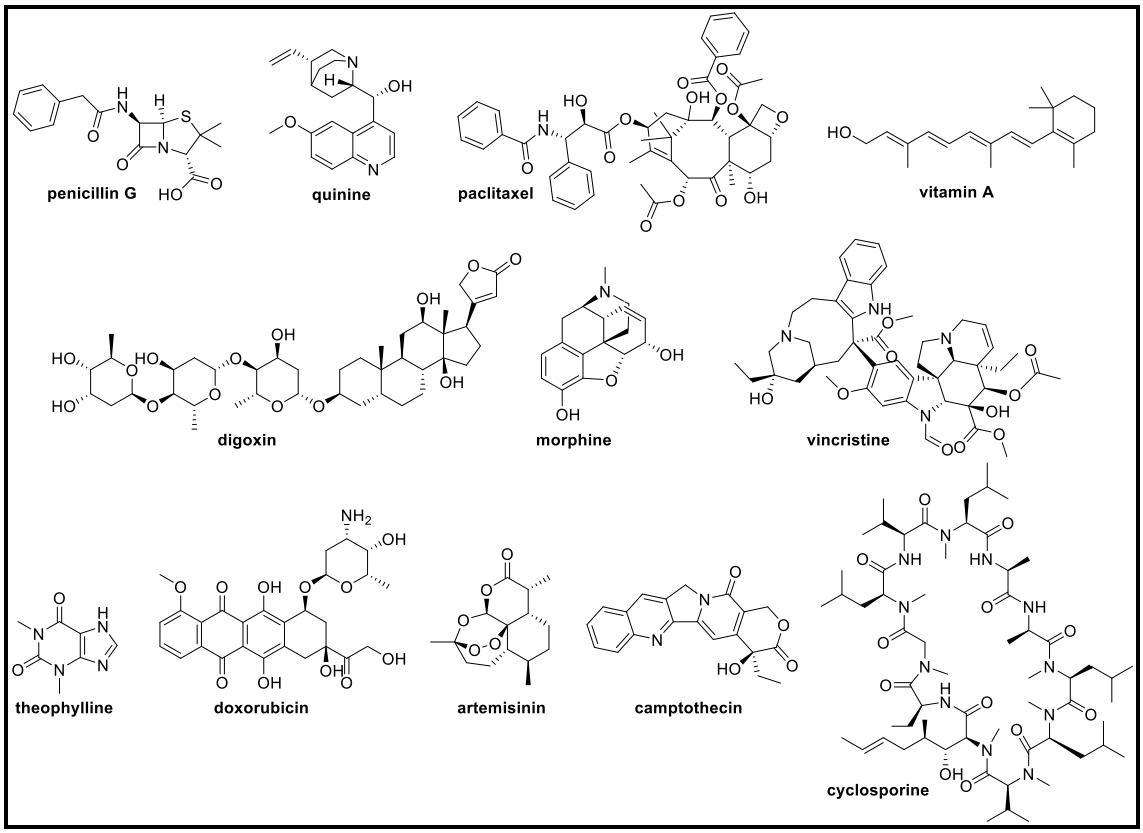

Figure 1.2. Chemical structures of some hallmarks of natural product derived drugs

Natural products have always been the most prolific source of leads in drug development. There are many natural product based drugs approved by the Food and Drug Administration (FDA) which include huperzine, galantamine, and elliptinium from plants; ziconotide and exenatide from animals; daptomycin from microbes; natural product based synthetic or semi-synthetic compounds such as caspofungin, micafungin, everolimus, tigecycline, and telithromycin. These compounds cover a series of therapeutic indications such as anti-diabetic,

anti-infective, and anti-cancer, among others, with a great diversity in their chemical structures (Figure 1.3).[5]

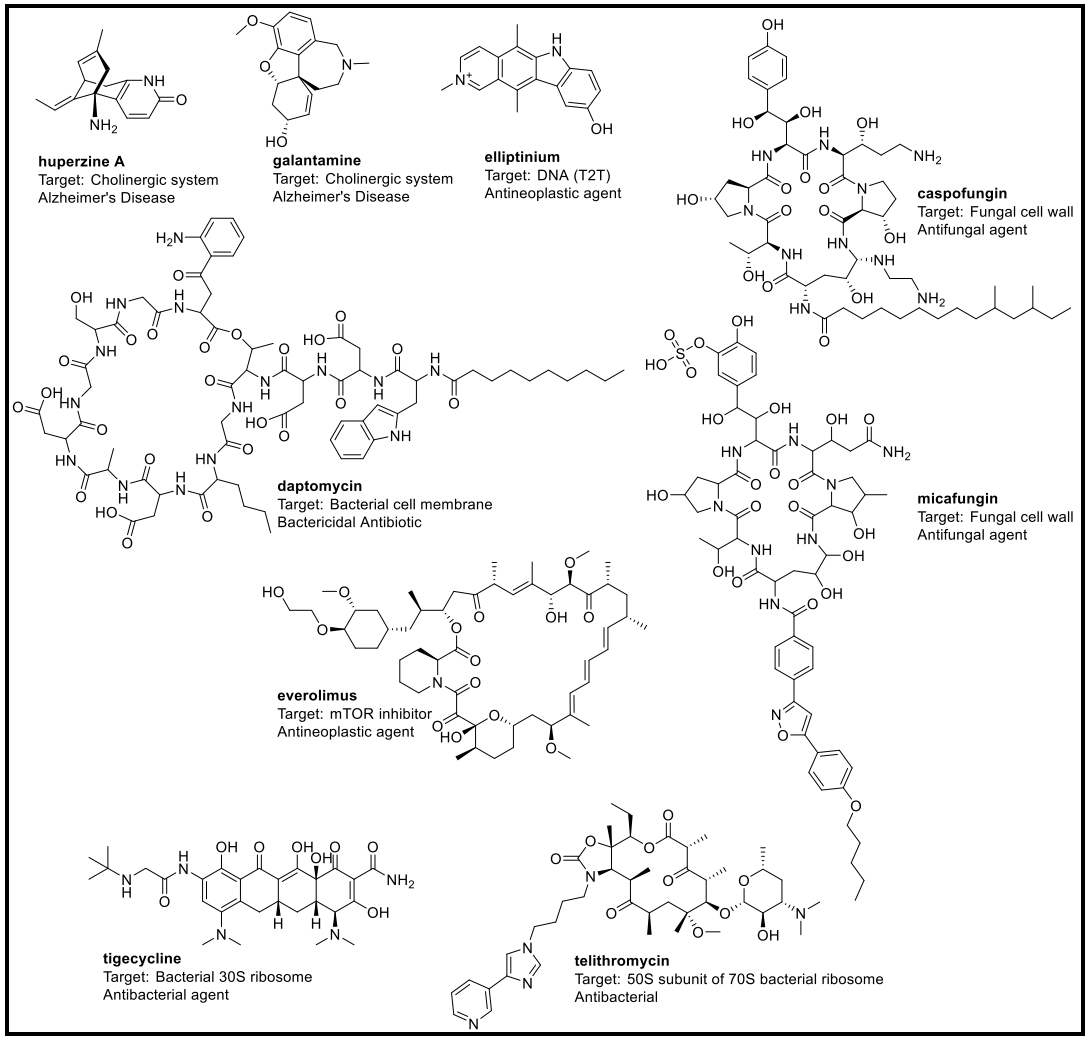

Figure 1.3. Chemical structures of approved natural products and natural product based synthetic or semi-synthetic compounds

Natural products play a significant role in the lead-discovery of drug development for the treatment of human diseases. Figure 1.4 demonstrates the number of new active substances (NASs) or NCEs approved over the years between 1981 to 2014. There are 175 molecules that were approved for the treatment of cancer between 1940s to 2014, of which 85 molecules were either from natural products or natural product derivatives. In 2014, 10 of the 44 approved small

molecule drugs were either unaltered natural products, botanical drugs, or natural product derivatives, accounting for 25% of the approved NCEs. The role of natural products in the drug discovery of small molecules was ~ 40% between 2000-2008, ~ 20% in 2009, 45% in 2010, and ~ 13% in 2013. Natural products exhibit a continued and overwhelming contribution for the expansion of chemotherapeutic armamentarium.[9]

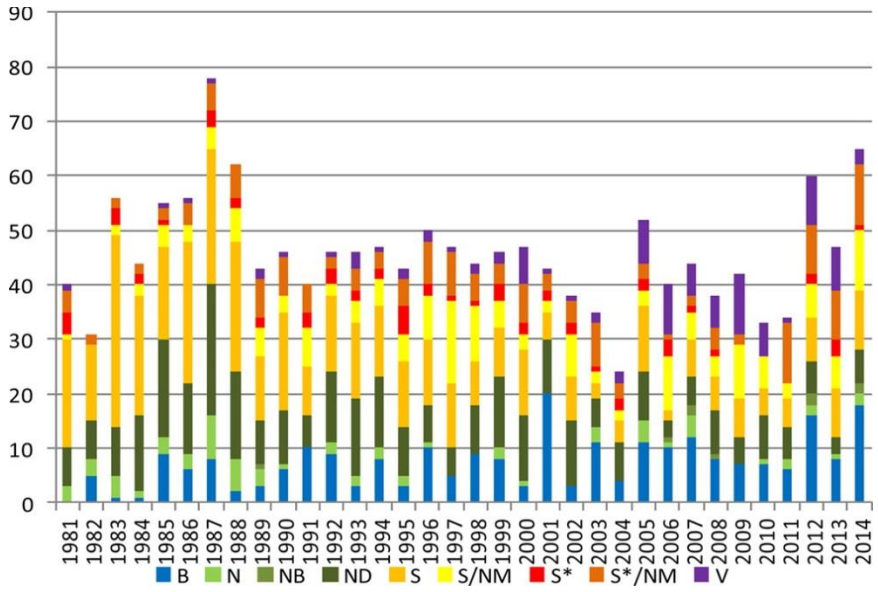

Figure 1.4. New drugs approved by FDA. B: biological macromolecule; N: unaltered natural product; NB: botanical drug (mixture); ND: natural product derivative; S: synthetic drug; S*: synthetic drug with natural product (NP) pharmacophore; /NM: mimic of natural product; V: vaccine. Reprinted with permission from ACS Publications: Newman, D. J.; Cragg, G. M. *J. Nat. Prod*. **2016**, *79*, 629-661, Copyright © 2016 The American Chemical Society and American Society of Pharmacognosy. [**Open access article**]

1.1.4. Role of Plants in Lead Discovery

Plants played a significant role in the development of traditional medicine systems. WHO estimated that approximately 80% of the Asian and African population still depend on traditional medicine for primary healthcare.[10] Plants play a crucial secondary role in the health-care sectors,

where 70-80% of people in developed countries use some form of complementary or alternative medicine such as acupuncture. Currently, herbal treatments gained popularity in traditional medicine and are highly lucrative in international marketplace. Plant products have an extensive history of use in the treatment of various diseases.[10]

Plant-derived compounds may not directly serve as drugs, but provide leads for the development of potential analogs to treat various diseases. Plants helped researchers to better understand the disease, provided efficient and novel therapies possessing unique mechanisms of action, opened distinctive research avenues, and provided inspiration in the development of novel and future therapeutic agents. Plants represent a vast diversity on earth, but only a fraction of that has been explored. It is therefore expected that plants can deliver potential bioactive compounds and have the potential for development into selective therapeutic agents.[10]

1.1.5. Challenges in Drug Discovery from Plants

There are many challenges in natural-product based drug discovery, which include access and adequate supply, tediousness in working with natural products, and the complexities involved in natural product chemistry.[8] Solubility is a common problem seen in the screening of extracts and the screening of extract libraries itself is problematic. Some of these issues could be alleviated using new techniques such as pre-fractionation of extracts. The isolation of active compounds could be facilitated using techniques like liquid chromatography-mass spectrometry (LC-MS) and liquid chromatography-nuclear magnetic resonance (LC-NMR), but the drug-development from lead compounds isolated from plants have unique challenges. In general, natural products are isolated in small quantities which are insufficient for lead optimization, development, and clinical trials. Hence, collaborations with medicinal and synthetic chemists would help explore the possibilities of semi- or total-synthesis. Another way of improving the

development of natural product compounds is the creation of natural product libraries, which combine the natural product features with combinatorial chemistry.[11]

A common and recurring concern with the isolation of compounds from plants, is their activity "hits" in multiple assays due to their interference with assay readout, rather than the specific target/compound interactions, termed as "pan-assay interference compounds" or PAINS.[12] Some of the PAINS-type behaviors include redox reactivity, metal chelation, membrane disruption, aggregation, covalent protein labeling, structural decomposition, and fluorescence interference. There are several compound classes that fall under PAINS or potential PAINS. The other category include *invalid* metabolic panaceas (IMPS) that are located in the natural products, inside the center of the hyberbolic black hole (occurrence-bioactivity-effort space). IMPS are the prototypes of the improbable metabolic panaceas with feeble performance as drug leads. IMPS include other factors in addition to PAINS characteristics such as the presence of a reactive Michael acceptor, chemical aggregation, and fluorescence activity. The above mentioned factors are other challenges to be faced with isolation of compounds from plants.[12]

1.2. Psychoactive Substances

New psychoactive substances (NPS) refer to a wide range of compounds that elicit psychotomimetic effects. These include stimulants which are congeners of synthetic cathinones or amphetamine. They have street market names which include 'plant food', 'designer drugs', 'research chemicals', or 'bath salts'. However, NPS are not restricted to amphetamine like compounds, but also to cannabimimetics, hallucinogens, and sedative-hypnotics. NPS cannot be considered harmless as they not only exert psychostimulant effects, but can also cause lethal side-effects at higher doses.[13] Based on their psychotropic effects, NPS can be classified into

various categories such as stimulants, entactogens/empathogens such as 3,4-methylenedioxymethamphetamine (MDMA), hallucinogens, or as amphetamines, cathinones, phenethylamines, benzofurans, tryptamines, piperazines, piperidines/pipradols, and aminoindans, based on their chemical family. The synthetic cannabinoids include various chemically diverse substances that act on the CB_1 receptor and are mostly hallucinogenic along with some stimulant properties.[14]

1.2.1. Opioid Receptor Subtypes

There are three types of opioid receptors that were initially identified: μ, δ, and κ in the mid-1970s. These opioid receptors were named after the drugs used in the study of these receptors: mu or μ coming from morphine which is known to induce miosis, hypothermia, bradycardia and analgesia, delta or δ from deferens induces analgesia as significant potentiators of mu-agonists, and kappa or κ known from ketocyclazocine inducing sedation, flexor-depression, miosis effects.[15] In 1996, an alternative terminology was proposed by the International Union of Basic and Clinical Pharmacology Committee on Receptor Nomenclature and Drug Classification (NC-IUPHAR) which was rejected, and later a reconstituted Opioid Receptor Nomenclature Subcommittee (ORNS) proposed a reversal to the original nomenclature along with adding further commendations to the opioid receptor family and nociceptin/orphanin FQ (N/OFQ), a receptor which is selectively activated by an endogenous ligand.[16] All the opioid receptors are members of one family of proteins and can be grouped as a single receptor family. The differences in these receptors arise from the gene duplication events during evolution.[16] The opioid receptors are G-protein coupled receptors (GPCRs) that are significant for the regulation of nociception, awareness, and mood. These opioid GPCRs are activated by various endogenous peptides and a number of small-molecule agonists, from interactions with the orthosteric site that

is located in the extracellular portion of the seven transmembrane (7TM) bundle.[17] The following table gives a summary of the opioid receptors and their endogenous ligands.

Table 1.1. Opioid receptors and their endogenous ligands[16,18,19,20,21]

Opioid Receptors	**Other Nomenclature**	**Endogenous Ligand(s)**	**Agonists**	**Antagonists**
μ, mu, or MOP	MOR, OP_3	β-endorphin, enkephalins, endomorphin-1, endomorphin-2	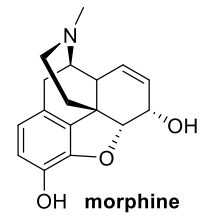 morphine 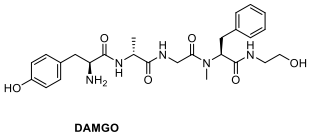 DAMGO	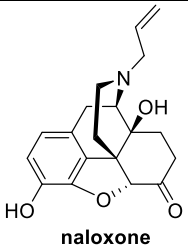 naloxone 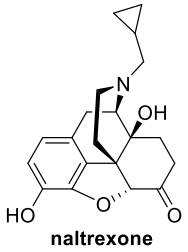 naltrexone
δ, delta, or DOP	DOR, OP_1	Enkephalins, β-endorphin	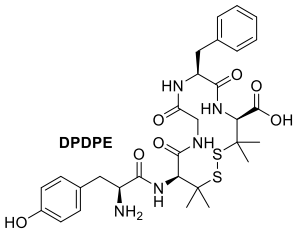 DPDPE	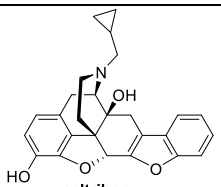 naltriben 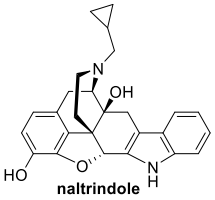 naltrindole

κ, kappa, or KOP	KOR, OP_2	Dynorphin A, dynorphin B, α-neoendorphin	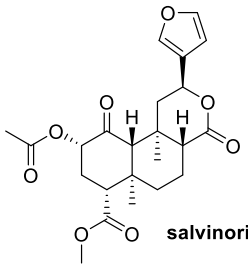 salvinorin A 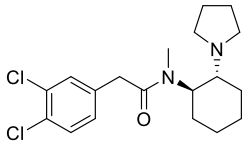 U50488	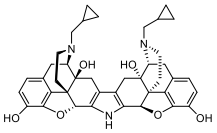 Norbinaltorphimine [norBNI]
NOP	ORL_1, OP_4	N/OFQ	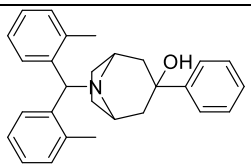 SCH 221510	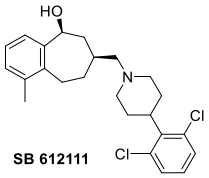 SB 612111

Opioid receptors are extensively distributed in the human body and are significantly involved in various physiological processes, which include pain signaling in the peripheral and central nervous systems, respiration, reproduction, immunological response, growth, opioid induced constipation or abdominal pain, and opioid induced bowel dysfunction. The amino acid sequences in these opioid receptors are roughly 60% identical, indicating their common origin.[18]

1.2.2. Cannabinoid Receptor Subtypes

The endocannabinoid system include two cannabinoid receptors: CB_1 and CB_2. CB_1 receptors are located in high density in various areas of the brain and mediates the behavioral effects of the endocannabinoids. CB_1 and CB_2 receptors are also members of GPCRs with a protein structure characterized by 7TM and a *C*-terminal domain which associates with arrestins or G-proteins.[22]

Table 1.2. Cannabinoid receptors and their endogenous ligands[22,23]

Cannabinoid Receptors	Endogenous Ligands	Agonists	Antagonists
CB_1	2-AG	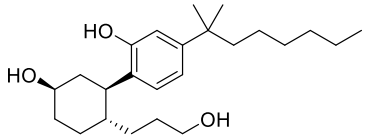 CP55940	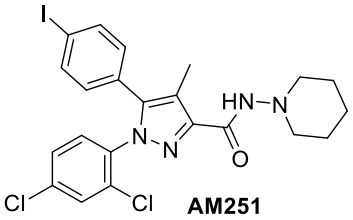 AM251 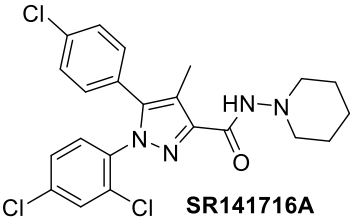 SR141716A
CB_2	2-AG	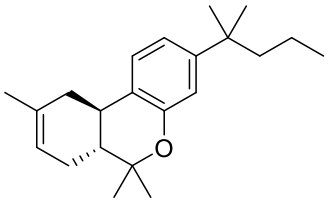 JWH-133 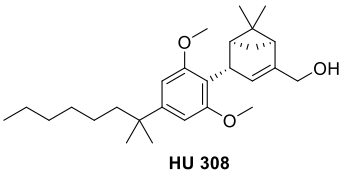 HU 308	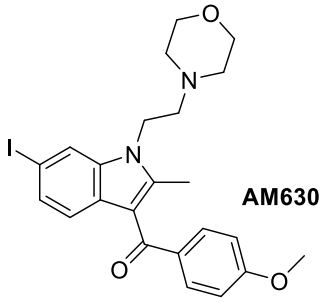 AM630 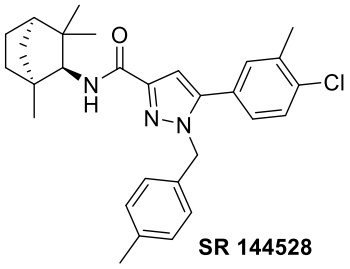 SR 144528

Other endogenous cannabinoid receptor ligands that were isolated include *N*-arachidonoylethanolamine [anandamide], noladin ether,[24] virodhamine,[25] *N*-arachidonyldopamine, and docosatetraenylethanolamide.[26] Activation of CB_1 receptors result in antinociception, decrease in body temperature and spontaneous activity, memory-disruption, and

catalepsy.[22] Activation of CB_2 receptors result in immunomodulatory properties without any psychotropic effects.[27]

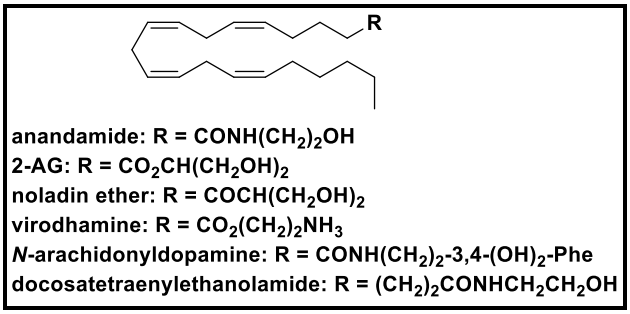

Figure 1.5. Chemical structures of cannabinoid receptor endogenous ligands, agonists, and antagonists[28,29]

1.2.3. Therapeutic Potentials of Opioid and Cannabinoid Receptor Modulators

Opioids are the most ancient and potent drugs that are used in the treatment of severe, acute pain including cancer pain. However, the continued use of opioids in chronic non-malignant pain includes the risks of abuse, addiction, and overdosage along with adverse side-effects such as respiratory depression, cognitive deficit, constipation, dizziness, nausea, endocrinopathy, sedation, and cardiac arrhythmia.[30]

Simultaneous activation of one or more opioid receptor types, selective target of hetero-oligomers, and opioid ligands which differentially activate discrete intracellular signalling cascades are few approaches to limit the tolerance of chronic opioid administration. The design of novel heteromer selective antibodies, agonists, or antagonists will help modulate the receptor complexes, and evaluate the analgesic potency. The identification of the signalling pathways responsible for the heterologous desensitization, and the cellular adaptations under chronic morphine exposure along with the development of the bivalent agonists, might help in the development of novel drugs for the prevention of acute or chronic tolerance or to extend the analgesic efficacy.[31] Partial agonists occupy the major portion of receptors compared to full

agonists in order to produce a response of equivalent magnitude. Mixed agonists/antagonists acts as agonists at low concentrations and antagonists at high doses. Such compounds exhibit high analgesic effects, and may produce acute withdrawal syndrome when administered with a pure agonist. All three opioid receptors facilitate analgesia with different side effects due to variable regional expression, functional activity of receptors, and plasticity in various parts of peripheral and central organ systems.[30]

The characterization of the CB receptor-independent and CB receptor-dependent mechanisms could be helpful in the development of multi-targeted polypharmacological compounds for diseases involving multiple mechanisms, especially the neurodegenerative and neuropsychiatric diseases, where the endocannabinoid system dysregulation plays a significant role.[32]

My research is focused on the role of natural products in drug discovery. Part of my research involved the investigation of psychoactive medicinal plants that targeted opioid and cannabinoid receptors. *Banisteriopsis caapi* is one of the psychoactive medicinal plants that exhibited activity against opioid and cannabinoid receptors. The coming sections will discuss the neurological disorders associated with not only opioid and cannabinoid receptors, but also monoamine oxidase (MAO) isoenzymes along with their current therapies, highlighting the role of opioid and cannabinoid receptors and MAOs in the pathogenesis of these neurological disorders.

1.3. Neurological Disorders

According to the 2010 Global Burden of Disease-study (GBD), the burden of substance use disorders and neurological disorders were individually estimated. Neurological disorders include disorders such as Parkinson's disease, epilepsy, and dementia. Neurological disorders

accounted for 28.6% of disability adjusted life years, while substance use disorders accounted for 14.7% Between the years of 1990 and 2010, absolute daily-adjusted life years (DALYs) for neurological, substance use, and mental disorders increased from 182 million to 258 million DALYs, accounting for 41% raise (Figure 1.7).[33]

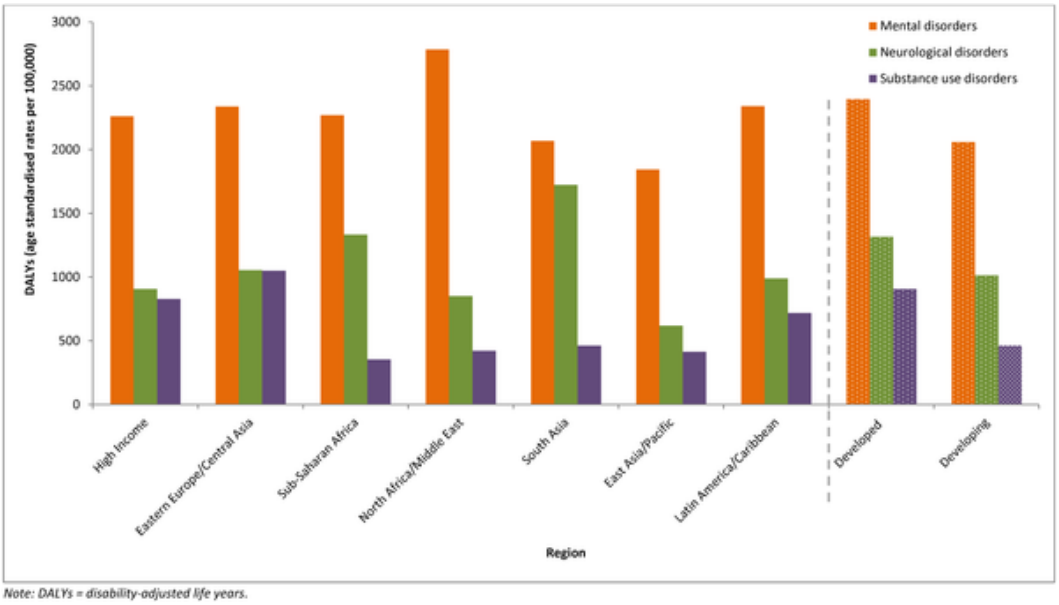

Figure 1.6. DALY rates of neurological, substance use, and mental disorders by region. Reprinted with permission from Whiteford, H. A.; Ferrari, A. J.; Degenhardt, L.; Feigin, V.; Vos, T. *PLOS One*, **2010**, *10*, e0116820. Copyright © 2015 Whiteford et al. [**Open access article**]

1.4. Parkinson's Disease (PD)

PD is the second most common neurodegenerative disorder following Alzheimer's disease (AD). In industrialized areas, PD affects 1% of all population over 60 years of age. The prevalence of PD is increasing over the years and is expected to double by 2030.[34] The incidence of PD seen in high income countries is 14 per 100,000 people in total population and 160 per 100,000 in people aged 65 years or older. In United States, the disease frequency was estimated to be 1.3% in females and 2% in males in individuals aged 40 years. The prevalence of age-related PD is lower in Africa than in the Americas and Europe, which reflects both mortality and

incidence, while the incidence in Asia is similar to that in the Americas and Europe. The incidence of PD is usually low in people below 50 years of age, and increases rapidly with age.[35]

1.4.1. Pathogenesis

PD is one of the common central nervous system (CNS) neurodegenerative disorders. The core pathology of PD includes the loss of dopaminergic nigral neurons and the formation of α-synuclein containing Lewy bodies.[36] Genetic mutations and environmental toxins are considered to be some of the etiological triggers that are linked to PD, with an unknown pathway leading to cell-death. The most common pathway underlying in both the sporadic and genetic forms of the disorder, is the defective dopamine sequestration into the vesicles, resulting in the production of the reactive oxygen species in cytoplasm. This is the primary reason for the death of dopaminergic neurons in PD.[37]

There are various pathogenic mechanisms resulting in the loss of dopaminergic neurons in PD. The first neurodegenerative change in PD is the loss of terminals in the striatum, followed by the accumulation of the aggregated proteins, Lewy neurites, in the nigral processes. The Lewy body like inclusions in the nigrostriatal terminals are accompanied by retrograde degeneration, and further accumulation of Lewy bodies, resulting in reactive gliosis and cell death. There are only three known mutant proteins resulting in PD among several monogenic familial forms: α-synuclein, parkin, and ubiquitin carboxy-terminal hydrolase L1 (UCHL1). The mutations in α-synuclein results in the loss of normal function, and toxic effects of altered forms, thereby promoting dopamine accumulation in the cytoplasm. This would primarily lead to oxidative stress at nigrostriatal terminals where dopamine is synthesized and stored, triggering the above mentioned neurodegenerative changes. Mutations in parkin and UCHL1 promote buildup of dopamine in the cytoplasm by decreasing the clearance of α-synuclein toxic forms, which could

penetrate vesicles and result in the escape of small molecules like dopamine into the cytoplasm. Hence, the role of α-synuclein is evident in the recycling of synaptic vesicles, thereby resulting in the accumulation of the cytoplasmic dopamine, which is the final detrimental event causing the death of nigral dopaminergic neurons in PD.[37]

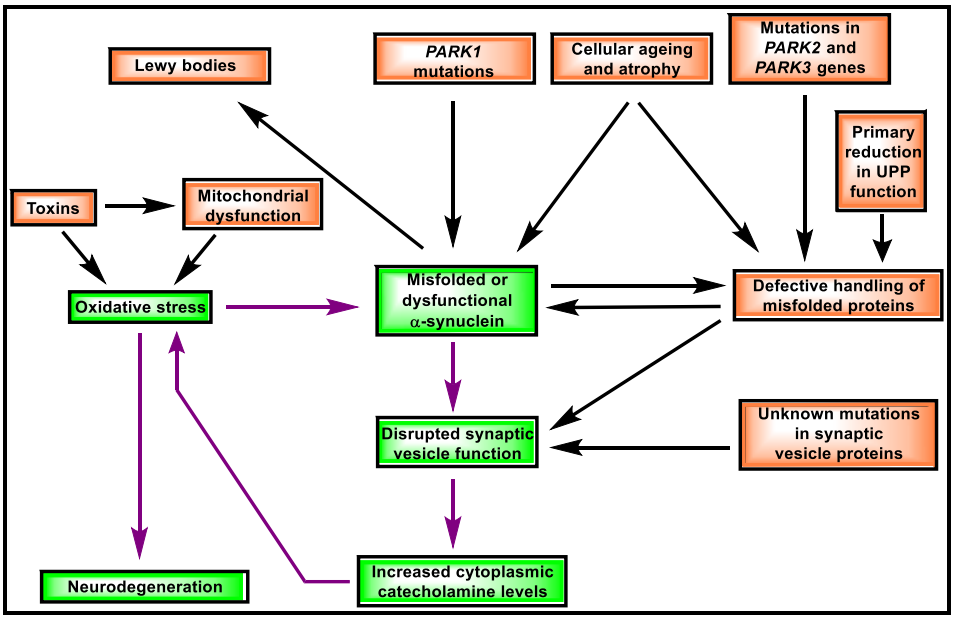

Figure 1.7. A common pathway leading to nigral degeneration in PD. The terms highlighted in green and purple arrows represent the deleterious processes that lead to cell-death. The mutations in the genes for α-synuclein (*PARK1*), parkin (*PARK2*), and ubiquitin carboxy-terminal hydrolase L1 (*PARK5*) and defects in ubiquitin-proteasome pathway (UPP) result in dopamine accumulation in the cytoplasm. Reprinted with permission from Lotharius, J.; Brundin, P. *Nat. Rev. Neurosci.* **2002**, *3*, 932-942. Copyright © 2002 Nature Publishing Group. [**Permission# 4200060836415**]

Dopamine is synthesized in the cytoplasm and then sequestered to the monoaminergic vesicles. If unstored, dopamine will be auto-oxidized to superoxide radical [$O_2{*}^-$], hydrogen peroxide (H_2O_2), and dopamine-quinone which is a cytotoxic by-product of dopamine. Alternatively, it can be oxidized by MAO to H_2O_2 and 3,4-dihydroxyphenylacetic acid

(DOPAC), an inert metabolite. Presynaptic terminals are enriched with α-synuclein, where 50% is cytosolic and the other 50% is associated with the synaptic membranes. The secondary structure of α-synuclein is converted from predominant random coil to 83% α-helix when bound to phospholipid membranes. Mutation in Ala30Pro results in the impairment of the ability of the protein to bind to small phospholipid vesicles, while the mutation in Ala53Thr prevents its coalition with planar lipid membranes. α-synuclein has a significant neuronal function of regulating the synaptic vesicles formation through phospholipase D2 (PLD2) interactions from early endosomes. Mutations in α-synuclein could reduce the number of vesicles necessary for dopamine storage, resulting in dopamine accumulation in the cytoplasm, and thereby, increasing the oxidative stress levels.[37]

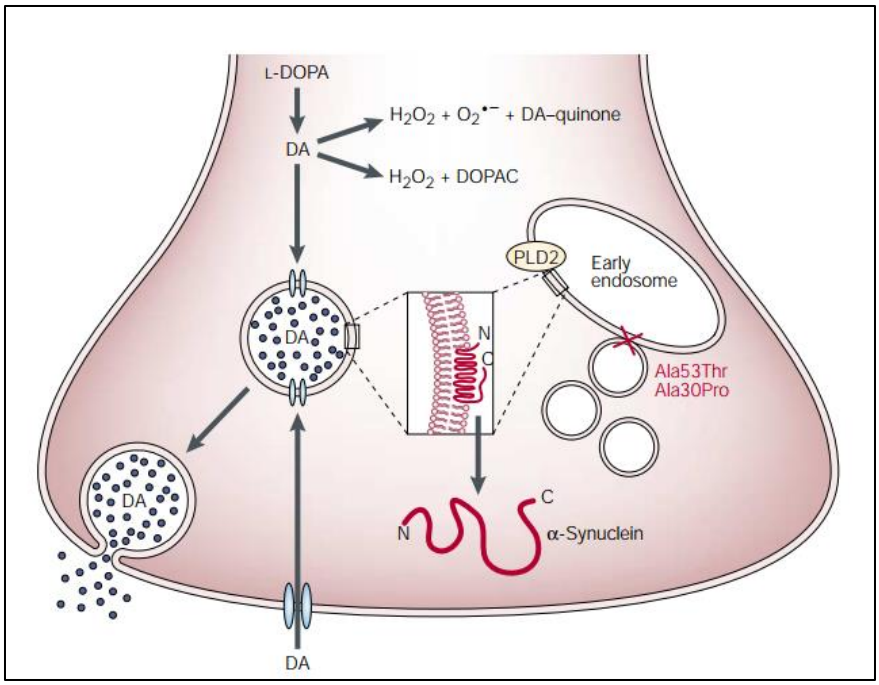

Figure 1.8. α-synuclein and intracellular dopamine storage. Reprinted with permission from Lotharius, J.; Brundin, P. *Nat. Rev. Neurosci.* **2002**, *3*, 932-942. Copyright © 2002 Nature Publishing Group. [**Permission# 4200060836415**]

Dopamine metabolism can result in the formation of various cytotoxic molecules including hydroxyl radicals [OH*], superoxide anions [$O^{2}*^{-}$], and dopamine-quinone species [SQ*]. The breakdown of dopamine occurs spontaneously in the presence of iron, or is catalyzed by MAO in a reaction which generates H_2O_2. Though cells are not damaged by H_2O_2, the formation of hydroxyl radicals by Fenton reaction can result in cytotoxicity. In general, these cells use various antioxidant systems to scavenge these deleterious molecules. Glutathione (GSH) peroxidase uses reduced glutathione to detoxify the H_2O_2, while the oxidized glutathione (GSSG) is reduced by GSSG reductase and is reused. The electrophilic centers of several potentially toxic compounds are converted to thioether bonds by GSH-*S*-transferase. Superoxide is coverted to H_2O_2 by superoxide dismutase, while catalase converts H_2O_2 to molecular oxygen and water. The balance between the production and elimination due to an abnormal increase of reactive oxygen species is tilted in PD, resulting in an enhanced oxidative stress.[37]

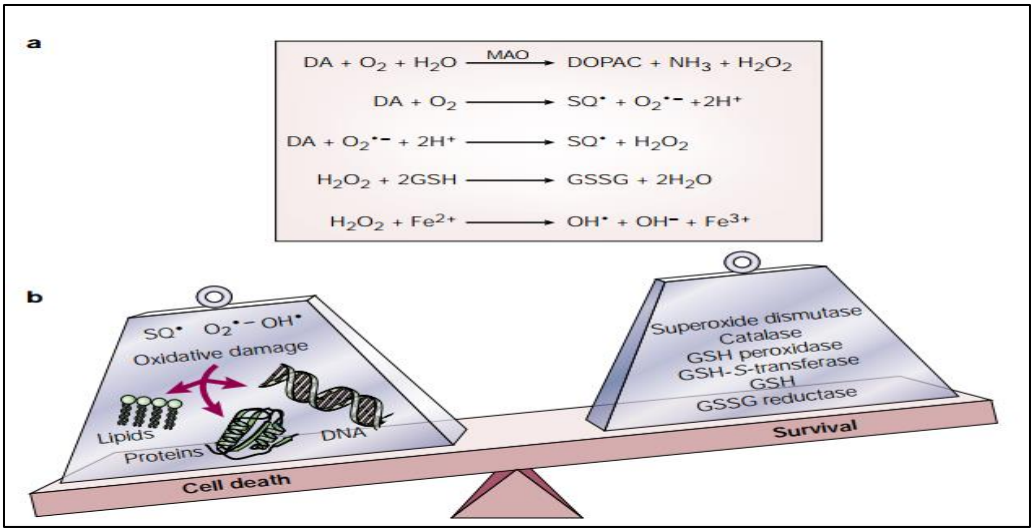

Figure 1.9. a. Metabolism of dopamine in normal person. **b.** Pathogenesis in PD. Reprinted with permission from Lotharius, J.; Brundin, P. *Nat. Rev. Neurosci.* **2002**, *3*, 932-942. Copyright © 2002 Nature Publishing Group. [**Permission# 4200060836415**]

1.4.2. Risk Factors

There is an increased risk in developing parkinsonism or PD from contact with toxic environmental substances such as agricultural chemicals or drinking well-water, and specific living conditions such as farming and rural living. Environmental factors such as metals, herbicides, and pesticides result in increased levels of α-synuclein in the brain, thereby causing parkinsonian symptoms. Evidence showed the presence of an insecticide, dieldrin, which is a lipid-soluble, long lasting mitochondrial poison in patients with PD. Further evidence showed that PD is associated with the exposure to pesticides, resulting in the impairment of the mitochondrial function by inhibition of the mitochondrial complex I or by increase in oxidative stress.[38]

1.4.3. Diagnosis

Patients with PD experience both nonmotor and motor symptoms. The motor symptoms of PD include rigidity, tremor, bradykinesia, and postural instability, while the nonmotor symptoms include depression, autonomic dysfunction, sleep disorders, and olfactory disturbances.[38] Parkinsonian disorders can be categorized into four different types: primary/idiopathic parkinsonism, secondary/acquired/symptomatic parkinsonism, heredodegenerative parkinsonism, and multiple system degeneration which includes parkinsonism along with its syndromes. Several features of PD such as tremor, postural instability, early gait abnormality such as freezing, response to levodopa, and pyramidal tract findings differentiate it from other parkinsonian disorders. There will be differences in the postsynaptic dopamine receptor density in patients with PD, which would result in poor response to levodopa therapy. Recent positron emission tomography (PET) imaging studies also showed relative preservation of dopamine receptors in progressive supranuclear palsy (PSP), proposing

downstream changes as probable mechanism for lack of response. Excellent initial responses are seen in patients with multiple systems atrophy (MSA), but they often develop levodopa related orofacial dyskinesias and the antiparkinsonian efficacy is lost. Although levodopa improvement differentiates PD, it does not distinguish PD with other parkinsonian disorders. Sub-cutaneous injection of apomorphine is used to distinguish PD from other parkinsonian disorders; nonetheless, this is not a superior test compared to levodopa therapy and contributes less to diagnostic evaluation.[39]

Neuroimaging techniques are also useful to differentiate PD from other parkinsonian disorders. Prospective imaging studies include [^{18}F]-fluorodopa PET, [^{11}C]-raclopride imaging of D2 dopamine receptors, single photo emission tomography of the striatal dopamine reuptake sites, and high 1.5 T field strength heavily T_2 weighted magnetic resonance imaging (MRI). One of the studies suggested that the brain parenchyma sonography could be highly specific for the differentiation of PD from atypical parkinsonism, but abnormal hyperechogenicity is also seen in both PD and essential tremor. Though these neuroimaging techniques are promising, there is the need for further improvement and resolution in sensitivity before their diagnostic potential is completely realized.[39]

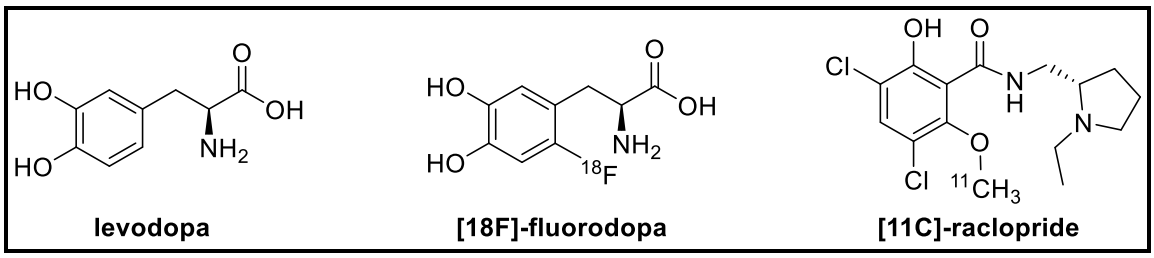

Figure 1.10. Chemical structures of levodopa, [^{18}F]-fluorodopa, and [^{11}C]-raclopride

1.4.4. Current Therapies

There is no cure for PD. Motor symptoms are clinically the major features of PD onset and progression. Since the 1960s, the treatment of PD has been focused on the supplement or

replacement of dopamine (DA). Currently, there are two major approaches in improving the dopaminergic activity in the brain: using exogenous agents to augment the secretion of dopamine and to target the related neurotransmission pathways.[40] The most effective treatment to-date is levodopa that benefits almost all the PD patients; however, the long term use of levodopa could result in motor complications, such as levodopa-induced dyskinesia (LID), "on-off", and "wearing-off" phenomena that can result in mild and non-disabling to incapacitating. Advanced stage PD patients have their motor complications emerged, and need a modified dosage, change in levodopa formulation, and combination with other drug treatments.[41] These include MAO-B inhibitors (rasagiline, selegiline, and safinamide), catechol-*O*-methyltransferase (COMT) inhibitors (entacapone, tolcapone), DA receptor agonists (apomorphine), anticholinergics (orphenadrine, trihexyphenidyl, procyclidine), and amantadine. Unfortunately, some of these drugs have some serious complications. Apomorphine shows the development of neuropsychiatric complications such as impulse control disorders, severe nausea, and vomiting. COMT inhibitors such as tolcapone exhibit life-threatening hepatotoxicity along with gastrointestinal symptoms. Amantadine could be used in early or late PD but its effects may wane with time, while the use of anticholinergics is limited due to their cognitive side effects.[40]

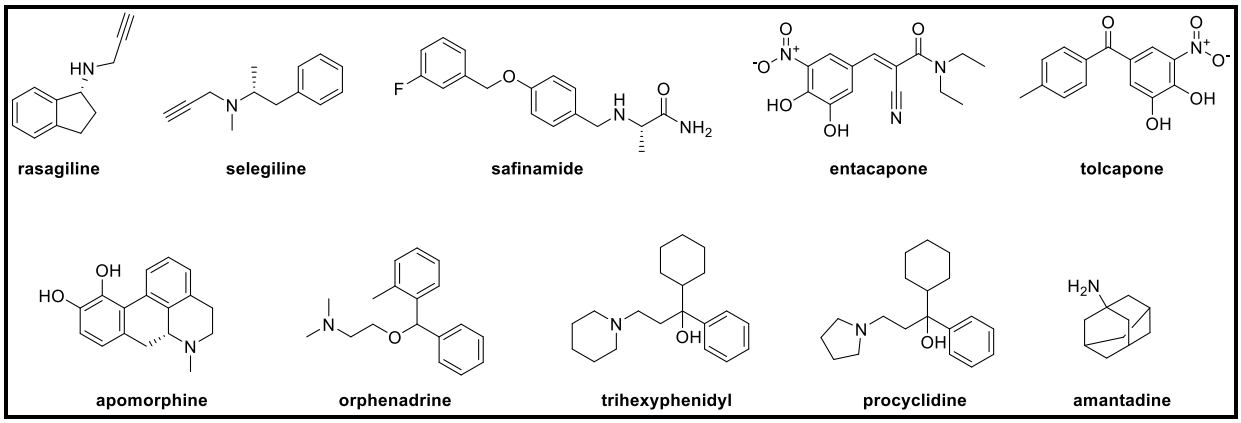

Figure 1.11. Chemical structures of rasagiline, selegiline, safinamide, entacapone, tolcapone, apomorphine, orphenadrine, trihexyphenidyl, procyclidine, and amantadine.

1.4.5. Agents Under Investigation

Since there is no cure for PD, the treatment for PD is aimed at treating the symptoms. Amino acid decarboxylase catalyzes L-Dopa to dopamine in the pre-synapse. DA is then released into the synaptic cleft, where it binds to D1-like [D1 and D5] and D2-like [D2, D3, and D4] receptors. In the glia cells, DA is metabolized to 3-methoxytyramine (3-MT) by COMT or to DOPAC by MAO-B isoenzyme. Dopamine transporters can also reuptake DA into the pre-synapse. Hence, the treatment options include L-Dopa, D1-like and D2-like dopamine agonists, COMT-, and MAO-B inhibitors. Figure 1.13 shows the various stages at which the PD drugs are targeted.[42]

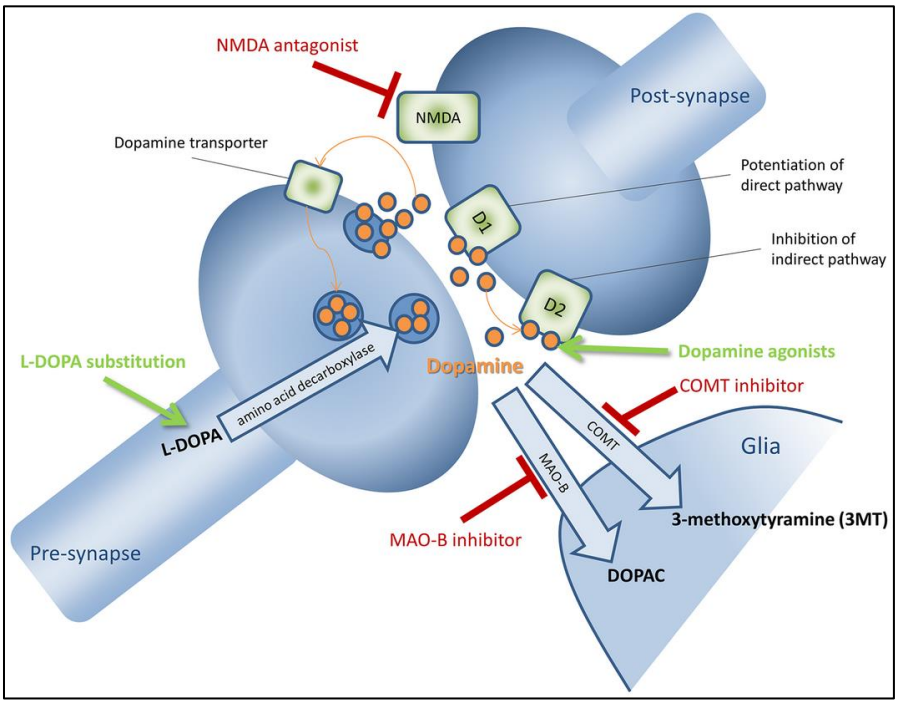

Figure 1.12. Current and investigational agents for the treatment of PD. Reprinted with permission from Oertel, W.; Schulz, J. B. *J. Neurochem.* **2016**, *139*, 325-337. Copyright © 1999-2017 John Wiley & Sons, Inc. [**Permission# 4200061422503**]

Table 1.3 shows the examples of drugs that are in various phases of clinical trials for PD. The drugs that are in the development for PD include adenosine 2a receptor (A2A) receptor antagonists, alpha-2 adrenergic receptor antagonists, glutamate receptor-5 antagonists, mixed action drugs, gene therapy, and neuroprotective targets. A2A receptor antagonists enhances the motor function by inhibiting the γ-amino butyric acid (GABA) release. Alpha-2 adrenergic receptor antagonists help in the management of dyskinesias, since the depletion of noradrenergic neurones is an additional component in the pathophysiology of PD. Overactivity of glutamate receptor-5 antagonists is linked with levodopa-induced dyskinesia and PD symptoms.[40, 43]

Table 1.3. PD drugs under development in the pipeline.

Structure/Name	FDA Status	Target
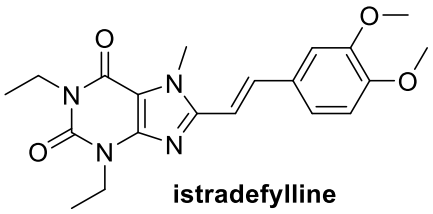 istradefylline	Phase III	A2A receptor antagonist
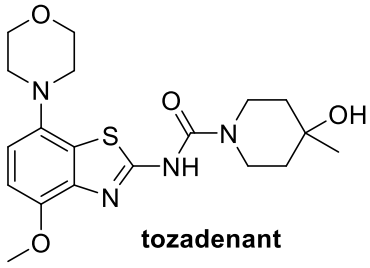 tozadenant	Phase III	A2A receptor antagonist
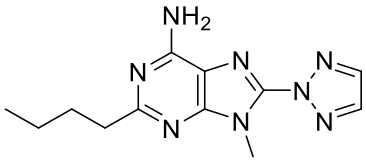 ST1535	Phase I	A2A receptor antagonist

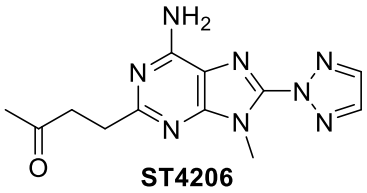 ST4206	Unknown	A2A receptor antagonist
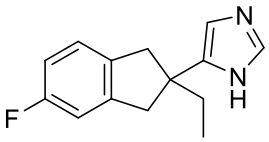 fipamezole	Phase II	Alpha-2 adrenergic receptor antagonist
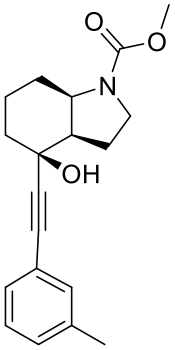 mavoglurant/AFQ056	Phase II	Glutamate receptor-5 antagonist

Table 1.4 represents the compounds that were discontinued from various phases of clinical trials for the treatment of PD. Preladenant is a non-xanthine A2A antagonist. Preladenant was orally active and exhibited good pharmacokinetic (PK) properties and excellent *in vivo* activity against parkinsonian symptoms. Preladenant was discontinued after phase III clinical trials due to the lack of evidence regarding its efficacy compared with placebo. Vipadenant is another non-xanthine compound that exhibited good oral bioavailability along with brain penetration and long plasma half-life. Despite promising phase II trials, vipadenant was discontinued in June 2010 by Vernalis and Biogen.[43] Although pardoprunox was effective in early PD, it was discontinued due to tolerability issues.[40]

Table 1.4. Discontinued PD drugs.[43]

Structure/Name	FDA Status	Target
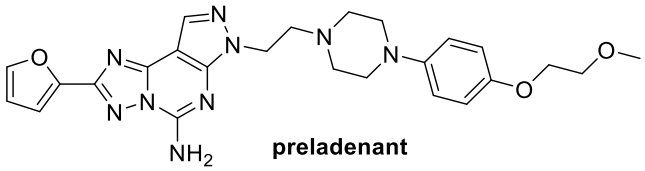 preladenant	Discontinued after phase III	A2A receptor antagonist
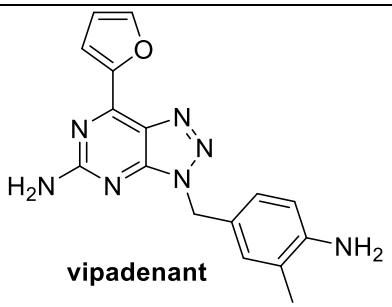 vipadenant	Discontinued after Phase III	A2A receptor antagonist
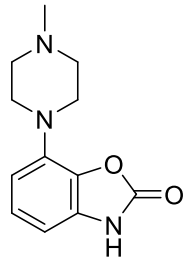 pardoprunox	Discontinued after phase III	Partial dopamine [D_2, D_3] agonist and full serotonin receptor agonist [$5HT_{1A}$]

1.5. Monoamine Oxidases

Over the past decade, the focus of MAOs has increased tremendously in the drug-discovery and development efforts. The human MAO is tightly linked with the outer mitochondrial membrane encoded with distinct genes on the X-chromosome. Human MAO is characterized into two subtypes: MAO-A and MAO-B. MAOs are specialized flavin adenine dinucleotide [FAD] dependent enzymes, which catalyze the oxidative deamination reaction of

endogenous, dietary and xenobiotic amines. There are approximately 90 members in the human flavoproteome, of which MAO-A and –B are two of the six enzymes which are linked covalently through a flavin cofactor. Only MAO and L-pipecolate oxidase have FAD linked to the 8α-methyl position of flavin through a cysteine-modified residue. MAO catalyzes the enantiospecific pro-*R* α-carbon oxidation of amine substrates to the imine products that usually undergo hydrolysis in order to produce an amine, aldehyde, and H_2O_2. H_2O_2 is a by-product of oxygen utilization through flavin regeneration.[44]

There are 5 crystal structures for MAO-A and 38 crystal structures for MAO-B since 2002 which help reveal the differences in the active site and substrate binding architectures in both MAOs. MAO-A and –B share about 70% sequence homology, with structural differences that would highly affect their functional specificity towards the inhibitor or substrate accomodation and catalysis. Human MAO-A crystallizes as a monomer, while human MAO-B crystallizes as a dimer. Human MAO-A has a monopartite cavity with a volume that extends to 550 Å along with an extended entrance conformation [residues 108-118]. The critical residues for ligand selectivity in MAO-A are Phe208–Ile335 but Phe208 is not known to function as a gating residue. The surrounding protein region of the active site in both the MAOs are hydrophobic in nature.[44]

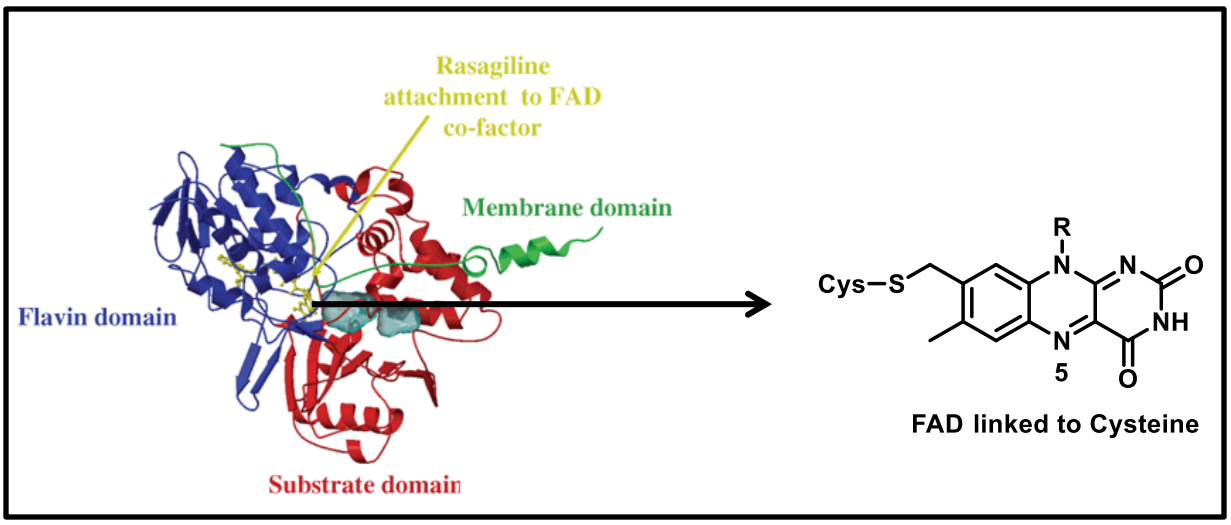

Figure 1.13. Crystal structure of human MAO-B. Reprinted with permission from Youdim, M. B. H.; Bakhle, Y. S. *Br. J. Pharmacol.* **2006**, *147*, S287-S296. Copyright © 2017 The British Pharmacological Society. [**Permission# 4200070173884**]

MAO-B crystallizes as a dimer and includes a bipartite cavity with a distinct substrate and entrance cavities. The entrance cavity is hydrophobic in nature and is approximately 290 Å in volume and is covered by residues 99-112 as an entrance loop. The larger substrate cavity is approximately 420 Å in volume, and extends to the entrance cavity from the flavin cofactor. Ile199 and Tyr326 are the amino acids that function as gating residues between the substrate and entrance cavities and are significant for both inhibitor and substrate recognition. The aromatic cage region in MAO-A is formed by Tyr407/Tyr444, while Tyr398/Tyr435 residues form the cage in MAO-B. These residues are perpendicular to the isoalloxazine ring that is covalently linked, and forms a 'bent' conformation.

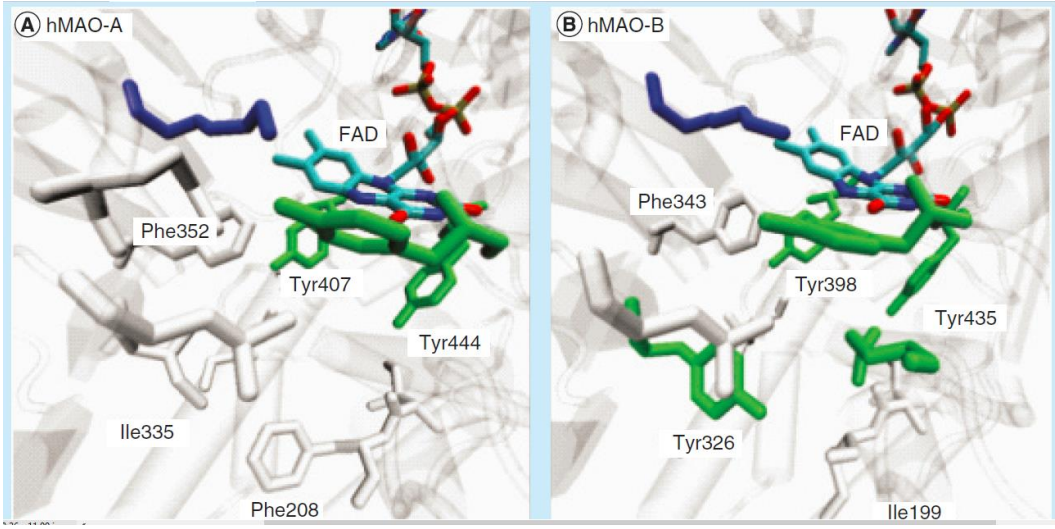

Figure 1.14. Differences in the human MAO-A and MAO-B architectures. Reprinted with permission from Chajkowski-Scarry, S.; Rimoldi, J. M. *Future Med. Chem.* **2014**, *6*, 697-717. Copyright © 2017 Future Science Group. [**Permission# 4200681286869**]

1.6. Monoamine Oxidases as PD Targets

MAOs are the key enzymes that are involved in the catalysis of the major inactivation pathway of catecholamine neurotransmitters such as dopamine, noradrenaline, and adrenaline along with 5-hydroxytryptamine as well. The initiation and progress of neurodegeneration depends on the augmented levels of oxidative-stress in the brain. Selective inhibition of MAOs in the brain contribute significantly in decreasing such stress. There are complex interactions undergoing between the MAOs and the free levels of iron in brain that may result in practical outcomes for depressive disorders. The concept of neuroprotection has been generated based on the clinical observations and consequent pharmacological analysis, reflecting the possibility of halting, slowing, maybe reversing of neurodegeneration in PD or AD. These aspects of MAOs and their inhibition indicates the importance of this pharmacological area and their therapeutics.[45]

1.6.1. MAO-B as a Target for PD

Iproniazid was the original MAO inhibitor that was effectively used in the treatment of depression, until its clinical value was negotiated due to side-effects. Due to its hydrazine structure, iproniazid caused liver toxicity. This problem was overcomed by the development of other non-hydrazine MAO inhibitors like tranylcypromine, but these induced another significant side-effect called the 'cheese reaction'.[45]

Figure 1.15. Chemical structures of iproniazid and tranylcypromine

Tyramine and other indirectly acting sympathomimetic amines present in certain foods such as cheeses and fermented drinks like wine and beer induce the cheese reaction. Dietary amines are metabolized in the liver and gut-wall by MAO under normal circumstances, and prevent them from entry into the systemic circulation. But in the presence of MAO inhibitors, this protective system is disturbed and so, tyramine and other monamines are not metabolized and hence enter the circulation; thereby releasing noradrenaline from peripheral adrenergic neurons, resulting in the release of severe hypertensive response, which could be fatal in certain cases. These serious side-effects discouraged the use of MAO inhibitors as antidepressants and paved way into looking into other areas.[45]

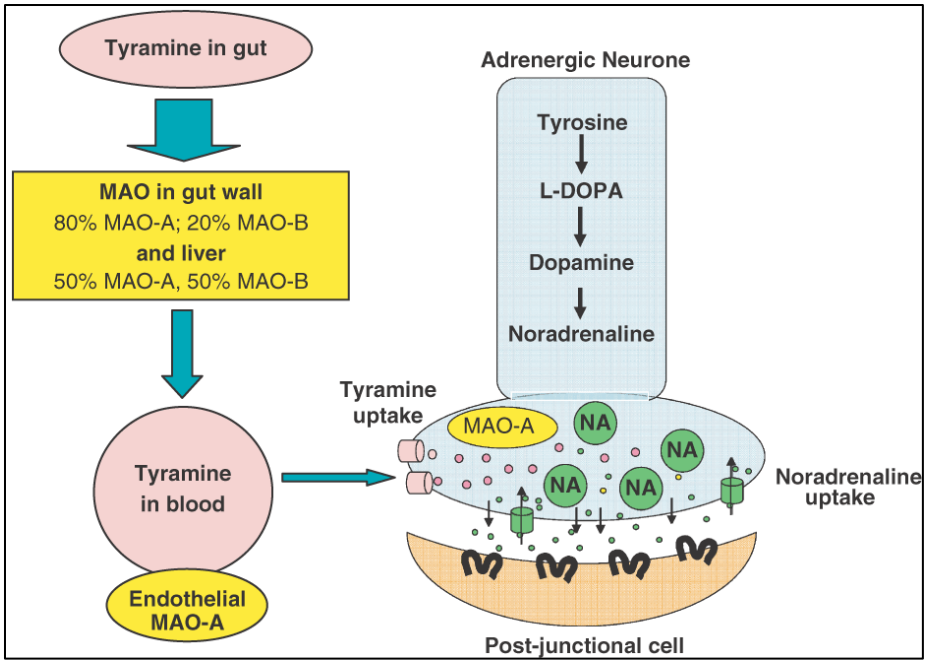

Figure 1.16. The 'cheese reaction'. Reprinted with permission from Youdim, M. B. H.; Bakhle, Y. S. *Br. J. Pharmacol.* **2006**, *147*, S287-S296. Copyright © 2017 The British Pharmacological Society. [**Permission# 4187860840706**]

The use of MAO inhibitors for the treatment of depressive disorders declined sharply after the realization of serious cardiovascular reactions due to 'cheese effect'; the fact that selective MAO-B inhibition does not cause cheese effect has facilitated the development of selective MAO-B inhibitors for the symptomatic treatment of PD. Three selective MAO-B inhibitors namely selegiline, rasagiline, and safinamide are the currently approved FDA drugs that are used for the symptomatic treatment of PD. Hence MAO-B inhibitors have projected these drugs in the drug therapy of PD due to the potential of this group of drugs in the treatment of other neurodegenerative disorders.[46]

1.7. Summary

Natural products are the most effective source of various drug leads. Artemisinin and taxol are examples of successful compounds which have been isolated from natural sources (plants). Natural products continue to provide wide structural diversity which is higher than any other source, and offer the opportunities of finding new lead compounds which are active against various biological targets. Less than 10% of the world's diversity has been explored so far and so, there are more natural lead compounds that are awaiting discovery. Due to the continued need for novel drug-like leads against various challenging biological targets, the chemical diversity from natural products are relevant for the future of drug-discovery.

The opium poppy is an ancient medicinal plant that is the major source for narcotic analgesics. The most common treatment for severe, chronic pain are opium alkaloids like morphine and similar drugs. But opioid drugs are known for their detrimental and unpleasant side effects. Hence, there is the need to develop novel agents for the management of neuropathic pain with fewer or no adverse-effects. We ultimately aim to identify new compounds with selective affinity for opioid and cannabinoid receptors. In Chapter 2, we describe the isolation and structural characterization of the secodary metabolites from *Banisteriopsis caapi* with radioligand displacement values to opioid and cannabinoid receptors. Radioligand displacement studies for opioid receptor subtypes and cannabinoid receptor subtypes were performed on the active fractions and purified bioactive compounds.

There is the need to develop new MAO inhibitors that are selective to MAO-B along with potency and minimal side-effects. We ultimately aim to develop new PD drugs targeting MAO-B with no or minimal selectivity to MAO-A. MAO inhibition assays, enzyme kinetics and mechanism studies, time-dependent enzyme inhibition assay, and analysis of inhibitor binding

and reversibility with MAO-A and –B studies were performed on the purified bioactive compounds, following which molecular modeling studies were carried out to support our data. In Chapter 3, we describe the isolation and structural elucidation of secondary metabolites from *Calea urticifolia* with potent inhibition of MAOs. In Chapter 4, we present the molecular modeling studies on acacetin, a bioactive compound isolated from *C. urticifolia*, along with the design of selective MAO-B inhibitors. Finally, Chapter 5 demonstrates the syntheses and the biological results of the designed MAO-B inhibitors.

Part of this work has been published in the *14th Annual Oxford International Conference on the Science of Botanicals* (ICSB). *Planta Medica* 10:80, PD123, **2014** [DOI: 10.1055/s-0034-1382544

CHAPTER 2. ISOLATION AND STRUCTURAL ELUCIDATION OF BIOACTIVE SECONDARY METABOLITES FROM *BANISTERIOPSIS CAAPI*

Vedanjali Gogineni, Francisco León, Janet Lambert, and Stephen J. Cutler

2.1. Introduction

Banisteriopsis caapi belongs to the family Malpighiaceae and is native to South America. *B. caapi* is known by the common names ayahuasca, yajé, natemä and caapi.[47] The ayahuasca decoction which has *B. caapi* as the major constituent along with *Psychotria viridis* is a traditional drink used by the ethnic groups for medicinal, recreational, and ritual purposes.[48] *B. caapi* is known to be a rich source of harmine and tetrahydroharmine, with harmaline to a lesser extent, which are indole alkaloids with a carboline moiety. In South America, this ceremonial beverage is known to be the spiritual core of various indigenous religions. The known medicinal properties include anthelmintic, vasorelaxant and antimicrobial properties along with ethnopsychiatric, rehabilitative, and sociopsychotherapeutic functions.[47] The known properties along with our discovery of the affinity for opioid receptors by the crude extracts of *B. caapi*, led to the phytochemical study of this plant.

There are several reports on the isolation and activity of various constituents of *B. caapi*[47, 49,50] but none on its binding ability to the opioid receptors. Hence, we focused on the receptor binding ability of *B. caapi* to the opioid receptors: μ, κ, and δ.

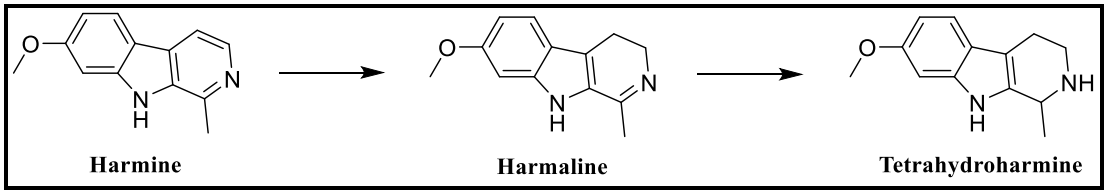

Figure 2.1. Chemical reduction of the major constituents during the decoction process

2.1.1. Specific Aims of the Research

Various efforts have been made to reduce addiction and increase the efficiency of morphine or codeine. Attempts are still being continued to reduce the abuse potential of these traditional agents. However, despite its disadvantages, the opioid receptors still play an important

role in health care and hence we focused on *Banisteriopsis caapi*, a plant native to the South America, which in our lab showed promising results in its binding ability to the opioid receptors. The plant was not screened previously for this ability and therefore we focused on identifying the compound(s) responsible for its opioid-receptor binding in order to determine the structure-activity relationship (SAR) and synthesize new analogs of the bioactive secondary metabolites.

In order to achieve the above goals, the following **specific aims** were considered:

1. To fractionate the crude methanolic extract of *B. caapi* and separate various constituents by means of polarity or nature of the compounds using bioassay-guided fractionation
2. To purify all the secondary metabolites present in the active fractions and the structural elucidation of the purified compounds
3. To perform radioligand displacement binding affinity studies for opioid and cannabinoid receptors on the purified bioactive compounds

2.2. Screening for Neurological Disorders

The isolation of *B. caapi* was carried out in our lab along with other plants including *Rhamnus purshiana*, *Arctostaphylos uva-ursi* and *Acacia xanthophloea*, among others. The dried extracts of these plants were assayed for opioid/cannabinoid activity and MAO inhibition. The ethanolic (EtOH) extract of *B. caapi* showed promising activity against opioid receptors and the following results were obtained as shown in Table 2.1. This activity was compared to the available literature on the plant, *B. caapi*, and was observed that the opioid activity has not been previously reported. Hence, the current idea of taking this research further and determining the responsible compound(s) for the receptor-binding, isolating them, and improving their binding affinities through synthesis of analogs, and performing a SAR analysis, could lead to the discovery and development of potentially novel therapeutic agents.

Table 2.1. Radioligand displacement binding affinity of various plant extracts

Sample Name	Sample Type	CB_2 %Inhibition	Delta %Inhibition	Kappa %Inhibition	Mu %Inhibition
Banisteriopsis caapi	**Leaves**	**28.8**	**79.1**	**64.9**	**73.0**
Rhamnus purshiana	Bark	-	30.0	-	20.9
Arctostaphylos uva-ursi	Leaves	8.0	0.5	-	23.9
Acacia xanthophloea	Root	-	24.8	-	27.6
Verbascum densiflorum	Aerial part	41.0	39.7	30.9	42.7
Rubus idaeus	Leaves	27.2	24.9	31.1	-
Datura stramonium	Seed	27.1	49.6	21.6	55.5
Hyoscyamus niger	Seed	24.8	27.1	-	9.5
Nerium oleander	Aerial part	-	14.5	23.1	-
Passiflora caerulea	Aerial part	-	58.9	25.3	48.6

***Concentrated at 1mg/mL and dissolved in DMSO**

2.3. Results and Discussion

2.3.1. Bioassay Guided Fractionation of *B. caapi*

The dried leaves of *B. caapi* are extracted with EtOH for at least 3 times and dried. The dried EtOH extract was divided into two equal portions and two different methods were employed to find better yield and activity. The first portion was subjected to organic treatment that includes successive extraction with hexane (Hex), dichloromethane (CH_2Cl_2), ethyl acetate (EtOAc), methanol (MeOH), and aqueous methanol. This extraction was done based on polarity and the dried portions were assayed for opioid-binding activity. The second portion of the dried EtOH extract was dissolved in MeOH: water (8:2), acidified with 1N HCl, and subjected to liquid-liquid partition with chloroform ($CHCl_3$) for 3 times, which yielded an organic and an aqueous portions. The aqueous layer was subjected to alkalinization using ammonium and was subjected to liquid-liquid extraction with $CHCl_3$ for at least 3 times. The organic layer was dried with sodium sulfate and dried in a rotavapor at low pressure. The organic layer was known to contain the alkaloids while the rest (like tannins) were seen in the aqueous layer. The obtained extracts were then assayed for opioid receptor binding affinities.

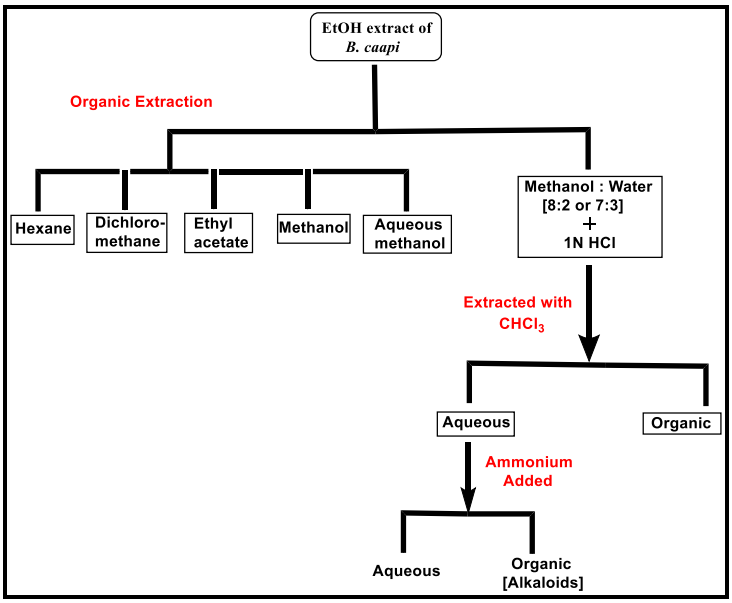

Figure 2.2. Isolation procedure of various extracts of *B. caapi*

The first portion of the dried EtOH extract was subjected to fractionation using silica gel column with 100% Hex increasing the polarity with EtOAc and MeOH and submitted for bioassay. The 50:50 Hex-EtOAc fraction showed the best radioligand displacement binding affinity [**Table 2.2**] for both cannabinoid and opioid receptors.

Table 2.2. Radioligand displacement binding affinity of *B. caapi* fractions

Fraction	CB_1 %Inhibition	CB_2 %Inhibition	Delta %Inhibition	Kappa %Inhibition	Mu %Inhibition
100% Hex	22.6	26.8	-	6.9	1.5
3:1 Hex-EtOAc	37.9	66.7	39.4	29.9	10.5
1:1 Hex-EtOAc	**86.0**	**86.9**	**79.3**	**55.8**	**62.9**
1:3 Hex-EtOAc	39.8	64.5	60.8	39.1	35.5
100% EtOAc	35.3	54.8	36.3	22.7	17.3
9:1 EtOAc-MeOH	34.1	57.3	55.6	25.9	28.6
3:1 EtOAc-MeOH	47.3	51.1	44.2	34.3	39.8
100% MeOH	64.4	43.8	30.3	15.6	19.5

***Concentrated at 1mg/mL and dissolved in DMSO**

Based on the radioligand displacement values [**Table 2.2**], the 50:50 Hex-EtOAc fraction (2.6280g) was further subjected to bioassay-guided fractionation using CH_2Cl_2, Hex, EtOAc, and MeOH with increasing polarity and submitted for bioassay. The 9:1 CH_2Cl_2-EtOAc fraction showed the best radioligand displacement [**Table 2.3**] for both cannabinoid and opioid receptors.

Table 2.3. Radioligand displacement binding affinity of *B. caapi* fractions

Sample	Fraction	CB_1 % Inhibition	CB_2 % Inhibition	Delta % Inhibition	Kappa % Inhibition	Mu % Inhibition
A	1:1 CH_2Cl_2-Hex	13.8	27.2	-	-	6.6
B	4:1 CH_2Cl_2-Hex	22.0	33.9	-	1.8	2.8
C	100% CH_2Cl_2	44.3	53.9	-	13.7	31.9
D	19:1 CH_2Cl_2-EtOAc	66.7	56.6	44.8	24.9	37.7
E	**9:1 CH_2Cl_2-EtOAc**	**91.4**	**92.2**	**85.9**	**61.6**	**69.9**
F	4:1 CH_2Cl_2-EtOAc	30.3	72.5	86.4	46.9	63.1
G	7:3 CH_2Cl_2-EtOAc	61.7	65.9	66.1	49.5	41.4
H	3:2 CH_2Cl_2-EtOAc	52.1	59.6	36.5	19.9	42.9
I	1:1 CH_2Cl_2-EtOAc	-	52.7	56.8	19.1	26.8
J	2:3 CH_2Cl_2-EtOAc	32.9	70.1	65.9	35.0	34.9
K	100% EtOAc	48.0	71.1	72.8	45.2	41.4
L	9:1 EtOAc-MeOH	66.0	55.9	85.5	45.6	56.9
M	100% MeOH	15.3	17.1	38.8	8.7	10.4

***Concentrated at 1mg/mL and dissolved in DMSO**

Based on the radioligand displacement values [**Table 2.3**], the 9:1 CH_2Cl_2-EtOAc and 8:2 CH_2Cl_2-EtOAc fractions (1.1960 g) were combined and subjected to bioassay-guided fractionation using CH_2Cl_2 and EtOAc that resulted in 12 sub-fractions that showed the following radioligand displacement values [**Table 2.4**] towards opioid and cannabinoid receptors.

Table 2.4. Radioligand displacement binding affinity of *B. caapi* sub-fractions

Fraction #	CB_1 %Inhibition	CB_2 %Inhibition	Delta %Inhibition	Kappa %Inhibition	Mu %Inhibition
EF 1 BC	47.7	84.4	50.0	7.2	34.0
EF 2 BC	16.5	65.6	-	3.2	2.6
EF 3 BC	**81.7**	**114.4**	**75.7**	**58.1**	**85.0**
EF 4 BC	69.8	64.8	58.9	30.8	76.6
EF 5 BC	55.6	109.4	94.2	39.1	89.0
EF 6 BC	48.0	108.5	72.4	59.5	53.6
EF 7 BC	-	61.5	30.3	0.7	33.4
EF 8 BC	14.5	30.9	30.5	15.6	41.4
EF 9 BC	28.2	10.9	89.7	14.3	46.9
EF 10 BC	4.1	33.2	38.4	4.5	52.6
EF 11 BC	20.5	14.8	26.6	38.3	76.5
EF 12 BC	37.9	6.6	-	-	16.2

***Concentrated at 1mg/mL and dissolved in DMSO**

The sub-fraction EF 3 BC (538 mg) showed interesting radioligand displacement values towards both opioid and cannabinoid receptors and hence was chosen for further fractionation. Sub-fraction 3 was subjected to gradient fractionation using Hex and EtOAc that yielded eight sub-fractions with the following radioligand displacement values towards opioid and cannabinoid receptors [**Table 2.5**].

Table 2.5. Radioligand displacement binding affinity of *B. caapi* sub-fraction 3

Fraction #	CB_1 %Inhibition	CB_2 %Inhibition	Delta %Inhibition	Kappa %Inhibition	Mu %Inhibition
EF 3.1	12.9	42.66	18.79	-	6.79
EF 3.2	33.5	48.80	-	-	-
EF 3.3	**71.9**	**89.20**	24.94	7.12	26.51
EF 3.4	**80.1**	**78.10**	63.93	44.05	53.82
EF 3.5	**97.0**	**89.55**	**91.00**	**95.42**	**89.01**
EF 3.6	**79.0**	**82.80**	58.84	60.70	55.64
EF 3.7	52.5	**80.77**	**86.45**	61.94	**100.0**
EF 3.8	13.3	63.40	63.68	1.20	34.99

***Concentrated at 1mg/mL and dissolved in DMSO**

Fractions 3.3 and 3.4 were combined and subjected to fractionation. These fractions along with 3.5, 3.6, and 3.7 were also subjected to fractionation and were assayed for radioligand displacement values towards opioid and cannabinoid receptors. DE 1, DE 2, DE 3, DE 5, and DE 4.1 showed the best radioligand displacement value towards CB_2 cannabinoid receptor [**Table 2.6**].

Table 2.6. Radioligand displacement binding affinity of *B. caapi* sub-fractions

Fraction	CB_1 %Inhibition	CB_2 %Inhibition	Delta %Inhibition	Kappa %Inhibition	Mu %Inhibition
BC 3.6 AD 1	19.2	56.4	-	-	-
BC 3.6 AD 2	11.5	15.0	10.8	-	-
BC 3.6 AD 4	-	4.4	13.6	-	13.8

BC 3.6 AD 5	-	3.4	-	-	-
BC 3.6 AD 6	11.4	18.6	-	0.7	-
BC 3.6 AD3 A1	2.0	1.9	10.9	-	2.8
BC 3.6 AD3 A2	5.1	2.9	6.7	-	2.9
BC 3.6 AD3 A3	9.6	2.5	4.5	2.5	3.4
BC 3.6 AD3 B1	-	-	7.4	-	-
BC 3.6 AD3 B2	-	-	3.7	-	1.2
BC 3.6 AD3 B3	-	-	3.2	-	6.8
BC 3.6 AD3 C1	6.3	1.0	-	1.2	11.5
BC 3.6 AD3 C2	10.6	12.2	14.7	-	-
BC 3.6 AD3 C3	9.4	4.6	4.2	-	-
BC 3.6 AD3 D1	11.6	3.3	-	-	0.4
BC 3.6 AD3 D2	17.5	3.1	4.6	-	9.3
BC 3.6 AD3 E	9.3	-	-	-	-
BC 3.6 I1	-	-	-	-	-
BC 3.6 I2	-	-	-	-	-
BC 3.6 I3	6.2	24.1	0.3	14.0	-
DE 1	54.9	**78.7**	-	7.8	5.6
DE 2	45.9	**75.1**	-	-	16.9
DE 3	38.2	**77.8**	-	7.2	5.2
DE 5	30.2	**72.2**	24.1	-	32.2
DE 4.1	44.6	**79.5**	-	-	1.8
DE 4.2	15.3	28.8	-	-	-

DE 4.3	-	9.7	-	-	3.1
DE 4.4	11.0	30.5	-	-	6.7
DE 4.5	**74.6**	**75.4**	**78.5**	62.2	**75.4**
DE 4.6	-	7.4	-	2.5	-
DE 4.7	-	-	-	12.0	-
DE 4.8	2.8	11.6	15.5	-	21.3
DE 4.9	34.4	**71.5**	**73.9**	51.8	**70.9**
DE 4.10	30.9	44.9	59.1	25.7	56.4
DE 4.11	10.5	14.7	32.9	26.0	36.2
DE 4.12	-	8.7	9.5	11.0	12.1
BC 4.4.1	10.7	34.4	-	-	-
BC 4.4.2	67.8	68.1	**90.4**	63.8	**87.4**
BC 4.4.3	11.0	17.3	9.0	10.2	42.9
BC 4.4.5	13.2	33.6	44.9	15.6	39.3
BC 4.4.6	9.6	24.4	27.4	-	14.0
BC 4.4.8	-	1.9	-	-	4.8
BC 4.4.9	-	-	-	-	19.7

: False positives [chlorophyll]

2.3.2. Molecular Structural Elucidation of Active Constituents

The structural elucidation of the active constituents was carried out based on a combination of spectrometric and spectroscopic experiments that include High Resolution Mass Spectroscopy (HRMS) and multidimensional nuclear magnetic resonance (NMR) Spectroscopy. To elucidate the structure of unknown chemical compounds, NMR spectroscopy is considered to

be the most powerful tool.[51] The planar structures of the new constituents are deduced from the ^{1}H-, ^{13}C- and 2D-NMR spectroscopic analyses. ^{1}H- ^{1}H- Correlation Spectroscopy (COSY) is used to determine the proton spin systems, while the Heteronuclear Multiple Quantum Correlation (HMQC) and Heteronuclear Multiple Bond Correlation (HMBC) 2D-NMR techniques are used to establish the single and multiple-bond connectivity. HMQC and HMBC are both proton-detected proton-carbon experiments but the former represents one bond correlations between carbons and protons while the later represents two and three bond correlations. HMBC experiments are considered powerful as the data is acquired with as little as 1 mg of sample along with the assignment of quaternary carbons from nearby protons.

Phytochemical investigation of the combined sub-fractions **K-M** from 50:50 Hex:EtOAc fraction when subjected to fractionation in a sephadex column using 1:1:1 Hex:CH_2Cl_2:MeOH, yielded the known triterpene, α-amyrin. The structure of the known compound was confirmed by comparison of its spectroscopic properties with published data.[52]

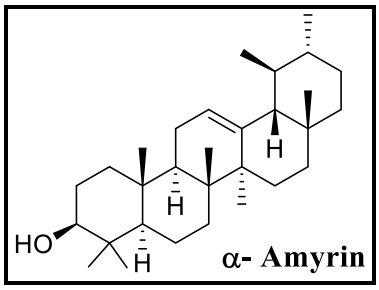

Figure 2.3. Chemical structure of α-amyrin

2.3.2.1. Structural Elucidation of the Bioactive Fractions

α-amyrin displayed the molecular formula $C_{30}H_{50}O$, assigned for its positive HRESIMS (*m*/*z* 426.3908 $[M + H]^{+}$). ^{1}H and ^{13}C NMR spectroscopic data were compared with reported data for α-amyrin and were found to be the same.[53] The palmitate of α-amyrin was previously reported from *B. caapi*.[54] α-amyrin has no known activity.

2.4. Experimental Methods

^{1}H and ^{13}C NMR spectra were obtained on Bruker model AMX 500 and 400 NMR spectrometers with standard pulse sequences, operating at 500 and 400 MHz in ^{1}H and 125 and 100 MHz in ^{13}C, respectively. The chemical shift values were reported in parts per million (ppm) from trimethylsilane (TMS) using known solvent chemical shifts. Coupling constants were recorded in hertz (Hz). Standard pulse sequences were used for COSY, DEPT, HMBC, HSQC, TOCSY, and NOESY. Column chromatography was carried out on silica-gel [70-230 mesh, Merck] and Sephadex LH-20 [GE Healthcare, Uppsala, Sweden]. TLC [silica gel 60 F254] was used to monitor the fractions obtained from column chromatography. Silica gel 60 PF254+366 plates (20 × 20 cm, 1 mm thick) were used to carry out the preparative TLC.

2.4.1. Plant Material

B. caapi was purchased from Bouncing Bear Botanicals Company, Lawrence, Kansas, United States, in May 2014. The leaves of *B. caapi* were investigated.

2.4.2. Chemicals

All the chemicals used were purchased from Sigma-Aldrich (Poole, Dorset, U.K.) with the following exceptions. [^{3}H]CP 55,940 (174.8 Ci/mmol), [^{3}H]DAMGO (53.4 Ci/mmol), [^{3}H]U-69,593 (42.7 Ci/mmol), and [^{3}H]enkephalin (45 Ci/mmol) were obtained from PerkinElmer Life Sciences Inc. (Boston, MA, USA) for the binding experiments. CP 55,940, DAMGO, DPDPE, and naloxone hydrochloride were all obtained from Tocris Bioscience (Ellisville, MO, USA).

2.4.3. Cell Culture

HEK293 cells (ATCC) were transfected stably with plasmids including cloned human cannabinoid receptor subtypes 1 and 2 obtained from Origene, Rockville, MD, USA. These cells

were preserved in a humidified incubator at 37 °C and 5% CO_2 in a Dulbecco's Modified Eagle's medium (DMEM) nutrient mixture F-12 HAM supplemented with 2 mM L-glutamine, 10% fetal bovine serum, 1000 IU/mL penicillin, 1000 μg/mL of streptomycin, and 0.5 mg/mL G418 antibiotic solution. HEK293 cells stably transfected with opioid receptor subtypes μ, δ, and κ, were used to perform the opioid receptor binding assays. These cells were maintained at 37 °C and 5% CO_2 in a DMEM nutrient mixture supplemented with 2 mM L-glutamine, 10% fetal bovine serum, penicillin–streptomycin, and either 0.2 mg/mL (δ and μ) or 0.5 mg/mL (κ) G418 or hygromycin B antibiotic solutions.

2.4.4. Membrane Preparation

Membranes for the radioligand binding assays were prepared by scraping the cells in cold Tris-HCl, pH 7.4, and centrifuged at 5200g at 4 °C for 10 min. The supernatant was then discarded, and the pellet resuspended in the same buffer, homogenized using a sonic dismembrator model 100 [Fisher Scientific, Pittsburgh, PA, USA] for 30 s, and centrifuged at 1000g at 4 °C for 10 min. The supernatant was saved, and the pellet underwent the suspension and sonication process two additional times under the same conditions. The supernatants were then combined and centrifuged at 23300g at 4 °C for 40 min. The pellet was resuspended and aliquoted into 2 mL vials and was stored at −80 °C. The total protein concentration was determined using a Pierce Bicinchoninic Acid Assay (BCA) protein assay kit [Thermo Scientific, Rockford, IL, USA] according to the manufacturer's instructions.[55] The optimal membrane and radioligand [K_D] concentrations for each receptor batch were established through membrane-evaluation and saturation binding experiments.

2.4.5. Radioligand Displacement for Cannabinoid Receptor Subtypes

Saturation experiments determine the receptor number and radioligand affinity for the membrane. Cannabinoid samples were incubated for 90 minutes at 37 °C with gentle agitation in 50 mM TrisHCl, 20 mM EDTA, 154 mM NaCl, 0.2% BSA, pH 7.4, and filtered through GF/C filterplates using a Perkin Elmer FilterMate Harvester. The assay plate was washed 10X with ice cold 50 mM TrisHCl, pH 7.4, 0.1% BSA. Radioactivity was quantified on a TopCount NXT Microplate Scintillation counter after the addition of MicroScint20 to the dried filterplate.

Percent displacement was calculated to represent the ability of the samples to displace the radioligand binding for a given cannabinoid or opioid receptor subtype.

% binding = 100 - (binding of compound - nonspecific binding)*100/specific binding.

If a purified compound exhibited > ~50% displacement, then a competitive radioligand binding assay was performed with a serial dilution of independent triplicate dilutions between 0.0017-300 µM for the test compound and between 0.017-3,000 nM for control compounds. The assays were tested with the same conditions stated above. The IC_{50} and K_i values were calculated by a non-linear curve fit model using GraphPad Prism 5.0 software (GraphPad Software, San Diego, California, USA).

2.4.6. Radioligand Displacement for Opioid Receptor Subtypes

Opioid binding assays were performed under the following conditions: 10 µM of each mixture was incubated with [^{3}H]-DAMGO (µ), [^{3}H]-U-69,593 (κ), or [^{3}H]-DPDPE (δ) for 60 minutes in a 96-well plate. Percent binding was calculated as the average of the triplicates tested at 10µM. Each sample concentration point of the compounds tested in dose response was in triplicates, and each compound showing activity was tested at least three times. The reaction was terminated via rapid vacuum filtration through GF/B filters pre-soaked with 0.3% BSA using a

Perkin Elmer 96-well Unifilter followed by 10 washes with 50 mM Tris-HCl. Plates were read using a Perkin Elmer Topcount. Total binding was defined as binding in the presence of 1.0% DMSO. Nonspecific binding was the binding observed in the presence of 10 μM DAMGO (μ), U-69,593 (κ), or DPDPE (δ). Specific binding was defined as the difference between total and nonspecific binding. Percent binding was calculated using the following formula:

% binding = 100 - (binding of compound - nonspecific binding)*100/specific binding.

Ki and IC_{50} values were calculated using Graph-Pad Prism 5; each point on the graph is representative of n=3. The binding assays of the fatty acids were performed as two independent experiments, and the results were obtained.

2.5. Summary

Bioassay-guided fractionation of *B. caapi* resulted in the isolation of a known triterpene, α-amyrin. Follow-up studies showed that α-amyrin did **not show** any radioligand displacement values towards cannabinoid and/or opioid receptors. The chemical structure of the isolated triterpene (α-amyrin) was confirmed on the basis of 1D and 2D NMR spectroscopic studies, which were compared with published data.[52] This project was discontinued due to the limited amounts of the bioactive fractions.

Part of this chapter has been published in the ***Journal of Natural Products*, 2016, *79* (10), 2538-2544** and has been formatted as per the University of Mississippi's guidelines for thesis preparation.

CHAPTER 3. ISOLATION AND STRUCTURAL ELUCIDATION OF BIOACTIVE SECONDARY METABOLITES FROM *CALEA URTICIFOLIA*

Vedanjali Gogineni, Francisco León, Khaled M. Elokely, Manal A. Nael, Narayan D. Chaurasiya, Babu L. Tekwani, and Stephen J. Cutler

3.1. Introduction

Asteraceae family includes over 1,600 genera and about 24,000 individual species, making it the largest family in the world with flowering plants. Most of the members from the Asteraceae family are known for their medicinal, economic and ornamental purposes.[56,57] *Calea* genus belongs to Heliantheae tribe and is known to include about 125 species inhabiting the subtropical and tropical regions of the world.[58] *Calea urticifolia*, known by various vernacular names including chilchaca, negrito, jaral de castilla, hierba del negro and juanislama,[59] is found to spread in Central America from Mexico to Panama, and the plant is used as folkloric medicine for the treatment of gastric ulcers and as a tropical bacteriocide.[59] Previous phytochemical studies on *C. urticifolia* revealed the presence of phenol derivatives,[60] and sesquiterpenoids including bisabolene[60] and germacrane[61,62,63] –types.

Sesquiterpene lactones are known for their extensive spectrum of biological activities including antitumor, antifungal, antibacterial, anti-inflammatory, phytotoxic, and cytotoxic properties,[64,65,66] along with their use against malaria, ulcers, dysentery, and ringworm infections.[67] The inhibitory action of sesquiterpene lactones resulted from the presence of highly electrophilic functional groups, by selectively alkylating through Michael-type addition to sulfhydryl proteins, in particular, to thiol groups, compared to other nucleophiles.[64,68] Various biological activities result from different skeletal types to understand the adaptive role of these constituents in plants, contributing to a complete understanding of these activities in pharmacological, botanical and medicinal disciplines.[69]

We found that the $CHCl_3$ extract of *C. urticifolia* displayed potent MAO enzymes' inhibition. There are no reports on its binding ability to the MAO isoenzymes and hence, we focused on the binding ability of *C. urticifolia* to the MAO enzymes.

3.1.1. Specific Aims of the Research

In order to achieve the above goals, the following **specific aims** were considered:

1. To isolate and extract the crude fractions of *C. urticifolia* and separate various constituents by means of polarity or nature of the compounds using bioassay-guided fractionation
2. To purify all the secondary metabolites present in the active fractions and the structural elucidation of the purified bioactive compounds
3. To perform MAO inhibition, enzyme-kinetics and mechanistic studies, and binding affinity studies on the purified bioactive compounds

3.2. Screening for Neurological Disorders

The isolation of *C. urticifolia* was carried out in our lab along with other plants including *Hyoscyamus niger*, *Passiflora caerulae*, *Acacia xanthophloea*, *Perovskia atriplicifolia*, and *Salix laevigata*. The dried extracts of these plants were assayed for opioid/cannabinoid activity and MAO inhibition. The $CHCl_3$ extract of *C. urticifolia* showed promising inhibition of MAOs and the following results were obtained as shown in **Table 3.1**. This activity was compared to the available literature on the plant, *C. urticifolia*, and was observed that the MAO inhibiton has not been previously reported. Hence, the current idea of taking this research further and determining the responsible compound(s) for the MAO inhibition, isolating them, and synthesizing analogs with improved selectivity and potency could lead to the discovery and development of potentially novel PD agents.

Table 3.1. Monoamine oxidase inhibition results of various plant extracts

Sample name	Extract type	MAO-A [IC_{50}][a]	MAO-B [IC_{50}][a]
Hyoscyamus niger	Seeds	57.072 ± 6.648[b]	13. 472 ± 0.892[b]
Passiflora caerulae	Aerial part	53.796 ± 3.193[b]	9.157 ± 0.989[b]
Acacia xanthophloea	Root	5.565 ± 0.071[b]	23.353 ± 3.324[b]
Calea urticifolia	**Leaves**	**2.491 ± 0.135[b]**	**1.857 ± 0.240[b]**
Perovskia atriplicifolia	Stems	36.546 ± 1.775[b]	10.959 ± 2.685[b]
Salix laevigata	Leaves	17.449 ± 0.356[b]	32.817 ± 8.646[b]
Clorgyline		0.003 ± 0.00005[c]	-
Deprenyl		-	0.088 ± 0.005[c]

[a]The IC_{50} values computed from the dose-response inhibition curves are mean ± SD of triplicate observations; [b]µg/mL; [c]µM

3.3. Results and Discussion

3.3.1. Bioassay Guided Fractionation of *C. urticifolia*

Bioassay-guided fractionation has been implemented for the isolation of the secondary metabolites from *C. urticifolia*. Based on the preliminary results, The leaves of *C. urticifolia* were extracted with $CHCl_3$ and concentrated under vacuum. The leaf extract was then fractionated in a silica gel column with 100% Hex increasing the polarity with EtOAc and MeOH, and the fractions were submitted for MAO inhibition assays. The 3:2 EtOAc-Hex fraction showed the best MAO inhibition [**Table 3.2**].

Table 3.2. MAO inhibition results of *C. urticifolia* fractions

Sample Code	Fraction	MAO-A [IC_{50}][a]	MAO-B [IC_{50}][a]
Cu-1	100% Hex	> 100[b]	> 100[b]
Cu-2	1:4 EtOAc-Hex	> 100[b]	59.85 ± 11.085[b]
Cu-3	1:4 EtOAc-Hex (**2**)	> 100[b]	11.61 ± 5.259[b]
Cu-4	2:3 EtOAc-Hex	12.006 ± 0.421[b]	14.11 ± 1.398[b]
Cu-5	**3:2 EtOAc-Hex**	**3.911 ± 0.443[b]**	**2.20 ± 0.007[b]**
Cu-6	4:1 EtOAc-Hex	8.757 ± 0.532[b]	8.13 ± 0.729[b]
Cu-7	100% EtOAc	31.676 ± 2.556[b]	16.89 ± 1.898[b]
Cu-8	1:9 MeOH-EtOAc	30.741 ± 1.795[b]	14.94 ± 1.475[b]
Cu-9	1:3 MeOH-EtOAc	15.680 ± 0.427[b]	27.48 ± 0.042[b]
Cu-10	1:1 MeOH-EtOAc	6.042 ± 0.351[b]	27.59 ± 3.954[b]
Cu-11	100% MeOH	3.175 ± 0.252[b]	23.29 ± 0.703[b]
	Phenelzine	0.249 ± 0.002[c]	0.056 ± 0.009[c]

[a]The IC_{50} values computed from the dose-response inhibition curves are mean ± SD of triplicate observations; [b]µg/mL; [c]µM

Based on the MAO inhibition, the 3:2 EtOAc-Hex fraction was subjected to further fractionation in a silica gel column using CH_2Cl_2 and EtOAc with increased polarities, and the sub-fractions were subjected for MAO inhibition assay. The sub-fractions Cu-5.5, Cu-5.6, Cu-5.7, Cu-5.8, Cu-5.10, and Cu-5.12 showed the best MAO inhibition [**Table 3.3**].

Table 3.3. MAO inhibition results of *C. urticifolia* sub-fractions

Sample Code	MAO-A [IC_{50}][a]	MAO-B [IC_{50}][a]
Cu 5.1	29.790 ± 1.7770[b]	12.018 ± 0.674[b]
Cu 5.2	> 100[b]	15.082 ± 0.009[b]
Cu 5.3	> 100[b]	53.904 ± 8.321[b]
Cu 5.4	78.691 ± 0.7879[b]	42.230 ± 0.038[b]
Cu 5.5	**1.009 ± 0.1070[b]**	**0.958 ± 0.085[b]**
Cu 5.6	**0.129 ± 0.0098[b]**	**0.145 ± 0.0072[b]**
Cu 5.7	**0.112 ± 0.0051[b]**	**0.132 ± 0.0290[b]**
Cu 5.8	**0.059 ± 0.0061[b]**	**0.069 ± 0.0017[b]**
Cu 5.10	**0.034 ± 0.0030[b]**	**0.036 ± 0.0002[b]**
Cu 5.12	**0.081 ± 0.0170[b]**	**0.058 ± 0.0067[b]**
Cu 5.14	1.749 ± 0.2110[b]	1.715 ± 0.386[b]
Clorgyline	0.0028 ± 0.0002[c]	-
Deprenyl	-	0.050 ± 0.0037[c]
Phenelzine	0.227 ± 0.034[c]	0.065 ± 0.0070[c]

[a]The IC_{50} values computed from the dose-response inhibition curves are mean ± SD of triplicate observations; [b]µg/mL; [c]µM

Figure 3.1 represents the isolation scheme of *C. urticifolia*. The isolation was performed in silica-gel columns. The active fractions and sub-fractions were purified to yield the bioactive compound/s along with other secondary metabolites. The purified fractions were submitted for MAO inhibition assay after each fractionation.

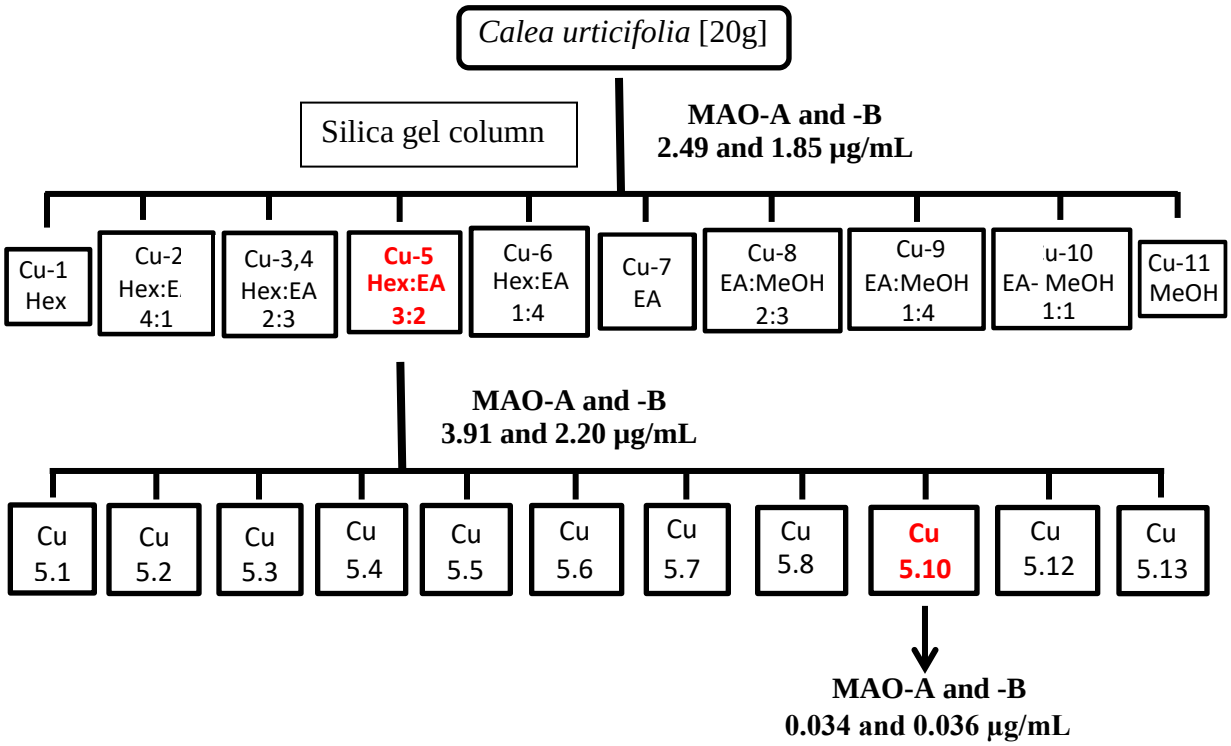

Figure 3.1. Isolation procedure of various extracts of *C. urticifolia*

Table 3.4 shows the summary of the active fractions that have been purified based on the highest inhibition. Since, the subfraction Cu 5.10 was identified as the most potent fraction, it was rechromatographed by silica gel which yielded acacetin upon further purification.

Table 3.4. Inhibition of recombinant human monoamine oxidase–A and –B by $CHCl_3$ extract, fractions, and acacetin isolated from *Calea urticifolia*

Compound	**Monoamine oxidase-A** **IC_{50} value[a]**	**Monoamine oxidase-B** **IC_{50} value[a]**
Calea urticifolia [$CHCl_3$ extract]	2.491 ± 0.135[b]	1.857 ± 0.240[b]
Fraction Cu-5	3.911 ± 0.443[b]	2.200 ± 0.007[b]
Subfraction Cu-5.10	0.034 ± 0.003[b]	0.036 ± 0.0002[b]
Acacetin	0.121 ± 0.0014[c]	0.049 ± 0.0007[c]
Phenelzine	0.238 ± 0.009[c]	0.143 ± 0.017[c]

[a]The IC_{50} values computed from the dose-response inhibition curves are mean ± SD of triplicate observations; [b]µg/mL; [c]µM

3.3.2. Molecular Structural Elucidation of the Active Constituents

The molecular structural elucidation of active constituents was similar to those mentioned earlier. Refer to page 47. Phytochemical investigation of the fractions Cu-5.5 and Cu-5.10 yielded acacetin, which was found to be the active constituent when MAO inhibition assay was performed. The phytochemical investigation of the fractions Cu-5.6, Cu-5.7, and Cu-5.8 yielded three novel bisabolenes: caleanolenes A-C, and three known germacranolides: 2,3-epoxyjuanislamin, calealactone B, and calein C [**Figure 3.2**]. The structures of the known compounds were confirmed by comparison of their spectroscopic properties with published data. Structural characterization of the new isolated compounds was based on extensive spectroscopic analysis, and the configuration of caleanolenes A-C was established by DP4 probability analysis, and ECD calculations.

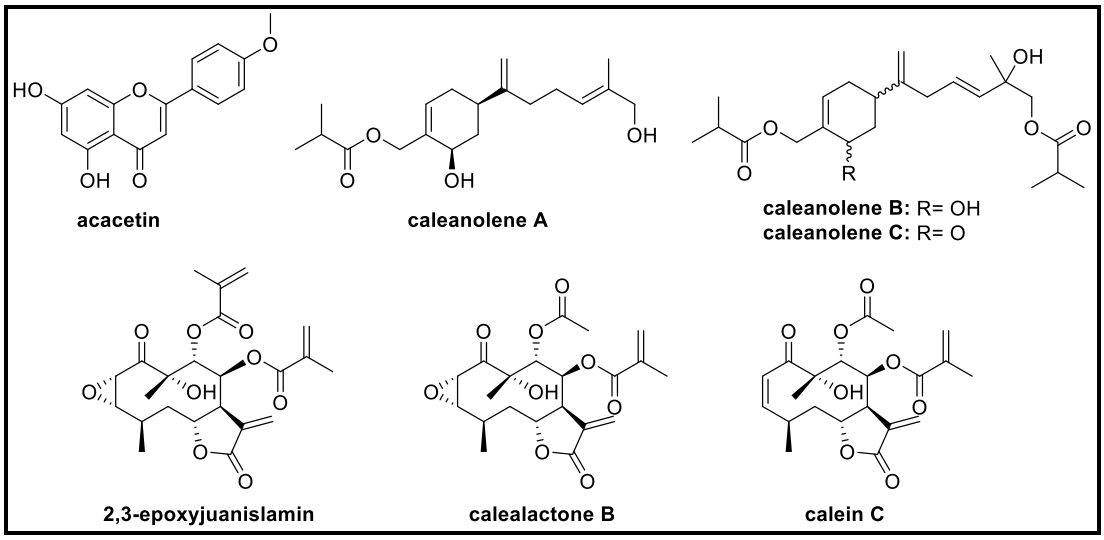

Figure 3.2. Chemical structures of the isolated secondary metabolites from *C. urticifolia*

3.3.2.1. Structural Elucidation of Acacetin and Evaluation of its MAO Activity

Acacetin displayed the molecular formula $C_{16}H_{12}O_5$, assigned for its positive HRESIMS (*m*/*z* 285.0908 $[M + H]^+$). ^1H and ^{13}C NMR spectroscopic data were compared with reported data for acacetin and were found to be the same.[70] This is the first report on isolation of acacetin from *C. urticifolia*.

Acacetin inhibited MAO-A and -B with IC_{50} values of 0.121 and 0.049 μM, respectively, which indicates a more preferential inhibition by acacetin of MAO-B over MAO-A [**Figure 3.3**]. Additionally, the potency of MAO inhibition by acacetin reported here is > 5-fold higher for MAO-A (0.121 μM vs 0.640 μM) and > 22-fold higher for MAO-B (0.049 μM vs 1.12 μM) compared to apigenin reported previously [**Table 3.5**].[71]

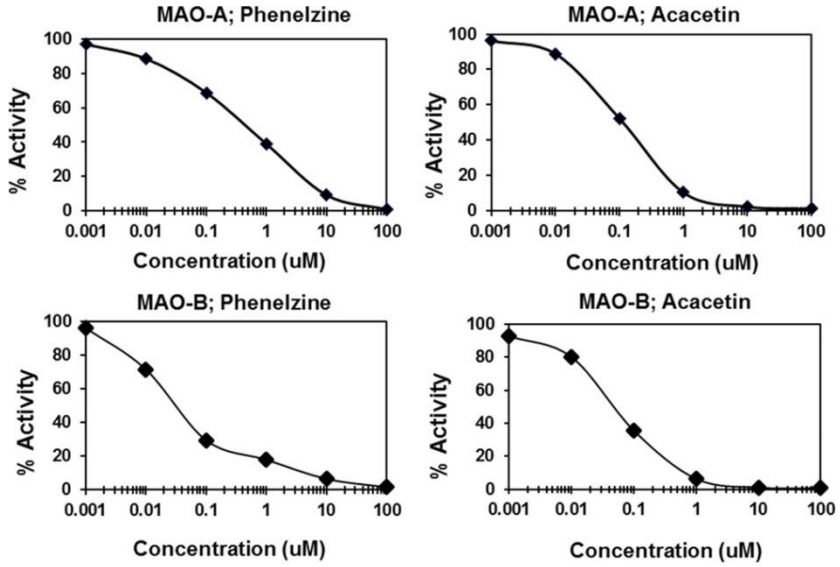

Figure 3.3. Concentration-response inhibition profile of recombinant human monoamine oxidase–A and –B by acacetin or phenelzine. Each point represents the mean value of at least three observations

Table 3.5. Inhibition of recombinant human monoamine oxidase–A and –B by acacetin isolated from *C. urticifolia* and related flavonoids[71,72]

Compound	**Monoamine oxidase-A** **IC_{50} value[a]**	**Monoamine oxidase-B** **IC_{50} value[a]**
Acacetin	0.121 ± 0.0014[b]	0.049 ± 0.0007[b]
Apigenin	0.640 ± 0.11[b]	1.12 ± 0.27[b]
Quercetin	2.44 ± 0.12[b]	38.66 ± 0.27[b]
Galangin	0.13 ± 0.01[b]	3.65 ± 0.150[b]
Naringenin	955 ± 129[b]	288 ± 18[b]
Phenelzine	0.238 ± 0.009[b]	0.143 ± 0.017[b]

[a]The IC_{50} values computed from the dose-response inhibition curves are mean ± SD of triplicate observations; [b]µM

The *in vitro* studies were reported to evaluate the mechanism and kinetics of the inhibition of human MAO-A and -B by acacetin. To understand the type of inhibition, we tested acacetin against both MAOs at different concentrations of a nonselective substrate (kynuramine). Two concentrations of acacetin were selected, one above and the other below its IC_{50} value. For every experiment, three sets of assays were performed at variable concentrations of the substrate: two concentrations of the inhibitor and one control without inhibitors. The data were analyzed by double-reciprocal Lineweaver–Burk plots to determine the K_i (i.e., inhibition/binding affinity) values. The results suggest that acacetin binds to human MAO-A at its active site and is therefore a competitive inhibitor [**Figure 3.4B**]. Similarly, MAO-B inhibition by acacetin was also competitive [**Figure 3.4D**].

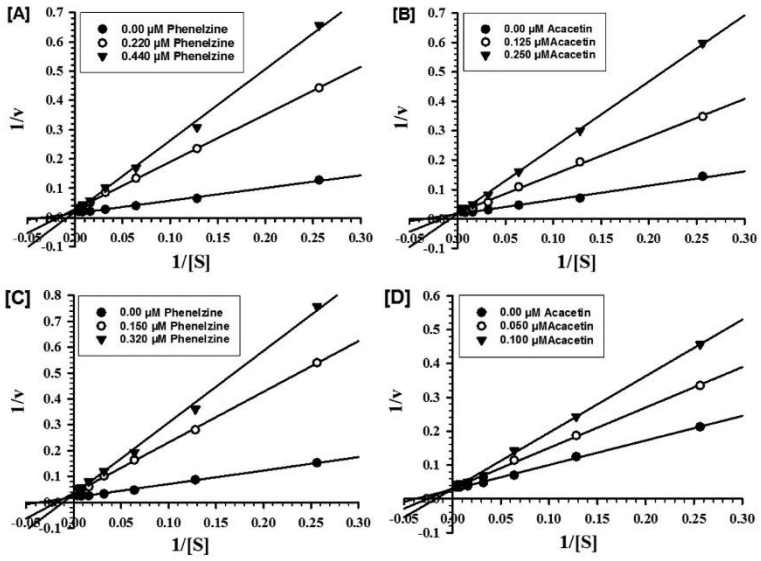

Figure 3.4. Kinetic characteristics of inhibition of recombinant human MAO-A analyzed with double-reciprocal Lineweaver-Burk plots. MAO-A and phenelzine (A) or acacetin (B), MAO-B with phenelzine (C) or acacetin (D). V = nmol/min/mg

K_i values were computed from the double-reciprocal plots [**Table 3.6**]. The binding affinities of acacetin with both MAOs were compared with phenelzine, a standard MAO

inhibitor.[73] While acacetin had binding affinities for MAO-A (K_i: 0.0592 μM) similar to those for MAO-B (K_i: 0.049 μM), it was twice as potent an inhibitor of MAO-B (IC_{50}: 0.049 μM) than MAO-A (IC_{50}: 0.121 μM) [**Table 3.6**].

Table 3.6. Inhibition/binding affinity constant (K_i) values for inhibition of recombinant human MAO–A and –B by acacetin and phenelzine[a]

Compound	Monoamine oxidase-A		Monoamine oxidase-B	
	***Ki* (μM)**	**Type of inhibition**	***Ki* (μM)**	**Type of inhibition**
Acacetin	0.0592 ± 0.0029	Competitive/ reversible	0.049 ± 0.0036	Competitive/ reversible
Phenelzine	0.163 ± 0.014	Mixed/irreversible	0.124 ± 0.004	Mixed/irreversible

[a]Values are mean ± SD of triplicate experiments

In order to analyze the time-dependent binding inhibition of MAO-A and -B, the enzymes were preincubated with each inhibitor for the indicated time (0–15 min) at concentrations that resulted in approximately 60–80% inhibition [**Figure 3.5**]. Simultaneously, controls without inhibitors were also evaluated. The activities of the enzymes were determined as mentioned in the experimental section, and the remaining enzyme activity percentage was plotted against the preincubation time to determine time-dependent inhibition. The results showed that inhibition of MAO-A and -B by acacetin was not time-dependent.

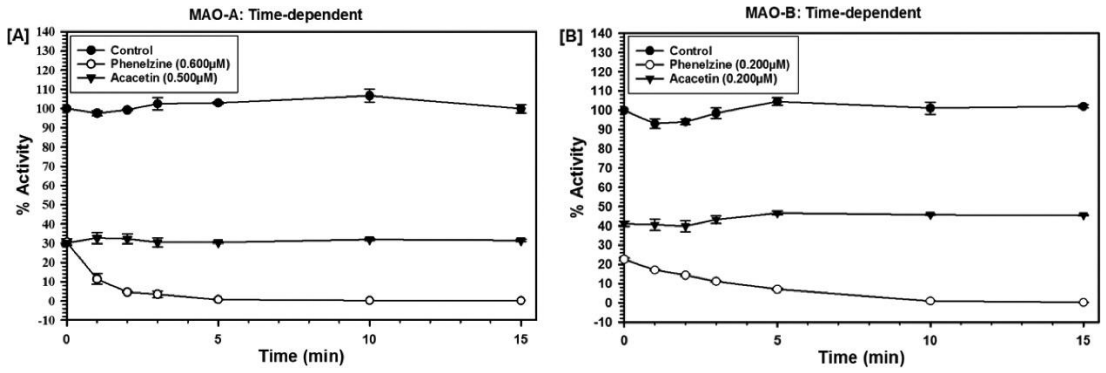

Figure 3.5. (A) Time-dependent inhibition of recombinant human MAO-A by phenelzine (0.600 μM) and acacetin (0.500 μM). **(B)** Time-dependent inhibition of recombinant human MAO-B by phenelzine (0.200 μM) and acacetin (0.200 μM). The remaining activity was expressed as % of activity. Each point represents mean ± SD of triplicate values.

The binding characteristics of acacetin were investigated by using dialysis to measure the dissociation of the enzyme–inhibitor complex. A high concentration of acacetin was incubated with the enzymes (MAO-A and -B) for 20 min. The enzyme–inhibitor complex mixtures were dialyzed overnight at 4 °C against buffer. The enzyme activies were analyzed before and after the dialysis [**Figure 3.6**]. During overnight dialysis, the recombinant human MAO-A lost about 10–15% of activity. Incubation of MAO-A with 15.0 μM acacetin inhibited more than 95% of the enzyme activity [**Figure 3.6A**]. After the dialysis, more than 90% enzyme activity was recovered from enzyme–acacetin incubation mixtures [**Figure 3.6A**]. Similarly, MAO-B lost about 10–15% of the enzyme activity during overnight dialysis. Acacetin incubation (5.0 μM) with MAO-B resulted in 90% inhibition of the enzyme activity, which was later fully recovered after the dialysis [**Figure 3.6B**]. These observations suggest that MAO inhibition by acacetin is reversible due to the dissociable nature of their enzyme–inhibitor complexes.

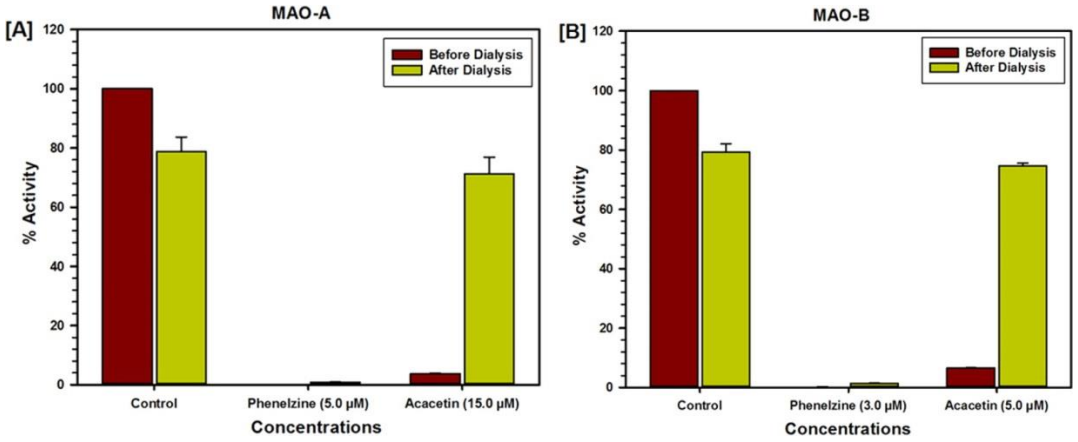

Figure 3.6. (A) Analysis of nature of binding of acacetin with recombinant human MAO-A by recovery of catalytic activity of the enzyme after equilibrium dialysis dissociation. **(B)** Analysis of nature of binding of acacetin with recombinant human MAO-B by recovery of catalytic activity of the enzyme after equilibrium dialysis dissociation. Each bar shows mean ± SD of triplicate values.

3.3.2.2. Structural Elucidation of the Remaining Bioactive Fractions

Caleanolene A was isolated as colorless oil. The molecular formula was determined as $C_{19}H_{30}O_4$, on the basis of its positive HRESIMS data (*m/z* 345.2040 $[M + Na]^+$). The IR spectrum showed absorption bands at 3353, 1736, 1013, 793 cm^{-1} indicating the presence of hydroxyl, ester, and olefinic functions. The ^1H NMR spectrum [**Table 3.7**] showed resonances that attributed to three methyl groups: one tertiary methyl at δ_H 1.68 (3H, s) and two secondary methyl groups at δ_H 1.19 (6H, d, *J* = 6.9 Hz), that could be assigned to the methyl groups of an isopropyl group; two oxygenated methylene groups at δ_H 4.40 (1H, d, *J* = 12.18 Hz), 4.98 (1H, d, *J* = 12.18 Hz) and 4.0 (2H, s br); one oxygenated methine group at δ_H 4.26 (1H, s br); four signals of vinylic protons at δ_H 4.80 (1H, s), 4.83 (1H, s), 5.41 (1H, t, *J* = 6.7 Hz), and 5.85 (1H, s br) corresponding to one methylene group and two separated tri substituent double bonds, respectively. The ^{13}C NMR [**Table 3.7**] and DEPT spectra disclosed 19 carbons which were

indicative of an isobutyryloxy group (δ_C 177.8; 34.1; 2C x 19.0). This data combined with the degrees of unsaturation suggested a ring system in the structure which is in agreement with a previous bisabolene skeleton reported from the Asteraceae family.[74,75]

Table 3.7. NMR spectroscopic data of caleanolenes A-C in $CDCl_3$

	Caleanolene A		**Caleanolene B**		**Caleanolene C[c]**	
position	δ_C [b]	δ_H mult. (*J*, Hz)	δ_C [b]	δ_H mult. (*J*, Hz)[a]	δ_C [b]	δ_H mult. (*J*, Hz)
1	31.5	2.21, m 2.00, m	31.9	2.21, m 1.99, m	31.9	2.58, m 2.30, m
2	129.5	5.85, s br	129.4	5.87, s br	146.7	6.96, dd (2.6, 5.8)
3	136.0		135.3		134.5	
4	67.5	4.26, m, m	67.4	4.27, s br	197.6	
5	37.1	2.17, m 1.56, ddd (9.7, 9.8, 12.4)	37.0	2.20, m 1.53, m	43.2	2.60, m 2.41, m
6	38.7	2.28, m	38.6	2.32, m	40.4	2.71, m
7	152.1		150.9		148.7	
8	34.0	2.11, m	37.4	2.80, d (6.4)	37.2	2.79, d (6.9)
9	26.1	2.19, m 2.10, m	127.9	5.77, ddd (6.7, 6.8, 15)	127.3	5.74, ddd (6.9, 7.8, 15)
10	125.5	5.41, t (6.7)	135.1	5.56, d (15)	135.6	5.56, d (15)
11	135.1		72.0		72.1	
12	68.8	4.00, s	70.8	4.08, d (11.2) 3.99, d (11.2)	70.7	4.08, d (11.1) 3.97, d (11.1)
13	13.7	1.68, s	24.9	1.32, s	24.9	1.29, s
14	108.5	4.83, s 4.80, s	109.8	4.87, s 4.80, s	111.2	4.87, s
15	65.3	4.98, d (12.1)	65.3	5.01, d (12) 4.40, d (12)	60.9	4.75, s
1′	177.8		177.7		177.1	
2′	34.1	2.59, quint (7)	34.1	2.61, , quint (7)	34.0	2.58, m
3′	19.0	1.19, m	19.0	1.20, m	19.0	1.16, m
4′	19.0	1.19, m	19.0	1.20, m	19.0	1.18, m
1″	----	----	177.4		177.6	
2″	----	----	34.0	2.61, , quint (7)	34.0	2.58, m
3″	----	----	19.0	1.20, m	19.0	1.16, m
4″	----	----	19.0	1.20, m	19.0	1.18, m

[a]Multiplicities were obtained from DEPT experiments; [b]Based on COSY, HSQC, HMBC, and ROESY experiments; [c]Spectra were recorded in $CDCl_3$.

The $^1H—^1H$ COSY experiment [**Figure 3.7**] disclosed three partial structures, $CHCH_2CHCH_2CH$; CH_2CH_2CH, and $CH(CH_3)_2$, corresponding to the C-2, C-1, C-6, C-5, C-4; C-8, C-9, C-10, and C-2′, C-1′, C-3′. HMBC correlations [**Figure 3.7**] of the oxymethylene $C\underline{H_2}$-

15 to the signal at δ_C 177.8 C-1′ corresponding to the link between the isobutyryloxy group and the bisabolene skeleton, and the correlations of the protons C$\underline{H_2}$-12 to C-10, C-11 and C-13 assisted in the linking of the second oxymethylene group. Additionally, the cross-peaks from C$\underline{H_2}$-15 to C-2, C-3, and C-4 helped to position the secondary hydroxyl and the double bond. The relative configuration of caleanolene A was deduced from the interpretation of the rotating frame overhauser effect (ROESY) spectra [**Figure 3.7**]. The ROESY correlation from C$\underline{H_2}$-12 (δ_H 4.0) to H-10 (δ_H 5.41) led to the conclusion that the stereochemistry of the C-10, C-11 double bond is *E*. The correlation from H-6 (δ_H 2.28) to H-4 (δ_H 4.26) clearly showed that these protons are on the same face.

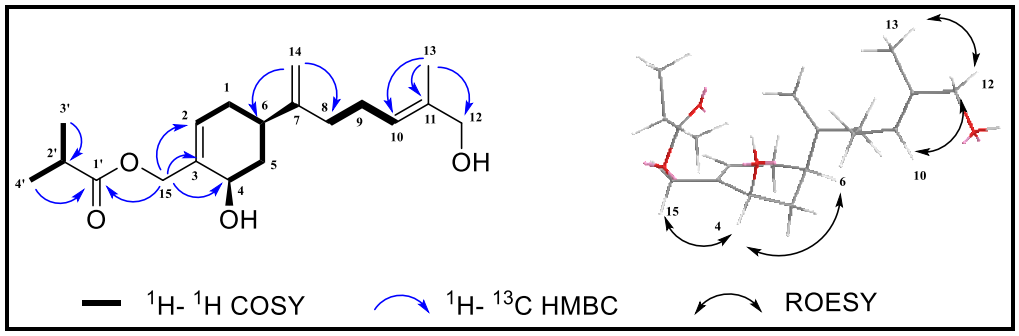

Figure 3.7. Selected COSY, HMBC, and ROESY correlations for caleanolene A

The absolute configuration of caleanolene A was established through experimental and theoretical electronic circular dichroism (ECD). The conformational space was searched using MacroModel (Schrödinger, LLC, New York) and the most abundant conformers according to Boltzmann distribution were optimized using the density functional theory (DFT) at m062x/6-31+G(d,p) level[76] [**Figure 3.8**].

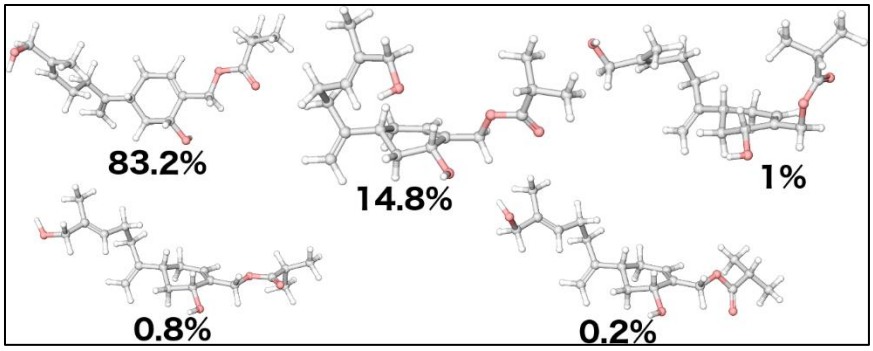

Figure 3.8. Geometry optimized conformers of caleanolene A using DFT at the m062x/6-31+G(d,p) level, and their contributions to the Boltzmann distribution

The calculated ECD spectra obtained using time-dependent density functional theory (TDDFT) at B3LYP/6–31G** level in a PCM (polarizable continuum model) methanol solvent model of the (4*S*, 6*S*) and (4*R*, 6*R*) stereoisomers are shown in **Figure 3.9**. The calculated (4*R*, 6*R*) stereoisomer showed excellent fit with the experimental data, with a negative Cotton effect at 210 nm [**Figure 3.9**]. Thus, the absolute configuration and the structure of the caleanolene A was established as (4*R*, 6*R*) 4,12-dihydroxy-15-isobutyryloxybisabola-2,7(14),10-triene.

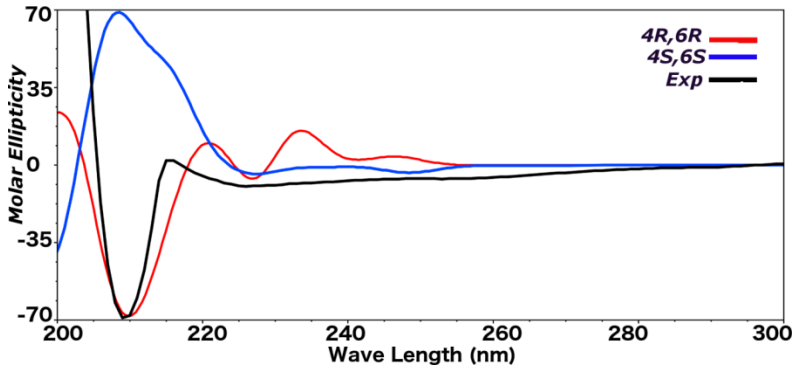

Figure 3.9. Experimental ECD spectrum of caleanolene A and calculated ECD spectra for the stereoisomers (4*R*, 6*R*) and (4*S*, 6*S*)

Caleanolene B possessed a molecular formula of $C_{23}H_{36}O_6$ as established by (+) HRESIMS data (*m/z* 431.2462 $[M + Na]^+$). The analysis of its ^1H, ^{13}C [**Table 3.7**], and HSQC NMR data revealed the existence of one sp^2 methylene at δ_H 4.87 (1H, s) and 4.80 (1H, s), three

sp^2 methines at δ_H 5.87 (1H, s br), 5.77 (1H, ddd, J = 6.7, 6.8, 15.0 Hz), and 5.56 (1H, d, J = 15.0 Hz), implying the presence of one tri-substituted, and two di-substituted double bonds. Secondary and tertiary hydroxyl groups were present at δ_C 67.4 and 72.0, respectively. Two isobutyryloxy groups were confirmed with the signals at δ_H 2.61 (2H, m), and 1.21-1.18 (12H, m); the location of these groups at C-12 and C-15 was determined through its HMBC spectrum with the correlations observed between the protons at CH_2 -12 at δ_H 3.99 (1H, d, J = 11.2 Hz) and 5.87 (1H, d, J = 11.2 Hz) and the signal at δ_C 177.4 C-1′ (detected by HMBC), and C$\underline{H_2}$-15 at δ_H 4.40 (1H, d, J = 12.0 Hz) and 5.01 (1H, d, J = 12.0 Hz) and the signal at δ_C 177.7 C-1″ (detected by HMBC). The stereochemistry of the C-9 and C-10 double bond was determined to be *E* by considering the coupling constant ($J_{9,10}$ = 15 Hz). The partial relative configuration of caleanolene B was deduced from a cross peak between H-4 and H-6 from the ROESY experiment, helping us to place these protons on the same face. However, the presence of the additional stereogenic center at C-11 enabled us to determine the absolute stereochemistry.

The stereochemical properties were depicted using computational quantum mechanical calculations, through the comparison of experimental with calculated data. The geometry optimized conformers representing all four possible stereoisomers were analyzed by applying TDDFT ECD and NMR calculations. The experimental and calculated ECD spectra were compared for each stereoisomer. The isomer (4*R*, 6*R*, 11*R*) showed perfect match with the experimental data [**Figure 3.10**]. The ECD spectra displayed a prominent negative Cotton effect at ~210 nm. The NMR tensors were obtained by calculating the gauge-including atomic orbitals (GIAO) shielding constants of the conformers within 2 kcal/mol of the global minimum. Vibrational analysis was performed to confirmed minima. The DP4 calculations[77] were executed at B3LYP/6-311+G(2d,p) level. The chemical shift (CS) values were calculated according to the

guide of the NMR CS assignment of small molecule structure.[78] The DP4 probability analysis of the experimental and calculated CS values supported the ECD results that the (4*R*, 6*R*, 11*R*) was most probable by ~ 87.4 %. Thus, caleanolene B was determined as (4*R*, 6*R*, 11*R*) 4,11-dihydroxy-12,15-diisobutyryloxybisabola-2,7(14),9-triene.

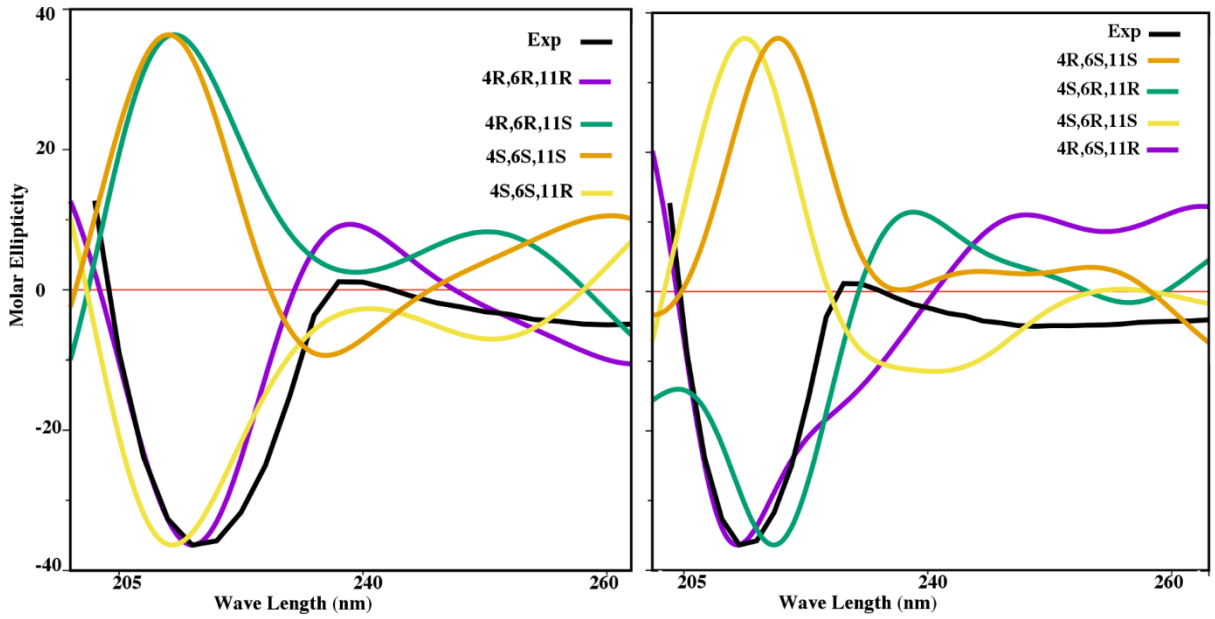

Figure 3.10. Experimental ECD spectrum of caleanolene B and calculated ECD spectra for all the possible stereoisomers

Caleanolene C, was purified as colorless oil and has the molecular formula of $C_{23}H_{34}O_6$ that was established by (+) HRESIMS data (*m/z* 429.2305 $[M + Na]^+$). The ^1H NMR spectra was similar to that of caleanolene B, suggesting that the two compounds are closely related in structure. The major difference between the two compounds is the absence of the methine proton corresponding to the secondary hydroxyl as in caleanolene B. A detailed comparison of the ^1H and ^{13}C NMR signals of caleanolenes B and C [**Table 3.7**] revealed that the secondary hydroxyl in C-4 was oxidized as an α,β-unsaturated ketone in caleanolene C (δ_C 197.6). Additionally, the low shift of the proton signal of H-2 δ_H 6.96 (1H, dd, *J* =2.6, 5.8 Hz) confirmed the presence of an α,β-unsaturated ketone. The structure was shown to be 4-oxo-11-hydroxy-12,15-

diisobutyryloxybisabola-2,7(14),9-triene. The absolute stereochemistry was deduced to be (6*R*, 11*R*) based on the matching of the calculated ECD spectrum with the experimental one [**Figure 3.11**].

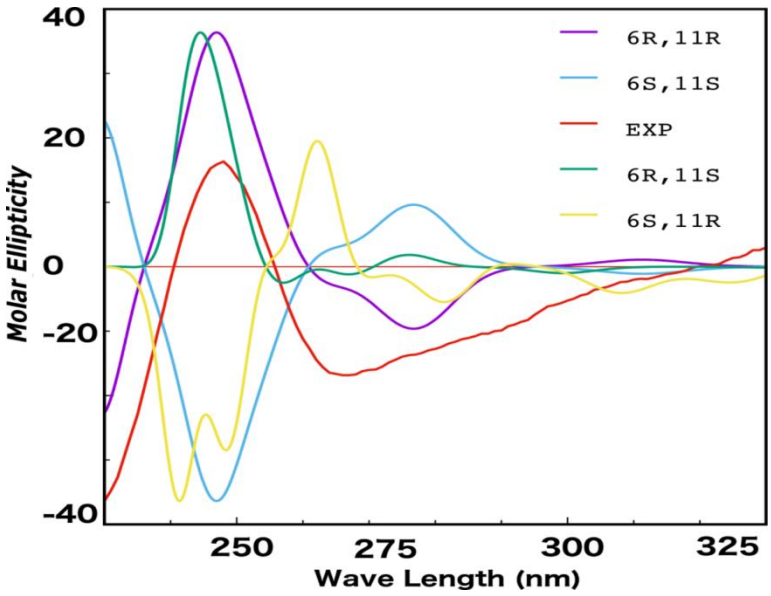

Figure 3.11. Experimental ECD spectrum of caleanolene C and calculated ECD spectra for all the possible stereoisomers

The isolated sesquiterpene lactones were assayed for their cytotoxic effects based on the previous reports that sesquiterpene lactones isolated from *C. urticifolia* have shown cytotoxic effects against U-937 lymphoma cell line,[62] and induced apoptosis in human tumor cell line HL-60.[79] These sesquiterpene lactones also showed inhibitory effects on adipocyte differentiation,[80] and inhibitory effects on melanin biosynthesis through suppression of tyrosine expression.[81] Based on these preceding bioassays, the sesquiterpenes caleanolene A, 2,3-epoxyjuanislamin, calealactone B, and calein C were assayed for their cytotoxic activities against CA46 and Raji lymphoma, and the MCF7 breast cancer cell lines [**Table 3.8**].

Table 3.8. Effects of caleanolene A, 2,3-epoxyjuanislamin, calealactone B, and calein C on the growth of the tumoral human cell lines.

Compound	IC_{50} (µM)		
	CA46	**RAJI**	**MCF7**
Caleanolene A	> 100	> 100	> 100
2,3-Epoxyjuanislamin	2.9 ± 0.3	12.3 ± 0.2	10.6 ± 0.1
Calealactone B	3.7 ± 0.6	17.5 ± 5.7	21.2 ± 4.8
Calein C	5.6 ± 0.6	11.7 ± 0.09	9.8 ± 0.6

Cells were cultured for 72h and the IC_{50} values were calculated as described in the experimental section. The data shown represent the means ± SE of 3-5 independent experiments with three determinations in each.

3.4. Experimental Methods

The general experimental methods were similar to those explained earlier. Refer to page 48.

3.4.1. Plant Material

The plant *Calea urticifolia* was collected from the University of El Salvador Campus, San Salvador, El Salvador, in July 2014 and was identified by a botanist, Jenny Menjivar. A voucher specimen (3220) has been deposited in the herbarium of the Natural History Museum of El Salvador.

3.4.2. Chemicals

Human recombinant monoamine oxidase-A and monoamine oxidase-B enzymes were obtained from BD Biosciences (Bedford, MA, USA). Kynuramine, clorgyline, deprenyl,

phenelzine, and DMSO were purchased from Sigma Chemical (St. Louis, MO, USA). Acacetin has been confirmed by comparing its experimental data with those reported in the literature.

3.4.3. Extraction and Isolation

The dried leaves were ground to a powder, yielding 325 g, which was extracted with $CHCl_3$ after maceration for 3 days. Removal of the solvent afforded a viscous residue (12.29 g). The extract showed good inhibition for MAO-A and -B with IC_{50} values of 2.49 and 1.85 μg/mL, respectively. The $CHCl_3$ extract (12 g) was fractionated on a flash silica gel column using a polarity gradient that resulted in 10 fractions [F-1 (Hex); F-2 (4:1 Hex–EtOAc); F-3 (3:2 Hex–EtOAc); F-4 (2:3 Hex–EtOAc); F-5 (1:4 Hex–EtOAc); F-6 (EtOAc); F-7 (9:1 EtOAc–MeOH); F-8 (75:25 EtOAc–MeOH); F-9 (1:1 EtOAc–MeOH); F-10 (MeOH)]. All fractions were tested for their biological activity. Fraction F-4 (2:3 Hex–EtOAc) showed IC_{50} values of 3.91 and 2.20 μg/mL for MAO-A and -B, respectively, and hence F-4 was further fractionated using a silica column. Eleven subfractions were obtained in order of polarity with CH_2Cl_2 to MeOH [F-4A (CH_2Cl_2), F-4B (98:2 CH_2Cl_2–EtOAc), F-4C (95:5 CH_2Cl_2–EtOAc), F-4D (9:1 CH_2Cl_2–EtOAc), F-4E (4:1 CH_2Cl_2–EtOAc), F-4F (7:3 CH_2Cl_2–EtOAc), F-4G (3:2 CH_2Cl_2–EtOAc), F-4H (1:1 CH_2Cl_2–EtOAc), F-4I (3:7 CH_2Cl_2–EtOAc), F-4J (EtOAc), F-4K (MeOH)], and these subfractions were subjected to bioassays. Subfraction F-4I showed a high percentage of inhibition for MAO-A and -B with IC_{50} values of 0.034 and 0.036 μg/mL, respectively. F-4I (3:7 CH_2Cl_2–EtOAc) was subjected to a silica gel column eluted with CH_2Cl_2–acetone (9:1) to furnish acacetin (18 mg) (0.005% from dried plant material and 0.15% from $CHCl_3$ extract).

Fractions eluted with CH_2Cl_2-EtOAc (9:1 and 4:1) were combined, concentrated, and submitted to Sephadex LH-20 CC using CH_2Cl_2-MeOH (1:1) to give three subfractions. Subfraction 2 was rechromatographed by CC eluted with CH_2Cl_2-MeOH (30:1) to obtain

calealactone B (25 mg), and a mixture of compounds, that was further submitted to Sephadex LH-20 CC using CH_2Cl_2-MeOH (2:1) and by repeated preparative TLC using Hex-EtOAc as mobile phase (1:1) to yield 2,3-epoxyjuanislamin (15 mg) and calein C (5 mg). In subfraction 3 a solid was precipitated, and was separated by filtration and crystallized from Hex-EtOAc, to yield more acacetin (15 mg). Fractions eluted with CH_2Cl_2-EtOAc (7:3 and 3:2) were combined and subjected to flash silica CC using CH_2Cl_2 and acetone mixtures of increasing polarity to obtain five subfractions. Subfraction four was initially rechromatographed by SPE column with CH_2Cl_2, and stepwise elution to MeOH, yielding four subfractions (20 mL each) (CH_2Cl_2; 50:1 CH_2Cl_2-MeOH; 20:1 CH_2Cl_2-MeOH; MeOH). Subfraction eluted with 50:1 CH_2Cl_2-MeOH was submitted to Sephadex LH-20 CC using CH_2Cl_2-MeOH (1:1), and by repeated preparative TLC using CH_2Cl_2-MeOH as mobile phase (50:1, 2 times) to yield compounds: caleanolene A (2.4 mg), caleanolene B (1.1 mg), and caleanolene C (1.6 mg).

Caleanolene A: colorless oil; $[\alpha]^{20}_D$ +22.8 (*c* 0.001, MeOH); IR (film, NaCl) ν_{max} 3353, 2921, 2852, 1736, 1642, 1453, 1378, 1258, 1013, 865, 793 cm^{-1}; CD (MeOH, *c* 0.35 x 10^{-3} M) $\Delta\varepsilon$ (nm) -58.3 (210); ^1H NMR and ^{13}C NMR data, see Table 3.3; HRESIMS *m/z* $[M+Na]^+$ 345.2042 (calcd. for $C_{19}H_{30}NaO_4$, 345.20418).

Caleanolene B: colorless oil; $[\alpha]^{20}_D$ -11.4 (*c* 0.001, MeOH); IR (film, NaCl) ν_{max} 3362, 2920, 2851, 1738, 1558, 1462, 1260, 1084, 1020, 800 cm^{-1}; CD (MeOH, *c* 0.35 x 10^{-3} M) $\Delta\varepsilon$ (nm) -27.4 (209); ^1H NMR and ^{13}C NMR data, see Table 3.3; HRESIMS *m/z* $[M+Na]^+$ 431.2456 (calcd. for $C_{23}H_{36}NaO_6$, 431.2410).

Caleanolene C: colorless oil; $[\alpha]^{20}_D$ +14.3 (*c* 0.001, MeOH); IR (film, NaCl) ν_{max} 3359, 2958, 2922, 2852,1691, 1551, 1463, 1258, 1085, 1013, cm^{-1}; CD (MeOH, *c* 0.35 x 10^{-3} M) $\Delta\varepsilon$

(nm) -4.79 (228), +2.10 (248), -2.17 (267); ^{1}H NMR and ^{13}C NMR data, see Table 3.3; HRESIMS *m/z* $[M+Na]^+$ 429.2298 (calcd. for $C_{23}H_{34}NaO_6$, 429.2253).

3.4.4. MAO Inhibition Assay

In order to investigate the effect of the isolated constituent acacetin from *C. urticifolia* on human recombinant MAO-A and MAO-B, the kynuramine deamination assay was performed in 96-well plates as previously reported.[82] A fixed concentration of substrate (kynuramine) and concentration response curve of inhibitor were used to determine the IC_{50} values. Kynuramine concentrations for MAO–A and –B were 80 and 50 μM, respectively. These concentrations were twice the apparent K_M value for substrate binding.[83] The concentrations run for fractions/constituents were from 0.001 to 100 μg/mL, acacetin from 0.001 to 100 μM for MAO-A and 0.01 to 100 μM for MAO-B, and phenelzine from 0.001 to 100 μM for MAO-A and phenelzine from 0.01 to 100 μM for MAO-B. Reactions were performed in 200 μL of 0.1 M potassium phosphate buffer, pH 7.4. The inhibitors and compounds were dissolved in DMSO, diluted in the buffer solution, and preincubated at 37 °C for 10 min (1.0% of DMSO final). Reactions were initiated by the addition of 50 μL of MAO-A (to 5 μg/mL) and -B (to 10 μg/mL), incubated for 20 min at 37 °C, and terminated immediately by the addition of 75 μL of 2 N NaOH. The enzyme product formation (4-hydroxyquinoline) was recorded fluorometrically using a SpectraMax M5 fluorescence plate reader (Molecular Devices, Sunnyvale, CA, USA) with an excitation (320 nm) and emission (380 nm) wavelength, using the Soft Max Pro program. The assays were calculated as percent of product formation compared to the corresponding control (enzyme–substrate reaction) without inhibitors. Controls including samples where the enzyme or the substrate was added after stopping the reaction were checked simultaneously to determine the interference with the fluorescence measurements. The

determination of IC_{50} values for MAO–A and –B inhibition by the selected samples was performed using varying concentrations of the inhibitor and fixed concentration of the substrate. The IC_{50} values were calculated from the concentration-dependent inhibition curves using XLFit software.

3.4.5. Enzyme Kinetics and Mechanism Studies

Assays were performed at varying concentrations of kynuramine (1.90 to 500 μM) for the determination of the enzyme inhibition constants (K_i) for inhibition of MAO–A and –B with acacetin. In addition to controls without inhibitors, two concentrations (one below and one above the IC_{50} values) of the inhibitors [for MAO-A phenelzine (0.450 and 0.900 μM), acacetin (0.125 and 0.250 μM), and for MAO-B phenelzine (0.050 and 0.100 μM), acacetin (0.045 and 0.090 μM)] were used to determine the K_M and V_{max} values of the inhibitor. The results were expressed as double-reciprocal Lineweaver–Burk plots, and the kinetic data namely K_M, V_{max}, and K_i values, were calculated by SigmaPlot 12.3 with the Enzyme-Kinetics module using the Michaelis–Menten equation. The results were also analyzed for type of inhibition.

3.4.6. Time-Dependent Enzyme Inhibition Assay

In order to evaluate the inhibitors binding to both MAOs, each enzyme was preincubated for variable time periods (0–15 min) with the inhibitor at a concentration that results in approximately > 60% inhibition to verify whether the inhibition of the catalytic function was time-dependent. The concentrations of the inhibitor used to test the time-dependent inhibition with 20 μg/mL MAO-A were acacetin (0.500 μM) and phenelzine (0.600 μM) and with 50 μg/mL MAO-B were acacetin (0.200 μM) and phenelzine (0.200 μM). Controls without inhibitors were also run. The enzyme activities were analyzed with the remaining enzyme

activity percentage plotted against the preincubation time to evaluate the time-dependent enzyme inhibition.

3.4.7. Analysis of Inhibitor Binding and Reversibility with MAO–A and –B

Many inhibitors result in the target enzyme inhibition by the formation of an enzyme–inhibitor complex, which may be accelerated in the presence of high inhibitor concentration. The reversibility of acacetin binding to, and inhibition of MAO, was analyzed by incubating the enzyme with high inhibitor concentration followed by an extensive dialysis of the enzyme–inhibitor complex and the recovery of enzyme catalytic activities. MAO-A (0.05 mg/mL protein) enzyme was incubated with acacetin (1.5 and 15.0 μM), and MAO-B (0.05 mg/mL protein) enzyme was incubated with acacetin (0.500 and 5.0 μM) in a total enzyme mixture of 1 mL volume including 100 mM potassium phosphate buffer (pH 7.4). After incubating for 20 min at 37 °C, the reaction was stopped by cooling the reaction on ice. The samples were then dialyzed against potassium phosphate buffer for 14 h at 4 °C (three buffer changes). The same procedure was run using control enzyme (without inhibitor), and the enzyme activity was determined before and after dialysis. After extensive dialysis of the enzyme–inhibitor mixture, recovery of the enzyme catalytic activity provided the necessary information regarding the reversibility/irreversibility of the inhibitor binding with the enzyme.

3.4.8. Molecular Modeling Calculations of Sesquiterpene Lactones

Conformational search was carried out using MacroModel.[84] We used mixed torsional/low-mode sampling method with intermediate torsion sampling. The energy window for saving conformers was defined as 5.02 kcal mol^{-1} to ensure thorough conformational search. The most abundant conformers according to Boltzmann distribution were subjected to DFT geometry optimization calculations protocol using Gaussian 09. The M06-2X functional with

the 6-31+G(d,p) basis set was used for geometry optimization and frequency calculations.[76] The NMR shielding tensors were calculated using the GIAO method of Gaussian 09 at B3LYP/ 6-311+G(2d,p) functional level.[76] To compute the ECD, we used TDDFT in Gaussian with B3LYP functional and 6-31G(d,p) basis set. PCM methanol solvent model was used.

3.5. Summary

Bioassay-guided fractionation of *C. urticifolia* resulted in the isolation of a flavonoid acacetin, as the most prominent MAO inhibitory constituent, with IC_{50} values of 121 and 49 nM for MAO-A and –B, respectively. Follow-up studies showed reversible binding of acacetin with human MAO-A and –B, resulting in competitive inhibition. Acacetin showed more preference towards MAO-B than to MAO-A, suggesting its potential for eliciting selective pharmacological effects that might be useful in the treatment of neurological and pyschiatric disorders. Further phytochemical investigation resulted in three novel bisabolenes: caleanolenes A-C, along with three known sesquiterpene lactones: 2,3-epoxyjuanislamin, calealactone B, and calein C. The chemical structures of the isolated compounds were determined on the basis of HRMS, IR, UV, and from 1D and 2D NMR spectroscopic studies. The configurations have been partly established using GIAO NMR and ECD calculations. The novel isolated compound: caleanolene A, and the known isolated compounds: 2,3-epoxyjuanislamin, calealactone B, and calein C were evaluated for cytotoxicity against the CA46 and Raji lymphoma, and the MCF7 breast cancer cell lines, with 2,3-epoxyjuanislamin showing the best activity in all cell lines (IC_{50} value range 2.8 to 5.8 μM). In addition, the binding modes of acacetin at the enzymatic site of MAO-A and –B were predicted through molecular modeling algorithms, illustrating the high improtance of ligand interaction with negative and positive free energy regions of the enzyme active site, described in the following chapter.

Part of this chapter has been published in the ***Journal of Natural Products*, 2016, *79* (10), 2538-2544** and has been formatted as per the University of Mississippi's guidelines for thesis preparation.

CHAPTER 4. MOLECULAR MODELING STUDIES OF ACACETIN ON MAO-A AND –B ISOENZYMES

Vedanjali Gogineni, Francisco León, Khaled M. Elokhely, Manal A. Nael, Stephen J. Cutler, and Christopher R. McCurdy

4.1. Introduction

Molecular modeling studies will help identify the important interactions between the lead compounds and the residues on the active site. Ligand docking helps in understanding the surface complementarities of the receptor and the ligand, and the interactions between the ligand and receptor.[85,86]

The modeling of MAO isoenzymes was done based on the available crystal structures downloaded from Research Collaboratory for Structural Bioinformatics (RCSB) protein data bank (PDB).[87] We believe that the computational insights gained in this study would provide a platform to other medicinal chemists working in the area of MAO research, for the design and synthesis of novel MAO-B analogs. This could in turn result in the identification of new synthetic compounds with improved selectivity and potency for MAO-B.

4.1.1. Specific Aims of the Research

In order to achieve the above goals, the following **specific aims** were considered:

1. To perform docking studies on acacetin to understand the binding modes of acacetin with the MAO active sites
2. To establish the SAR of the virtual compounds obtained through docking studies which will help understand the major functional groups necessary to improve the selectivity and potency towards MAO-B
3. To design selective MAO-B analogs which will be synthesized and biologically evaluated for MAO inhibition

4.2. Computational Methods

4.2.1. Protein Preparation and Receptor Grid Generation

The protein structural files of MAO-A (PDB ID: 2Z5Y)[88] and MAO-B (PDB ID: 4A79)[89] were downloaded from the protein databank repository.[87] Protein structures were prepared by Protein Preparation Wizard (PrepWizard)[90,91] of the Schrödinger suite to add missing hydrogen atoms, adjust bond orders, assign hydrogen bonds, and relax the protein–ligand complex. The missing loops and amino acid side chains were filled using Prime.[92] The center of the docking receptor grids was defined as the coordinate of cognate ligands. The potential of the nonpolar parts of the receptor was softened by scaling the van der Waals radius by a factor of 0.8 and partial charge cutoff of 0.25. The receptor thiol and hydroxyl groups were allowed to rotate for optimal hydrogen bond formation with predicted docked poses. Ligand sampling and preparation were performed using LigPrep[93] of Schrödinger by using the OPLS2005 force field[94] and charges. All possible ligand states at pH 7.4 were generated by Epik,[95] and the known ligand stereogenic centers were retained during preparation.

4.2.2. Docking and Scoring

The compounds were then docked using Glide[96] standard precision (SP) mode, and the top 5 poses were kept for analysis. The thermodynamic properties of the ligand binding pockets of MAO-A and MAO-B were then studied, in order to map the active site water molecules.[97] The protein structures were prepared by PrepWizard.[88] The partial charges of the amino acids were assigned by AmberFF94 charges, and the ligands with AM1BCC.[98,99] The thermodynamic properties of the complex, apo, and ligand were calculated separately by using a probe of explicit water molecules. Then, the excess free energy water molecules that are supposed to be displaced by the ligand were determined.

4.3. Design of Selective MAO-B Inhibitors

4.3.1. Observations of the Binding Modes of Acacetin

Acacetin binds more favorably to MAO-B [**Figure 4.1**] with a better Glide docking score of −8.1 kcal/mol, emodel of −64 kcal/mol, and MMGBSA binding Δ*G* of −76 kcal/mol than with MAO-A [**Figure 4.1**] (Glide docking score = −6.2 kcal/mol, emodel = −30 kcal/mol, and Δ*G* = −54 kcal/mol). Acacetin tightly bound to MAO-B by forming a network of hydrogen bonds with the surrounding water molecules and amino acid residues.

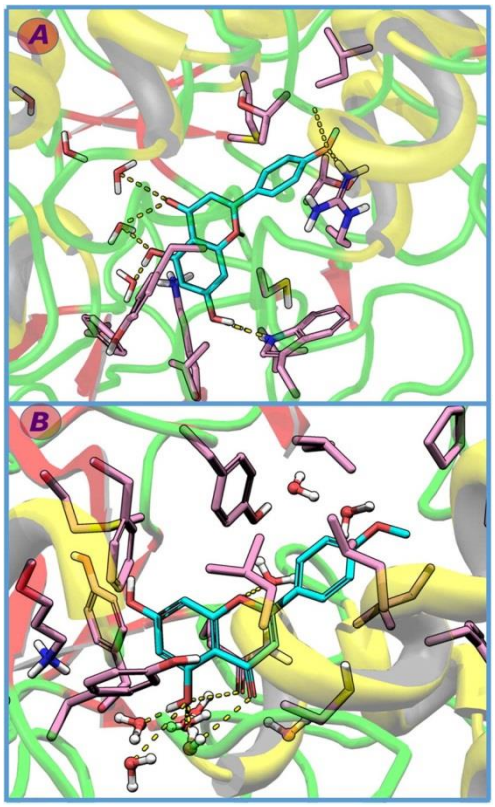

Figure 4.1. Binding modes of acacetin MAO-A (**A**) and with MAO-B (**B**)

The enzyme kinetics and binding studies of acacetin mentioned in chapter 3 inspired us to use docking simulation to investigate the binding modes of acacetin in the structurally similar ligand binding pockets of MAO-A and MAO-B. The active site of MAO-A contains six water molecules [**Figure 4.2**] that form more than two hydrogen bonds with nonwaters. MAO-B

encloses 10 water molecules in the active site. Tyr 326 in MAO-B, which corresponds to Ile 335 in MAO-A, plays an important role in imparting more polarity to the active site and attracting waters to the binding pocket [**Figure 4.2**]. Tyr 326 forms strong hydrogen bonds with two active site waters (W7b and W8b), while the Ile 335 of MAO-A is hydrophobic and only W6a is observed in close proximity to W7b. Five water molecules (W1–W5) have the same atomic coordinates in both enzymes, while one water (W6a) in MAO-A and five water molecules (W6b–W10b) in MAO-B are in different regions of the active site.

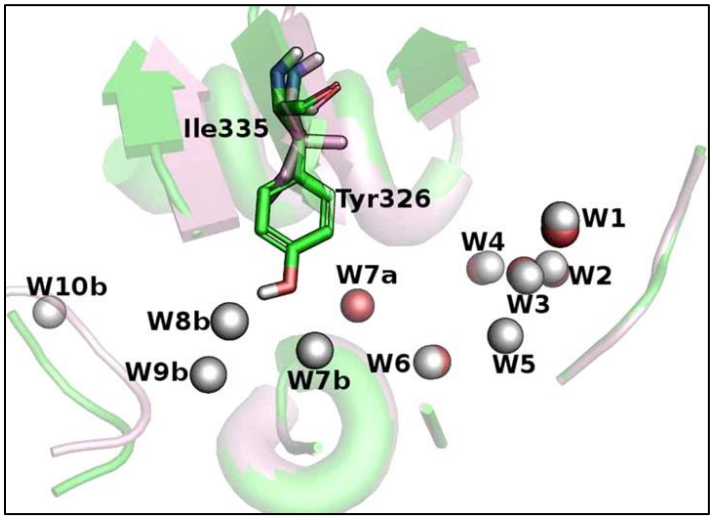

Figure 4.2. Active site water molecules in MAO-A and MAO-B. MAO-A is displayed as pink and MAO-B as green cartoon. Water molecules of MAO-A are shown as red and those of MAO-B as gray spheres.

The thermodynamic properties of the active sites of MAO-A and -B crystal structures were inspected using SZMAP. The negative free energy regions of the ligand binding pocket of MAO-A and -B show a high tendency to hold water molecules and high affinity towards polar functional groups. The positive free energy regions prefer nonpolar molecular increments [**Figure 4.3**]. Water molecules in the crystal structures of MAO-A were carefully checked for their existence in favorable or unfavorable regions. W1, W4, W5, and W6a of MAO-A are

favorably located in thermodynamic stable positions, while W2 and W3 are in unfavorable regions. This means, by displacing W2 and/or W3 with hydrophobic groups, MAO-A activity of the ligands will increase. By improving the interaction with the four waters in the favorable positions or by displacing them with polar groups, acacetin can be further modified to be a more potent MAO-A modulator. The binding site of MAO-B contains W1, W3, W5, W6b, W7b, W8b, W9b, and W10b in thermodynamically favorable locations. W2 of MAO-B exists in an unfavorable region similar to that of MAO-A. The active site of MAO-B holds more negative free energy regions compared to MAO-A and, in particular, close to Phe 208 (MAO-A) and Ile199 (MAO-B). Enhancement of MAO-B inhibition can be achieved by considering appropriate functional groups that interact with the negative and positive free energy regions of the binding site.

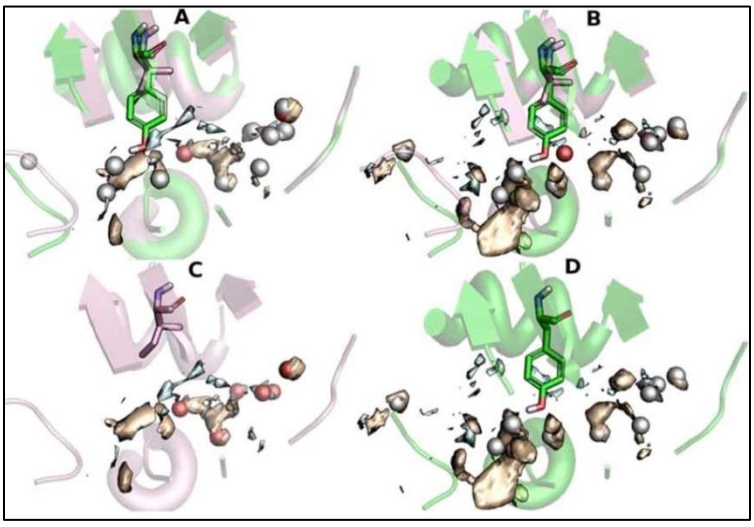

Figure 4.3. Thermodynamic properties of the ligand binding pockets of MAO-A and MAO-B. The regions that favor the presence of water molecules are shown as wheat-colored and those favoring nonpolar groups as pale cyan surfaces. The active sites of MAO-A and MAO-B are aligned A and B with the thermodynamic maps of MAO-A (**A**) and MAO-B (**B**), respectively.

Crystal structure water molecules that are in the wheat regions are supposed to be native ones, and those in the cyan areas are artificial because of crystallization. The thermodynamic map of MAO-A (**C**) shows less favorable regions for water and polar groups compared to that of MAO-B (**D**). Two water molecules are found in close proximity to Tyr 326 of MAO-B (**D**). Water molecules are shown as red for MAO-A and gray spheres for MAO-B.

Figure 4.4 represents the 2D interaction profiles of acacetin on MAO-A and MAO-B explaining the interactions between the ligand (acacetin) and the active sites. We observe a cationic-pi interaction between Arg51 of MAO-A and the aromatic ring of acacetin. Similarly, we observe a cationic-pi interaction between Tyr326 of MAO-B enzyme and the aromatic ring of acacetin. Water molecules in the active site interacted with the hydroxyl functional groups through hydrogen bonding in both the MAO isoenzymes.

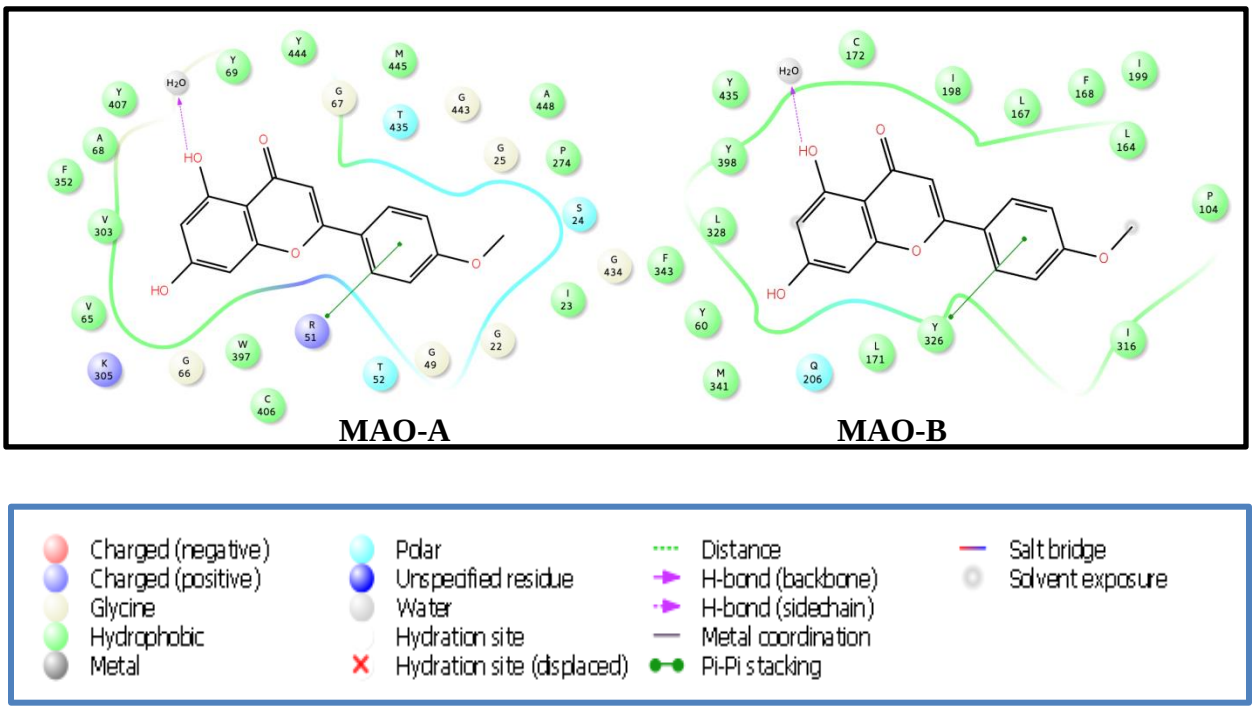

Figure 4.4. 2D interaction profiles of acacetin with MAO-A and MAO-B

The 2D interaction profile showed that there is opportunity for modifications at the R_1 and R_2 positions. R_2 has room for bulky groups such as nonpolar/lipophilic groups at R_2 position which is the 4′ position of the flavone skeleton of acacetin to make the analogs MAO-B selective. The OH present at R_1 position seems to show interaction with the MAO enzymes and there is room for small groups [**Figure 4.5**].

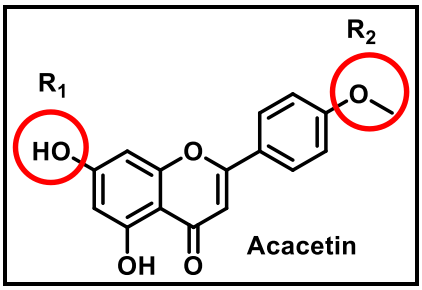

Figure 4.5. Crucial positions representing the modifications in acacetin

4.3.2. Structure-Activity Relationship of Acacetin

SAR is a correlation study between the drug-structure and its biological activity. SAR is essential for the design of compounds with high potency and less adverse effects. Developing SAR helps in determining the chemical groups at specified positions in the drug-structure, to improve the biological effects on the target. SAR is used by medicinal chemists to modify the drug-structures and test the modifications of the biological activities.

The SAR of acacetin is explained in **Figure 4.6**. The selectivity of MAO inhibition (MAO-A *vs* MAO-B) depends on the substituents present on the B ring, and the presence of the double-bond present in position 2 and 3 of C ring. The presence of hydrophilic groups in the para position of B ring favors MAO-A inhibition, while the presence of lipophilic groups favors MAO-B inhibition. Shifting of B ring from postion-2 to position-3 decreases MAO-B inhibition.

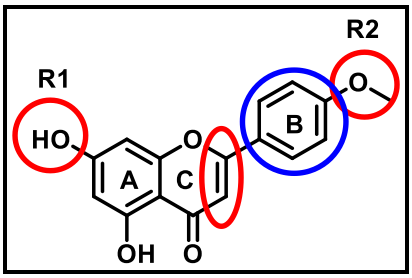

Figure 4.6. Structure-activity relationship of acacetin

4.4. Results and Discussion

Based on the understanding of the binding modes of acacetin and the structure-activity relationship, sixteen analogs of acacetin were designed [**Figure 4.7**]. The sixteen analogs were drawn in ChemDraw and saved as individual .sdf files. The files were uploaded to the Maestro interface of the Schrödinger suite and were minimized to acquire their 3D conformations. The 3D structures were then prepared using LigPrep, which prepares the ligands at certain pH ranges [pH 7.4 used]. The sixteen analogs were docked in the active sites of both MAO-A and –B using Glide docking to retrieve their docking scores and poses [**Table 4.1**].

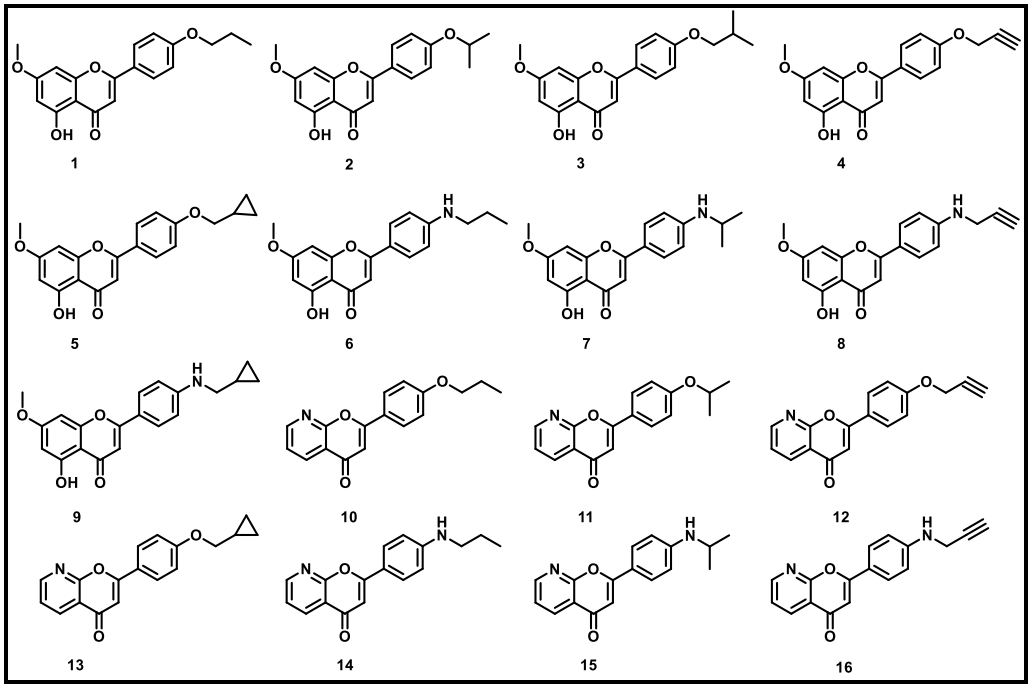

Figure 4.7. Chemical structures of the 16 acacetin analogs

Table 4.1 shows the docking scores of acacetin and the sixteen acacetin analogs that were designed based on the SAR of acacetin. All the derivatives scored better than acacetin in MAO-B. All the sixteen compounds were synthesized and were assayed for their MAO-B inhibitory activity and potency.

Table 4.1. Docking scores of acacetin analogs

Compound	**MAO-A** **Docking score [kcal/mol]**	**MAO-B** **Docking score [kcal/mol]**
1	-	-15.243
2	-	-15.102
3	-	-15.663
4	-	-15.545
5	-	-16.172
6	-	-15.451
7	-	-14.912
8	-	-15.866
9	-	-16.084
10	-2.240	-15.129
11	-	-14.667
12	0.127	-14.989
13	-	-15.756
14	-	-14.807
15	-	-14.936
16	-	-15.452

Acacetin	-6.2	-8.1

4.5. Summary

We designed sixteen acacetin analogs to study the effect of non-polar substituents. The analogs were designed based on the binding modes and the SAR of acacetin. Liphophilic groups were introduced on the R_2 position to improve the MAO-B selectivity of these analogs. Two different series (flavonoid and pyridine) were designed to understand their selectivity towards MAO-B. Similarly oxygen and nitrogen substituents were used on the B ring with both flavonoid and pyridine series, to study the difference in their affinity for MAO-B. Furthermore, these analogs also showed excellent docking scores for MAO-B supporting our design.

CHAPTER 5. SYNTHESIS OF DESIGNED SELECTIVE MAO-B INHIBITORS

Vedanjali Gogineni, Francisco León, Manal A. Nael, Narayan D. Chaurasiya, Babu L. Tekwani, Stephen J. Cutler, Christopher R. McCurdy, and John M. Rimoldi

5.1. Specific Aims of the Research

The following specific aims were outlined:

1. To synthesize analogs that were designed based on the docking studies of acacetin (See Chapter 4)
2. To purify the synthesized analogs and perform mass and HPLC purity analysis on the purified compounds
3. To perform MAO inhibition, enzyme-kinetics and mechanistic studies, and binding affinity studies on the synthesized analogs

5.2. Chemistry

The synthesis of the flavonoid series was achieved through the methods illustrated in Scheme 1.

Scheme 5.1. Synthesis of (oxygenated) flavonoid series [**1-4**]

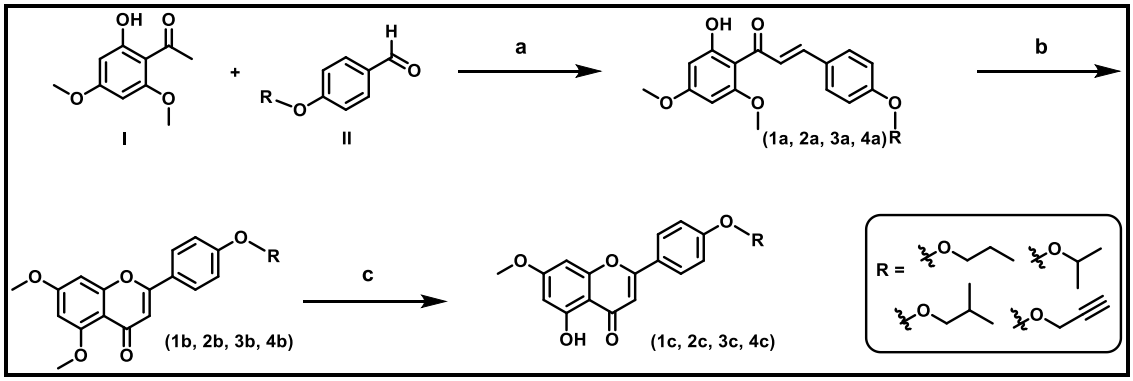

Reagents and conditions: (a) NaOH 50%, EtOH, rt, 16-20 h (b) I_2, DMSO, 140 °C, 4-6 h (c) 1N BBr_3, CH_2Cl_2, rt, 1-3 h

Chalcones **1a, 2a, 3a, 4a** were afforded through Schmidt condensation by reacting 2′-hydroxy-4′,6′-dimethoxyacetophenone **I** and the corresponding 4-benzaldehydes **II** with 50%

sodium hydroxide in ethanol. The intermediate flavonoids **1b, 2b, 3b, 4b** were prepared by treatment of the chalcones with iodine crystals in minimal amount of DMSO by undergoing cyclization. The final compounds **1c, 2c, 3c, 4c** were prepared by demethylation of the OH in the 5^{th} position of the 'A' ring, when the intermediates **1b, 2b, 3b, 4b** were treated with boron tribromide (BBr_3) in CH_2Cl_2.

Scheme 5.2. Synthesis of (oxygenated) flavonoid series with cyclopropane substituent [**5**]

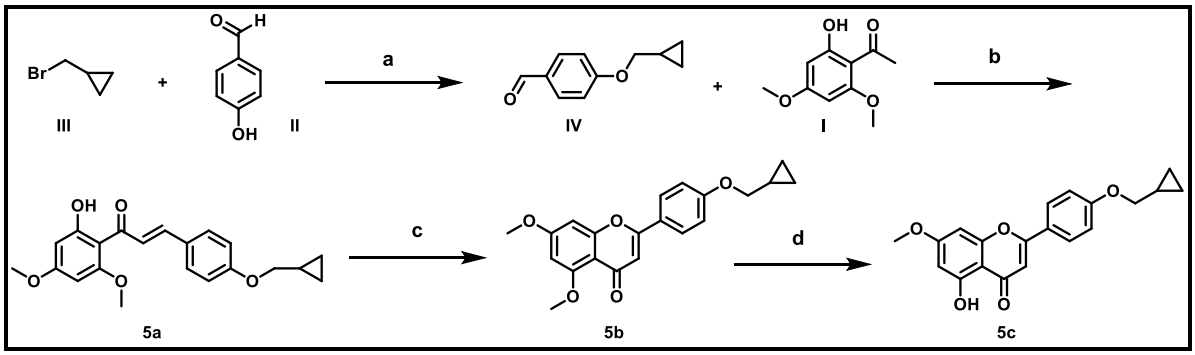

Reagents and conditions: (a) acetone, K_2CO_3, reflux 24 h (b) NaOH 50%, EtOH, rt, 16-20 h (c) I_2, DMSO, 140 °C, 4-6 h (d) 1N BBr_3, CH_2Cl_2, rt, 1-3 h

4-(cyclopropylmethoxy)benzaldehyde **IV** was afforded by reacting (bromomethyl)cyclopropane **III** with 4-hydroxybenzaldehyde **II** with acetone and potassium carbonate. Chalcone **5a** was prepared through Schmidt condensation by treatment of the cyclopropyl aldehyde **IV** with 2′-hydroxy-4′,6′-dimethoxyacetophenone **I** and 50% sodium hydroxide in ethanol. The intermediate flavonoid **5b** was prepared by the treatment of the chalcone with iodine crystals in minimal amount of DMSO by undergoing cyclization. The final compound **5c** was prepared by demethylation of the OH in the 5^{th} position of the 'A' ring, when the intermediate **5b** was treated with boron tribromide in dichloromethane.

Scheme 5.3. Synthesis of (nitrogenated) flavonoid series [**6-9**]

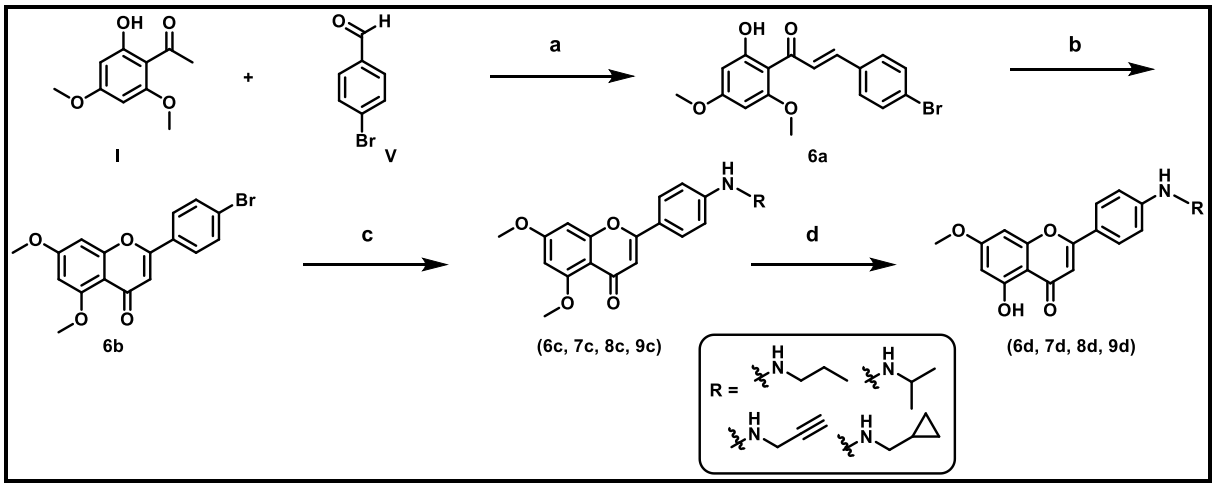

Reagents and conditions: (a) NaOH 50%, EtOH, rt, 16-20 h (b) I_2, DMSO, 140 °C, 4-6 h (c) NaO^tBu, $Pd_2(dba)_3$, corresponding amines [propylamine, isopropylamine, propargylamine, and (aminomethyl)cyclopropane], BINAP, toluene, 80 °C, 48 h (d) 1N BBr_3, CH_2Cl_2, rt, 1-2 h

Compounds **6-9** were prepared as shown in scheme 3. The brominated chalcone **6a** was produced by treating 2′-hydroxy-4′,6′-dimethoxyacetophenone **I** with 4-bromobenzaldehyde **V** through Schmidt condensation with 50% sodium hydroxide in ethanol. The brominated flavonoid **6b** was prepared from the treatment of the chalcone with iodine crystals in minimal amount of DMSO by undergoing cyclization. The intermediates **6c, 7c, 8c, 9c** were prepared by treating compound **6b** with sodium tert-butoxide, tris(dibenzylideneacetone)dipalladium, 1,1′-binaphthalene-2,2′-diylbis(diphenylphosphine), and the corresponding amines such as propylamine, isopropylamine, propargylamine, and (aminomethyl)cyclopropane in toluene. The final compounds **6d, 7d, 8d, 9d** were prepared by demethylation of the OH in the 5th position of the ‘A’ ring, when the intermediates **6c, 7c, 8c, 9c** were treated with boron tribromide in dichloromethane.

Scheme 5.4. Synthesis of (oxygenated) pyridine series [**10-12**]

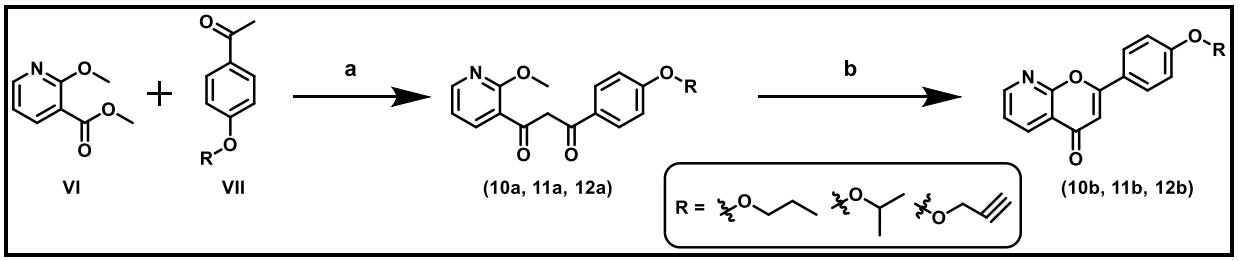

Reagents and conditions. (a) NaH, DMF, rt, 17 h (b) pyridinium hydrochloride, 190 °C, 17 h

The diketo intermediates **10a, 11a, 12a** were formed from reacting methyl-2-methoxy nicotinate **VI** and the corresponding 4′-acetophenones **VII** in the presence of sodium hydride and dimethyl formamide. The final oxygenated pyridine compounds **10b, 11b, 12b** were accomplished from the treatment of the corresponding diketo intermediates **10a, 11a, 12a** with pyridinium hydrochloride through cyclization.

Scheme 5.5. Synthesis of 2-(4-(cyclopropylmethoxy)phenyl)-4*H*-pyrano[2,3-*b*]pyridin-4-one [**13**]

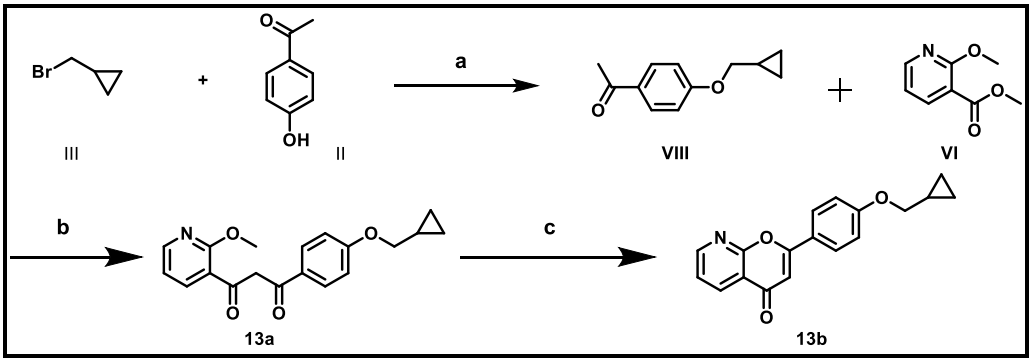

Reagents and conditions. (a) acetone, K_2CO_3, reflux 24 h (b) NaH, DMF, rt, 17 h (c) pyridinium hydrochloride, 190 °C, 17 h

The 1-(4-(cyclopropylmethoxy)phenyl)ethan-1-one **VIII** was formed by treating (bromomethyl)cyclopropane **III** and 4′-hydroxy acetophenone **II** in the presence of acetone and potassium carbonate. The intermediate **13a** was prepared by treating **VIII** with methyl-2-

methoxy nicotinate **VI** in the presence of sodium hydride and dimethyl formamide. The final compound **13b** was furnished from treating the intermediate **13a** with pyridinium hydrochloride.

Scheme 5.6. Synthesis of (nitrogenated) pyridine series [**14-16**]

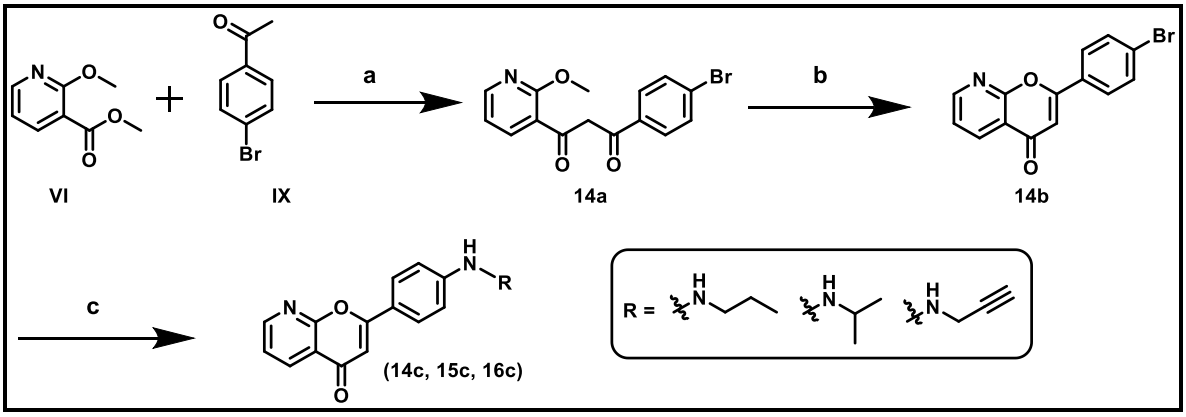

Reagents and conditions. (a) NaH, DMF, rt, 19 h (b) pyridinium hydrochloride, 190 °C, 4 h (c) NaO^tBu, $Pd_2(dba)_3$, corresponding amines [propylamine, isopropylamine, and propargylamine], BINAP, toluene, 80 °C, 48 h

The brominated diketo compound **14a** was prepared by reacting methyl-2-methoxy nicotinate **VI** and 4′-bromo acetophenone **IX** with sodium hydride and dimethyl formamide. Upon further treatment of the compound **14a** with pyridinium hydrochloride resulted in the formation of the intermediate **14b**. Final compounds **14c, 15c, 16c** were accomplished from the treatment of the intermediate **14b** with sodium tert-butoxide, tris(dibenzylideneacetone)dipalladium, 1,1′-binaphthalene-2,2′-diylbis(diphenylphosphine), and the corresponding amines such as propylamine, isopropylamine, and propargylamine in toluene.

5.3. Results and Discussion

We screened a total of 38 compounds which also included the intermediates along with the final compounds for MAO inhibition assay. The potent compounds from **Table 5.1** were evaluated for the mechanism and kinetics of the inhibition of human MAO-A and B.

Table 5.1. Inhibition of recombinant human monoamine oxidase-A and –B by the synthesized analogs

Synthesized Analogs	MAO-A [IC_{50}][a,b]	MAO-B [IC_{50}][a,b]
1a	0.515 ± 0.024	0.40 ± 0.024
1b	> 100	**1.70 ± 0.076**
1c	48.78 ± 2.01	**0.033 ± 0.0042**
2a	0.117 ± 0.05	**0.049 ± 0.0035**
2b	> 100	**2.64 ± 0.0880**
2c	30.74 ± 0.023	**0.016 ± 0.0070**
3a	0.42 ± 0.002	0.22 ± 0.0211
3b	> 100	7.23 ± 2.1438
3c	> 100	**0.031 ± 0.0070**
4a	9.42 ± 1.78	8.33 ± 0.7871
4b	> 100	> 100
4c	62.70 ± 5.21	**0.049 ± 0.0014**
5a	1.30 ± 0.09	0.90 ± 0.035
5b	> 100	22.82 ± 2.098
5c	-	-
6a	12.349 ± 0.249	-
6b	87.830 ± 5.449	28.407 ± 2.639
6c	-	22.097 ± 2.479
6d	85.484 ± 1.585	**1.554 ± 0.137**

7c	37.492 ± 0.476	9.447 ± 0.113
7d	40.500 ± 2.374	**0.417 ± 0.012**
8c	-	-
8d	-	-
9c	39.095 ± 5.144	12.727 ± 0.290
9d	39.114 ± 0.555	2.185 ± 0.088
10a	6.50 ± 1.22	**0.23 ± 0.003**
10b	**0.104 ± 0.0014**	**0.020**
11a	10.13 ± 0.085	0.161 ± 0.0022
11b	**0.0875 ± 0.0035**	**0.010 ± 0.0014**
12a	58.44 ± 0.184	3.98 ± 0.297
12b	-	-
13a	11.10 ± 0.025	0.367 ± 0.0044
13b	**0.207 ± 0.006**	**< 0.1**
14a	-	3.458 ± 0.829
14b	3.909 ± 0.452	**0.284 ± 0.029**
14c	0.569 ± 0.003	**0.138 ± 0.012**
15c	0.389 ± 0.008	**< 0.1**
16c	-	-
Acacetin	0.105 ± 0.0014	0.042 ± 0.0021
Clorgyline	0.0039 ± 0.0002	2.15 ± 0.212
Deprenyl	33.00 ± 1.411	0.046 ± 0.0014
Harmine	0.0031 ± 0.0003	39.000 ± 1.412

[a]The IC_{50} values computed from the dose-response inhibition curves are mean ± SD of triplicate observations; [b]μM; * Highlighted items represent the potent analogs

Based on the results, we found that the flavonoid series were more potent and selective compared to the pyridine series. The reason behind the flavonoid series being more potent than the pyridine series could be explained from the fact that the flavonoid series were large enough to completely occupy the MAO-B active site. Among the flavonoid series, we observed that the oxygen substituents showed more selectivity towards MAO-B compared to the nitrogen series.

5.4. Experimental Methods

The general experimental methods were similar to those mentioned in page 48. $CDCl_3$ and CD_3OD were used as solvents and TMS was used as an internal standard.

5.4.1. Chemicals

All the chemicals used were purchased from Sigma-Aldrich. Human recombinant monoamine oxidase-A and monoamine oxidase-B enzymes were obtained from BD Biosciences (Bedford, MA, USA). Kynuramine, clorgyline, deprenyl, phenelzine, and DMSO were purchased from Sigma Chemical (St. Louis, MO, USA). Purified acacetin from previous project has been used.

5.4.2. MAO Inhibition Assay

Refer to page 77.

5.4.3. Enzyme Kinetics and Mechanism Studies

Refer to page 78.

5.4.4. Time-Dependent Enzyme Inhibition Assay

Refer to page 78.

5.4.5. Analysis of Inhibitor Binding and Reversibility with MAO-A and –B

Refer to page 79.

Preparation of the Chalcone (*E*) 4-Propyloxy-4',6'-Dimethoxy-2'-Hydroxychalcone [1a]: A mixture of equimolar amounts of 2′-hydroxy-4′,6′-dimethoxyacetophenone (300 mg, 1.53 mmol) and 4-n-propoxybenzaldehyde (251 mg, 1.53 mmol) was taken in a round-bottomed flask (RBF) and 10 mL of 50% sodium hydroxide in ethanol was added and left for 16 h at rt. The resulting yellow precipitate was then suction filtered and washed with Hex and CH_2Cl_2 to yield **1a** (342 mg, 65%). ^{1}H NMR (400 MHz, $CDCl_3$) δ_H 14.41 (s, C-2′-OH), 7.79 (s br, 2H, H-α and H-β), 7.55 (d, *J* = 8.5 Hz, 1H, H-2 and H-6), 6.91 (d, *J* = 8.5 Hz, 2H, H-3 and H-5), 6.10 (d, *J* = 1.8 Hz, 1H, H-3′), 5.96 (d, *J* = 1.8 Hz, 1H, H-5′), 3.97 (t, *J* = 6.5, 2H, H_2-1″), 3.93 (s, 3H, OCH_3), 3.85 (s, 3H, OCH_3), 1.83 (dt, *J* = 6.5, 7.4 Hz, 2H, H_2-2″), 1.05 (t, *J* = 7.4 Hz, 3H, CH_3-3″). ^{13}C NMR (100 MHz, $CDCl_3$) δ_C 192.6 (C=O), 168.3 (C-2′), 166.0 (C-4′), 162.4 (C-6′), 161.0 (C-4), 142.6 (C-β), 130.1 (C-2 and C-6), 128.1 (C-1), 124.9 (C-α), 114.8 (C-3 and C-5), 106.3 (C-1′), 93.8 (C-3′), 91.2 (C-5′), 69.6 (C-1″), 55.8 (OCH_3), 55.5 (OCH_3), 22.5 (C-2″), 10.5 (C-3″). ESIMS *m/z* 343.0897 $[M+H]^+$ (calcd $C_{20}H_{22}O_5$ 342.1467).

Preparation of Oxygenated Intermediate Flavonoid 5,7-Dimethoxy-4'-Propyloxyflavone [1b]: The chalcone **1a** (200 mg, 0.584 mmol) was treated with 3-4 mol% of iodine crystals with minimal amount of DMSO at 140 °C for 4-6 h. The resulting white precipitate was extracted with CH_2Cl_2 and was removed by filtration. The filtrate was transferred into a separatory funnel, where the layers were separated as aqueous and organic layers. The organic layer was washed with sodium thiosulfate ($Na_2S_2O_3$), dried (Na_2SO_4), and concentrated. The intermediate flavonoid **1b** was then purified in a silica column using 100% CH_2Cl_2, 50:1 CH_2Cl_2-MeOH, 9:1 CH_2Cl_2-MeOH, 1:1 CH_2Cl_2-MeOH, and 100% MeOH (128 mg, 64%). ^{1}H NMR (400 MHz,

$CDCl_3$) δ_H 7.80 (d, *J* = 8.9 Hz, 2H, H-2′ and H-6′), 6.98 (d, *J* = 8.9 Hz, 2H, H-3′ and H-5′), 6.59 (s, 1H, H-3), 6.57 (d, *J* = 2.3 Hz, 1H, H-6), 6.37 (d, *J* = 2.3 Hz, 1H, H-8), 3.99 (t, *J* = 6.6 Hz, 2H, H_2-1″), 3.96 (s, OCH_3), 3.91 (s, OCH_3), 1.84 (dt, *J* = 6.5, 7.4 Hz, 2H, H_2-2″), 1.06 (t, *J* = 7.4 Hz, 3H CH_3-3″). ^{13}C NMR (100 MHz, $CDCl_3$) δ_C 177.7 (C-4), 163.9 (C-2), 161.6 (C-5), 160.9 (C-4′), 160.7 (C-9), 159.8 (C-7), 127.5 (C-2′ and C-6′), 123.5 (C-1′), 114.8 (C-3′ and C-5′), 109.2 (C-10), 107.6 (C-3), 96.0 (C-8), 92.8 (C-6), 69.7 (C-1″), 56.4 (OCH_3), 55.7 (OCH_3), 22.5 (C-2″), 10.5 (C-3″). ESIMS *m/z* 341.0738 $[M+H]^+$ (calcd $C_{20}H_{20}O_5$ 340.1311).

Preparation of Final Oxygenated Flavonoid 7-Methoxy-4'-Propyloxy-5-Hydroxyflavone [1c]: The intermediate **1b** (128 mg, 0.377 mmol) was treated with double the moles of 1N boron tribromide (189 mg, 0.754 mmol) in the presence of CH_2Cl_2 at rt, for 1-3 h. The reactant solution was diluted with 10:1 CH_2Cl_2:MeOH and then washed with brine and water. Na_2SO_4 was added to the solution and left overnight. The solution was then filtered into an RBF, dried, and concentrated. The flavonoid **1c** was purified in a silica column using 30:1 CH_2Cl_2-MeOH (35 mg, 29%). ^{1}H NMR (400 MHz, $CDCl_3$) δ_H 12.83 (s, C-5-OH), 7.82 (d, *J* = 8.9 Hz, 2H, H-2′ and H-6′), 7.00 (d, *J* = 8.9 Hz, 2H, H-3′ and H-5′), 6.56 (s, 1H, H-3), 6.47 (d, *J* = 2.2 Hz, 1H, H-6), 6.35 (d, *J* = 2.2 Hz, 1H, H-8), 4.00 (t, *J* = 6.6 Hz, 2H, H_2-1″), 3.88 (s, OCH_3), 1.86 (ddd, *J* = 6.6, 7.4 Hz, 2H, H_2-2″), 1.08 (t, *J* = 7.4 Hz, 3H, CH_3-3″). ^{13}C NMR (100 MHz, $CDCl_3$) δ_C 182.4 (C-4), 165.4 (C-7), 164.0 (C-2), 162.2 (C-4′), 162.1 (C-5), 157.6 (C-9), 127.7 (C-2′ and C-6′), 123.5 (C-1′), 115.0 (C-3′ and C-5′), 105.5 (C-10), 104.2 (C-3), 98.0 (C-8), 92.5 (C-6), 69.8 (C-1″), 55.8 (OCH_3), 22.5 (C-2″), 10.5 (C-3″). ESIMS *m/z* 327.0637 $[M+H]^+$ (calcd $C_{19}H_{18}O_5$ 326.1154).

Preparation of the Chalcone (*E*) 4-Isopropyloxy-4',6'-Dimethoxy-2'-Hydroxychalcone [2a]: Procedure for the preparation of the chalcone **2a** is similar to the preparation of the chalcone 1a except for the use of 4-isopropoxybenzaldehyde (251 mg, 1.53 mmol). The chalcone **2a** was

purified in a silica column using 4:1 Hex-EtOAc, 3:1 Hex-EtOAc, 4:1 EtOAc-Hex, 100% EtOAc, and 100% MeOH (411 mg, 79%). ^{1}H NMR (400 MHz, $CDCl_3$) δ_H 14.43 (s, C-2′-OH), 7.80 (s br, 2H, H-α and H-β), 7.55 (d, *J* = 8.7 Hz, 2H, H-2 and H-6), 6.91 (d, *J* = 8.7 Hz, 2H, H-3 and H-5), 6.12 (d, *J* = 2.3, 1H, H-3′), 5.97 (d, *J* = 2.3, 1H, H-5′), 4.62 (sept, *J* = 6.0 Hz, 1H, H-1″), 3.93 (s, 3H, OCH_3), 3.84 (s, 3H, OCH_3), 1.37 (d, *J* = 6.0 Hz, 6H, CH_3-2″ and CH_3-3″). ^{13}C NMR (100 MHz, $CDCl_3$) δ_C 192.6 (C=O), 168.3 (C-2′), 166.0 (C-4′), 162.4 (C-6′), 159.8 (C-4), 142.6 (C-β), 130.1 (C-2 and C-6), 127.9 (C-1), 124.9 (C-α), 115.9 (C-3 and C-5), 106.4 (C-1′), 93.8 (C-3′), 91.2 (C-5′), 70.0 (C-1″), 55.8 (OCH_3), 55.6 (OCH_3), 22.0 (C-2″ and C-3″). ESIMS *m/z* 343.0876 $[M+H]^+$ (calcd $C_{20}H_{22}O_5$ 342.1467).

Preparation of Oxygenated Intermediate Flavonoid 5,7-Dimethoxy-4'-Isopropyloxyflavone [2b]: Procedure is similar to the preparation of the intermediate flavonoid **1b**. The intermediate flavonoid **2b** was purified in a silica column using 1:1 Hex-EtOAc, 100% EtOAc, 20:1 EtOAc-MeOH, and 100% MeOH (78 mg, 52%). ^{1}H NMR (400 MHz, $CDCl_3$) δ_H 7.78 (d, *J* = 8.9 Hz, 2H, H-2′ and H-6′), 6.95 (d, *J* = 8.9, 2H, H-3′ and H-5′), 6.56 (s, 1H, H-3), 6.53 (d, *J* = 2.3, 1H, H-6), 6.34 (d, *J* = 2.3, 1H, H-8), 4.62 (sept, *J* = 6.0 Hz, 1H, H-1″), 3.93 (s, 3H, OCH_3), 3.89 (s, 3H, OCH_3), 1.36 (d, *J* = 6.0 Hz, 6H, CH_3-2″ and CH_3-3″). ^{13}C NMR (100 MHz, $CDCl_3$) δ_C 177.6 (C-4), 163.8 (C-2), 160.8 (C-5), 160.7 (C-4′), 160.5 (C-9), 159.8 (C-7), 127.6 (C-2′ and C-6′), 123.3 (C-1′), 115.8 (C-3′ and C-5′), 109.2 (C-3), 109.2 (C-10), 107.5 (C-3), 96.0 (C-8), 92.8 (C-6), 70.1 (C-1″), 56.4 (OCH_3), 55.7 (OCH_3), 21.9 (C-2″ and C-3″). ESIMS *m/z* 341.0796 $[M+H]^+$ (calcd $C_{20}H_{20}O_5$ 340.1311).

Preparation of Final Oxygenated Flavonoid 7-Methoxy-4'-Isopropyloxy-5-Hydroxyflavone [2c]: Procedure is similar to the preparation of the final flavonoid **1c**. The final flavonoid **2c** was purified in a silica column using 7:3 Hex-EtOAc and 1:1 Hex-EtOAc (6 mg, 10%). ^{1}H NMR

(400 MHz, $CDCl_3$) δ_H 12.83 (s, C-5-OH), 7.83 (d, *J* = 8.9 Hz, 2H, H-2′ and H-6′), 6.99 (d, *J* = 8.9 Hz, 2H, H-3′ and H-5′), 6.58 (s, 1H, H-3), 6.49 (d, *J* = 2.2 Hz, 1H, H-6), 6.37 (d, *J* = 2.2 Hz, 1H, H-8), 4.66 (sept, *J* = 6.0 Hz, 1H, H-1″), 3.89 (s, 3H, OCH_3), 1.40 (d, *J* = 6.0 Hz, 6H, CH_3-2″ and CH_3-3″). ^{13}C NMR (100 MHz, $CDCl_3$) δ_C 182.4 (C-4), 165.4 (C-7), 164.1 (C-2), 162.2 (C-4′), 161.1 (C-5), 157.3 (C-9), 128.0 (C-2′ and C-6′), 123.1 (C-1′), 115.9 (C-3′ and C-5′), 105.5 (C-10), 104.2 (C-3), 98.0 (C-8), 92.6 (C-6), 70.2 (C-1″), 55.8 (OCH_3), 21.9 (C-2″ and C-3″). ESIMS *m/z* 327.0724 $[M+H]^+$ (calcd $C_{19}H_{18}O_5$ 326.1154).

Preparation of the Chalcone (*E*) 4-Isobutyloxy-4',6'-Dimethoxy-2'-Hydroxychalcone [3a]: Procedure is similar to the preparation of the chalcone **1a** except for the use of 4-isobutoxy benzaldehyde (273 mg, 1.53 mmol). The chalcone **3a** was purified in a silical column using CH_2Cl_2 (436 mg, 80%). ^{1}H NMR (500 MHz, $CDCl_3$) δ_H 14.45 (s, C-2′-OH), 7.82 (s, br, 2H, H-α and H-β), 7.57 (d, *J* = 8.8 Hz, 2H, H-2 and H-6), 6.94 (d, *J* = 8.8 Hz, 2H, H-3 and H-5), 6.13 (d, *J* = 2.4 Hz, 1H, H-3′), 5.99 (d, *J* = 2.4 Hz, 1H, H-5′), 3.94 (s, 3H, OCH_3), 3.86 (s, 3H, OCH_3), 3.79 (d, *J* = 6.6 Hz, 2H, H_2-1″), 2.13 (sept, *J* = 6.7 Hz, 1H, H-2″), 1.06 (d, *J* = 6.7 Hz, 6H, CH_3-3″ and CH_3-4″). ^{13}C NMR (125 MHz, $CDCl_3$) δ_C 192.6 (C=O), 168.4 (C-2′), 166.0 (C-4′), 162.4 (C-6′), 161.1 (C-4), 142.6 (C-β), 130.1 (C-2 and C-6), 128.0 (C-1), 124.9 (C-α), 114.9 (C-3 and C-5), 106.4 (C-1′), 93.8 (C-3′), 91.2 (C-5′), 74.5 (C-1″), 55.8 (OCH_3), 55.6 (OCH_3), 28.2 (C-2″), 19.2 (C-3″ and C-4″). ESIMS *m/z* 357.0610 $[M+H]^+$ (calcd $C_{21}H_{24}O_5$ 356.1624).

Preparation of Oxygenated Intermediate Flavonoid 5,7-Dimethoxy-4'-Isobutyloxyflavone [3b]: Procedure is similar to the preparation of the intermediate flavonoid **1b**. The intermediate flavonoid **3b** was purified in a silica column using 1:1 Hex-EtOAc, 8:2 EtOAc-Hex, 100% EtOAc, 20:1 EtOAc, and 9:1 EtOAc-MeOH (113 mg, 57%). ^{1}H NMR (400 MHz, $CDCl_3$) δ_H 7.73 (d, *J* = 8.6 Hz, 2H, H-2′ and H-6′), 6.92 (d, *J* = 8.4 Hz, 2H, H-3′ and H-5′), 6.52 (s, 1H, H-

3), 6.48 (d, *J* = 1.4 Hz, 1H, H-6), 6.29 (d, *J* = 1.6 Hz, 1H, H-8), 3.89 (s, 3H, OCH_3), 3.85 (s, 3H, OCH_3), 3.73 (d, *J* = 6.5 Hz, 2H, H_2-1″), 2.07 (sept, *J* = 6.7 Hz, 1H, H-2″), 1.00 (d, *J* = 6.7 Hz, 6H, CH_3-3″ and CH_3-4″). ^{13}C NMR (100 MHz, $CDCl_3$) δ_C 177.6 (C-4), 163.8 (C-2), 161.7 (C-5), 160.7 (C-4′ and C-9), 159.7 (C-7), 127.4 (C-2′ and C-6′), 123.4 (C-1′), 114.8 (C-3′ and C-5′), 109.0 (C-10), 107.4 (C-3), 96.0 (C-8), 92.8 (C-6), 74.5 (C-1″), 56.3 (OCH_3), 55.7 (OCH_3), 28.2 (C-2″), 19.2 (C-3″ and C-4″). ESIMS *m/z* 355.0958 $[M+H]^+$ (calcd $C_{21}H_{22}O_5$ 354.1467).

Preparation of Final Oxygenated Flavonoid 7-Methoxy-4'-Isobutyloxy-5-Hydroxyflavone [3c]: Procedure is similar to the preparation of the final flavonoid **1c**. The final flavonoid **3c** was purified in a silica column using 7:3 EtOAc-Hex and 100% EtOAc (40 mg, 44%). ^{1}H NMR (400 MHz, $CDCl_3$) δ_H 12.83 (s, C-5-OH), 7.81 (d, *J* = 8.9 Hz, 2H, H-2′ and H-6′), 7.00 (d, *J* = 8.9 Hz, 2H, H-3′ and H-5′), 6.56 (s, 1H, H-3), 6.47 (d, *J* = 2.2 Hz, 1H, H-6), 6.36 (d, *J* = 2.2 Hz, 1H, H-8), 3.88 (s, 3H, OCH_3), 3.80 (d, *J* = 6.6 Hz, 2H, H_2-1″), 2.14 (sept, *J* = 6.6 Hz, 1H, CH_3-2″), 1.07 (d, *J* = 6.7 Hz, 6H, CH_3-3″ and CH_3-4″). ^{13}C NMR (100 MHz, $CDCl_3$) δ_C 182.4 (C-4), 165.4 (C-7), 164.1 (C-2), 162.3 (C-4′), 162.1 (C-5), 157.6 (C-9), 127.9 (C-2′ and C-6′), 123.1 (C-1′), 114.9 (C-3′ and C-5′), 105.5 (C-10), 104.1 (C-3), 98.0 (C-8), 92.5 (C-6), 74.6 (C-1″), 55.7 (OCH_3), 28.2 (C-2″), 19.2 (C-3″ and C-4″). ESIMS *m/z* 341.0737 $[M+H]^+$ (calcd $C_{20}H_{20}O_5$ 340.1311).

Preparation of the Chalcone (*E*) 4-Propargyloxy-4',6'-Dimethoxy-2'-Hydroxychalcone [4a]: Procedure is similar to the preparation of the chalcone **1a** except for the use of 4-(prop-2-ynyloxy)benzaldehyde (245 mg, 1.53 mmol). The chalcone **4a** was purified in a silica column using 100% CH_2Cl_2 (326 mg, 63%). ^{1}H NMR (500 MHz, $CDCl_3$) δ_H 14.38 (s, C-2′-OH), 7.84 (d, *J* = 15.6 Hz, 1H, H-β), 7.79 (d, *J* = 15.6 Hz, 1H, H-α), 7.60 (d, *J* = 8.8 Hz, 2H, H-2 and H-6), 7.03 (d, *J* = 8.8 Hz, 2H, H-3 and H-5), 6.14 (d, *J* = 2.3 Hz, 1H, H-3′), 5.99 (d, *J* = 2.3 Hz, 1H, H-5′), 4.76 (d, *J* = 2.4 Hz, 2H, H_2-1″), 3.94 (s, 3H, OCH_3), 3.86 (s, 3H, OCH_3), 2.57 (t, *J* = 2.4 Hz,

1H, H-3″). ^{13}C NMR (125 MHz, $CDCl_3$) δ_C 192.6 (C=O), 168.4 (C-2′), 166.1 (C-4′), 162.5 (C-6′), 159.1 (C-4), 142.1 (C-β), 130.0 (C-2 and C-6), 129.2 (C-1), 125.7 (C-α), 115.3 (C-3 and C-5), 106.4 (C-1′), 93.8 (C-3′), 91.3 (C-5′), 78.1 (C-2″), 75.9 (C-3″), 55.9 (2C, OCH_3, C-1″), 55.6 (OCH_3). ESIMS *m/z* 339.0599 $[M+H]^+$ (calcd $C_{20}H_{18}O_5$ 338.1154)

Preparation of Oxygenated Intermediate Flavonoid 5,7-Dimethoxy-4'-Propargyloxyflavone [4b]: Procedure is similar to the preparation of the intermediate flavonoid **1b**. The intermediate flavonoid **4b** was purified in a silica column using 1:1 Hex-EtOAc, 100% EtOAc, 20:1 EtOAc-MeOH, 9:1 EtOAc-MeOH, 1:1 EtOAc-MeOH, and 100% MeOH (87 mg, 54%). ^{1}H NMR (400 MHz, $CDCl_3$) δ_H 7.82 (d, *J* = 8.9 Hz, 2H, H-2′ and H-6′), 7.07 (d, *J* = 8.9 Hz, 2H, H-3′ and H-5′), 6.58 (s, 1H, H-3), 6.54 (d, *J* = 2.3 Hz, 1H, H-6), 6.36 (d, *J* = 2.3 Hz, 1H, H-8), 4.76 (d, *J* = 2.4 Hz, 2H, H_2-1″), 3.94 (s, 3H, OCH_3), 3.90 (s, 3H, OCH_3), 2.57 (t, *J* = 2.4 Hz, 1H, H-3″). ^{13}C NMR (100 MHz, $CDCl_3$) δ_C 177.6 (C-4), 163.9 (C-2), 160.9 (C-5), 160.4 (C-4′), 159.8 (C-9), 159.8 (C-7), 127.5 (C-2′ and C-6′), 124.7 (C-1′), 115.2 (C-3′ and C-5′), 109.2 (C-10), 107.9 (C-3), 96.1 (C-8), 92.8 (C-6), 77.9 (C-2″), 76.1 (C-3″), 56.4 (C-1″), 55.9 (OCH_3), 55.7 (OCH_3). ESIMS *m/z* 337.0495 $[M+H]^+$ (calcd $C_{20}H_{16}O_5$ 336.0998)

Preparation of Final Oxygenated Flavonoid 7-Methoxy, 4'-Propargyloxy-5-Hydroxyflavone [4c]: Procedure is similar to the preparation of the final flavonoid **1c**. The final flavonoid **4c** was purified in a silica column with 7:3 Hex-EtOAc, 1:1 Hex-EtOAc, 100% EtOAc, 20:1 EtOAc-MeOH, and 9:1 EtOAc-MeOH (14 mg, 28%). ^{1}H NMR (400 MHz, $CDCl_3$) δ_H 12.79 (s, C-5-OH), 7.88 (d, *J* = 8.9 Hz, 2H, H-2′ and H-6′), 7.12 (d, *J* = 8.9 Hz, 2H, H-3′ and H-5′), 6.60 (s, 1H, H-3), 6.50 (d, *J* = 2.2 Hz, 1H, H-6), 6.39 (d, *J* = 2.2 Hz, 1H, H-8), 4.80 (d, *J* = 2.3 Hz, 2H, H_2-1″), 3.90 (s, 3H, OCH_3), 2.59 (t, *J* = 2.3 Hz, 1H, H-3″). ^{13}C NMR (100 MHz, $CDCl_3$) δ_C 182.4 (C-4), 165.5 (C-7), 163.8 (C-2), 162.2 (C-4′), 160.4 (C-5), 157.7 (C-9), 128.0 (C-2′ and C-

6′), 124.4 (C-1′), 115.4 (C-3′ and C-5′), 105.6 (C-10), 104.6 (C-3), 98.1 (C-8), 92.6 (C-6), 77.7 (C-2″), 76.2 (C-3″), 55.9 (C-1″), 55.8 (OCH_3). ESIMS *m/z* 323.0367 $[M+H]^+$ (calcd $C_{19}H_{14}O_5$ 322.0841).

Preparation of 4-(Cyclopropyl Methoxy)Benzaldehyde [Compound IV]: (Bromomethyl)cyclopropane (400 mg, 2.96 mmol) was added to 4-hydroxy benzaldehyde (724 mg, 5.92 mmol) and were dissolved in 15 mL of acetone and potassium carbonate (1.6 g, 11.9 mmol). The mixture was then refluxed for 36 h until the reaction went through and then diluted with EtOAc and washed with water. This compound **IV** was purified in a silica column using 95:5 Hex-EtOAc (380 mg, 73%). ^{1}H NMR (400 MHz, $CDCl_3$) δ_H 9.82 (s, 1H, CHO), 7.76 (d, *J* = 8.8 Hz, 2H, H-2 and H-6), 6.94 (d, *J* = 8.8 Hz, 2H, H-3 and H-5), 3.84 (dd, *J* = 8.1, 10.9 Hz, 2H, H_2-1′), 1.27 – 1.21 (m, 1H, H-2′), 0.64 – 0.61 (m, 2H, H-3′a and H-4′a), 0.34 – 0.32 (m, 2H, H-3′b and H-4′b). ^{13}C NMR (100 MHz, $CDCl_3$) δ_C 190.7 (CHO), 164.0 (C-4), 131.9 (C-2 and C-6), 129.8 (C-1), 114.8 (C-3 and C-5), 73.0 (C-1′), 10.0 (C-2′), 3.2 (C-3′ and C-4′).

Preparation of the Chalcone (*E*) 4-(Cyclopropyl Methoxy)-4',6'-Dimethoxy-2'-Hydroxychalcone [5a]: Procedure is similar to the preparation of the chalcone **1a** except for the use of 4-(cyclopropyl methoxy)benzaldehyde (**compound IV**) (270 mg, 1.53 mmol). The chalcone **5a** was purified in a silica column with 4:1 CH_2Cl_2-Hex, 100% CH_2Cl_2, 20:1 CH_2Cl_2-MeOH, and 9:1 CH_2Cl_2-MeOH (287 mg, 53%). ^{1}H NMR (400 MHz, $CDCl_3$) δ_H 14.42 (s, C-2′-OH), 7.84 (s, br, 2H, H-α and H-β), 7.55 (d, *J* = 8.7 Hz, 2H, H-2 and H-6), 6.93 (d, *J* = 8.7 Hz, 2H, H-3 and H-5), 6.11 (d, *J* = 2.3 Hz, 1H, H-3′), 5.97 (d, *J* = 2.3 Hz, 1H, H-5′), 3.86 (s, 2H, H_2-1″), 3.92 (s, 3H, OCH_3), 3.84 (s, 3H, OCH_3), 1.31 – 1.27 (m, 1H, H-2″), 0.67 (dd, *J* = 4.9, 12.9 Hz, 2H, H-3″a and H-4″a), 0.38 (dd, *J* = 4.9, 10.3 Hz, 2H, H-3″b and H-4″b). ^{13}C NMR (100 MHz, $CDCl_3$) δ_C 192.6 (C=O), 168.3 (C-2′), 166.0 (C-4′), 162.4 (C-6′), 160.8 (C-4), 142.5 (C-β),

130.1 (C-2 and C-6), 128.2 (C-1), 125.0 (C-α), 114.9 (C-3 and C-5), 106.3 (C-1′), 93.8 (C-3′), 91.2 (C-5′), 72.9 (C-1″), 55.8 (OCH_3), 55.5 (OCH_3), 10.2 (C-2″), 3.2 (C-3″ and C-4″). ESIMS *m/z* 355.0575 $[M+H]^+$ (calcd $C_{21}H_{22}O_5$ 354.1467).

Preparation of Oxygenated Intermediate Flavonoid 5,7-Dimethoxy-4'(Cyclopropyl Methoxy)Flavone [5b]: Procedure is similar to the preparation of the intermediate flavonoid **1b**. The intermediate flavonoid **5b** was purified in a silica column using 1:1 Hex-EtOAc, 100% EtOAc, 20:1 EtOAc-MeOH, 9:1 EtOAc-MeOH, and 1:1 EtOAc-MeOH (120 mg, 78%). ^{1}H NMR (400 MHz, $CDCl_3$) δ_H 7.78 (d, *J* = 9.0 Hz, 2H, H-2′ and H-6′), 6.97 (d, *J* = 9.0 Hz, 2H, H-3′ and H-5′), 6.56 (s, 1H, H-3), 6.53 (d, *J* = 2.3 Hz, 1H, H-6), 6.34 (d, *J* = 2.3 Hz, 1H, H-8), 3.93 (s, 3H, OCH_3), 3.89 (s, 3H, OCH_3), 3.85 (d, *J* = 6.9 Hz, 2H, H_2-1″), 1.25 (t, *J* = 7.2, 1H, H-2″), 0.66 (dd, *J* = 4.8, 12.9 Hz, 2H, H-3″a and H-4″a), 0.37 (dd, *J* = 4.8, 10.6 Hz, 2H, H-3″b and H-4″b). ^{13}C NMR (100 MHz, $CDCl_3$) δ_C 177.6 (C-4), 163.9 (C-2), 161.5 (C-5), 160.8 (C-4′), 160.7 (C-9), 159.8 (C-7), 127.5 (C-2′ and C-6′), 123.6 (C-1′), 114.9 (C-3′ and C-5′), 109.1 (C-10), 107.5 (C-3), 96.0 (C-8), 92.8 (C-6), 72.9 (C-1″), 56.4 (OCH_3), 55.7 (OCH_3), 10.1 (C-2″), 3.2 (C-3″ and C-4″). ESIMS *m/z* 353.0805 $[M+H]^+$ (calcd $C_{21}H_{20}O_5$ 352.1311).

Preparation of Brominated Chalcone (*E*) 4-Bromo-4',6'-Dimethoxy-2'-Hydroxychalcone [6a]: A mixture of equimolar amounts of 2′-hydroxy-4′,6′-dimethoxyacetophenone (300 mg, 1.53 mmol) and the 4-bromobenzaldehyde (285 mg, 1.53 mmol) was taken in a RBF and 10 mL of 50% sodium hydroxide in ethanol was added and left for 16 h at rt. The resulting yellow precipitate was then suction filtered and washed with Hex and CH_2Cl_2. The brominated chalcone **6a** was then purified in a silica column using 10% EtOAc and Hex (361 mg, 65%). ^{1}H NMR (400 MHz, $CDCl_3$) δ_H 14.23 (s, C-2′-OH), 7.89 (d, *J* = 15.6 Hz, 1H, H-β), 7.71 (d, *J* = 15.6 Hz, 1H, H-α), 7.55 (d, *J* = 8.4 Hz, 2H, H-2 and H-6), 7.47 (d, *J* = 8.4 Hz, 2H, H-3 and H-5), 6.13 (d,

J = 2.2 Hz, 1H, H-3′), 5.98 (d, *J* = 2.2 Hz, 1H, H-5′), 3.93 (s, 3H, OCH_3), 3.86 (s, 3H, OCH_3). ^{13}C NMR (100 MHz, $CDCl_3$) δ_C 192.3 (C=O), 168.4 (C-4′), 166.4 (C-6′), 162.5 (C-2′), 140.8 (C-β), 134.5 (C-1), 132.1 (C-3 and C-5), 129.7 (C-2 and C-6), 128.1 (C-α), 124.2 (C-4), 106.3 (C-1′), 93.8 (C-3′), 91.3 (C-5′), 55.9 (OCH_3), 55.6 (OCH_3). ESIMS *m/z* 363.1418 $[M+H]^+$ (calcd $C_{17}H_{15}BrO_4$ 362.0154).

Preparation of Brominated Intermediate Flavonoid 5,7-Dimethoxy-4'-Bromoflavone [6b]: The brominated chalcone [**6a**] (200 mg, 0.551 mmol) was treated with 3-4 mol% of iodine crystals with minimal amount of DMSO at 140 °C for 4-6 h. The resulting white precipitate was extracted with CH_2Cl_2 and was removed by filtration. The filtrate was transferred into a separatory funnel, where the layers were separated as aqueous and organic layers. The organic layer was washed with $Na_2S_2O_3$, dried Na_2SO_4, and concentrated. The intermediate flavonoid **6b** was purified in a silica column with 1:1 Hex-EtOAc, 3:2 EtOAc-Hex, 4:1 EtOAc-Hex, and 9:1 EtOAc-Hex (134 mg, 67%). ^1H NMR (400 MHz, $CDCl_3$) δ_H 7.72 (d, *J* = 8.7 Hz, 2H, H-3′ and H-5′), 7.62 (d, *J* = 8.7 Hz, 2H, H-2′ and H-6′), 6.64 (s, 1H, H-3), 6.55 (d, *J* = 2.3 Hz, 1H, H-6), 6.37 (d, *J* = 2.3 Hz, 1H, H-8), 3.95 (s, 3H, OCH_3), 3.91 (s, 3H, OCH_3). ^{13}C NMR (100 MHz, $CDCl_3$) δ_C 177.3 (C-4), 164.2 (C-2), 160.9 (C-5), 159.8 (C-9), 159.5 (C-7), 132.2 (C-3′ and C-5′), 130.4 (C-1′), 127.3 (C-2′ and C-6′), 125.8 (C-4′), 109.2 (C-10 and C-3), 96.3 (C-8), 92.8 (C-6), 56.4 (OCH_3), 55.8 (OCH_3). ESIMS *m/z* 361.1324 $[M+H]^+$ (calcd $C_{17}H_{13}BrO_4$ 359.9997).

Preparation of Nitrogenated Intermediate Flavonoid 5,7-Dimethoxy-4'-Aminopropylflavone [6c]: Sodium tert-butoxide (17 mg, 0.18 mmol), tris(dibenzylideneacetone)dipalladium (11 mg, 0.012 mmol), and 1,1′-binaphthalene-2,2′-diylbis(diphenylphosphine) (8 mg, 0.012 mmol) were dissolved in 5 mL of toluene. To this, the brominated intermediate flavonoid **6b** (50 mg, 0.138 mmol) and propylamine (11 mg, 0.18

mmol) were added dropwise with stirring at rt, and the mixture was refluxed at 80 °C for 48 h. The nitrogenated intermediate flavonoid was purified in a silica column using 7:3 EtOAc-Hex, 9:1 EtOAc-Hex, 100% EtOAc, and 9:1 EtOAc-MeOH (24 mg, 52%). ^{1}H NMR (500 MHz, $CDCl_3$) δ_H 7.67 (d, *J* = 10.9 Hz, 2H, H-2′ and H-6′), 6.61 (d, *J* = 10.9 Hz, 2H, H-3′ and H-5′), 6.52 (d, *J* = 2.6 Hz, 1H, H-6), 6.50 (s, 1H, H-3), 6.33 (d, *J* = 2.5 Hz, 1H, H-8), 3.92 (s, 3H, OCH_3), 3.88 (s, 3H, OCH_3), 3.13 (t, *J* = 9.0 Hz, 2H, H_2-1″), 1.66 (ddd, *J* = 9.2, 18.2, 9.0 Hz, 2H, H_2-2″), 1.00 (t, *J* = 9.2 Hz, 3H, CH_3-3″). ^{13}C NMR (125 MHz, $CDCl_3$) δ_C 177.8 (C-4), 163.6 (C-2), 161.6 (C-5), 160.7 (C-4′), 159.7 (C-9), 150.9 (C-7), 127.5 (C-2′ and C-6′), 119.0 (C-1′), 112.1 (C-3′ and C-5′), 109.2 (C-10), 105.8 (C-3), 95.8 (C-8), 92.8 (C-6), 56.3 (OCH_3), 55.7 (OCH_3), 45.2 (C-1″), 22.5 (C-2″), 11.5 (C-3″). ESIMS *m/z* 340.2991 $[M+H]^+$ (calcd $C_{20}H_{21}NO_4$ 339.1471).

Preparation of Nitrogenated Final Compound 7-Methoxy-4'-Aminopropyl-5-Hydroxyflavone [6d]: The nitrogenated intermediate flavonoid **6c** (15 mg, 0.044 mmol) was treated with double the moles of 1N boron tribromide (22 mg, 0.088 mmol) in the presence of CH_2Cl_2 at rt, for 1-3 h. The reactant solution was diluted with 10:1 CH_2Cl_2:MeOH and then washed with brine and water. Na_2SO_4 was added to the solution and left overnight. The solution was then filtered into an RBF, dried, and concentrated. The final compound **6d** was purified in a silica column using 1:1 Hex-EtOAc (11 mg, 77%). ^{1}H NMR (500 MHz, $CDCl_3$) δ_H 12.90 (s, C-5-OH), 7.65 (d, *J* = 8.8 Hz, 2H, H-2′ and H-6′), 6.58 (d, *J* = 8.7 Hz, 2H, H-3′ and H-5′), 6.43 (s, 1H, H-3), 6.39 (d, *J* = 2.2 Hz, 1H, H-6), 6.27 (d, *J* = 2.2 Hz, 1H, H-8), 3.80 (s, 3H, OCH_3), 3.10 (t, *J* = 7.2 Hz, 2H, H_2-1″), 1.62 (ddd, *J* = 7.4, 7.2, 7.3 Hz, 2H, H_2-2″), 0.96 (t, *J* = 7.4 Hz, 3H, CH_3-3″). ^{13}C NMR (125 MHz, $CDCl_3$) δ_C 182.3 (C-4), 165.2 (C-7), 164.4 (C-2), 162.1 (C-5 and C-4′), 157.6 (C-9), 128.0 (C-2′ and C-6′), 127.5 (C-1′), 114.0 (C-3′ and C-5′), 105.4 (C-10),

103.0 (C-3), 97.9 (C-8), 92.5 (C-6), 55.8 (OCH_3), 29.7 (C-1″), 22.1 (C-2″), 11.5 (C-3″). ESIMS *m/z* 326.2691 $[M+H]^+$ (calcd $C_{19}H_{19}NO_4$ 325.1314).

Preparation of Nitrogenated Intermediate Flavonoid 5,7-Dimethoxy-4'-Aminoisopropylflavone [7c]: Procedure is similar to the preparation of the intermediate flavonoid **6c** except for the use of isopropylamine (11 mg, 0.18 mmol). The intermediate flavonoid **7c** was purified in a silica column using 9:1 EtOAc-Hex (37 mg, 79%). ^{1}H NMR (400 MHz, $CDCl_3$) 7.65 (d, *J* = 8.7 Hz, 2H, H-2′ and H-6′), 6.58 (d, *J* = 8.7 Hz, 2H, H-3′ and H-5′), 6.50 (d, *J* = 2.2 Hz, 1H, H-6), 6.48 (s, 1H, H-3), 6.31 (d, *J* = 2.2 Hz, 1H, H-8), 3.90 (s, 3H, OCH_3), 3.86 (s, 3H, OCH_3), 3.67 (sept, *J* = 6.4 Hz, 1H, H-1″), 1.22 (d, *J* = 6.4 Hz, 6H, H-2″ and H-3″). ^{13}C NMR (100 MHz, $CDCl_3$) δ_C 177.7 (C-4), 163.6 (C-2), 161.5 (C-5), 160.7 (C-4′), 159.7 (C-9), 150.0 (C-7), 127.5 (C-2′ and C-6′), 118.8 (C-1′), 112.5 (C-3′ and C-5′), 109.1 (C-10), 105.7 (C-3), 95.8 (C-8), 92.8 (C-6), 56.3 (OCH_3), 55.6 (OCH_3), 43.9 (C-1″), 22.7 (C-2″ and C-3″). ESIMS *m/z* 340.3005 $[M+H]^+$ (calcd $C_{20}H_{21}NO_4$ 339.1471).

Preparation of Nitrogenated Final Compound 7-Methoxy-4'-Aminoisopropyl-5-Hydroxyflavone [7d]: Procedure is similar to the preparation of the final compound **6d**. The final compound **7d** was purified in a silica column with 9:1 Hex-EtOAc (16 mg, 83%). ^{1}H NMR (500 MHz, $CDCl_3$) 13.00 (s, C-5-OH), 7.74 (d, *J* = 8.9 Hz, 2H, H-2′ and H-6′), 6.64 (d, *J* = 8.9 Hz, 2H, H-3′ and H-5′), 6.52 (s, 1H, H-3), 6.48 (d, *J* = 2.3 Hz, 1H, H-6), 6.37 (d, *J* = 2.3 Hz, 1H, H-8), 3.90 (s, 3H, OCH_3), 3.75 (sept, *J* = 6.3 Hz, 1H, H-1″), 1.29 (d, *J* = 6.3 Hz, 6H, CH_3-2″ and CH_3-3″). ^{13}C NMR (125 MHz, $CDCl_3$) δ_C 182.4 (C-4), 165.1 (C-7), 164.9 (C-2), 162.1 (C-4′), 157.6 (C-5), 150.5 (C-9), 128.1 (C-2′ and C-6′), 118.6 (C-1′), 112.6 (C-3′ and C-5′), 105.5 (C-10), 102.4 (C-3), 97.8 (C-8), 92.5 (C-6), 55.7 (OCH_3), 44.1 (C-1″), 22.8 (C-2″ and C-3″). ESIMS *m/z* 326.2691 $[M+H]^+$ (calcd $C_{19}H_{19}NO_4$ 325.1314).

Preparation of Nitrogenated Intermediate Flavonoid 5,7-Dimethoxy-4'-(Cyclopropyl Methylamino)Flavone [9c]: Procedure is similar to the preparation of the intermediate flavonoid **6c** except for the use of (aminomethyl)cyclopropane (13 mg, 0.18 mmol). The intermediate flavonoid **9c** was purified in a silica column using 7:3 EtOAc-Hex, 100% EtOAc, 10:1 EtOAc-MeOH, and 100% MeOH (40 mg, 83%). ^{1}H NMR (500 MHz, $CDCl_3$) 7.66 (d, *J* = 8.5 Hz, 2H, H-2′ and H-6′), 6.66 (d, *J* = 8.7 Hz, 2H, H-3′ and H-5′), 6.56 (s, 1H, H-3), 6.41 (d, *J* = 2.2 Hz, 1H, H-6), 6.38 (d, *J* = 2.2 Hz, 1H, H-8), 3.97 (s, 3H, OCH_3), 3.92 (s, 3H, OCH_3), 3.05 (d, *J* = 6.9 Hz, 2H, H_2-1″), 1.12 (m, 1H, H-2″), 0.61 (dd, *J* = 6.0, 13.6 Hz, 2H, H-3″a and H-4″a), 0.30 (dd, *J* = 5.5, 10.5 Hz, 2H, H-3″b and H-4″b). ^{13}C NMR (125 MHz, $CDCl_3$) δ_C 177.8 (C-4), 163.7 (C-2), 161.5 (C-5), 160.8 (C-4′), 160.9 (C-9), 159.8 (C-7), 127.5 (C-2′ and C-6′), 119.3 (C-1′), 112.3 (C-3′ and C-5′), 109.3 (C-10), 106.0 (C-3), 96.3 (C-8), 92.8 (C-6), 56.5 (OCH_3), 55.7 (OCH_3), 48.5 (C-1″), 10.7 (C-2″), 3.6 (C-3″ and C-4″). ESIMS *m/z* 352.2586 $[M+H]^+$ (calcd $C_{21}H_{21}NO_4$ 351.1471).

Preparation of Nitrogenated Final Compound 7-Methoxy-4'-(Cyclopropyl Methylamino)-5-Hydroxyflavone [9d]: Procedure is similar to the preparation of the final compound **6d**. The final compound **9d** was purified in a sephadex column with 1:1 Hex-EtOAC (2 mg, 7%). ^{1}H NMR (500 MHz, $CDCl_3$) 13.00 (s, C-5-OH), 7.75 (d, *J* = 8.8 Hz, 2H, H-2′ and H-6′), 6.67 (d, *J* = 8.8 Hz, 2H, H-3′ and H-5′), 6.53 (s, 1H, H-3), 6.48 (d, *J* = 2.1 Hz, 1H, H-6), 6.37 (d, *J* = 2.1 Hz, 1H, H-8), 3.90 (s, 3H, OCH_3), 3.07 (d, *J* = 6.9 Hz, 2H, H_2-1″), 1.14 (m, 1H, H-2″), 0.63 (dd, *J* = 5.9, 13.0 Hz, 2H, H-3″a and H-4″a), 0.31 (dd, *J* = 4.9, 9.9 Hz, 2H, H-3″b and H-4″b). ^{13}C NMR (125 MHz, $CDCl_3$) δ_C 182.4 (C-4), 165.1 (C-7), 164.9 (C-2), 162.1 (C-4′), 157.6 (C-5), 151.3 (C-9), 128.1 (C-2′ and C-6′), 118.9 (C-1′), 112.3 (C-3′ and C-5′), 105.5 (C-10), 102.5 (C-3), 97.8 (C-

8), 92.5 (C-6), 55.7 (OCH_3), 48.4 (C-1″), 10.7 (C-2″), 3.6 (C-3″ and C-4″). ESIMS *m/z* 338.2880 $[M+H]^+$ (calcd $C_{20}H_{19}NO_4$ 337.1314).

Preparation of Oxygenated Diketo Intermediate 1-3′(2′-Methoxypyridin-3′-yl)-(4″-(Propyloxy)Phenyl)Propane-1,3-Dione [10a]: A mixture of equimolar amounts of methyl-2-methoxy nicotinate (500 mg, 2.99 mmol) and 1-(4-propoxyphenyl)ethanone (533 mg, 2.99 mmol) was used to prepare the oxygenated diketo intermediate **10a**. Methyl-2-methoxy nicotinate (500 mg, 2.99 mmol) and double the molar amounts of sodium hydride (144 mg, 5.98 mmol) were taken in a RBF and dissolved in 2.5 mL of dry dimethyl formamide. A solution of 1-(4-propoxyphenyl)ethanone (533 mg, 2.99 mmol) dissolved in 2 mL of dry dimethyl formamide was added dropwise and left at rt, for 2 h. Monosodium phosphate (NaH_2PO_4) was added to adjust the pH to 7.4 and the solution was then washed with CH_2Cl_2 in a separating funnel and dried in Na_2SO_4 and left overnight. The solution was then filtered into an RBF, dried, and concentrated. The diketo intermediate **10a** was purified in a silica column using 9:1 Hex-EtOAc, 4:1 Hex-EtOAc, and 1:1 Hex-EtOAc (71 mg, 8%). ^{1}H NMR (400 MHz, $CDCl_3$) δ_H 8.31 (dd, *J* = 1.8, 7.5 Hz, 1H, H-6′), 8.27 (dd, *J* = 1.8, 4.8 Hz, 1H, H-4′), 7.95 (d, *J* = 8.8 Hz, 2H, H-2″ and H-6″), 7.02 (dd, *J* = 4.8, 7.5 Hz, 1H, H-5′), 6.96 (d, *J* = 8.8 Hz, 2H, H-3″ and H-5″), 4.11 (s, 3H, OCH_3), 3.99 (t, *J* = 6.6 Hz, 2H, H_2-1‴), 1.83 (m, 2H, H_2-2‴), 1.06 (t, *J* = 7.4 Hz, 3H, CH_3-3‴). ^{13}C NMR (100 MHz, $CDCl_3$) δ_C 187.7 (C-3), 178.8 (C-1), 162.9 (C-2′), 161.5 (C-4″), 149.5 (C-4′), 139.0 (C-6′), 129.5 (C-2″ and C-6″), 128.3 (C-1″), 118.7 (C-1′), 117.1 (C-5′), 114.4 (C-3″ and C-5″), 97.2 (C-2), 69.7 (C-1‴), 53.9 (OCH_3), 22.5 (C-2‴), 10.4 (C-3‴). ESIMS *m/z* 314.0791 $[M+H]^+$ (calcd $C_{18}H_{19}NO_4$ 313.1314).

Preparation of Final Oxygenated Pyridine Compound 2-(4′-Propyloxyphenyl)-4*H*-Pyrano[2,3-*b*]Pyridin-4-one [10b]: The oxygenated diketo intermediate **10a** (48 mg, 0.17

mmol) was treated with 10 times the amount of pyridinium hydrochloride (480 mg, 4.154 mmol) and heated at 190 °C for 4 h. The resultant solution was diluted with water, neutralized with sodium bicarbonate ($NaHCO_3$) and extracted with EtOAc. Na_2SO_4 was added and left overnight. The solution was then filtered into an RBF, dried, and concentrated. The final pyridine compound **10b** was purified in a silica column using 1:1 CH_2Cl_2-Hex (37 mg, 86%). ^{1}H NMR (400 MHz, $CDCl_3$) δ_H 8.66 (dd, *J* = 1.6, 4.3 Hz, 1H, H-7), 8.55 (dd, *J* = 1.8, 7.6 Hz, 1H, H-5), 7.90 (d, *J* = 8.8 Hz, 2H, H-2′ and H-6′), 7.42 (dd, *J* = 4.6, 7.6 Hz, 1H, H-6), 6.96 (d, *J* = 8.8 Hz, 2H, H-3′ and H-5′), 6.73 (s, 1H, H-3), 3.96 (t, *J* = 6.5 Hz, 2H, H_2-1″), 1.81 (ddd, *J* = 7.2, 6.8, 7.1 Hz, 2H, H_2-2″), 1.02 (t, *J* = 7.4 Hz, 3H, CH_3-3″). ^{13}C NMR (100 MHz, $CDCl_3$) δ_C 178.5 (C-4), 164.1 (C-9), 162.4 (C-2), 160.7 (C-4′), 152.9 (C-7), 136.2 (C-5), 128.3 (C-2′ and C-6′), 122.8 (C-1′), 122.0 (C-6), 118.7 (C-10), 115.0 (C-3′ and C-5′), 106.0 (C-3), 69.7 (C-1″), 22.4 (C-2″), 10.4 (CH_3-3″). ESIMS *m/z* 282.1133 $[M+H]^+$ (calcd $C_{17}H_{15}NO_3$ 281.1052).

Preparation of Oxygenated Diketo Intermediate 1-3′(2′-Methoxypyridin-3′-yl)-(4″-(Isopropyloxy)Phenyl)Propane-1,3-Dione [11a]: Procedure is similar to the preparation of the diketo intermediate **10a** except for the use of 1-(4-isopropoxy phenyl)ethan-1-one (533 mg, 2.99 mmol). The compound **11a** was purified in a silica column using 9:1 Hex-EtOAc (221 mg, 24%). ^{1}H NMR (500 MHz, $CDCl_3$) δ_H 8.29 (dd, *J* = 1.9, 7.6 Hz, 1H, H-6′), 8.24 (dd, *J* = 1.9, 4.8 Hz, 1H, H-4′), 7.94 (d, *J* = 8.8 Hz, 2H, H-2″ and H-6″), 6.98 (dd, *J* = 4.8, 7.5 Hz, 1H, H-5′), 6.92 (d, *J* = 8.8 Hz, 2H, H-3″ and H-5″), 4.62 (sept, *J* = 6.0 Hz, 1H, H-1‴), 4.09 (s, 3H, OCH_3), 1.35 (d, *J* = 6.0 Hz, 6H, CH_3-2‴ and CH_3-3‴). ^{13}C NMR (125 MHz, $CDCl_3$) δ_C 187.7 (C-3), 178.7 (C-1), 161.8 (C-2′), 161.4 (C-4″), 149.5 (C-4′), 139.0 (C-6′), 129.6 (C-2″ and C-6″), 128.0 (C-1″), 118.7 (C-1′), 117.1 (C-5′), 115.3 (C-3″ and C-5″), 97.2 (C-2), 70.1 (C-1‴), 53.9 (OCH_3), 21.9 (CH_3-2‴ and CH_3-3‴). ESIMS *m/z* 314.2995 $[M+H]^+$ (calcd $C_{18}H_{19}NO_4$ 313.1314).

Preparation of Final Oxygenated Pyridine Compound 2-(4′-Isopropyloxyphenyl)-4*H*-Pyrano[2,3-*b*]Pyridin-4-one [11b]: Procedure is similar to the preparation of the final pyridine compound **10b**. The final pyridine compound **11b** was purified in a silica column with 1:1 Hex-EtOAc (18 mg, 20%). ^{1}H NMR (400 MHz, $CDCl_3$) δ_H 8.70 (dd, *J* = 2.5, 5.7 Hz, 1H, H-7), 8.60 (dd, *J* = 2.5, 9.6 Hz, 1H, H-5), 7.95 (d, *J* = 8.92 Hz, 2H, H-2′ and H-6′), 7.46 (dd, *J* = 5.7, 9.5 Hz, 1H, H-6), 7.00 (d, *J* = 8.96 Hz, 2H, H-3′ and H-5′), 6.78 (s, 1H, H-3), 4.66 (sept, *J* = 7.5 Hz, 1H, H-1″), 1.38 (d, *J* = 7.5 Hz, 6H, CH_3-2″ and CH_3-3″). ^{13}C NMR (100 MHz, $CDCl_3$) δ_C 178.5 (C-4), 164.2 (C-9), 161.3 (C-2), 160.7 (C-4′), 152.9 (C-7), 136.3 (C-5), 128.4 (C-2′ and C-6′), 122.7 (C-1′), 122.0 (C-6), 118.8 (C-10), 115.9 (C-3′ and C-5′), 106.0 (C-3), 70.2 (C-1″), 21.9 (CH_3-2″ and CH_3-3″). ESIMS *m/z* 282.1133 $[M+H]^+$ (calcd $C_{17}H_{15}NO_3$ 281.1052).

Preparation of Oxygenated Diketo Intermediate 1-3′(2′-Methoxypyridin-3′-yl)-(4″-(Propargyloxy)Phenyl)Propane-1,3-Dione [12a]: Procedure is similar to the preparation of the diketo intermediate **10a** except for the use of 1-(4-(prop-2-yn-1-yloxy)phenyl)ethan-1-one (521 mg, 2.99 mmol). The diketo intermediate **12a** was purified in a silica column using 9:1 Hex-EtOAc, 7:3 Hex-EtOAc, and 100% EtOAc (30 mg, 3%). ^{1}H NMR (400 MHz, $CDCl_3$) δ_H 8.33 (dd, *J* = 1.9, 7.5 Hz, 1H, H-6′), 8.29 (dd, *J* = 1.9, 4.8 Hz, 1H, H-4′), 7.99 (d, *J* = 8.9 Hz, 2H, H-2″ and H-6″), 7.08 (d, *J* = 8.9 Hz, 2H, H-3″ and H-5″), 7.04 (dd, *J* = 4.9, 7.6 Hz, 1H, H-5′), 4.78 (d, *J* = 2.4 Hz, 2H, H-1‴), 4.13 (s, OCH_3), 2.58 (t, *J* = 2.4 Hz, 1H, H-3‴). ^{13}C NMR (100 MHz, $CDCl_3$) δ_C 187.4 (C-3), 179.3 (C-1), 161.5 (C-2′), 161.0 (C-4″), 149.6 (C-4′), 139.1 (C-6′), 129.5 (C-2″ and C-6″), 129.4 (C-1″), 118.7 (C-1′), 117.2 (C-5′), 114.8 (C-3″ and C-5″), 97.4 (C-2), 76.1 (C-1‴), 55.9 (C-2‴), 54.0 (OCH_3), 53.4 (C-3‴). ESIMS *m/z* 310.0542 $[M+H]^+$ (calcd $C_{18}H_{15}NO_4$ 309.1001).

Preparation of 4-(Cyclopropyl)Acetophenone [Compound VIII]: (Bromomethyl)cyclopropane (400 mg, 2.96 mmol) was added to 4′-hydroxy acetophenone (806 mg, 5.92 mmol) and were dissolved in 15 mL of acetone and potassium carbonate (1.6 g, 11.9 mmol). The mixture was then refluxed for 24 h until the reaction went through and then diluted with EtOAc and washed with water. This compound **VIII** was purified in a silica column using 9:1 Hex-EtOAc, 7:3 Hex-EtOAc, and 100% EtOAc (551 mg, 98%). ^{1}H NMR (400 MHz, $CDCl_3$) δ_H 7.72 (d, *J* = 8.9 Hz, 2H, H-2 and H-6), 6.72 (d, *J* = 8.9 Hz, 2H, H-3 and H-5), 3.66 (d, *J* = 6.9 Hz, 2H, H_2-1′), 2.34 (s, CH_3), 1.06 (m, 1H, H-2′), 0.48 (m, 2H, H-3′a and H-4′a), 0.20 (m, 2H, H-3′b and H-4′b). ^{13}C NMR (100 MHz, $CDCl_3$) δ_C 196.2 (C=O), 162. 8 (C-4), 130.4 (C-2 and C-6), 129.9 (C-1), 114.0 (C-3 and C-5), 72.6 (C-1′), 26.0 (CH_3), 10.0 (C-2′), 3.1 (C-3′ and C-4′). ESIMS *m/z* 191.1628 $[M+H]^+$ (calcd $C_{12}H_{14}O_2$ 190.0994).

Preparation of Oxygenated Diketo Intermediate 1-3′(2′-Methoxypyridin-3′-yl)-(4′′-(Cyclopropyl Methyloxy)Phenyl)Propane-1,3-Dione [13a]: Procedure is similar to the preparation of the diketo intermediate **10a** except for the use of 1-(4-cyclopropyl methoxy)phenyl)ethan-1-one (300 mg, 1.58 mmol). The diketo intermediate **13a** was purified in a silica column using 9:1 Hex-EtOAc (73 mg, 14%). ^{1}H NMR (400 MHz, $CDCl_3$) δ_H 8.32 (dd, *J* = 2.0, 7.5 Hz, 1H, H-6′), 8.28 (dd, *J* = 2.0, 4.9 Hz, 1H, H-4′), 7.96 (d, *J* = 8.9 Hz, 2H, H-2′′ and H-6′′), 7.04 (dd, *J* = 4.9, 7.5 Hz, 1H, H-5′), 6.98 (d, *J* = 8.9 Hz, 2H, H-3′′ and H-5′′), 4.12 (s, OCH_3), 3.89 (d, *J* = 6.9 Hz, 2H, H-1′′′), 1.26 (m, 1H, H-2′′′), 0.68 (dd, *J* = 6.1, 13.0 Hz, 2H, H-3′′′a and H-4′′′a), 0.39 (dd, *J* = 4.8, 10.6 Hz, 2H, H-3′′′b and H-4′′′b). ^{13}C NMR (100 MHz, $CDCl_3$) δ_C 187.6 (C-3), 178.9 (C-1), 162.8 (C-2′), 161.5 (C-4′′), 149.5 (C-4′), 139.1 (C-6′), 129.5 (C-2′′ and C-6′′), 128.4 (C-1′′), 118.8 (C-1′), 117.1 (C-5′), 114.5 (C-3′′ and C-5′′), 97.3 (C-2),

73.0 (C-1‴), 53.9 (OCH_3), 10.1 (C-2‴), 3.3 (C-3‴ and C-4‴). ESIMS *m/z* 326.2691 $[M+H]^+$ (calcd $C_{19}H_{19}NO_4$ 325.1314).

Preparation of Final Oxygenated Pyridine Compound 2-(4′-Cyclopropyl Methoxyphenyl)-4*H*-Pyrano[2,3-*b*]Pyridin-4-one [13b]: 2-(4′-cyclopropyl methoxyphenyl)-4*H*-pyrano[2,3-*b*]pyridin-4-one was not yielded when procedure similar to **10b** was followed. **13b** was prepared when (Bromomethyl)cyclopropane (11 mg, 0.084 mmol) was added to 2-(4′-hydroxyphenyl)-4*H*-pyrano[2,3-*b*]pyridin-4-one (20 mg, 0.084 mmol) and were dissolved in 5 mL of acetone and potassium carbonate (46 mg, 0.336 mmol). The mixture was then refluxed for 24 h until the reaction went through and then diluted with EtOAc and washed with water. The final pyridine compound **13b** was purified in a silica column with 1:1 Hex-EtOAc (13 mg, 52%). ^{1}H NMR (500 MHz, $CDCl_3$) δ_H 8.72 (dd, *J* = 2.0, 4.6 Hz, 1H, H-7), 8.62 (dd, *J* = 2.0, 7.7 Hz, 1H, H-5), 7.98 (d, *J* = 8.9 Hz, 2H, H-2′ and H-6′), 7.48 (dd, *J* = 4.6, 7.7 Hz, 1H, H-6), 7.04 (d, *J* = 8.9 Hz, 2H, H-3′ and H-5′), 6.81 (s, 1H, H-3), 3.92 (d, *J* = 7.0 Hz, 2H, H-1″), 1.33 (m, 1H, H-2″), 0.70 (dd, *J* = 6.1, 13.0 Hz, 2H, H-3″a and H-4″a), 0.41 (dd, *J* = 4.9, 10.7 Hz, 2H, H-3″b and H-4″b). ^{13}C NMR (125 MHz, $CDCl_3$) δ_C 178.6 (C-4), 164.2 (C-9), 162.3 (C-2), 160.7 (C-4′), 153.0 (C-7), 136.3 (C-5), 128.4 (C-2′ and C-6′), 123.1 (C-1′), 122.1 (C-6), 118.8 (C-10), 115.1 (C-3′ and C-5′), 106.1 (C-3), 73.1 (C-1″), 10.1 (C-2″), 3.3 (C-3″ and C-4″). ESIMS *m/z* 294.0721 $[M+H]^+$ (calcd $C_{18}H_{15}NO_3$ 293.1052).

Preparation of Brominated Diketo Intermediate 1-3′(2′-Methoxypyridin-3′-yl)-(4″-Bromophenyl)Propane-1,3-Dione [14a]: A mixture of equimolar amounts of methyl-2-methoxy nicotinate (500 mg, 2.99 mmol) and 4′-bromo acetophenone (595 mg, 2.99 mmol) was used to prepare the brominated diketo intermediate **14a**. Methyl-2-methoxy nicotinate (500 mg, 2.99 mmol) and double the molar amounts of sodium hydride (144 mg, 5.98 mmol) were taken

in a RBF and dissolved in 2.5 mL of dry dimethyl formamide. A solution of 4′-bromo acetophenone (595 mg, 2.99 mmol) dissolved in 2 mL of dry dimethyl formamide was added dropwise and left at rt, for 2 h. NaH_2PO_4 was added to adjust the pH to 7.4 and the solution was then washed with CH_2Cl_2 in a separating funnel and dried in Na_2SO_4 and left overnight. The solution was then filtered into an RBF, dried, and concentrated. The diketo intermediate **14a** was purified in a silica column using 9:1 Hex-EtOAc (313 mg, 31%). ^{1}H NMR (500 MHz, $CDCl_3$) δ_H 8.35 (dd, *J* = 2.0, 7.5 Hz, 1H, H-6′), 8.33 (dd, *J* = 2.0, 4.9 Hz, 1H, H-4′), 7.87 (d, *J* = 8.5 Hz, 2H, H-2″ and H-6″), 7.66 (d, *J* = 8.5 Hz, 2H, H-3″ and H-5″), 7.08 (dd, *J* = 4.9, 7.5 Hz, 1H, H-5′), 4.14 (s, OCH_3). ^{13}C NMR (125 MHz, $CDCl_3$) δ_C 186.1 (C-3), 181.2 (C-1), 161.6 (C-2′), 150.2 (C-4″), 139.4 (C-4′), 134.8 (C-6′), 132.1 (C-2″ and C-6″), 128.9 (C-3″ and C-5″), 127.2 (C-1″), 118.2 (C-1′), 117.1 (C-5′), 97.4 (C-2), 54.1 (OCH_3). ESIMS *m/z* 334.1347 $[M+H]^+$ (calcd $C_{15}H_{12}BrNO_3$ 333.0001).

Preparation of Brominated Intermediate 2-(4′-Bromophenyl)-4*H*-Pyrano[2,3-*b*]Pyridin-4-one [14b]: The brominated diketo intermediate **[14a]** (250 mg, 0.748 mmol) was treated with 10 times the amount of pyridinium hydrochloride (2.5 g, 21.6 mmol) and heated at 190 °C for 4 h. The resultant solution was diluted with water, neutralized with $NaHCO_3$ and extracted with EtOAc. Na_2SO_4 was added and left overnight. The solution was then filtered into an RBF, dried, and concentrated to yield **14b** (196 mg, 87%). ^{1}H NMR (400 MHz, $CDCl_3$) δ_H 8.73 (dd, *J* = 2.0, 4.6 Hz, 1H, H-7), 8.61 (dd, *J* = 2.0, 7.7 Hz, 1H, H-5), 7.88 (d, *J* = 8.6 Hz, 2H, H-2′ and H-6′), 7.68 (d, *J* = 8.6 Hz, 2H, H-3′ and H-5′), 7.49 (dd, *J* = 4.6, 7.7 Hz, 1H, H-6), 6.85 (s, 1H, H-3). ^{13}C NMR (100 MHz, $CDCl_3$) δ_C 178.5 (C-4), 163.0 (C-2), 160.6 (C-9), 153.4 (C-7), 136.4 (C-5), 132.5 (C-2′ and C-6′), 130.0 (C-1′), 128.0 (C-3′ and C-5′), 126.9 (C-4′), 122.4 (C-6), 118.7 (C-10), 107.8 (C-3). ESIMS *m/z* 302.1248 $[M+H]^+$ (calcd $C_{14}H_8BrNO_2$ 300.9738).

Preparation of Final Nitrogenated Pyridine Compound 2-(4′-Propyloxyphenyl)-4*H*-Pyrano[2,3-*b*]Pyridin-4-one [14c]: Sodium tert-butoxide (25 mg, 0.255 mmol), tris(dibenzylideneacetone)dipalladium (16 mg, 0.017 mmol), and 1,1′-binaphthalene-2,2′-diylbis(diphenylphosphine) (11 mg, 0.017 mmol) were dissolved in 5 mL of toluene. To this, the brominated pyridine intermediate **14b** (50 mg, 0.17 mmol) and propylamine (15 mg, 0.255 mmol) were added dropwise with stirring at rt, and the mixture was refluxed at 80 °C for 48 h. The final pyridine compound **14c** was purified in a silica column using 20:1 Hex-EtOAc, 9:1 Hex-EtOAc, and 1:1 Hex-EtOAc (21 mg, 45%). ^{1}H NMR (500 MHz, $CDCl_3$) δ_H 8.69 (dd, *J* = 1.9, 4.5 Hz, 1H, H-7), 8.60 (dd, *J* = 1.8, 7.6 Hz, 1H, H-5), 7.86 (d, *J* = 8.6 Hz, 2H, H-2′ and H-6′), 7.44 (dd, *J* = 4.6, 7.6 Hz, 1H, H-6), 6.73 (s, 1H, H-3), 6.67 (d, *J* = 8.6 Hz, 2H, H-3′ and H-5′), 3.19 (t, *J* = 7.2 Hz, 2H, H_2-1″), 1.70 (dd, *J* = 7.4, 14.7 Hz, 2H, H_2-2″), 1.04 (t, *J* = 7.4 Hz, CH_3-3″). ^{13}C NMR (125 MHz, $CDCl_3$) δ_C 178.4 (C-4), 165.0 (C-9), 163.02 (C-2), 152.6 (C-4′), 151.7 (C-7), 136.1 (C-5), 128.5 (C-2′ and C-6′), 121.8 (C-1′), 118.9 (C-6), 118.3 (C-10), 112.3 (C-3′ and C-5′), 104.2 (C-3), 45.1 (C-1″), 22.5 (C-2″), 11.6 (CH_3-3″). ESIMS *m/z* 281.2853 $[M+H]^+$ (calcd $C_{17}H_{16}N_2O_2$ 280.1212).

Preparation of Final Nitrogenated Pyridine Compound 2-(4′-Isopropyloxyphenyl)-4*H*-Pyrano[2,3-*b*]Pyridin-4-one [15c]: Procedure is similar to the preparation of the final pyridine compound **14c** except for the use of isopropylamine (15 mg, 0.255 mmol). The final compound **15c** was purified in a silica column using 20:1 Hex-EtOAc, 9:1 Hex-EtOAc, and 1:1 Hex-EtOAc (25 mg, 54%). ^{1}H NMR (500 MHz, $CDCl_3$) δ_H 8.67 (dd, *J* = 1.6, 4.3 Hz, 1H, H-7), 8.58 (dd, *J* = 1.8, 7.6 Hz, 1H, H-5), 7.84 (d, *J* = 8.8 Hz, 2H, H-2′ and H-6′), 7.43 (dd, *J* = 4.6, 7.6 Hz, 1H, H-6), 6.71 (s, 1H, H-3), 6.64 (d, *J* = 8.8 Hz, 2H, H-3′ and H-5′), 3.73 (sept, *J* = 6.3 Hz, 1H, H-1″), 1.26 (d, *J* = 6.3 Hz, 6H, CH_3-2″ and CH_3-3″). ^{13}C NMR (125 MHz, $CDCl_3$) δ_C 178.4 (C-

4), 165.0 (C-9), 160.7 (C-2), 152.6 (C-4′), 150.8 (C-7), 136.1 (C-5), 128.5 (C-2′ and C-6′), 121.8 (C-1′), 118.9 (C-6), 118.0 (C-10), 112.6 (C-3′ and C-5′), 104.1 (C-3), 44.0 (C-1″), 22.8 (CH_3-2″ and CH_3-3″). ESIMS *m/z* 281.2853 $[M+H]^+$ (calcd $C_{17}H_{16}N_2O_2$ 280.1212).

5.5. Drawbacks/Pitfalls

The synthesis of the flavonoid and pyridine series of various subsituents involved various conditions and times. But the synthesis of certain compounds did not go through with the schemes used for other substituents. For example, the flavonoid with the O-methyl cyclopropyl was not yielded when the intermediate flavonoid **[5b]** was treated with boron tribromide for 1-3 h. The methyl cyclopropyl substituent was lost even when the reaction was tried for shorter time to prevent the loss of the methyl cyclopropyl substituent (10 min). Moreover, no methylation was seen on position-7 of the 'A' ring. Boron trichloride (BCl_3) was also tried instead of boron tribromide. **5c** was not accomplished during the synthesis of oxygenated flavonoid series.

There was problem in the synthesis of the flavonoid with the propargylamine substituent. The treatment of the brominated flavonoid **[6b]** with the treatment of sodium tert-butoxide, tris(dibenzylideneacetone)dipalladium, and 1,1′-binaphthalene-2,2′-diylbis(diphenylphosphine) with propargylamine in the presence of toluene did not yield either the intermediate flavonoid **[8c]** or the final flavonoid **[8d]**. The propargylamine substituent was lost even with reduced solvents and time.

The synthesis of the pyridine compound with the O-methyl propyl substituent **[12b]** was not furnished when the diketo intermediate with the O-methyl propyl substituent **[12a]** was treated with pyridinium hydrochloride. Similarly, the synthesis of the pyridine compound with the propargylamine substituent **[16c]** was not accomplished when the brominated intermediate **[14b]** was treated with sodium tert-butoxide, tris(dibenzylideneacetone)dipalladium, and 1,1′-

binaphthalene-2,2′-diylbis(diphenylphosphine) with propargylamine in the presence of toluene. Different reactant concentrations and varying times were used but to no avail.

Getting good yields was another challenge that is generally involved with any synthesis. Since, the main focus of my project is to initially furnish the designed analogs, methodologies to improve the yields were not developed.

5.6. Summary

The synthesis of the designed analogs was successfully performed. The synthesized analogs were subjected to MAO inhibition assays. The potent analogs were further assayed for enzyme kinetics and mechanism studies along with time-dependent enzyme inhibition assay and the analysis of inhibitor binding and reversibility with MAO-A and –B studies. The flavonoid compounds with O-propyl **[1c]**, O-isopropyl **[2c]**, O-isobutyl **[3c]**, and O-propargyl **[4c]** substituents showed about 1500, 2000, 3500, and 1300-fold difference respectively, in their selectivity towards MAO-B *vs* MAO-A.

CHAPTER 6. FUTURE PLANS

We designed flavonoid and pyridine series with different substituents to study the interaction of these analogs on MAO-A and –B. We also studied the effect of the flavonoid and pyridine skeleton on these isoenzymes. The MAO-inhibition studies of these analogs showed that the flavonoid series exhibited more selectivity towards MAO-B *vs* MAO-A. Hence, we plan to conduct *in vivo* studies on these analogs to understand their potential as therapeutic compounds.

We plan to dock the hit compounds which were identified as potent MAO-B compounds in the active site of the MAO-B to understand their binding interactions. The interactions of these analogs on these active sites would help understand the binding modes, to design novel scaffolds as PD hits, and to achieve higher MAO-B selectivity because selective MAO-B compounds are known to possess less adverse-effects.

Since we studied the interactions of the flavonoid and pyridine series on MAO isoenzymes, one of the future plans is to study the effect of other substituents on the 'C' ring. Then, we will compare these results with the potent flavonoid compounds on the MAO enzymes. This strategy would be helpful to identify the substituents that play a significant role in MAO-B selectivity. We would also consider the cytotoxicity studies and the promiscuity of the synthesized analogs on the MAO-B enzyme. PK studies will be done on the potent and selective compounds along with the drug-metabolism studies, to understand how the compounds are excreted and what the active and inactive metabolites are. Understanding the routes of metabolism would significantly affect the drug's efficacy and safety, and also the directions for use. If the elimination occurs primarily through metabolism, then the principal routes of metabolism should be understood. If the elimination occurs through a single metabolic pathway, then the individual differences in the metabolic-rates would lead to large differences in the

concentration of the drug and the metabolites in the blood and tissue. The major goals of the drug-metabolism studies are to characterize and identify the major metabolites of the synthesized compounds and the specific enzymes involved in its metabolism; to evaluate the impacts of these metabolites on the drug's safety and efficacy; and to utilize this information to maximize its intellectual property.

BIBLIOGRAPHY

1. Ji, H. F.; Li, X. J.; Zhang, H. Y. Natural Products and Drug Discovery. *EMBO Rep.* **2009**, 10, 194–200.
2. Cragg, G. M.; Newman, D. J. Natural Products: A Continuing Source of Novel Drug Leads. *Biochim. Biophys. Acta, Gen. Subj.* **2013**, 1830, 3670–3695.
3. Cragg, G. M.; Newman, D. J.; Snader, K. M. Natural Products in Drug Discovery and Development. *J. Nat. Prod.* **1997**, 60, 52–60.
4. Koehn, F. E.; Carter, G. T. The Evolving Role of Natural Products in Drug Discovery. *Nat. Rev. Drug Discovery* **2005**, 4, 206–220.
5. Harvey, A. L. Natural Products in Drug Discovery. *Drug Discovery Today* **2008**, 13, 894–901.
6. Croteau, R.; Kutchan, T. M.; Lewis, N. G. Natural Products (Secondary Metabolites). *Biochem. Mol. Biol. Plants* **2000**, 24, 1250–1319.
7. Petit, J.; Meurice, N.; Kaiser, C.; Maggiora, G., Softening the Rule of Five—Where to Draw the Line? Bioorg. Med. Chem. **2012**, 20, 5343–5351.
8. Cheuka, P. M.; Mayoka, G.; Mutai, P.; Chibale, K. The Role of Natural Products in Drug Discovery and Development against Neglected Tropical Diseases. *Molecules* **2016**, 22, 58.
9. Newman, D. J.; Cragg, G. M. Natural Products as Sources of New Drugs from 1981 to 2014. *J. Nat. Prod* **2016**, 79, 629–661.
10. Khazir, J.; Mir, B. A.; Pilcher, L.; Riley, D. L. Role of Plants in Anticancer Drug Discovery. *Phytochem. Lett.* **2014**, 7, 173–181.
11. Jachak, S. M.; Saklani, A. Challenges and Opportunities in Drug Discovery from Plants. *Curr. Sci.* **2007**, 92, 1251–1257.
12. Nelson, K. M.; Dahlin, J. L.; Bisson, J.; Graham, J.; Pauli, G. F.; Walters, M. A. The Essential Medicinal Chemistry of Curcumin: Miniperspective. *J. Med. Chem.* **2017**, 60, 1620–1637.
13. Sitte, H. H.; Freissmuth, M. Amphetamines, New Psychoactive Drugs and the Monoamine Transporter Cycle. *Trends Pharmacol. Sci.* **2015**, 36, 41–50.
14. Liechti, M. E. Novel Psychoactive Substances (Designer Drugs): Overview and Pharmacology of Modulators of Monoamine Signalling. *Swiss Med. Wkly.* **2015**, 145, w14043.
15. Dhawan, B. N.; Cesselin, F.; Raghubir, R.; Reisine, T.; Bradley, P. B.; Portoghese, P. S.; Hamon, M. International Union of Pharmacology. XII. Classification of Opioid Receptors. *Pharmacol. Rev.* **1996**, 48, 567–592.
16. Cox, B. M.; Christie, M. J.; Devi, L.; Toll, L.; Traynor, J. R. Challenges for Opioid Receptor Nomenclature: IUPHAR Review 9. *Br. J. Pharmacol.* **2015**, 172, 317–323.
17. Fenalti, G.; Giguere, P. M.; Katritch, V.; Huang, X.-P.; Thompson, A. A.; Cherezov, V.; Roth, B. L.; Stevens, R. C. Molecular Control of δ-Opioid Receptor Signaling. *Nature* **2014**, 506, 191–196.
18. Sobczak, M.; Sałaga, M.; Storr, M. A.; Fichna, J. Physiology, Signaling, and Pharmacology of Opioid Receptors and Their Ligands in the Gastrointestinal Tract: Current Concepts and Future Perspectives. *J. Gastroenterol.* **2014**, 49, 24–45.
19. Ong, E. W.; Cahill, C. M. Molecular Perspectives for Mu/Delta Opioid Receptor Heteromers as Distinct, Functional Receptors. *Cells* **2014**, 3, 152–179.

20. Fichna, J.; Sobczak, M.; Mokrowiecka, A.; Cygankiewicz, A. I.; Zakrzewski, P. K.; Cenac, N.; Sałaga, M.; Timmermans, J. -P.; Vergnolle, N.; Małecka-Panas, E.; Krajewska, W. M.; Storr. M. Activation of the Endogenous Nociceptin System by Selective Nociceptin Receptor Agonist SCH 221510 Produces Antitransit and Antinociceptive Effect: A Novel Strategy for Treatment of Diarrhea-Predominant IBS. *Neurogastroenterol. Motil.* **2014**, 26, 1539–1550.
21. Lohman, R.-J.; Harrison, R. S.; Ruiz-Gómez, G.; Hoang, H. N.; Shepherd, N. E.; Chow, S.; Hill, T. A.; Madala, P. K.; Fairlie, D. P. Chapter One-Helix-Constrained Nociceptin Peptides Are Potent Agonists and Antagonists of ORL-1 and Nociception. *Vitam. Horm.* **2015,** *97*, 1–55.
22. Breivogel, C. S.; Vaghela, M. S. The Effects of Beta-Arrestin1 Deletion on Acute Cannabinoid Activity, Brain Cannabinoid Receptors and Tolerance to Cannabinoids in Mice. *J. Recept. Signal Transduction* **2015**, 35, 98–106.
23. Rom, S.; Persidsky, Y. Cannabinoid Receptor 2: Potential Role in Immunomodulation and Neuroinflammation. *J. Neuroimmune Pharmacol.* **2013**, 8, 608–620.
24. Sugiura, T.; Waku, K. Cannabinoid Receptors and Their Endogenous Ligands. *J. Biochem.* **2002**, 132, 7–12.
25. Porter, A. C.; Sauer, J.-M.; Knierman, M. D.; Becker, G. W.; Berna, M. J.; Bao, J.; Nomikos, G. G.; Carter, P.; Bymaster, F. P.; Leese, A. B.; Felder, C. C. Characterization of a Novel Endocannabinoid, Virodhamine, with Antagonist Activity at the CB1 Receptor. *J. Pharmacol. Exp. Ther.* **2002**, 301, 1020–1024.
26. Chen, J.; Paudel, K. S.; Derbenev, A. V.; Smith, B. N.; Stinchcomb, A. L. Simultaneous Quantification of Anandamide and Other Endocannabinoids in Dorsal Vagal Complex of Rat Brainstem by LC–MS. *Chromatographia* **2009**, 69, 1–7.
27. Zhang, M.; Martin, B. R.; Adler, M. W.; Razdan, R. K.; Jallo, J. I.; Tuma, R. F. Cannabinoid CB2 Receptor Activation Decreases Cerebral Infarction in a Mouse Focal Ischemia/Reperfusion Model. *J. Cereb. Blood Flow Metab.* **2007**, 27, 1387–1396.
28. Sun, Y.; Bennett, A. Cannabinoids: A New Group of Agonists of PPARs. *PPAR Res.* **2007,** 2007. *DOI: 10.1155/2007/23513*
29. Hanuš, L.; Gopher, A.; Almog, S.; Mechoulam, R. Two New Unsaturated Fatty Acid Ethanolamides in Brain That Bind to the Cannabinoid Receptor. *J. Med. Chem.* **1993**, 36, 3032–3034.
30. Stein, C. Opioid Receptors. *Annu. Rev. Med.* **2016**, 67, 433–451.
31. Parsadaniantz, S. M.; Rivat, C.; Rostène, W.; Réaux-Le Goazigo, A. Opioid and Chemokine Receptor Crosstalk: A Promising Target for Pain Therapy? *Nat. Rev. Neurosci.* **2015**, 16, 69–78.
32. Sharma, C.; Sadek, B.; Goyal, S. N.; Sinha, S.; Kamal, M. A.; Ojha, S. Small Molecules from Nature Targeting G-Protein Coupled Cannabinoid Receptors: Potential Leads for Drug Discovery and Development. *Evidence-Based Complementary Altern. Med.* **2015**, 2015.
33. Whiteford, H. A.; Ferrari, A. J.; Degenhardt, L.; Feigin, V.; Vos, T. The Global Burden of Mental, Neurological and Substance Use Disorders: An Analysis from the Global Burden of Disease Study 2010. *PloS One* **2015**, 10, e0116820.
34. Ambrosio, L.; Portillo, M. C.; Rodríguez-Blázquez, C.; Rodriguez-Violante, M.; Castrillo, J. C. M.; Arillo, V. C.; Garretto, N. S.; Arakaki, T.; Dueñas, M. S.; Álvarez, M.; Ibáñez, I. P.; Carvajal, A.; Martinez-Martin, P. Living with Chronic Illness Scale: International Validation of a New Self-Report Measure in Parkinson's Disease. *Parkinson's Dis.* **2016**, 2, 16022.

35. Ascherio, A.; Schwarzschild, M. A. The Epidemiology of Parkinson's Disease: Risk Factors and Prevention. *Lancet Neurol.* **2016**, 15, 1257–1272.
36. Barker, R. A.; Drouin-Ouellet, J.; Parmar, M. Cell-Based Therapies for Parkinson Disease - Past Insights and Future Potential. *Nat. Rev. Neurol.* **2015**, 11, 492–503.
37. Lotharius, J.; Brundin, P. Pathogenesis of Parkinson's Disease: Dopamine, Vesicles and α-Synuclein. *Nat. Rev. Neurosci.* **2002**, 3, 932–942.
38. Klingelhoefer, L.; Reichmann, H. Pathogenesis of Parkinson Disease-The Gut-Brain Axis and Environmental Factors. *Nat. Rev. Neurol.* **2015**, 11, 625–636.
39. Jankovic, J. Parkinson's Disease: Clinical Features and Diagnosis. *J. Neurol., Neurosurg. Psychiatry* **2008**, 79, 368–376.
40. Jones, T.; Murray, R. Current Research In and Development of Treatments for Parkinson's Disease. *Management* **2017**, 12, 17.
41. Dong, J.; Cui, Y.; Li, S.; Le, W. Current Pharmaceutical Treatments and Alternative Therapies of Parkinson's Disease. *Curr. Neuropharmacol.* **2016**, 14, 339–355.
42. Oertel, W.; Schulz, J. B. Current and Experimental Treatments of Parkinson Disease: A Guide for Neuroscientists. *J. Neurochem.* **2016**, 139, 325–337.
43. Pinna, A. Adenosine A2A Receptor Antagonists in Parkinson's Disease: Progress in Clinical Trials from the Newly Approved Istradefylline to Drugs in Early Development and Those Already Discontinued. *CNS Drugs* **2014**, 28, 455–474.
44. Chajkowski-Scarry, S.; Rimoldi, J. M. Monoamine Oxidase A and B Substrates: Probing the Pathway for Drug Development. *Future Med. Chem.* **2014**, 6, 697–717.
45. Youdim, M. B. H.; Bakhle, Y. S. Monoamine Oxidase: Isoforms and Inhibitors in Parkinson's Disease and Depressive Illness. *Br. J. Pharmacol.* **2006**, 147, S287–S296.
46. Finberg, J. P. M. Update on the Pharmacology of Selective Inhibitors of MAO-A and MAO-B: Focus on Modulation of CNS Monoamine Neurotransmitter Release. *Pharmacol. Ther.* **2014**, 143, 133–152.
47. Callaway, J. C. Various Alkaloid Profiles in Decoctions of *Banisteriopsis caapi*. *J. Psychoact. Drugs* **2005**, 37, 151–155.
48. Gibbons, S.; Arunotayanun, W. Natural Product (Fungal and Herbal) Novel Psychoactive Substances. **2013**, 345–362.
49. Hashimoto, Y.; Kawanishi, K. New Alkaloids from *Banisteriopsis caapi*. *Phytochemistry* **1976**, 15, 1559–1560.
50. Schwarz, M. J.; Houghton, P. J.; Rose, S.; Jenner, P.; Lees, A. D. Activities of Extract and Constituents of *Banisteriopsis caapi* Relevant to Parkinsonism. *Pharmacol., Biochem. Behav.* **2003**, 75, 627–633.
51. Simpson, A. J.; Simpson, M. J.; Soong, R. Nuclear Magnetic Resonance Spectroscopy and Its Key Role in Environmental Research. *Environ. Sci. Technol.* **2012**, 46, 11488–11496.
52. Vázquez, L. H.; Palazon, J.; Navarro-Ocaña, A., The Pentacyclic Triterpenes α, β-amyrins: A Review of Sources and Biological Activities. In *Phytochemicals–A Global Perspective of Their Role in Nutrition and Health*, Rao, V., Ed.; InTech: Croatia, 2012, pp 487–502. ISBN: 978-953-51-0296-0.
53. Wehril, F. W.; Marchand, A. P.; Wehrli, S. Interpretation of Carbon-13 NMR Spectra. In *Inorganic, Organic, Physical and Analytical Chemistry*; Wiley: New York, **1988**, 20, 495.
54. de Siqueira, D. S.; dos Santos Pereira, A.; de Aquino Neto, F. R.; Cabral, J. A.; Ferreira, C. A. C.; Simoneit, B. R. T.; Elias, V. O. Determination of High Molecular Mass Compounds in Leaves of Amazonian Plants. *Quím. Nova* **2003**, 26, 633-640.

55. Rahman, A. -ur.; Choudhary, M. I.; Thomsen, W. J. Radioligand Binding Assays. In *Bioassay Techniques for Drug Development*; Harwood Academic Publishers: San Diego, **2005**, 167–188.
56. Gao, T.; Yao, H.; Song, J.; Zhu, Y.; Liu, C.; Chen, S. Evaluating the Feasibility of Using Candidate DNA Barcodes in Discriminating Species of the Large Asteraceae Family. *BMC Evol. Biol.* **2010**, 10, 324.
57. Bessada, S. M. F.; Barreira, J. C. M.; Oliveira, M. B. P. P. Asteraceae Species with Most Prominent Bioactivity and Their Potential Applications: A Review. *Ind. Crops Prod.* **2015**, 76, 604–615.
58. Camilotti, J. G.; Biu, C. C.; Farago, P. V.; dos Santos, V. L. P.; Franco, C. R. C.; Budel, J. M. Anatomical Characters of Leave and Stem of *Calea serrata* Less., Asteraceae. *Braz. Arch. Biol. Technol.* **2014**, 57, 867–873.
59. Torres-Rodríguez, M. L.; García-Chávez, E.; Berhow, M.; de Mejia, E. G. Anti-Inflammatory and Anti-Oxidant Effect of *Calea urticifolia* Lyophilized Aqueous Extract on Lipopolysaccharide-Stimulated RAW 264.7 Macrophages. *J. Ethnopharmacol.* **2016**, 188, 266–274.
60. Bohlmann, F.; Jakupovic, J. Neue Germacranolide aus *Calea urticifolia*. *Phytochemistry* **1979**, 18, 119–123.
61. Yamada, M.; Matsuura, N.; Suzuki, H.; Kurosaka, C.; Hasegawa, N.; Ubukata, M.; Tanaka, T.; Iinuma, M. Germacranolides from *Calea urticifolia*. *Phytochemistry* **2004**, 65, 3107–3111.
62. Herz, W.; Kumar, N. Sesquiterpene Lactones of *Calea zacatechichi* and *C. urticifolia*. *Phytochemistry* **1980**, 19, 593–597.
63. del Castillo, J. B.; Ferrero, M. T. M.; Luis, F. R.; Bueno, P. V.; Leonor, N. G.; Arévalo, S. C. Salvadorian Compositae. II. Juanislamin and 2,3-Epoxy-Juanislamin, Two New Sesquiterpenic Lactones from *Calea urticifolia*. *J. Nat. Prod.* **1981**, 44, 348–350.
64. Ren, Y.; Yu, J.; Douglas Kinghorn, A. Development of Anticancer Agents from Plant-Derived Sesquiterpene Lactones. *Curr. Med. Chem.* **2016**, 23, 2397–2420.
65. Fischer, N. H.; Lu, T.; Cantrell, C. L.; Castañeda-Acosta, J.; Quijano, L.; Franzblau, S. G. Antimycobacterial Evaluation of Germacranolides in Honour of Professor G.H. Neil Towers 75th birthday. *Phytochemistry* **1998**, 49, 559–564.
66. Merfort, I. Perspectives on Sesquiterpene Lactones in Inflammation and Cancer. *Curr. Drug Targets* **2011**, 12, 1560–1573.
67. Unger, C.; Kiss, I.; Vasas, A.; Lajter, I.; Kramer, N.; Atanasov, A. G.; Nguyen, C. H.; Chatuphonprasert, W.; Brenner, S.; Krieger, S.; McKinnon, R.; Peschel, A.; Kain, R.; Saiko, P.; Szekeres, T.; Kenner, L.; Hassler, M. R.; Diaz, R.; Frisch, R.; Dirsch, V. M.; Jäger, W.; de Martin, R.; Bochkov, V. N.; Passreiter, C. M.; Peter-Vörösmarty, B.; Mader, R. M.; Grusch, M.; Dolznig, H.; Kopp, B.; Zupko, I.; Hohmann, J.; Krupitza, G. The Germacranolide Sesquiterpene Lactone Neurolenin B of the Medicinal Plant *Neurolaena lobata* (L.) R.Br. ex Cass Inhibits NPM/ALK-Driven Cell Expansion and NF-κB-Driven Tumour Intravasation. *Phytomedicine* **2015**, 22, 862–874.
68. Gach, K.; Janecka, A. α-Methylene-γ-Lactones as a Novel Class of Anti-Leukemic Agents. *Anti-Cancer Agents Med. Chem.* **2014**, 14, 688–694.

69. Molnár, J.; Szebeni, G. J.; Csupor-Löffler, B.; Hajdú, Z.; Szekeres, T.; Saiko, P.; Ocsovszki, I.; Puskás, L. G.; Hohmann, J.; Zupkó, I. Investigation of the Antiproliferative Properties of Natural Sesquiterpenes from *Artemisia asiatica* and *Onopordum acanthium* on HL-60 Cells *in Vitro*. *Int. J. Mol. Sci.* **2016**, 17, 83.
70. Miyazawa, M.; Hisama, M. Antimutagenic Activity of Flavonoids from *Chrysanthemum morifolium*. *Biosci., Biotechnol., Biochem.* **2003**, 67, 2091–2099.
71. Chaurasiya, N. D.; Ibrahim, M. A.; Muhammad, I.; Walker, L. A.; Tekwani, B. L. Monoamine Oxidase Inhibitory Constituents of Propolis: Kinetics and Mechanism of Inhibition of Recombinant Human MAO-A and MAO-B. *Molecules* **2014**, 19, 18936–18952.
72. Olsen, H. T.; Stafford, G. I.; van Staden, J.; Christensen, S. B.; Jäger, A. K. Isolation of the MAO-Inhibitor Naringenin from *Mentha aquatica* L. *J. Ethnopharmacol.* **2008**, 117, 500–502.
73. Chiuccariello, L.; Cooke, R. G.; Miler, L.; Levitan, R. D.; Baker, G. B.; Kish, S. J.; Kolla, N. J.; Rusjan, P. M.; Houle, S.; Wilson, A. A.; Meyer, J. H. Monoamine Oxidase-A Occupancy by Moclobemide and Phenelzine: Implications for the Development of Monoamine Oxidase Inhibitors. *Int. J. Neuropsychopharmacol.* **2016**, 19, pyv078.
74. Saito, Y.; Takiguchi, K.; Gong, X.; Kuroda, C.; Tori, M. Three New Bisabolane-Type Sesquiterpenoids from *Cremanthodium rhodocephalum* (Asteraceae). *Heterocycles* **2012**, 86, 497–503.
75. Pavarini, D. P.; Nogueira, E. F.; Callejon, D. R.; Soares, D. M.; de Souza, G. E. P.; de Queiroz Cunha, F.; Lopes, J. L. C.; Lopes, N. P. Novel Bisabolane Derivative from "arnica-da-serra" (*Vernonieae*: Asteraceae) Reduces Pro-Nociceptive Cytokines Levels in LPS-Stimulated Rat Macrophages. *J. Ethnopharmacol.* **2013**, 148, 993–998.
76. Frisch, M. J.; Trucks, G. W.; Schlegel, H. B.; Scuseria, G. E.; Robb, M. A.; Cheeseman, J. R.; Scalmani, G.; Barone, V.; Mennucci, B.; Petersson, G. A.; Nakatsuji, H.; Caricato, M.; Li, X.; Hratchian, H. P.; Izmaylov, A. F.; Bloino, J.; Zheng, G.; Sonnenberg, J. L.; Hada, M.; Ehara, M.; Toyota, K.; Fukuda, R.; Hasegawa, J.; Ishida, M.; Nakajima, T.; Honda, Y.; Kitao, O.; Nakai, H.; Vreven, T.; Montgomery, J. A.; Peralta, J. E.; Ogliaro, F.; Bearpark, M.; Heyd, J. J.; Brothers, E.; Kudin, K. N.; Staroverov, V. N.; Kobayashi, R.; Normand, J.; Raghavachari, K.; Rendell, A.; Burant, J. C.; Iyengar, S. S.; Tomasi, J.; Cossi, M.; Rega, N.; Millam, J. M.; Klene, M.; Knox, J. E.; Cross, J. B.; Bakken, V.; Adamo, C.; Jaramillo, J.; Gomperts, R.; Stratmann, R. E.; Yazyev, O.; Austin, A. J.; Cammi, R.; Pomelli, C.; Ochterski, J. W.; Martin, R. L.; Morokuma, K.; Zakrzewski, V. G.; Voth, G. A.; Salvador, P.; Dannenberg, J. J.; Dapprich, S.; Daniels, A. D.; Farkas, O.; Foresman, J. B.; Ortiz, J. V.; Cioslowski, J.; Fox, D. J. Gaussian 09, Revision A02; Gaussian, Inc: Wallingford, CT, 2009.
77. Smith, S. G.; Goodman, J. M. Assigning Stereochemistry to Single Diastereoisomers by GIAO NMR Calculation: The DP4 Probability. *J. Am. Chem. Soc.* **2010**, 132, 12946-12959.
78. Willoughby, P. H.; Jansma, M. J.; Hoye, T. R. A Guide to Small-Molecule Structure Assignment Through Computation of (^{1}H and ^{13}C) NMR Chemical Shifts. *Nat. Protoc.* **2014**, 9, 643–660.
79. Nakagawa, Y.; Iinuma, M.; Matsuura, N.; Yi, K.; Naoi, M.; Nakayama, T.; Nozawa, Y.; Akao, Y. A Potent Apoptosis-Inducing Activity of a Sesquiterpene Lactone, Arucanolide, in HL60 cells: A Crucial Role of Apoptosis-Inducing Factor. *J. Pharmacol. Sci.* **2005**, 97, 242–252.
80. Matsuura, N.; Yamada, M.; Suzuki, H.; Hasegawa, N.; Kurosaka, C.; Ubukata, M.; Tanaka, T.; Iinuma, M. Inhibition of Preadipocyte Differentiation by Germacranolides from *Calea urticifolia* in 3T3-L1 Cells. *Biosci., Biotechnol., Biochem.* **2005**, 69, 2470–2474.

81. Ohguchi, K.; Ito, M.; Yokoyama, K.; Iinuma, M.; Itoh, T.; Nozawa, Y.; Akao, Y. Effects of Sesquiterpene Lactones on Melanogenesis in Mouse B16 Melanoma Cells. *Biol. Pharm. Bull.* **2009**, 32, 308–310.
82. Samoylenko, V.; Rahman, M. M.; Tekwani, B. L.; Tripathi, L. M.; Wang, Y.-H.; Khan, S. I.; Khan, I. A.; Miller, L. S.; Joshi, V. C.; Muhammad, I. *Banisteriopsis caapi*, A Unique Combination of MAO Inhibitory and Antioxidative Constituents for the Activities Relevant to Neurodegenerative Disorders and Parkinson's Disease. *J. Ethnopharmacol.* **2010**, 127, 357–367.
83. Parikh, S.; Hanscom, S.; Gagne, P.; Crespi, C.; Patten, C. A Fluorescent-Based, High-Throughput Assay for Detecting Inhibitors of Human Monoamine Oxidase A and B. **2002**.
84. *Schrödinger Release 2015-1: MacroModel, Schrödinger, LLC: New York, NY, 2015.*
85. Eguchi, M. Recent Advances in Selective Opioid Receptor Agonists and Antagonists. *Med. Res. Rev.* **2004**, 24, 182–212.
86. Pogozheva, I. D.; Przydzial, M. J.; Mosberg, H. I. Homology Modeling of Opioid Receptor-Ligand Complexes Using Experimental Constraints. *AAPS J.* **2005**, 7, E434–E448.
87. Berman, H. M.; Westbrook, J.; Feng, Z.; Gilliland, G.; Bhat, T. N.; Weissig, H.; Shindyalov, I. N.; Bourne, P. E. The Protein Data Bank. *Nucleic Acids Res.* **2000**, 28, 235–242.
88. Son, S.-Y.; Ma, J.; Kondou, Y.; Yoshimura, M.; Yamashita, E.; Tsukihara, T. Structure of Human Monoamine Oxidase A at 2.2-Å Resolution: The Control of Opening the Entry for Substrates/Inhibitors. *Proc. Natl. Acad. Sci. U. S. A.* **2008**, 105, 5739–5744.
89. Binda, C.; Aldeco, M.; Geldenhuys, W. J.; Tortorici, M.; Mattevi, A.; Edmondson, D. E. Molecular Insights into Human Monoamine Oxidase B Inhibition by the Glitazone Antidiabetes Drugs. *ACS Med. Chem. Lett.* **2012**, 3, 39–42.
90. Sastry, G. M.; Adzhigirey, M.; Day, T.; Annabhimoju, R.; Sherman, W. Protein and Ligand Preparation: Parameters, Protocols, and Influence on Virtual Screening Enrichments. *J. Comput. -Aided Mol. Des.* **2013**, 27, 221–234.
91. *Schrödinger Suite S. S. Protein Preparation Wizard*, Epik version 3.0, Schrödinger, LLC, New York, NY, Impact version 6.5, Schrödinger, LLC, New York, NY, 2014; Prime version 3.8, Schrödinger, LLC, New York, NY, 2014.
92. *Prime, version 3.8; Schrödinger, LLC: New York, NY, 2014.*
93. *LigPrep, version 3.2; Schrödinger, LLC: New York, NY, 2014.*
94. Shivakumar, D.; Williams, J.; Wu, Y.; Damm, W.; Shelley, J.; Sherman, W. Prediction of Absolute Solvation Free Energies Using Molecular Dynamics Free Energy Perturbation and the OPLS Force Field. *J. Chem. Theory Comput.* **2010**, 6, 1509–1519.
95. *Epik, version 3.0; Schrödinger, LLC: New York, NY, 2014*.
96. *Glide, version 6.5; Schrödinger, LLC: New York, NY, 2014*.
97. *SZMAP, version 1.2.0.7*: *OpenEye Scientific Software, Inc.: Santa Fe, NM, USA*. https://www.eyesopen.com. *(2012).*
98. Shulman, K. I.; Herrmann, N.; Walker, S. E. Current Place of Monoamine Oxidase Inhibitors in the Treatment of Depression. *CNS Drugs* **2013**, 27, 789–797.
99. Jakalian, A.; Jack, D. B.; Bayly, C. I. Fast, Efficient Generation of High-Quality Atomic Charges. AM1-BCC Model: II. Parameterization and Validation. *J. Comput. Chem.* **2002**, 23, 1623–1641.

LIST OF APPENDICES

APPENDIX A

NMR SPECTRAL DATA

^{1}H-NMR Spectrum of Acacetin

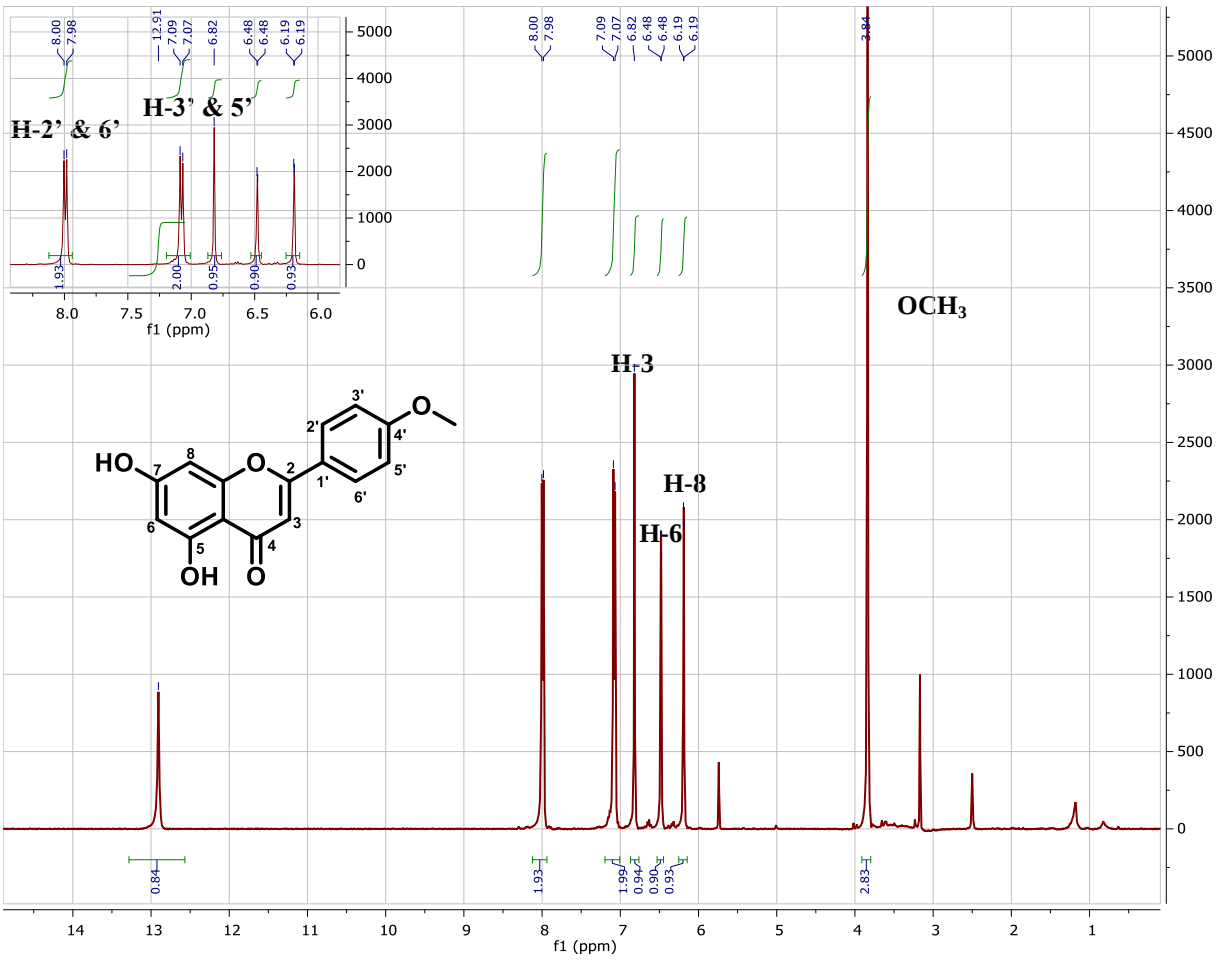

^{13}C-NMR Spectrum of Acacetin

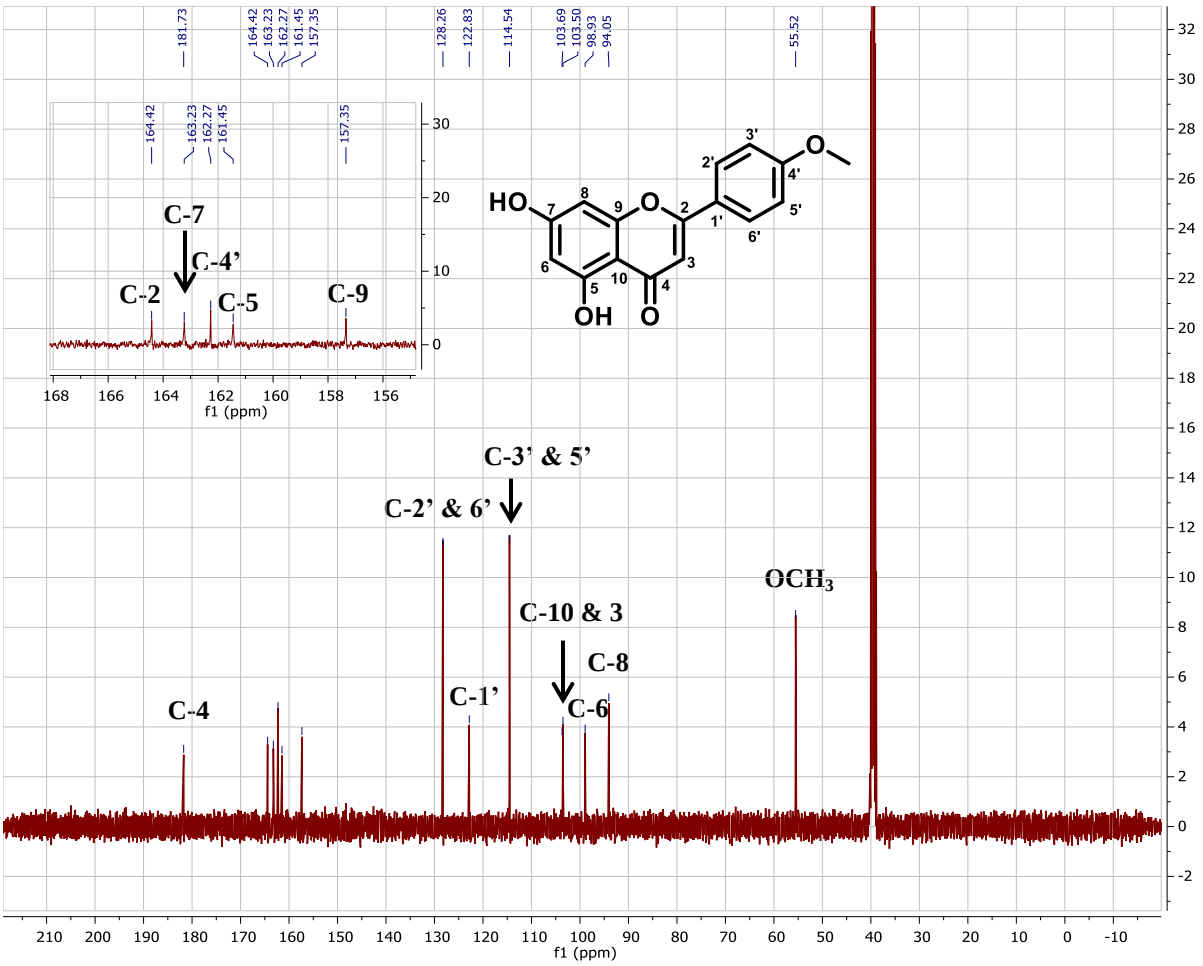

^{13}C NMR and DEPT135 Spectra of Acacetin

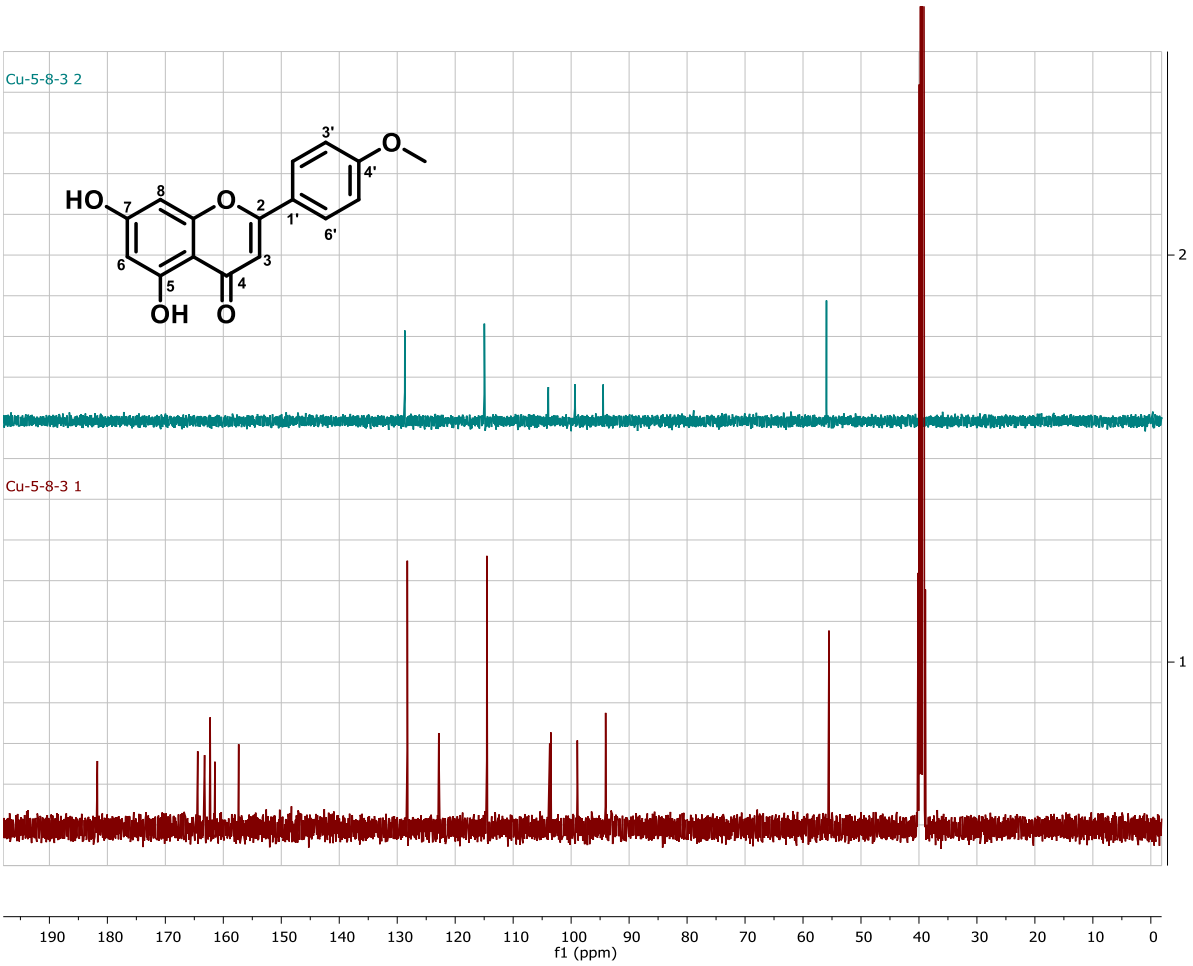

HMBC Spectrum of Acacetin

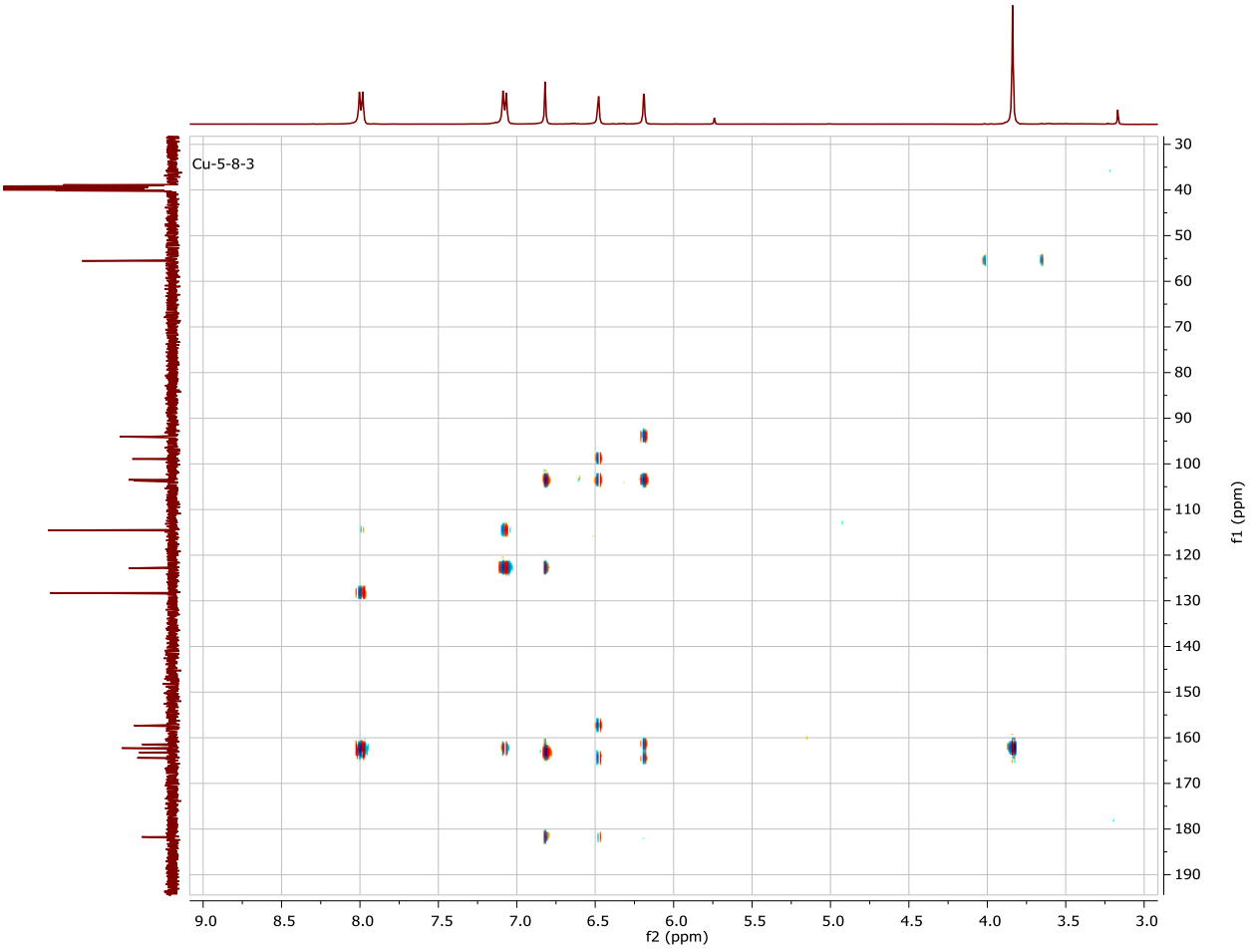

NOESY Spectrum of Acacetin

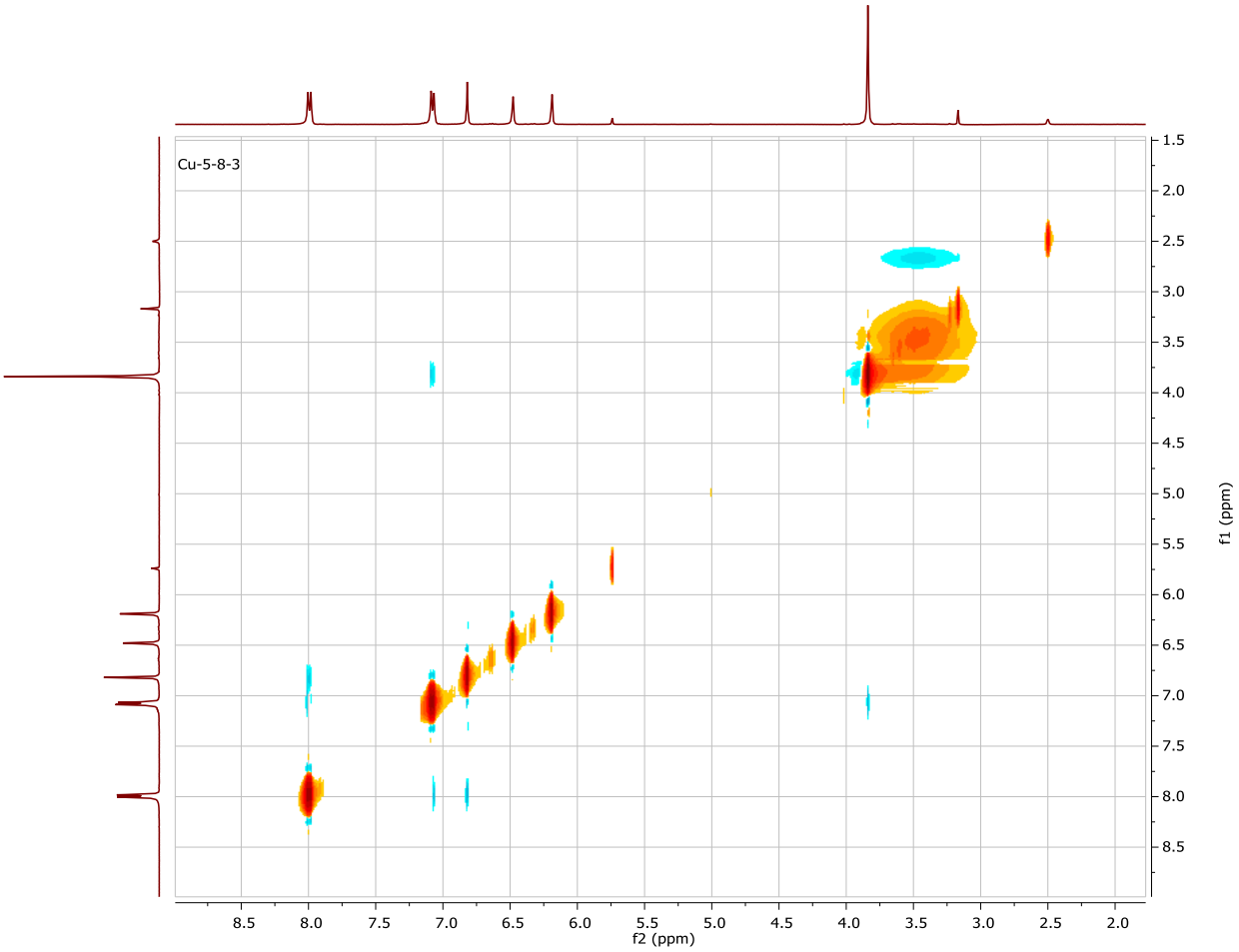

^{1}H-NMR Spectrum of Caleanolene A

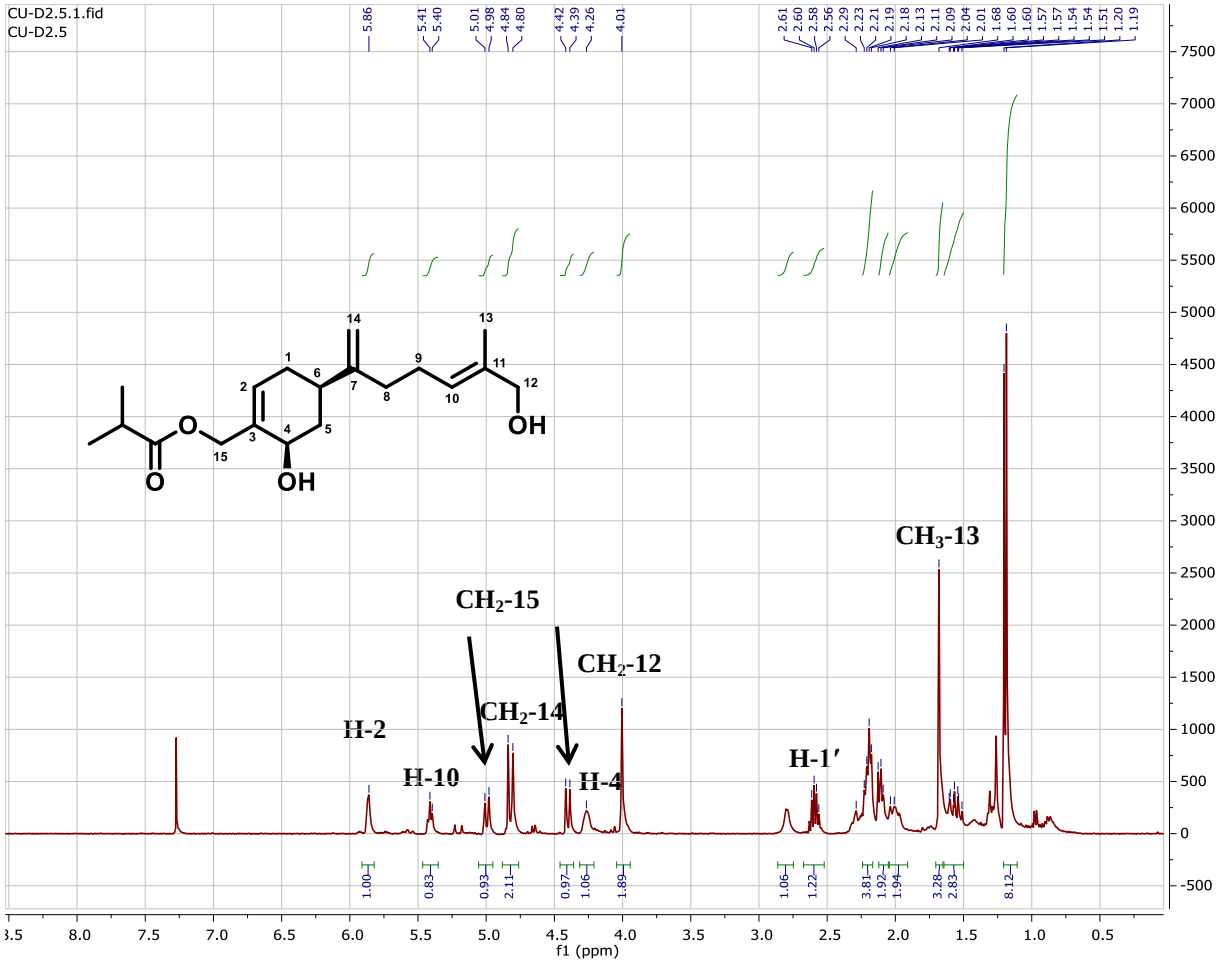

^{13}C Spectrum of Caleanolene A

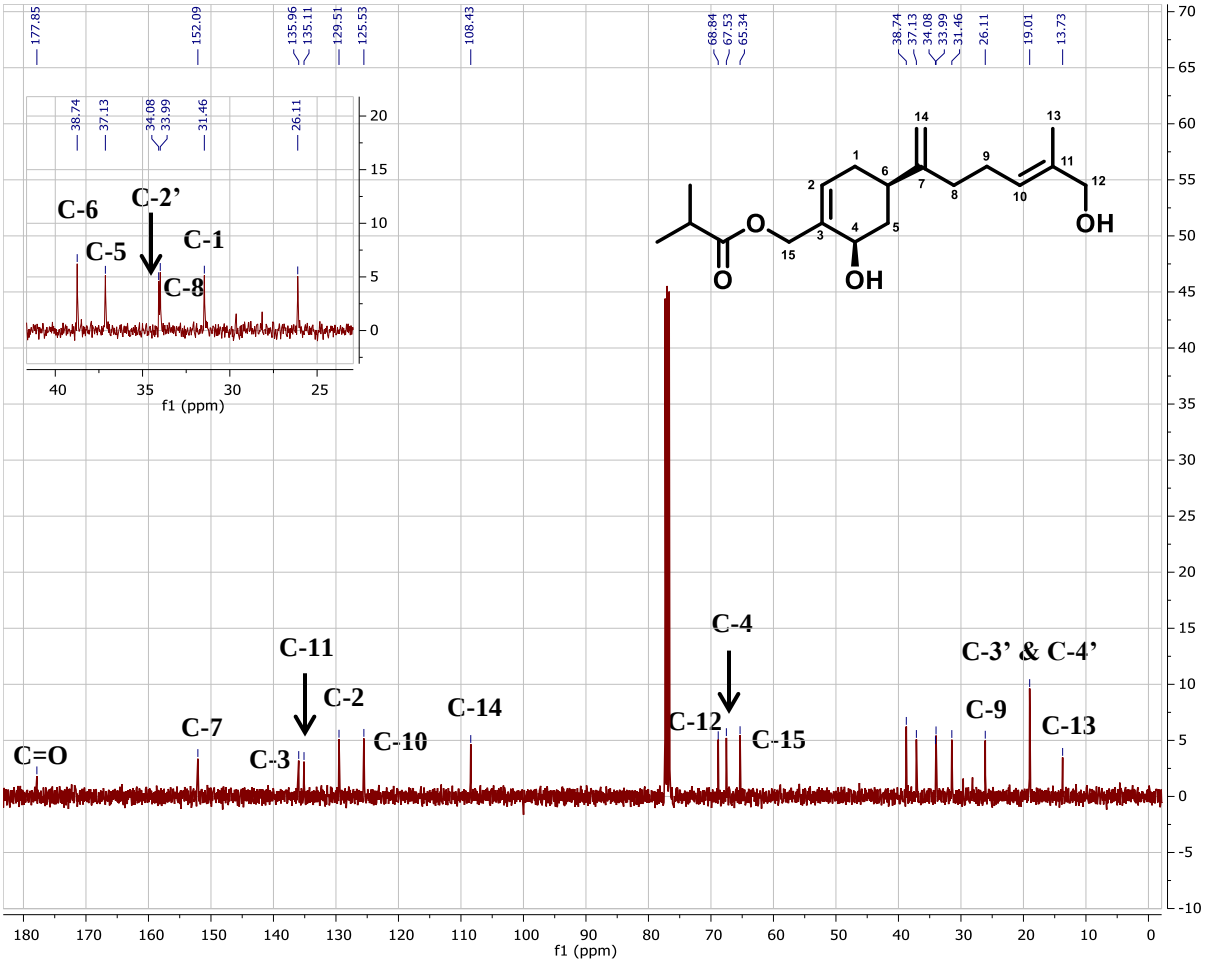

DEPT-135 and ^{13}C-spectra of Caleanolene-A

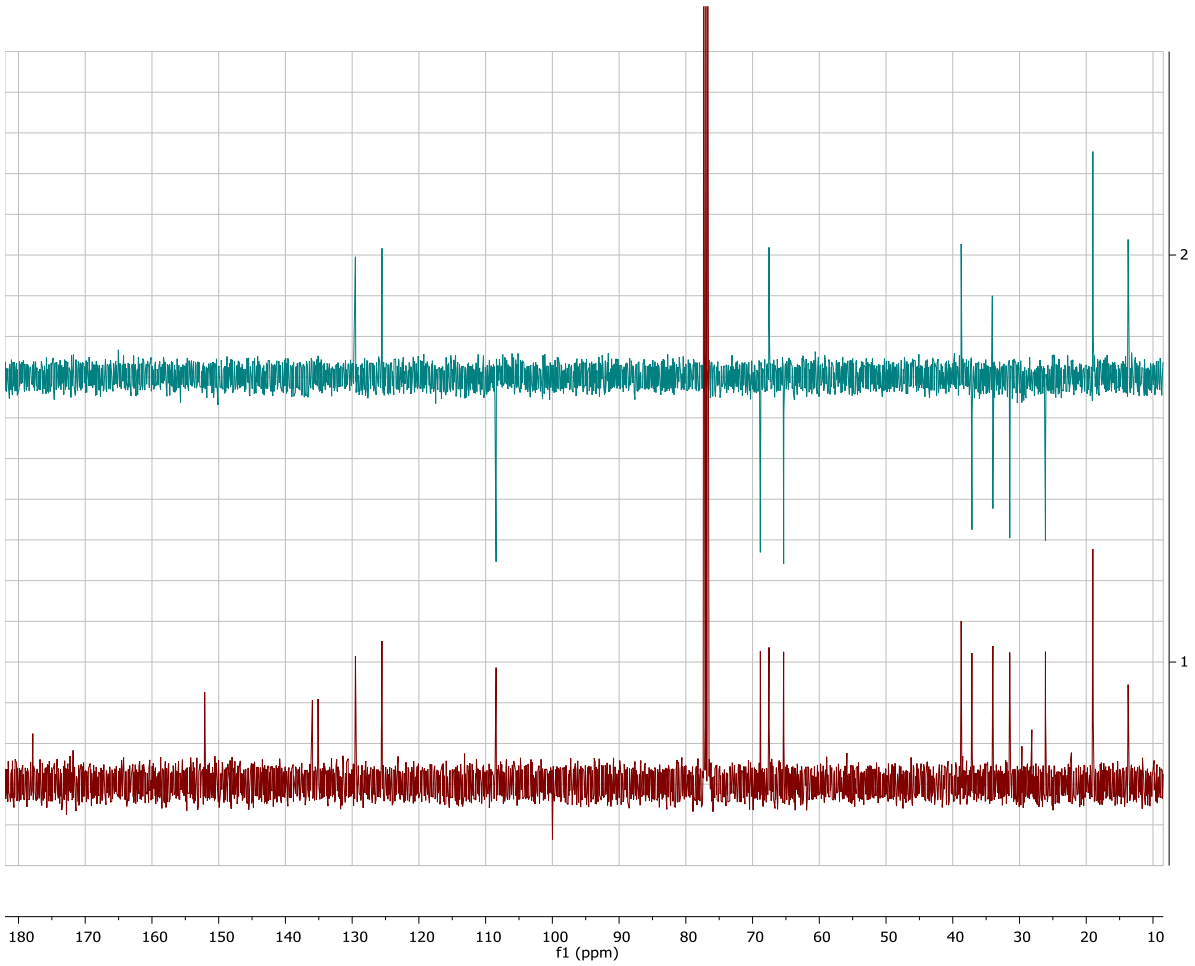

COSY Spectrum of Caleanolene-A

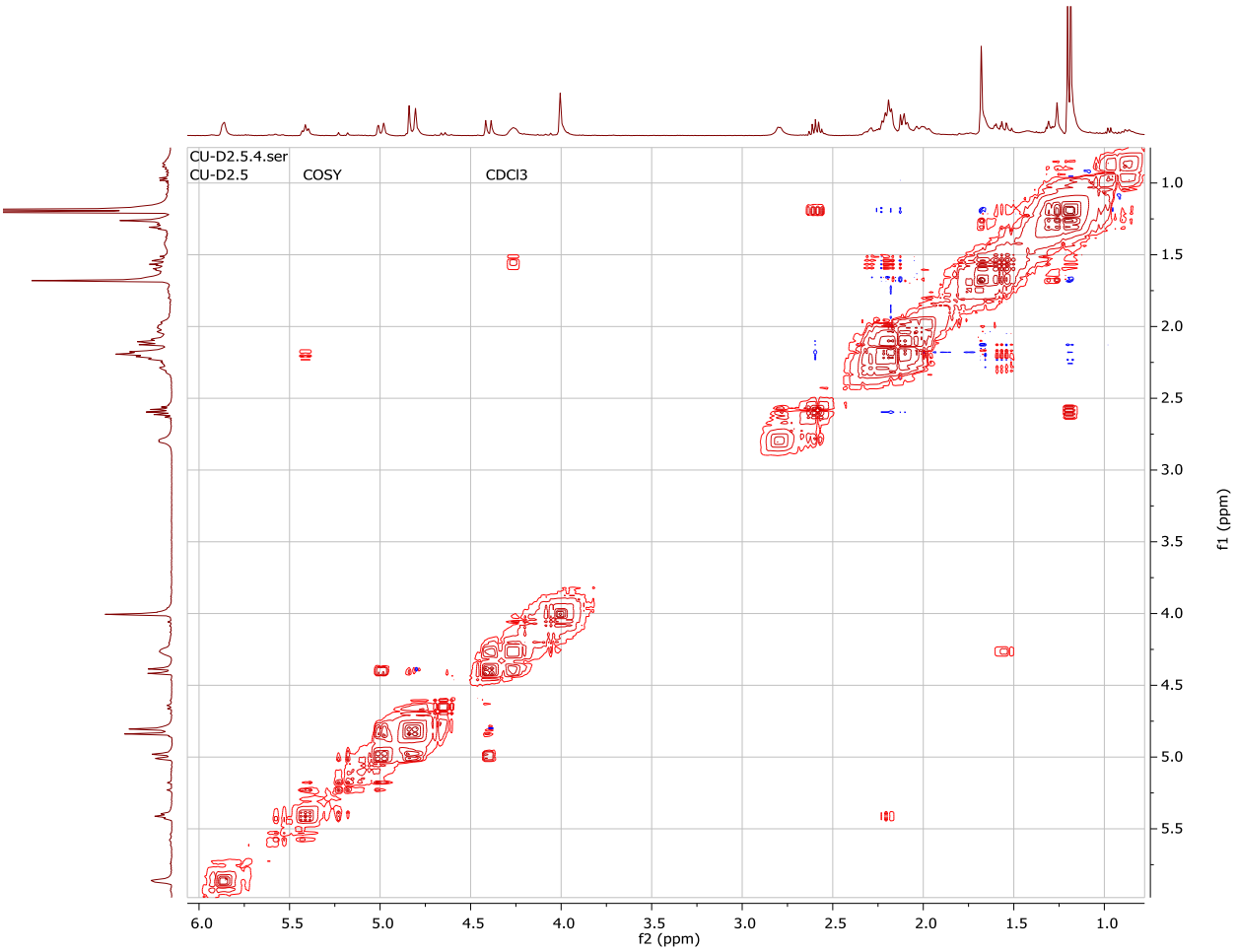

HSQC Spectrum of Caleanolene-A

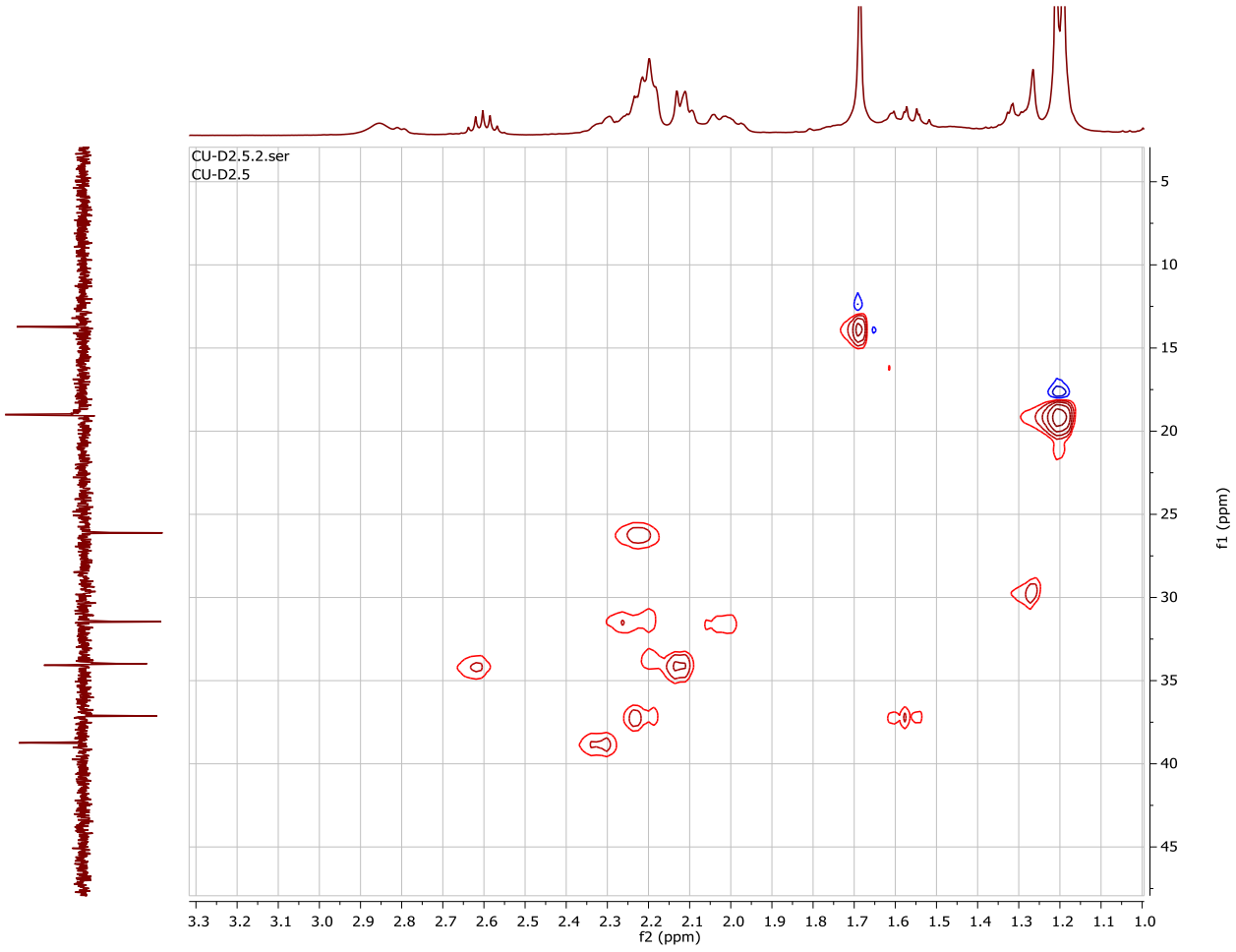

HMBC Spectrum of Caleanolene-A

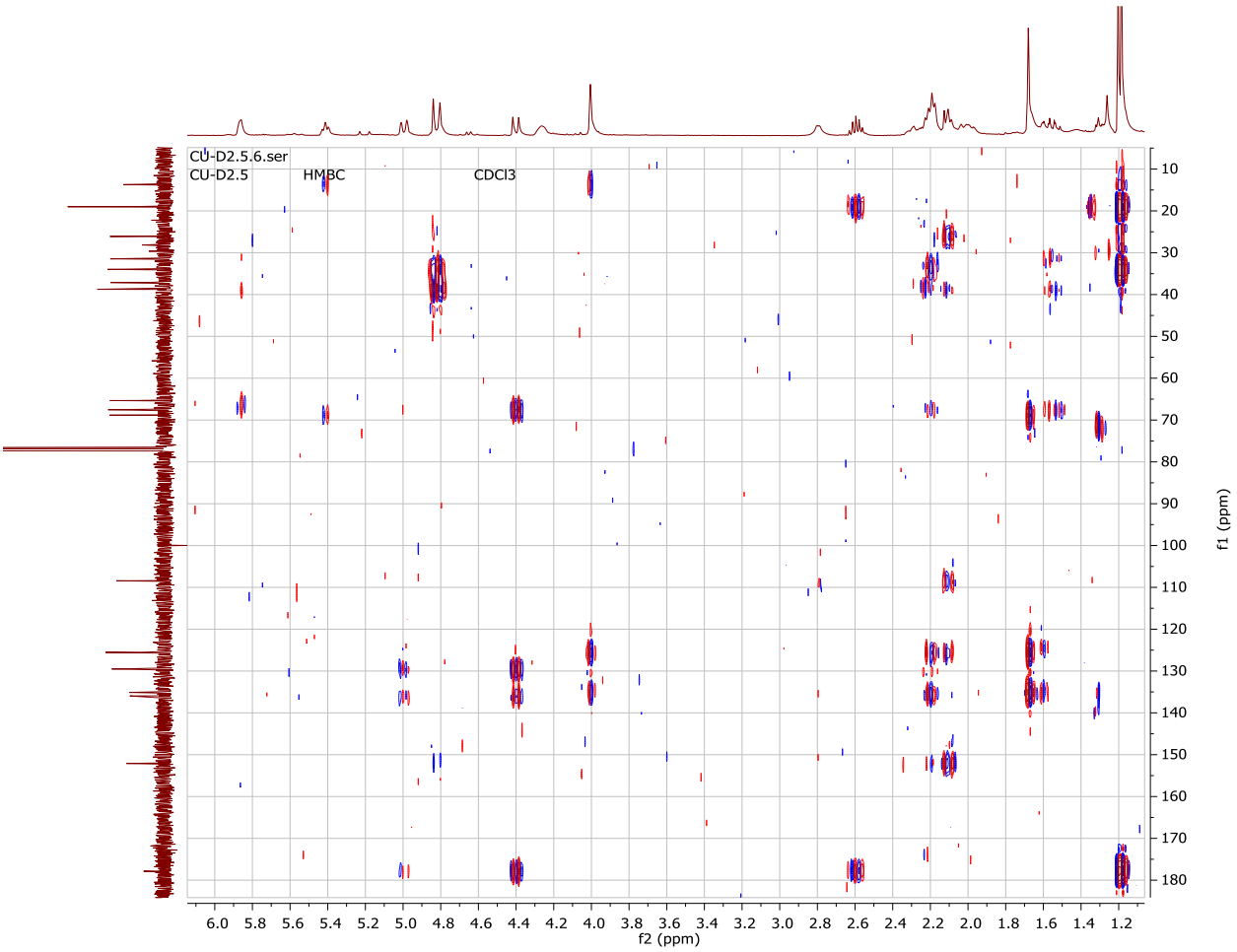

ROESY Spectrum of Caleanolene-A

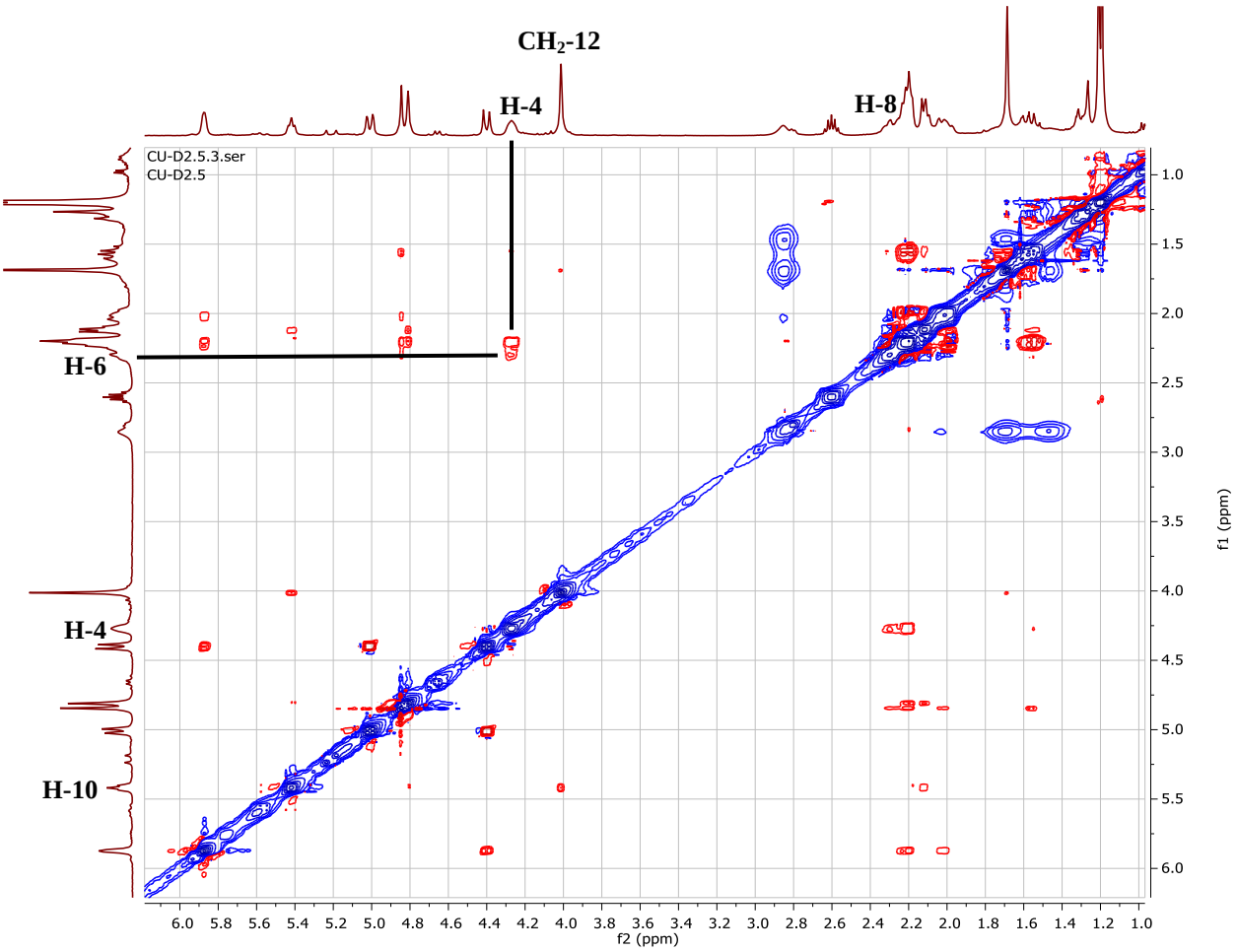

^{1}H-NMR Spectrum of Caleanolene-B

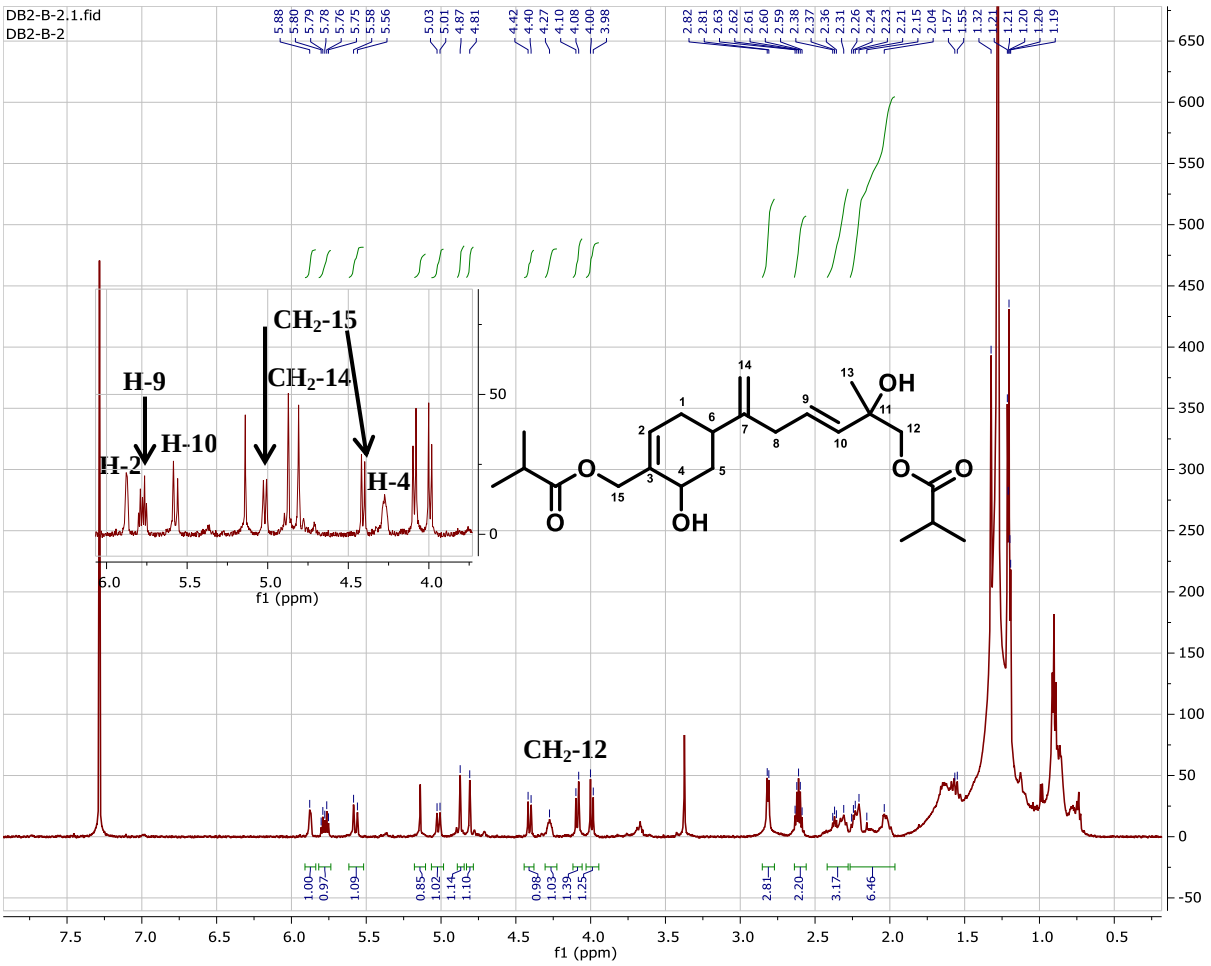

DEPT-135 and ^{13}C-Spectra of Caleanolene-B

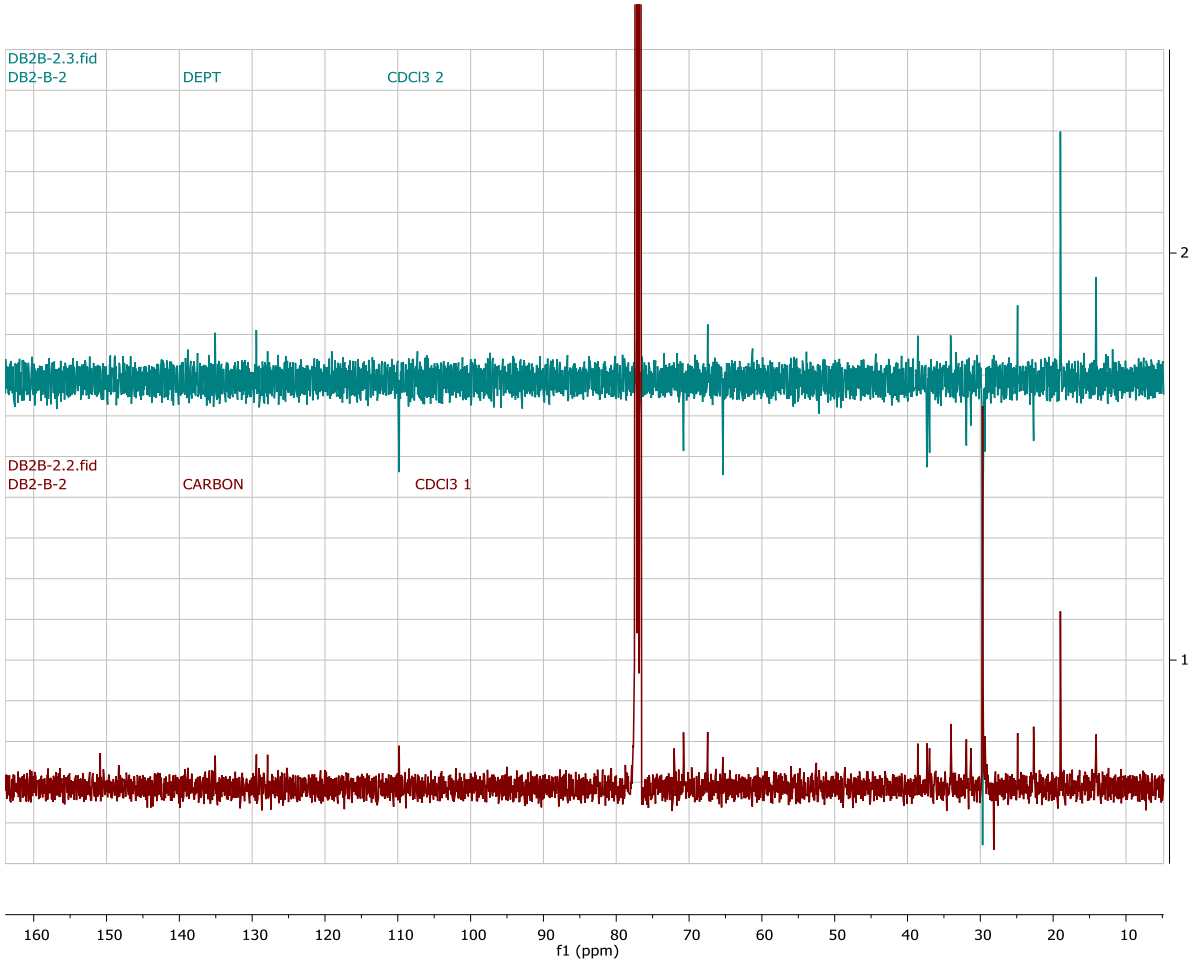

COSY Spectrum of Caleanolene-B

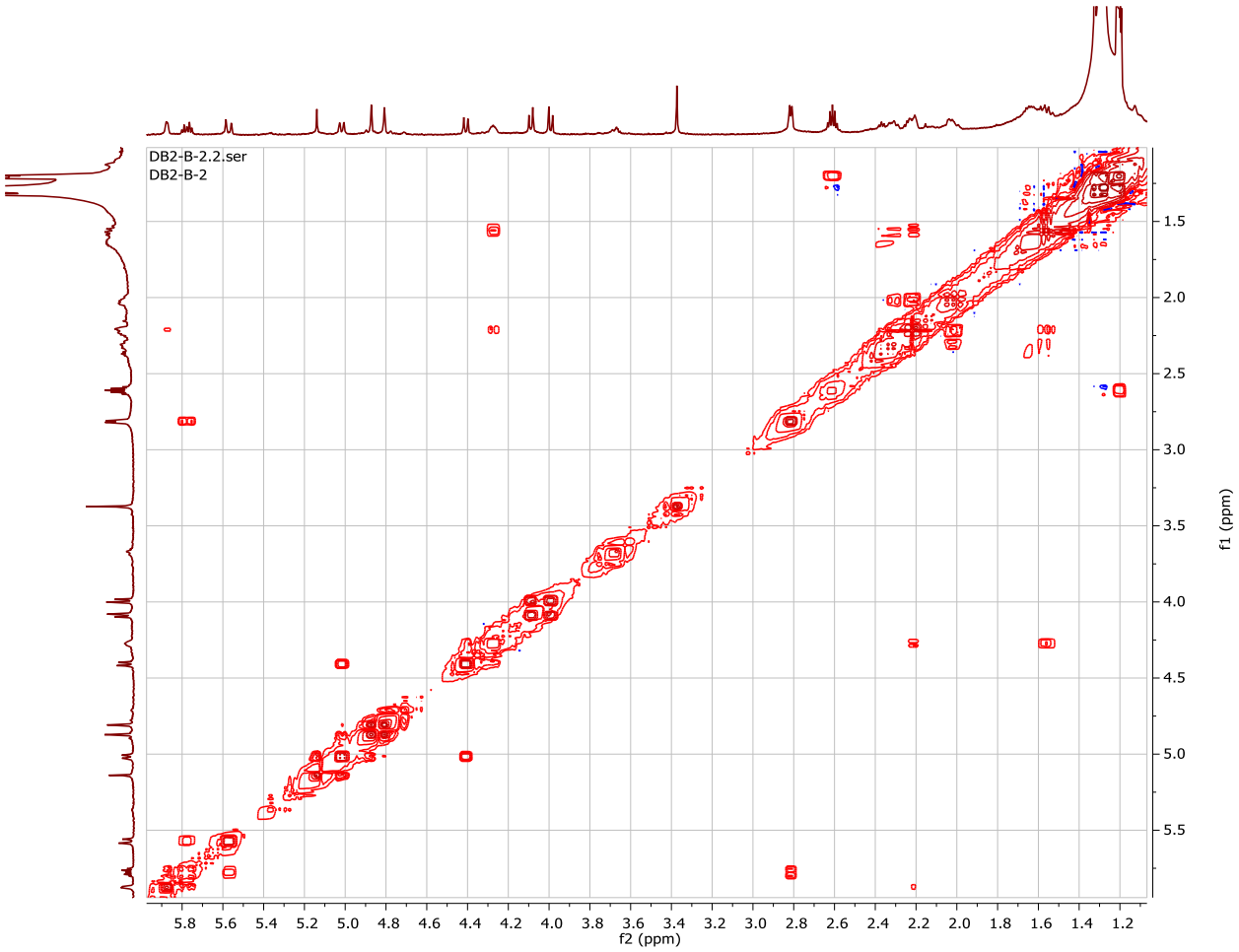

HMQC Spectrum of Caleanolene-B

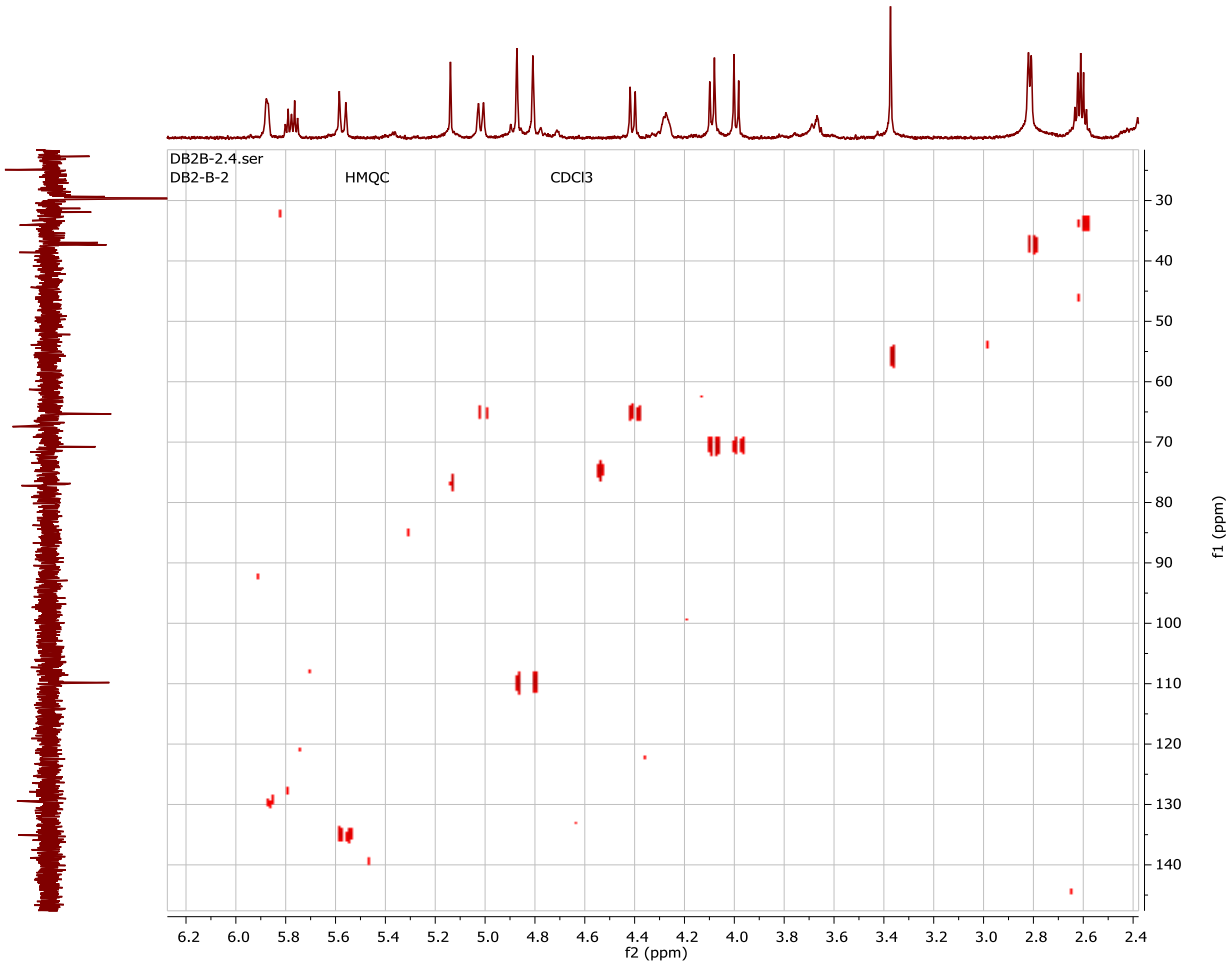

HMBC Spectrum of Caleanolene-B

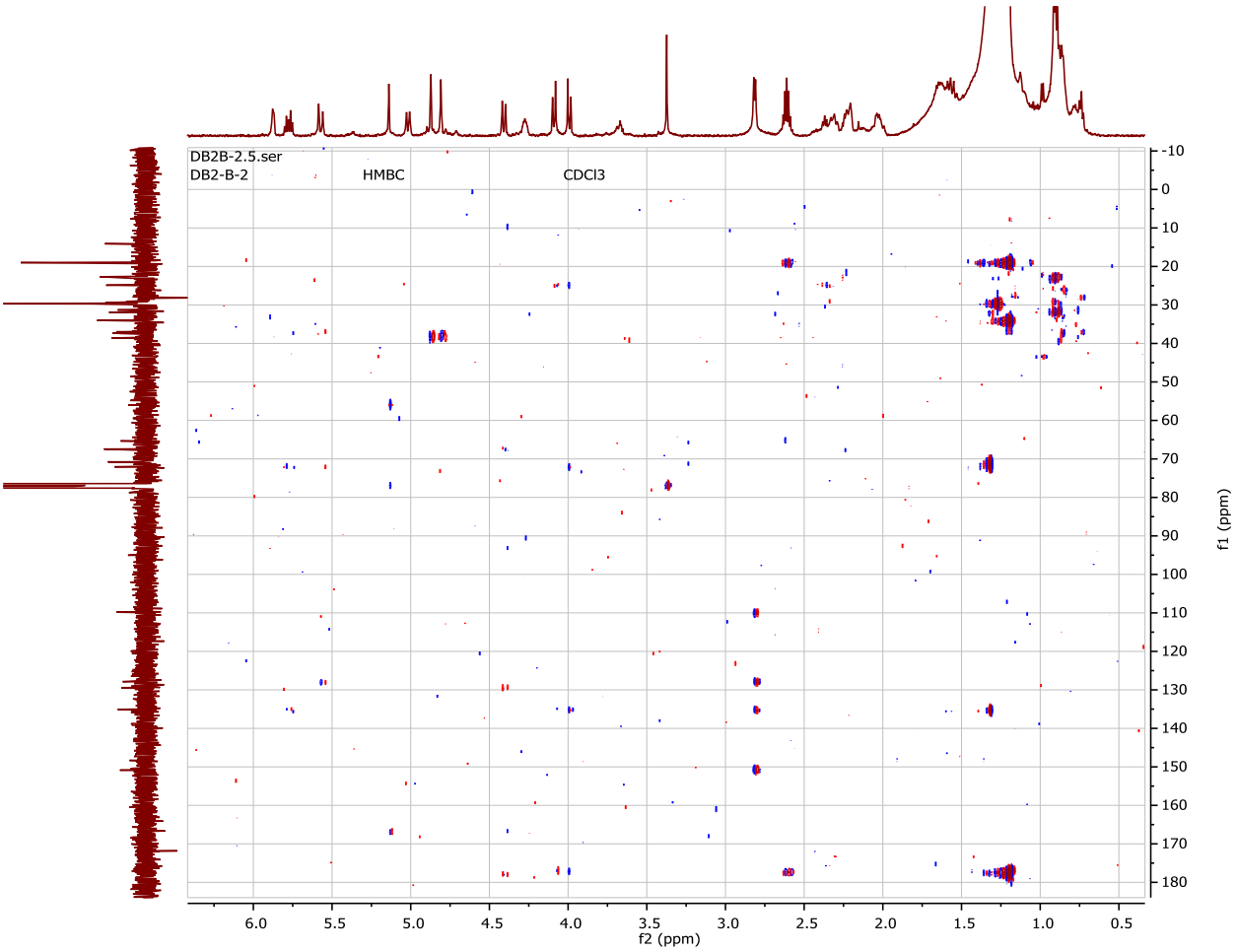

NOESY Spectrum of Caleanolene-B

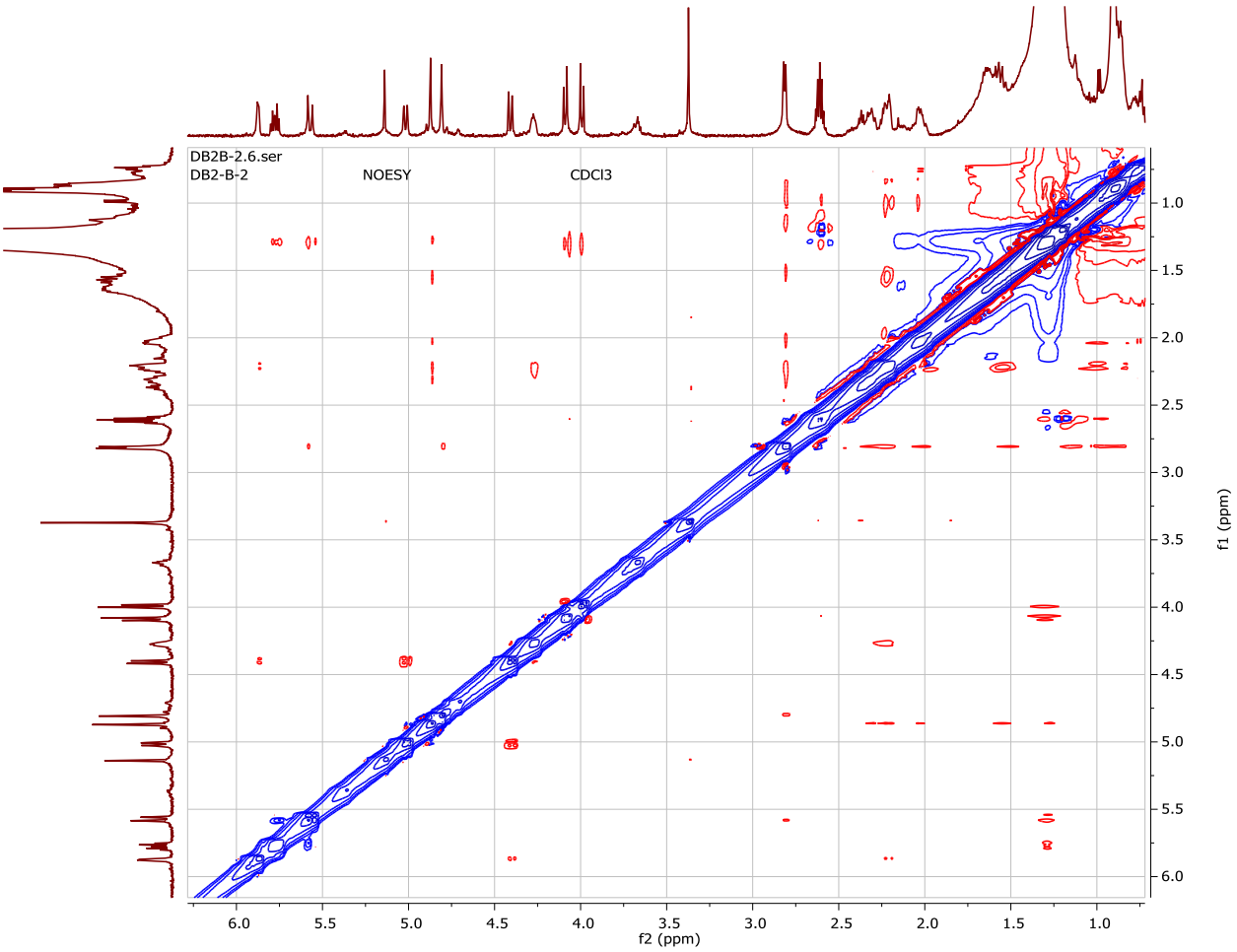

^{1}H-NMR Spectrum of Caleanolene-C

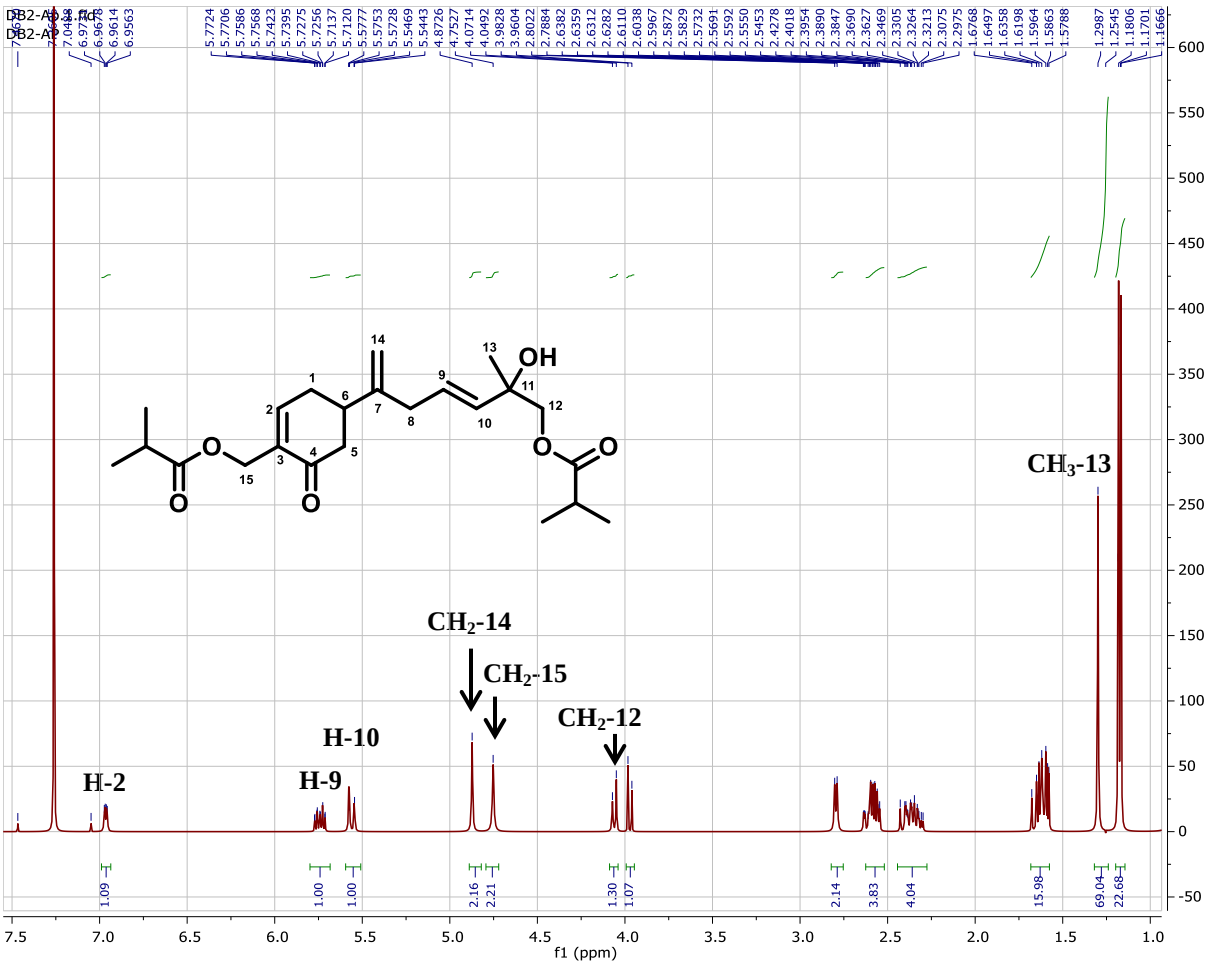

^{13}C-NMR Spectrum of Caleanolene-C

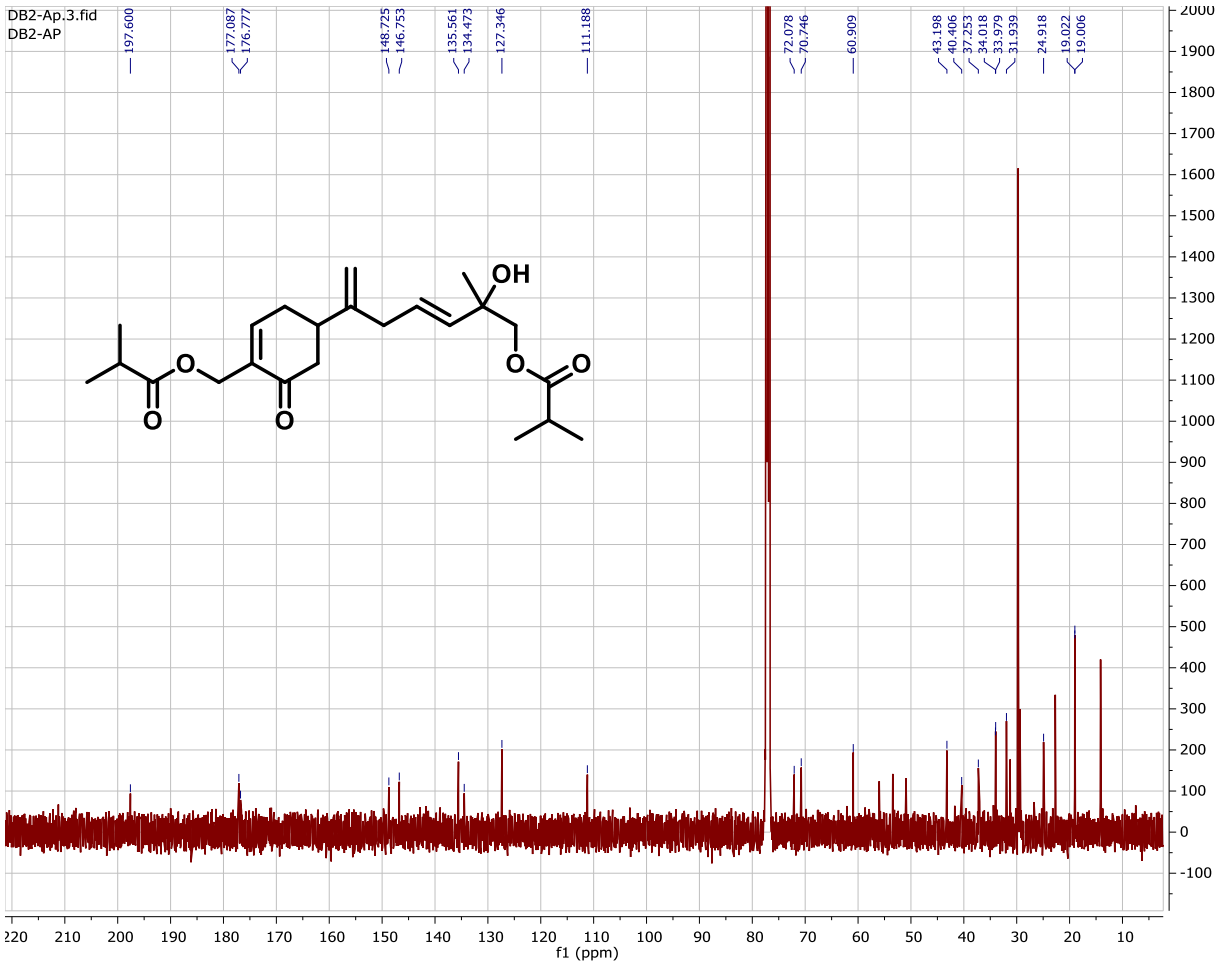

DEPT-135 Spectrum of Caleanolene-C

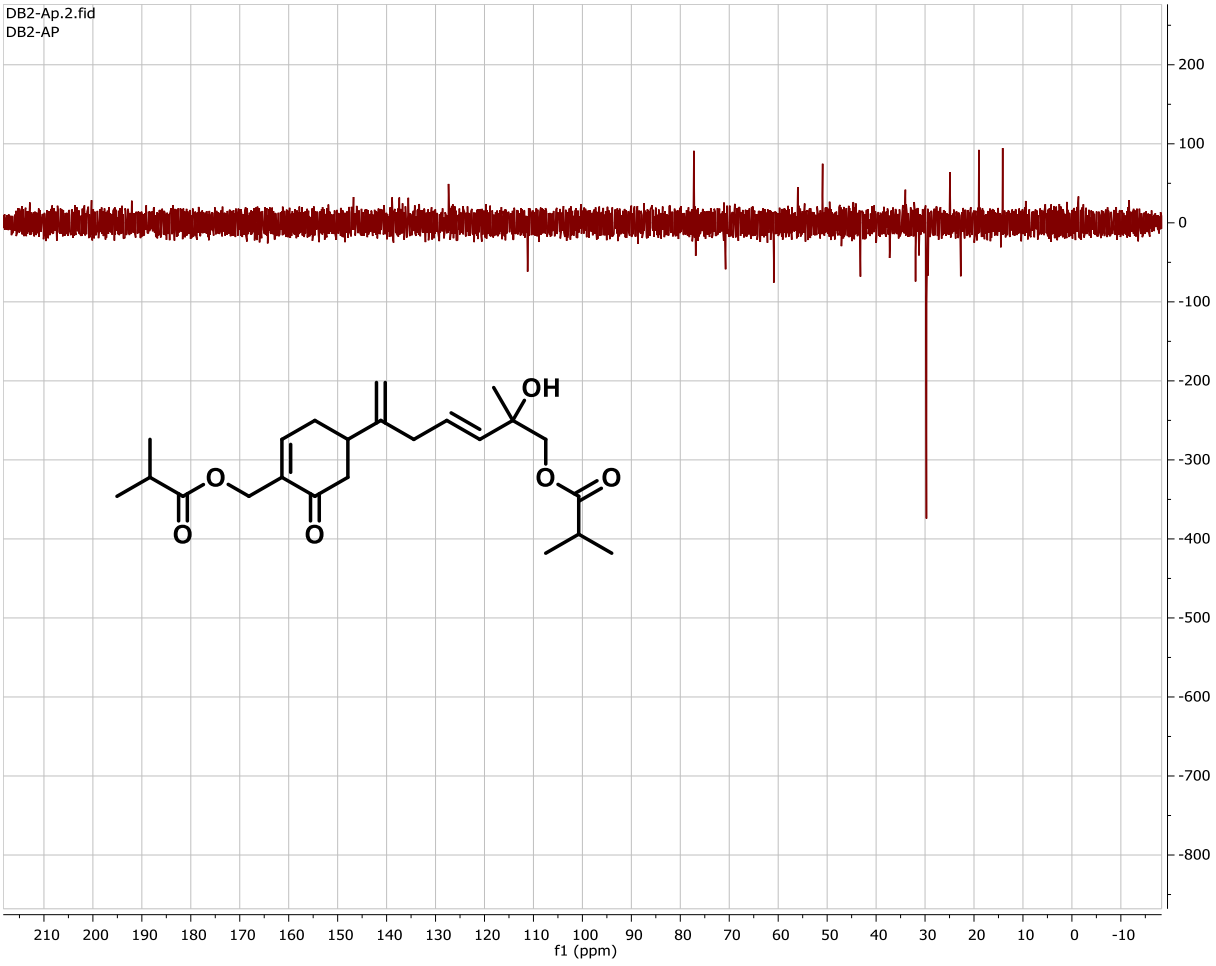

COSY Spectrum of Caleanolene-C

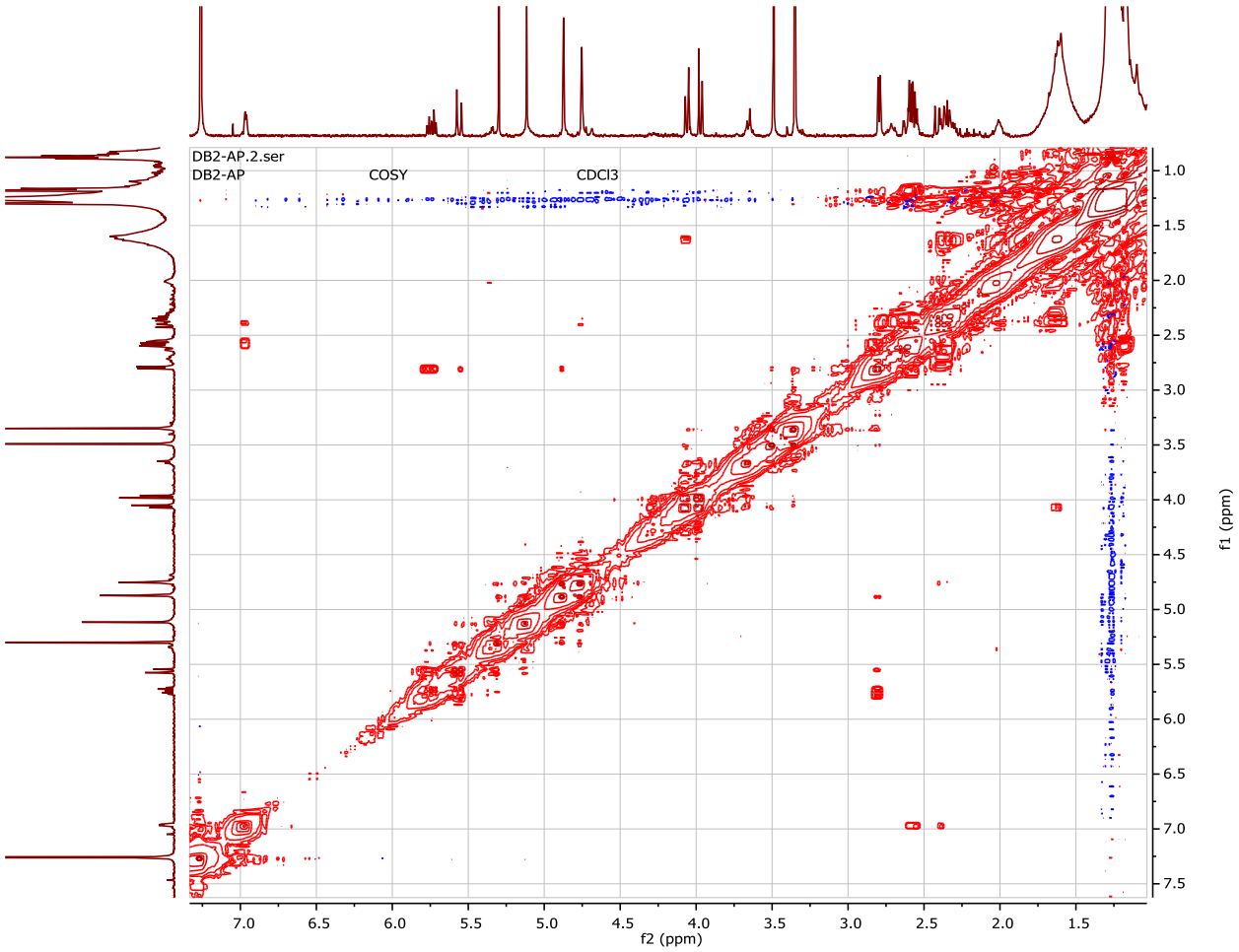

HSQC Spectrum of Caleanolene-C

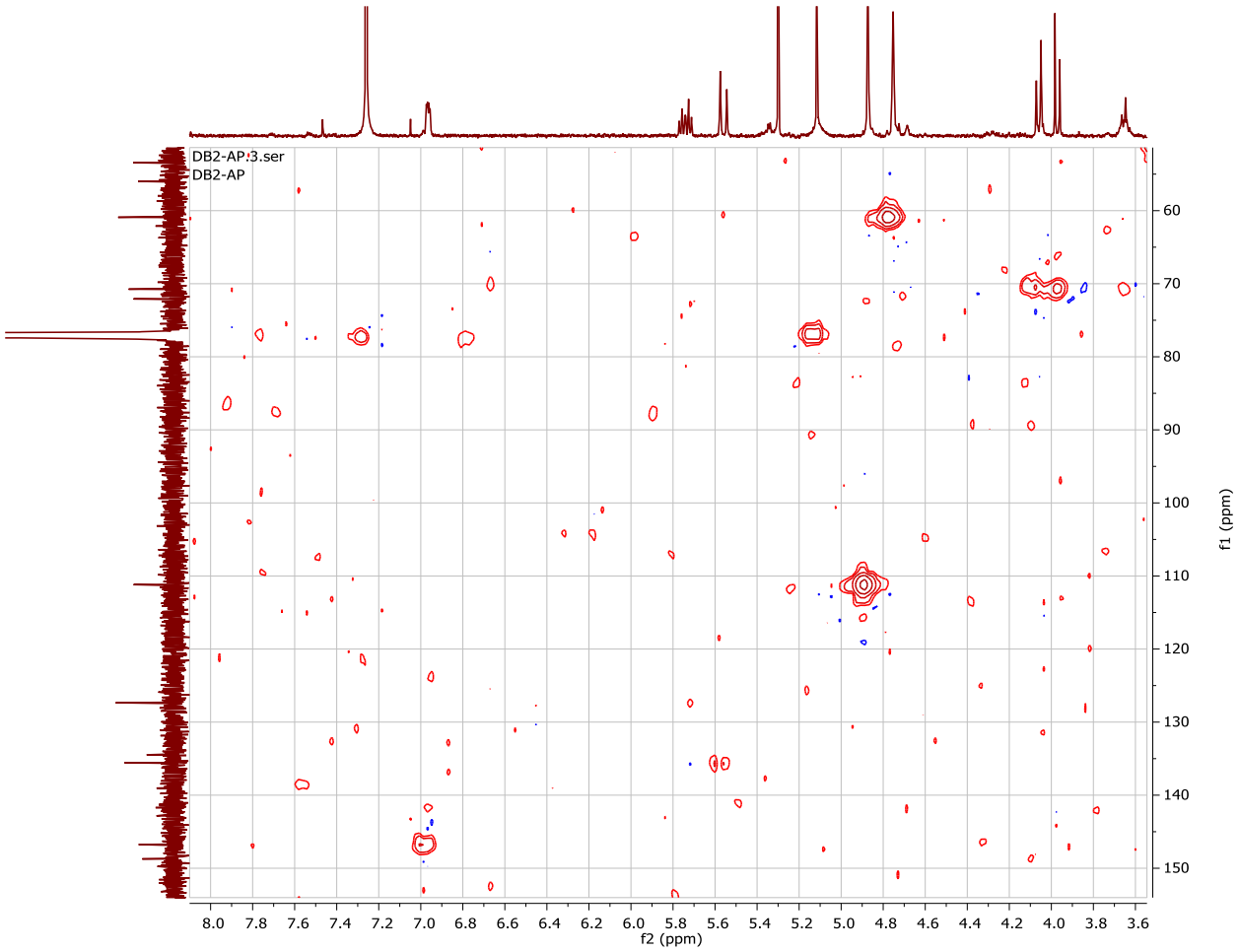

HMBC Spectrum of Caleanolene-C

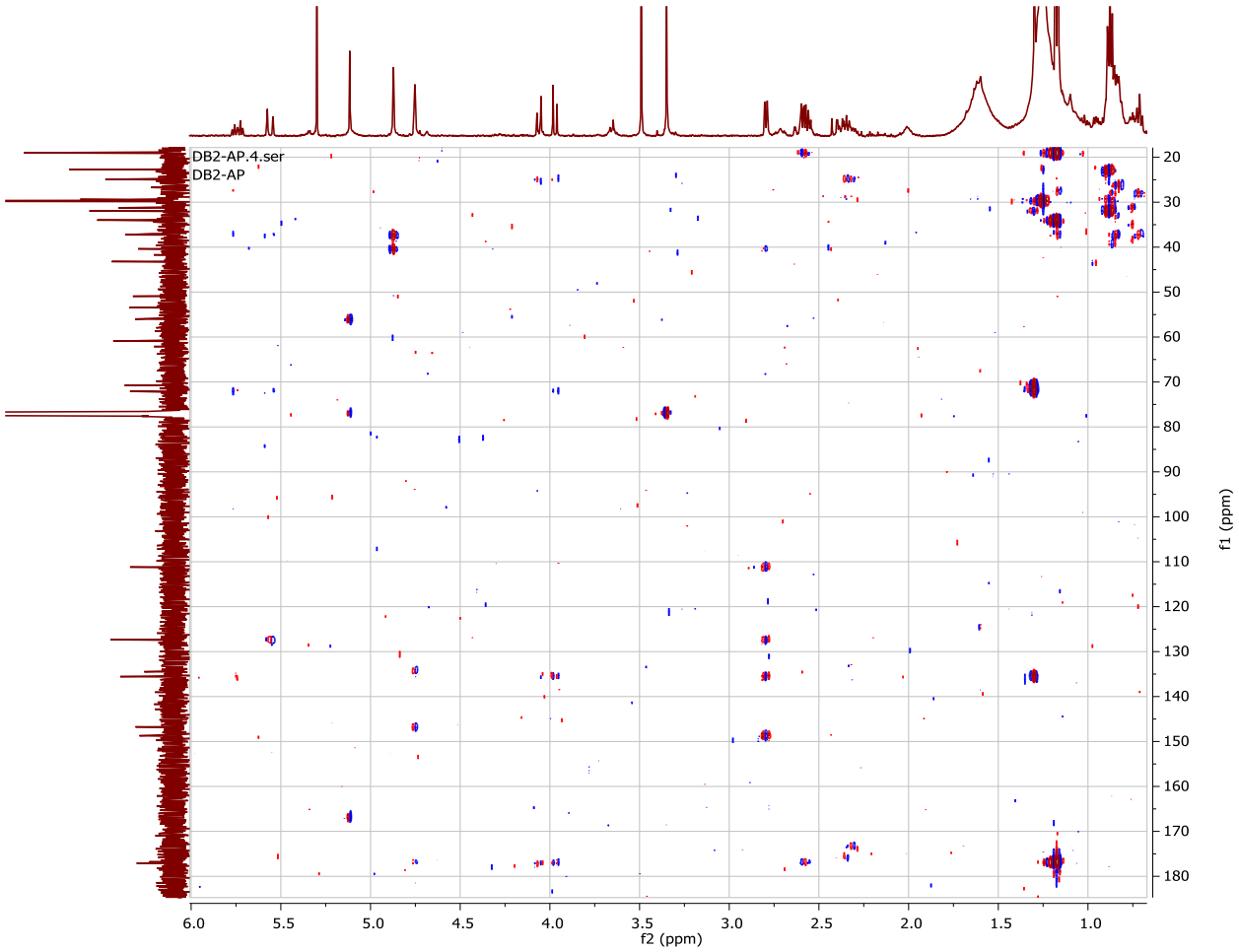

^{1}H-NMR Spectrum of 2,3-Epoxyjuanislamin

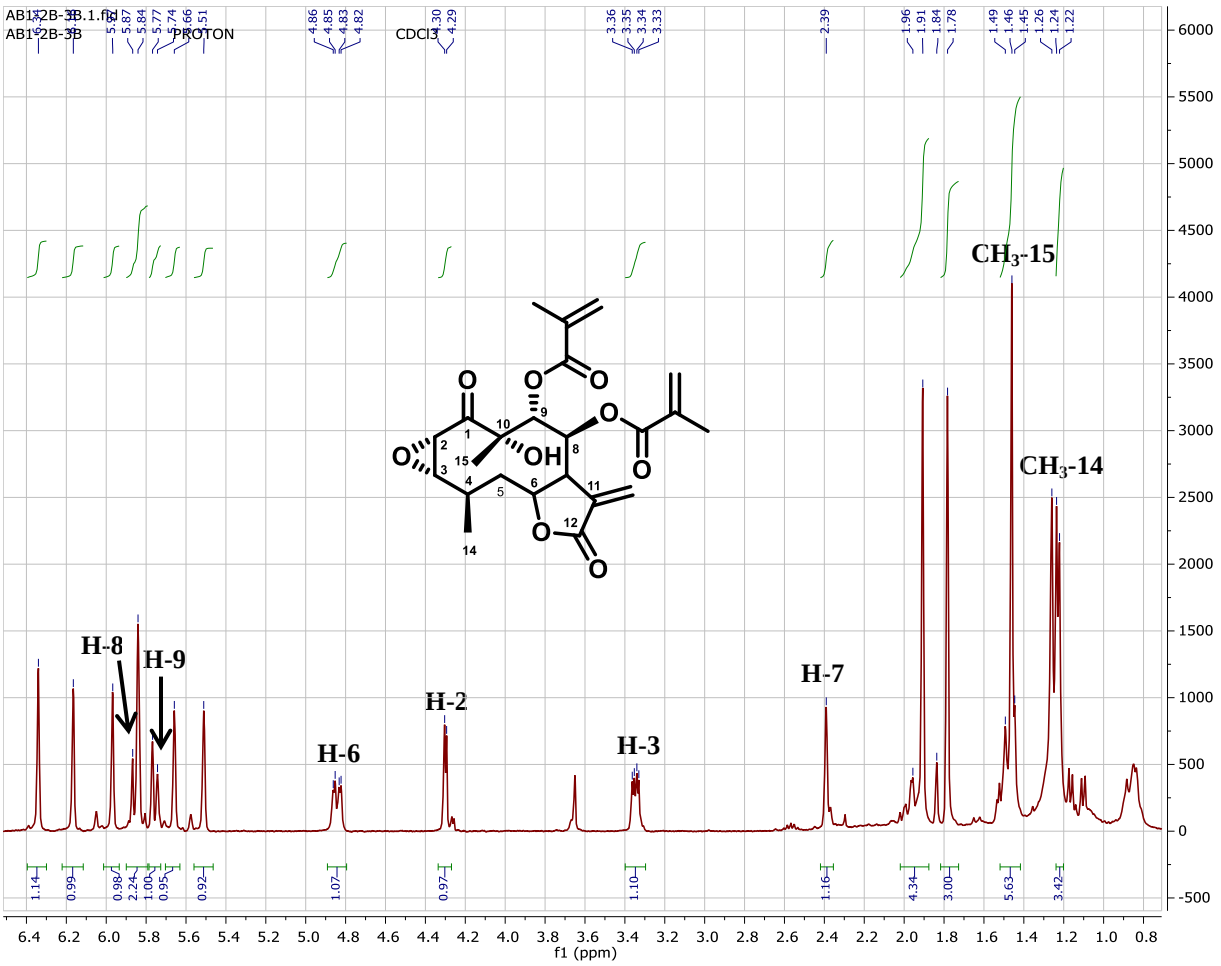

^{13}C-NMR Spectrum of 2,3-Epoxyjuanislamin

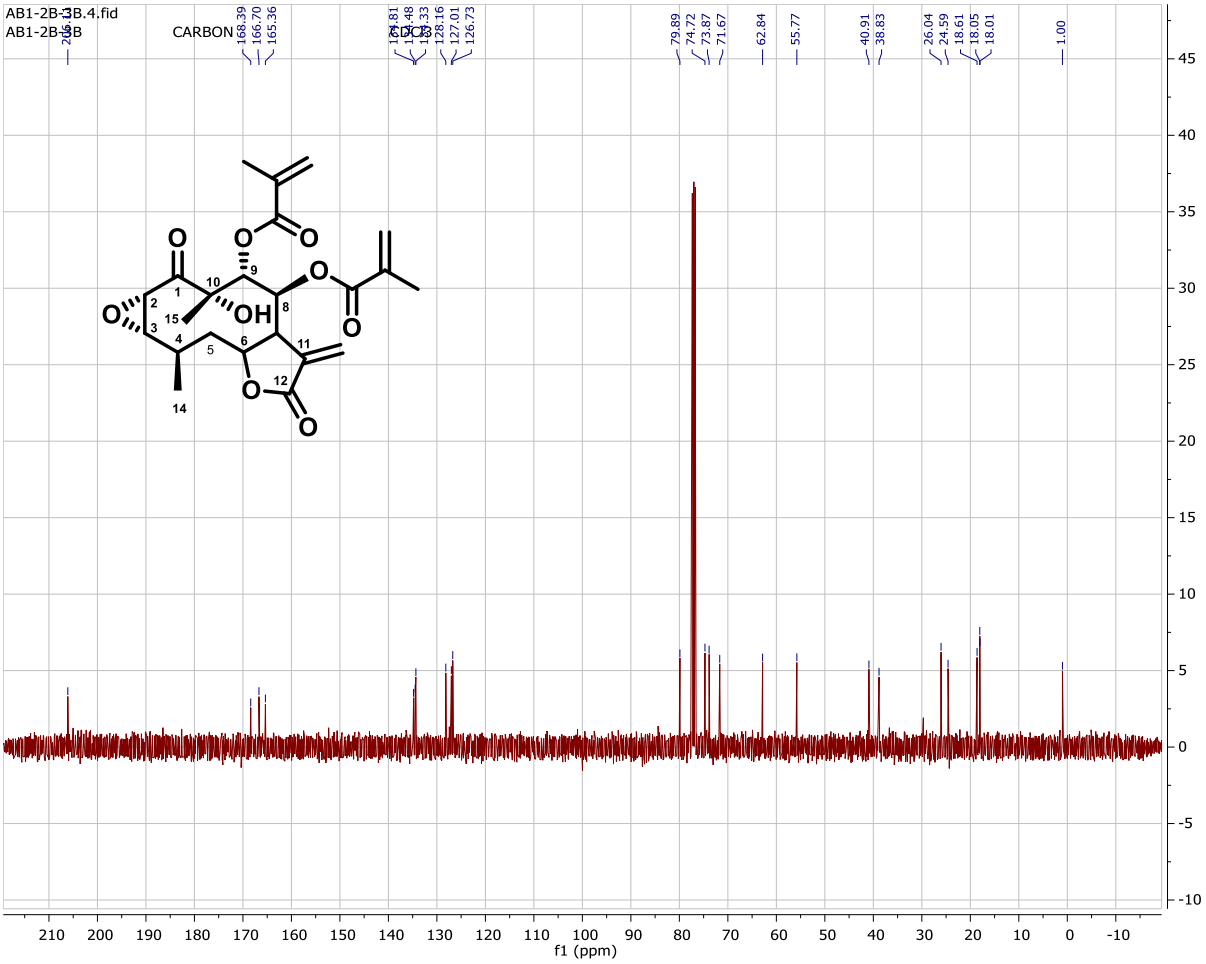

DEPT-135 and ^{13}C-NMR Spectra of 2,3-Epoxyjuanislamin

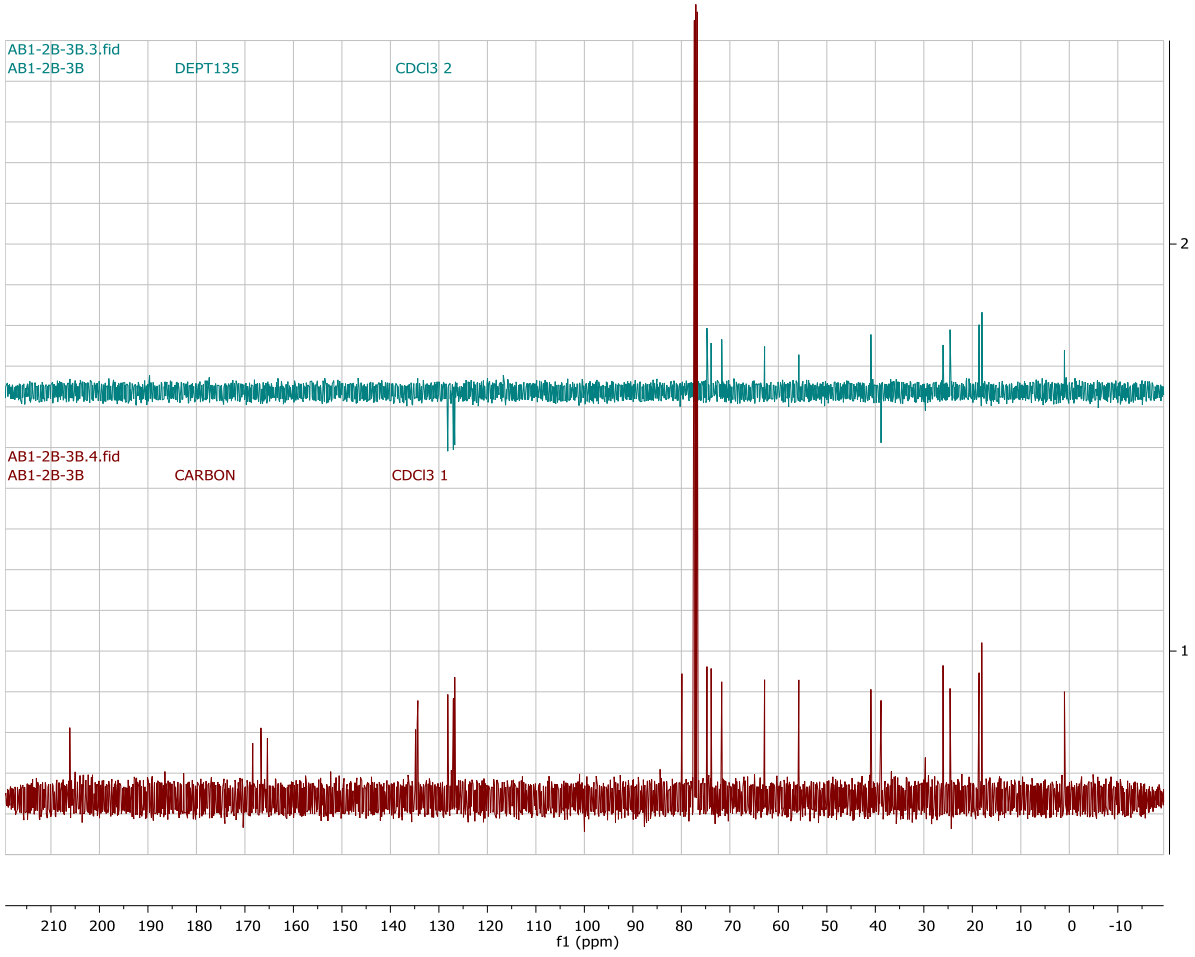

DEPT-135 Spectrum of 2,3-Epoxyjuanislamin

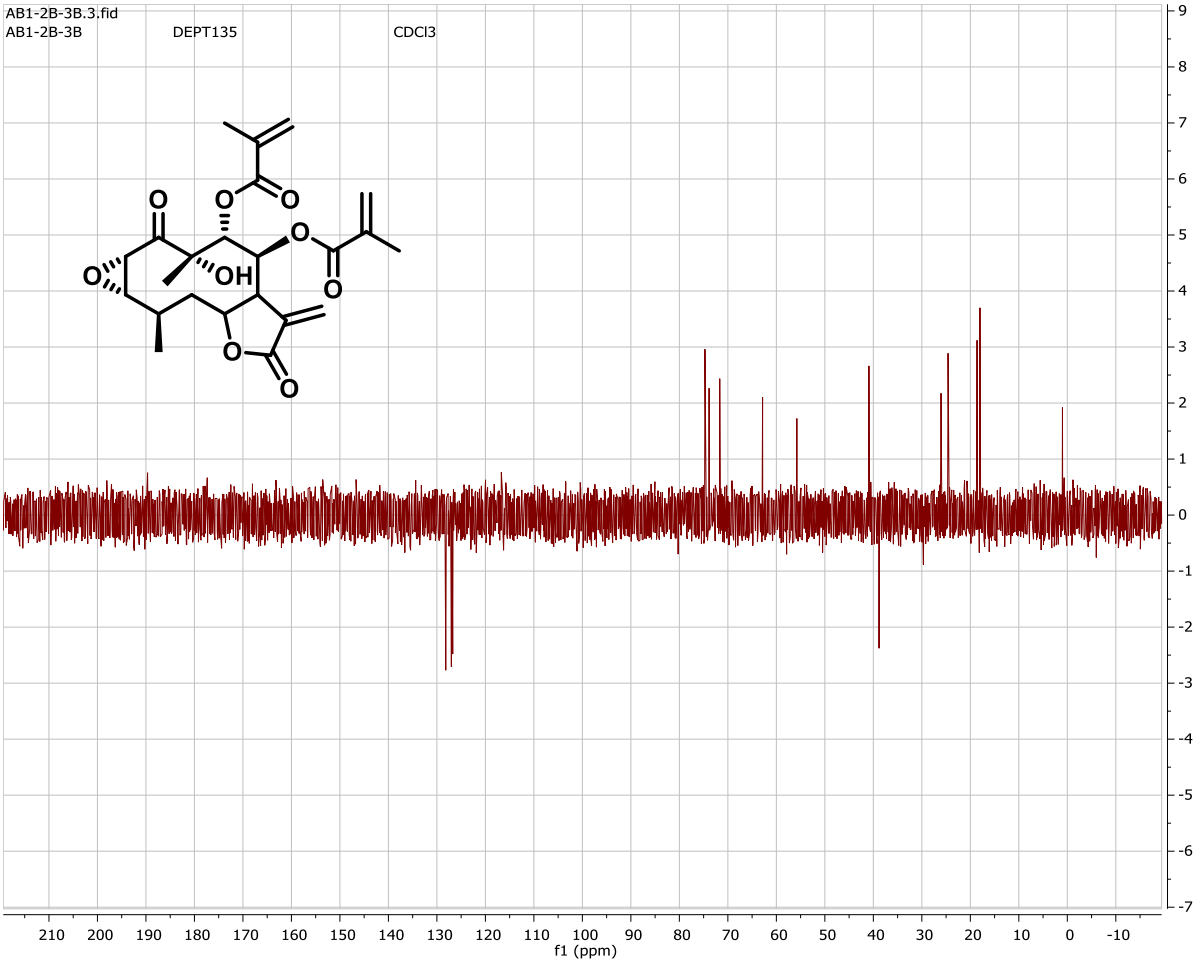

COSY Spectrum of 2,3-Epoxyjuanislamin

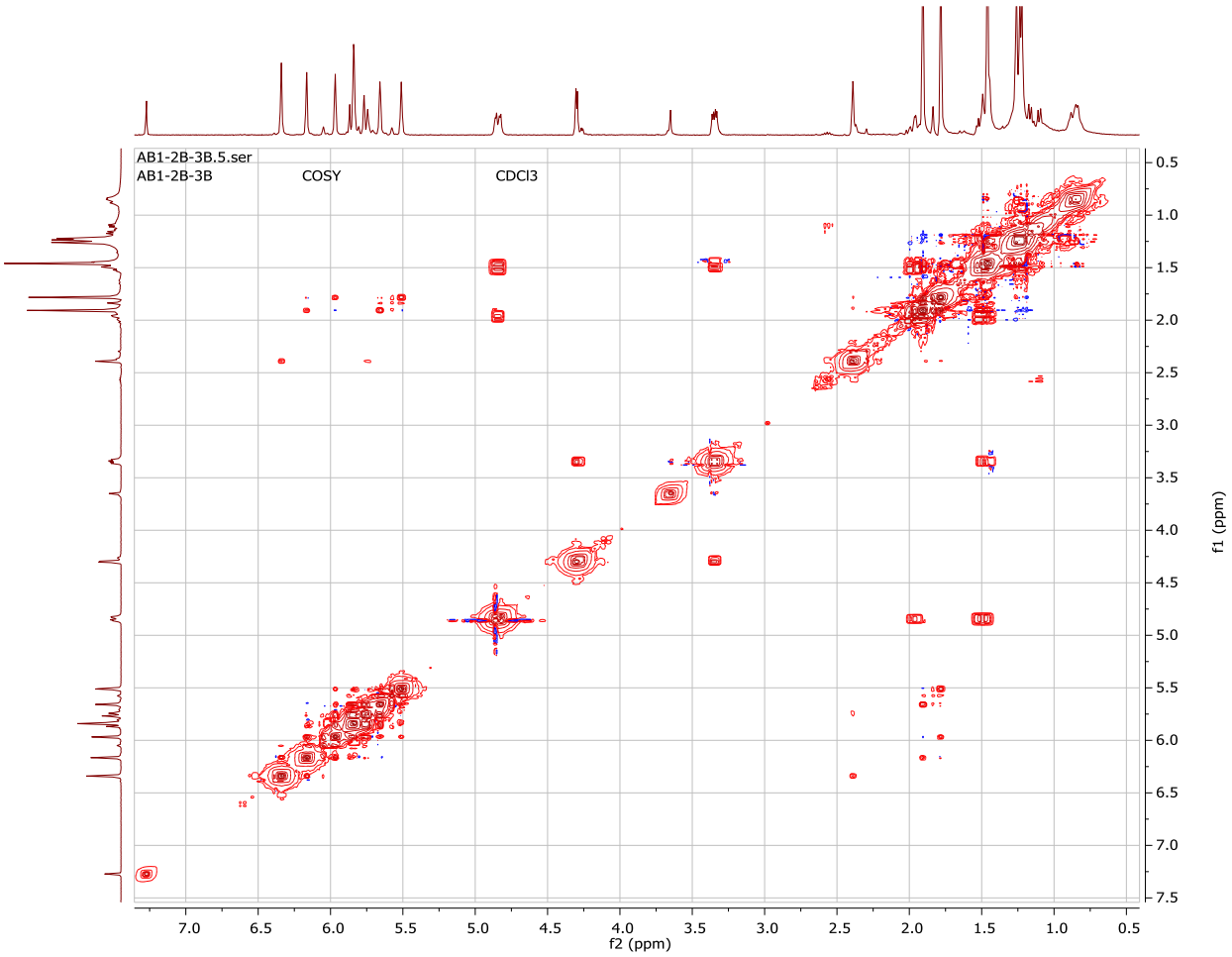

HMQC Spectrum of 2,3-Epoxyjuanislamin

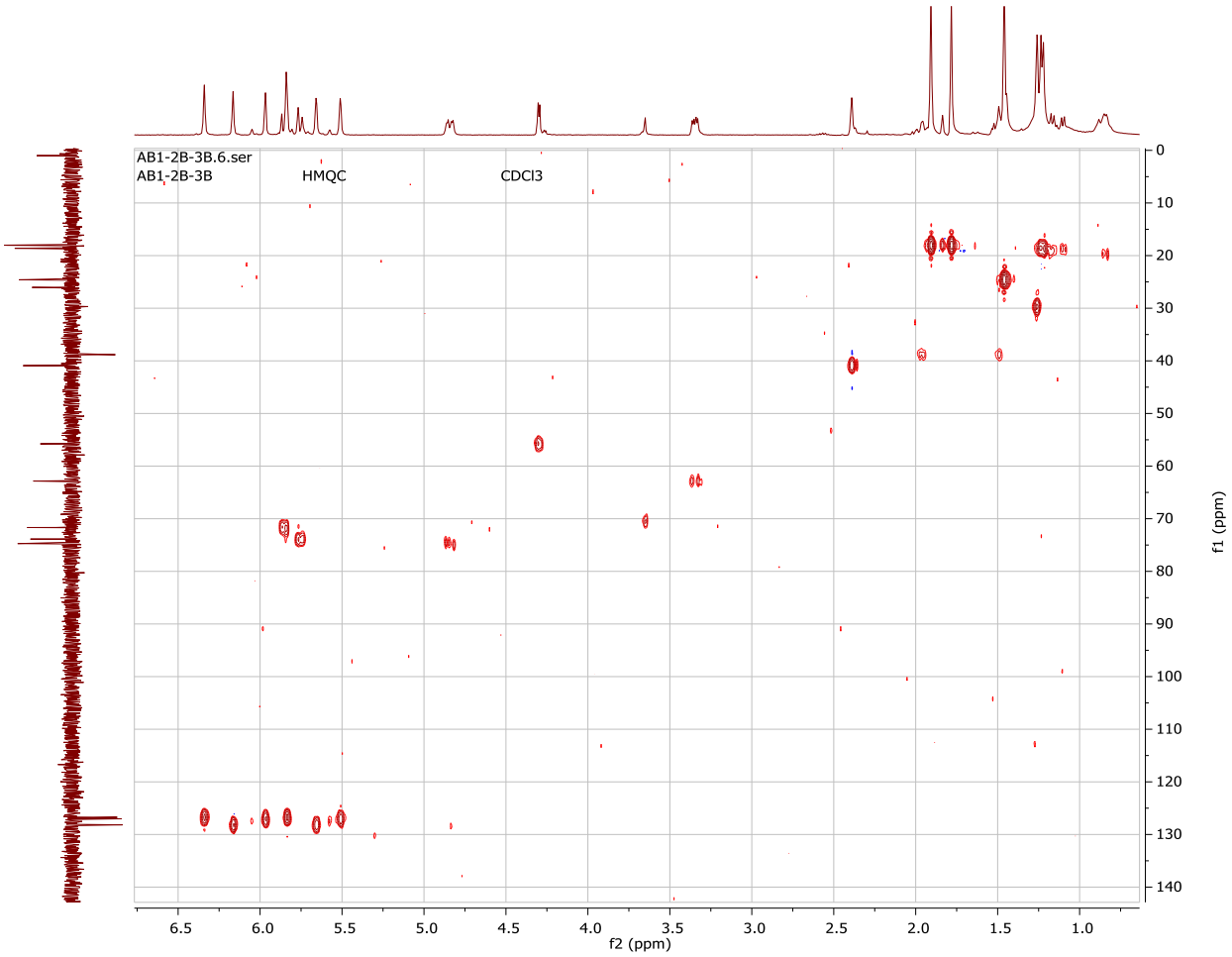

HMBC Spectrum of 2,3-Epoxyjuanislamin

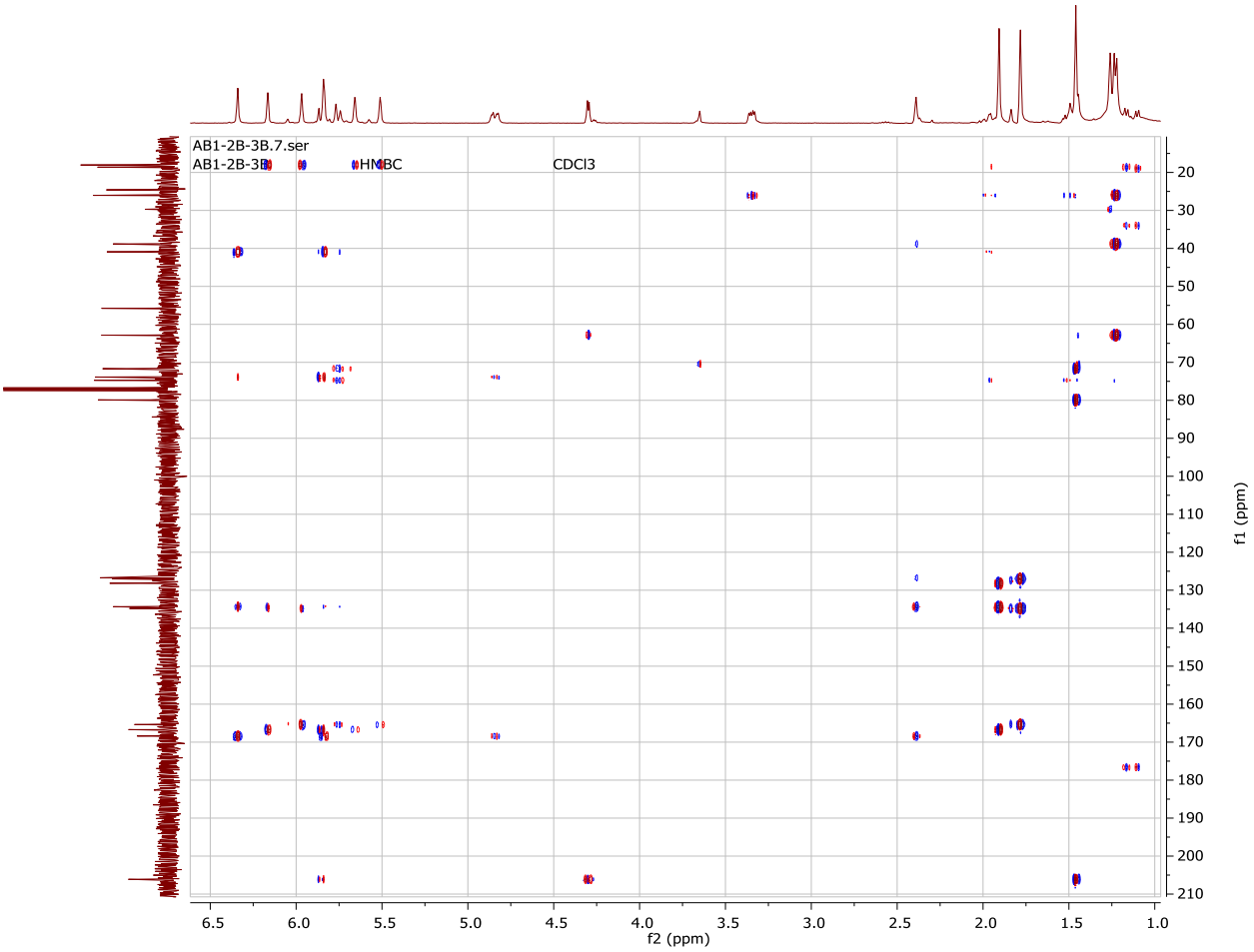

^{1}H-Spectrum of Calealactone-B

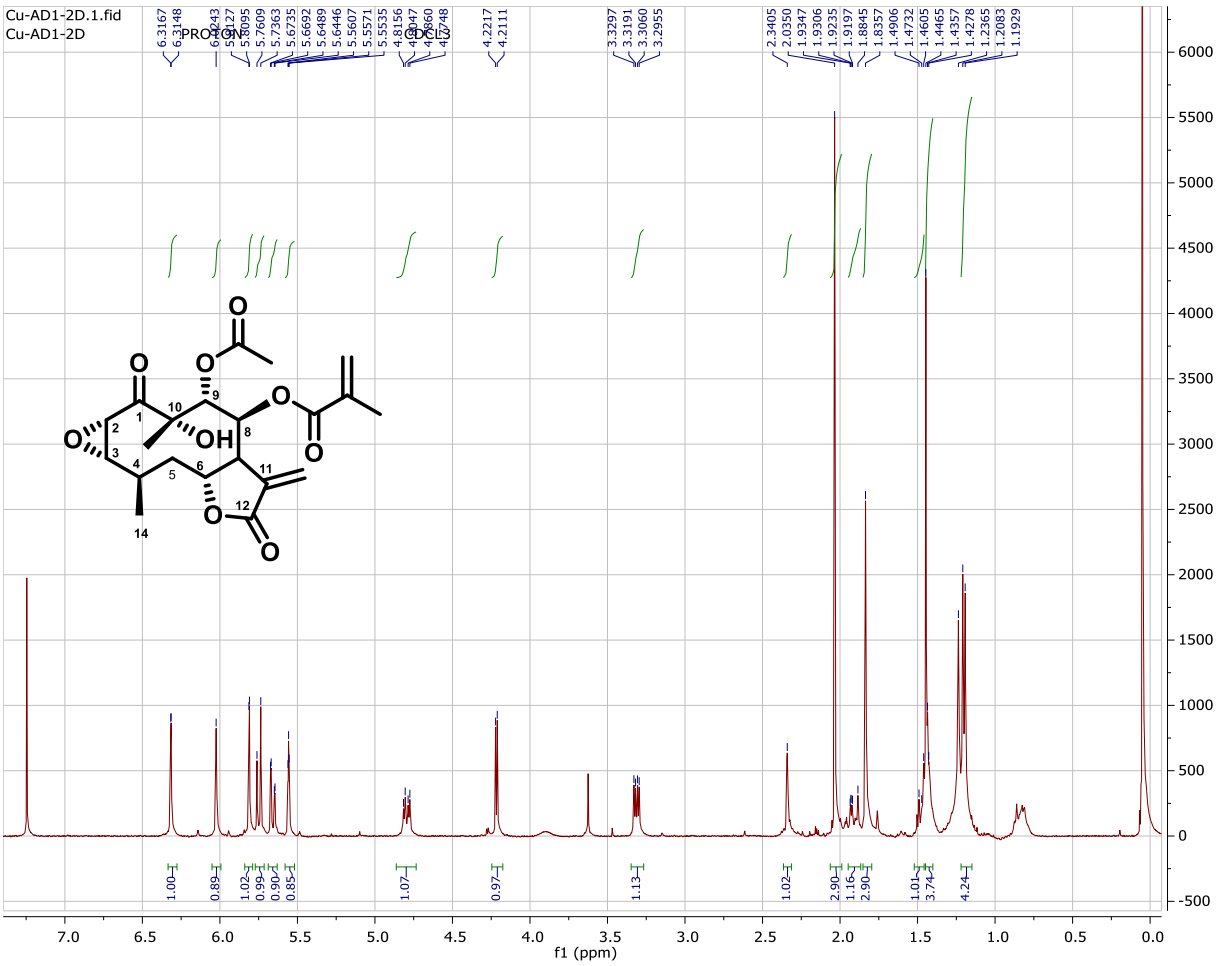

^{13}C-Spectrum of Calealactone-B

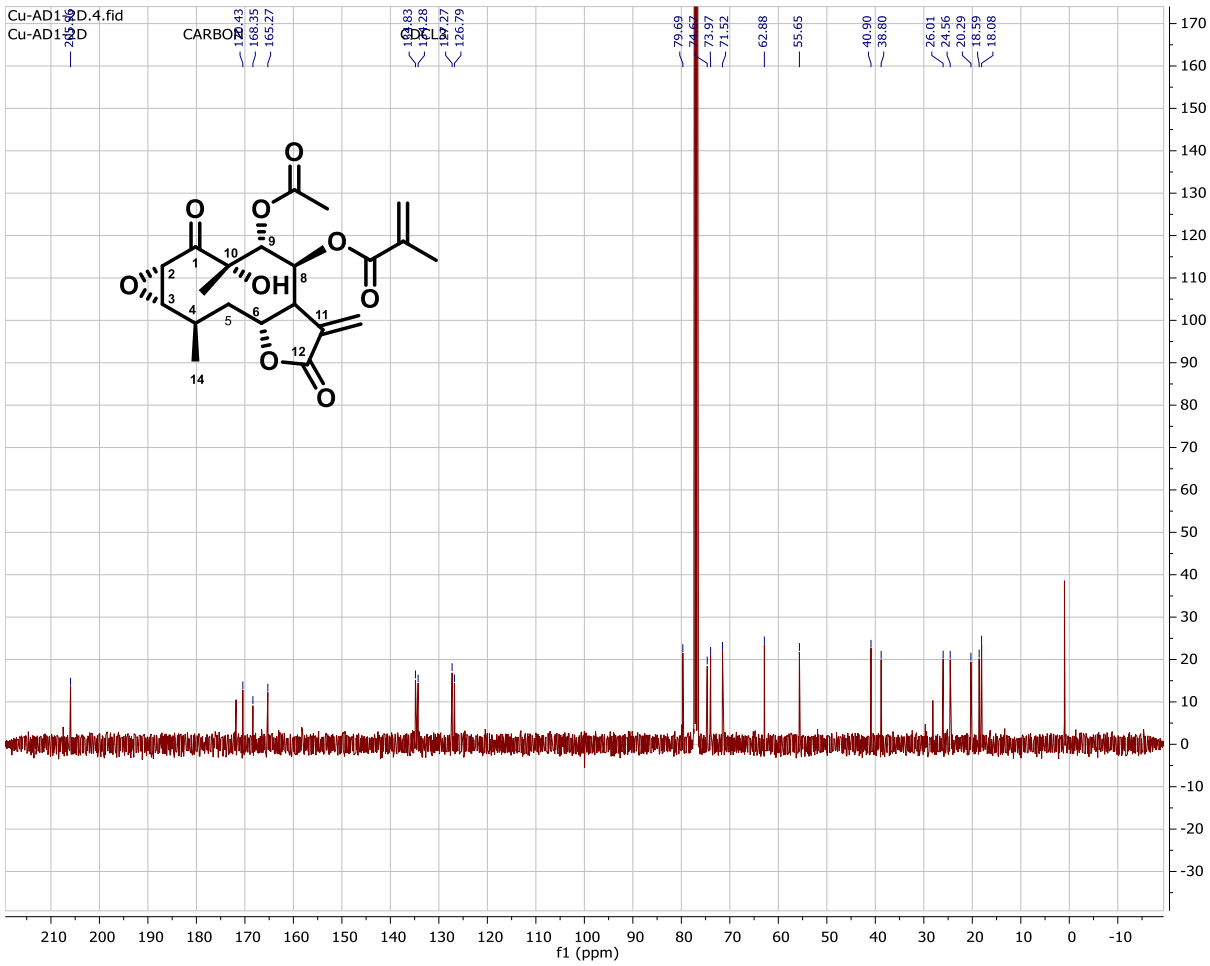

DEPT-135 and ^{13}C-Spectra of Calealactone-B

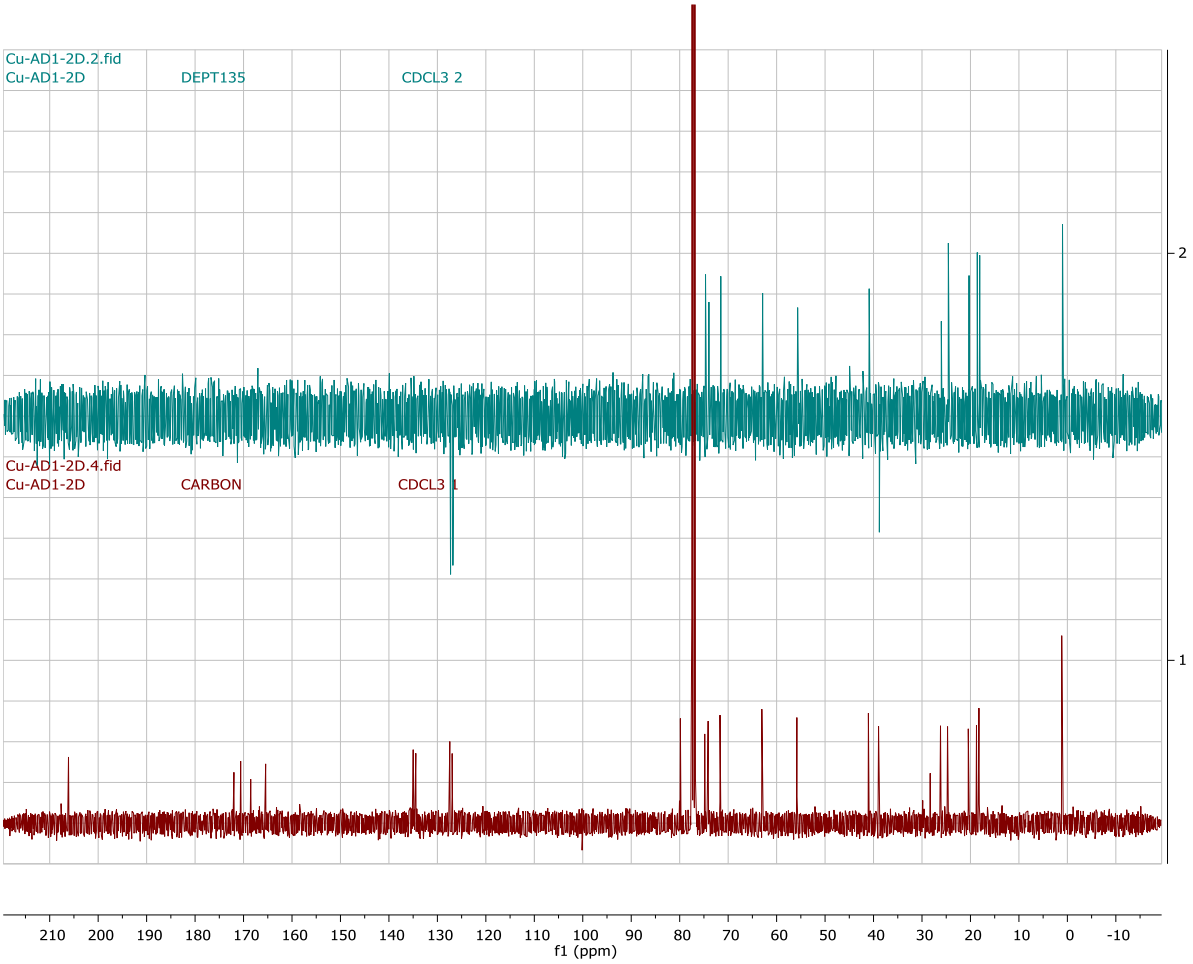

DEPT-135 Spectrum of Calealactone-B

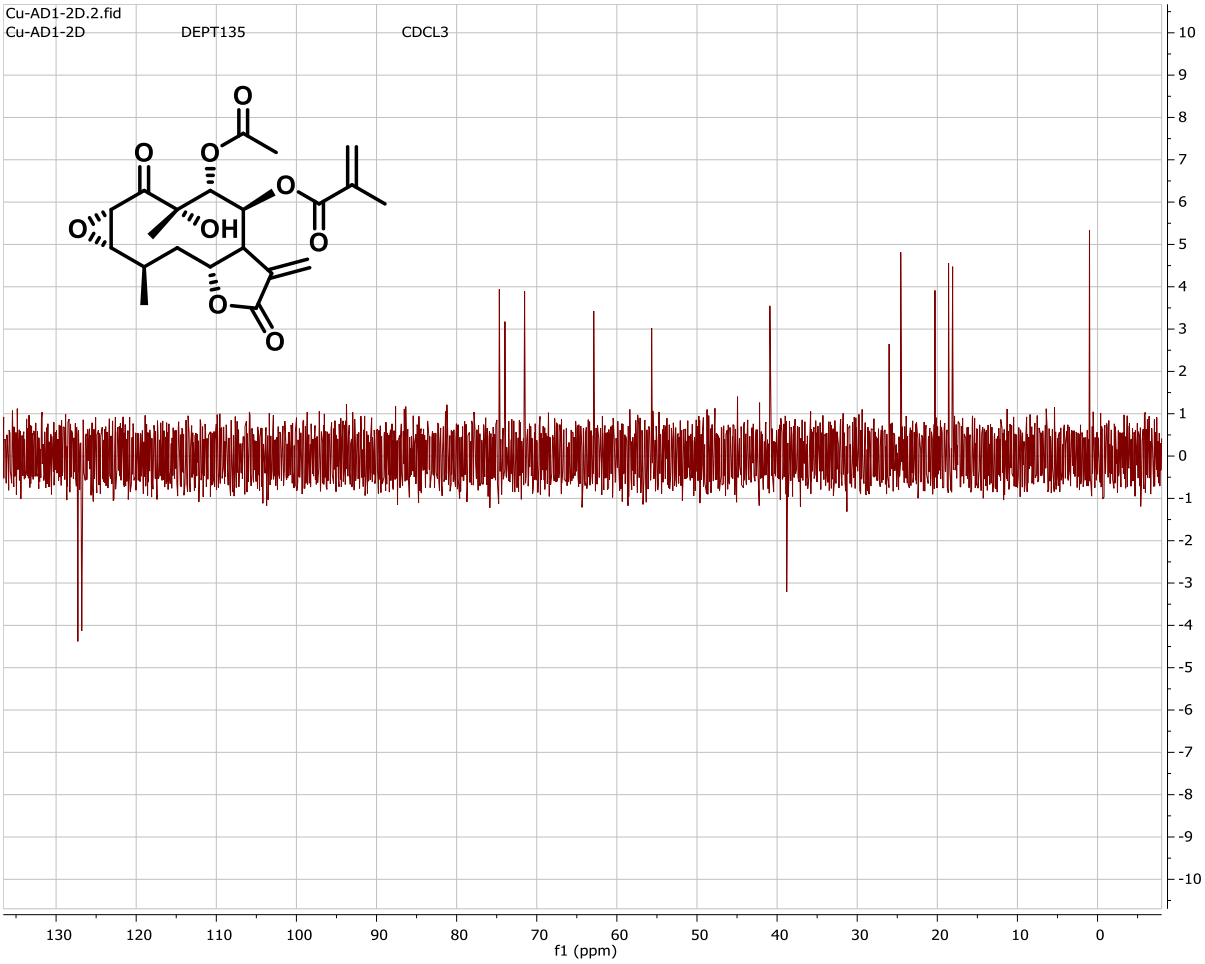

COSY Spectrum of Calealactone-B

HMQC Spectrum of Calealactone-B

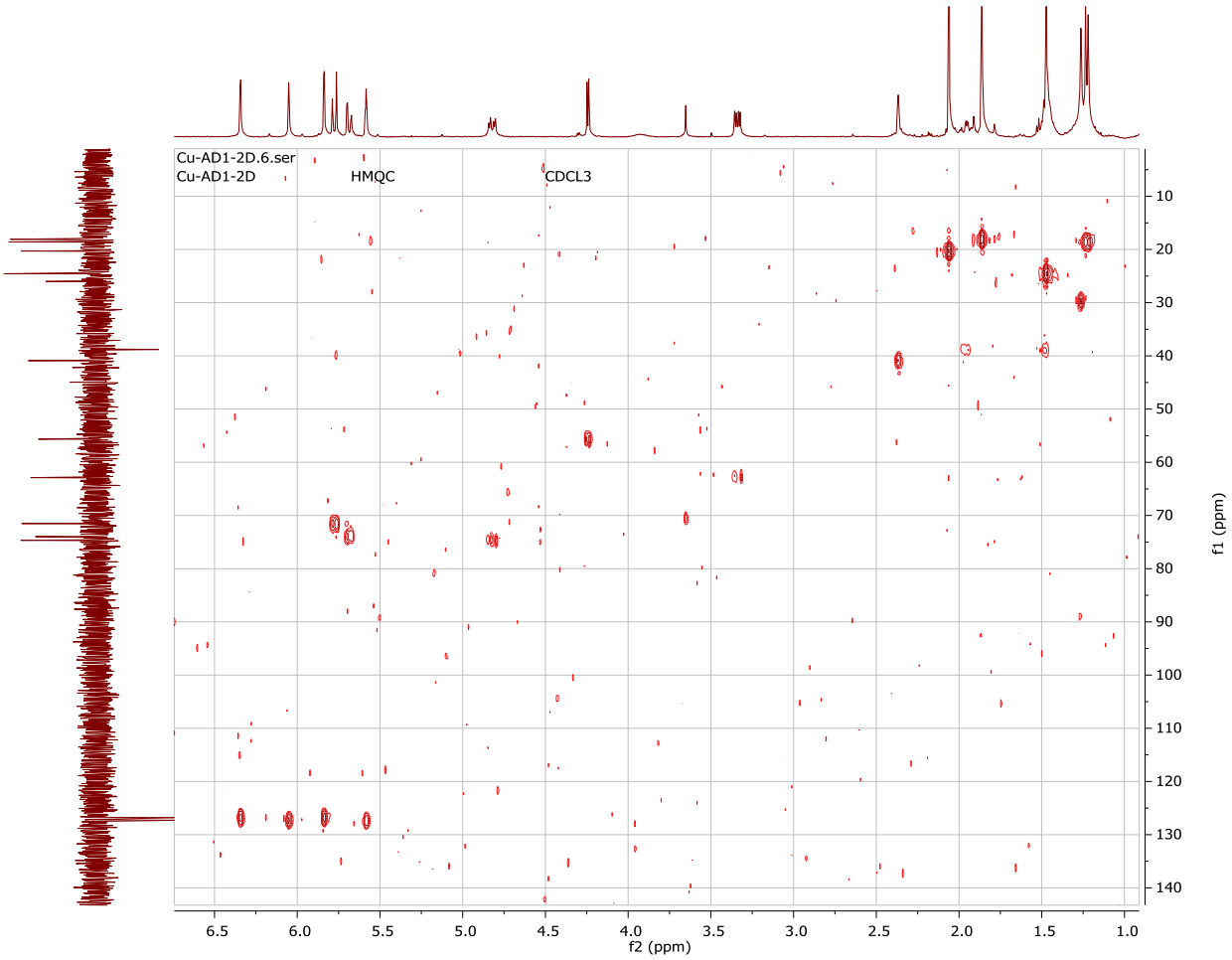

HMBC Spectrum of Calealactone-B

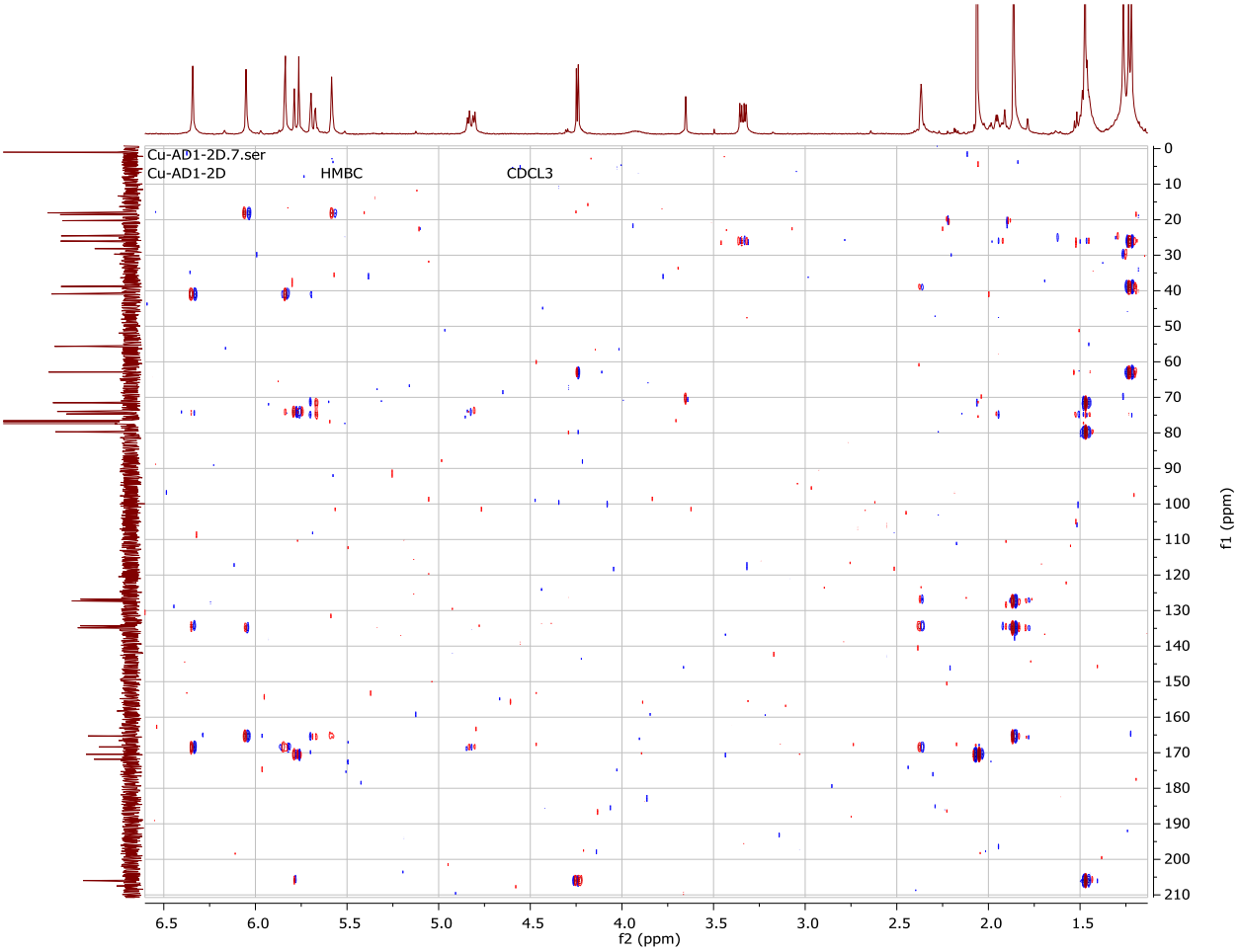

^{1}H-Spectrum of Calein-C

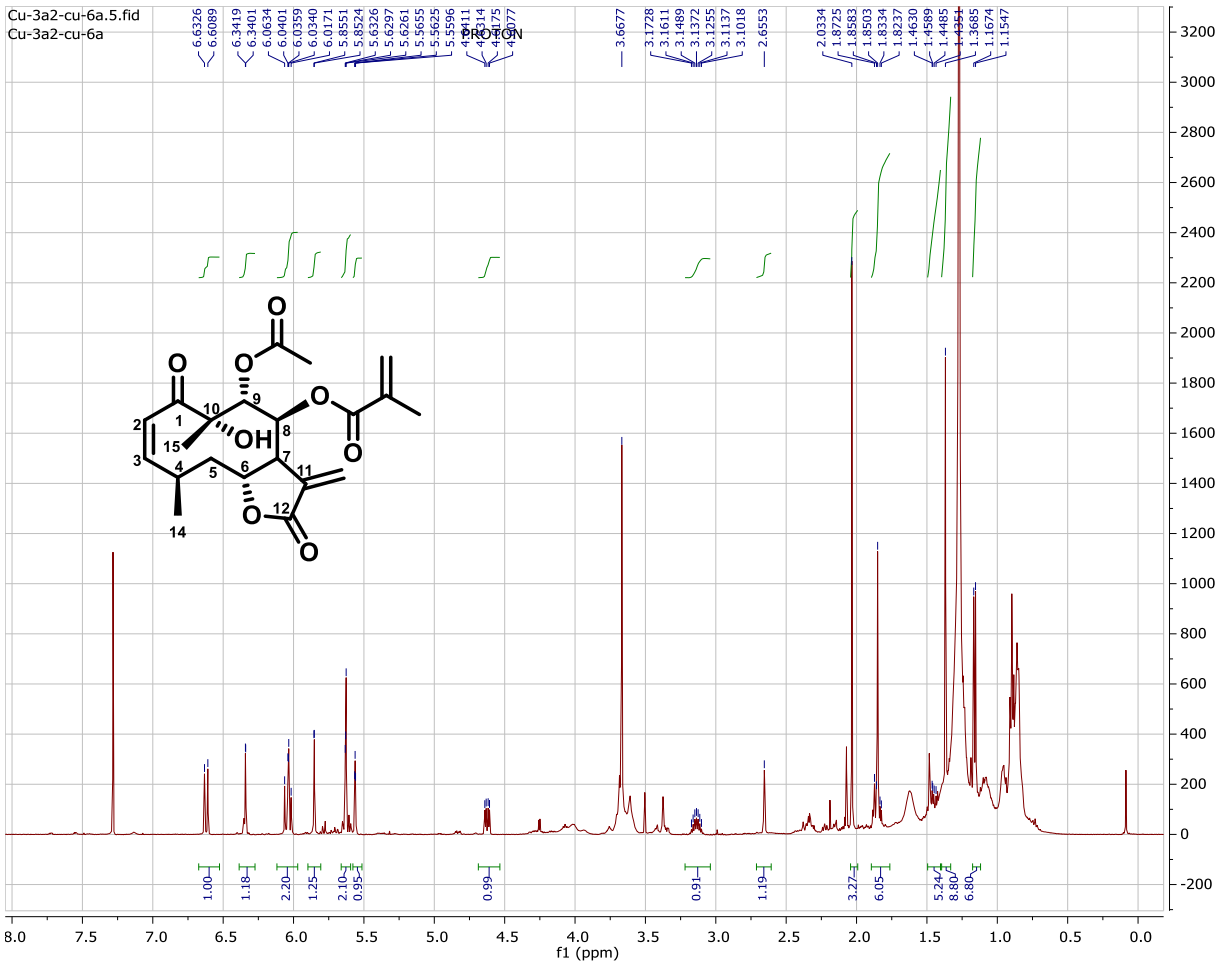

^{13}C-Spectrum of Calein-C

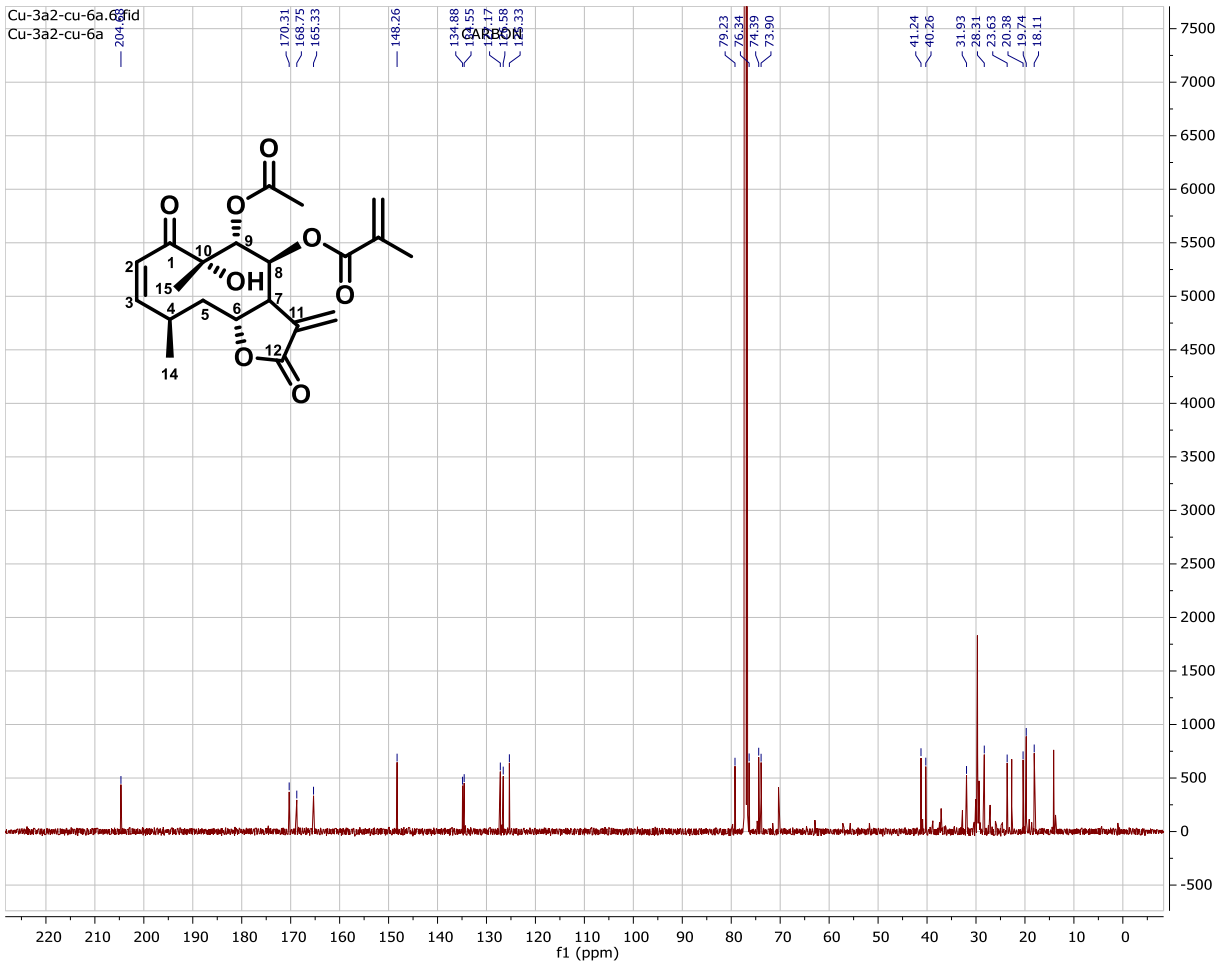

DEPT-135 Spectrum of Calein-C

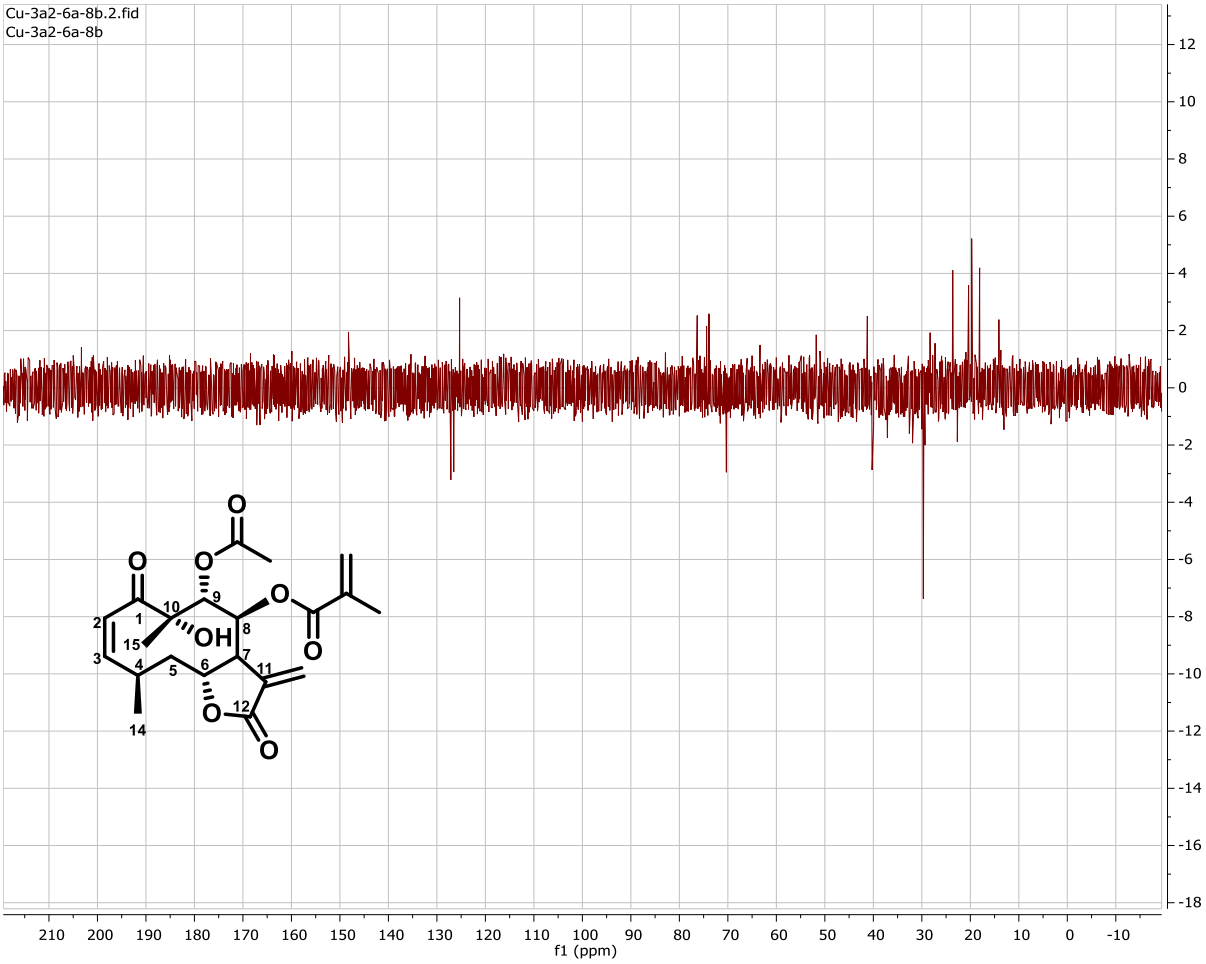

COSY-Spectrum of Calein-C

HMQC-Spectrum of Calein-C

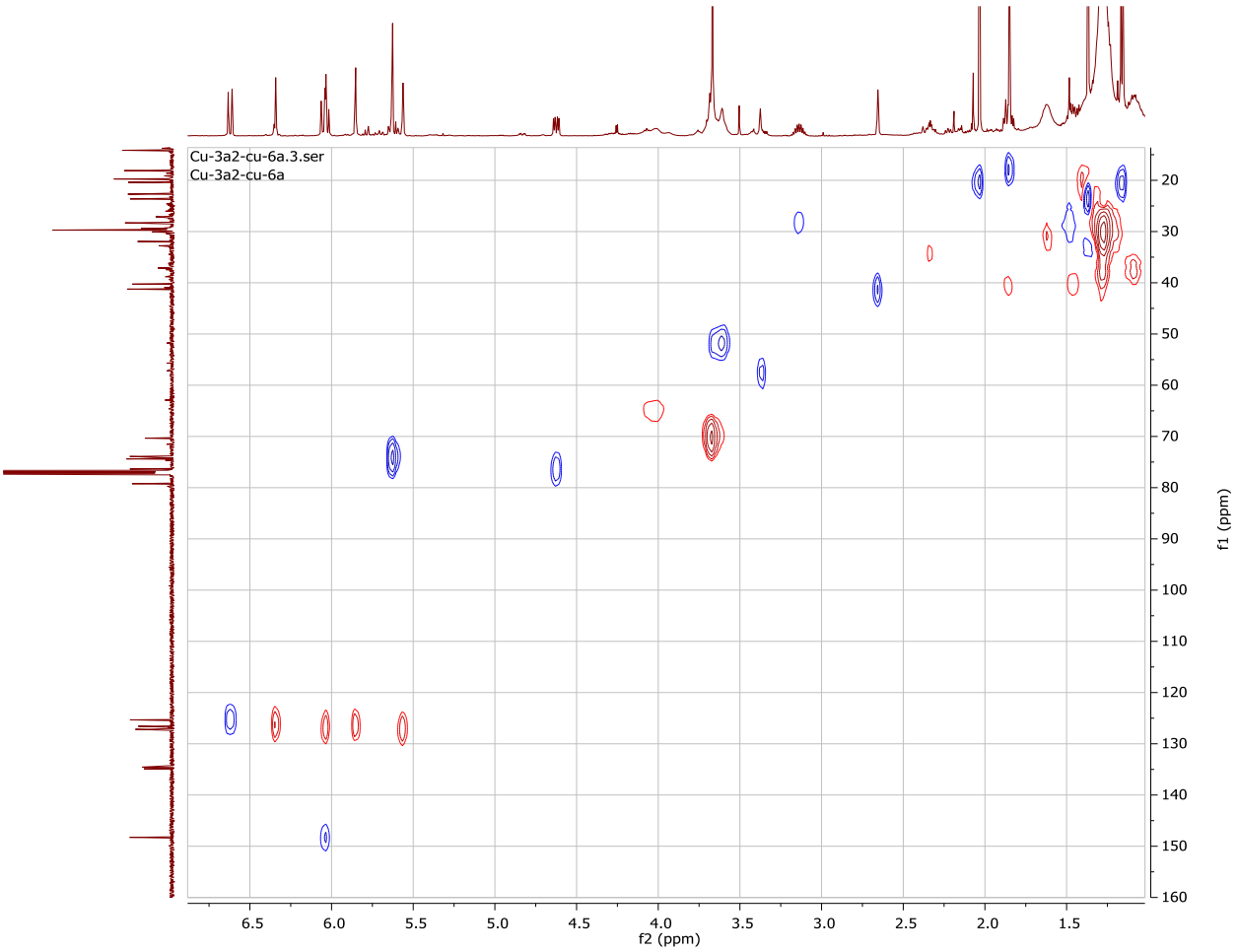

HMBC-Spectrum of Calein-C

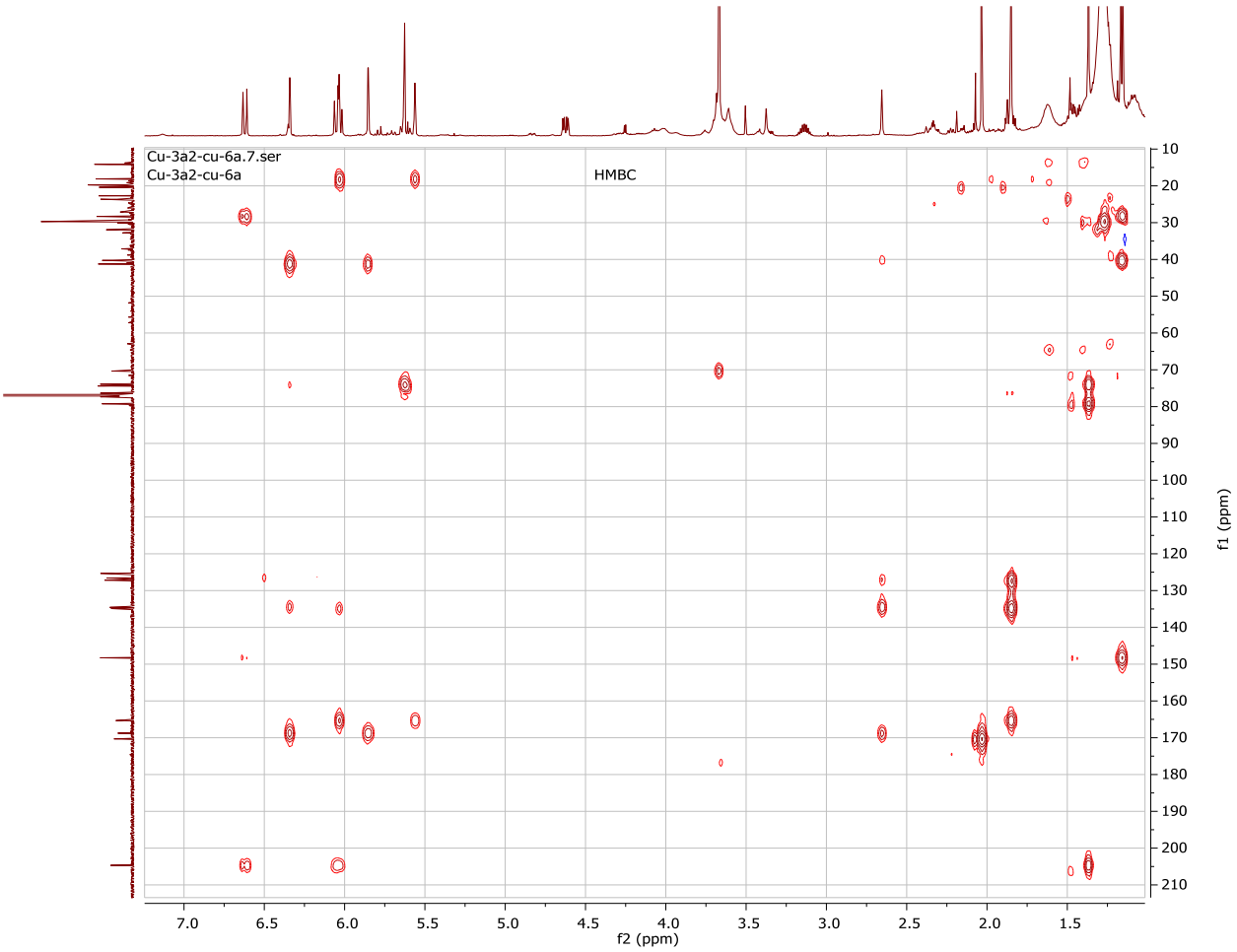

NOESY-Spectrum of Calein-C

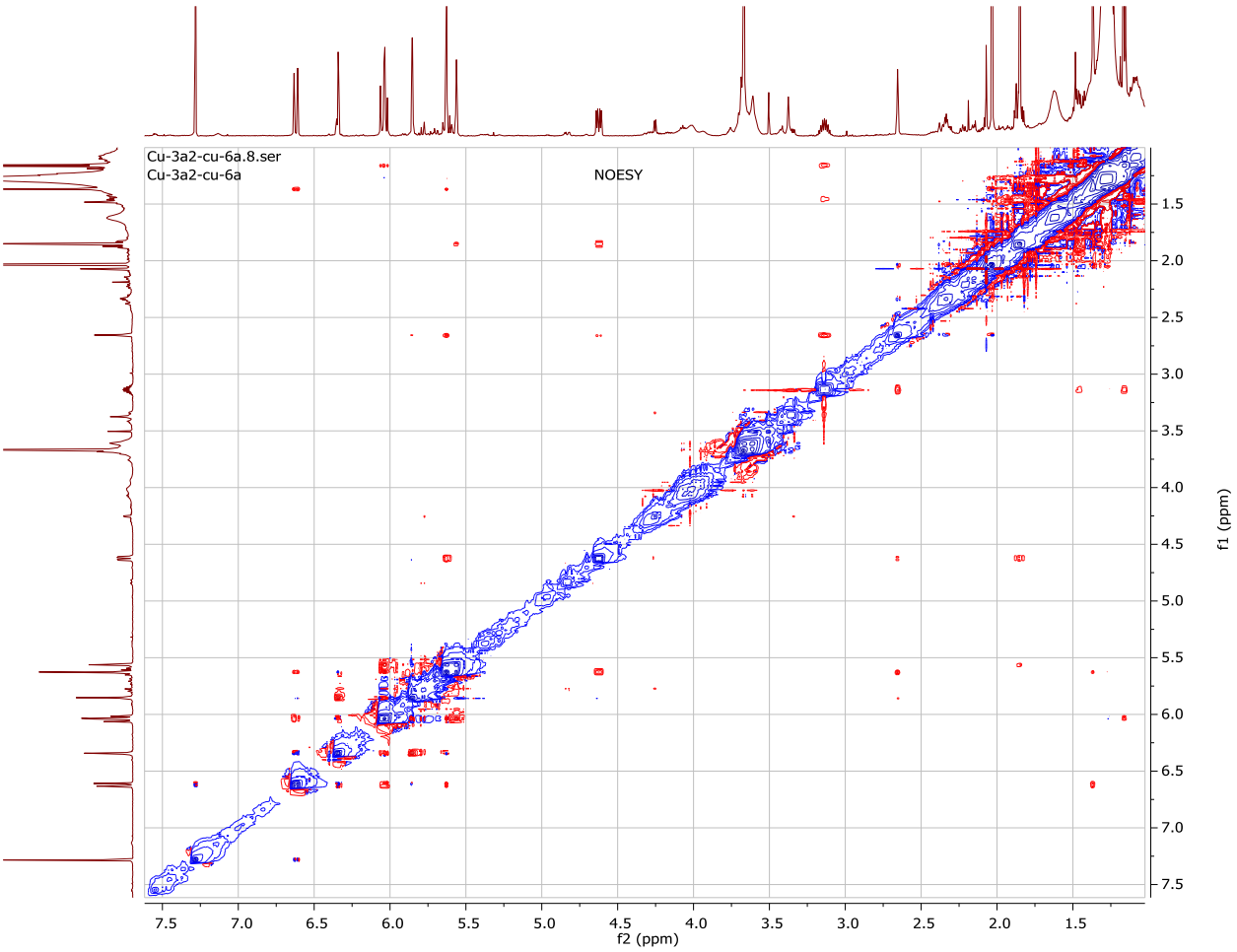

^{1}H-NMR Spectrum of Compound 1a

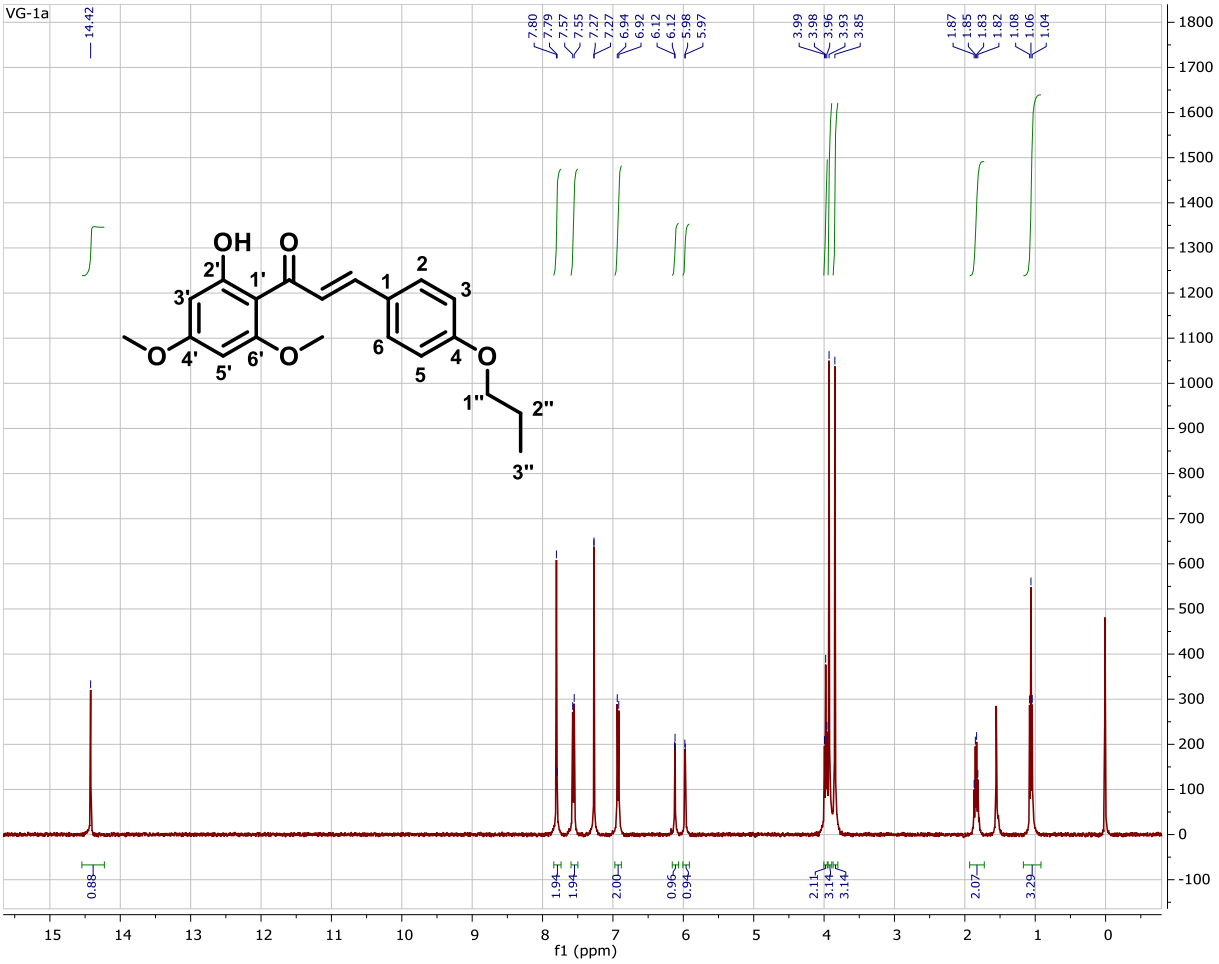

^{13}C-Spectrum of Compound 1a

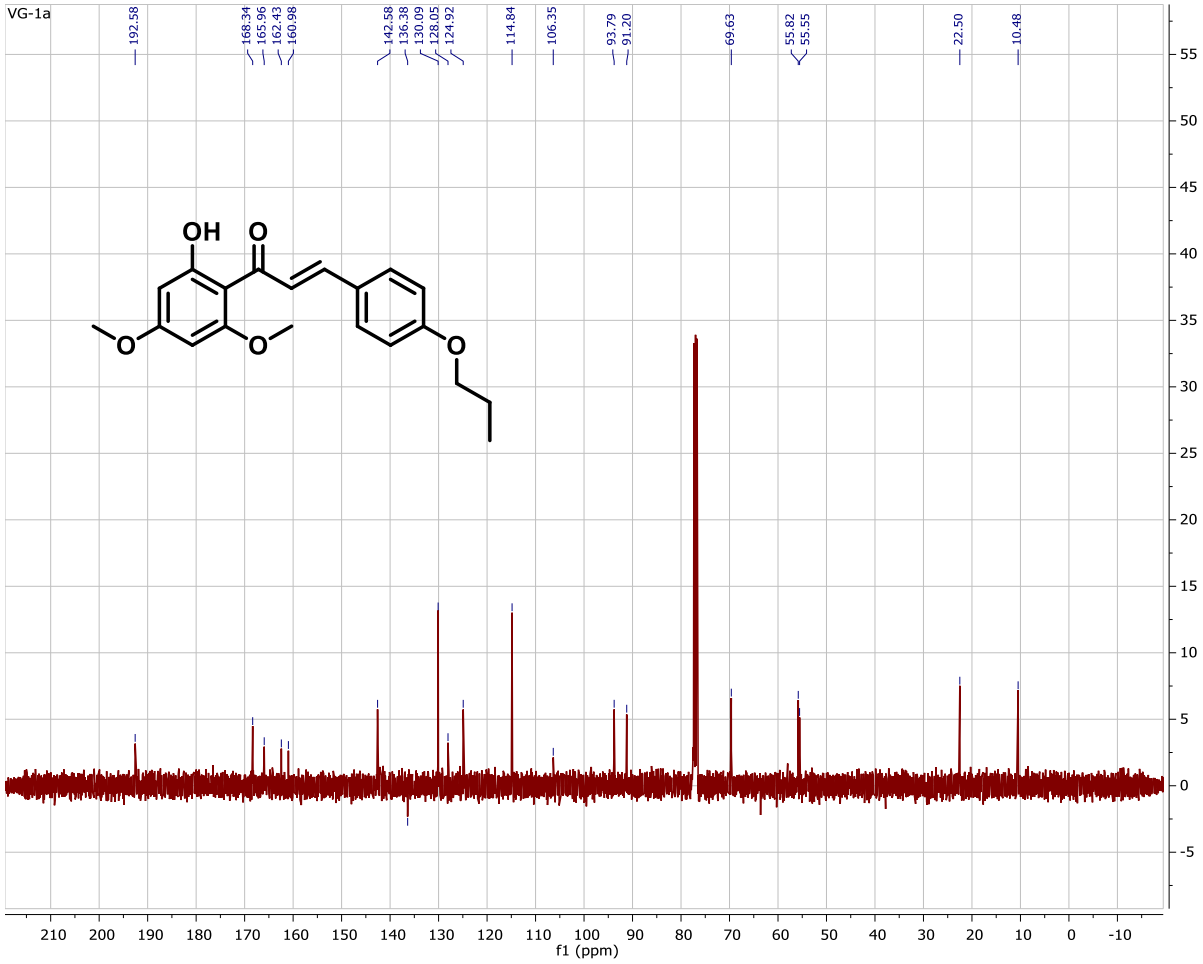

DEPT Spectrum of Compound 1a

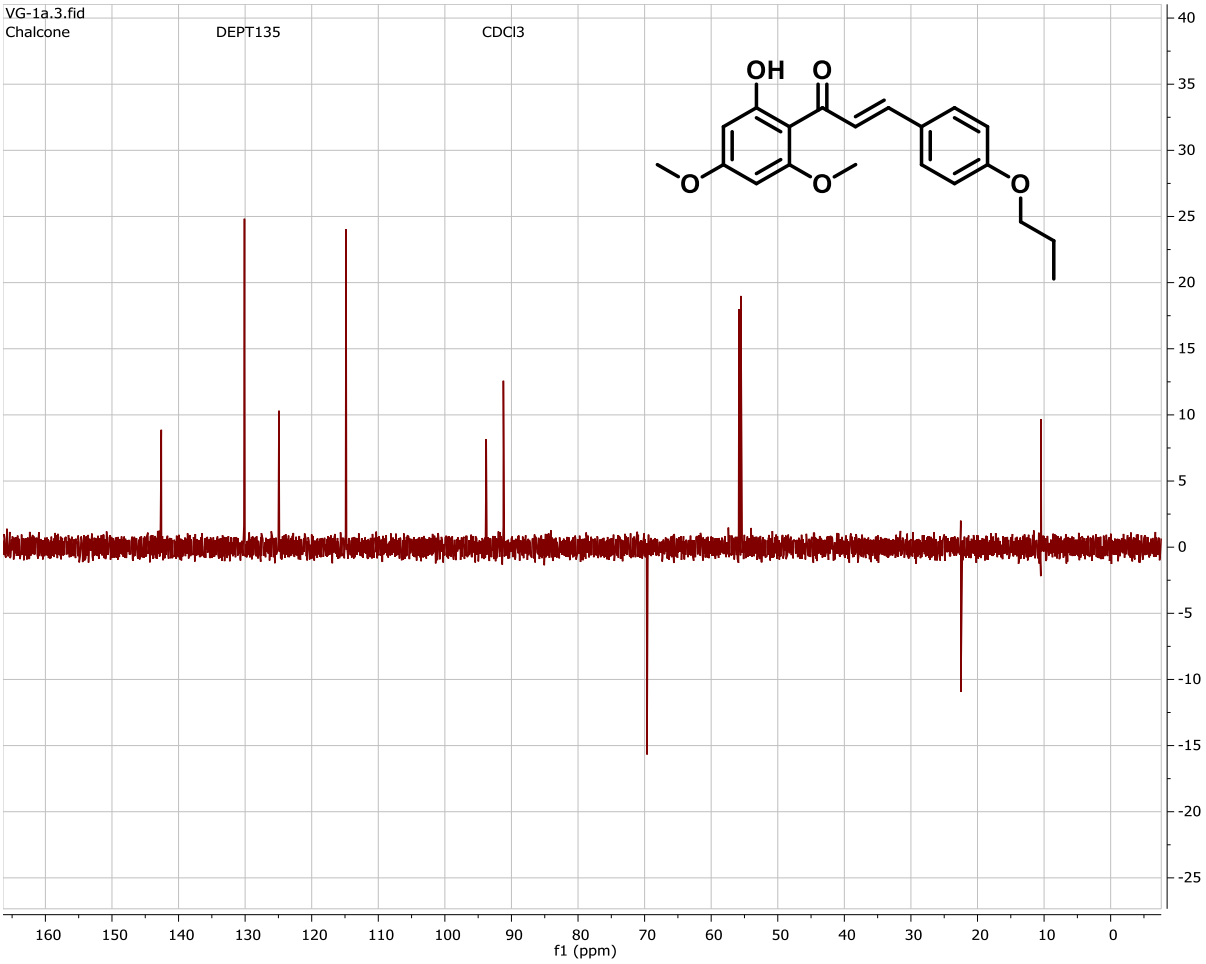

^{1}H-Spectrum of Compound 1b

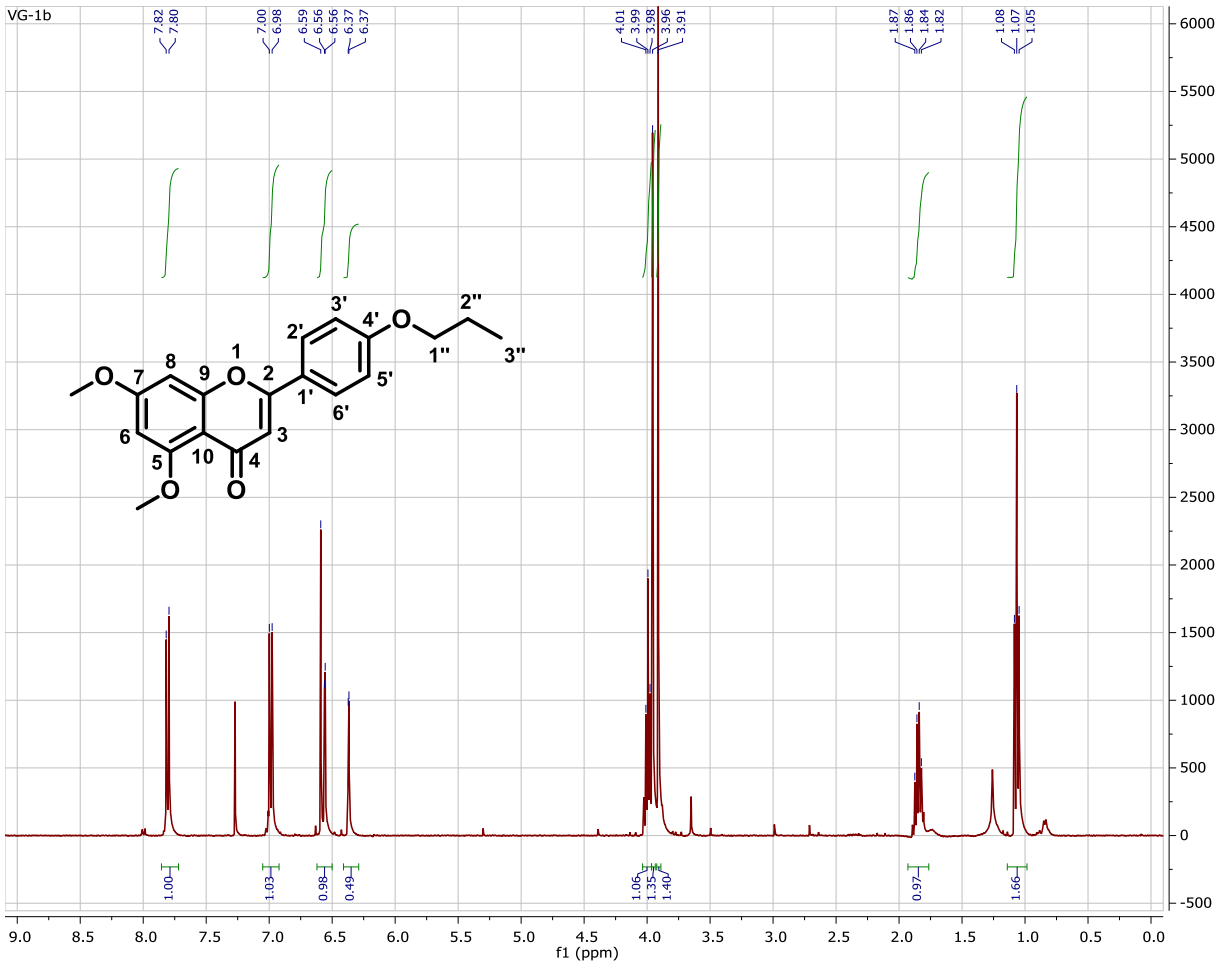

^{13}C-Spectrum of Compound 1b

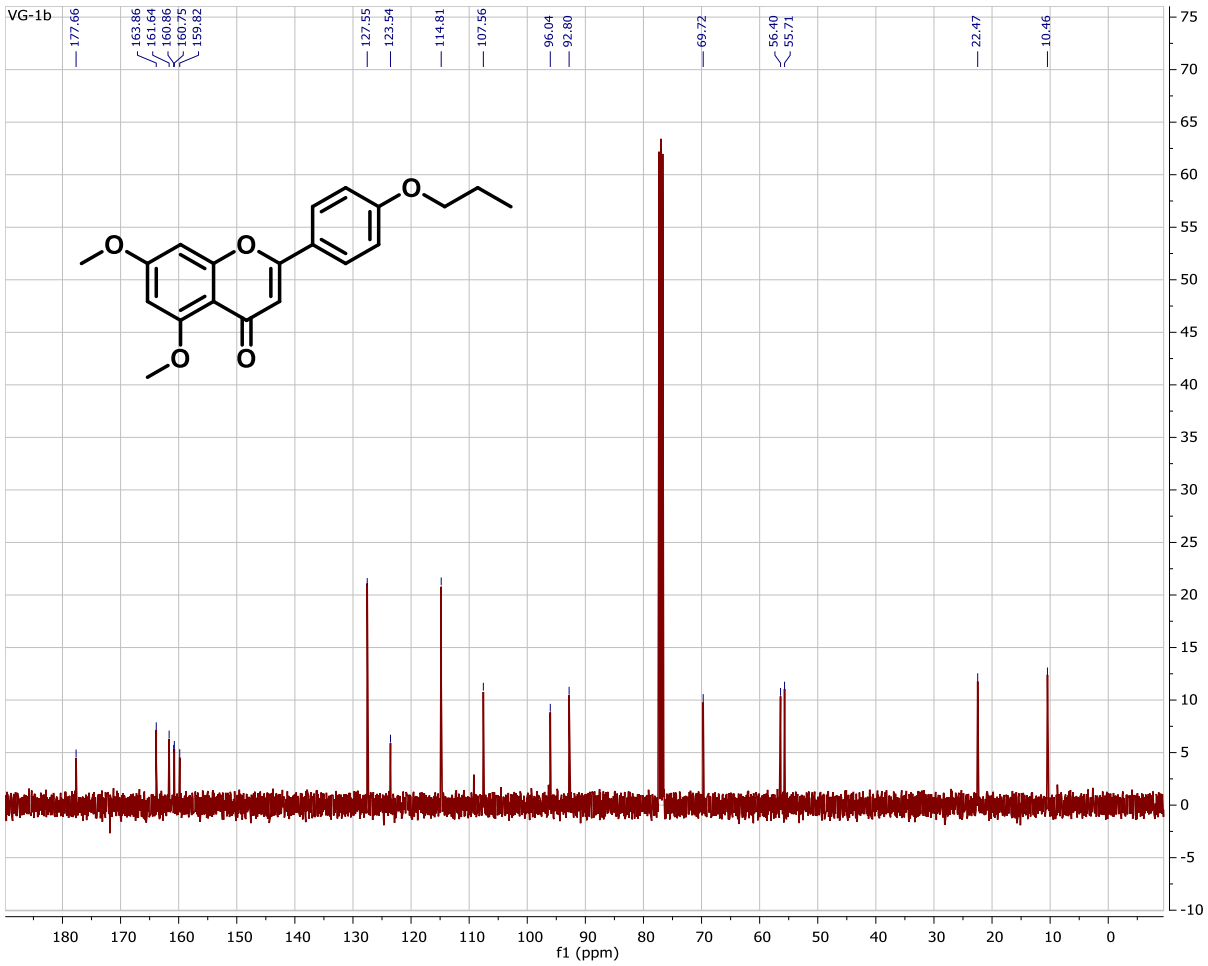

DEPT-135 Spectrum of Compound 1b

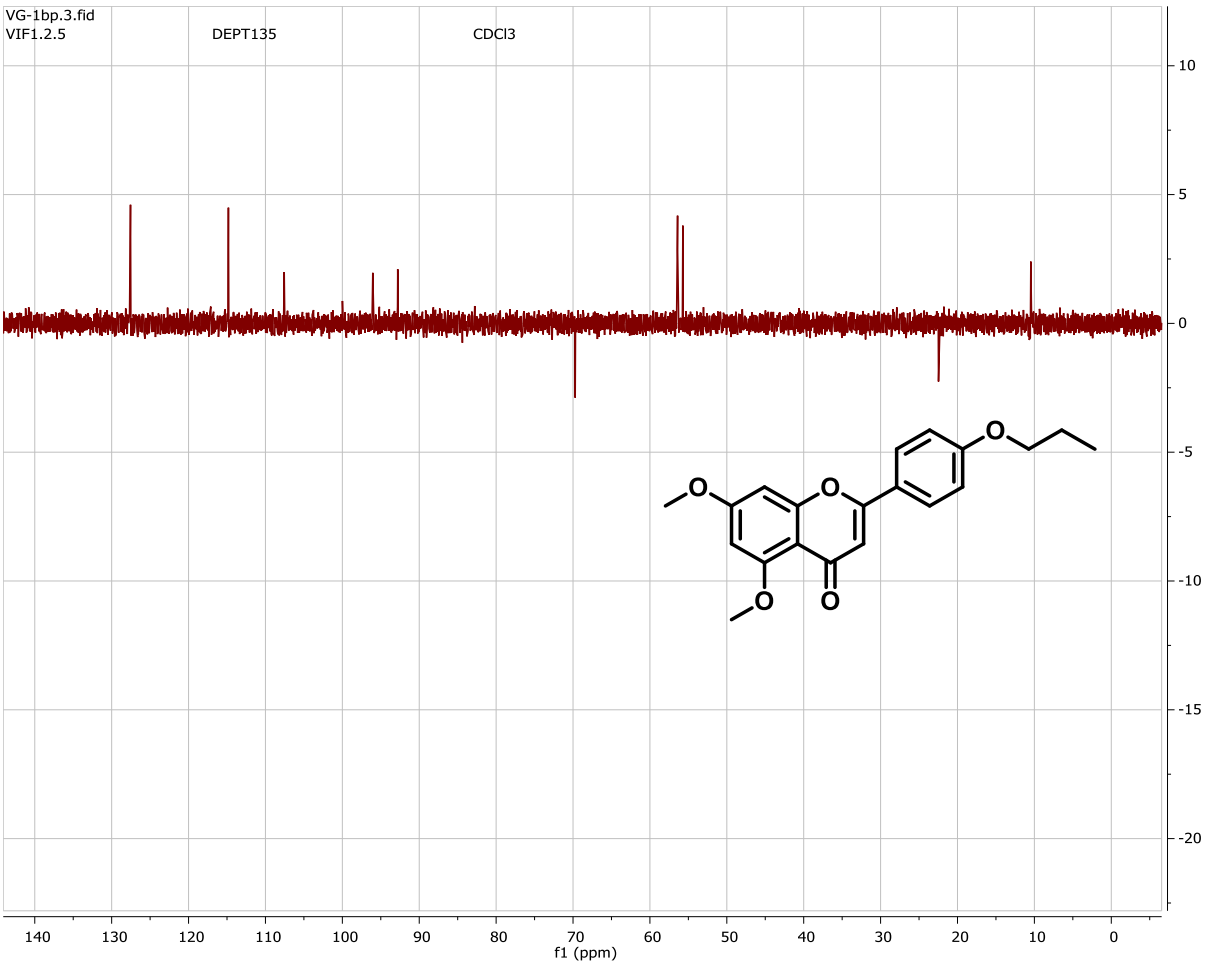

^{1}H-Spectrum of Compound 1c

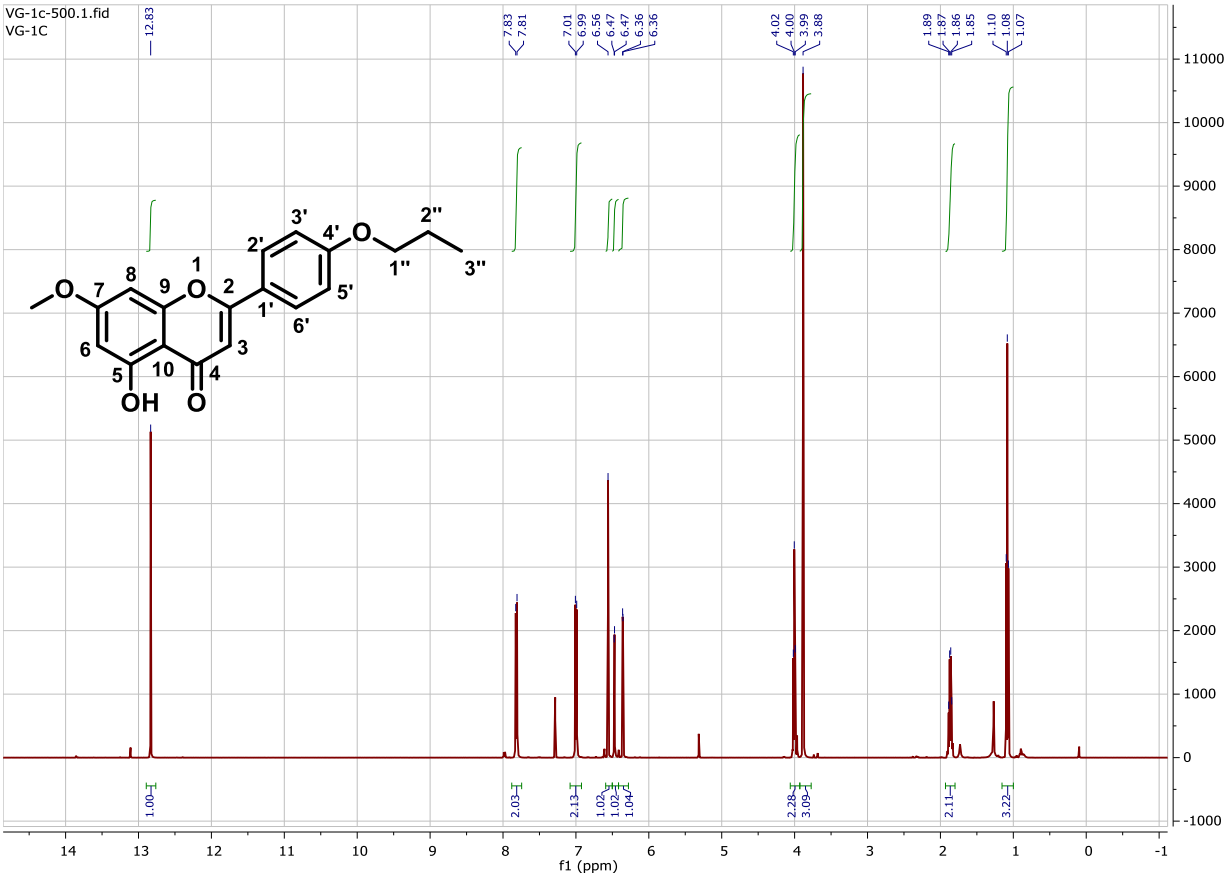

^{13}C-Spectrum of Compound 1c

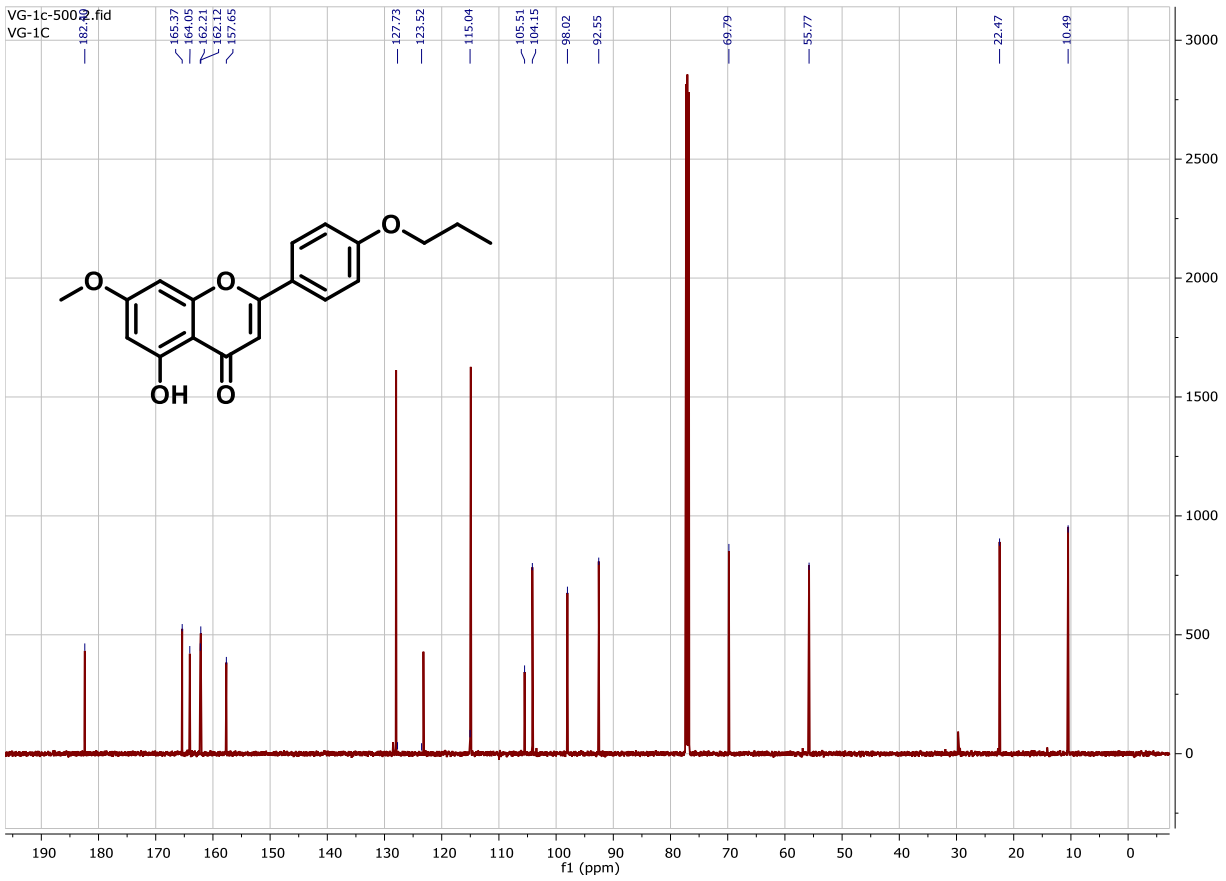

DEPT-135 and ^{13}C-Spectra of Compound 1c

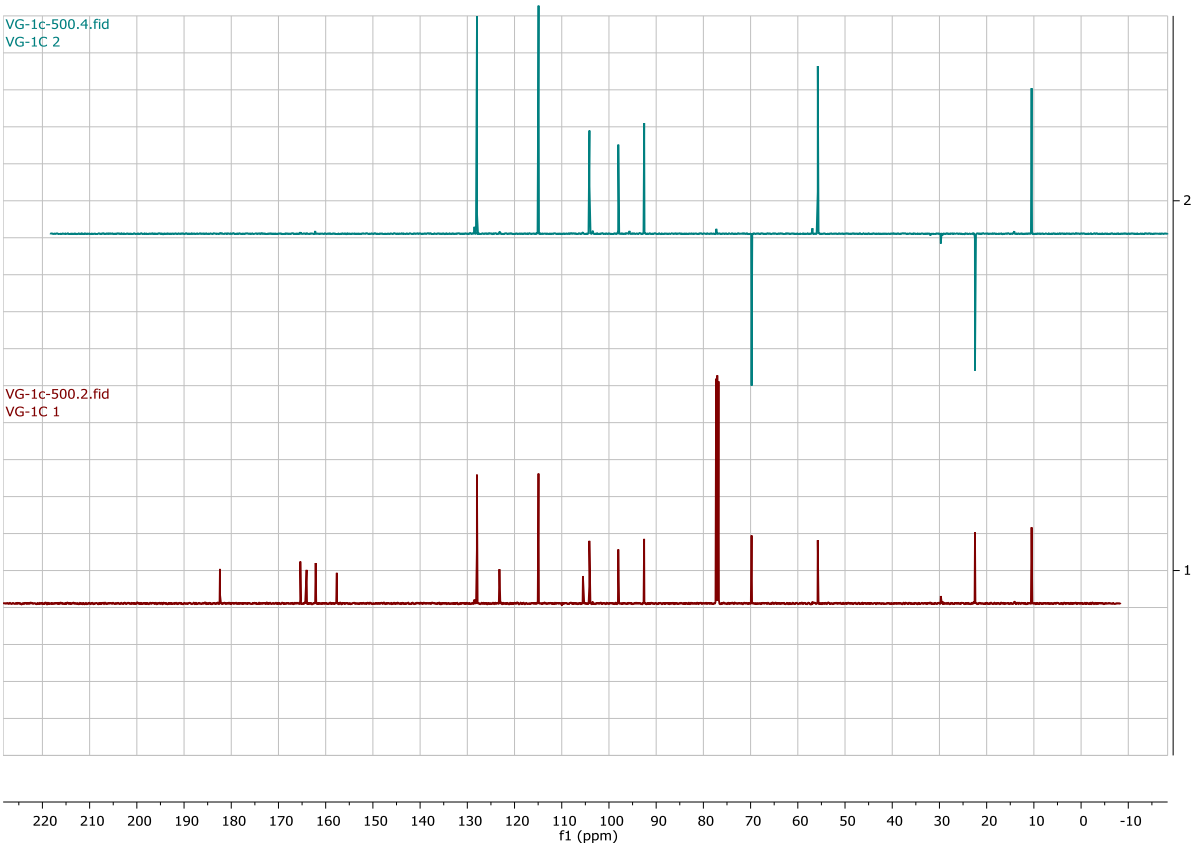

DEPT-135 Spectrum of Compound 1c

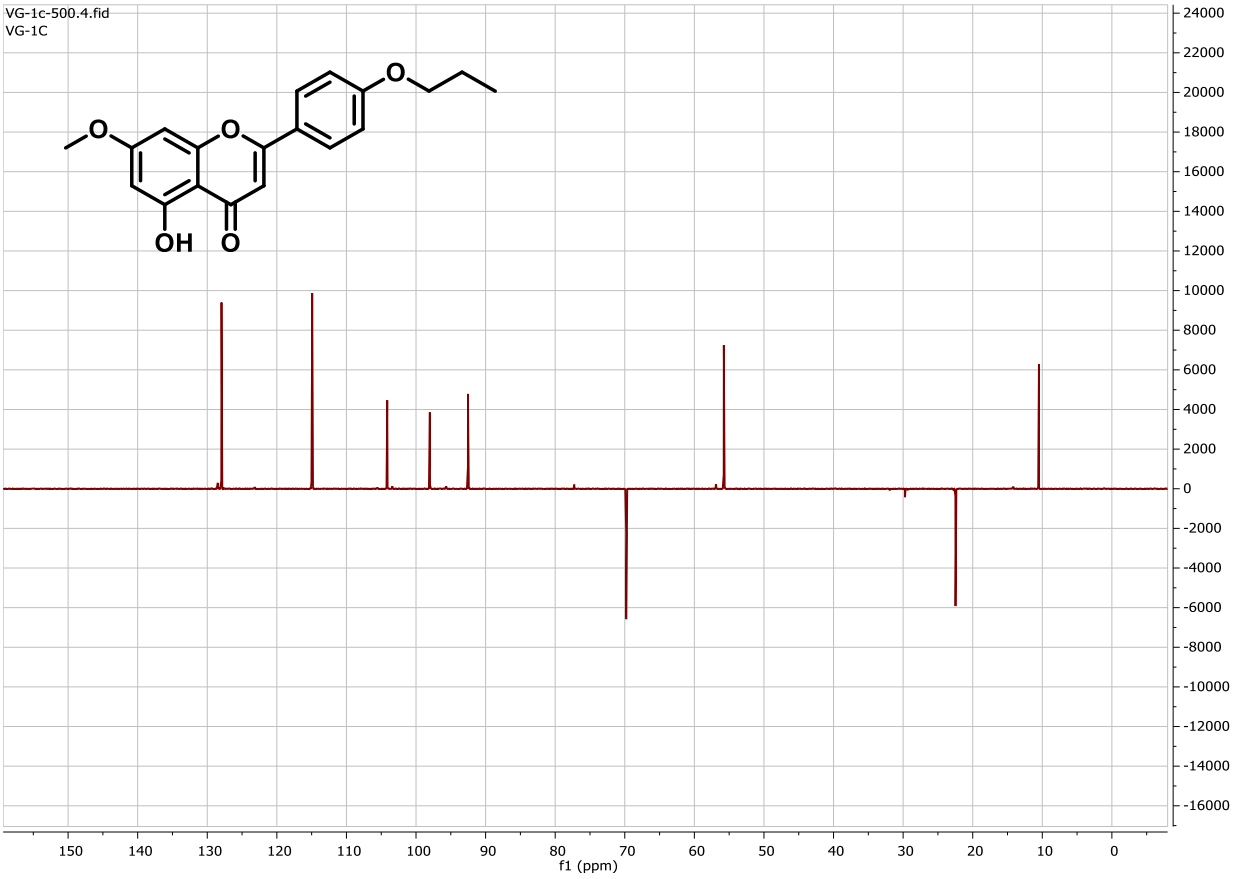

HSQC Spectrum of Compound 1c

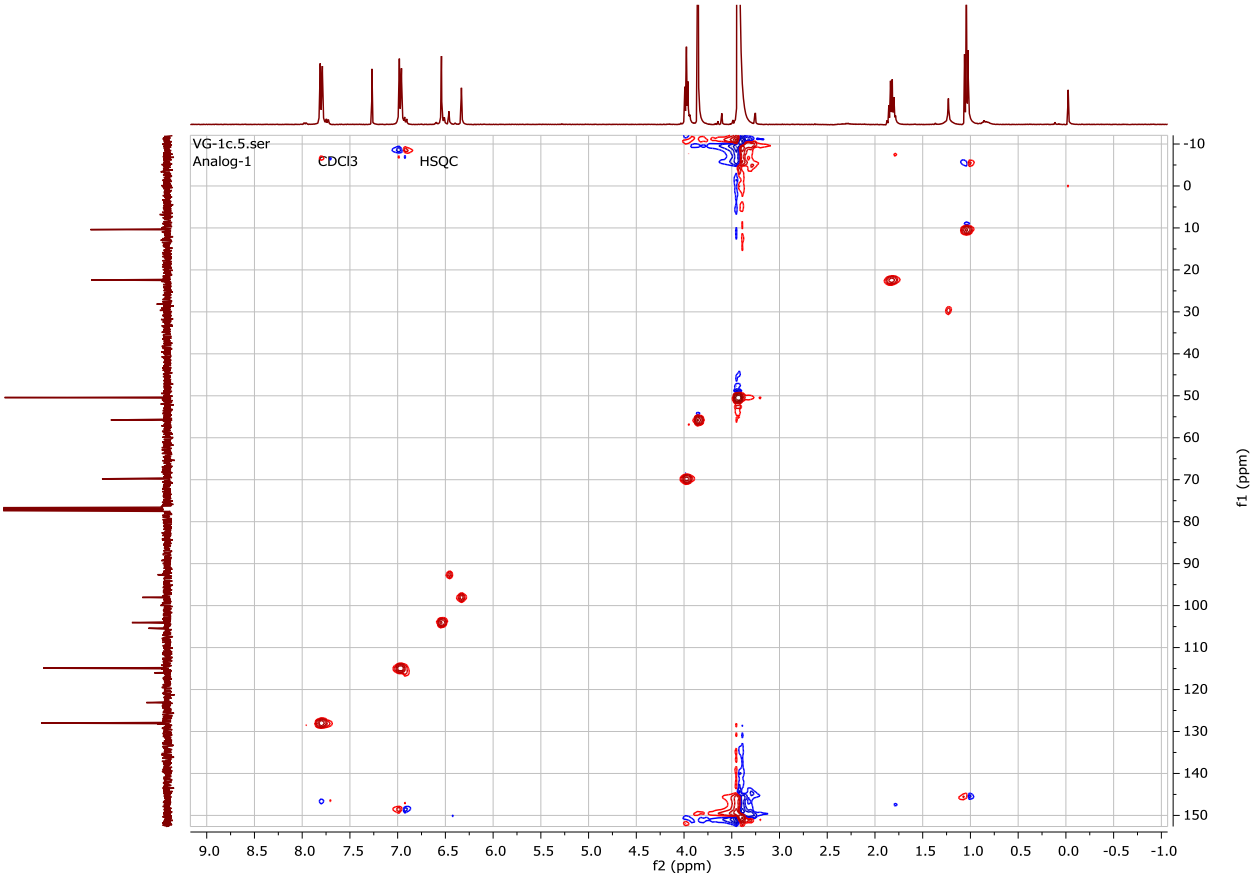

HMBC Spectrum of Compound 1c

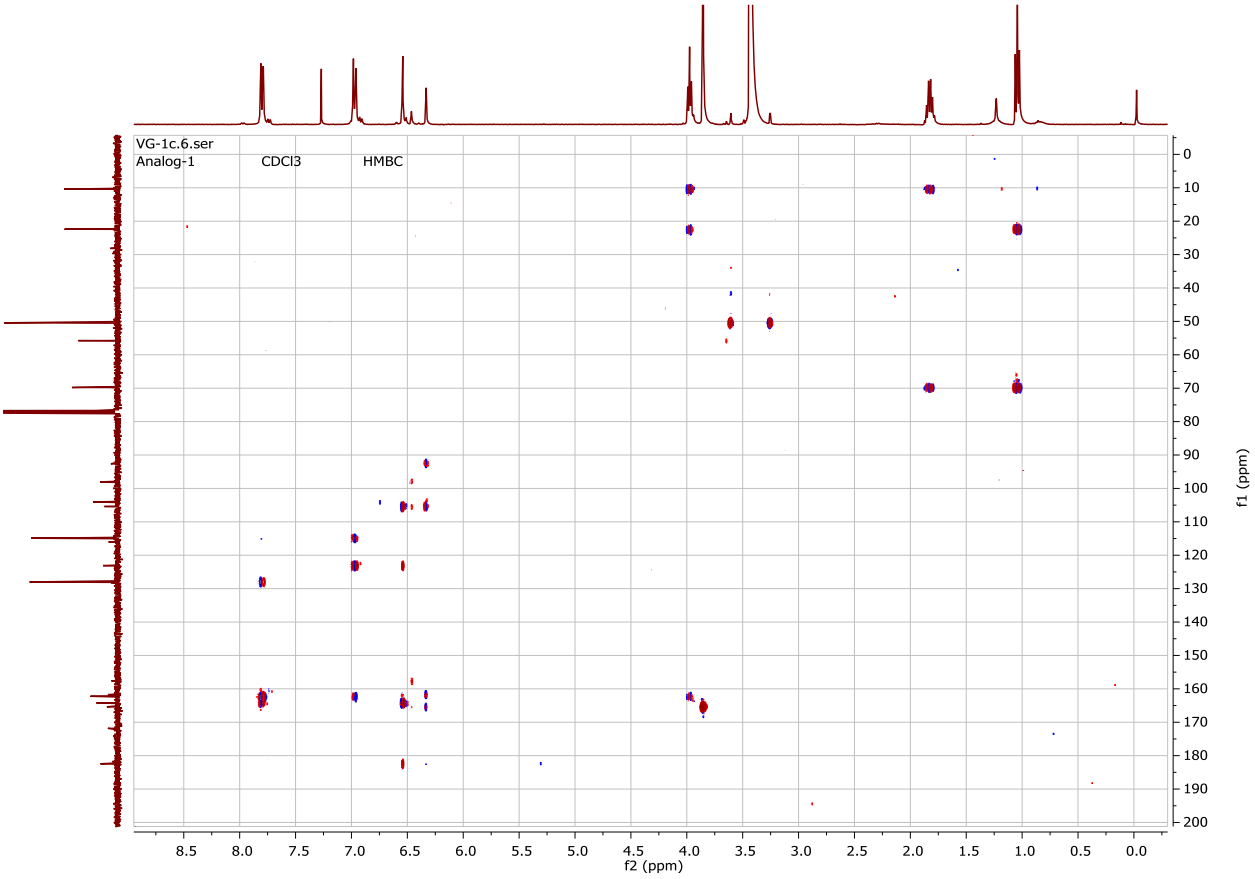

^{1}H-Spectrum of Compound 2a

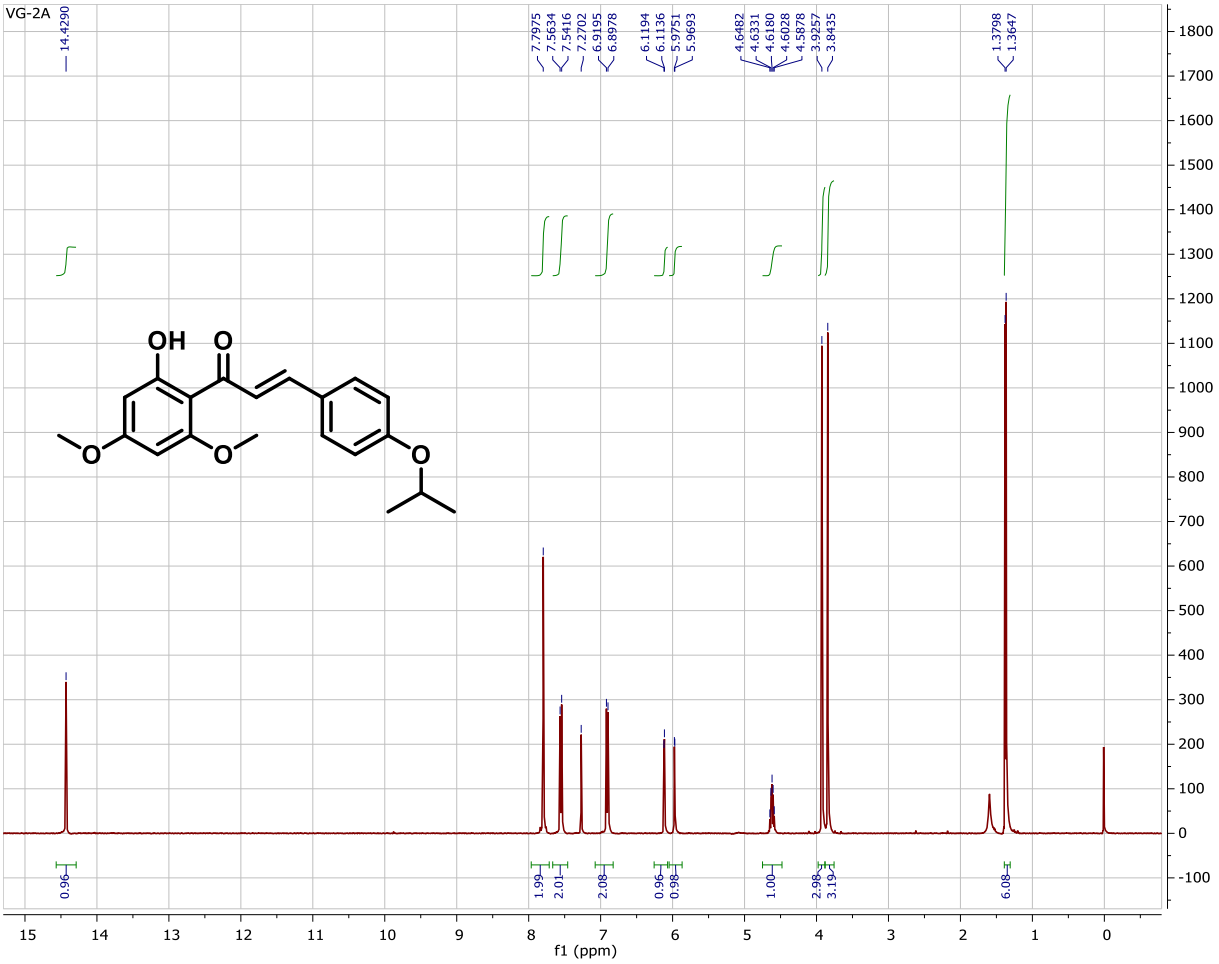

^{13}C-Spectrum of Compound 2a

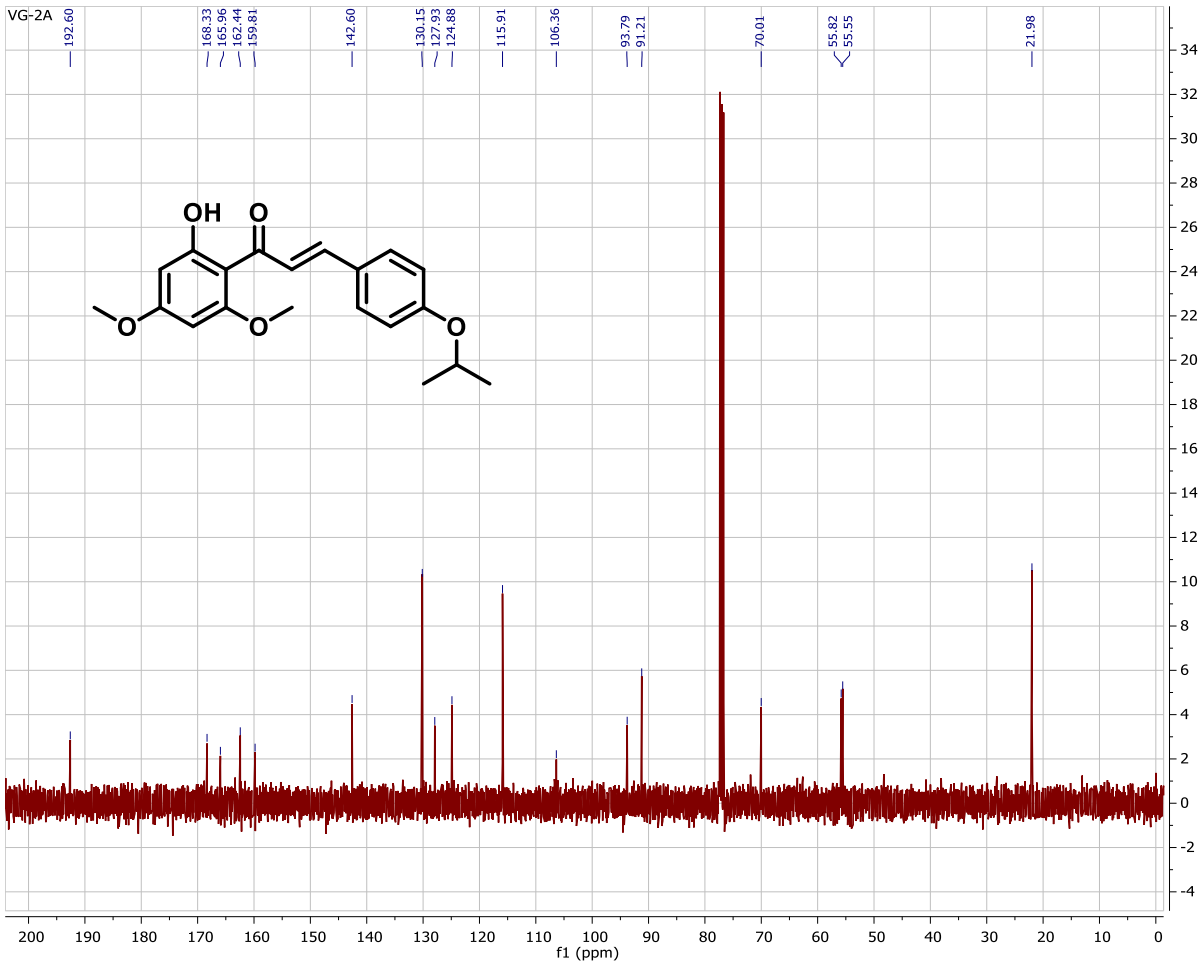

DEPT-135 Spectrum of Compound 2a

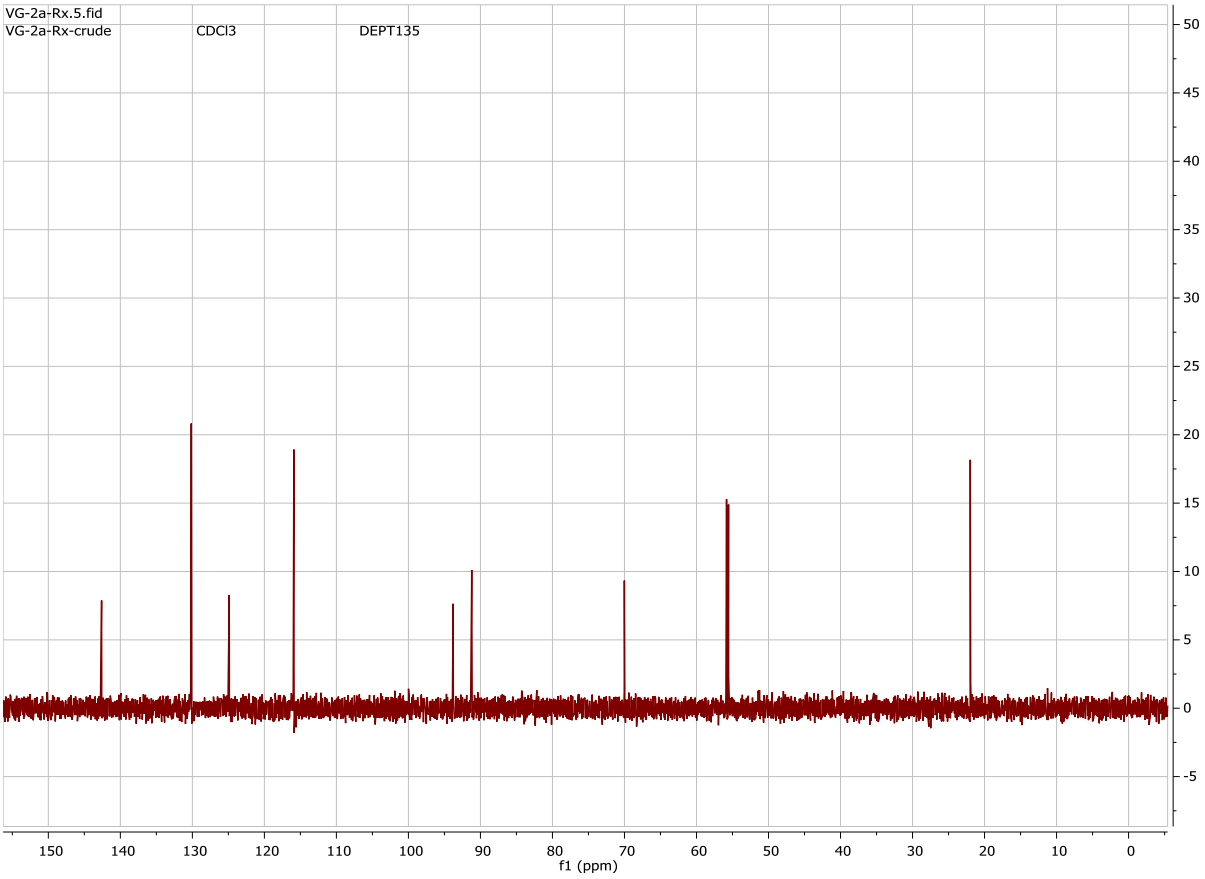

^{1}H-Spectrum of Compound 2b

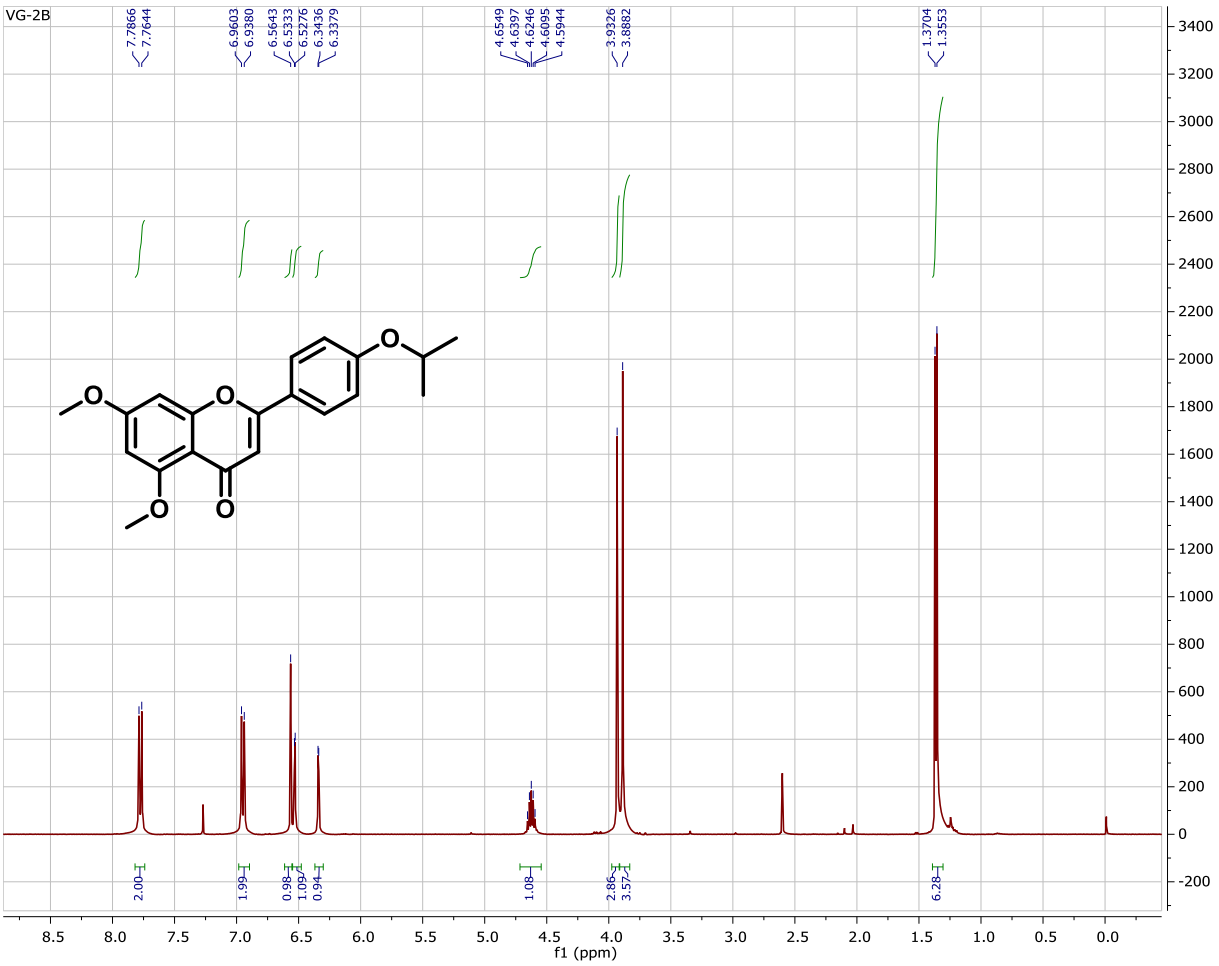

^{13}C-Spectrum of Compound 2b

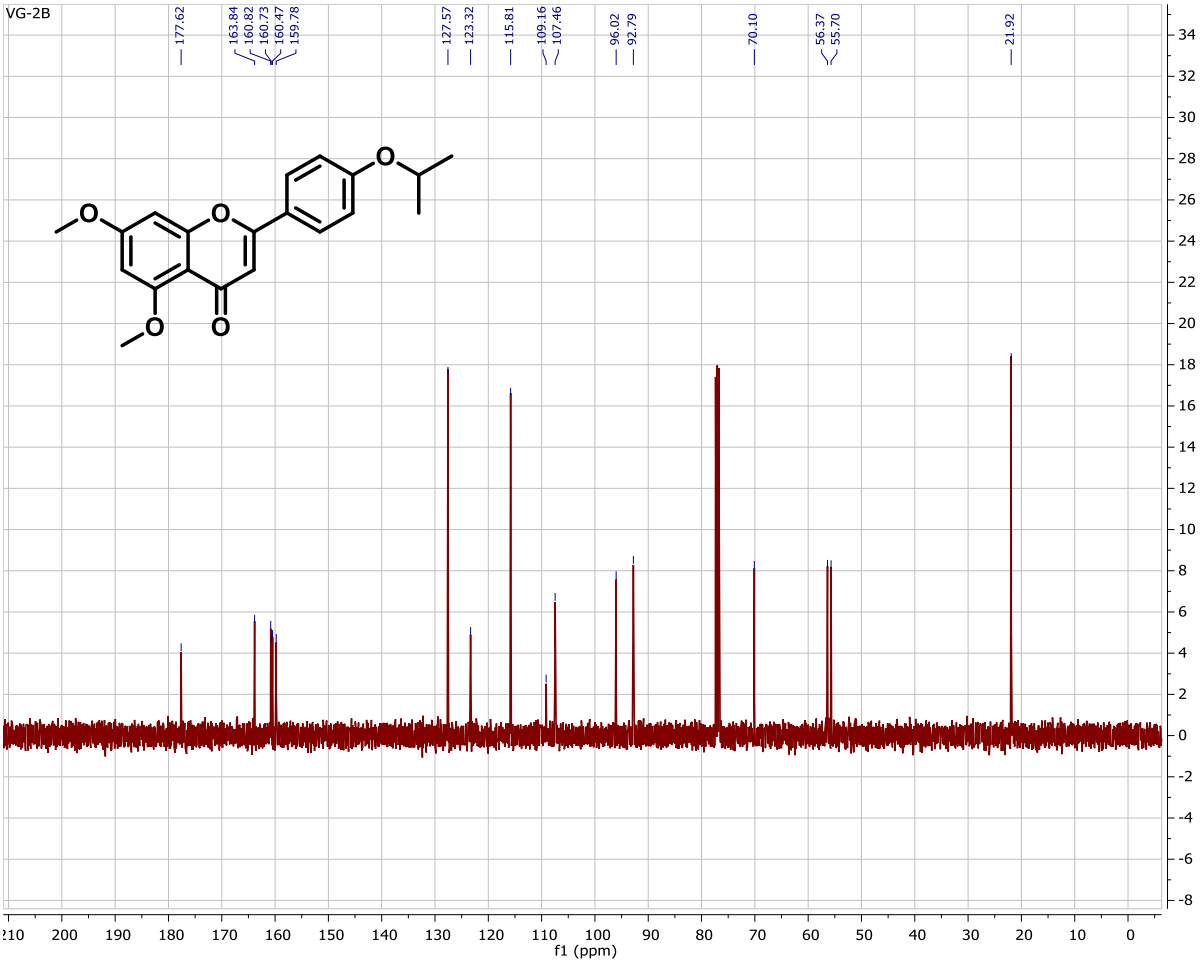

DEPT-135 Spectrum of Compound 2b

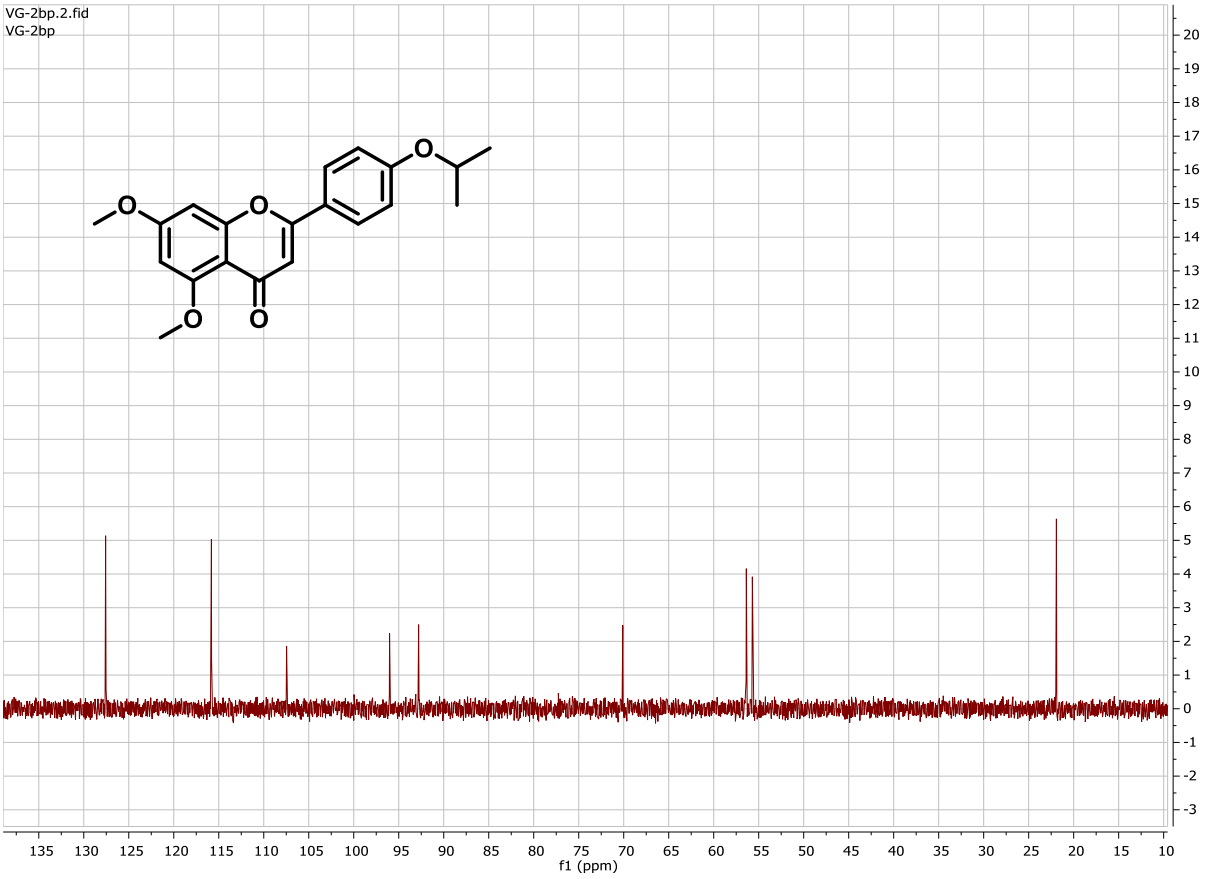

^{1}H-Spectrum of Compound 2c

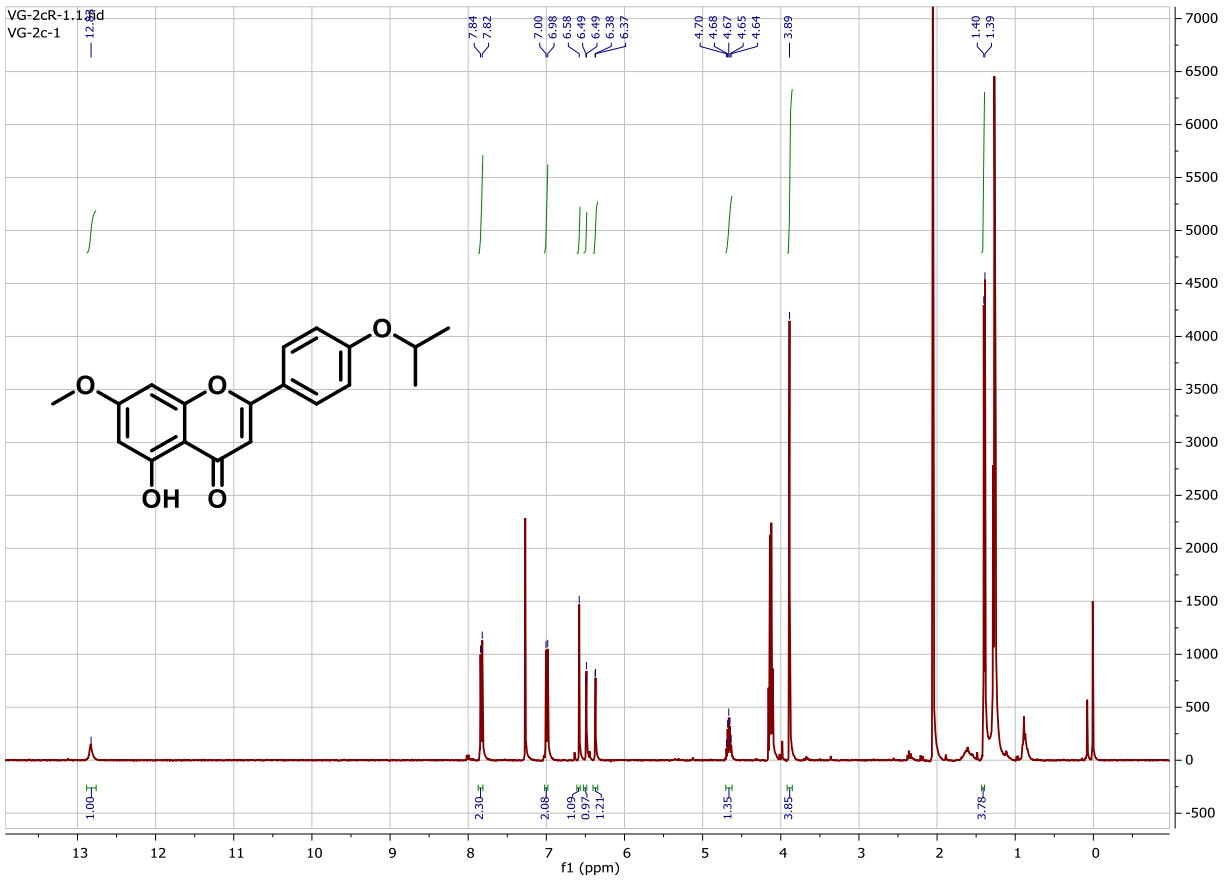

^{13}C-Spectrum of Compound 2c

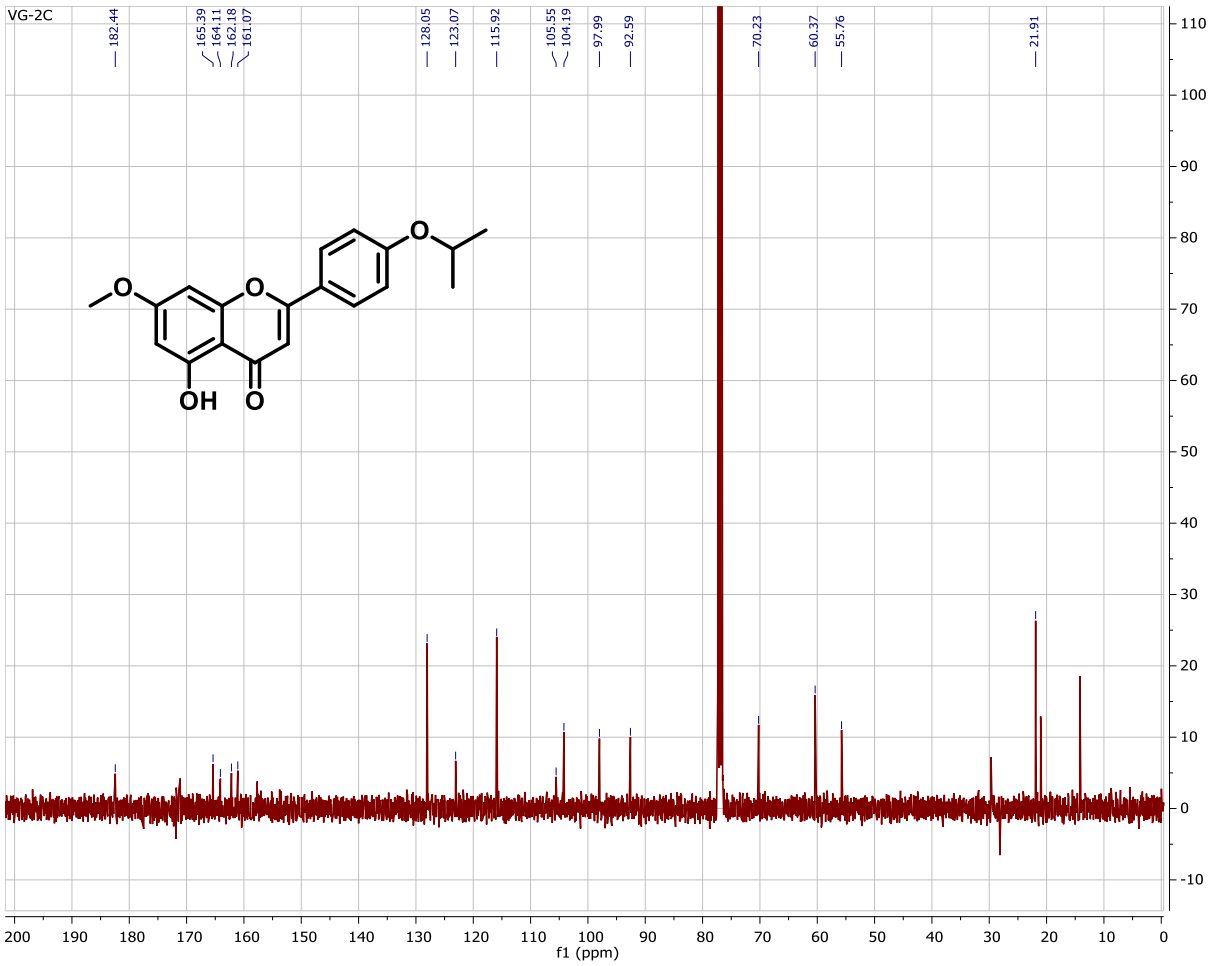

DEPT-135 Spectrum of Compound 2c

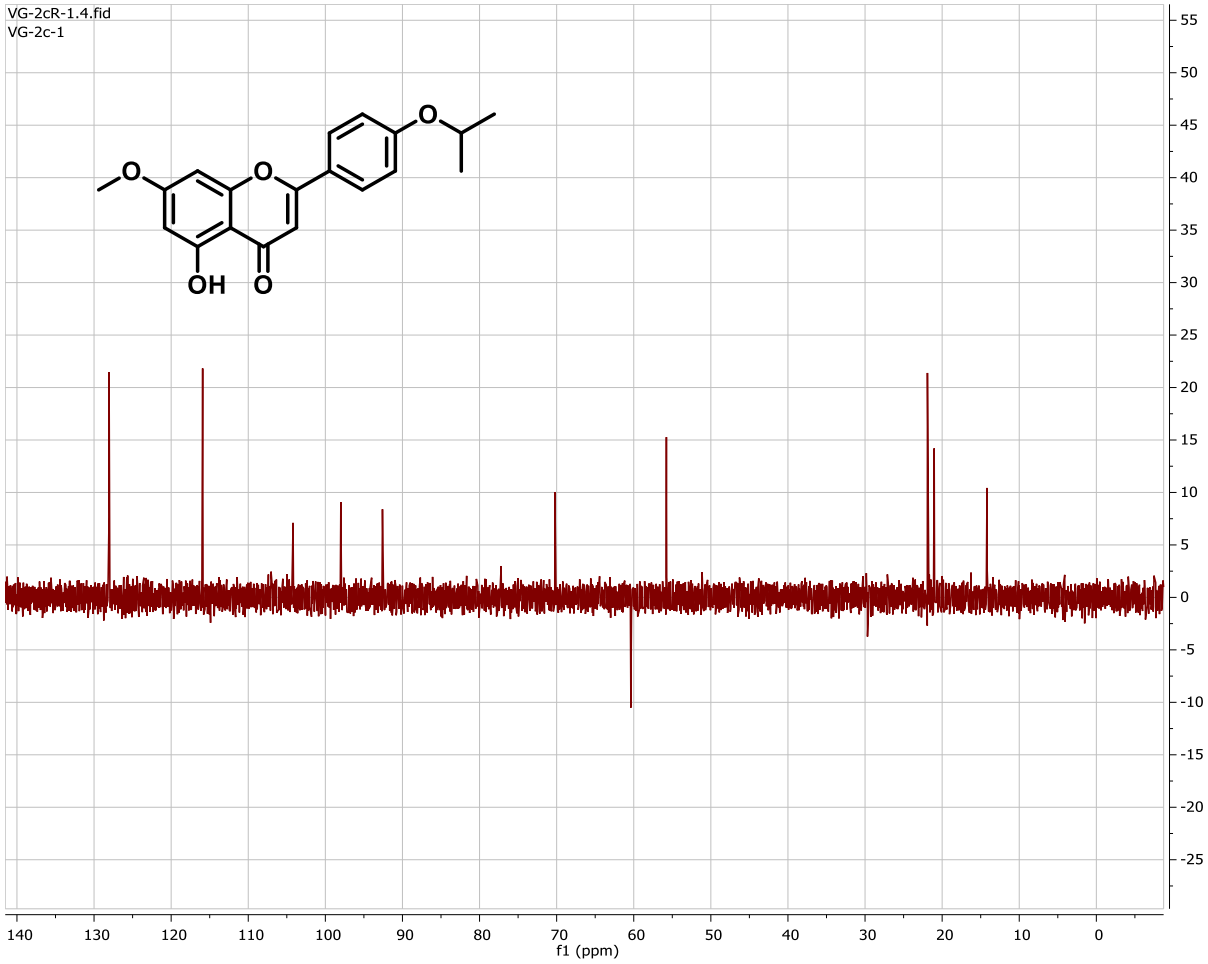

HSQC Spectrum of Compound 2c

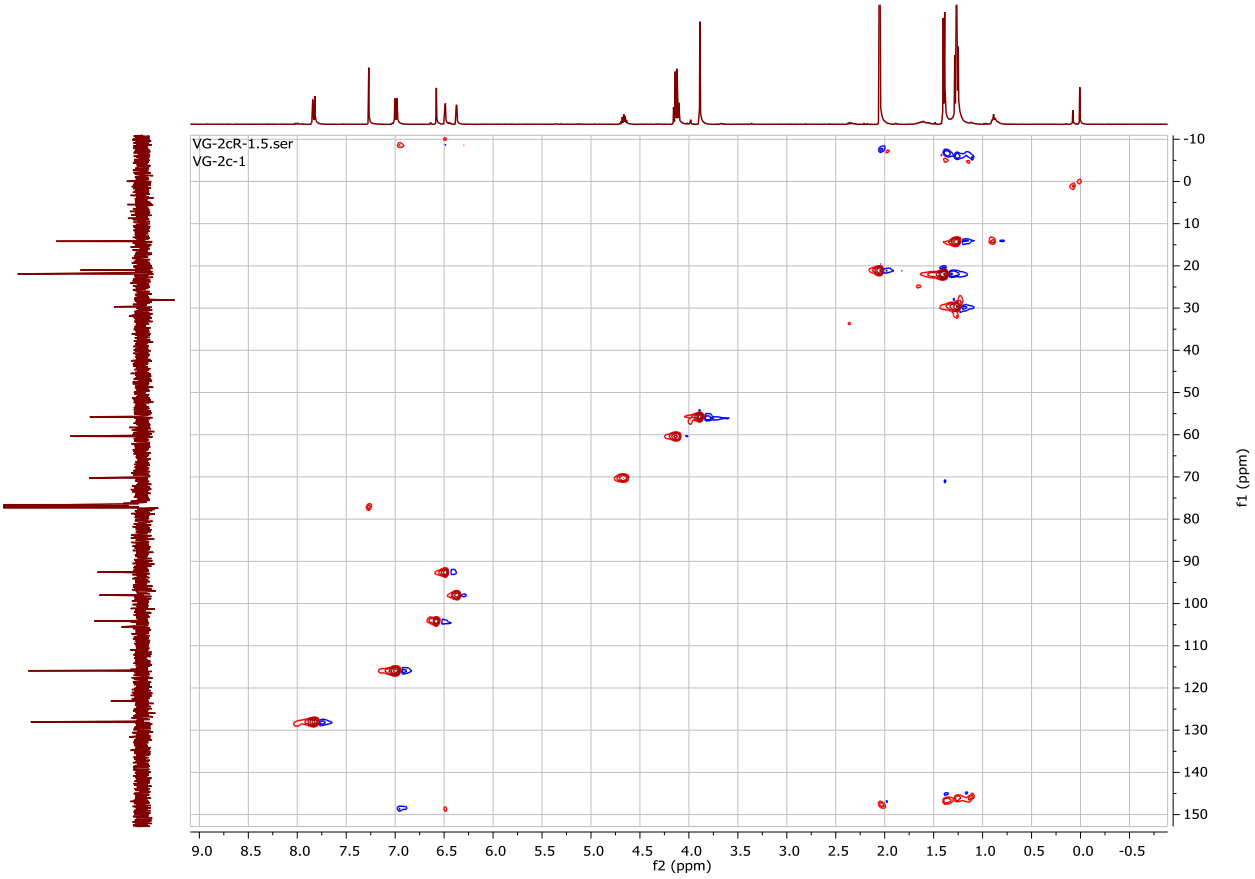

HMBC Spectrum of Compound 2c

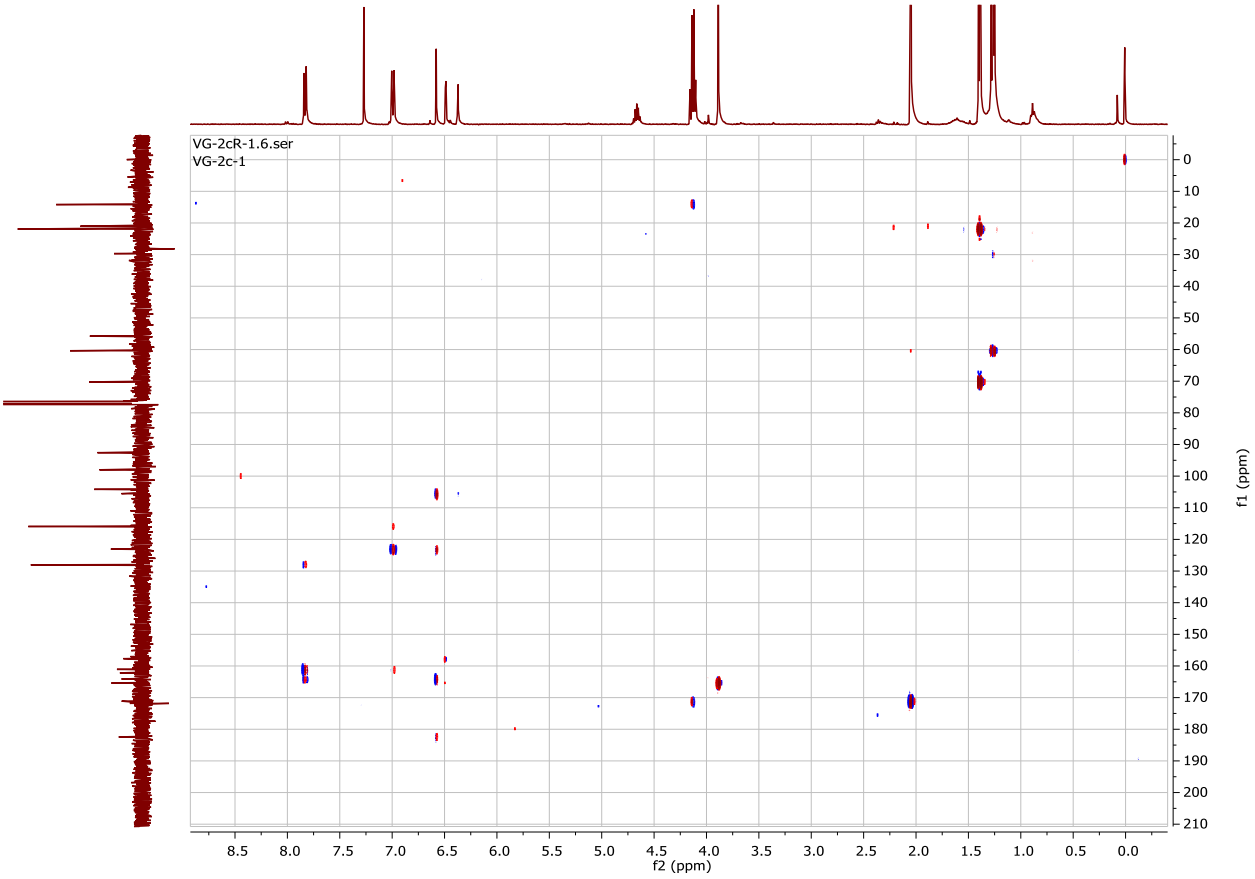

^{1}H-Spectrum of Compound 3a

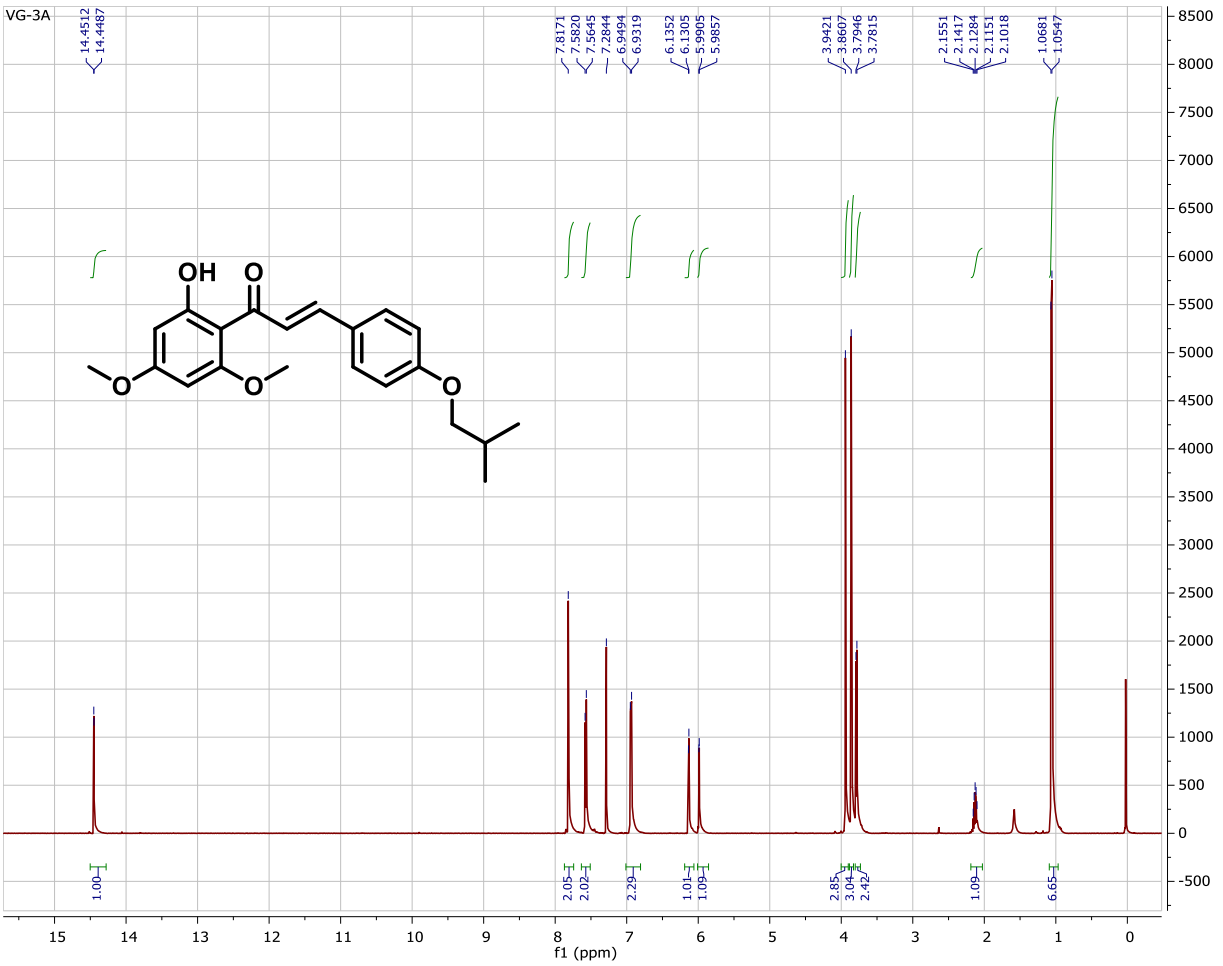

^{13}C-Spectrum of Compound 3a

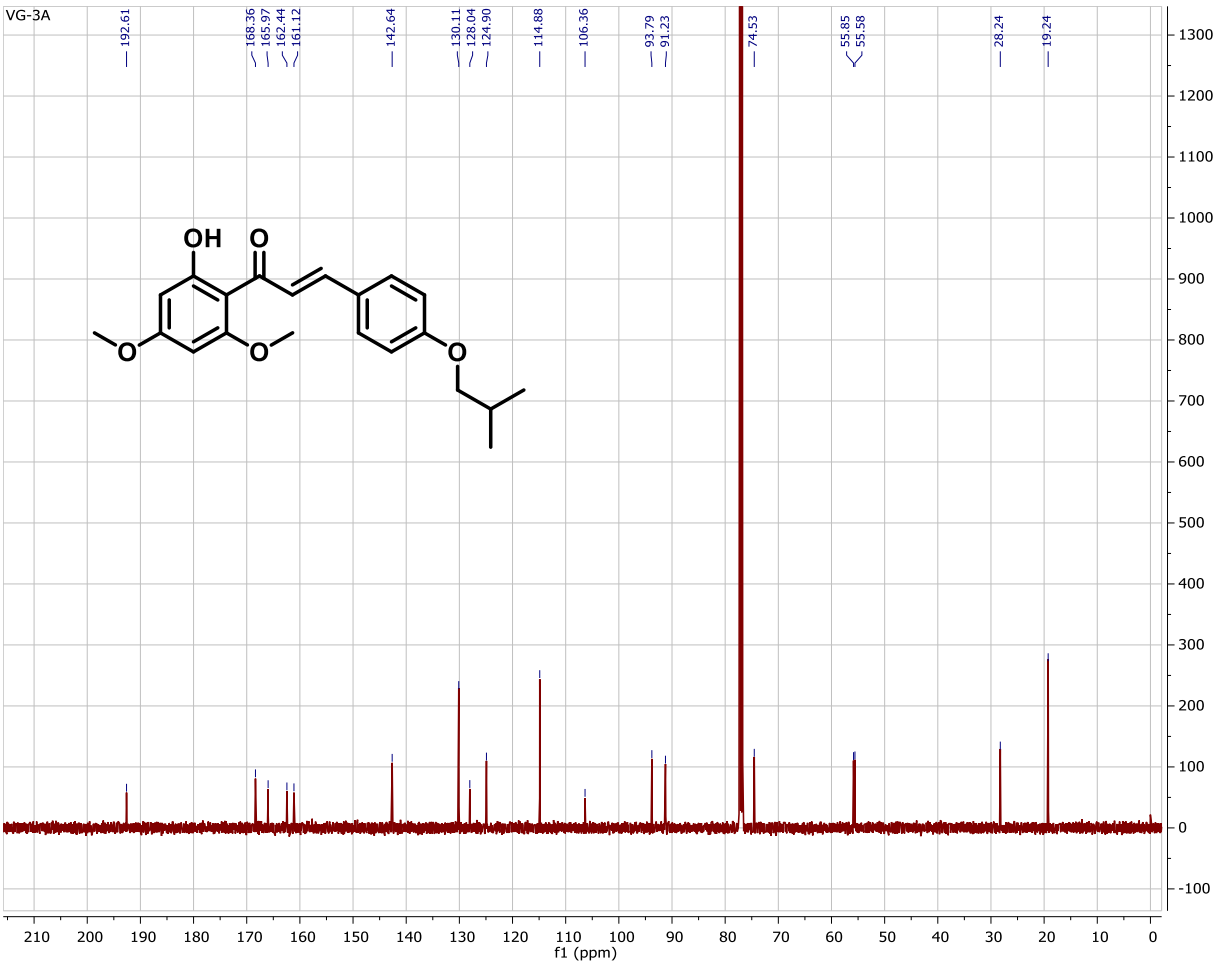

DEPT-135 Spectrum of Compound 3a

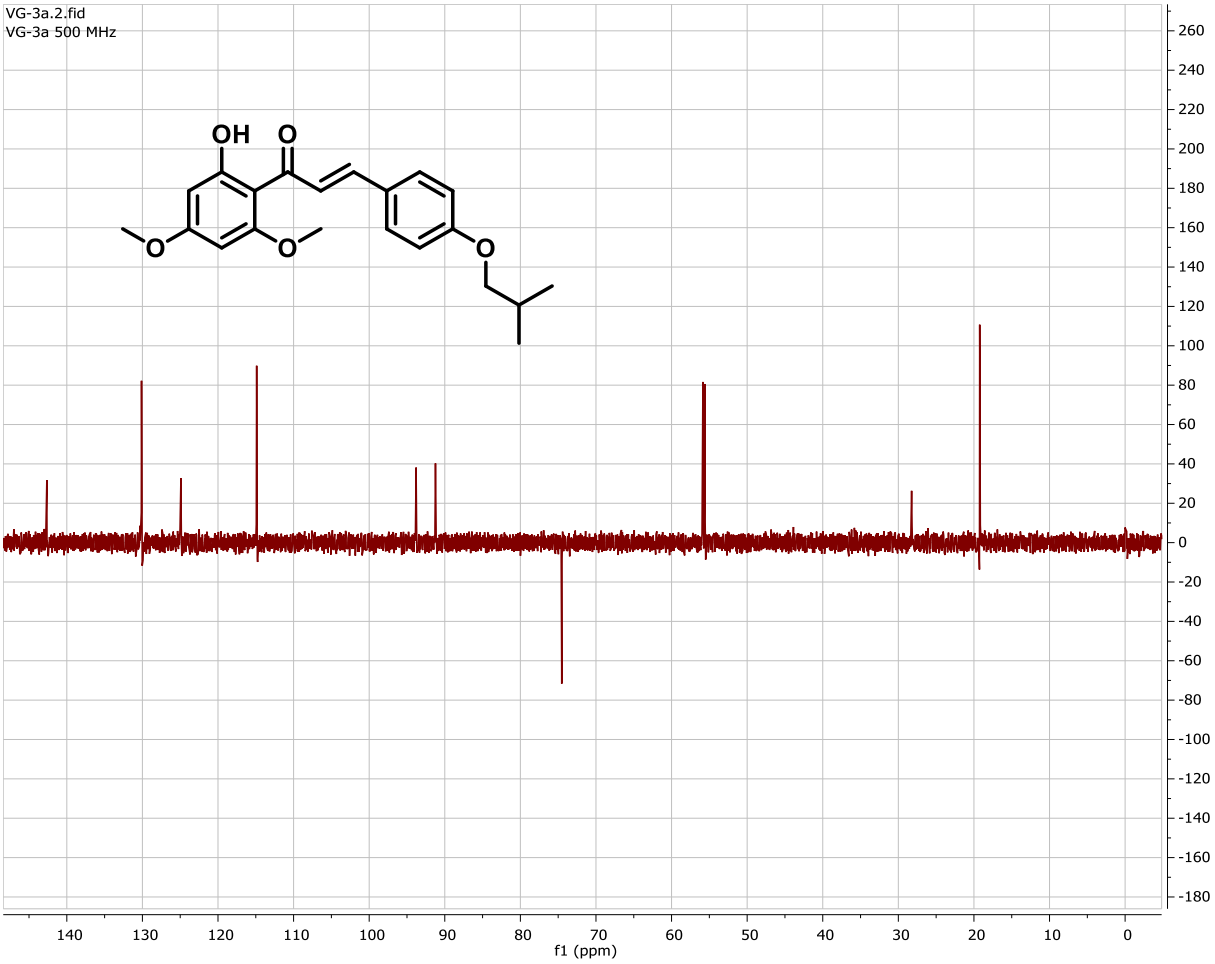

^{1}H-Spectrum of Compound 3b

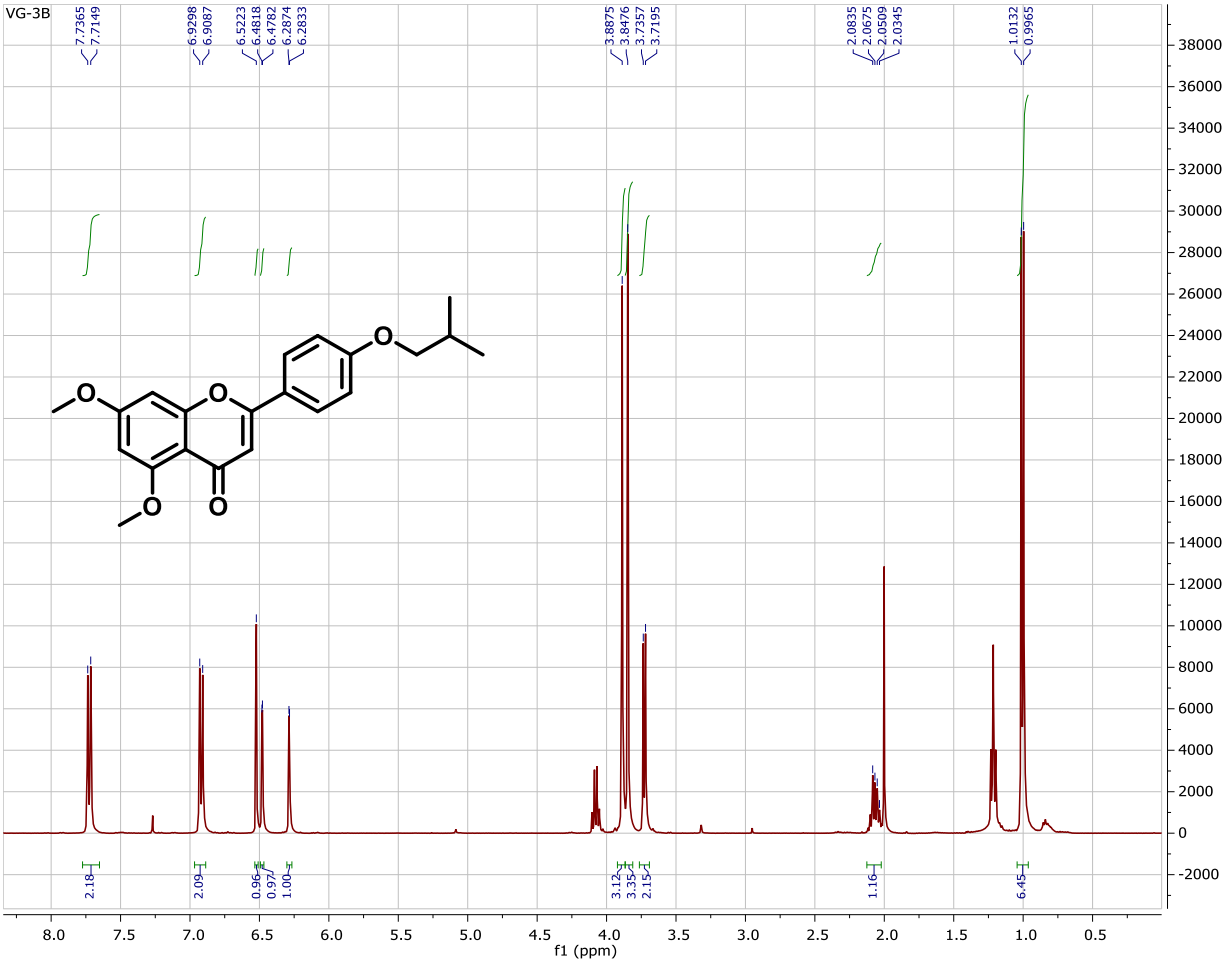

^{13}C-Spectrum of Compound 3b

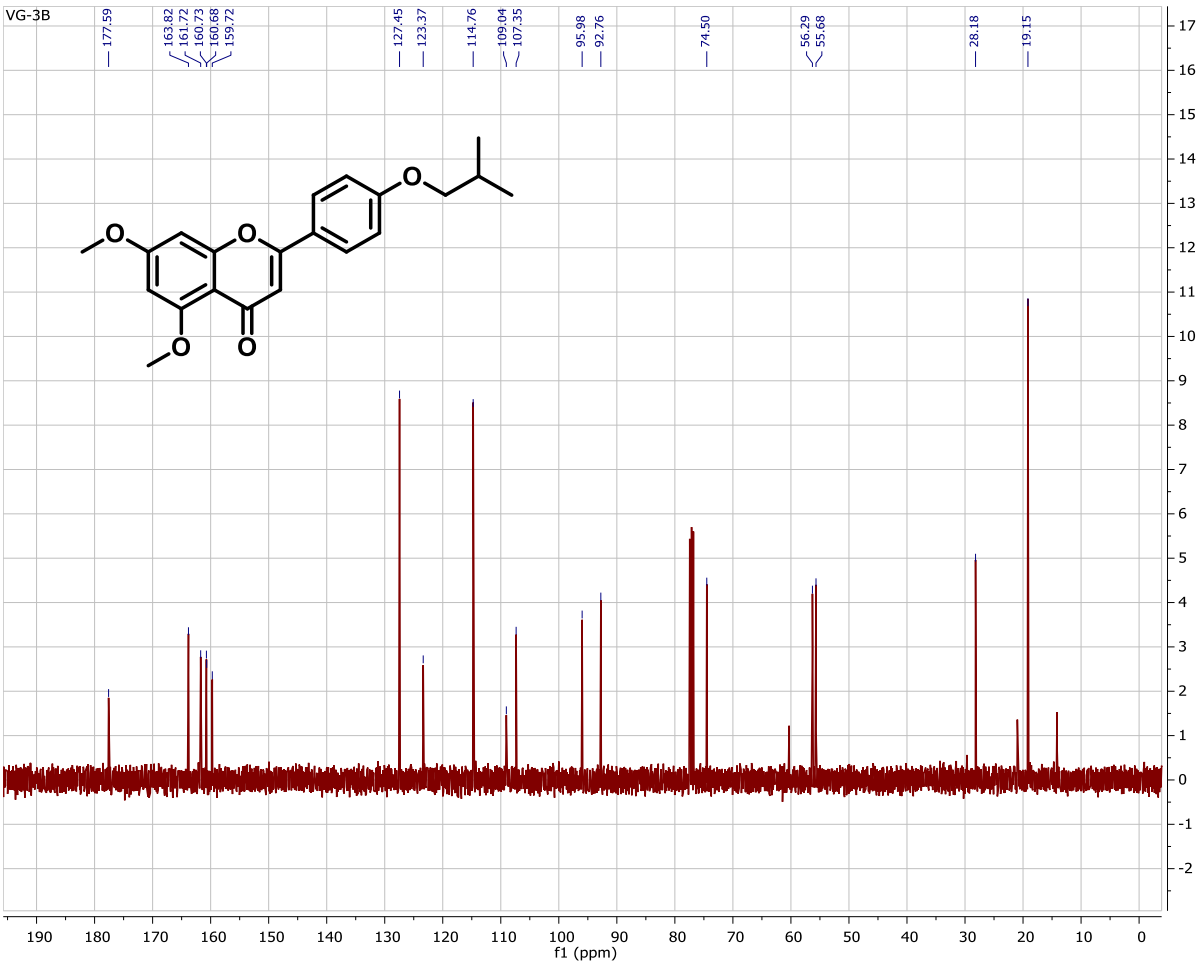

DEPT-135 Spectrum of Compound 3b

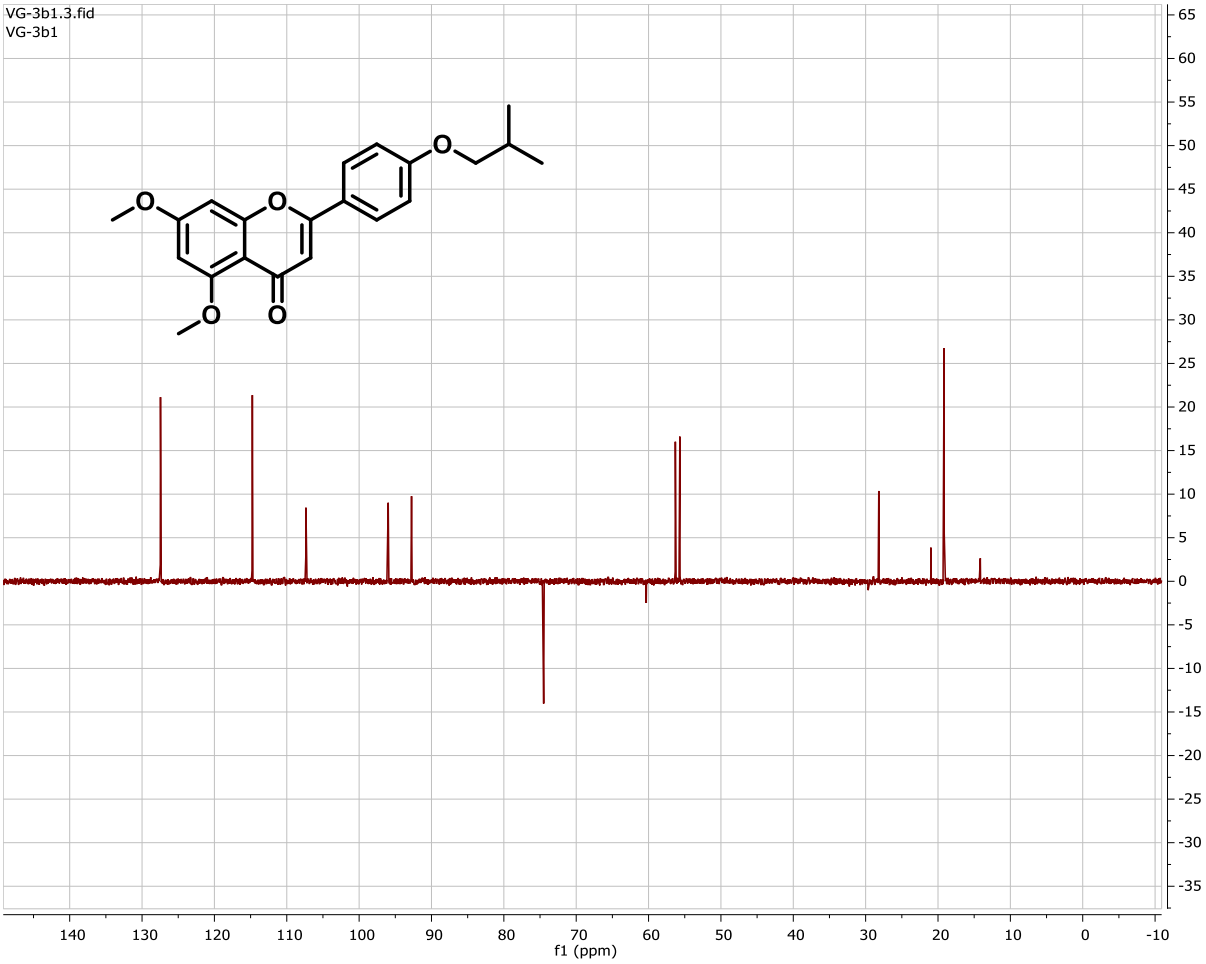

^{1}H-Spectrum of Compound 3c

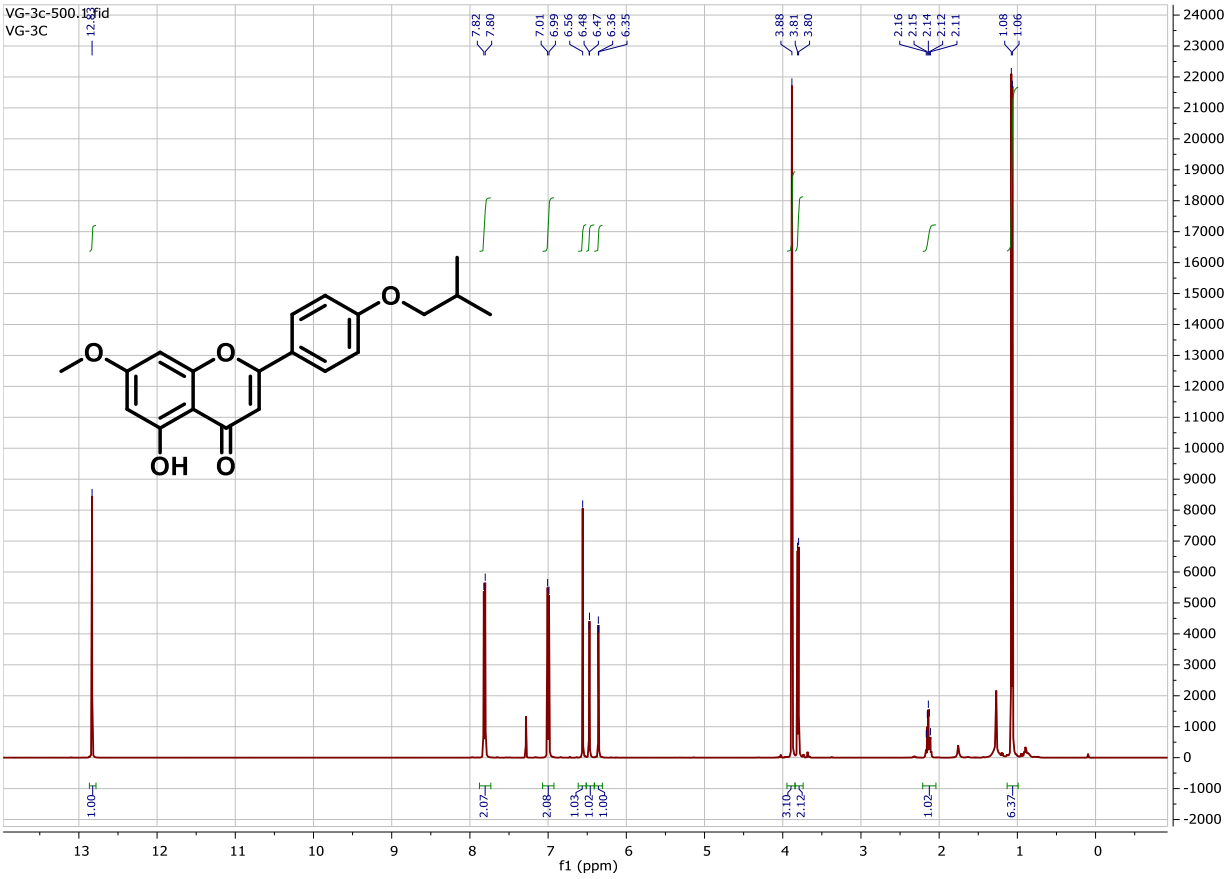

^{13}C-Spectrum of Compound 3c

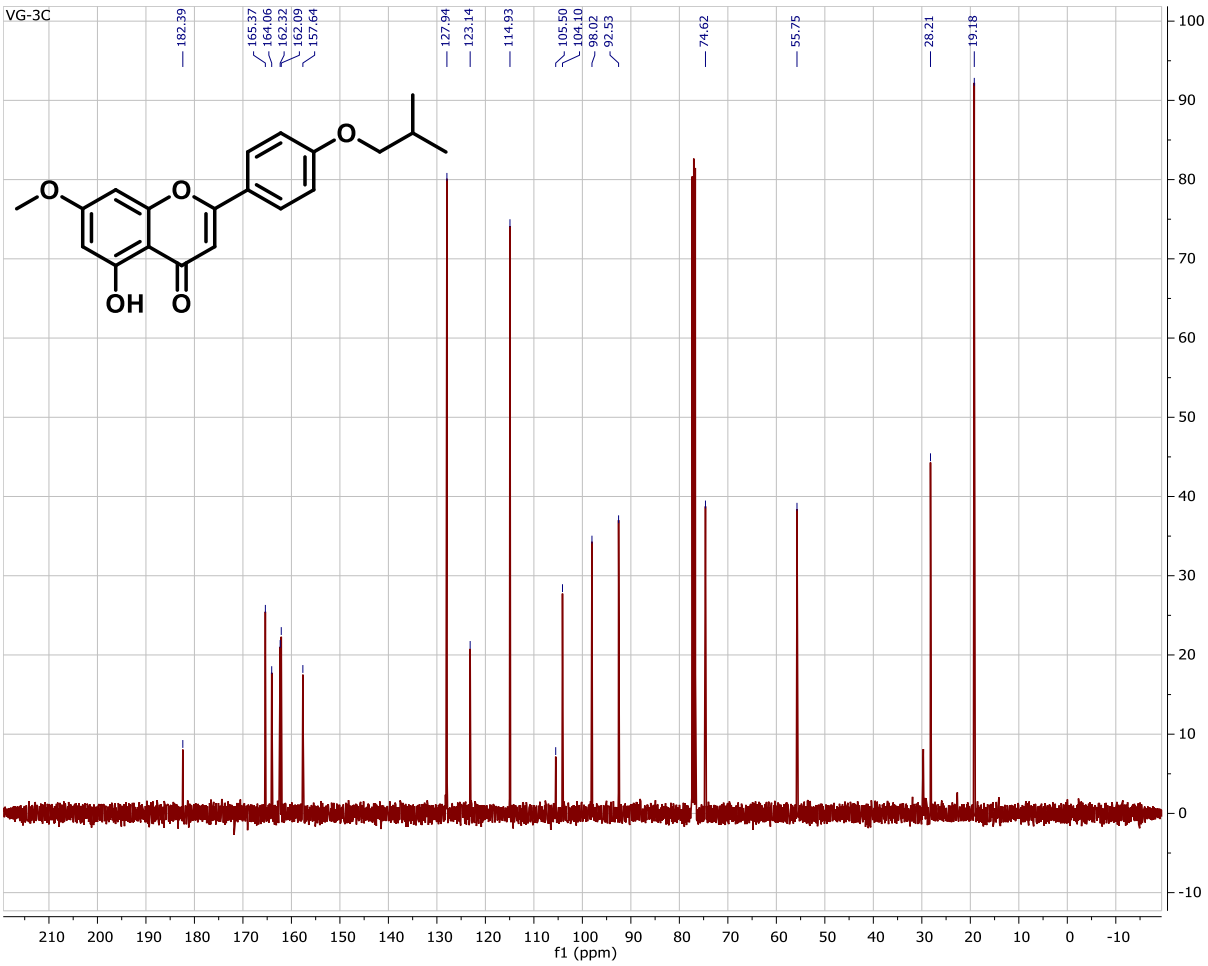

DEPT-135 Spectrum of Compound 3c

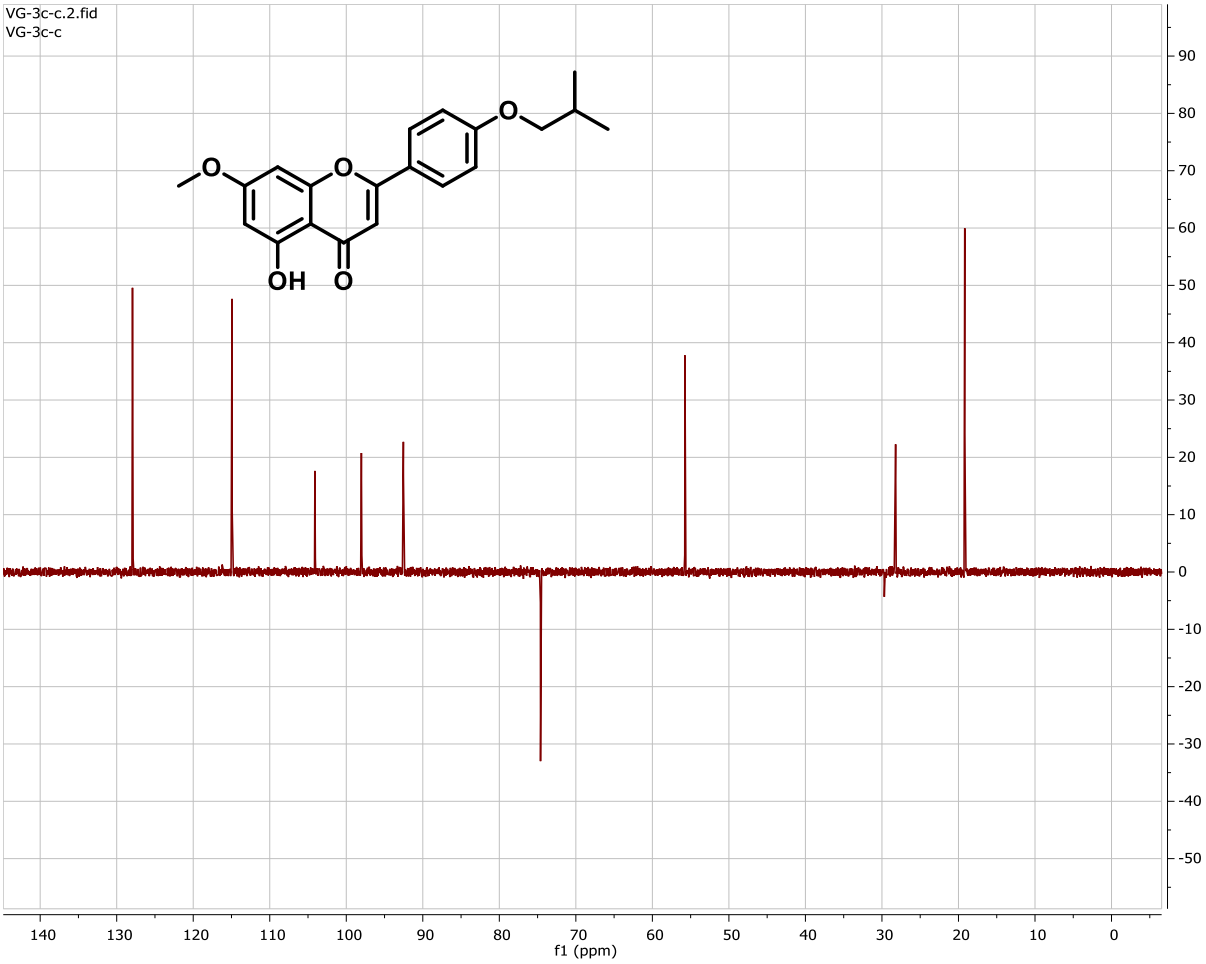

HSQC Spectrum of Compound 3c

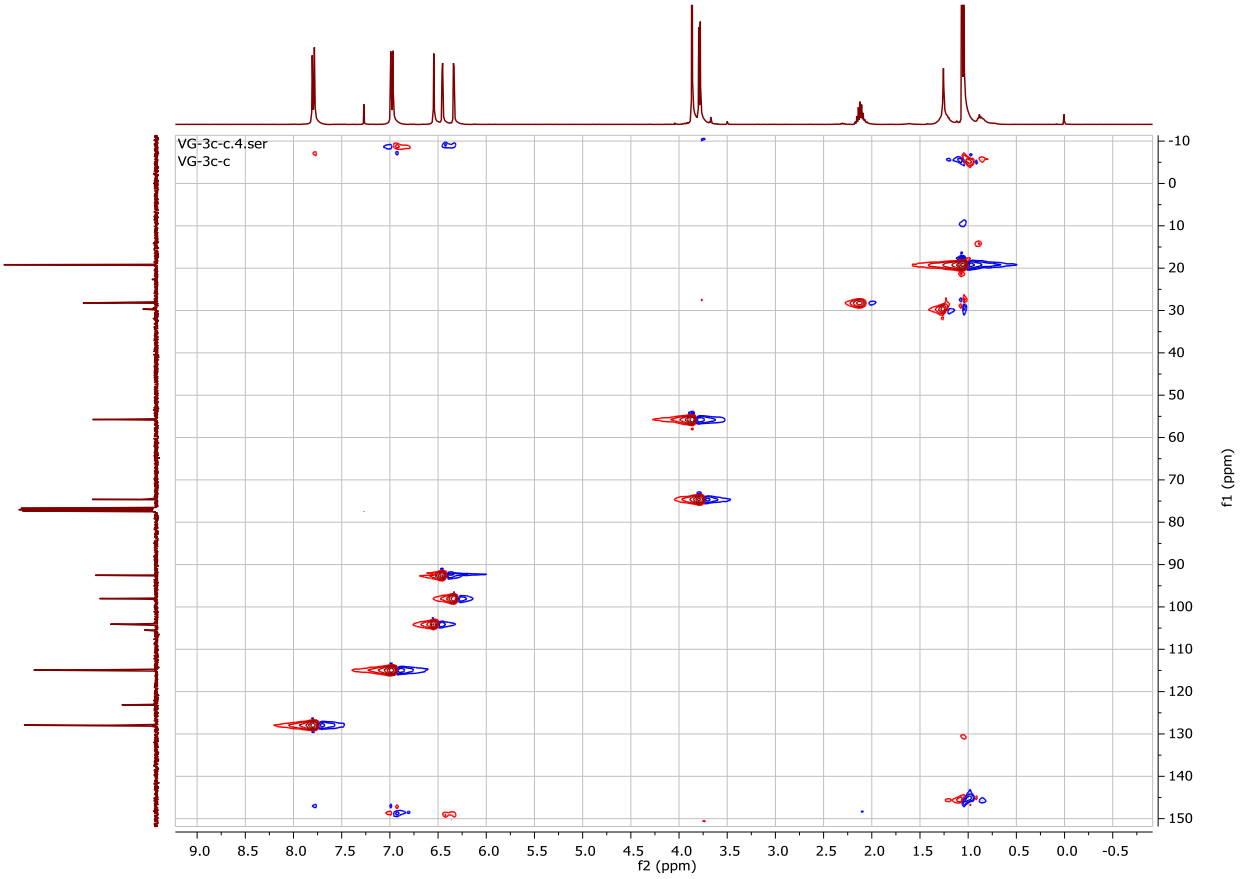

HMBC Spectrum of Compound 3c

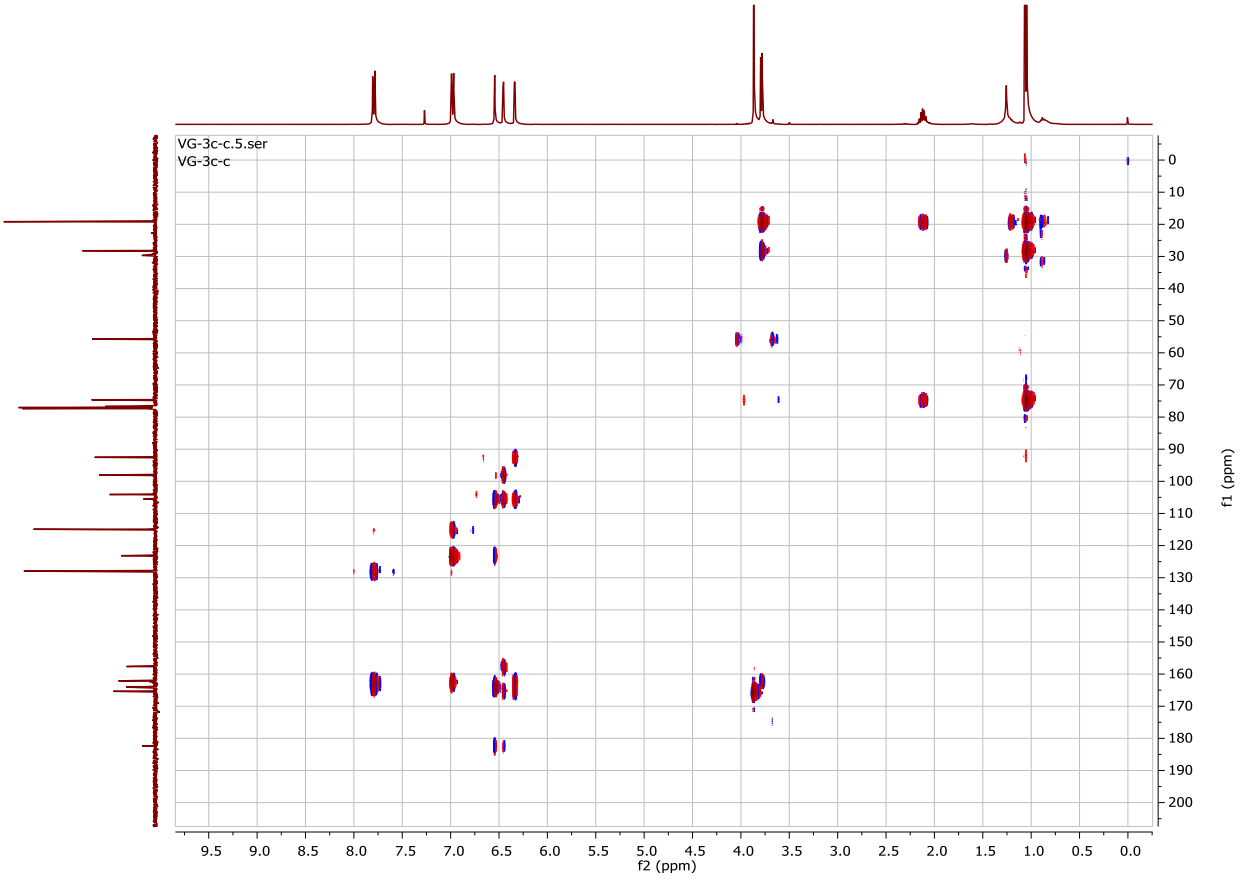

^{1}H-Spectrum of Compound 4a

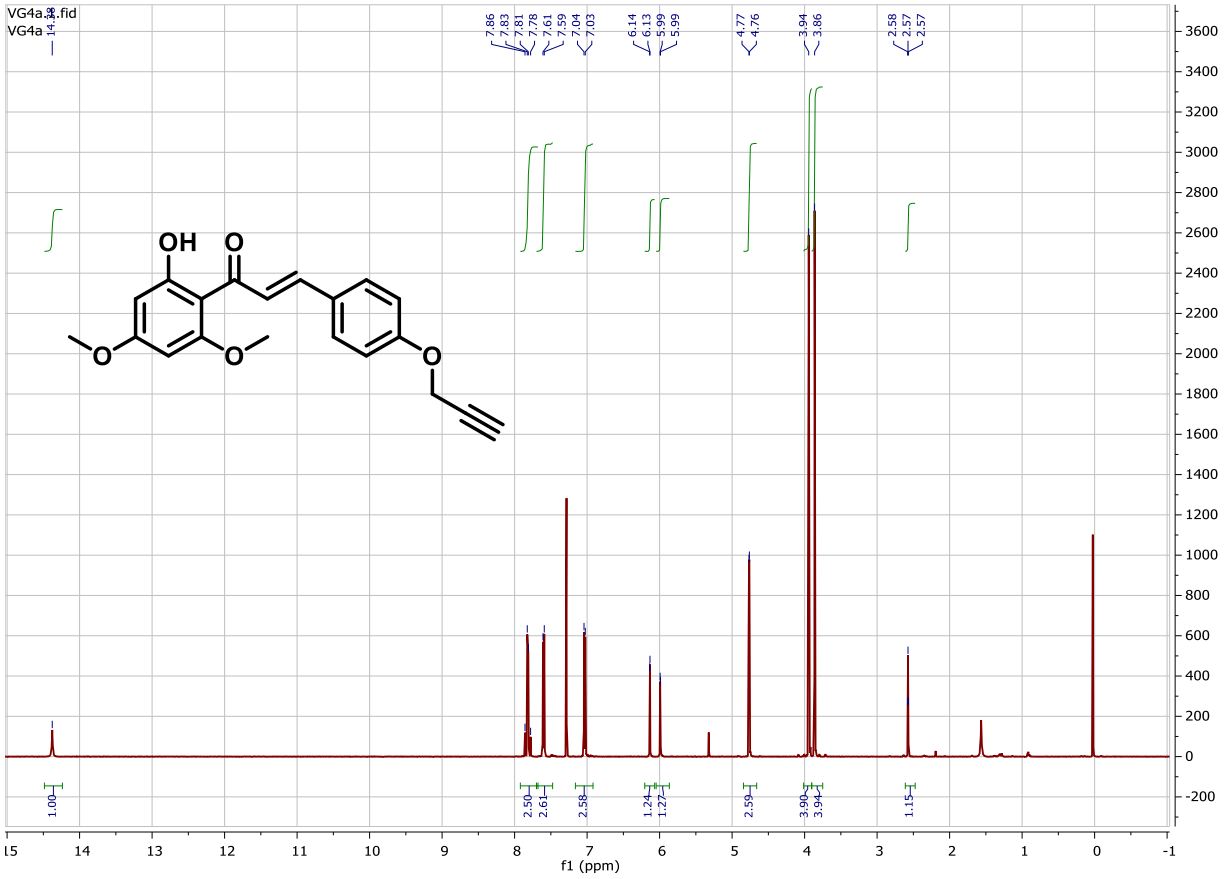

^{13}C-Spectrum of Compound 4a

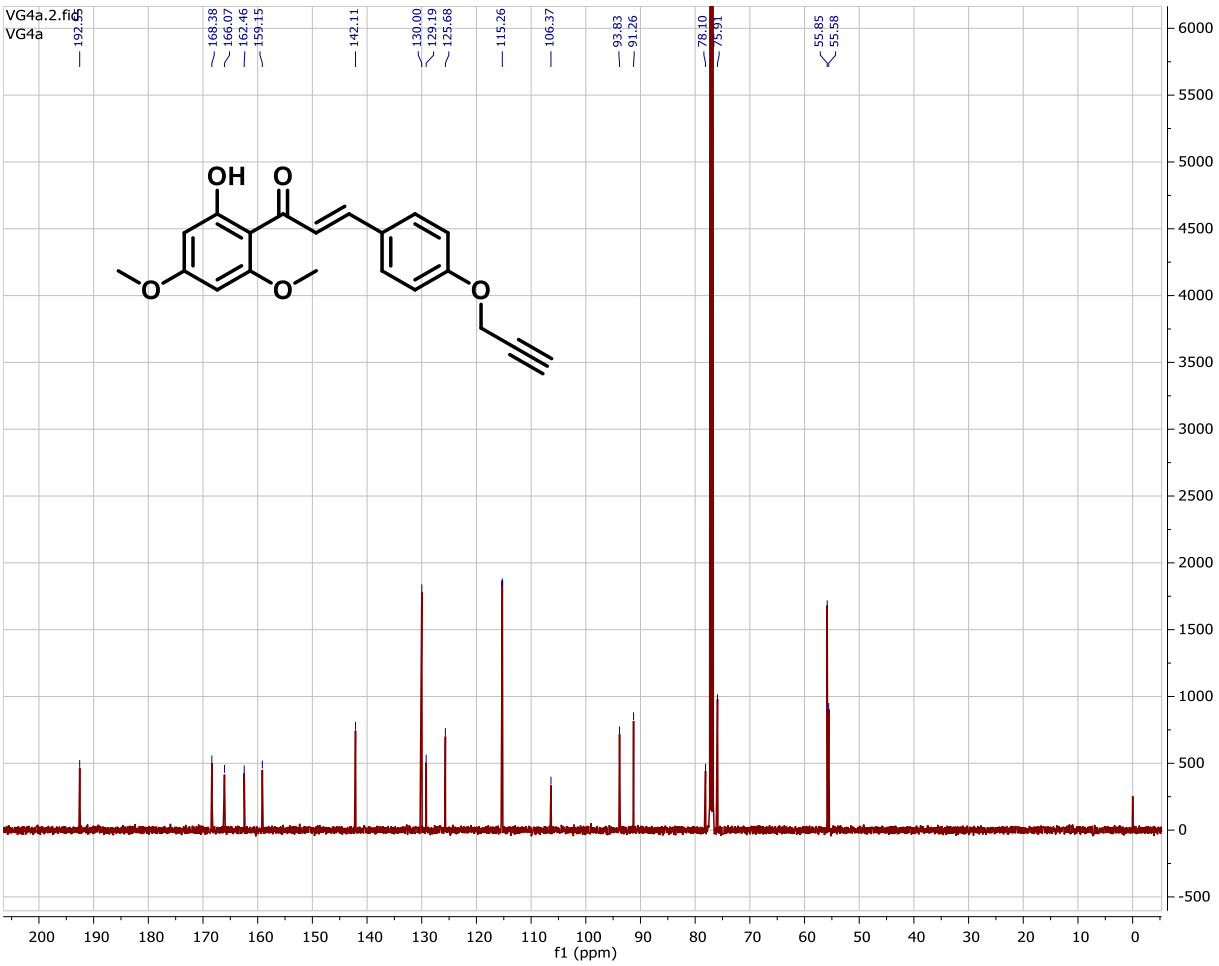

DEPT-135 Spectrum of Compound 4a

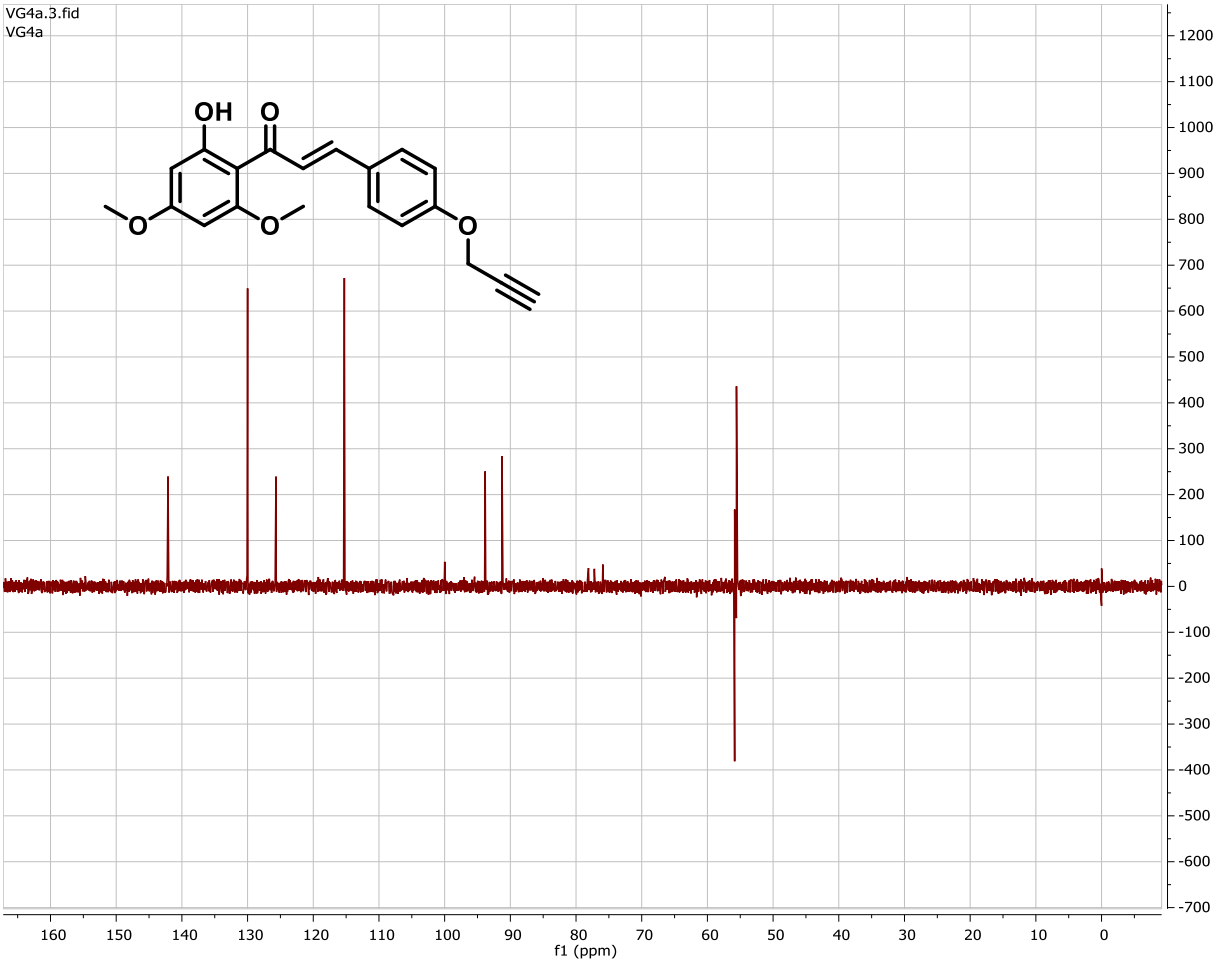

^{1}H-Spectrum of Compound 4b

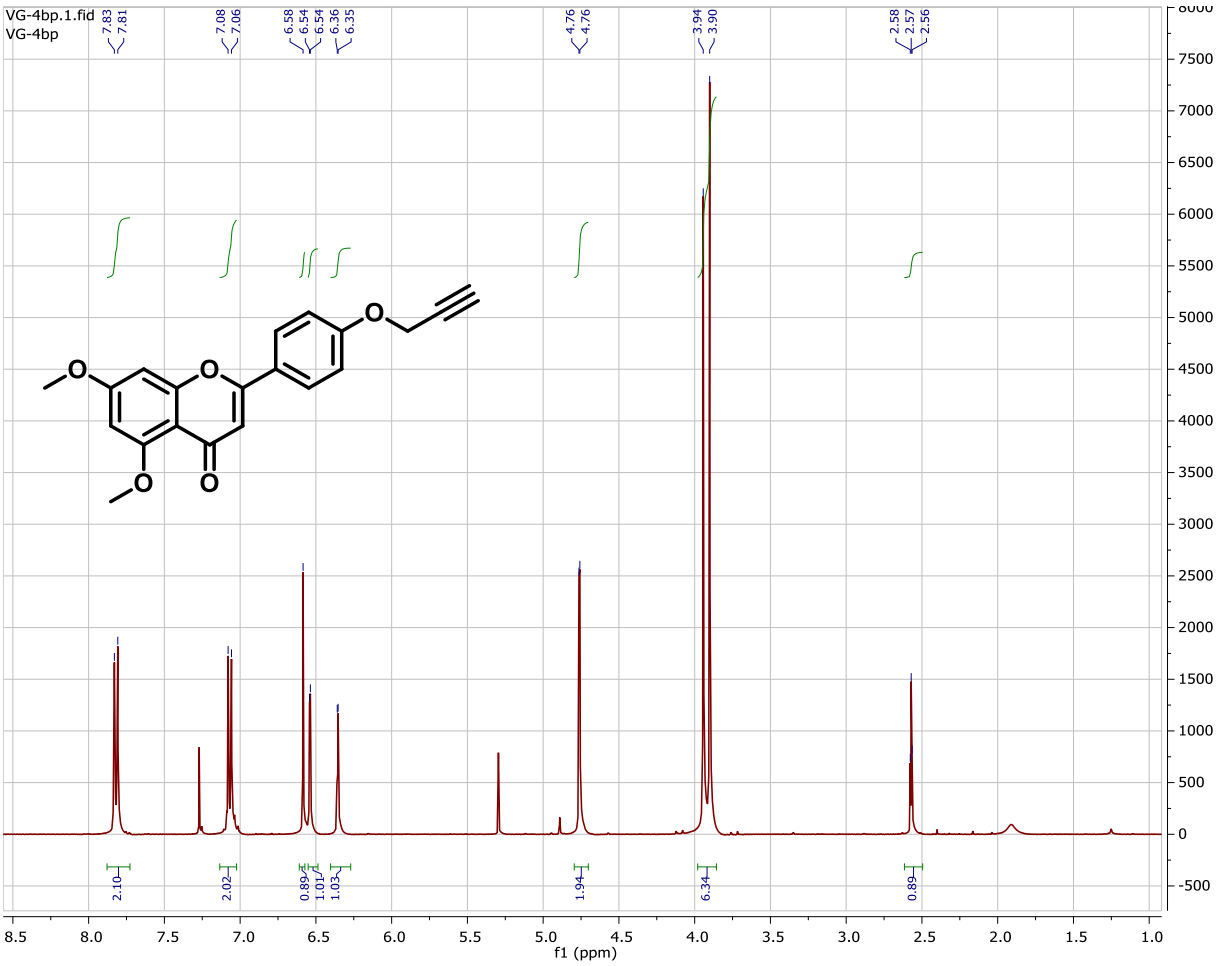

^{13}C-Spectrum of Compound 4b

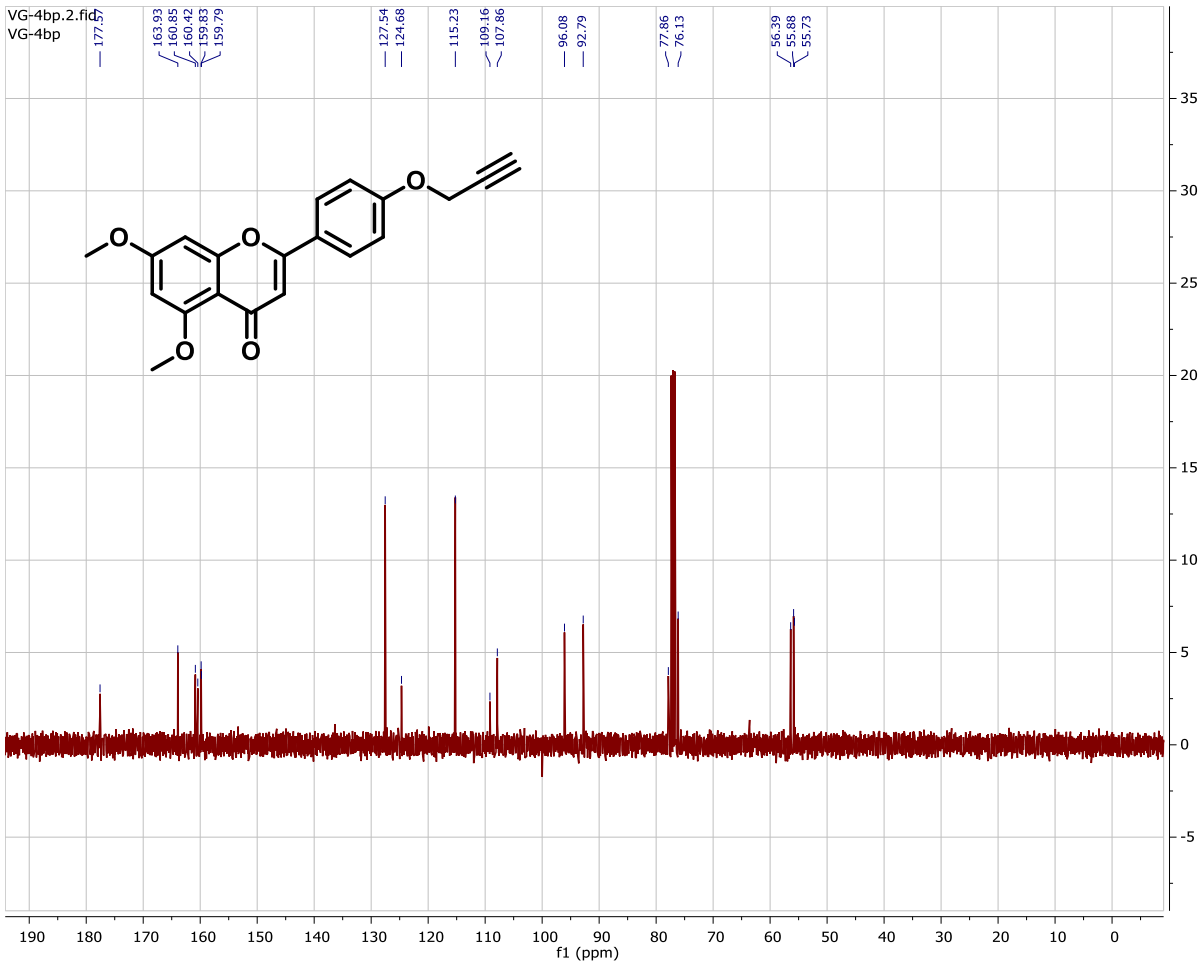

DEPT-135 Spectrum of Compound 4b

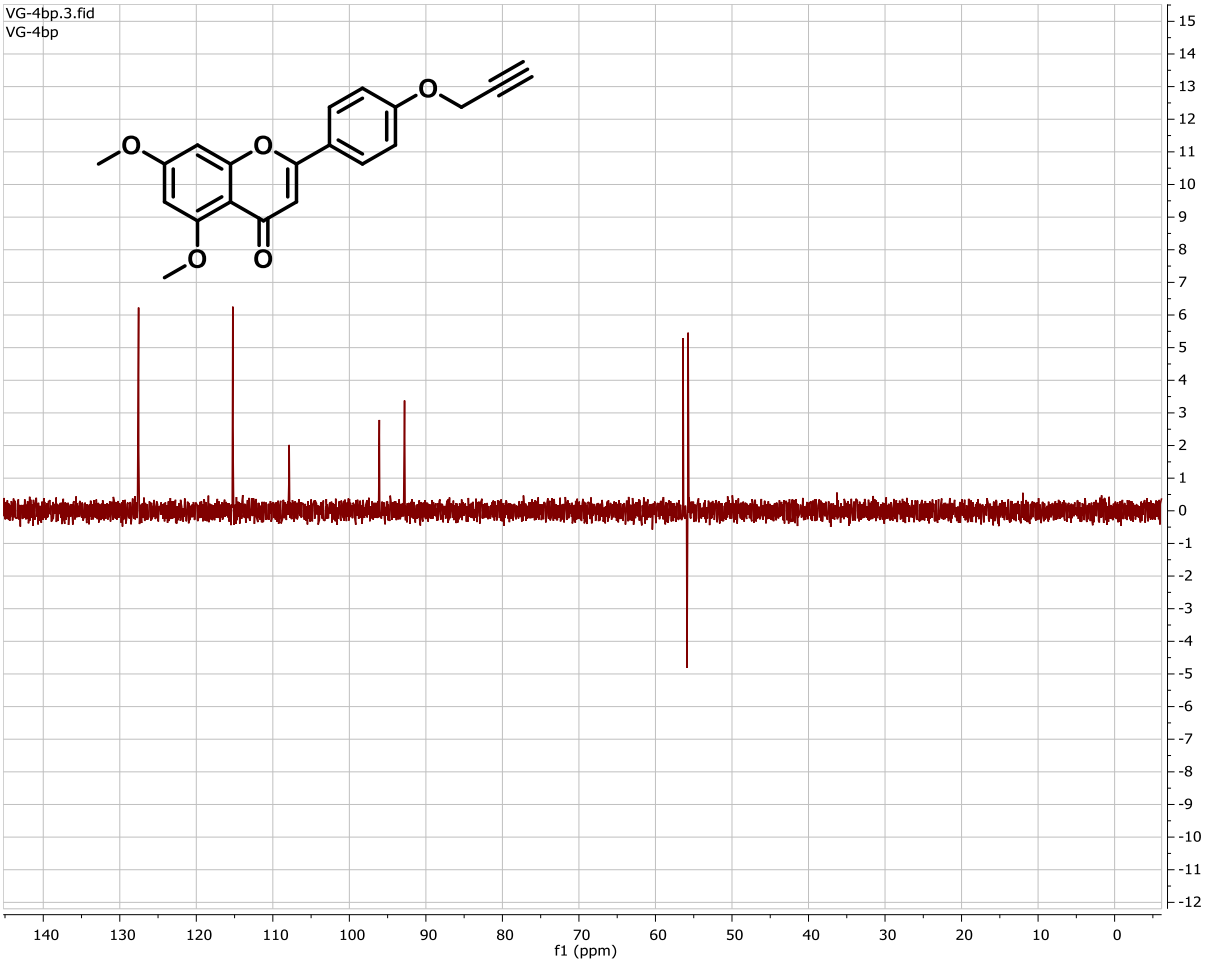

^{1}H-Spectrum of Compound 4c

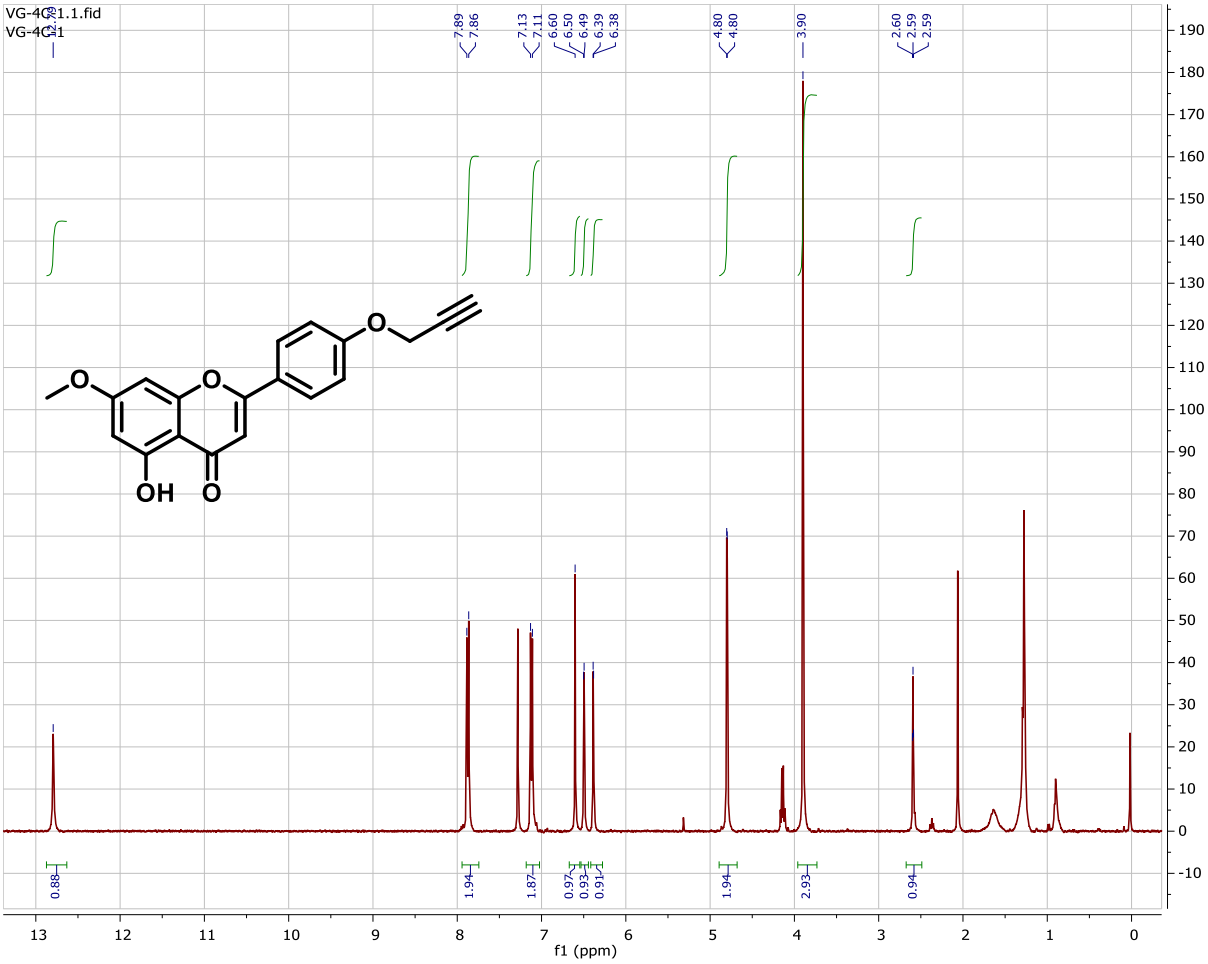

^{13}C-Spectrum of Compound 4c

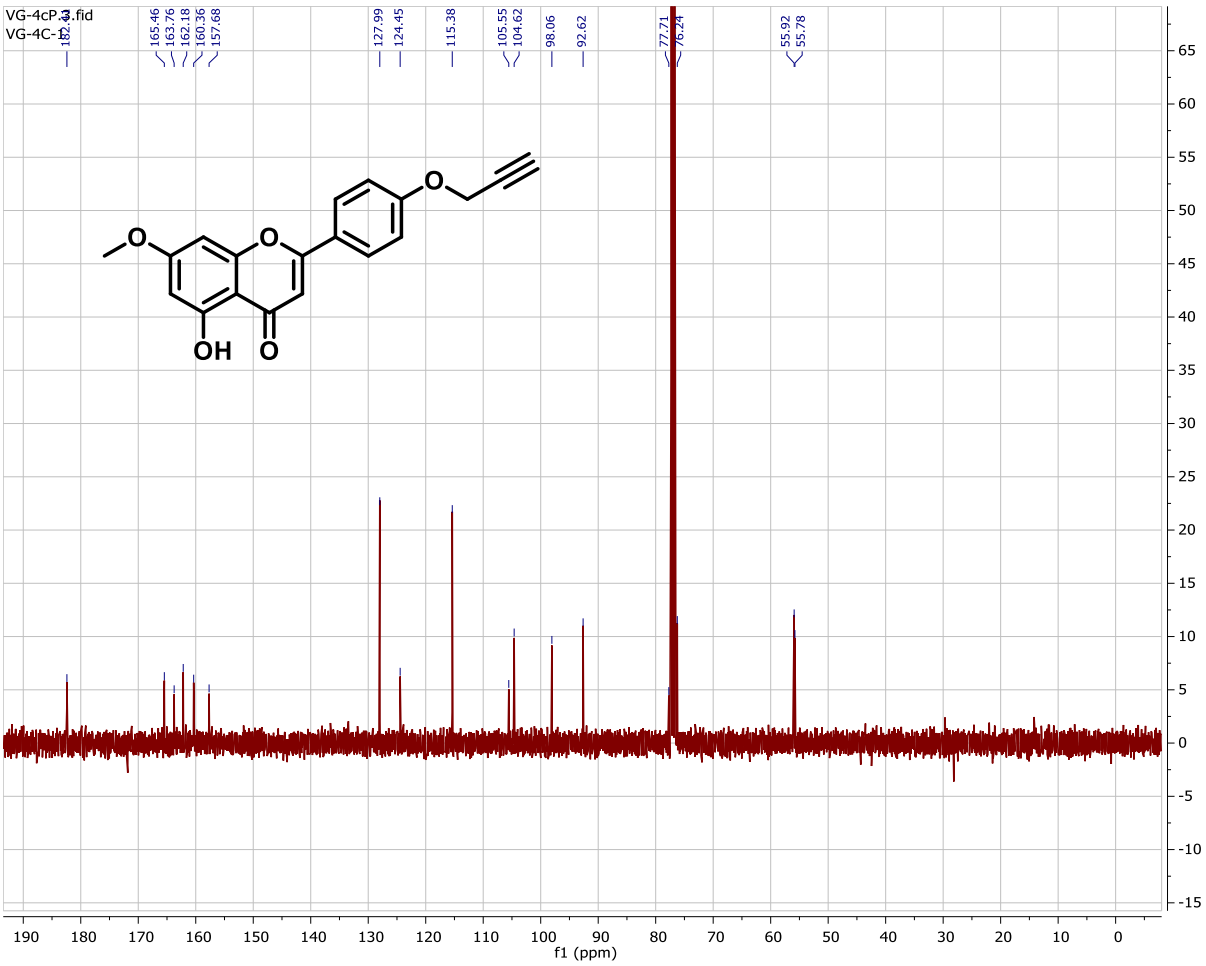

DEPT-135 Spectrum of Compound 4c

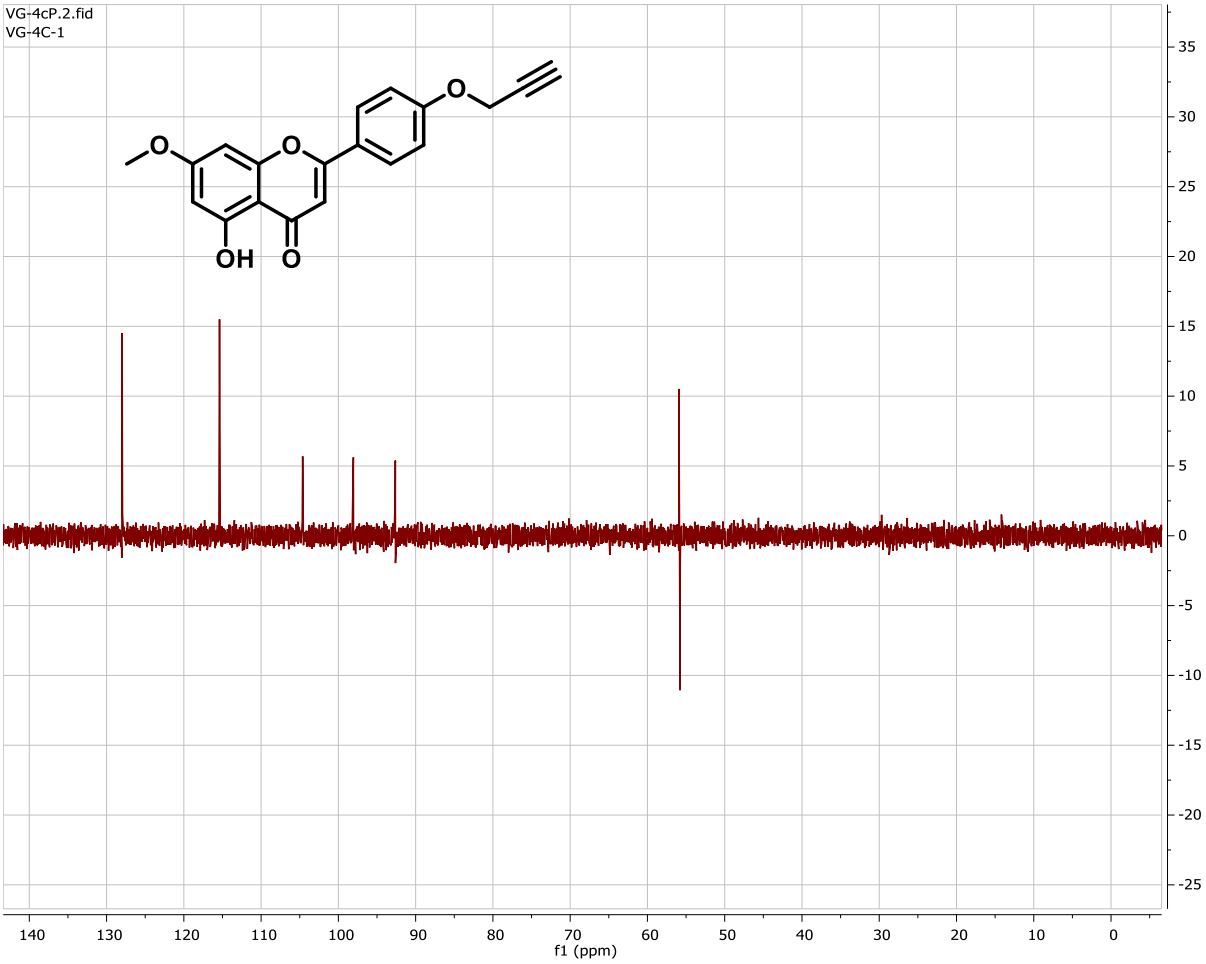

HSQC Spectrum of Compound 4c

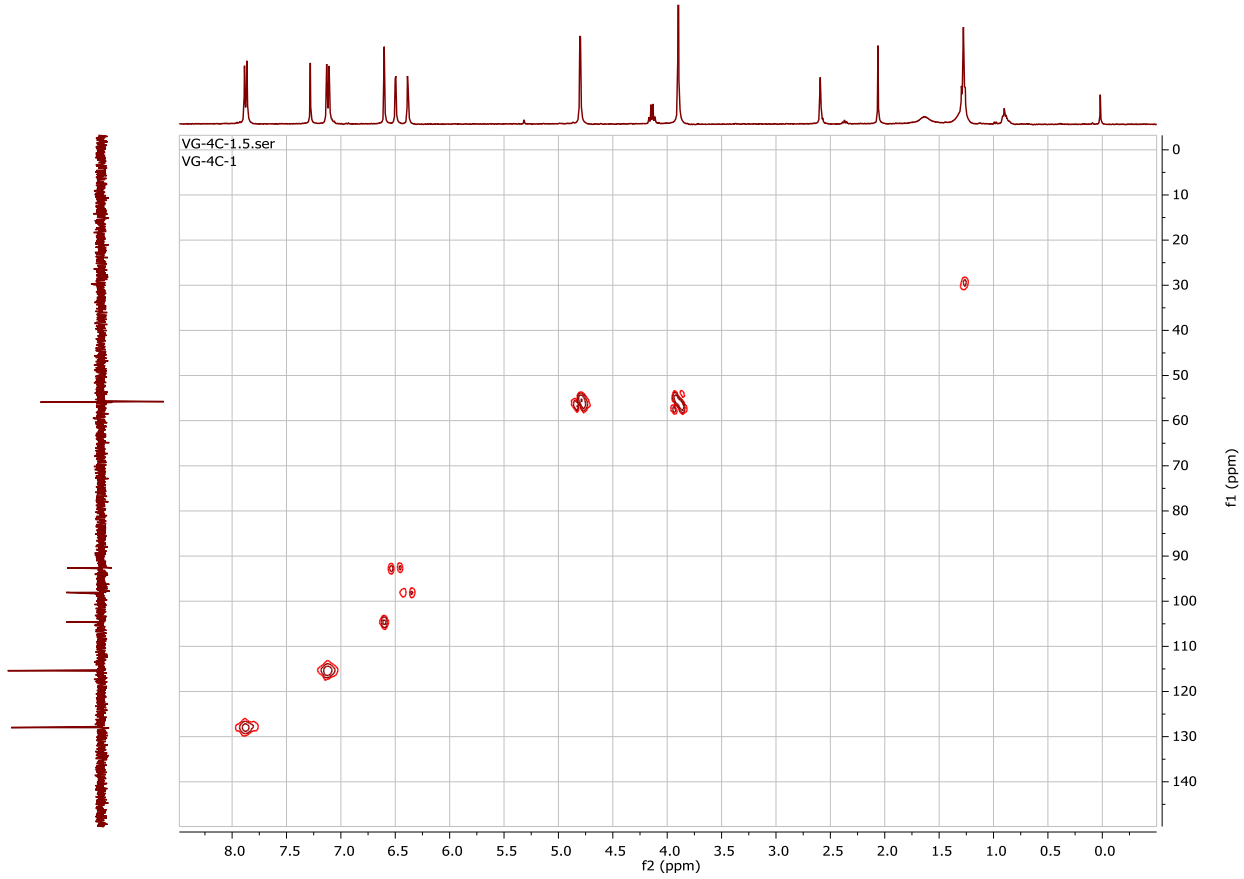

HMBC Spectrum of Compound 4c

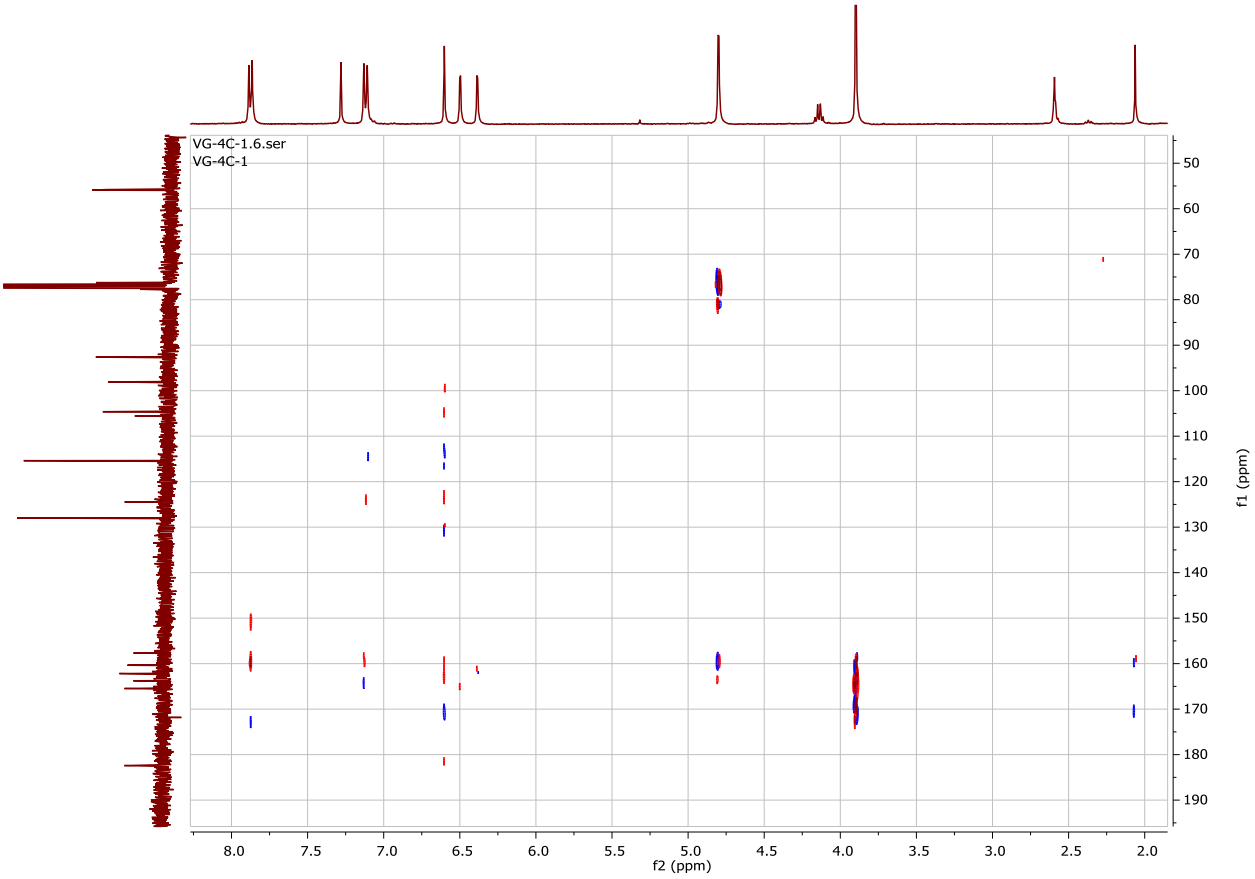

^{1}H-Spectrum of Compound IV

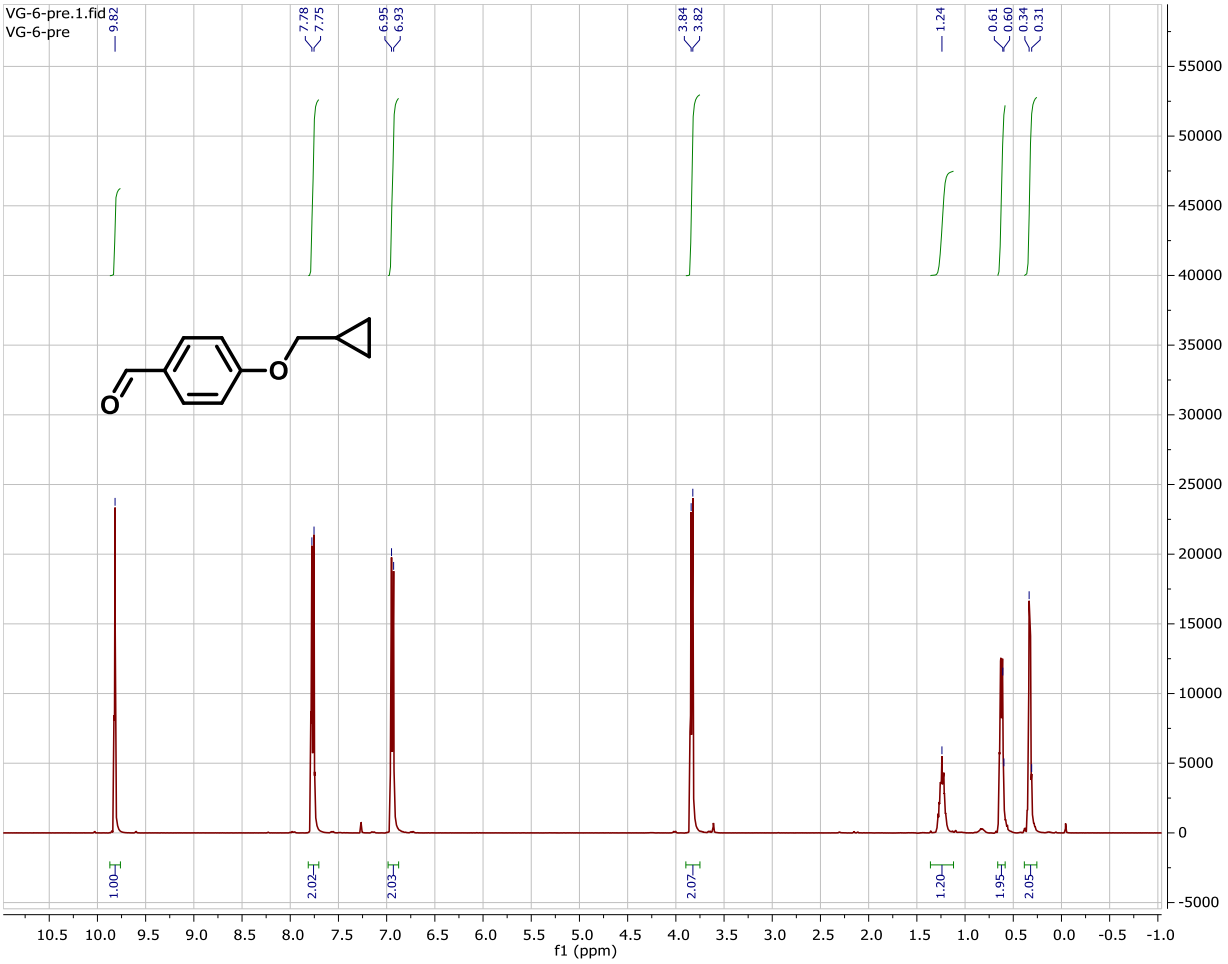

^{13}C-Spectrum of Compound IV

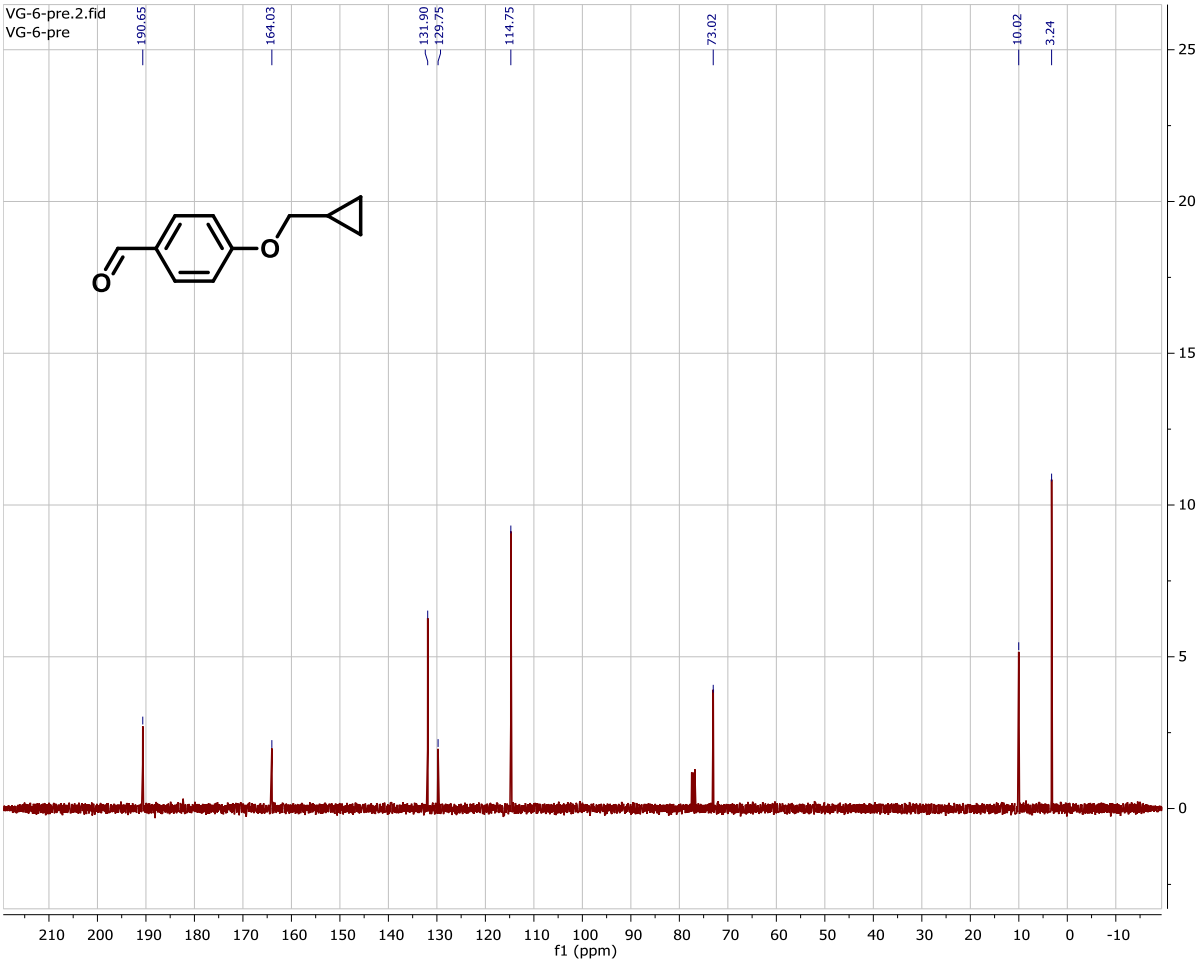

DEPT-135 Spectrum of Compound IV

^{1}H-Spectrum of Compound 5a

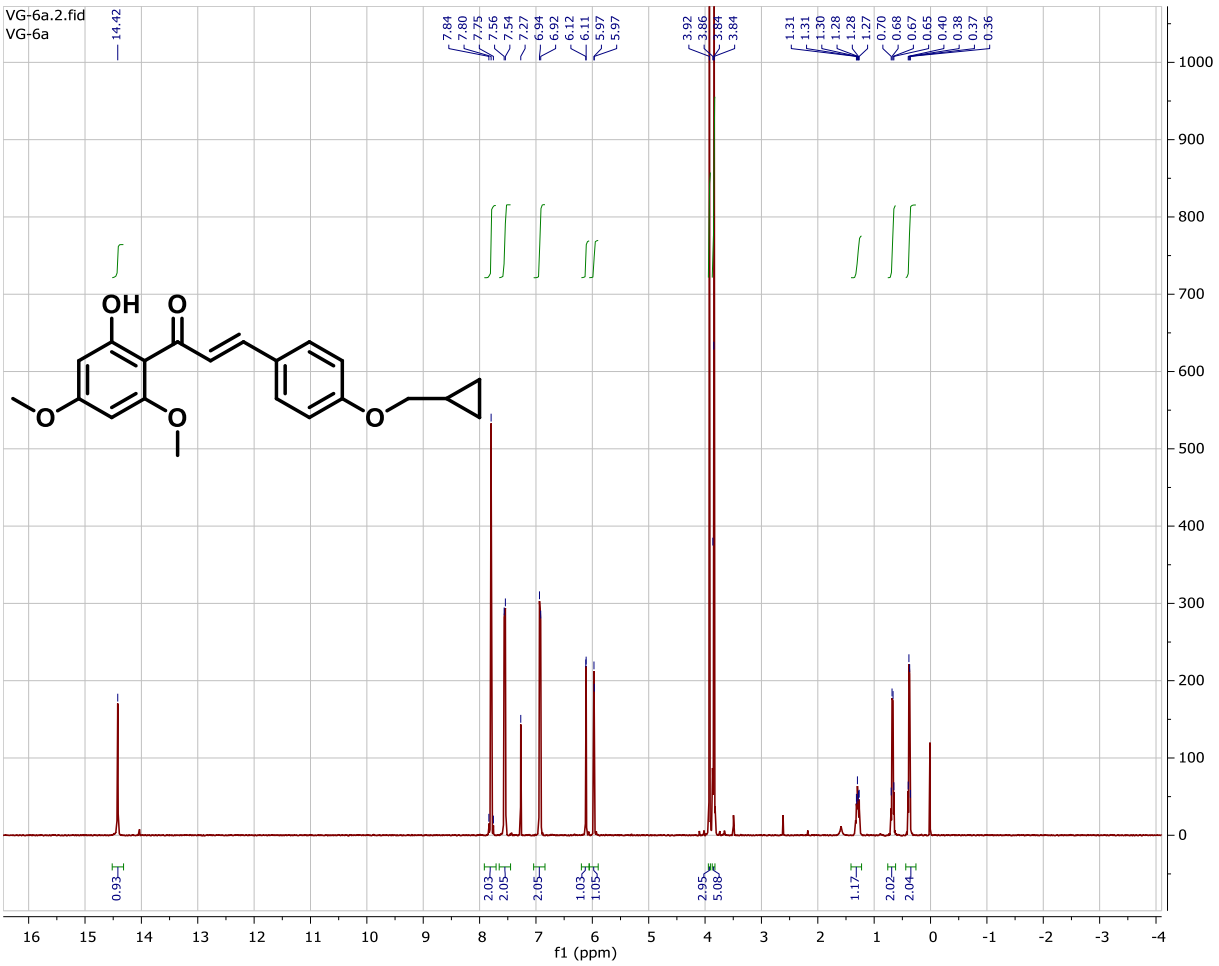

^{13}C-Spectrum of Compound 5a

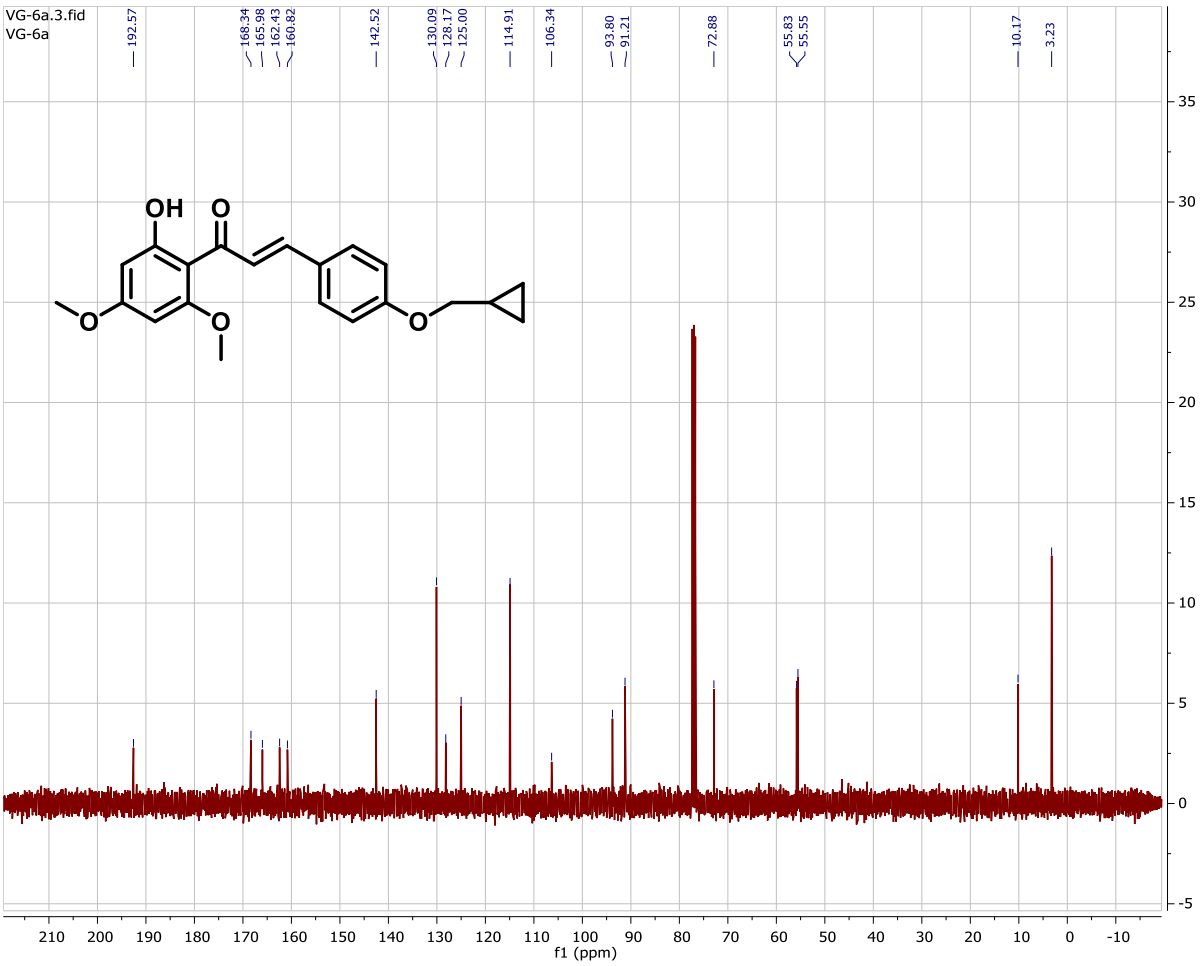

DEPT-135 Spectrum of Compound 5a

^{1}H-Spectrum of Compound 5b

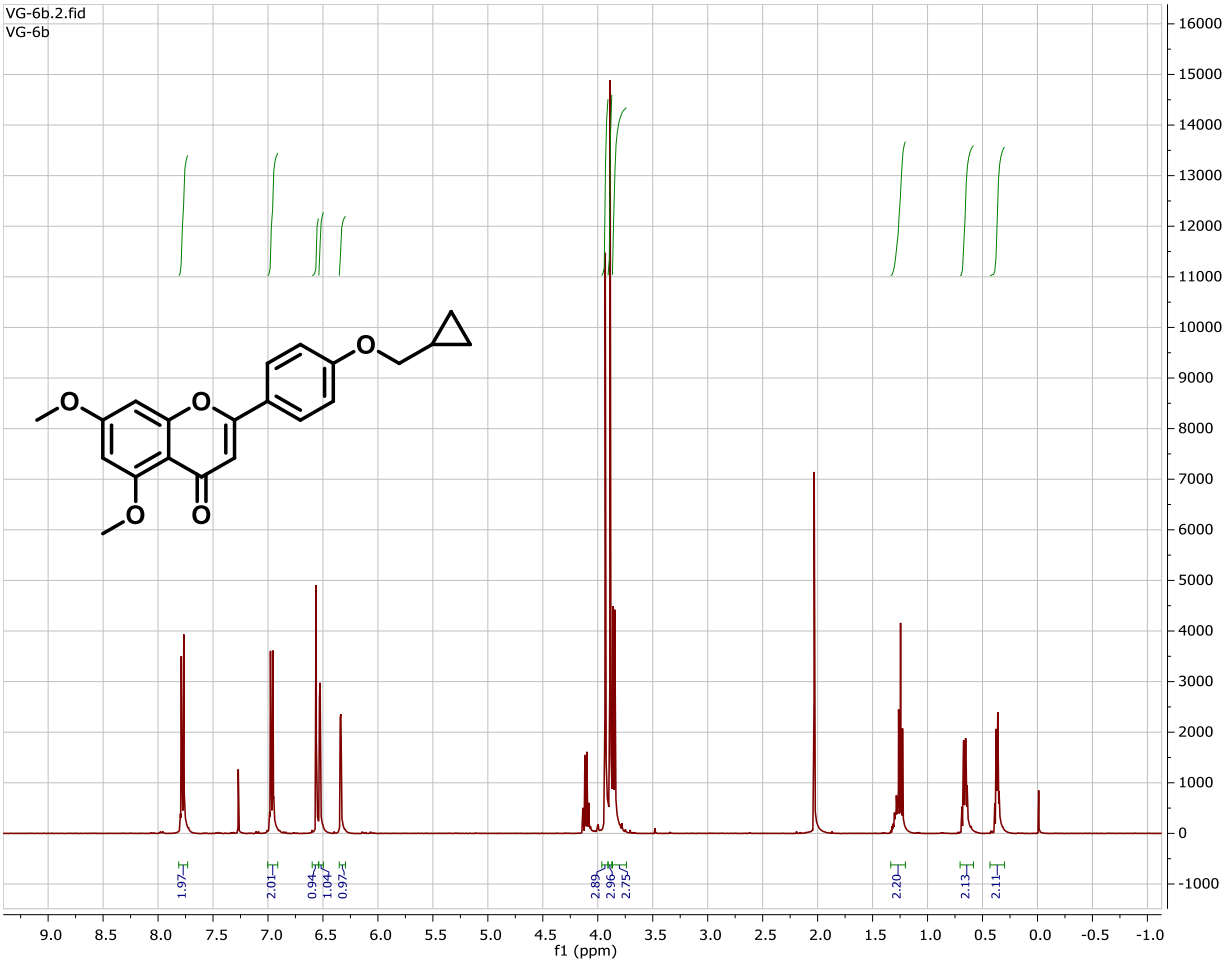

^{13}C-Spectrum of Compound 5b

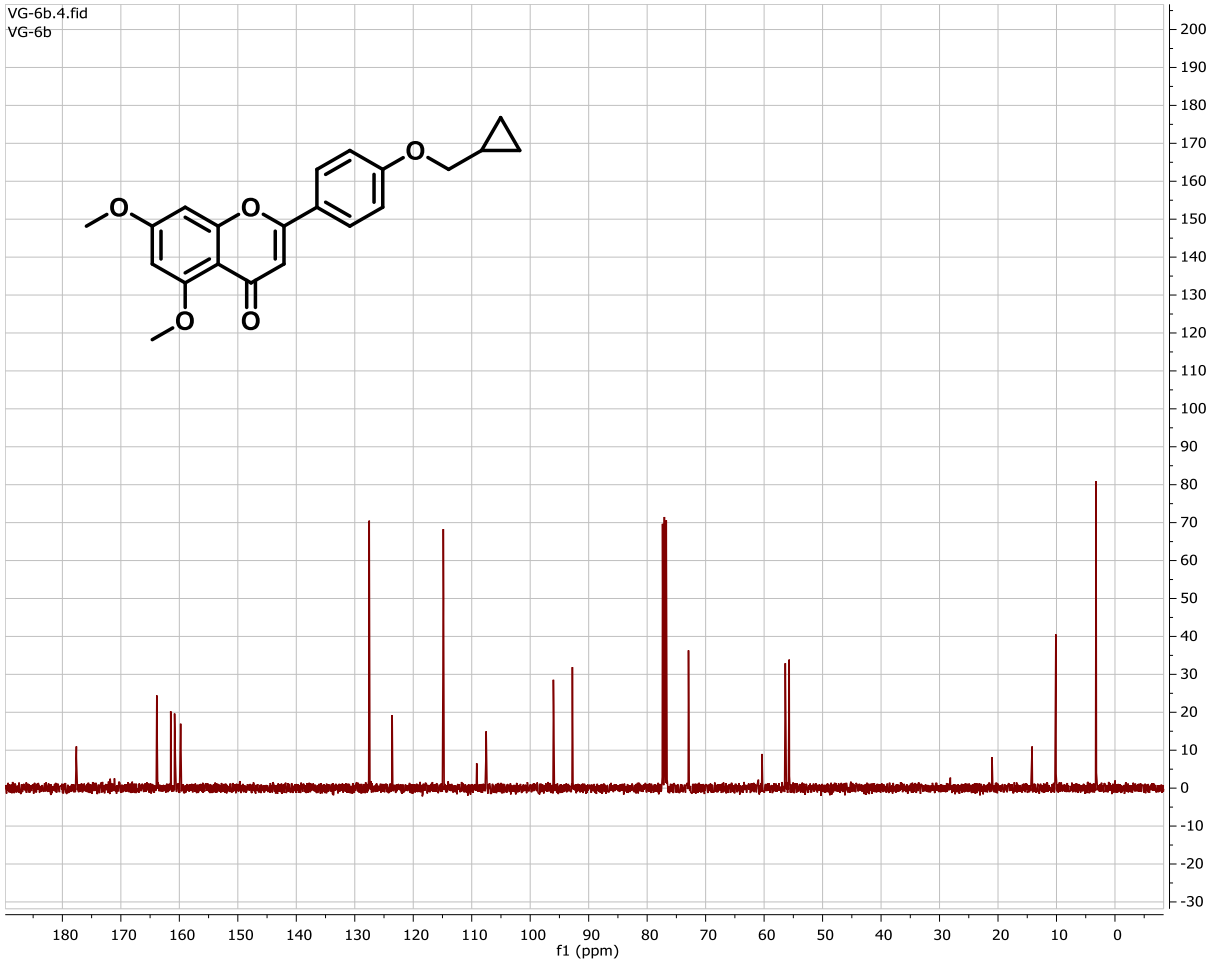

DEPT-135 Spectrum of Compound 5b

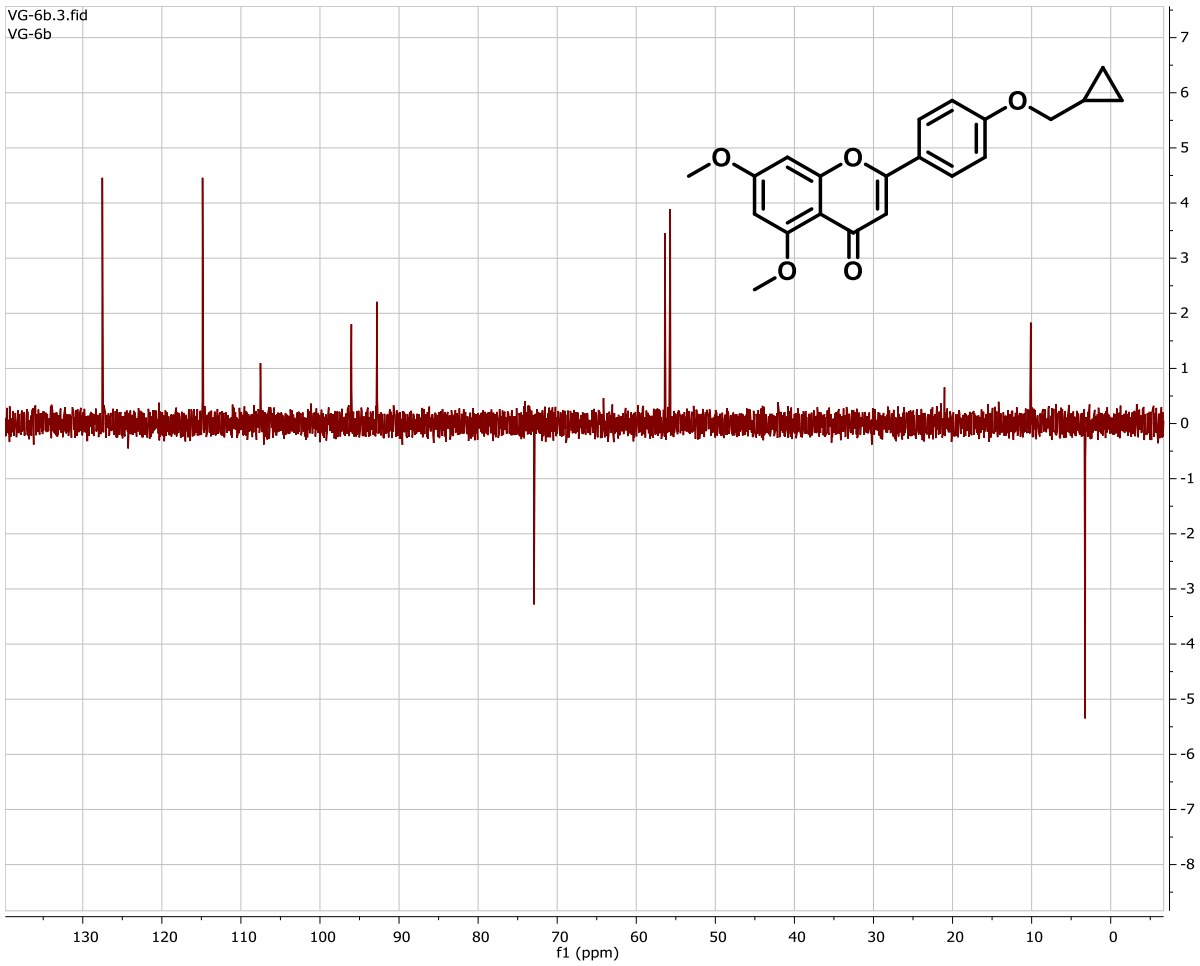

^{1}H-Spectrum of Compound 6a

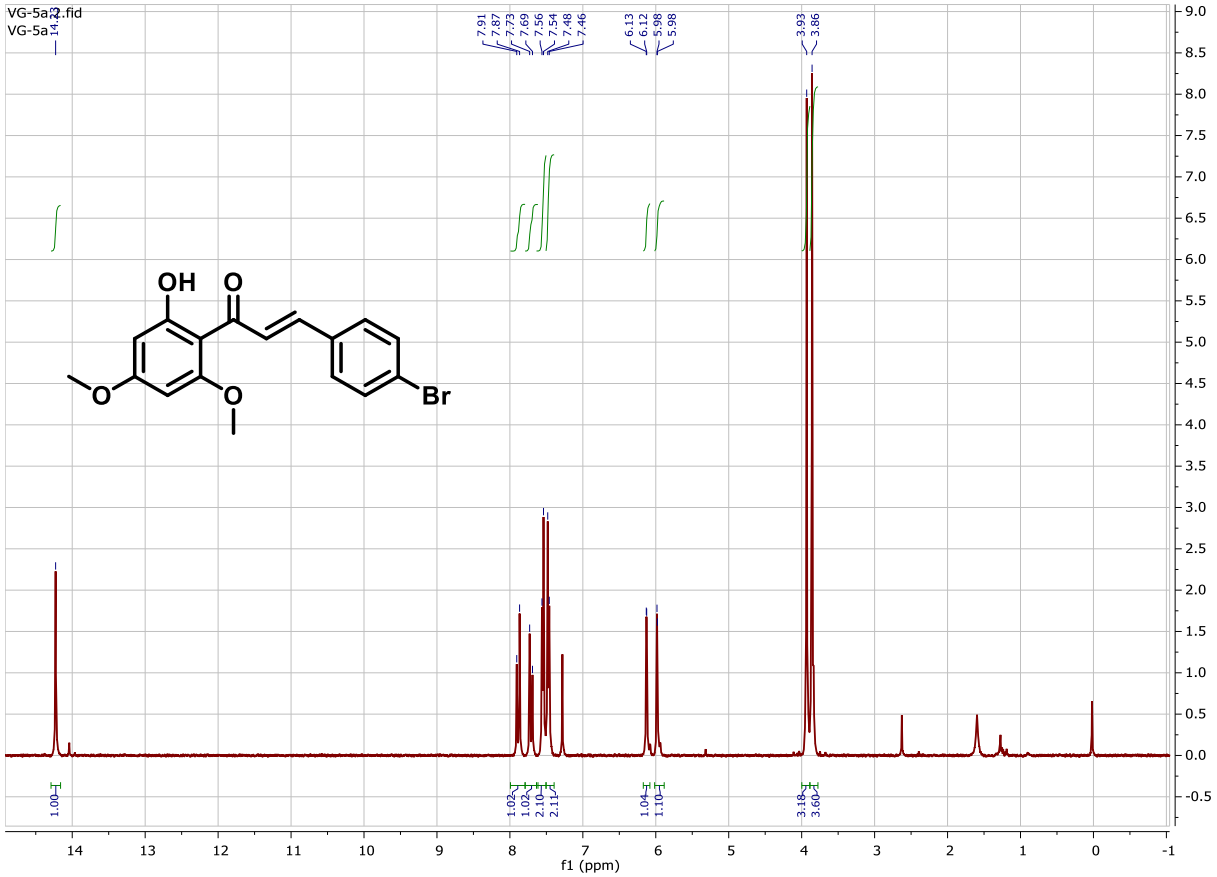

^{13}C-Spectrum of Compound 6a

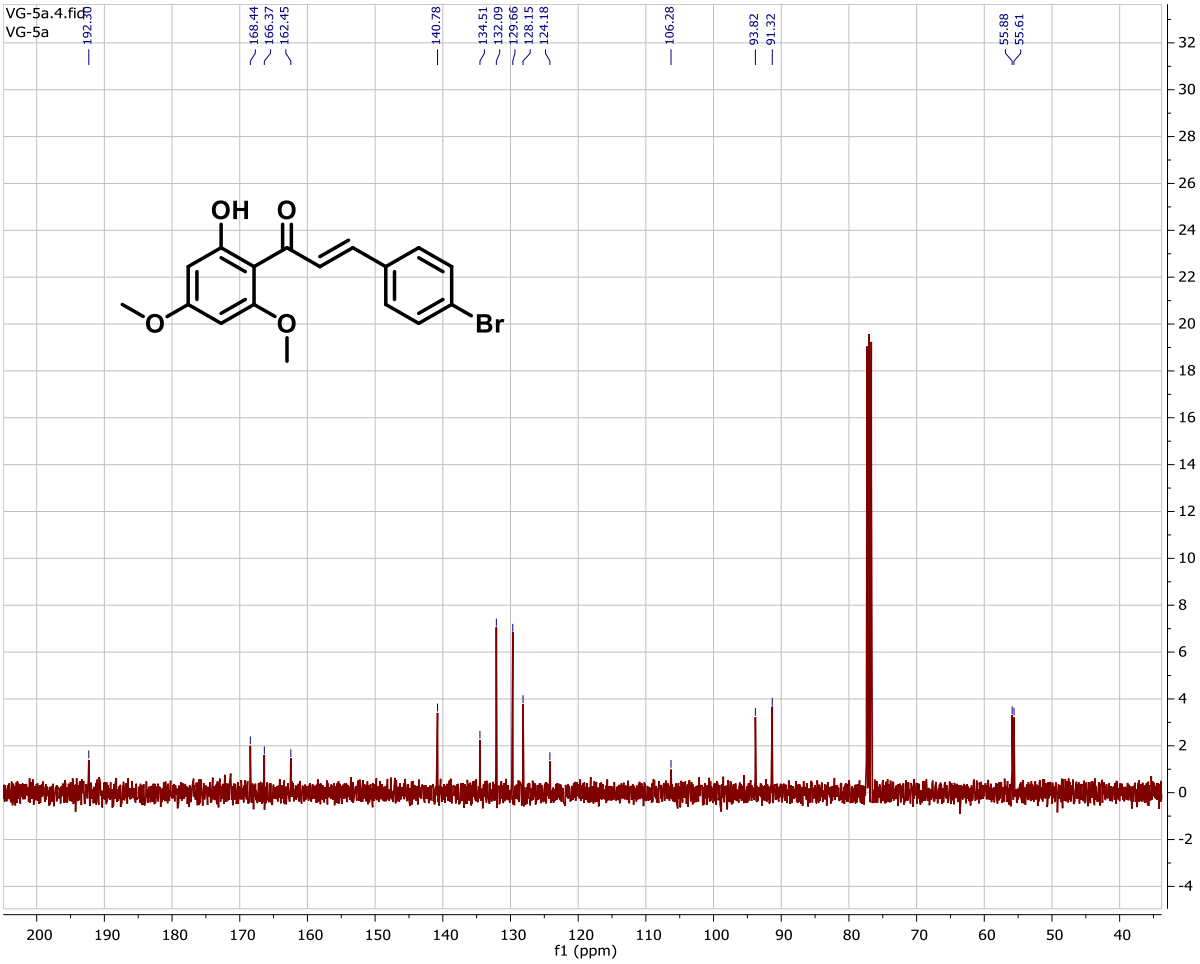

DEPT-135 Spectrum of Compound 6a

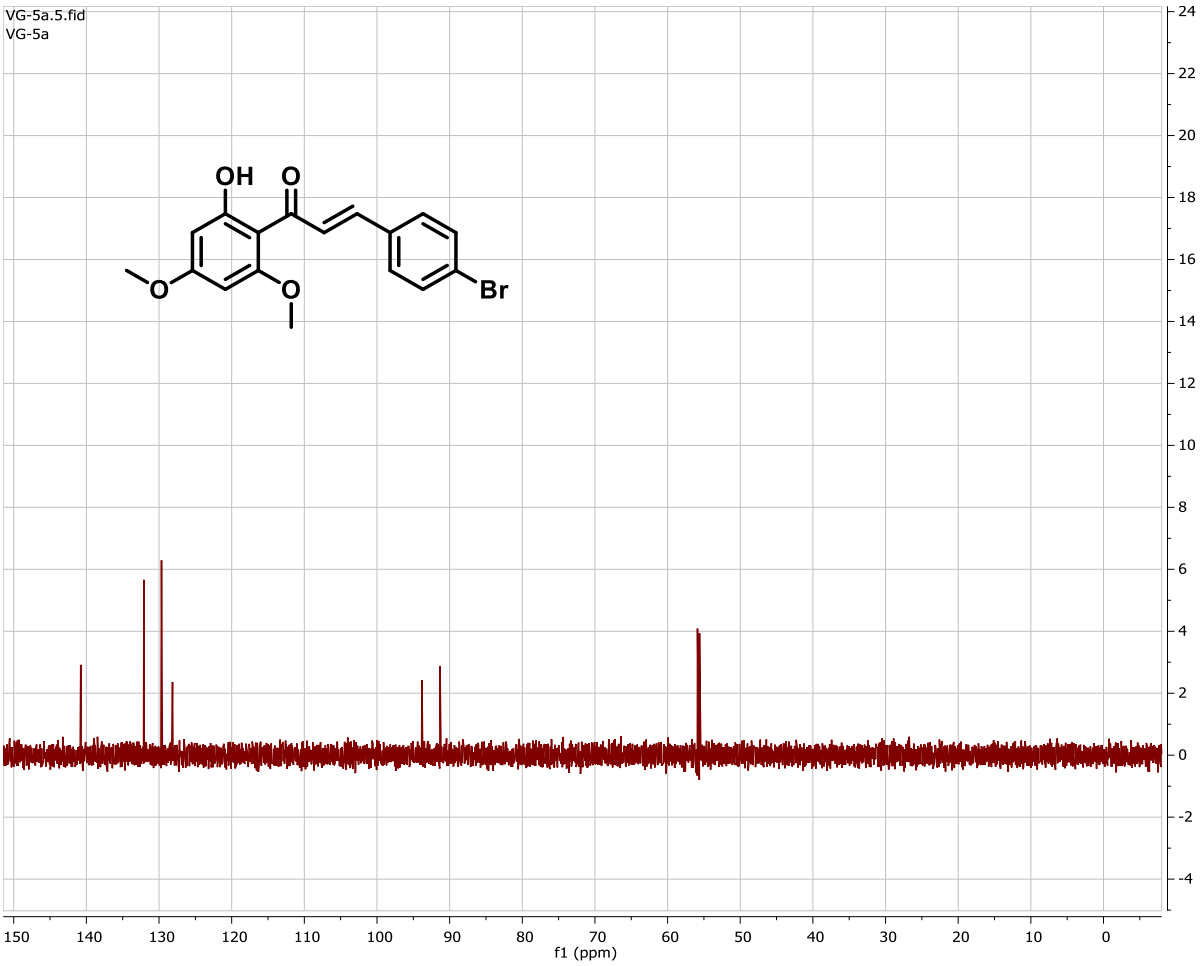

^{1}H-Spectrum of Compound 6b

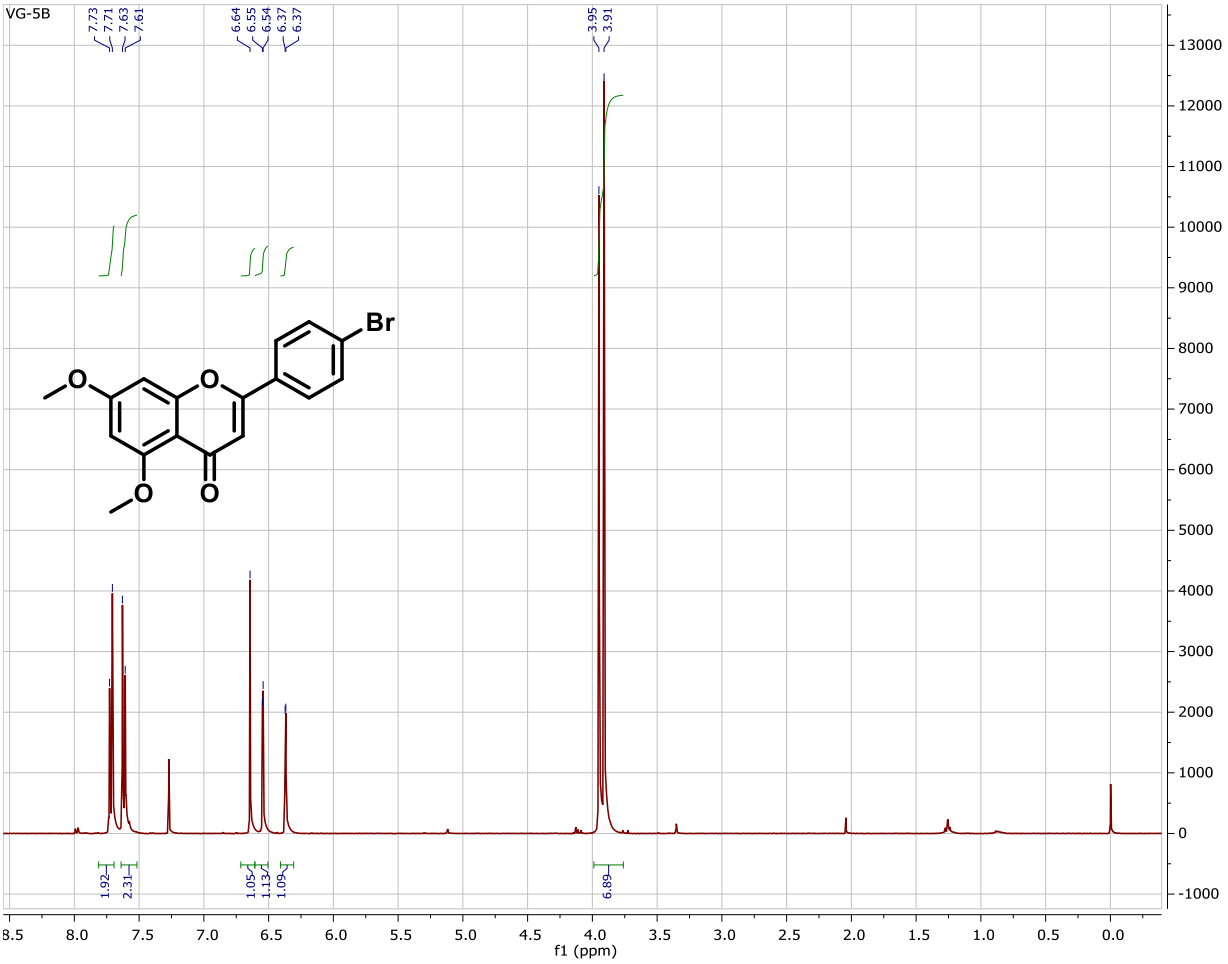

^{13}C-Spectrum of Compound 6b

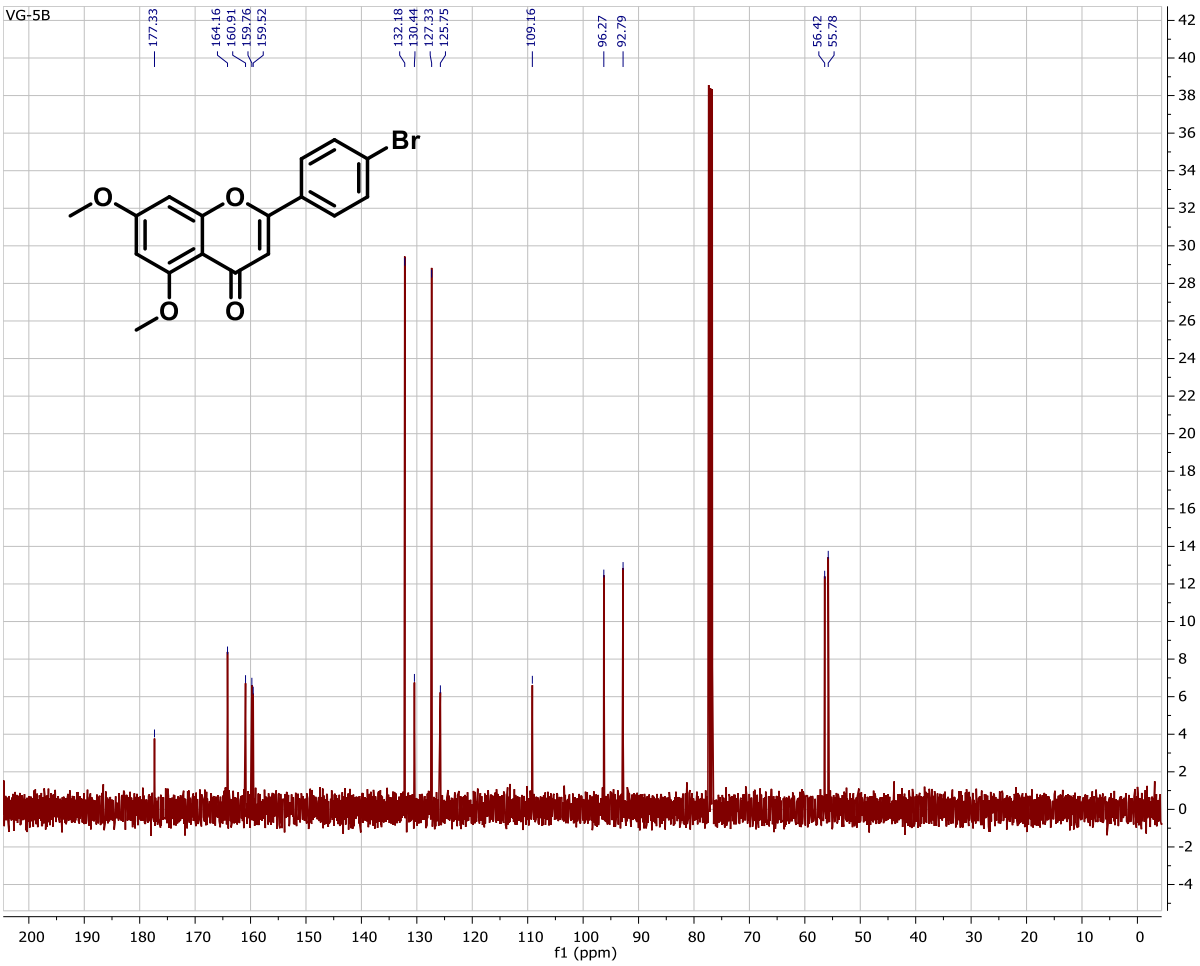

DEPT-135 Spectrum of Compound 6b

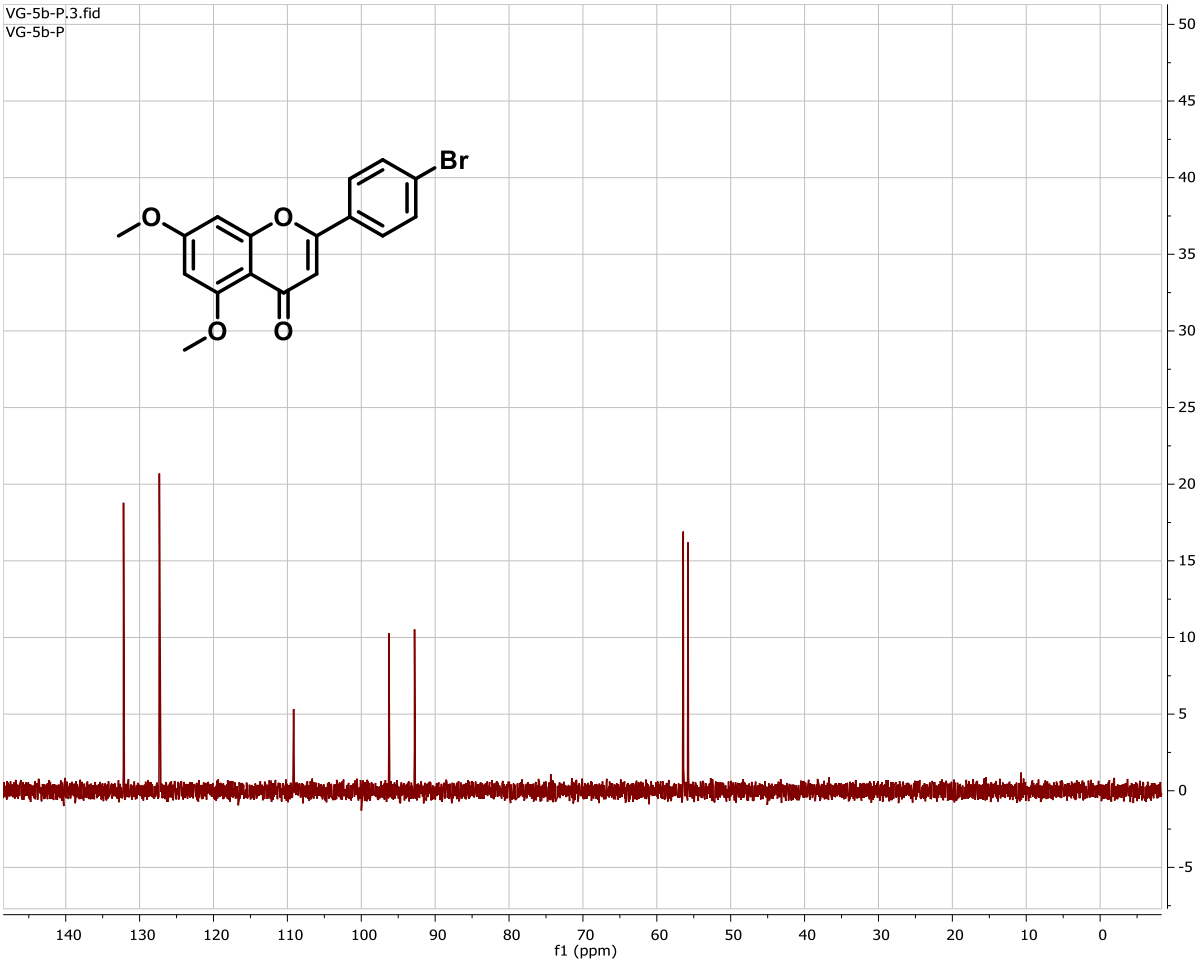

^{1}H-Spectrum of Compound 6c

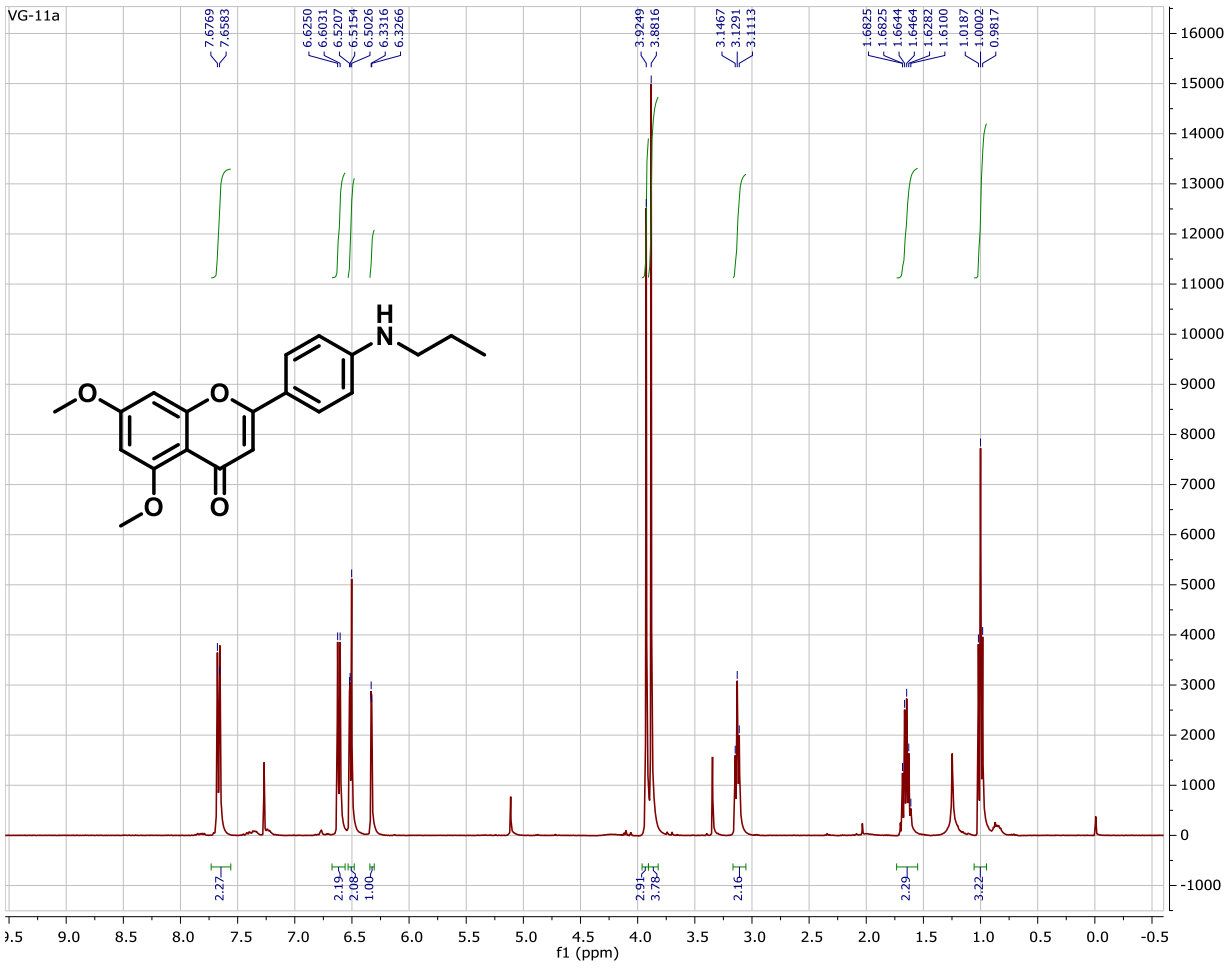

^{13}C-Spectrum of Compound 6c

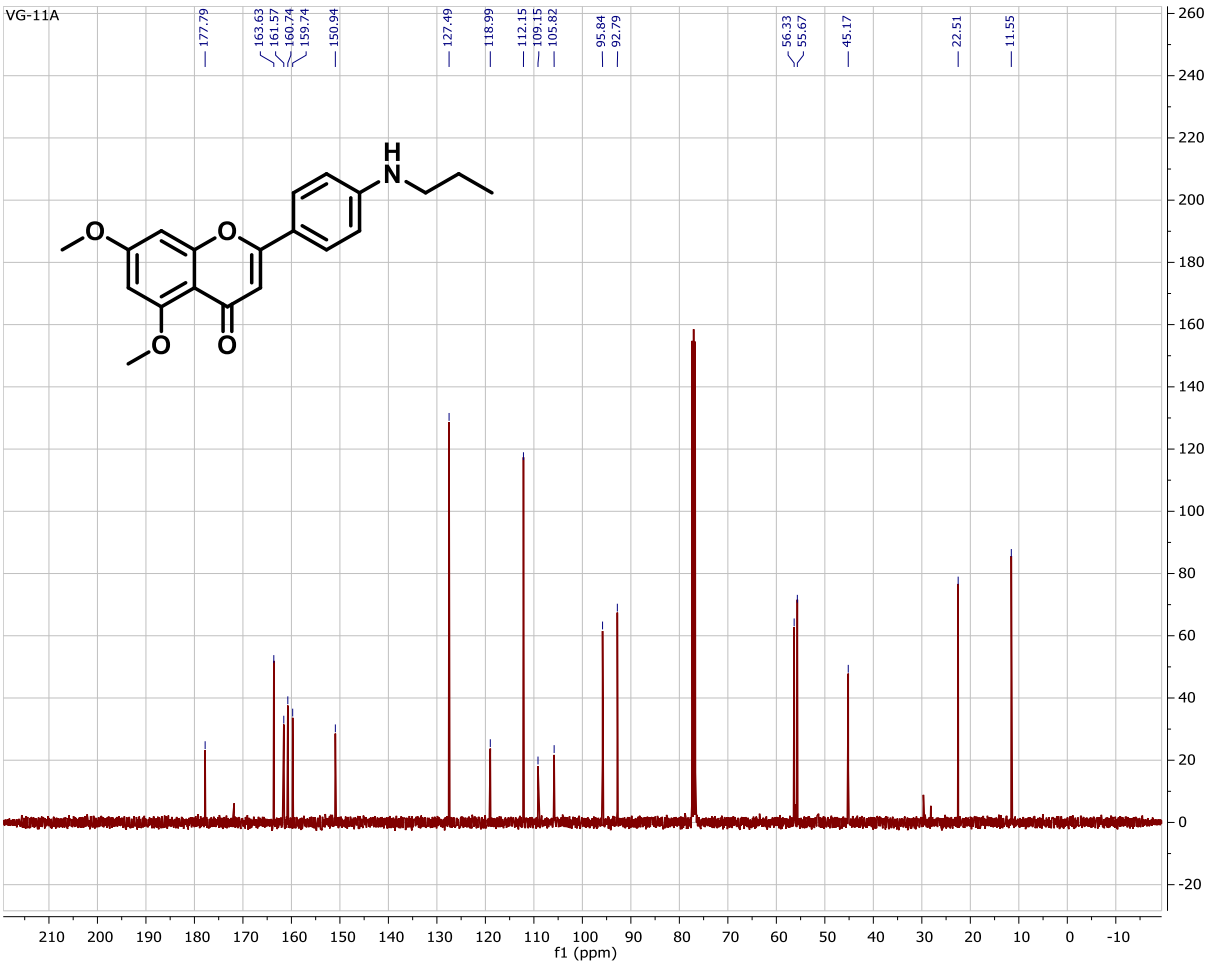

DEPT-135 Spectrum of Compound 6c

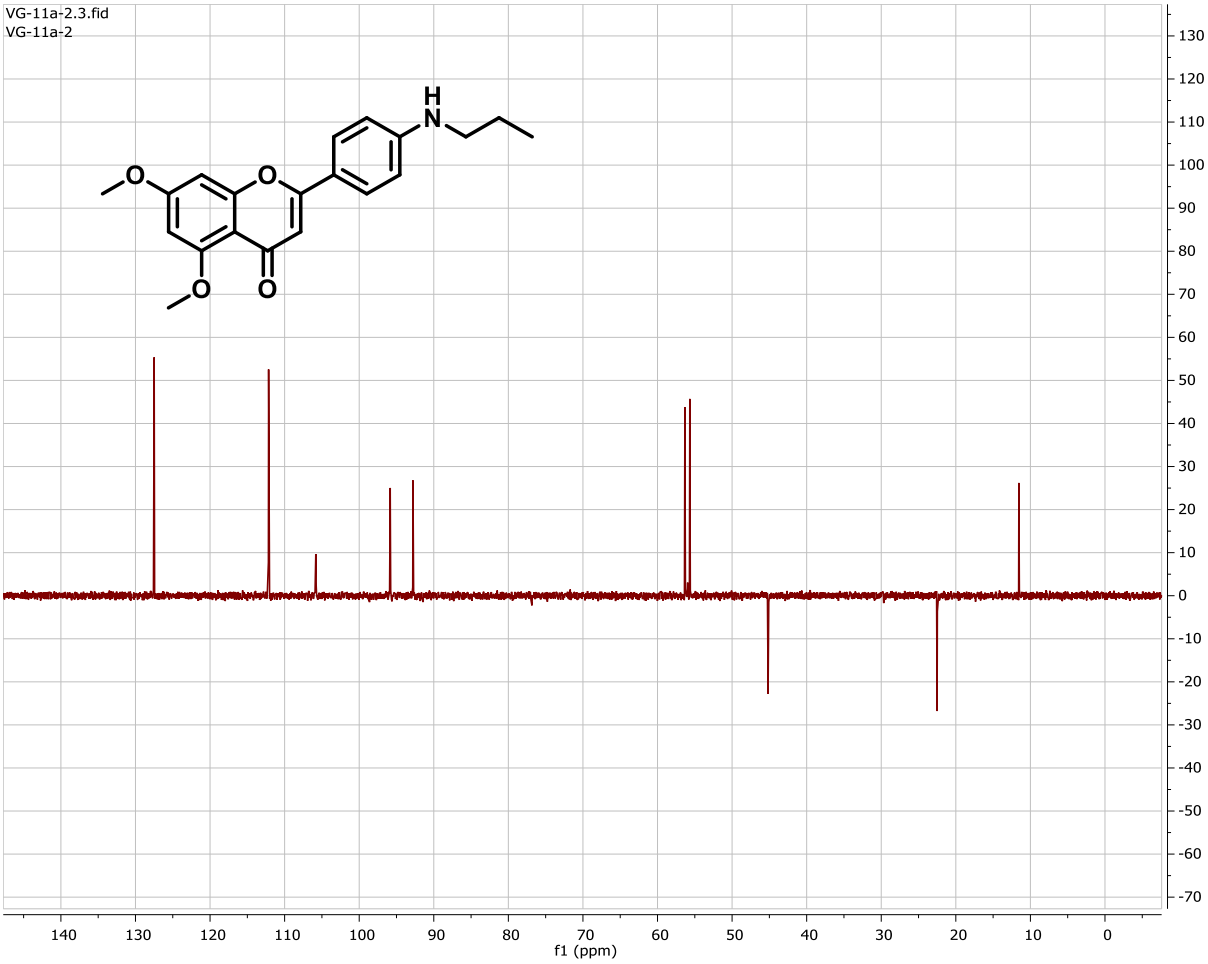

^{1}H-Spectrum of Compound 6d

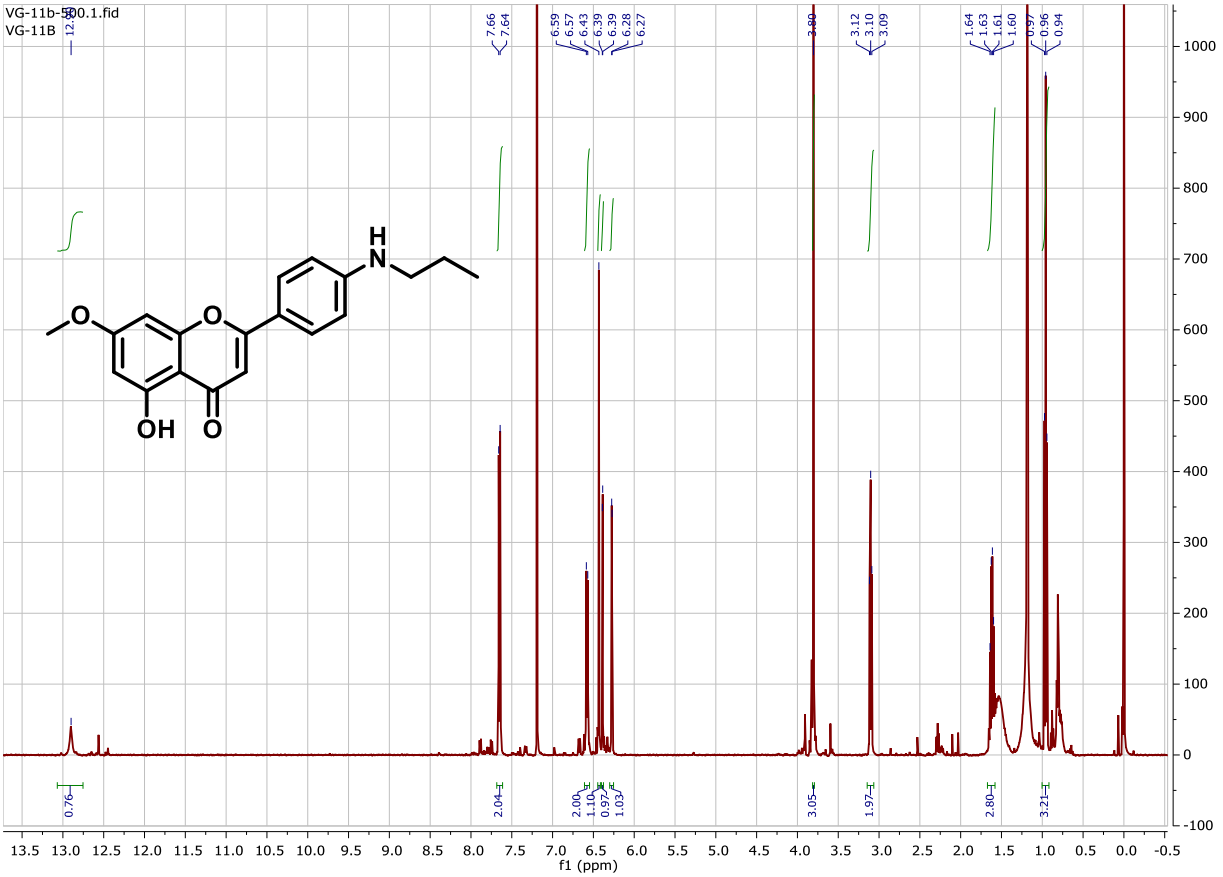

^{13}C-Spectrum of Compound 6d

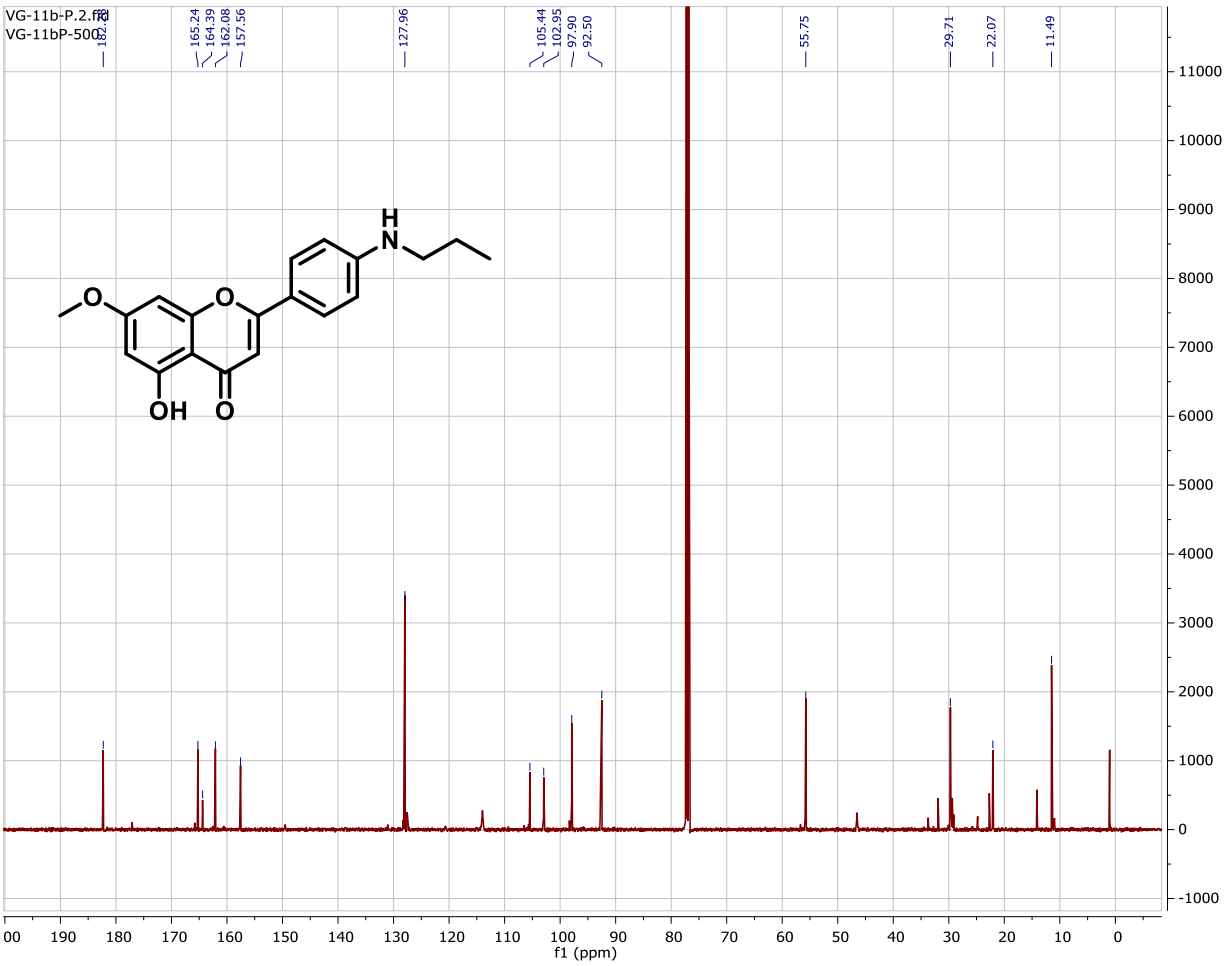

DEPT-135 Spectrum of Compound 6d

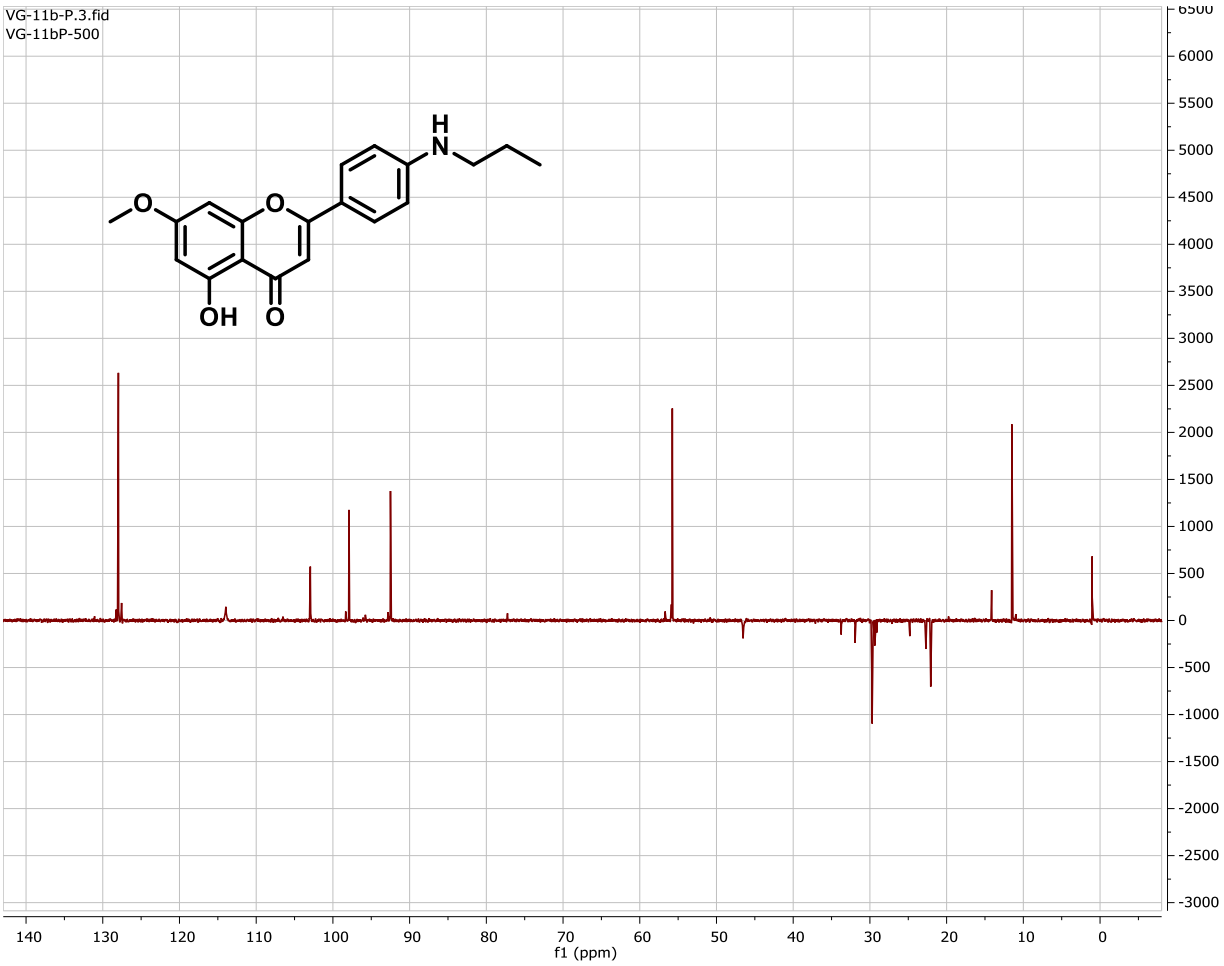

HSQC Spectrum of Compound 6d

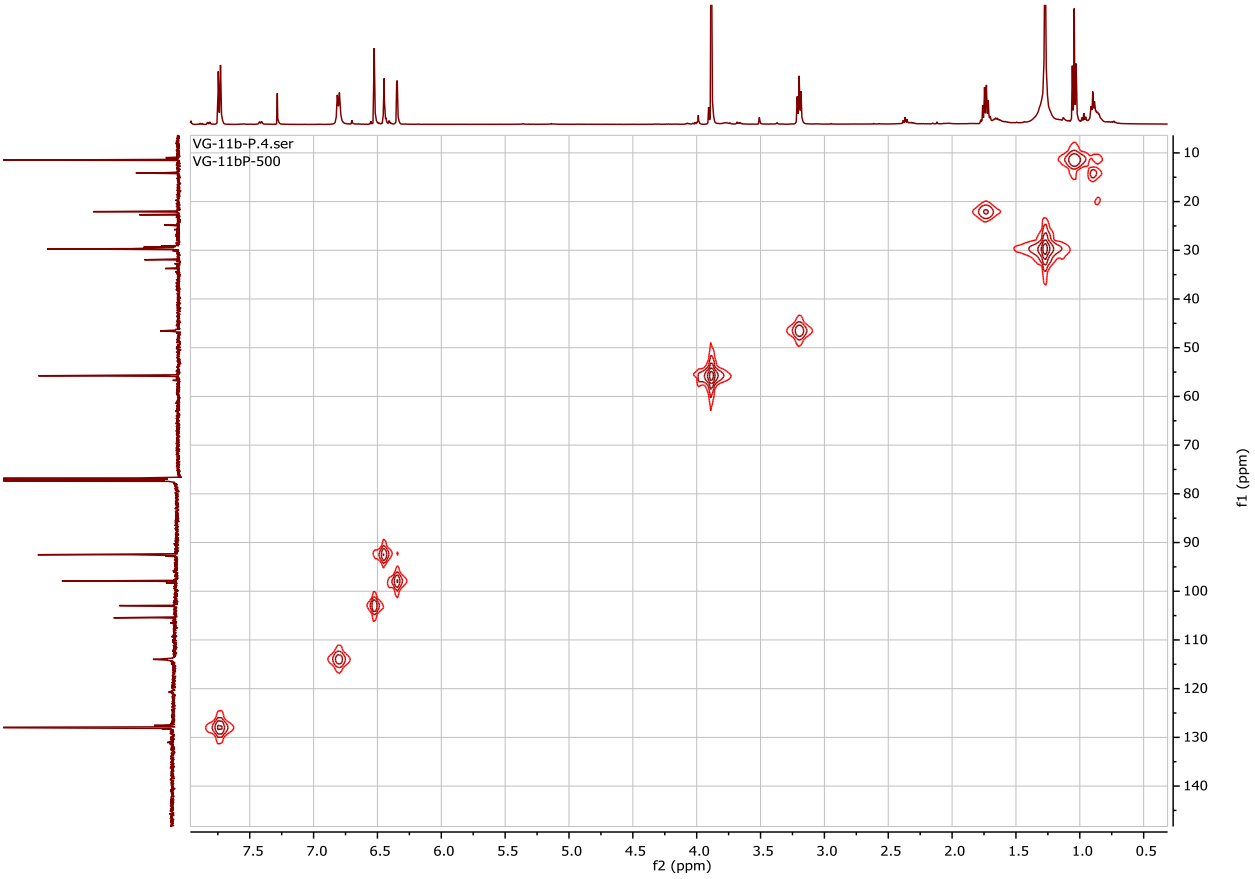

HMBC Spectrum of Compound 6d

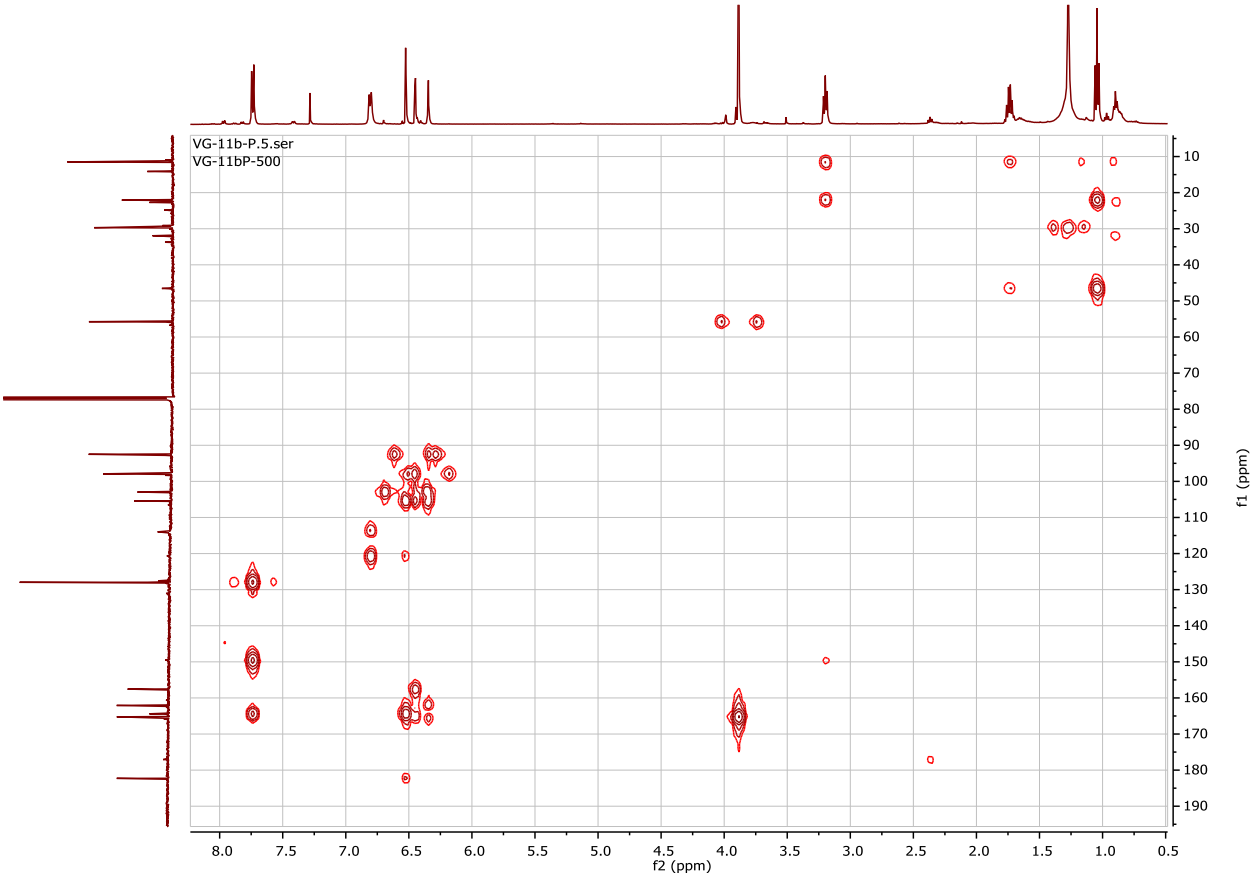

^{1}H-Spectrum of Compound 7c

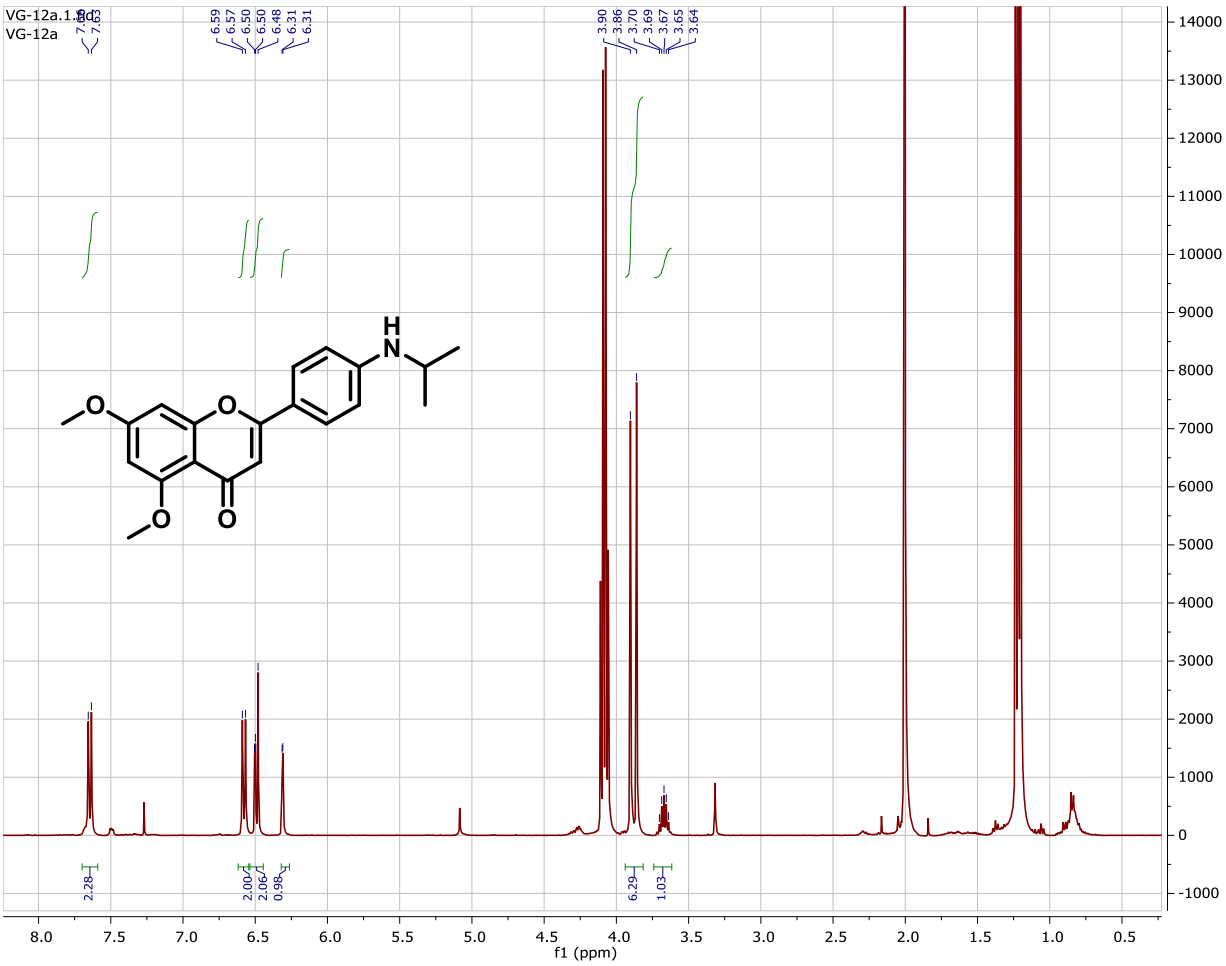

^{13}C-Spectrum of Compound 7c

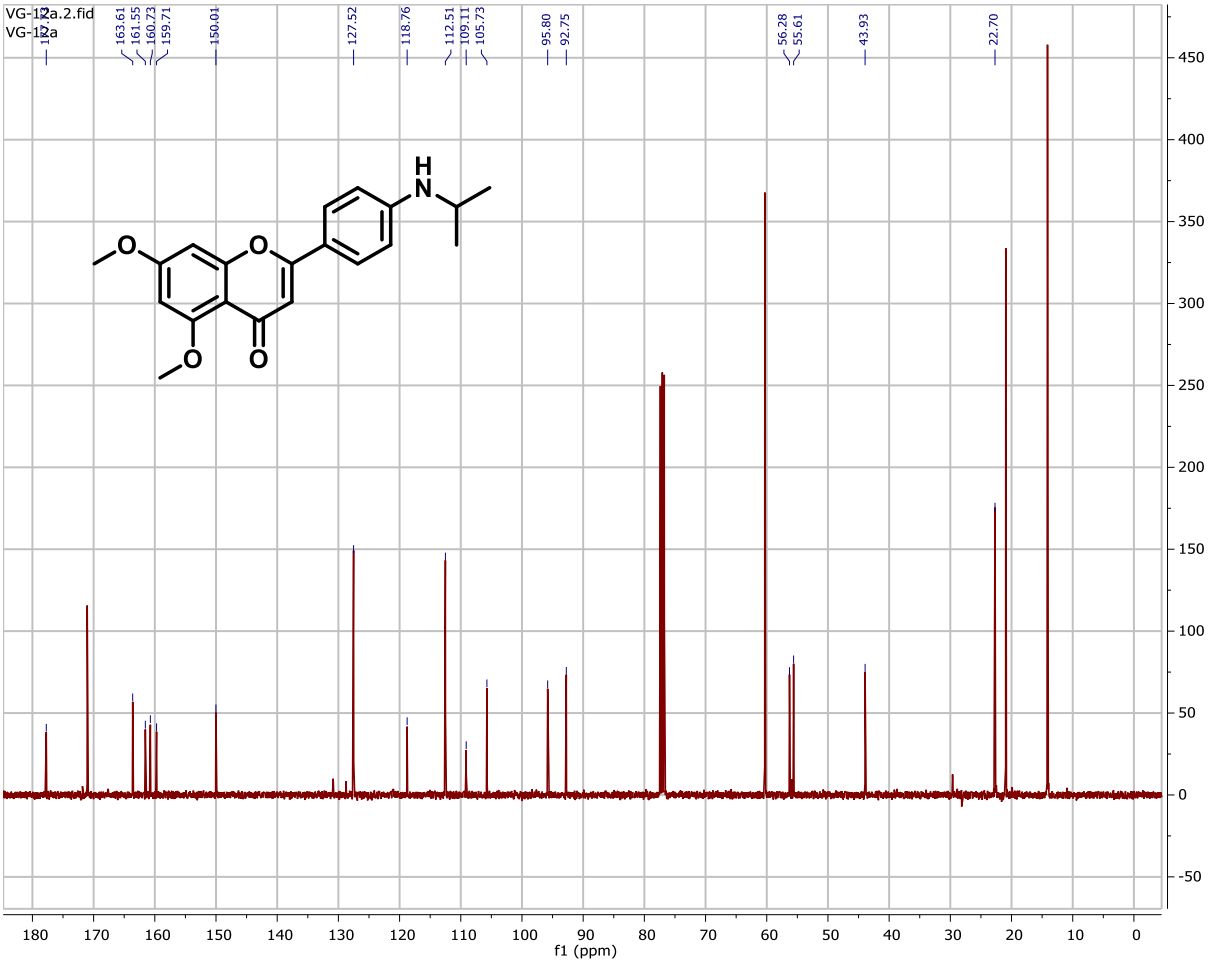

DEPT-135 Spectrum of Compound 7c

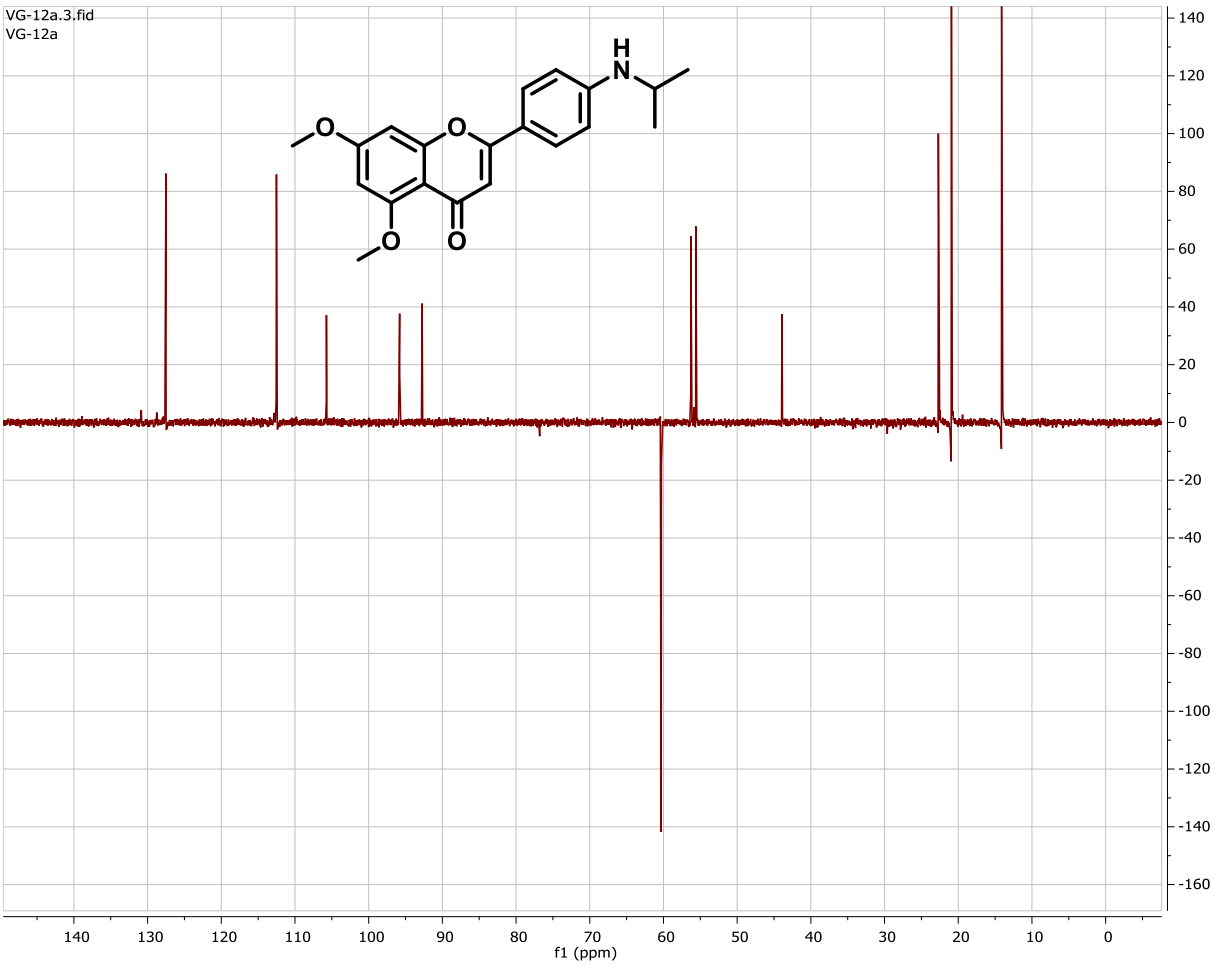

^{1}H-Spectrum of Compound 7d

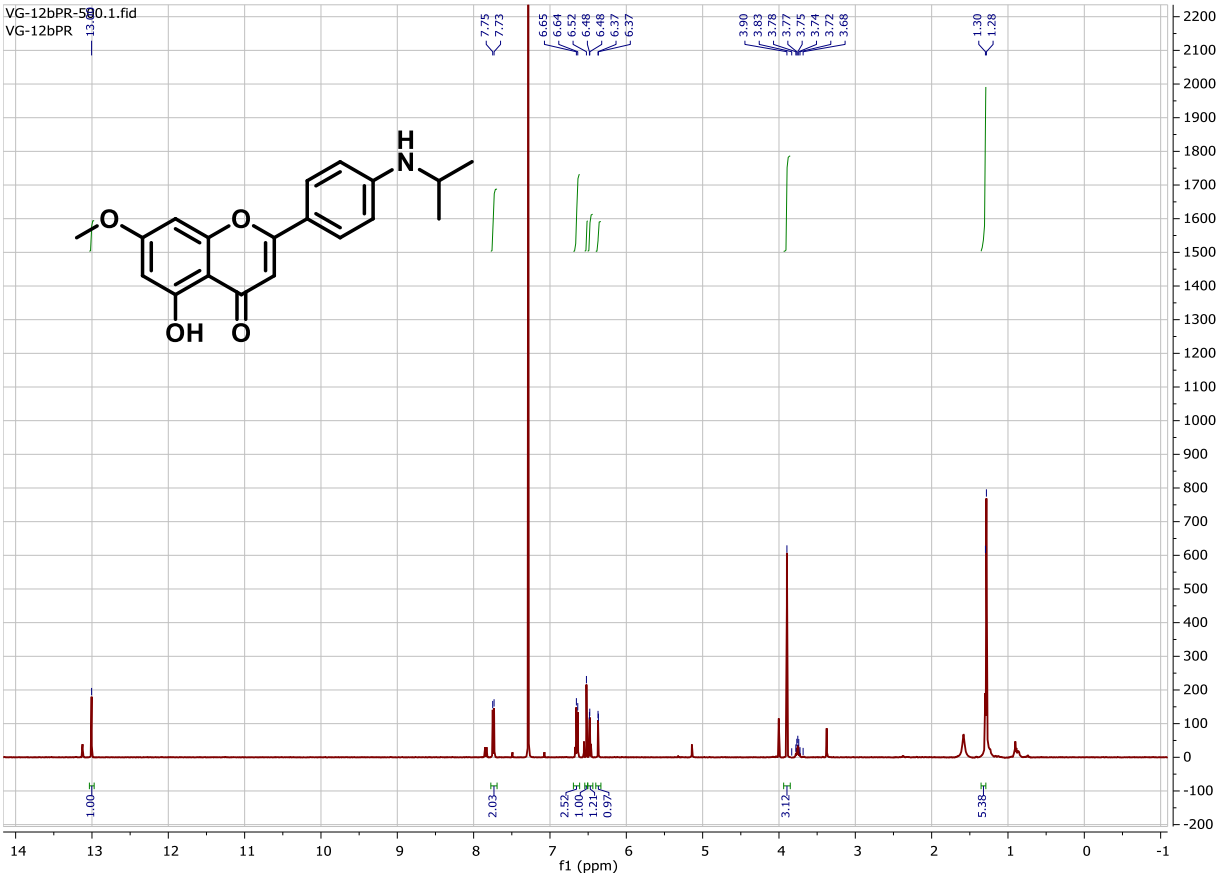

^{13}C-Spectrum of Compound 7d

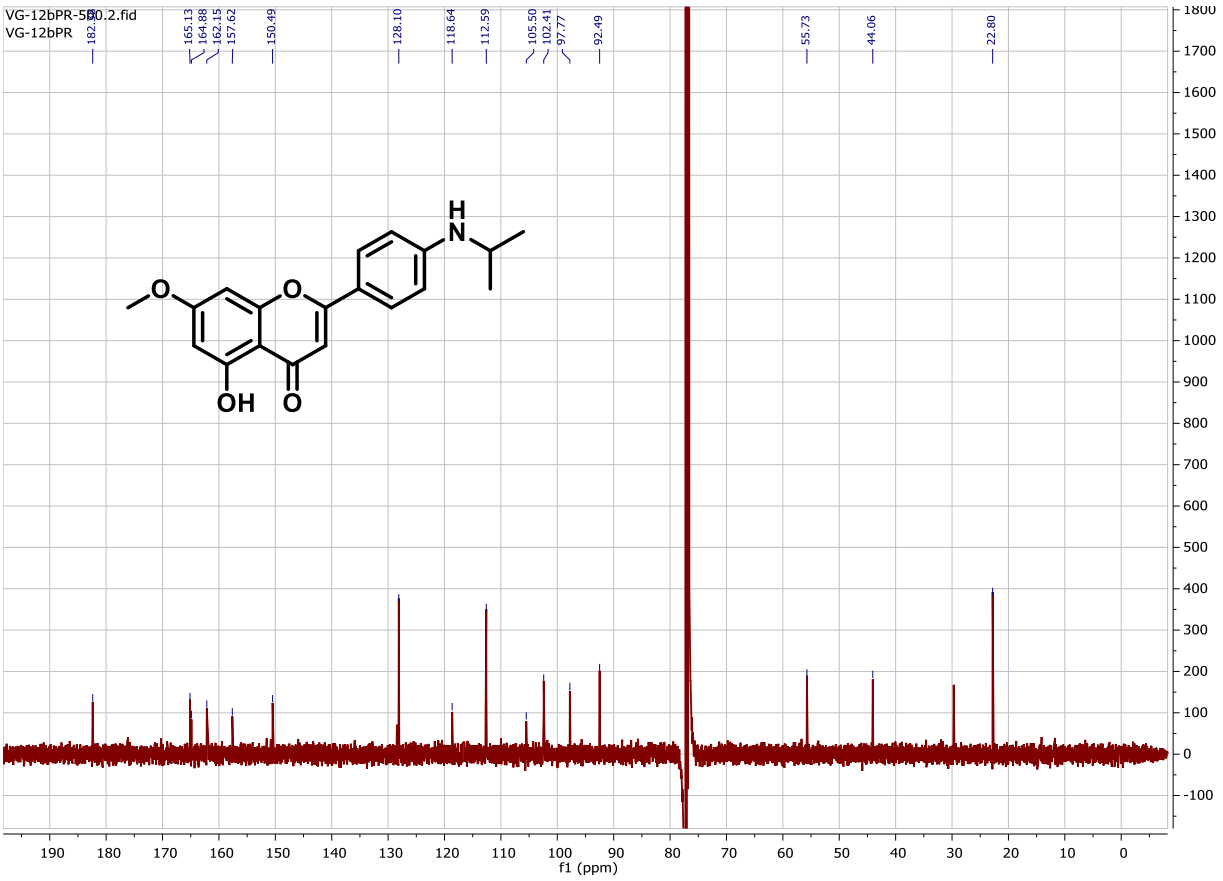

DEPT-135 Spectrum of Compound 7d

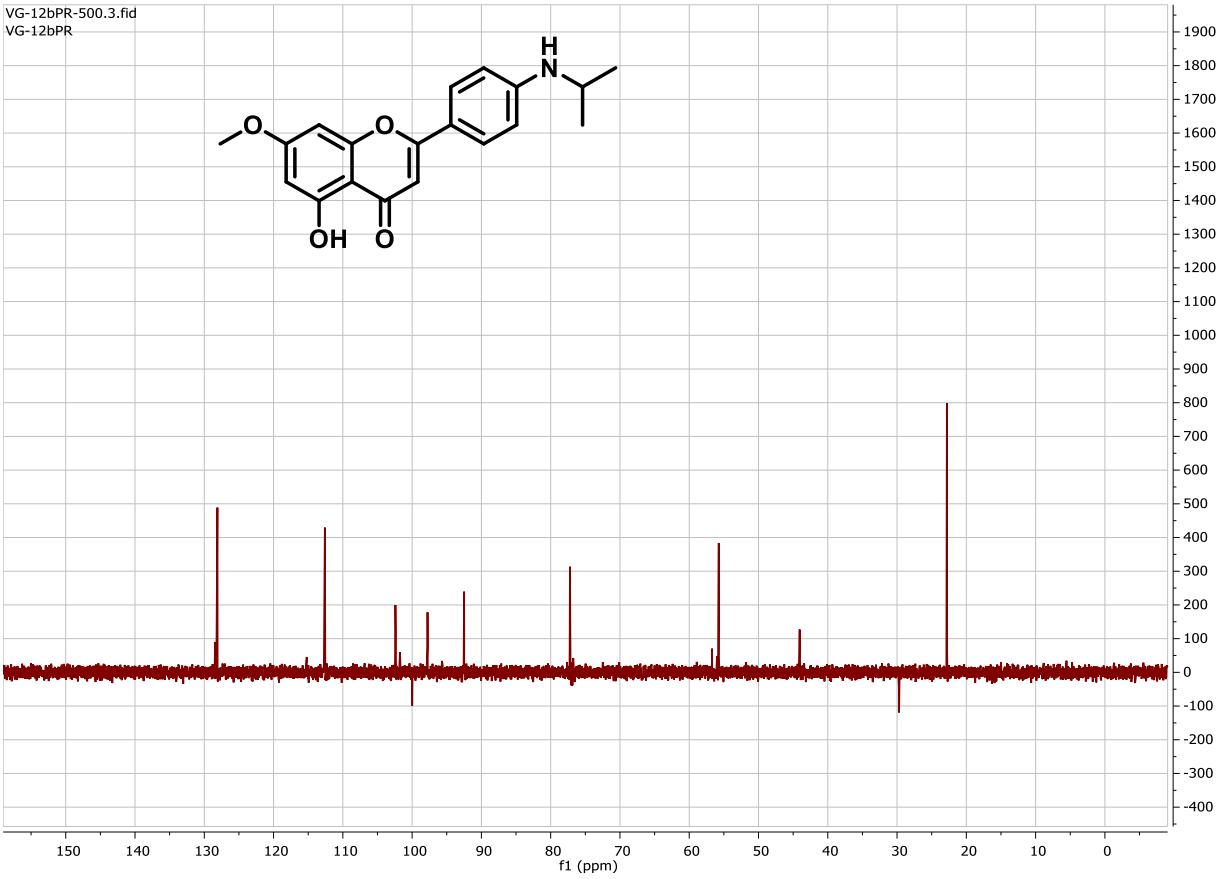

HSQC Spectrum of Compound 7d

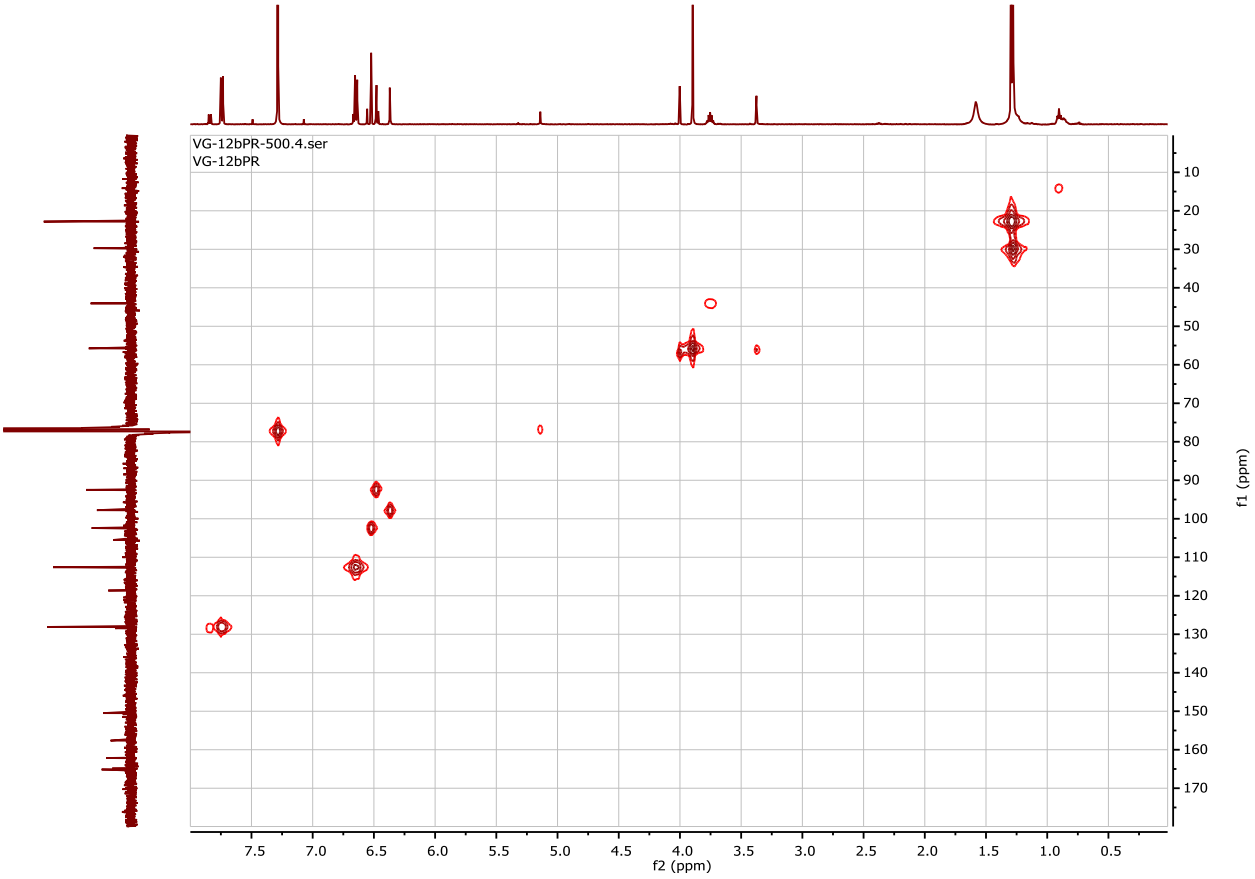

HMBC Spectrum of Compound 7d

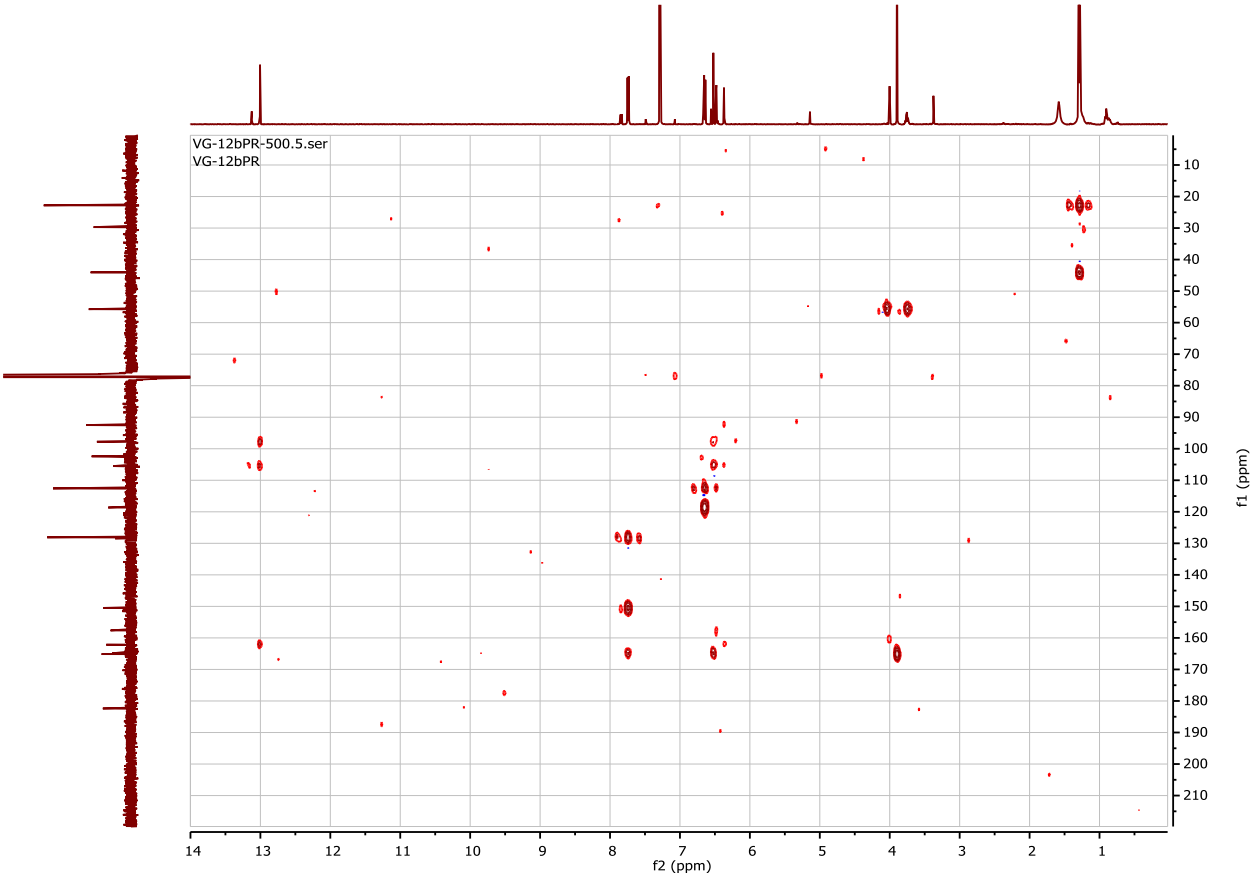

^{1}H-Spectrum of Compound 9c

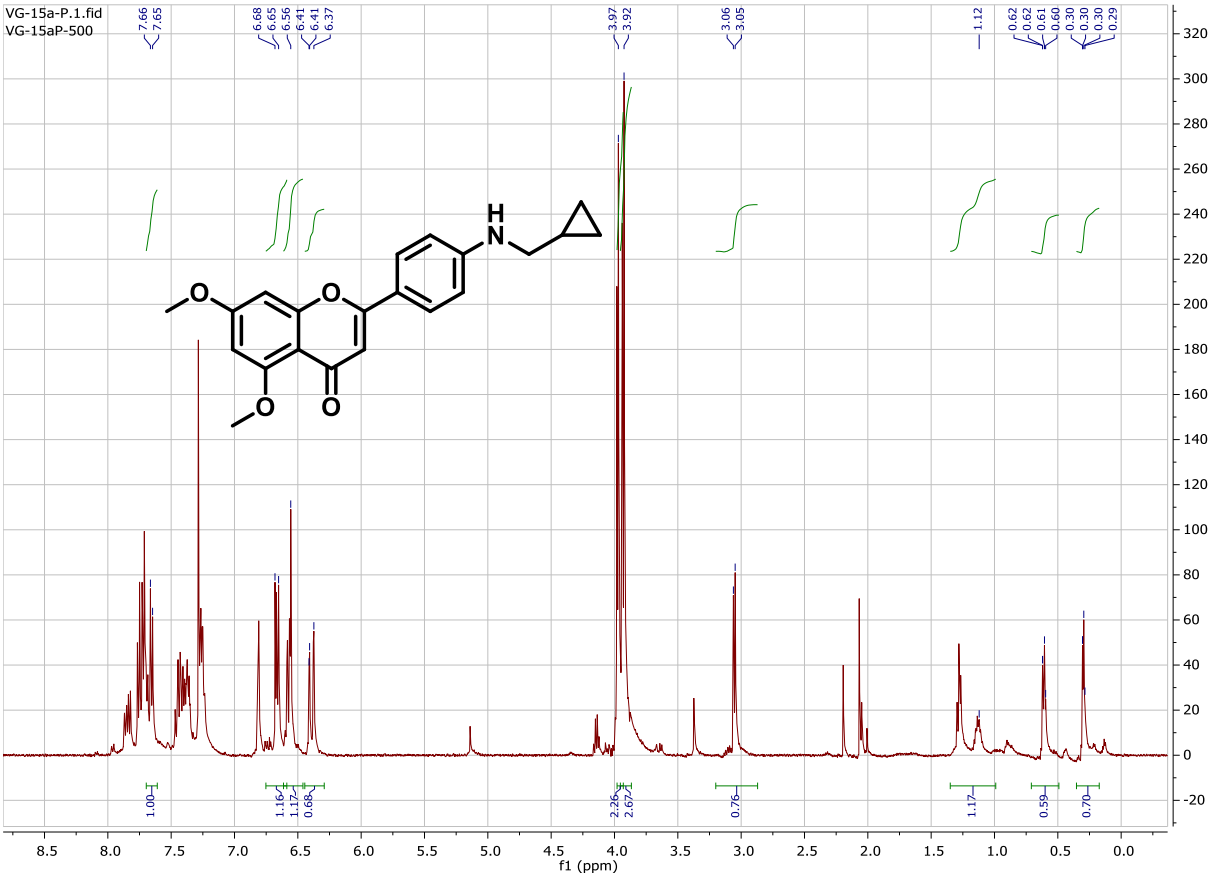

^{13}C-Spectrum of Compound 9c

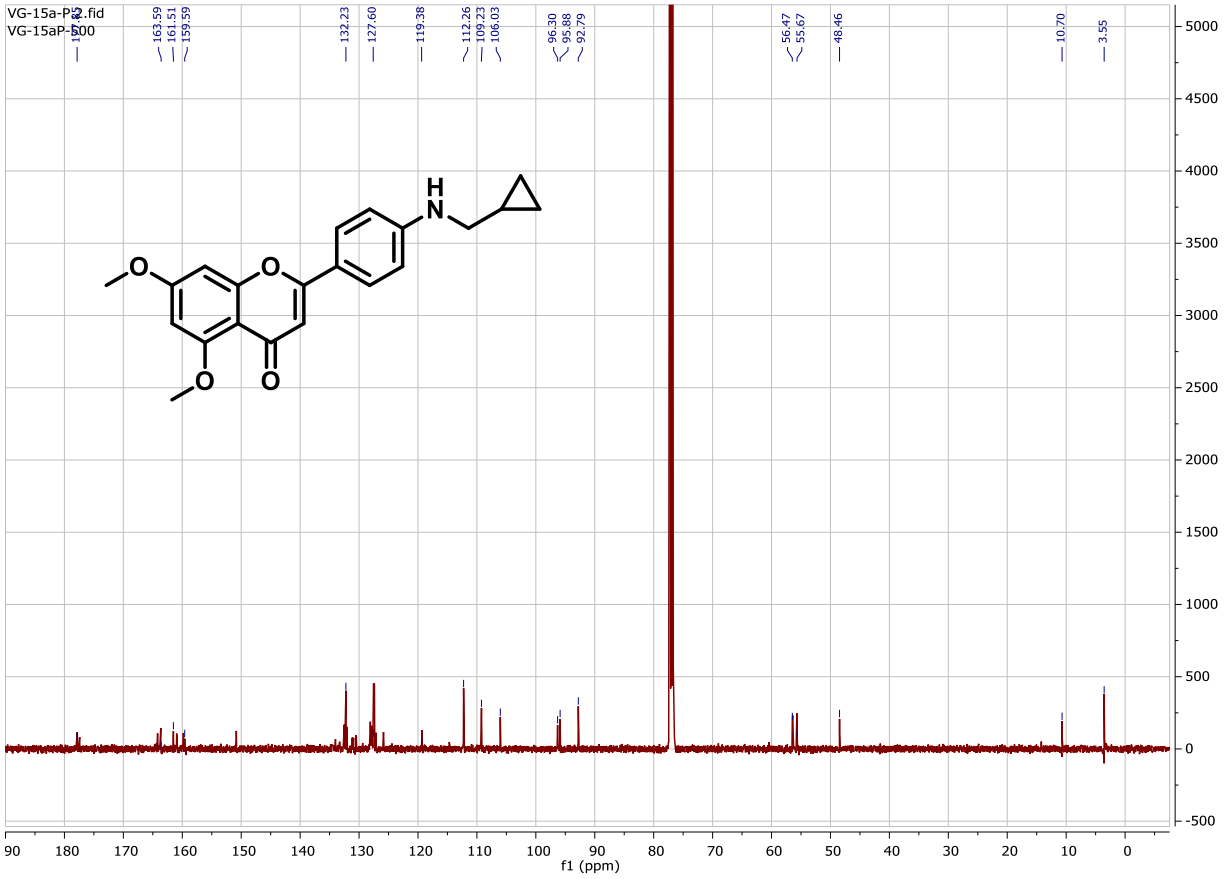

DEPT-135 Spectrum of Compound 9c

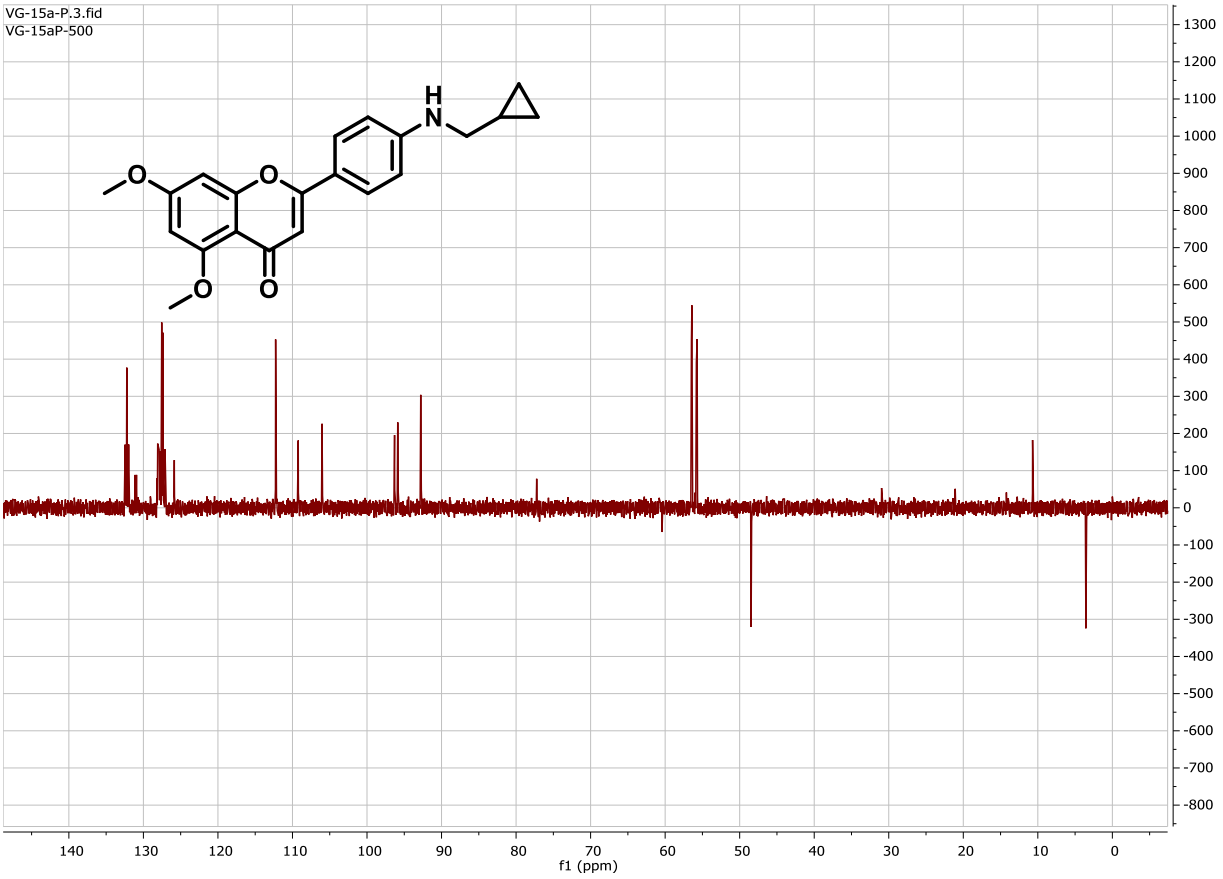

^{1}H-Spectrum of Compound 9d

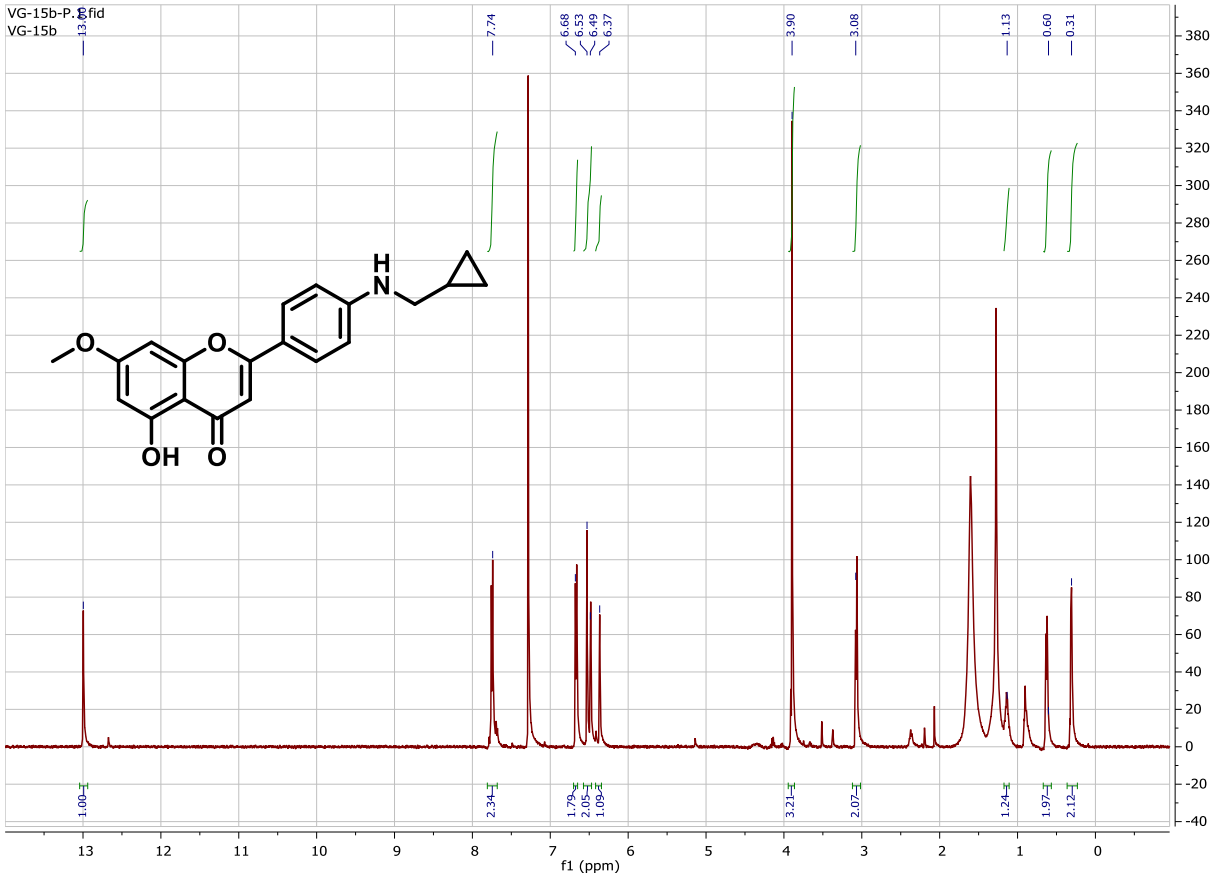

^{13}C-Spectrum of Compound 9d

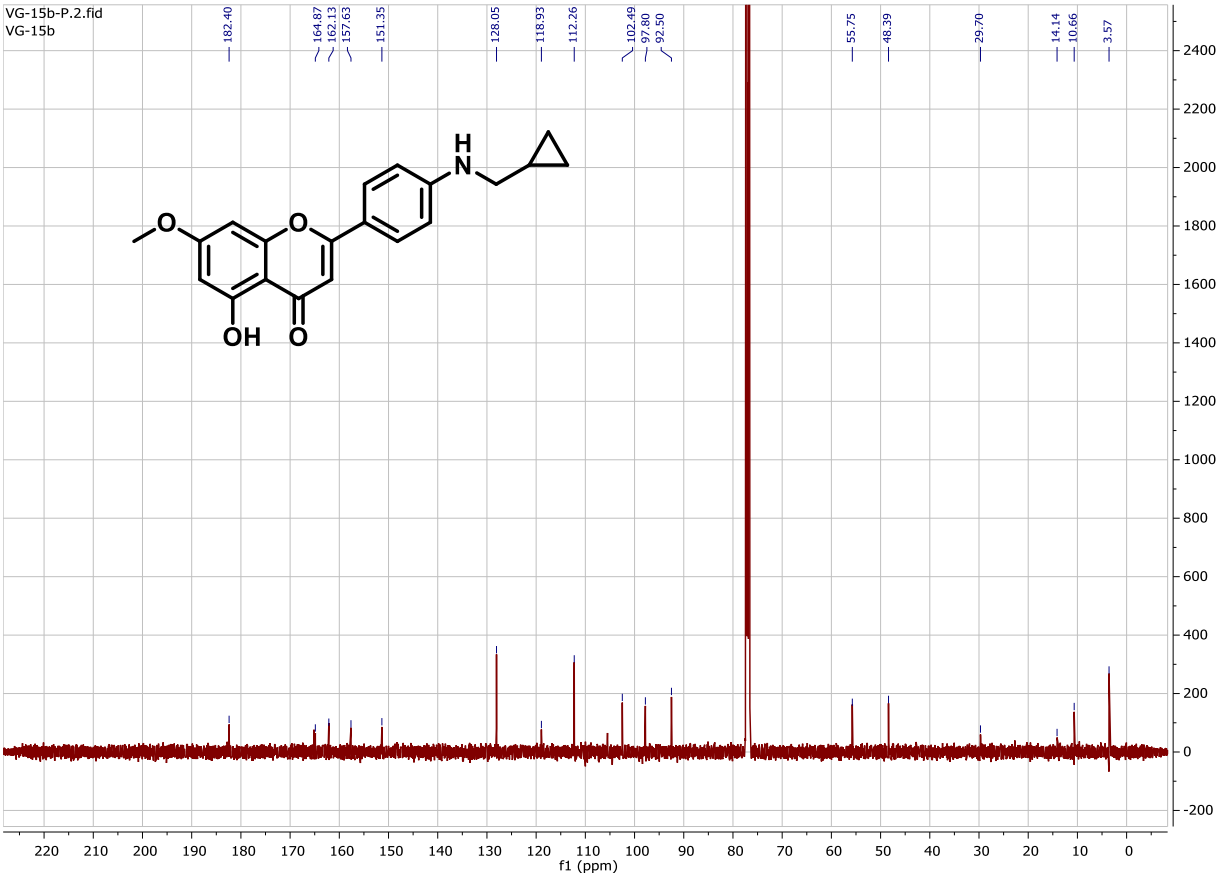

DEPT-135 Spectrum of Compound 9d

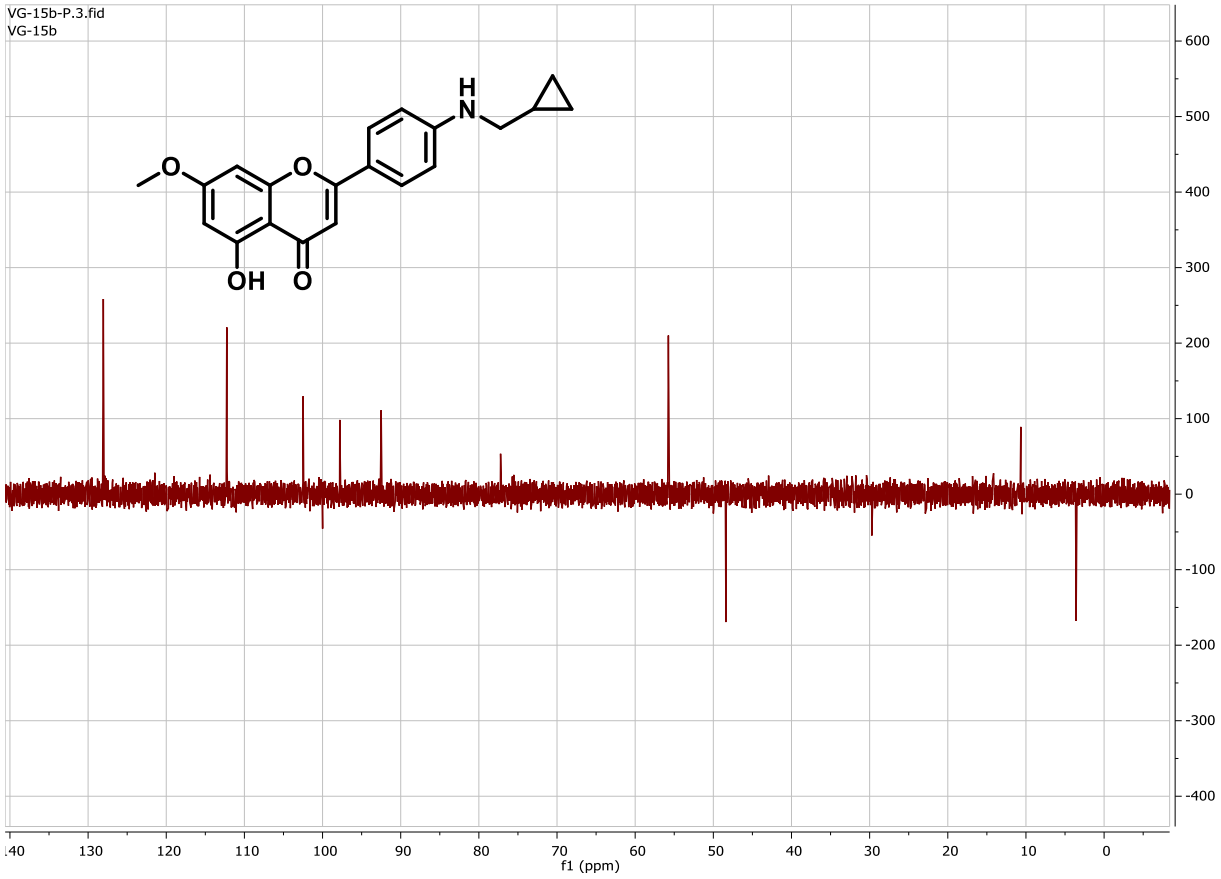

HSQC Spectrum of Compound 9d

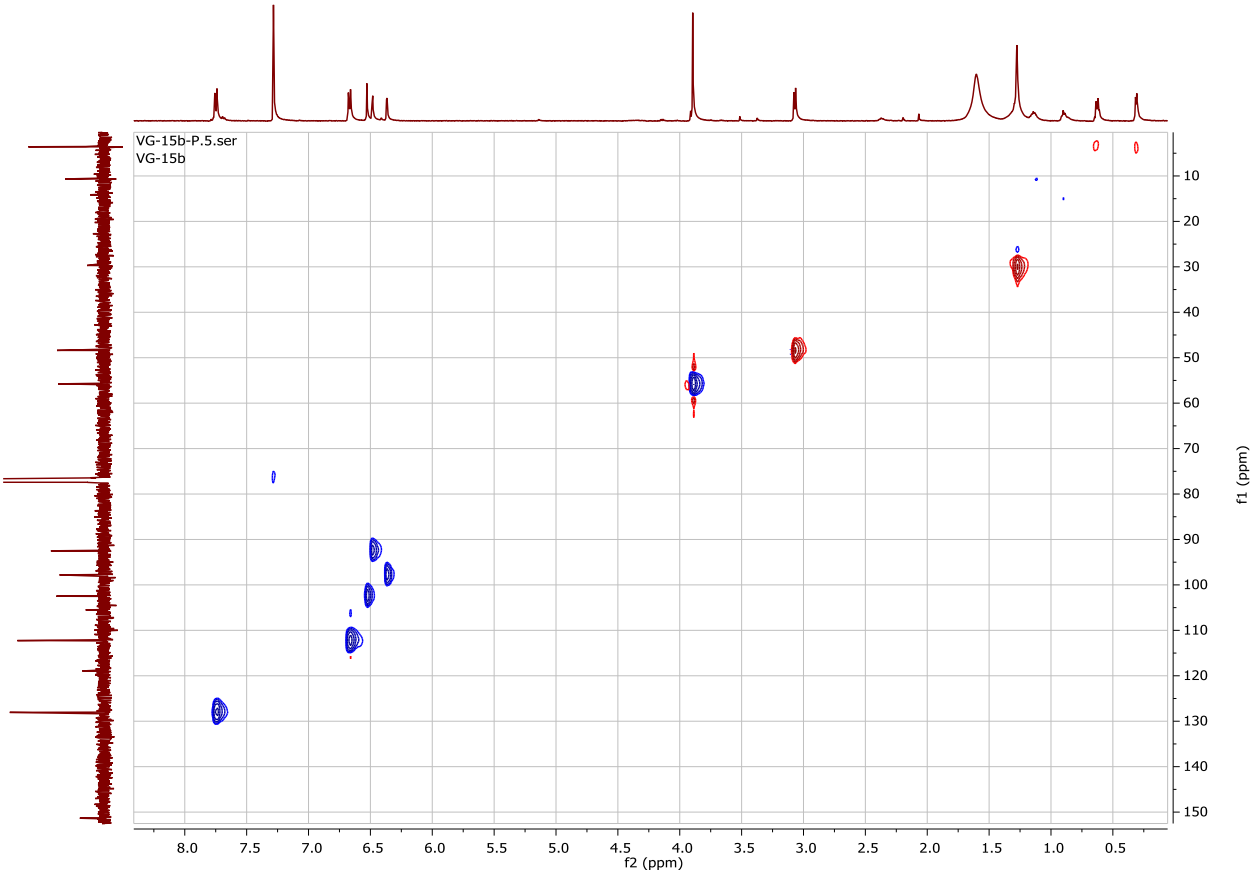

HMBC Spectrum of Compound 9d

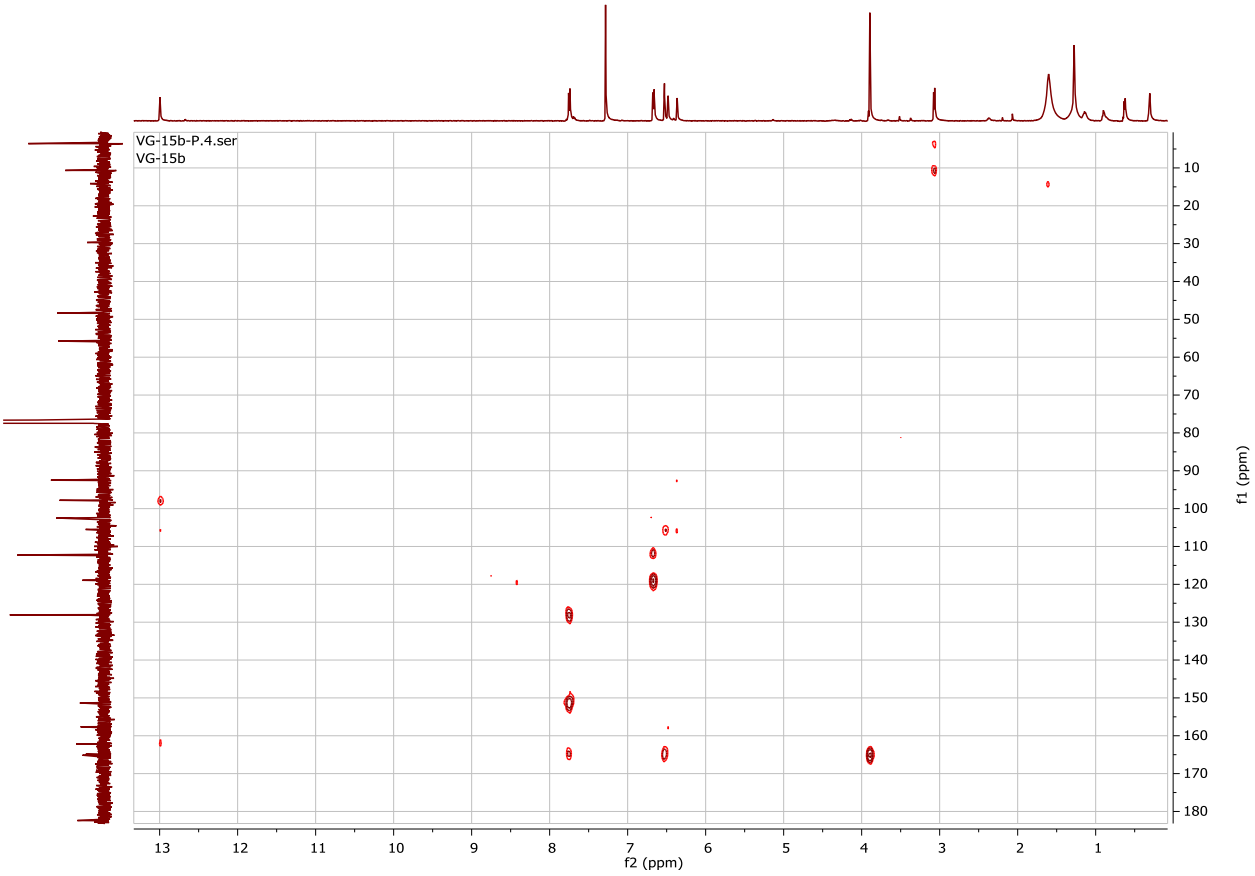

^{1}H-Spectrum of Compound 10a

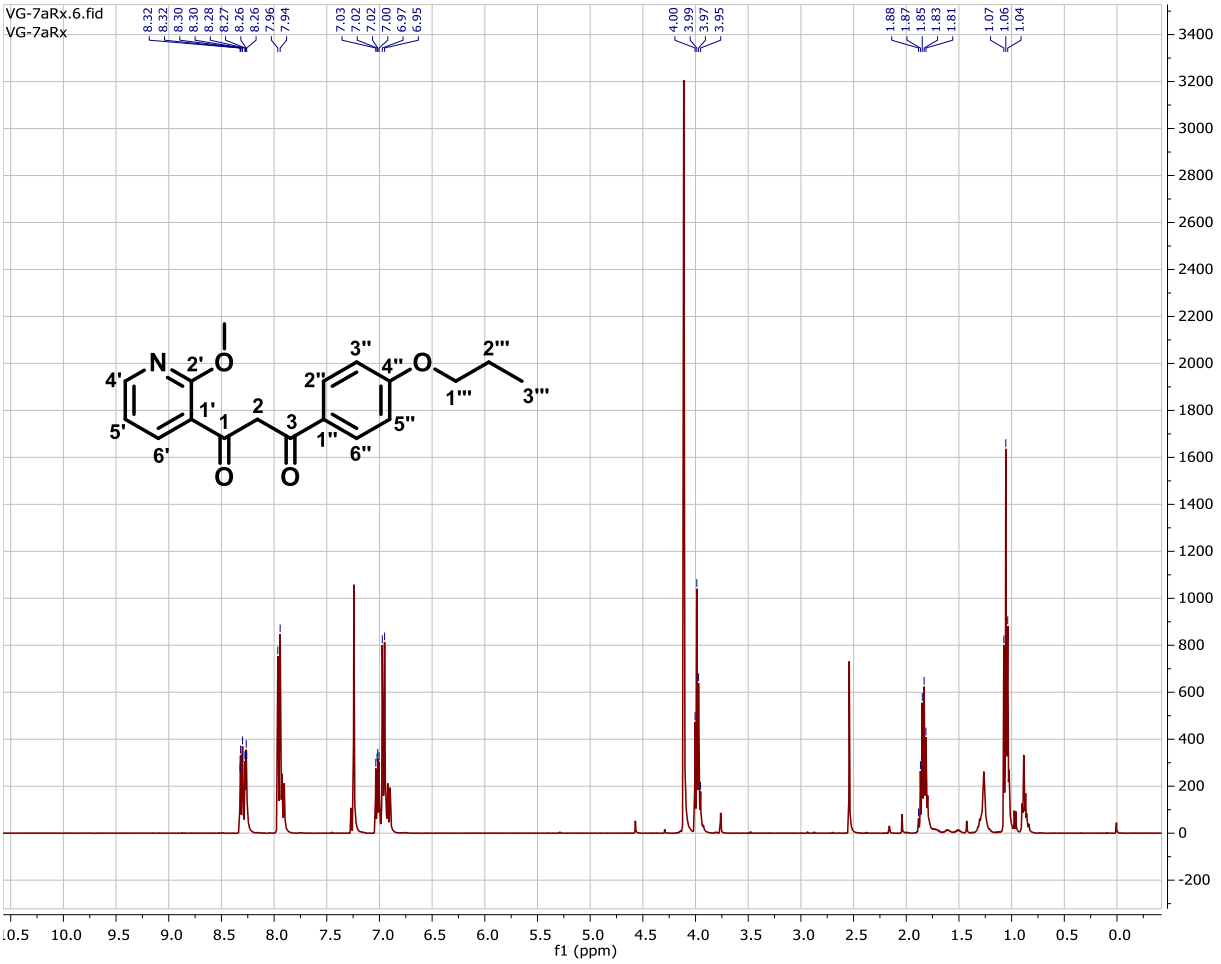

^{13}C-Spectrum of Compound 10a

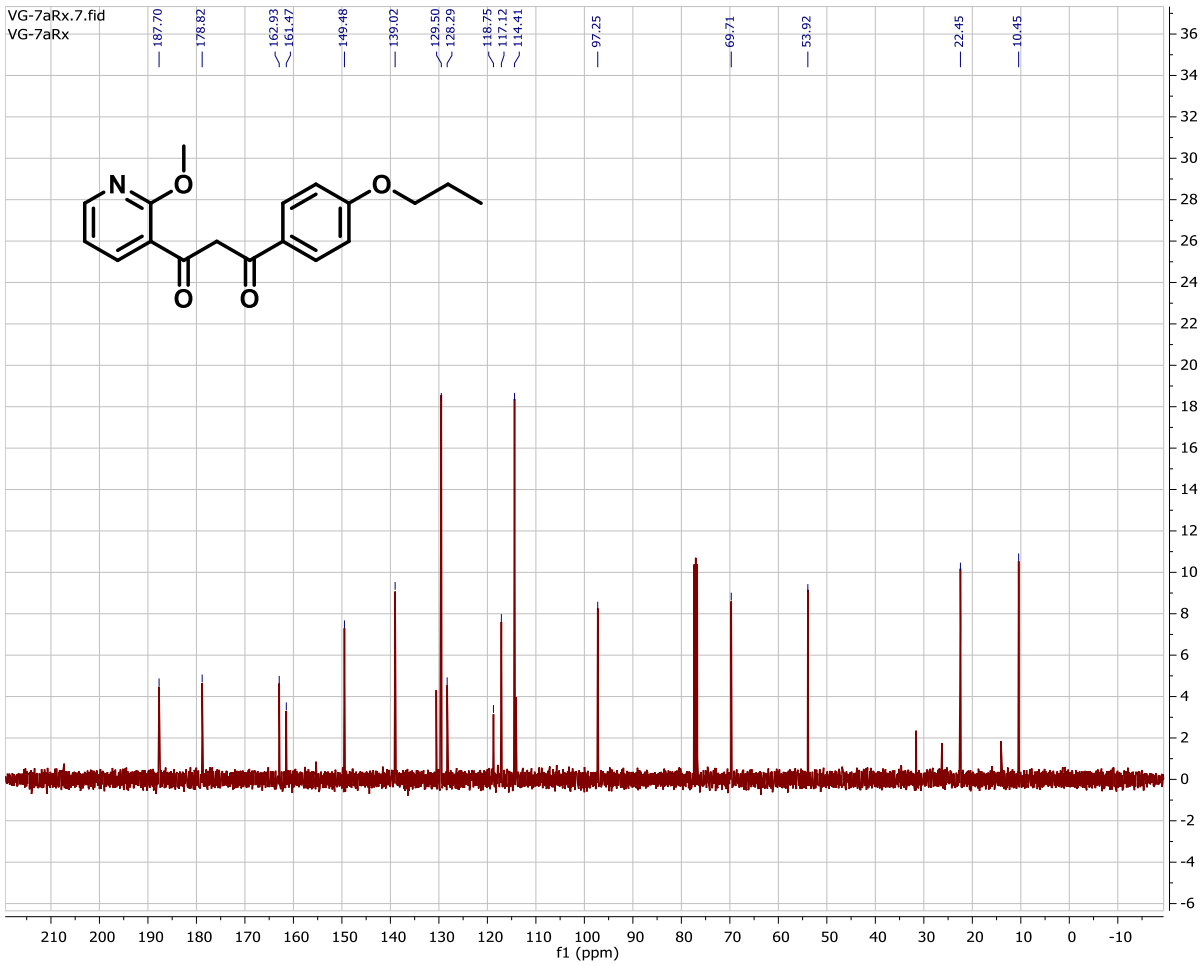

DEPT-135 Spectrum of Compound 10a

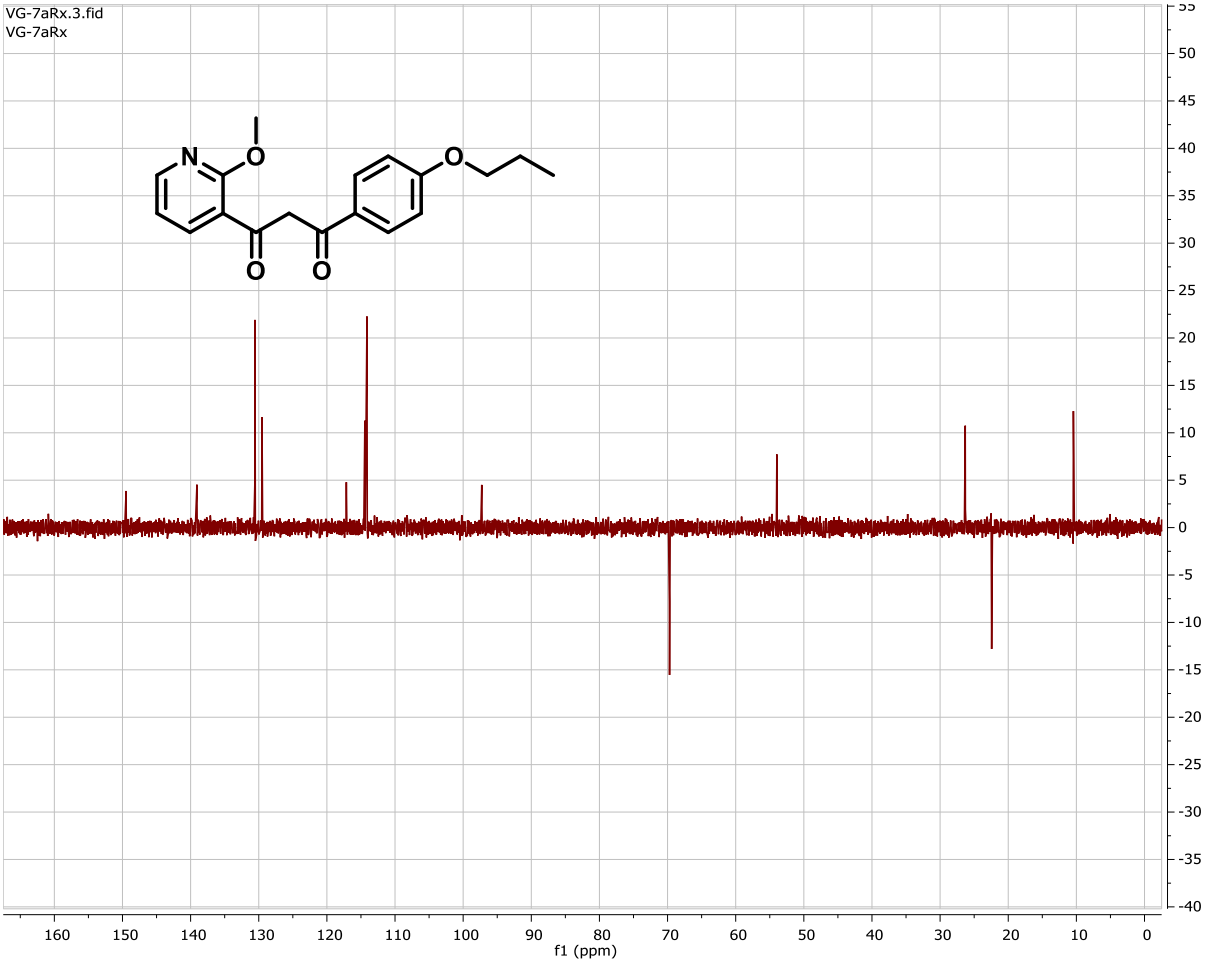

^{1}H-Spectrum of Compound 10b

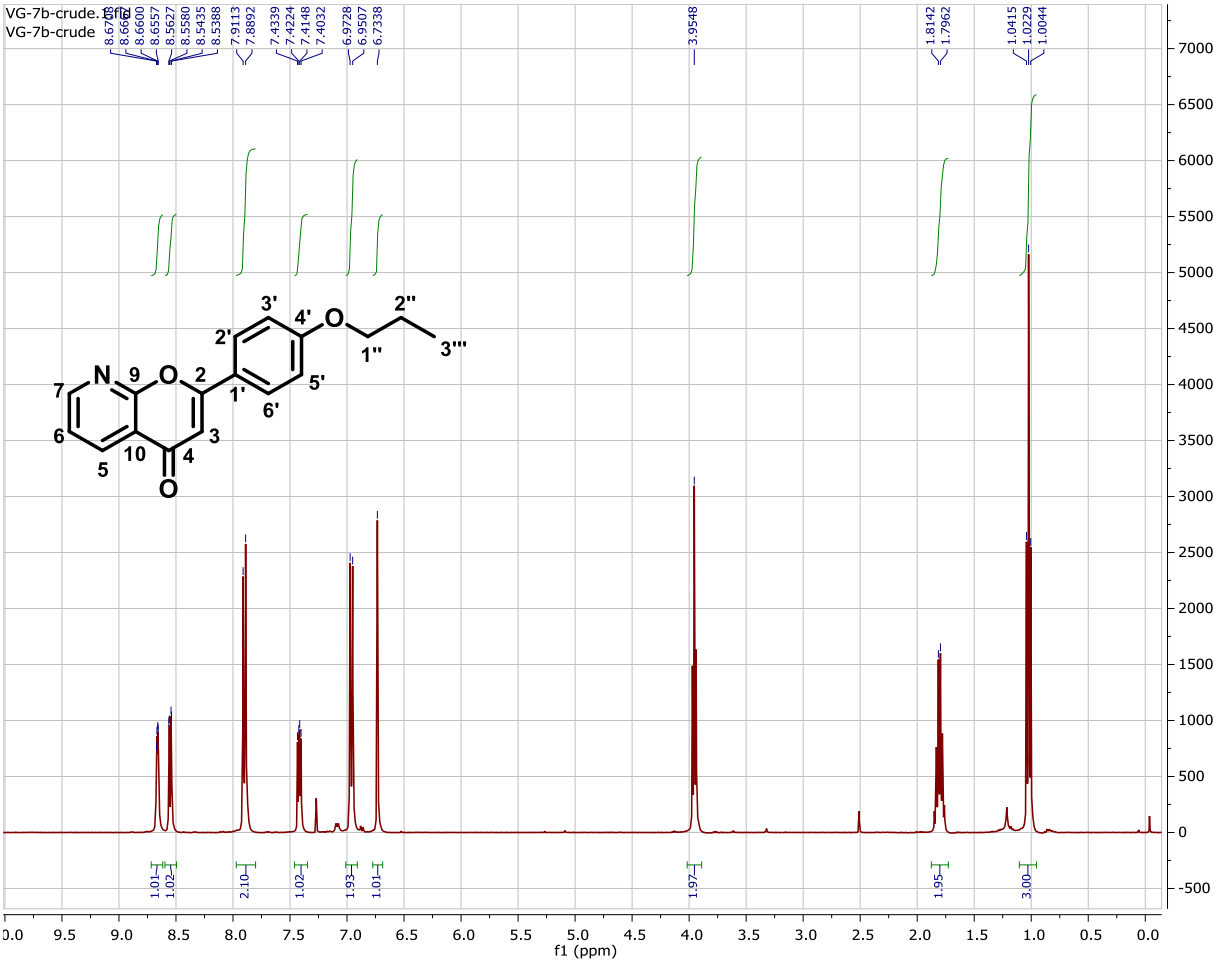

^{13}C-Spectrum of Compound 10b

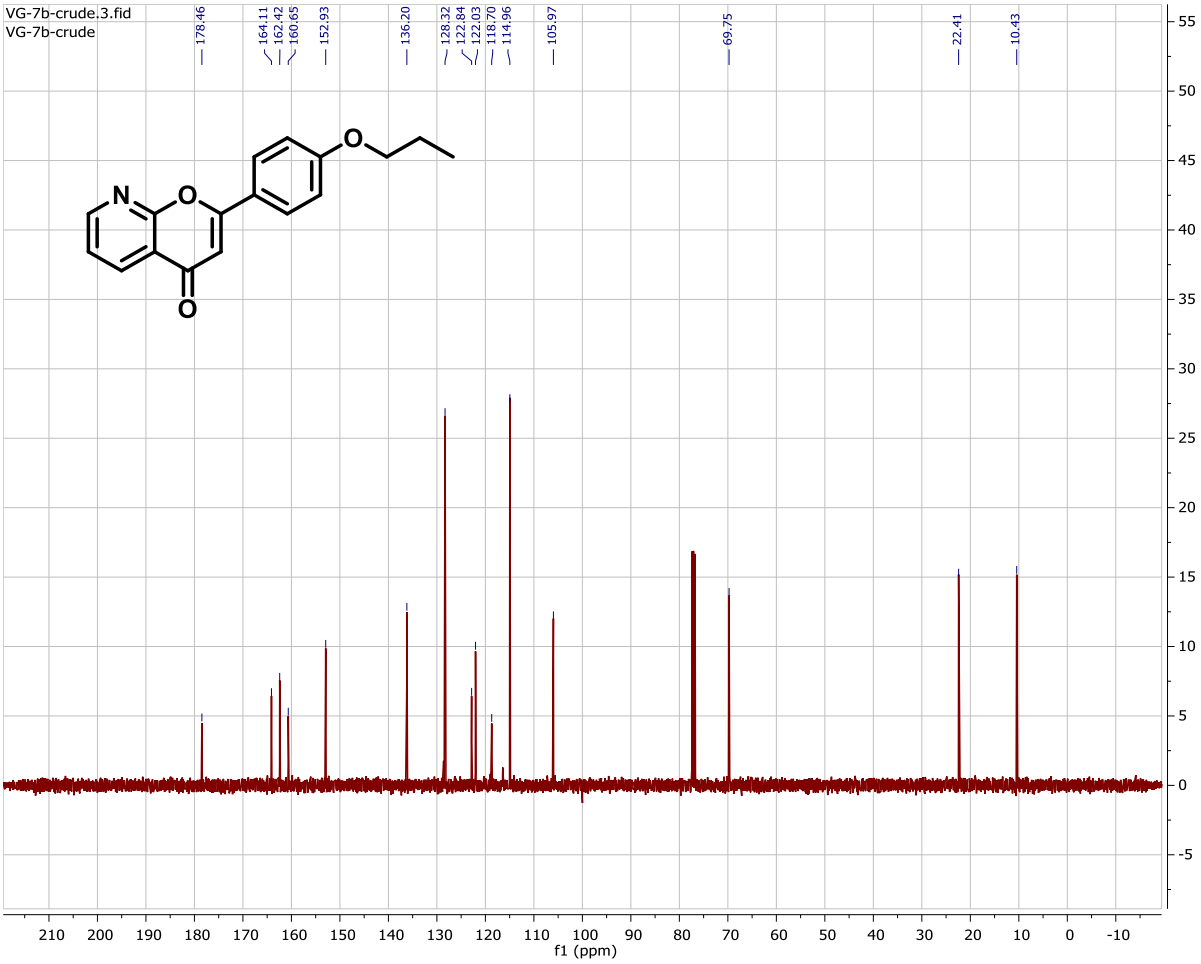

DEPT-135 Spectrum of Compound 10b

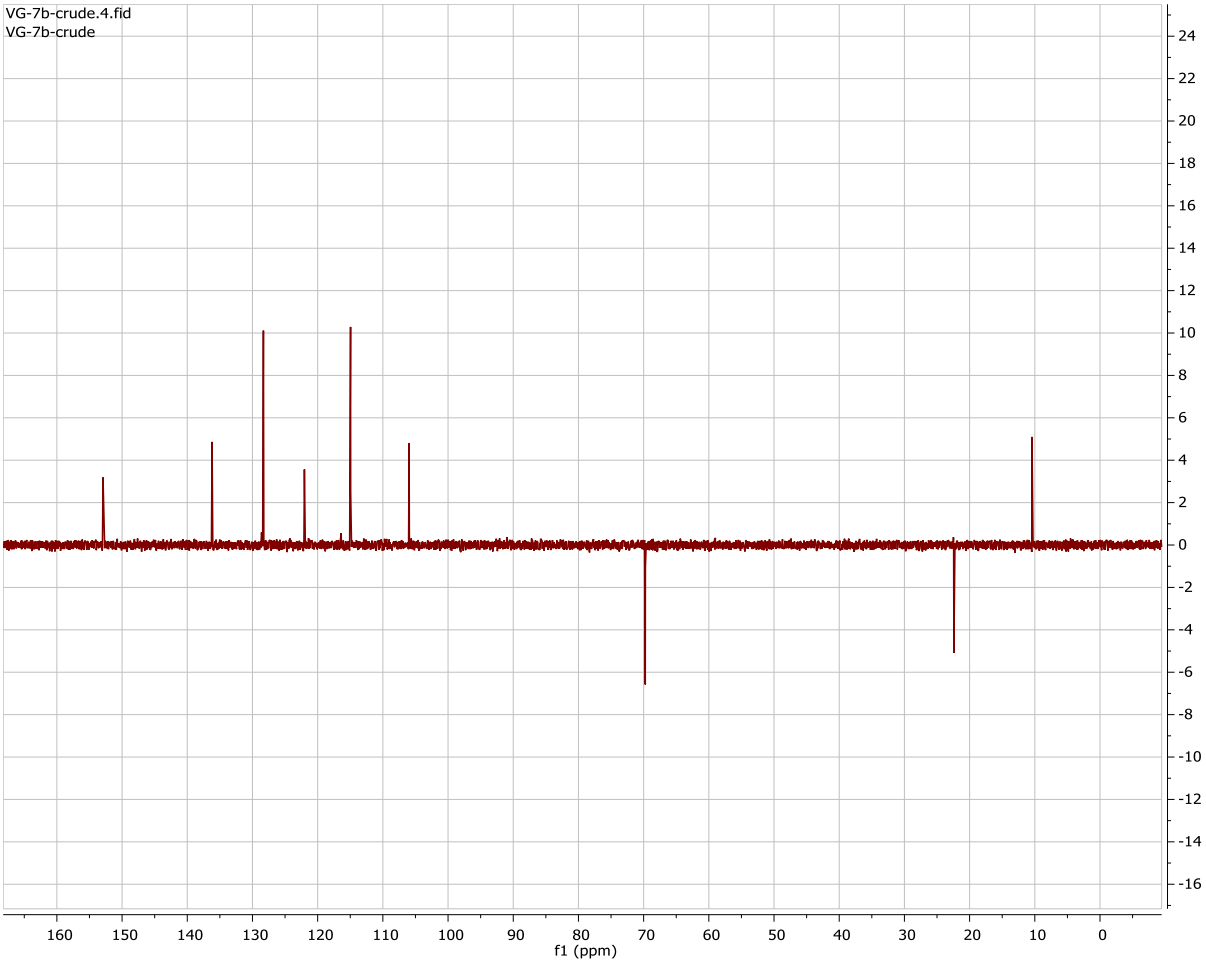

HSQC Spectrum of Compound 10b

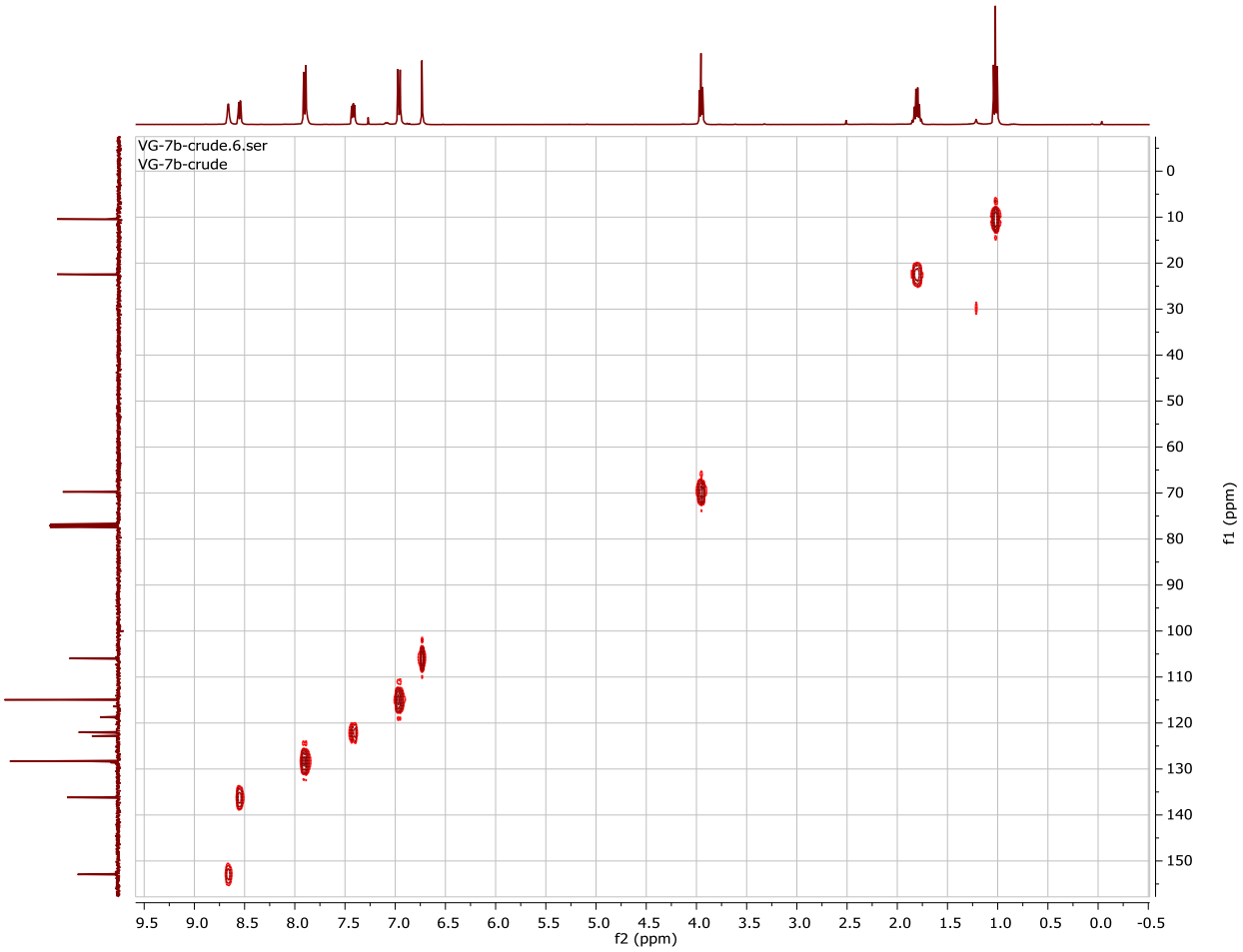

HMBC Spectrum of Compound 10b

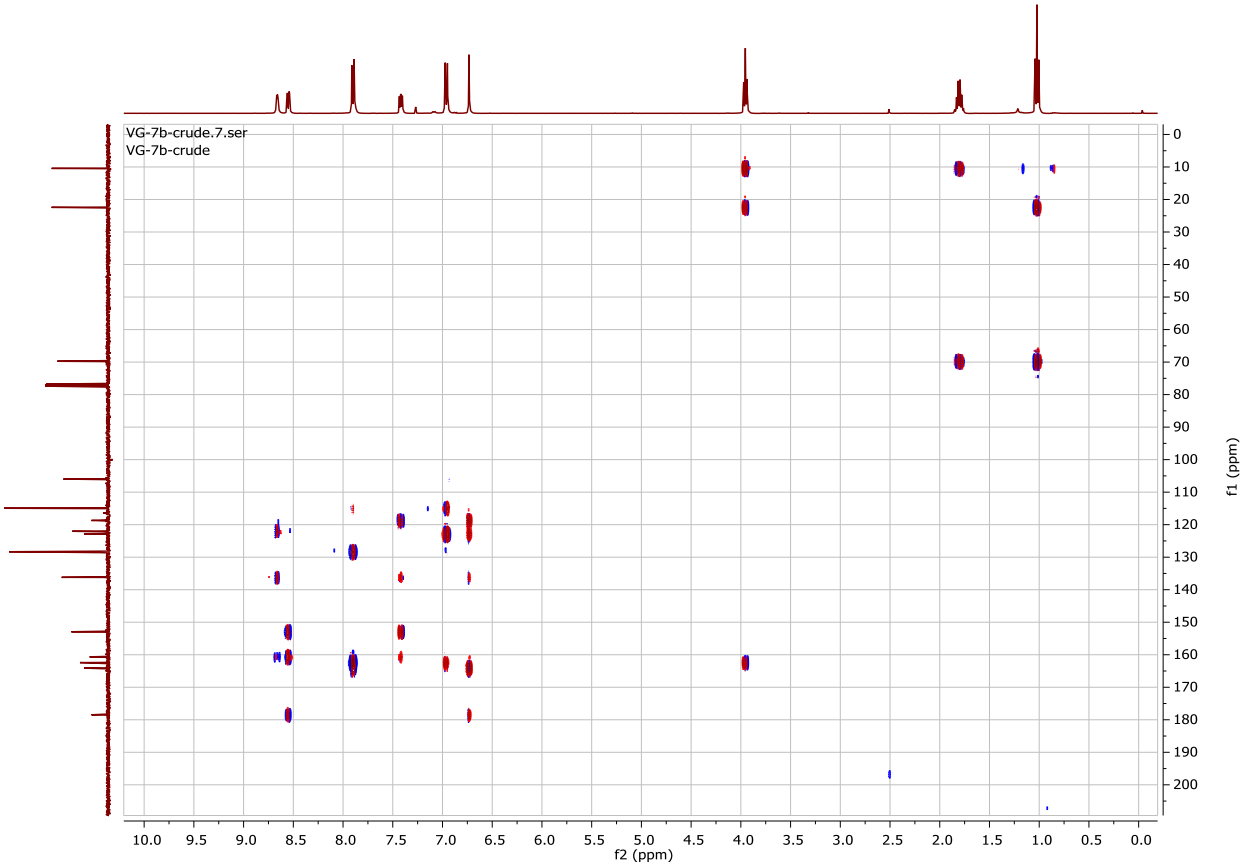

^{1}H-Spectrum of Compound 11a

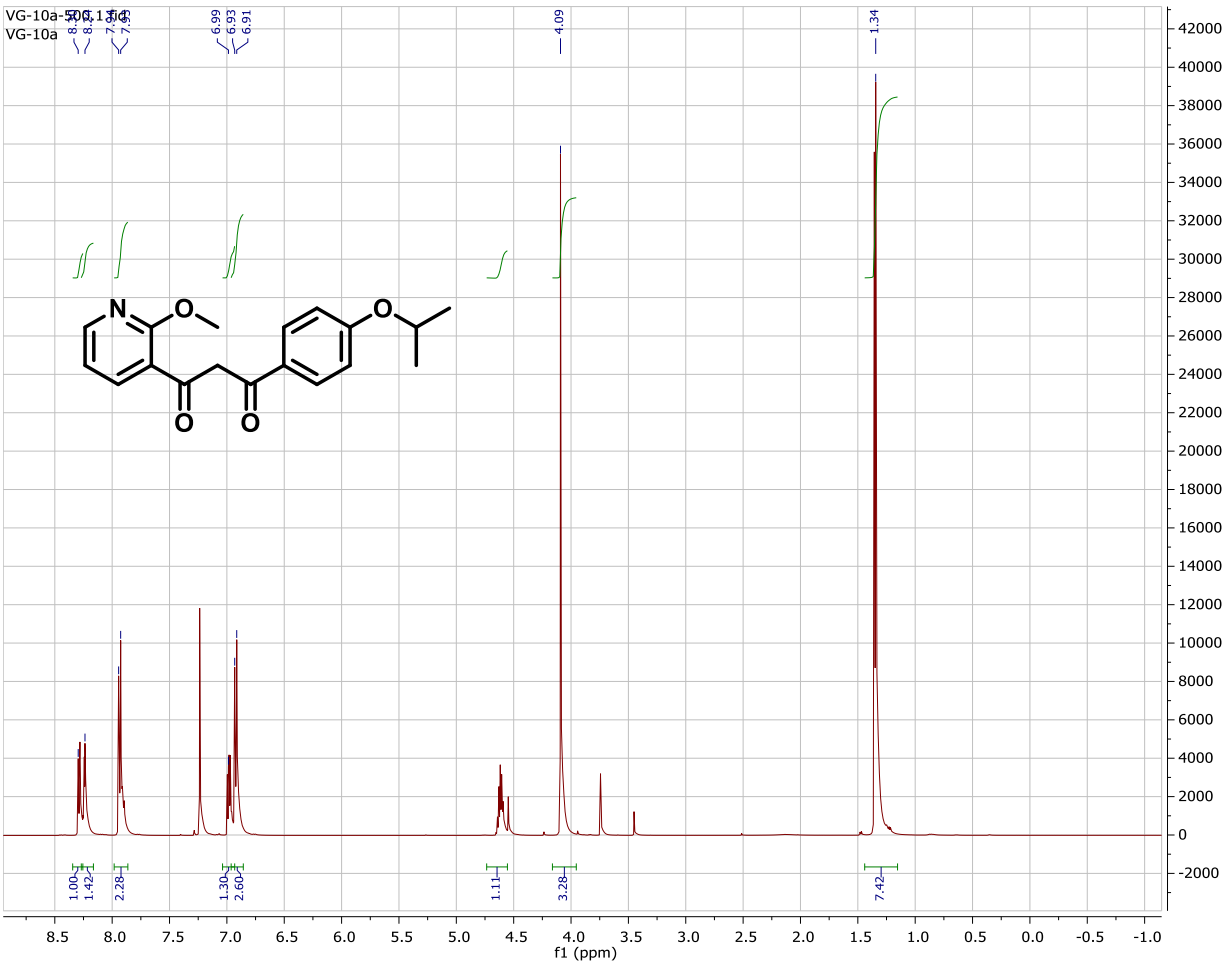

^{13}C-Spectrum of Compound 11a

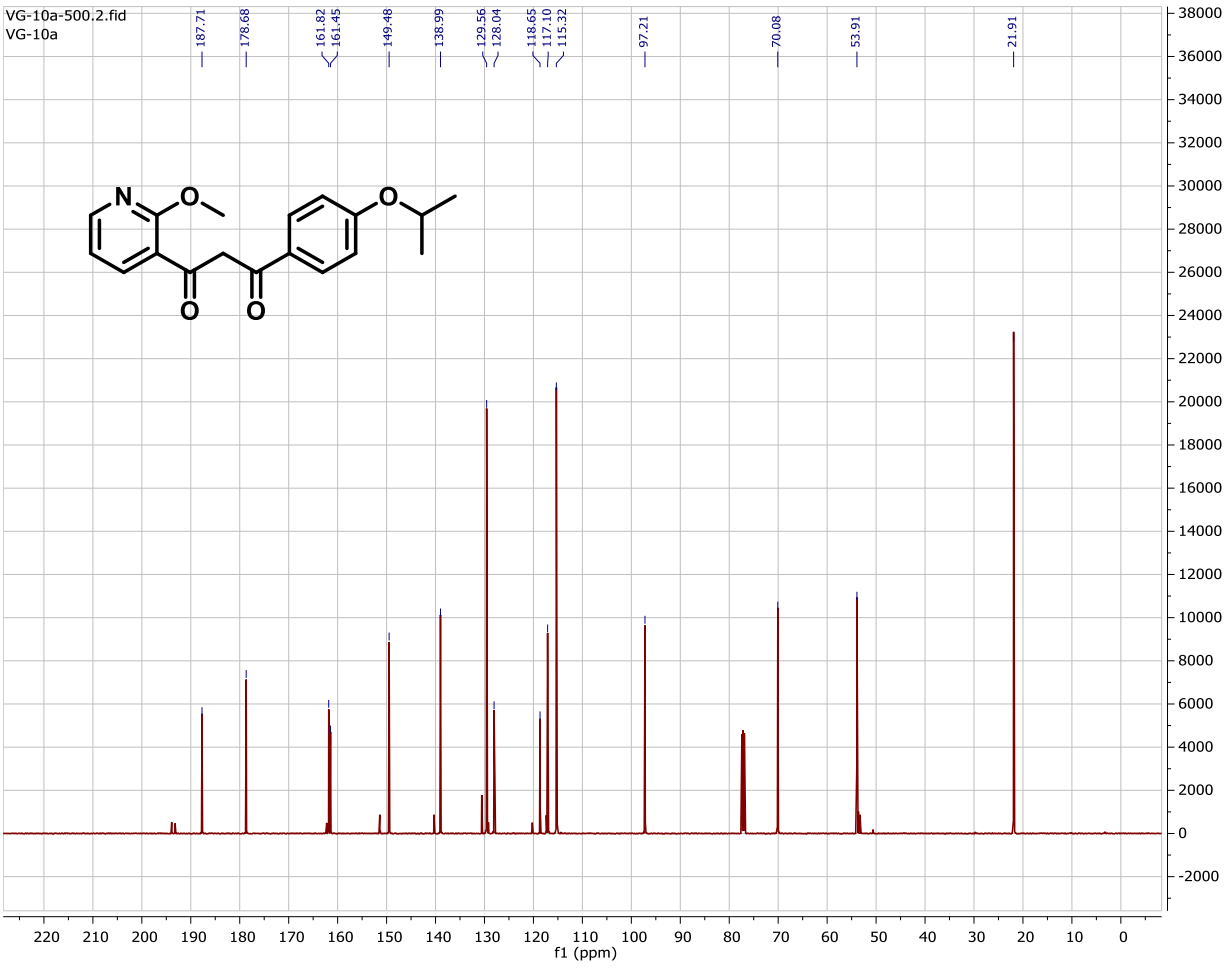

DEPT-135 Spectrum of Compound 11a

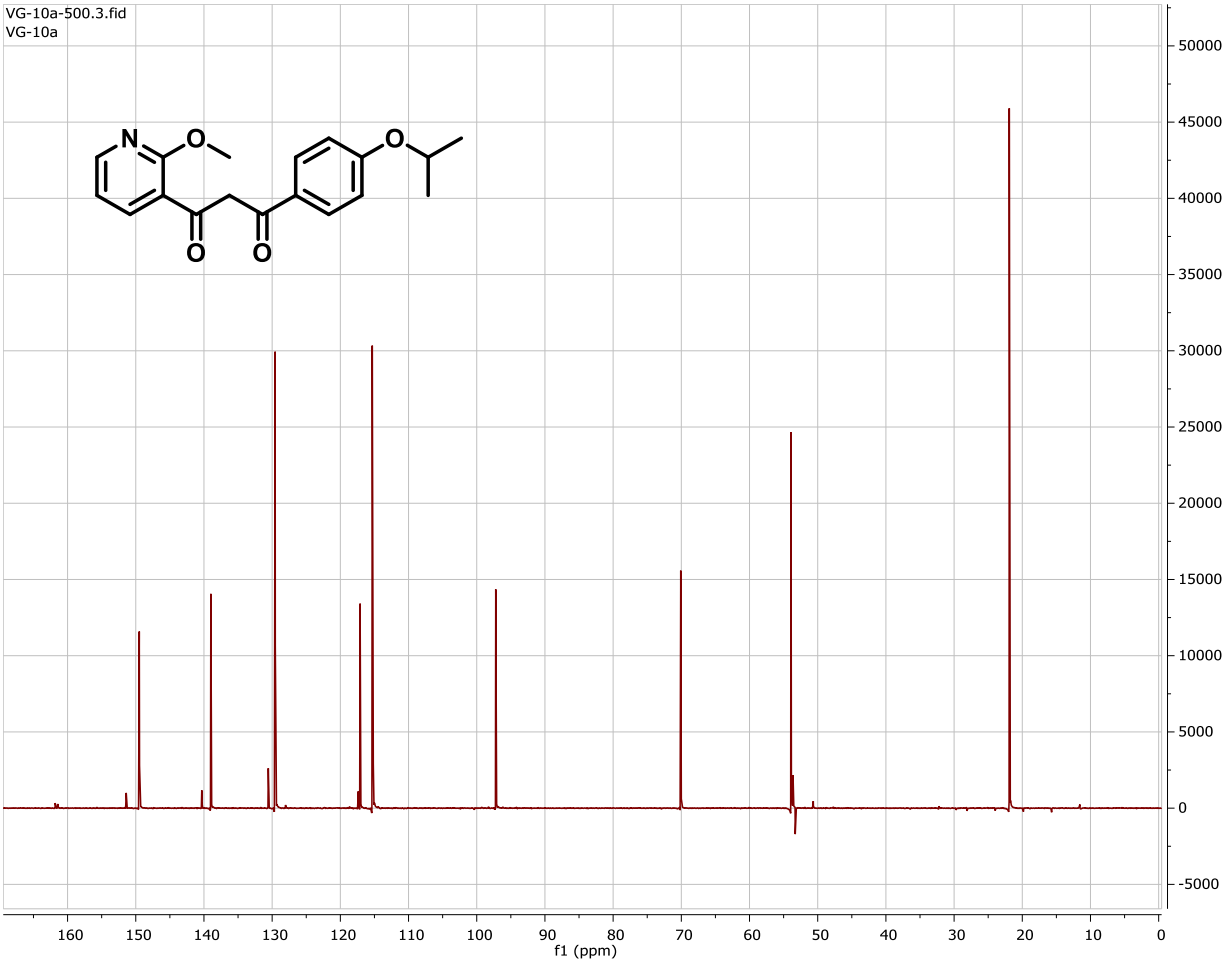

^{1}H-Spectrum of Compound 11b

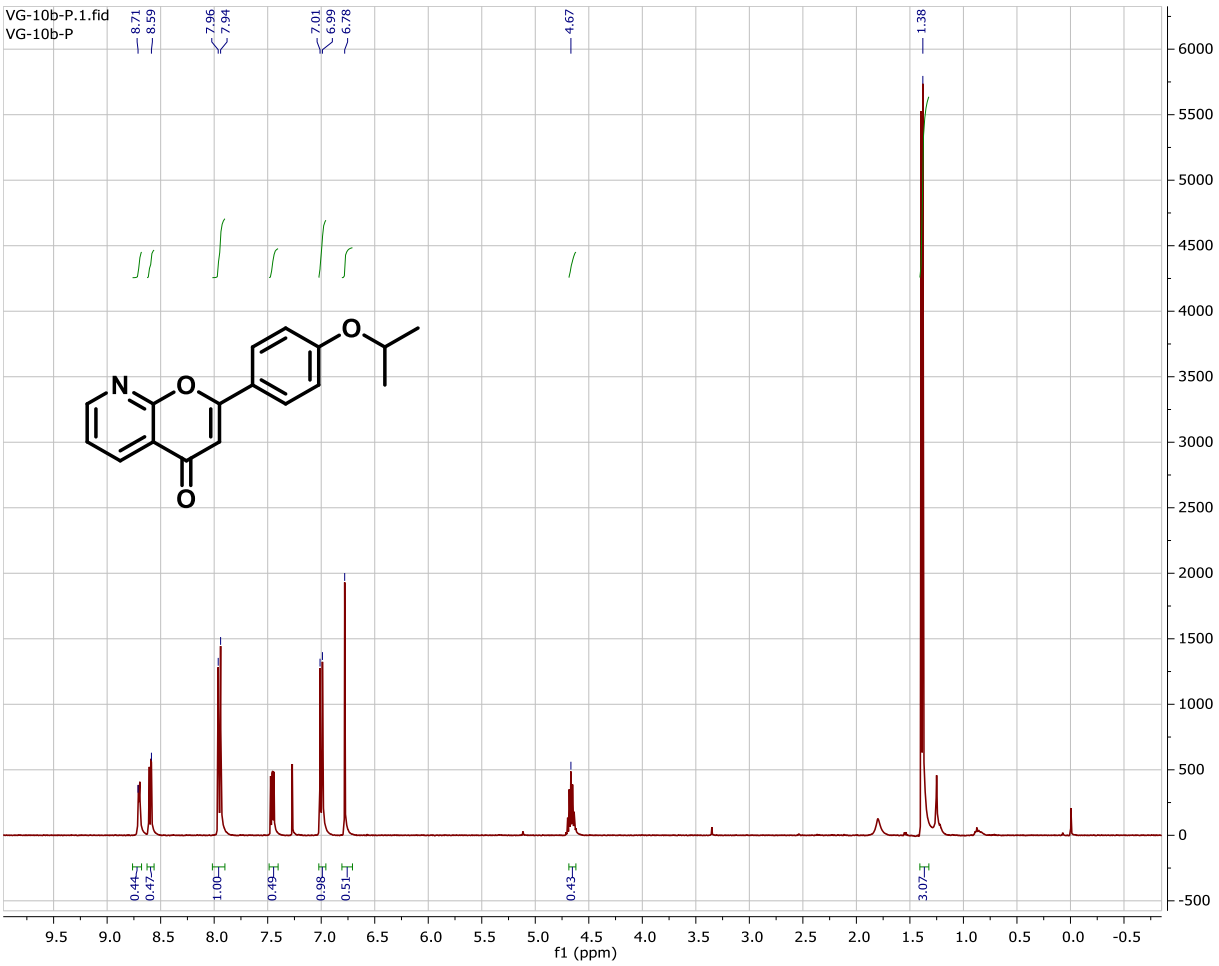

^{13}C-NMR Spectrum of Compound 11b

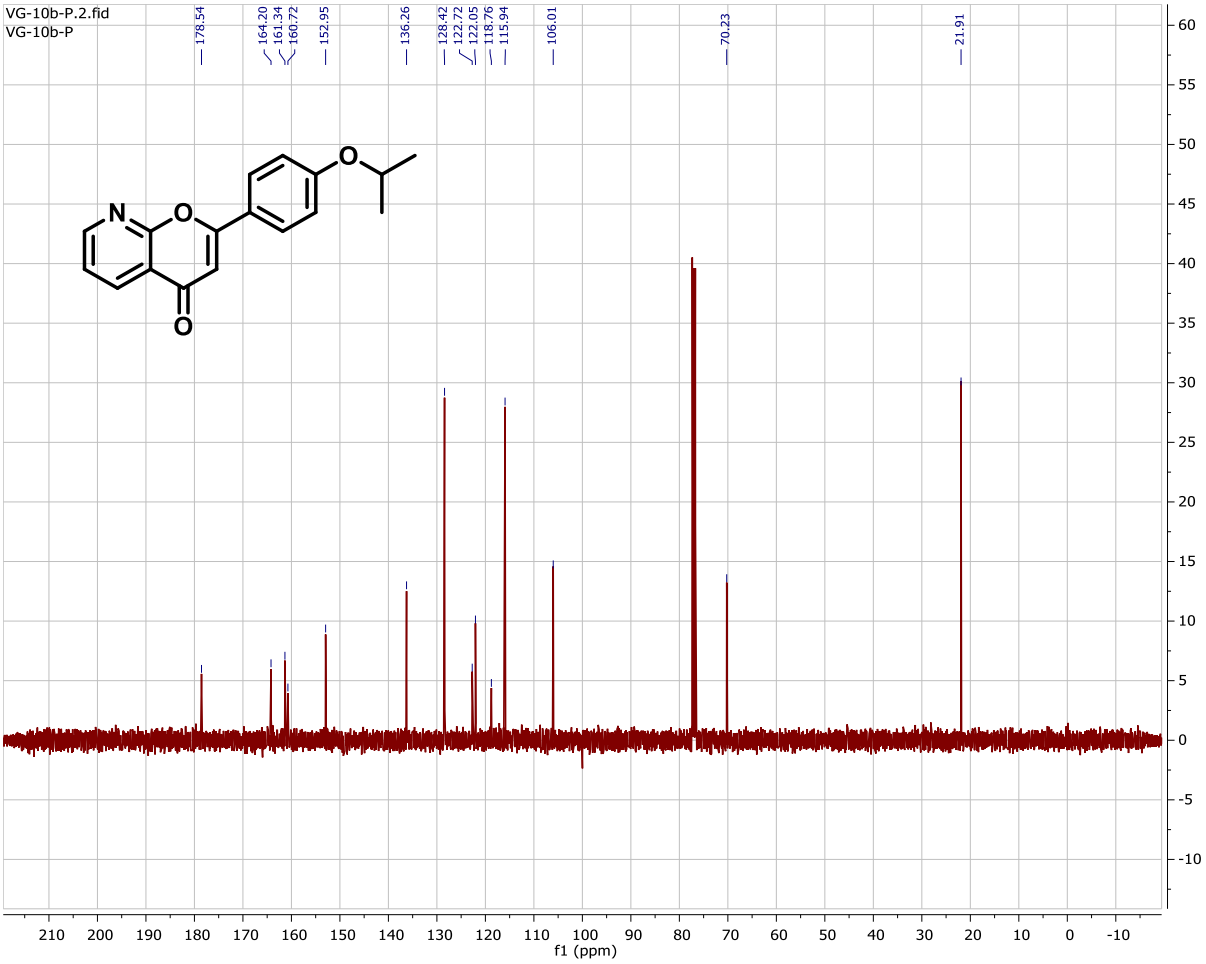

DEPT-135 Spectrum of Compound 11b

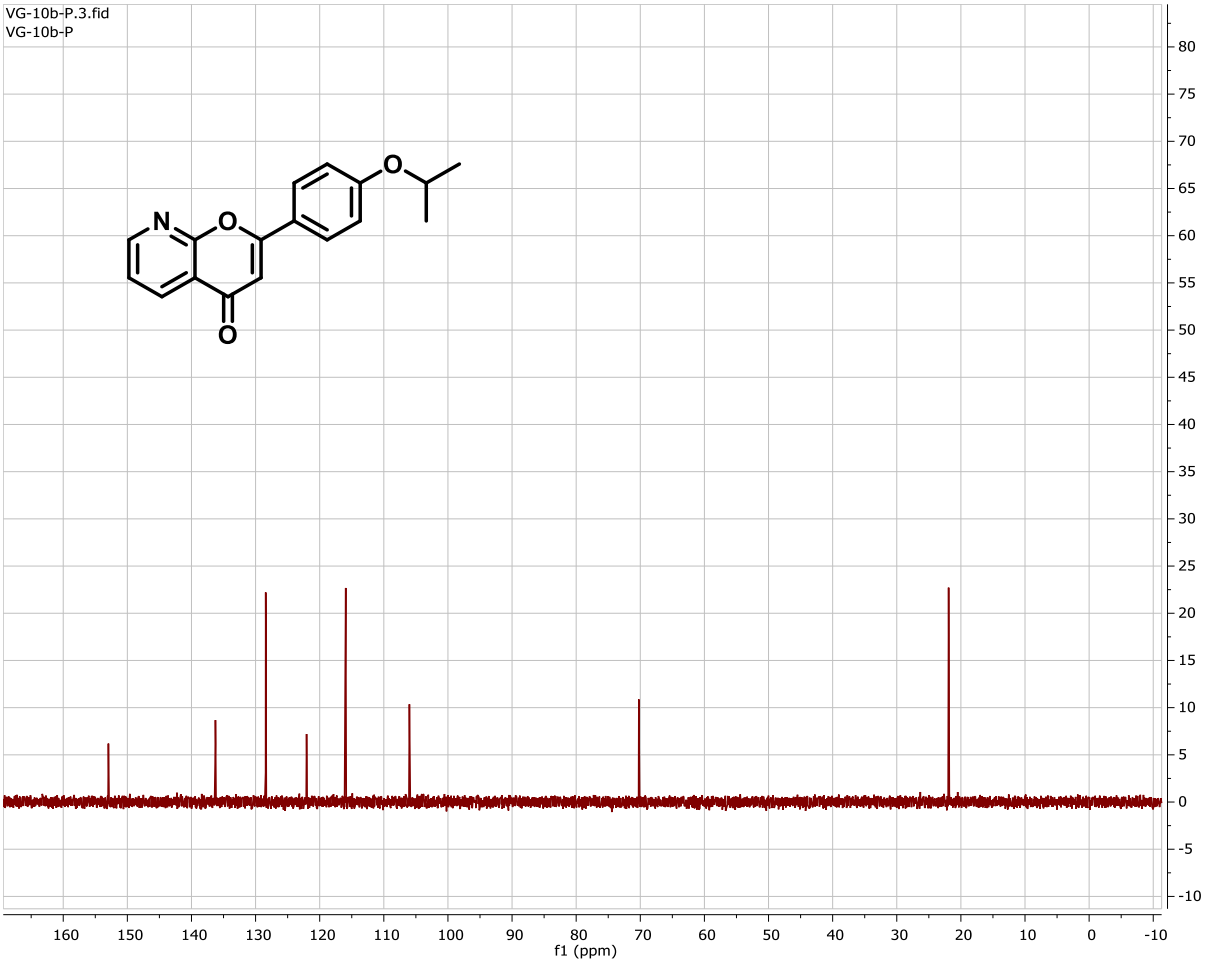

HSQC Spectrum of Compound 11b

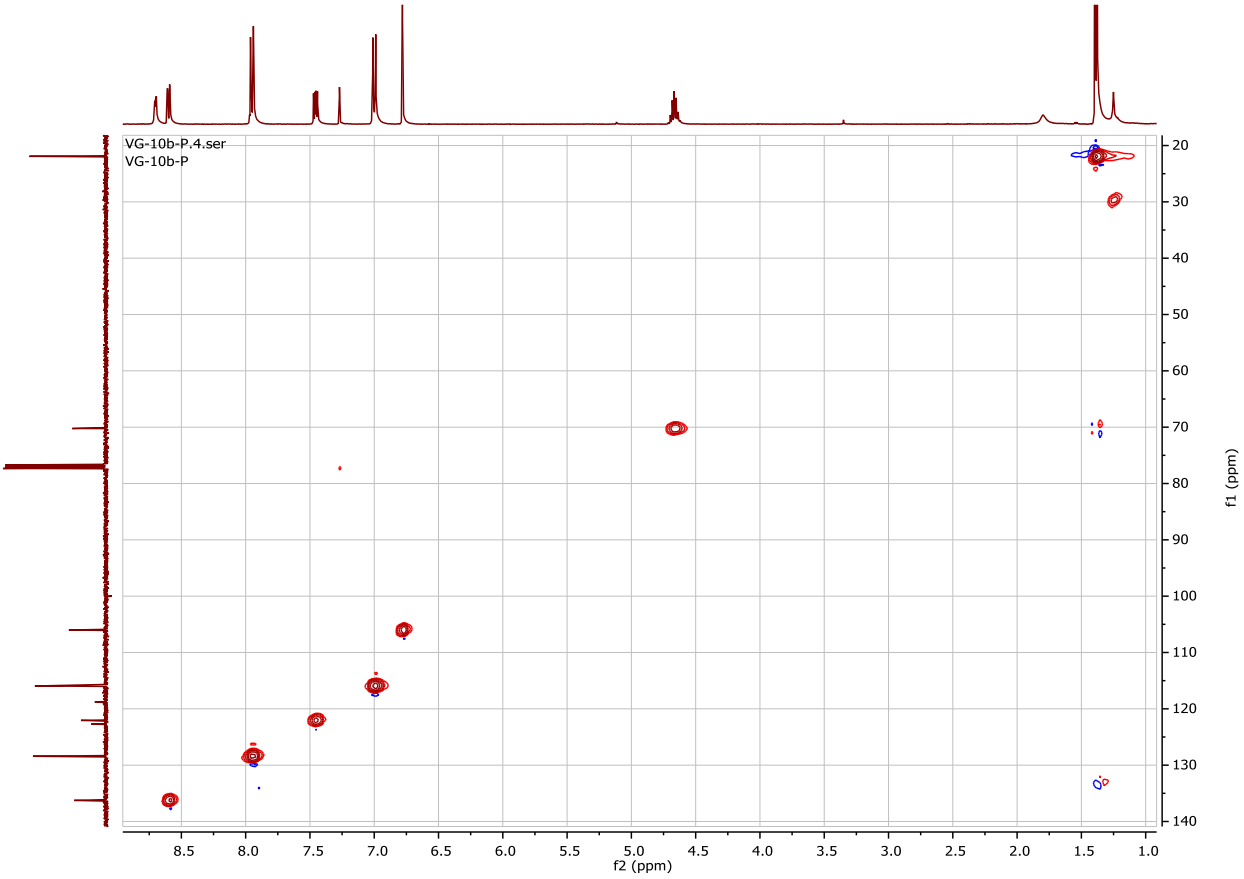

HMBC Spectrum of Compound 11b

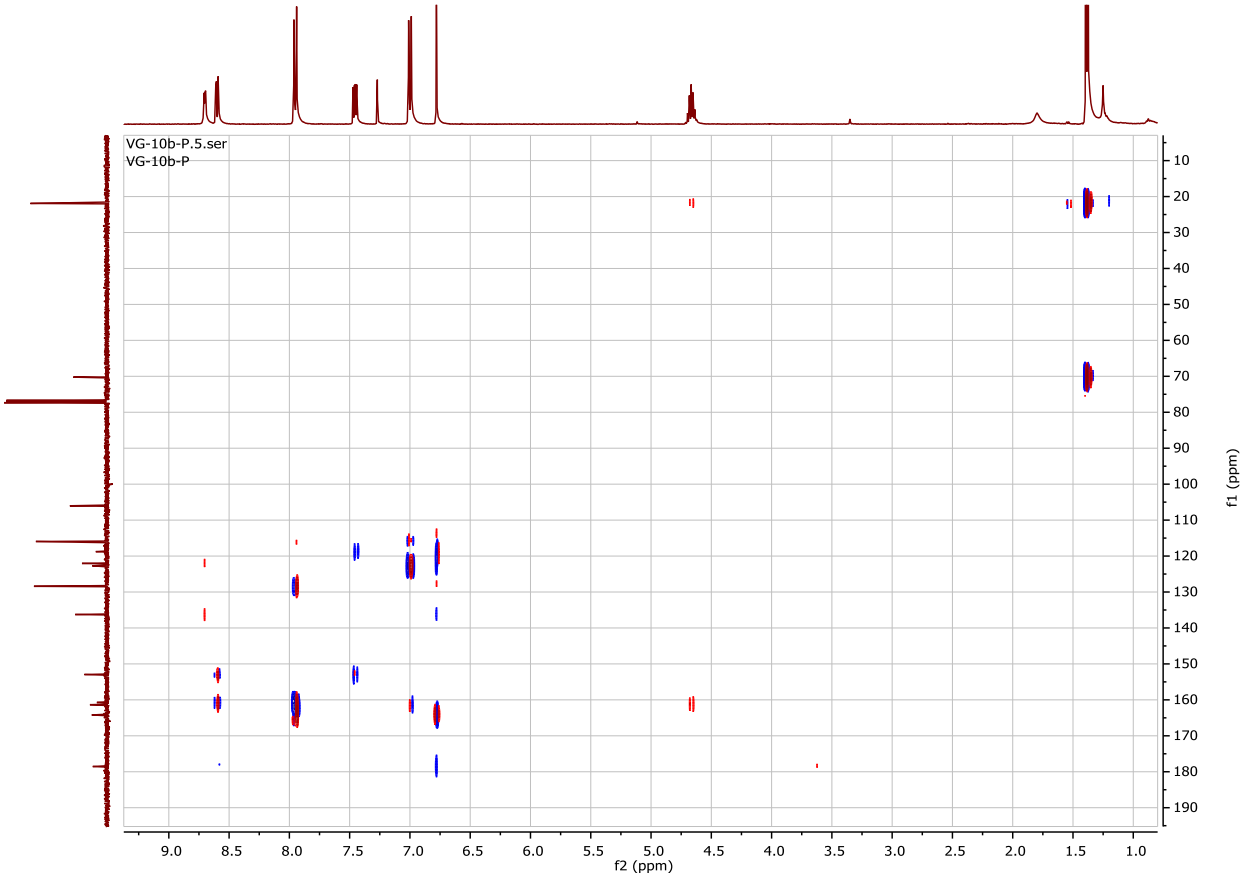

^{1}H-Spectrum of Compound 12a

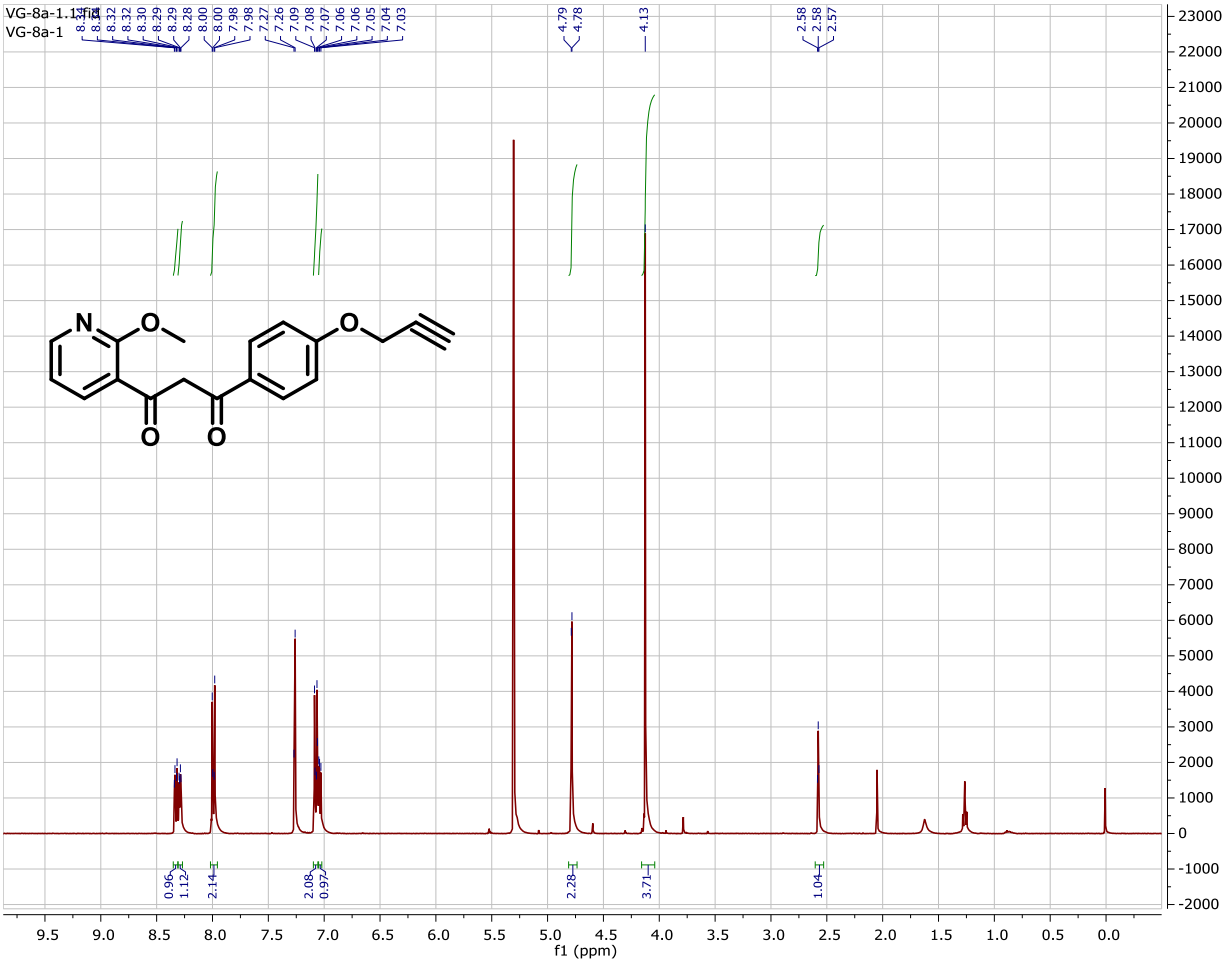

^{13}C-Spectrum of Compound 12a

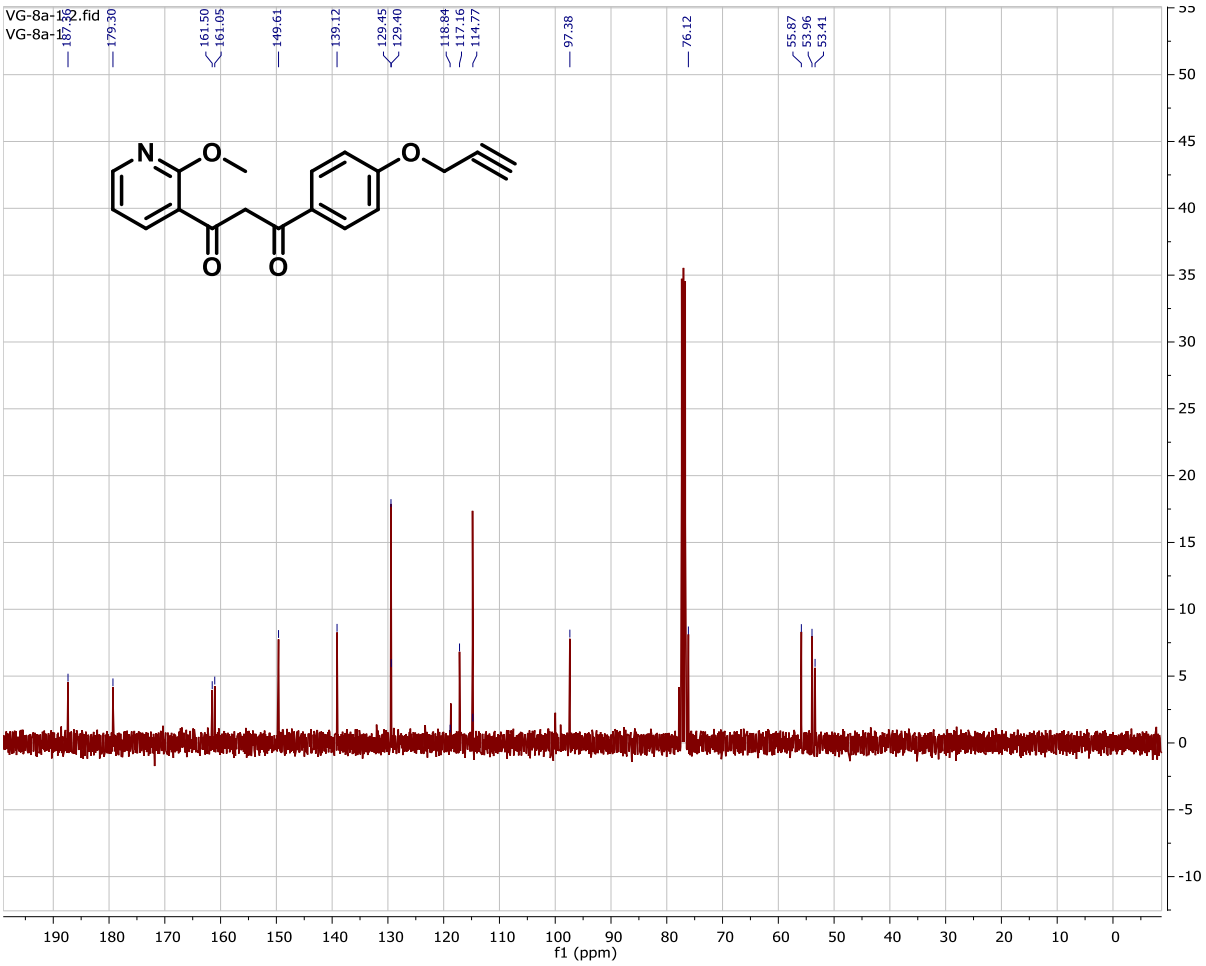

DEPT-135 Spectrum of Compound 12a

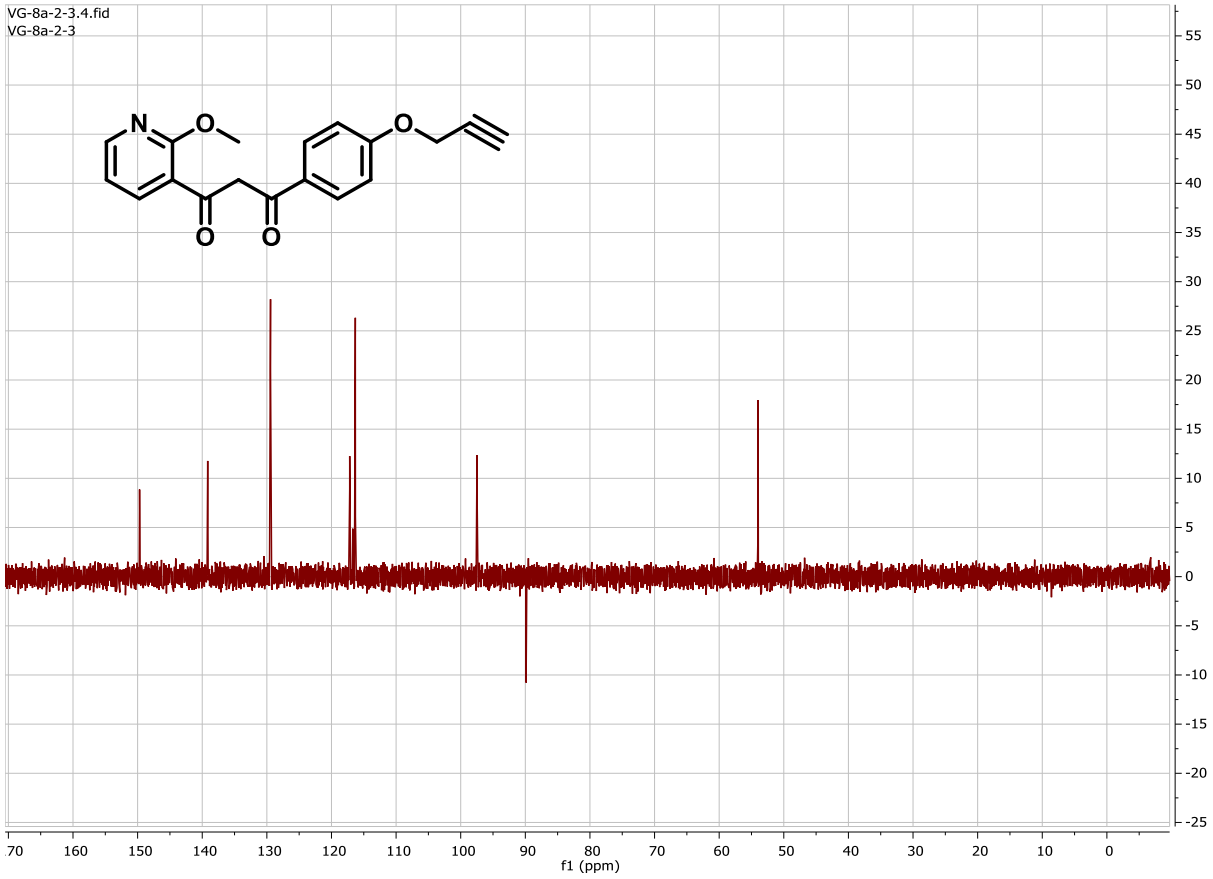

^{1}H-Spectrum of Compound VIII

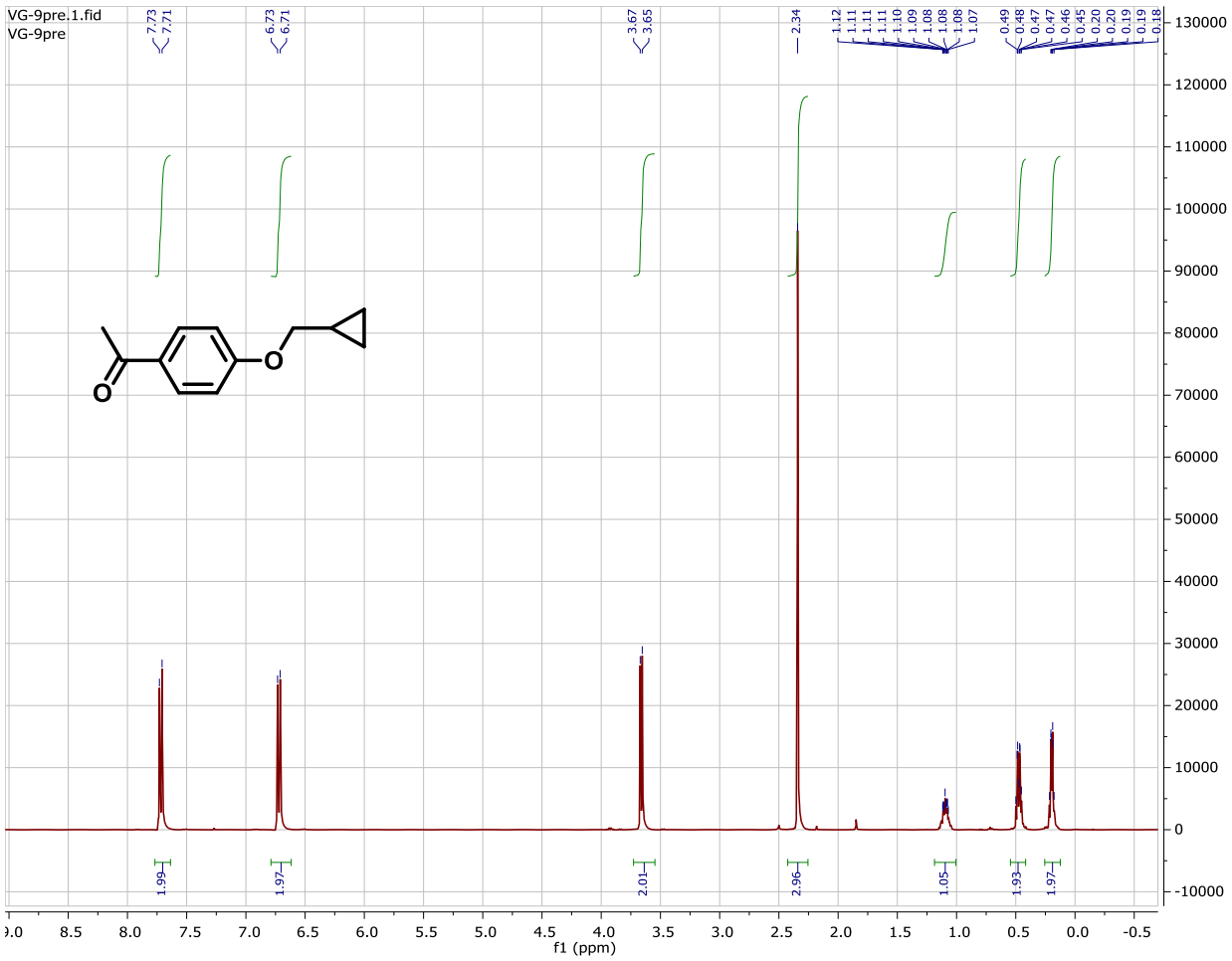

^{13}C-Spectrum of Compound VIII

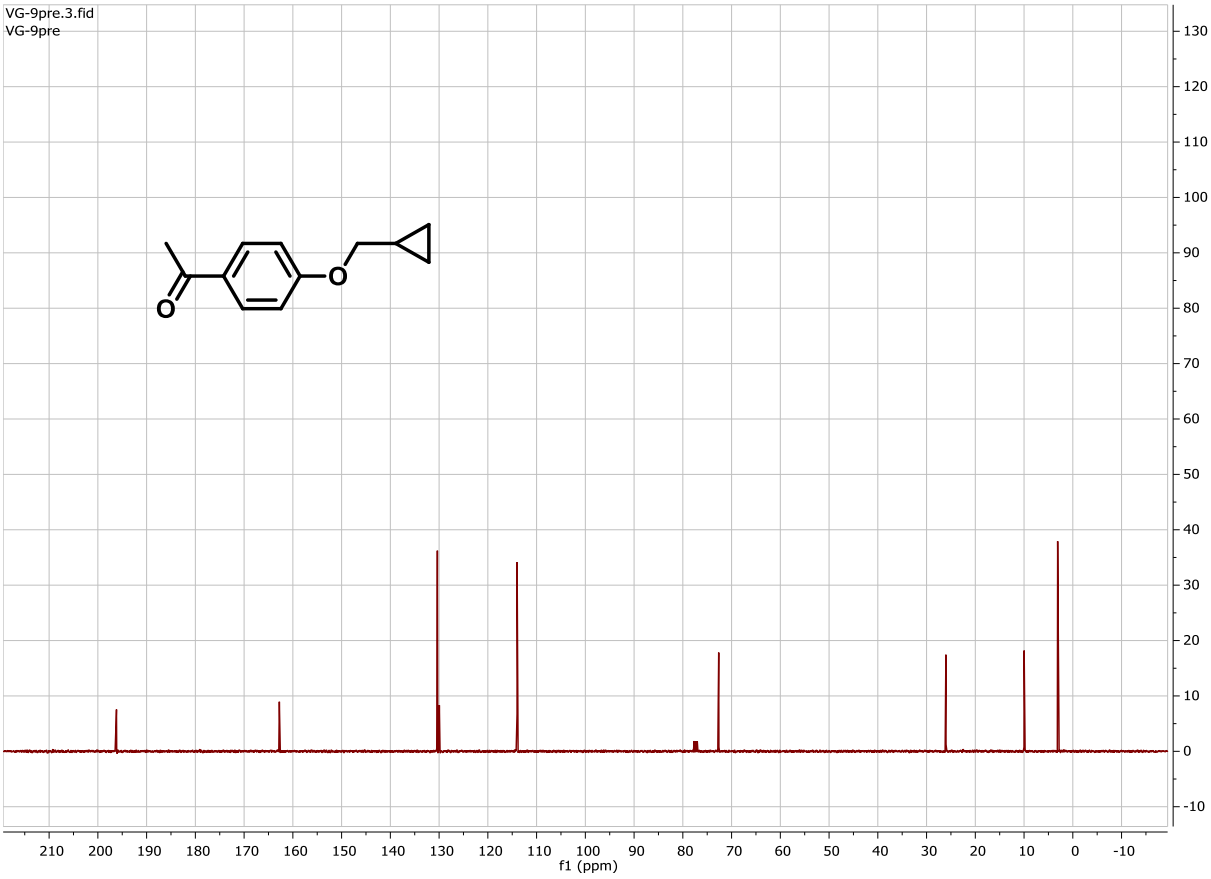

DEPT-135 Spectrum of Compound VIII

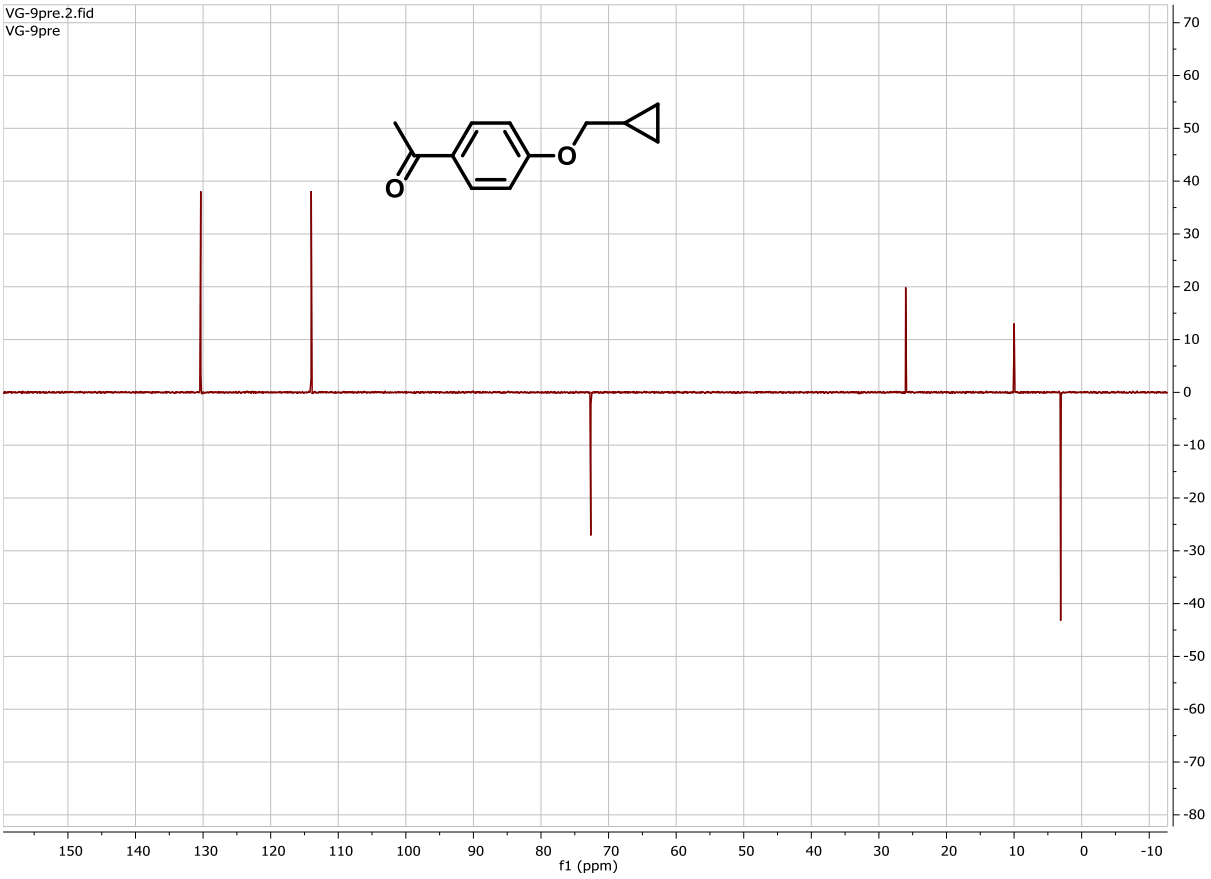

^{1}H-Spectrum of Compound 13a

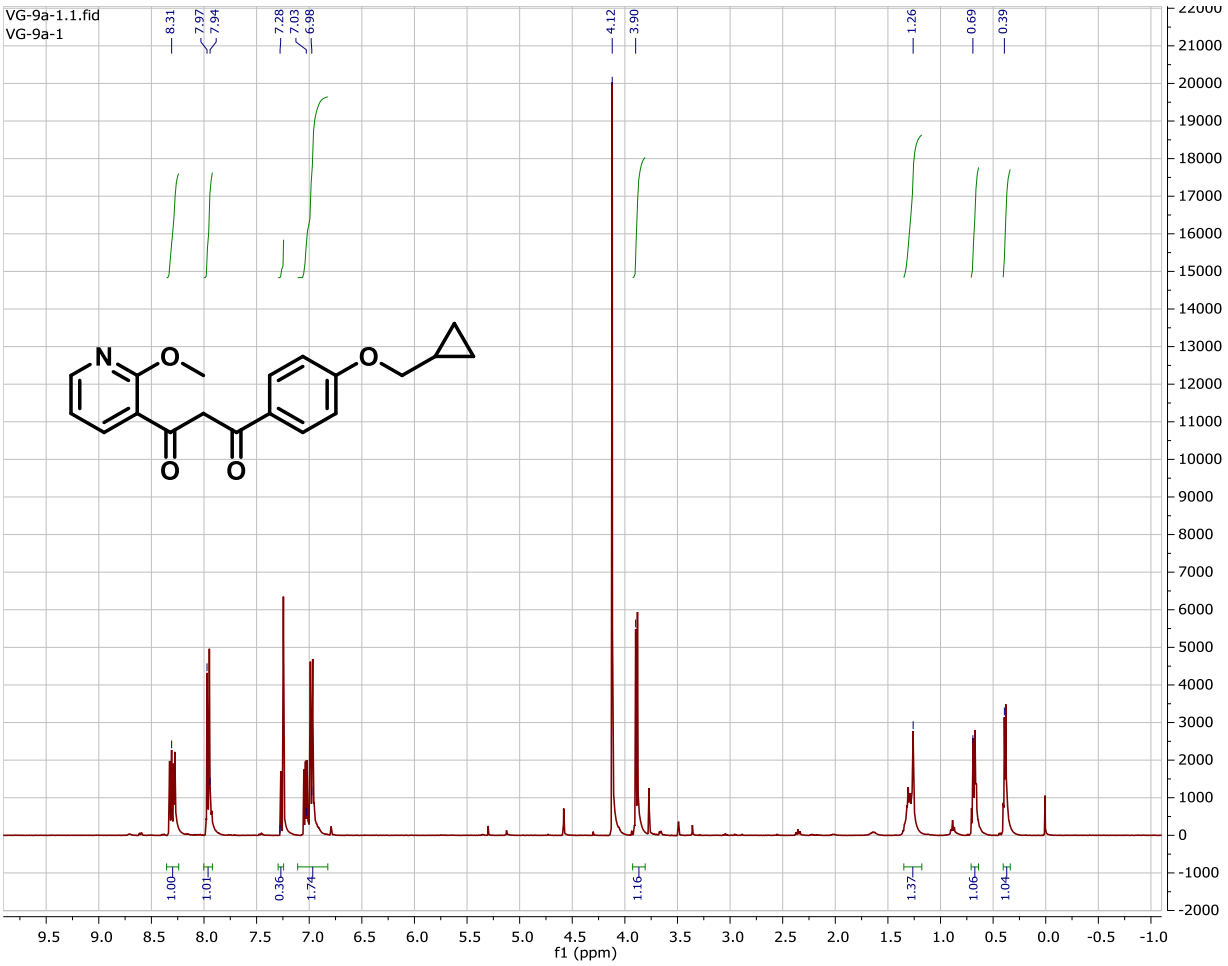

^{13}C-Spectrum of Compound 13a

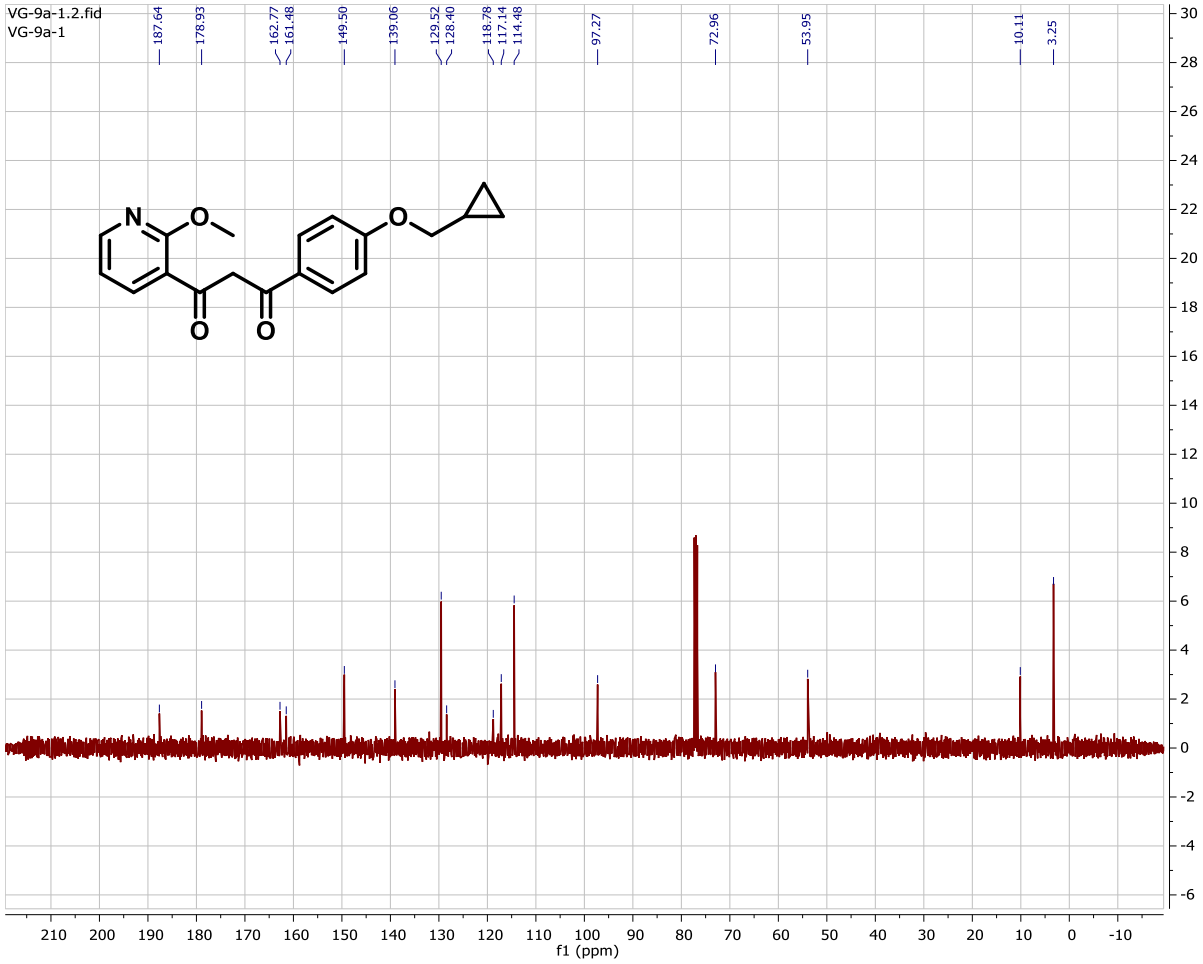

DEPT-135 Spectrum of Compound 13a

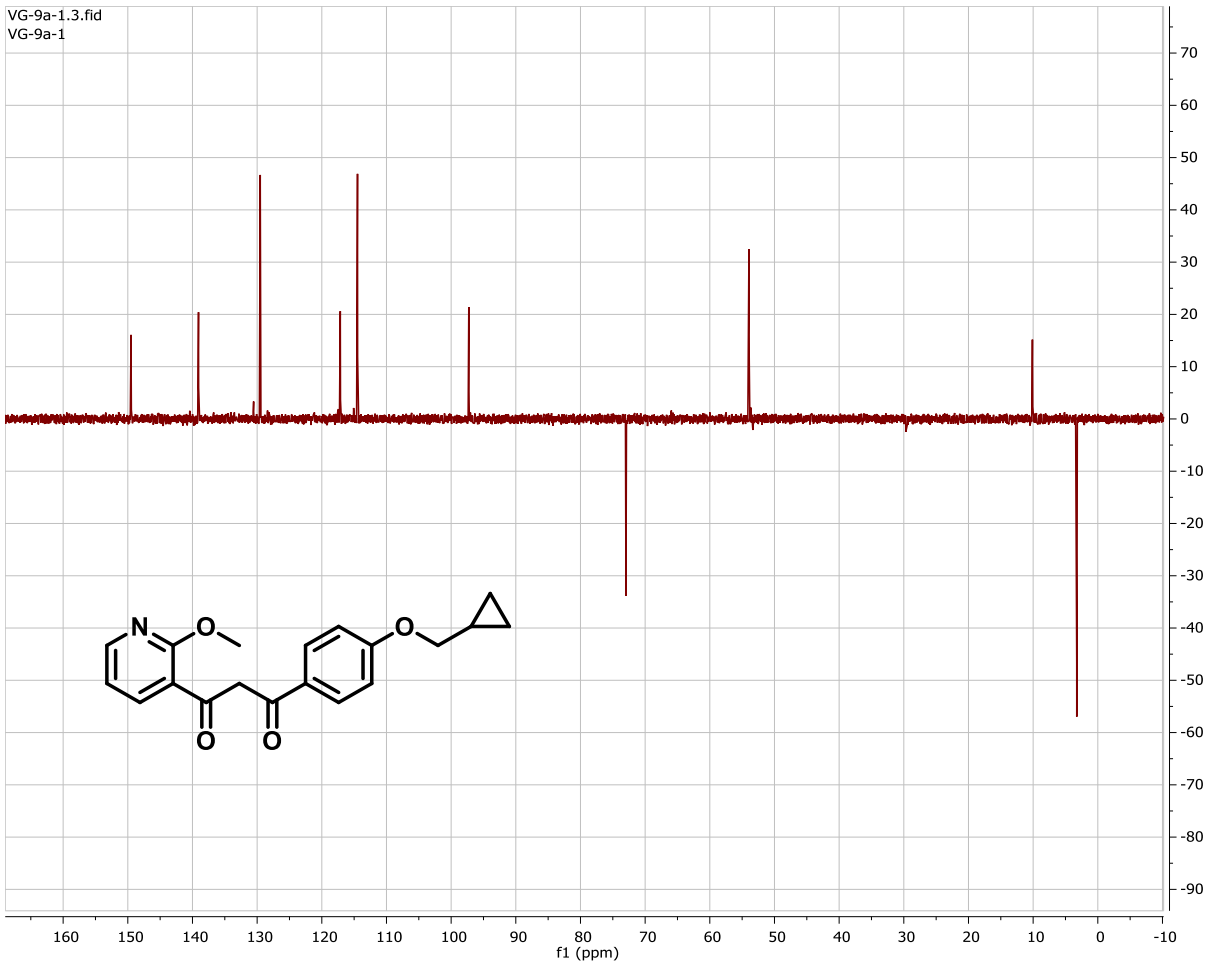

^{1}H-Spectrum of Compound 13b

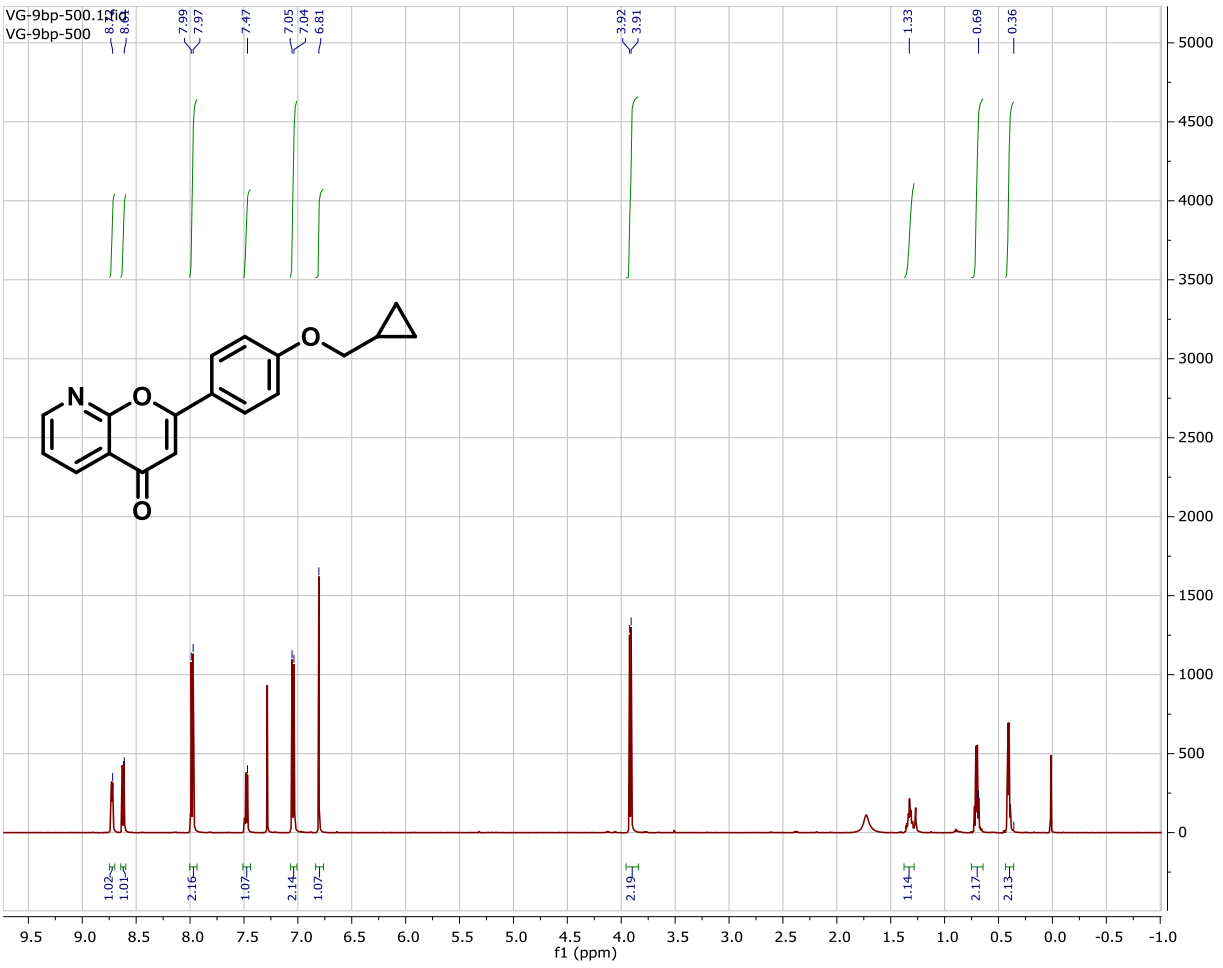

^{13}C-Spectrum of Compound 13b

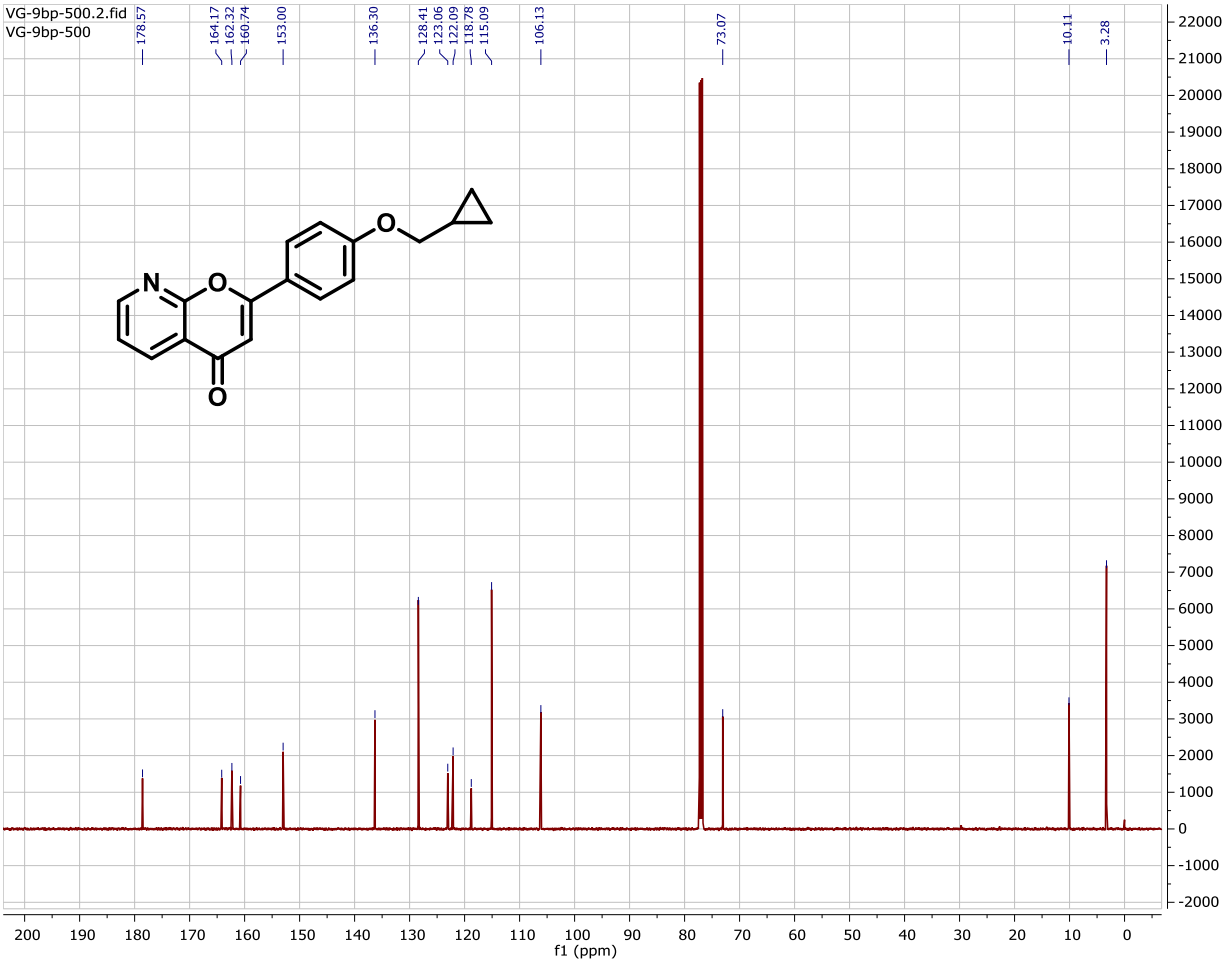

DEPT-135 Spectrum of Compound 13b

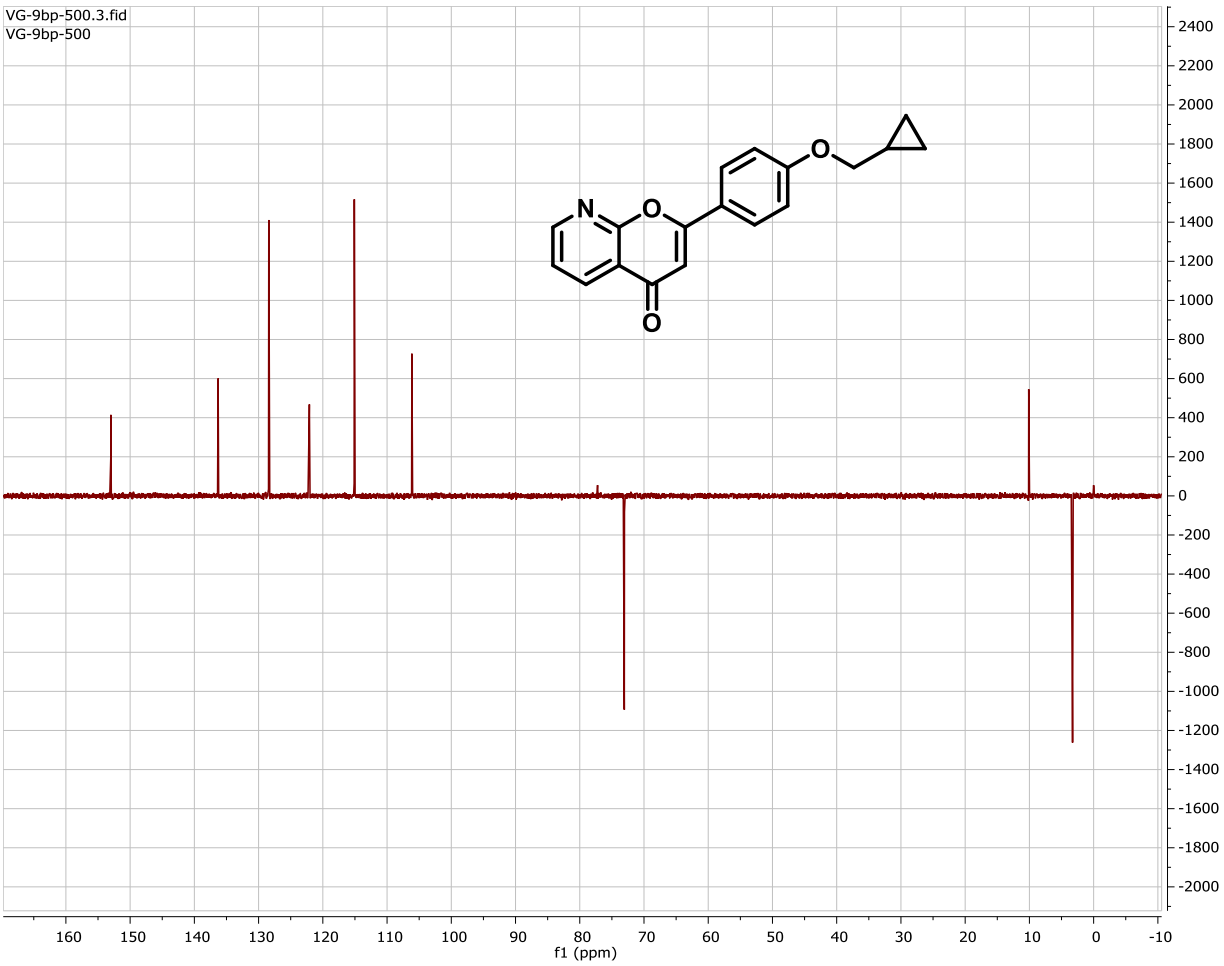

HSQC Spectrum of Compound 13b

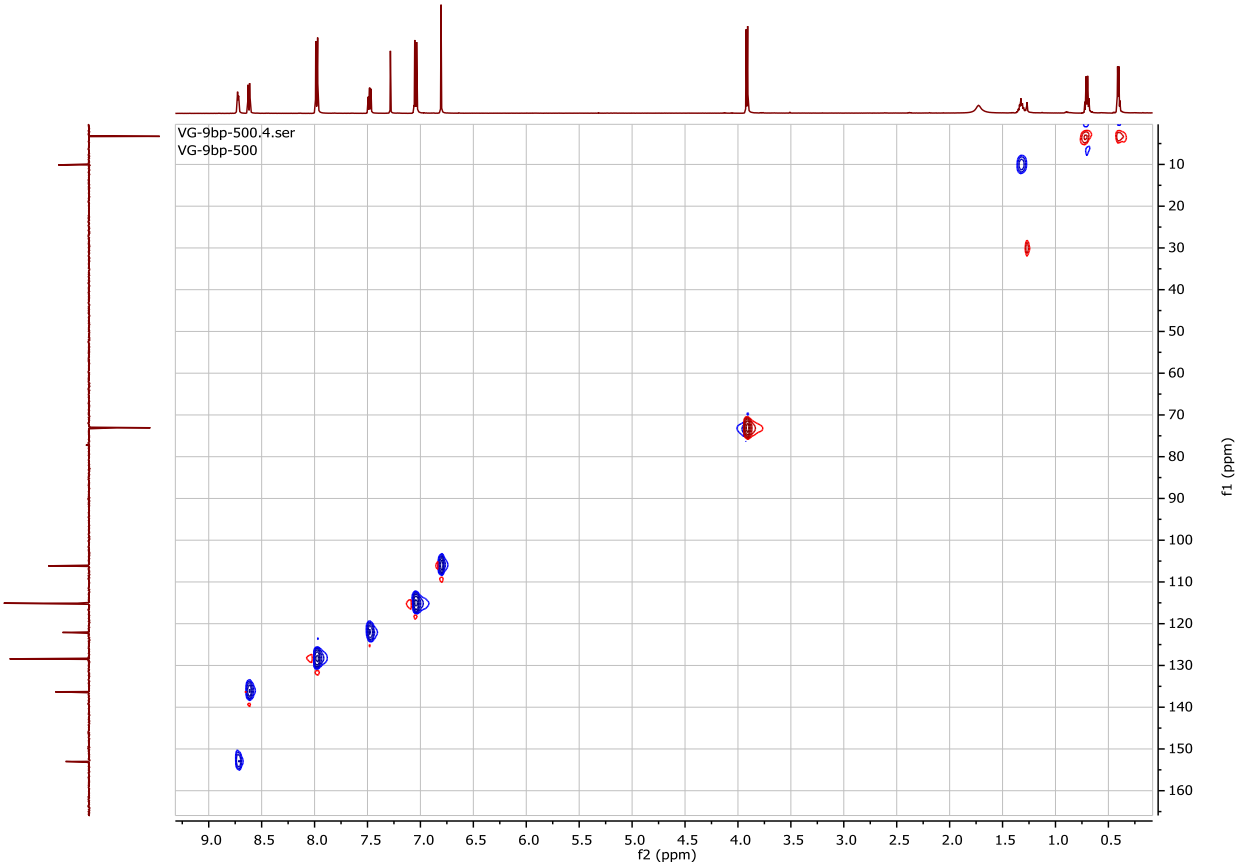

HMBC Spectrum of Compound 13b

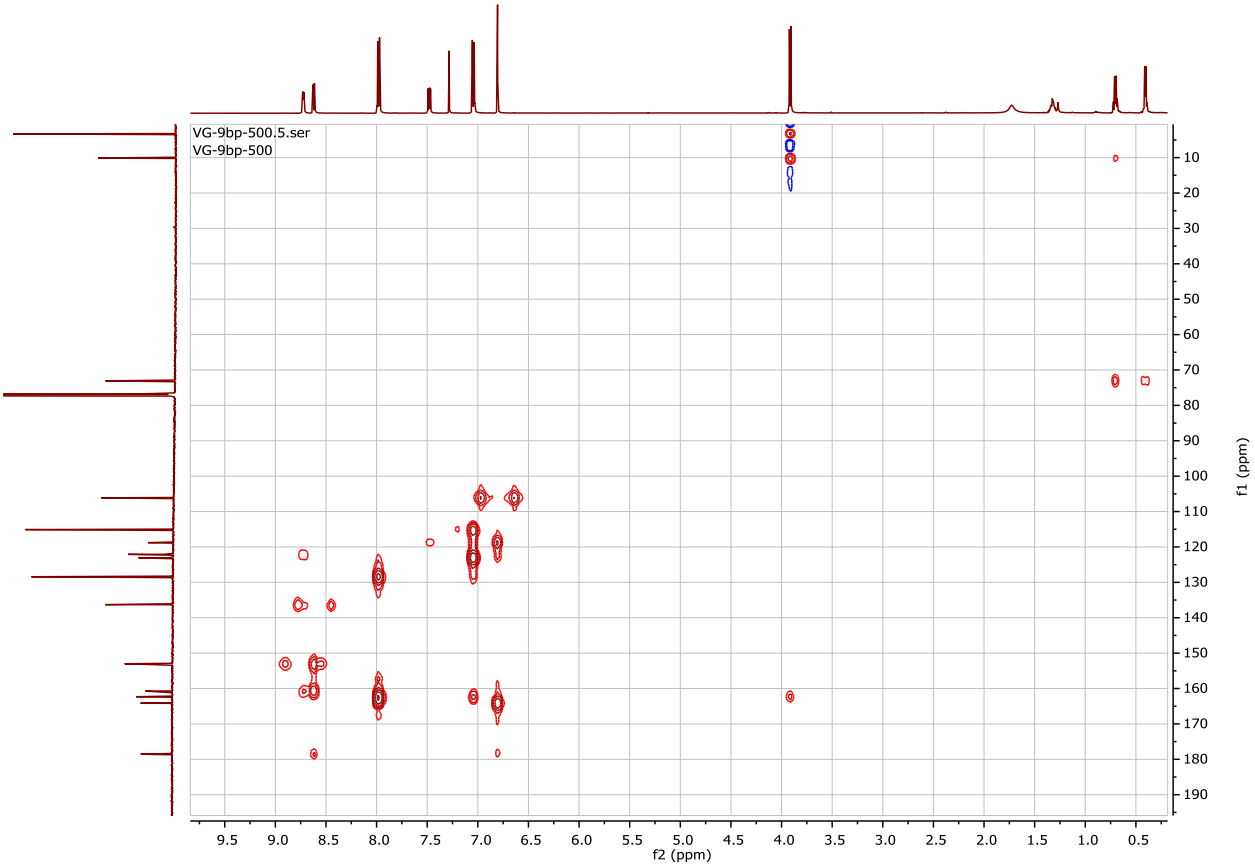

^{1}H-Spectrum of Compound 14a

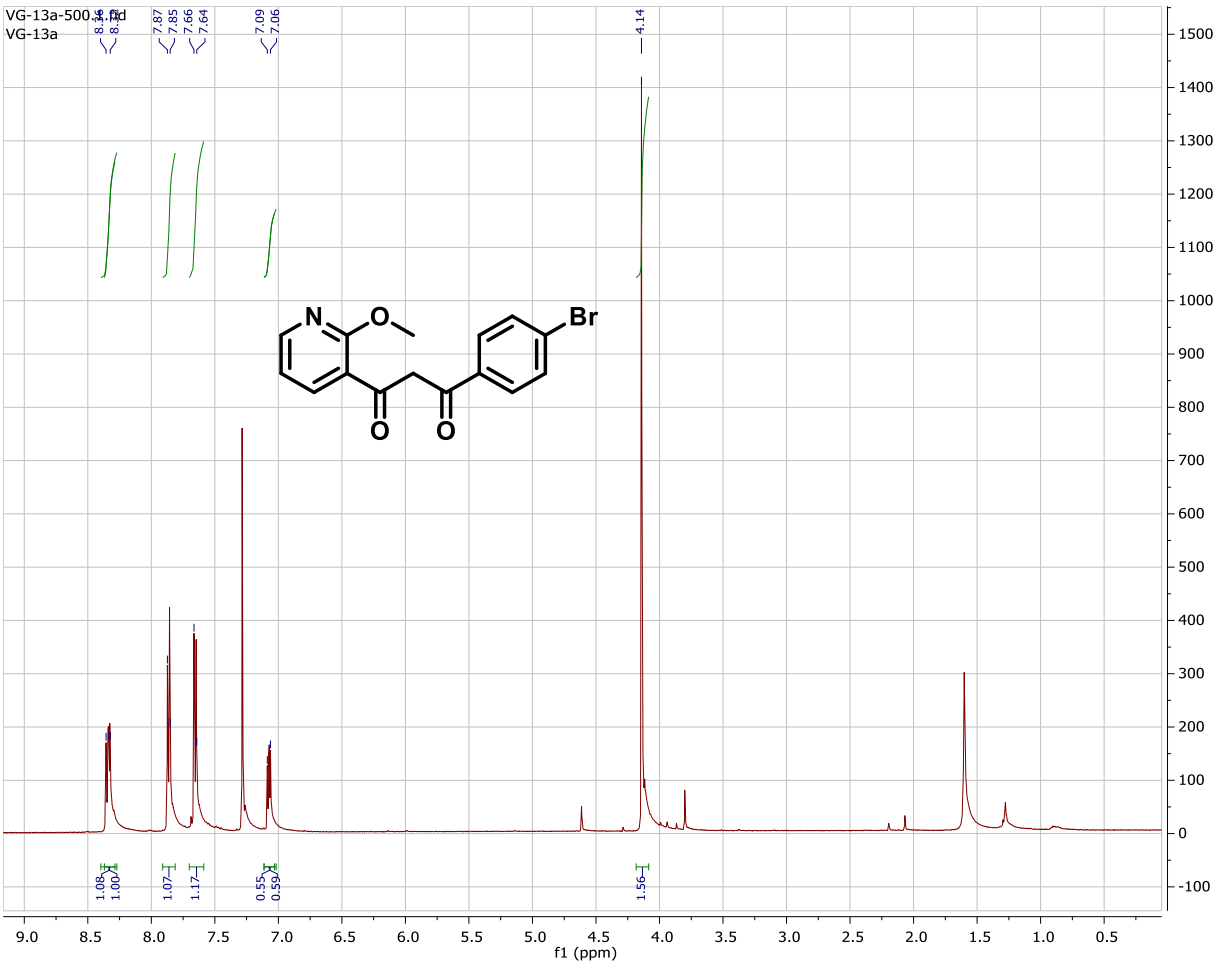

^{13}C-Spectrum of Compound 14a

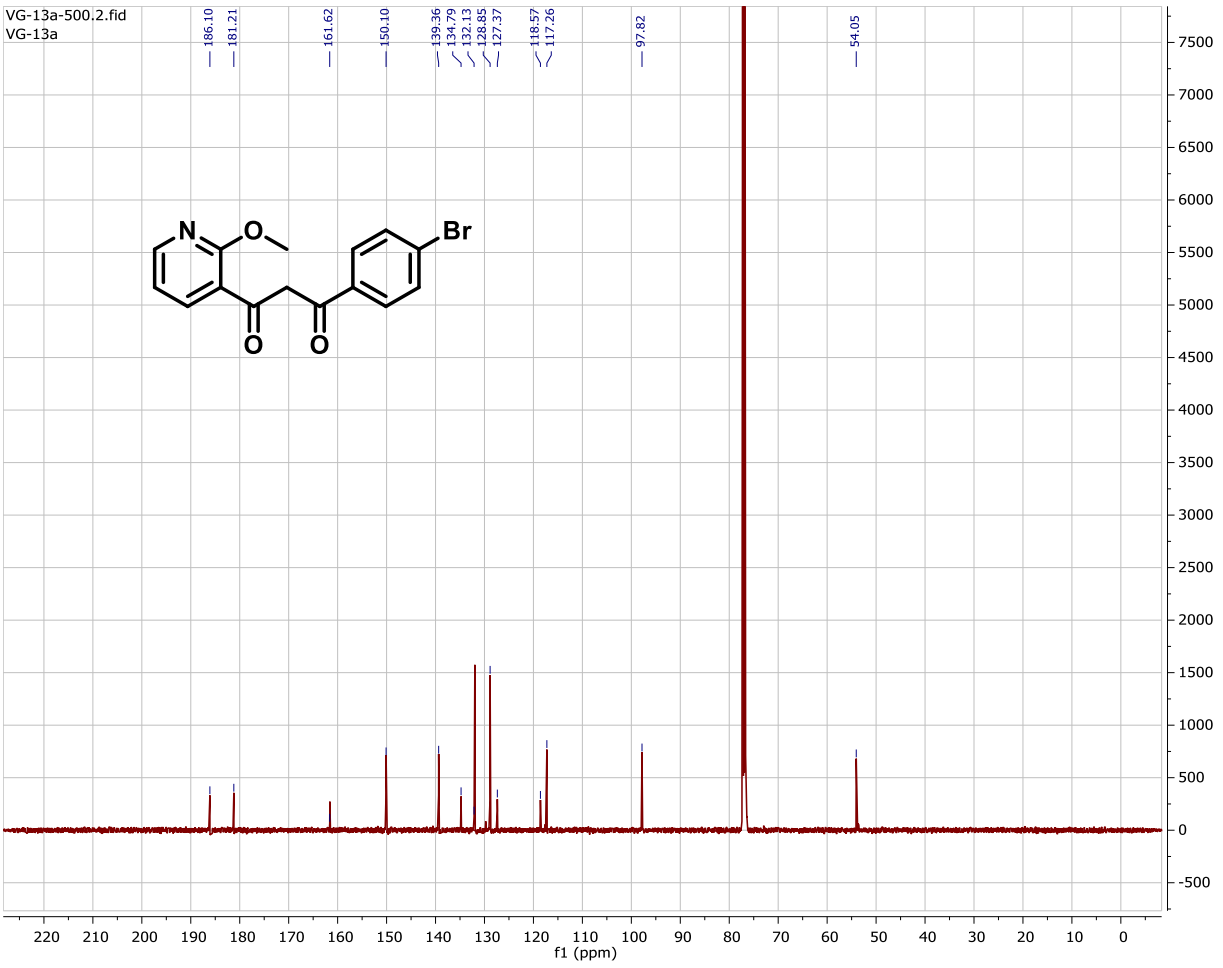

DEPT-135 Spectrum of Compound 14a

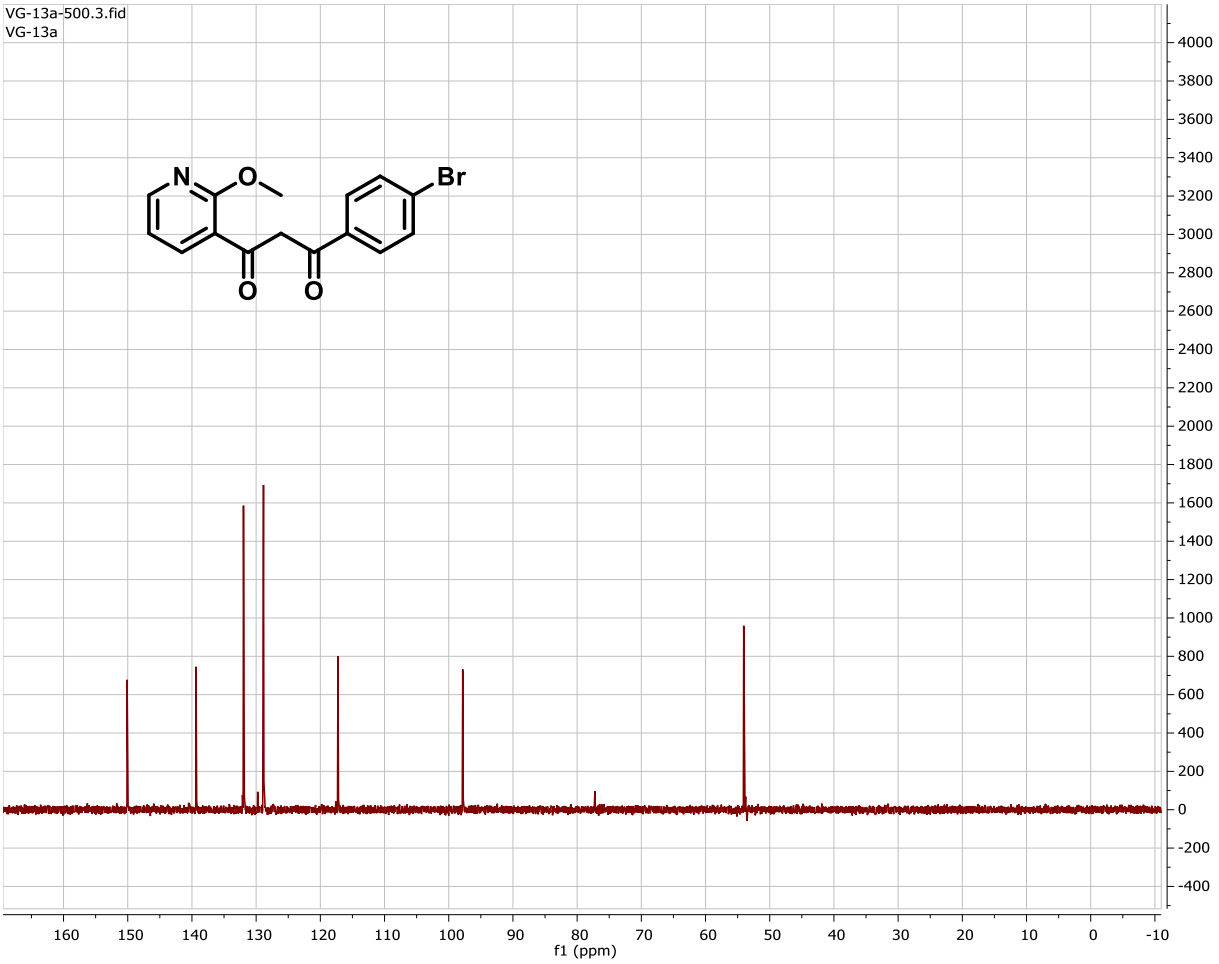

^{1}H-Spectrum of Compound 14b

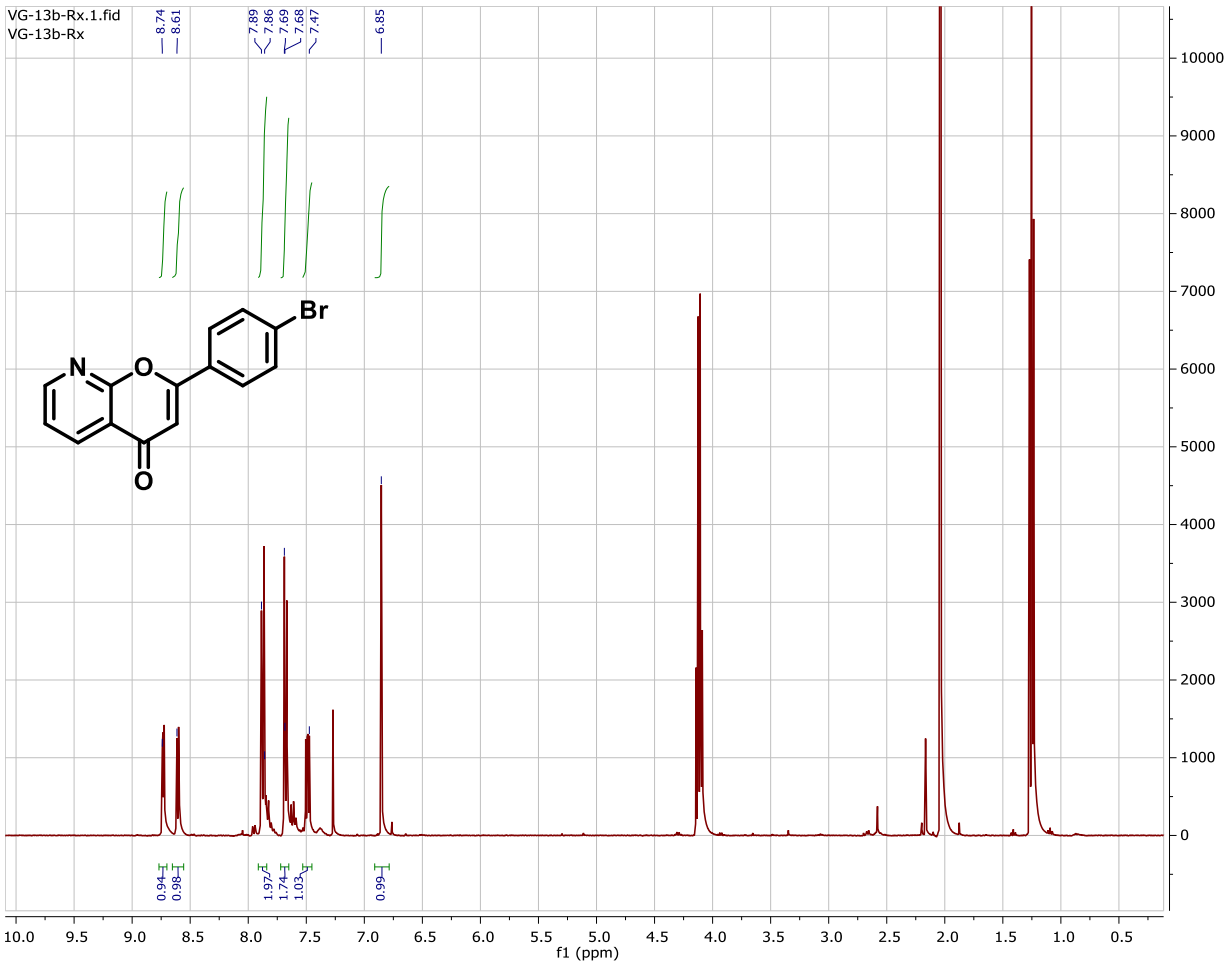

^{13}C-Spectrum of Compound 14b

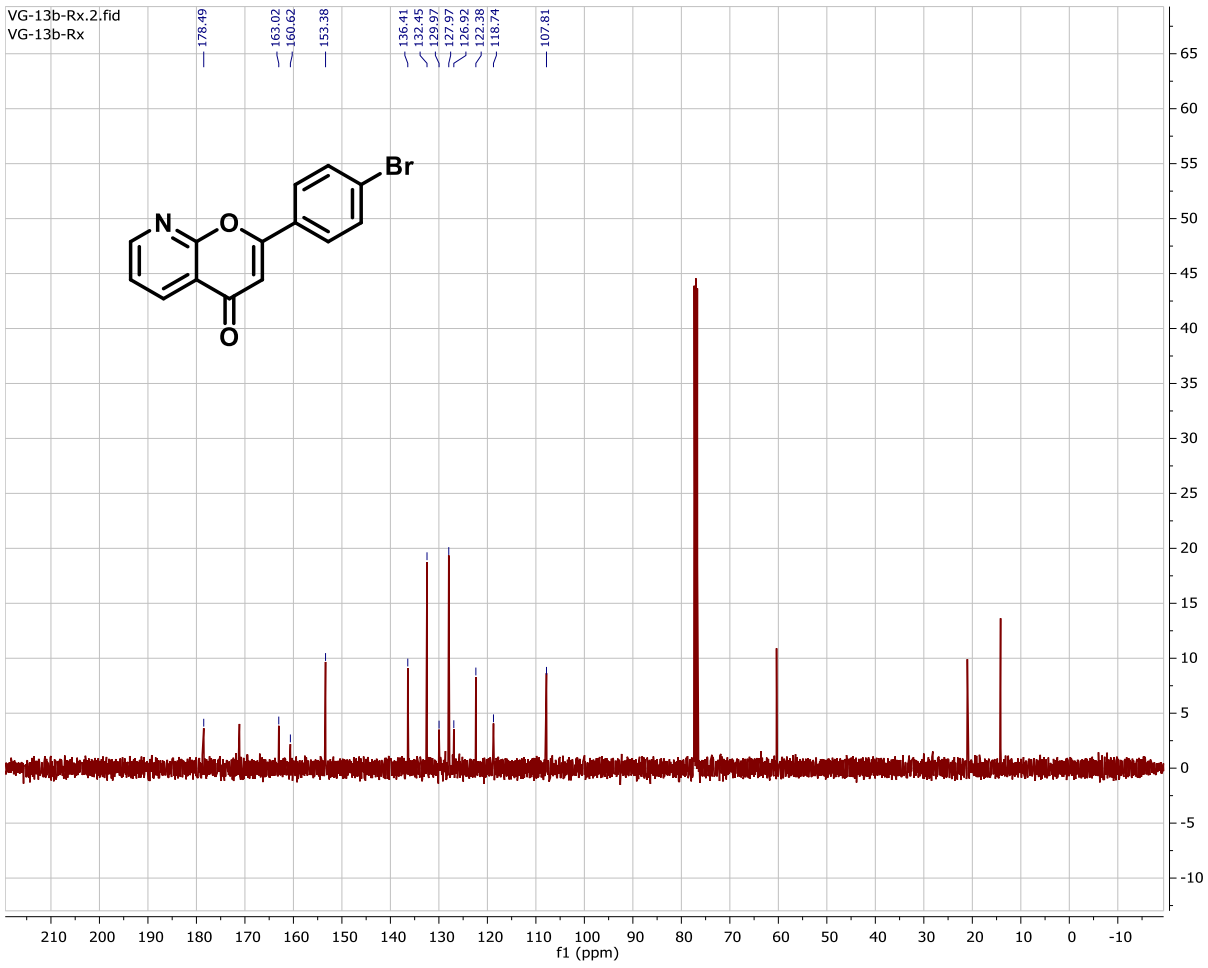

DEPT-135 Spectrum of Compound 14b

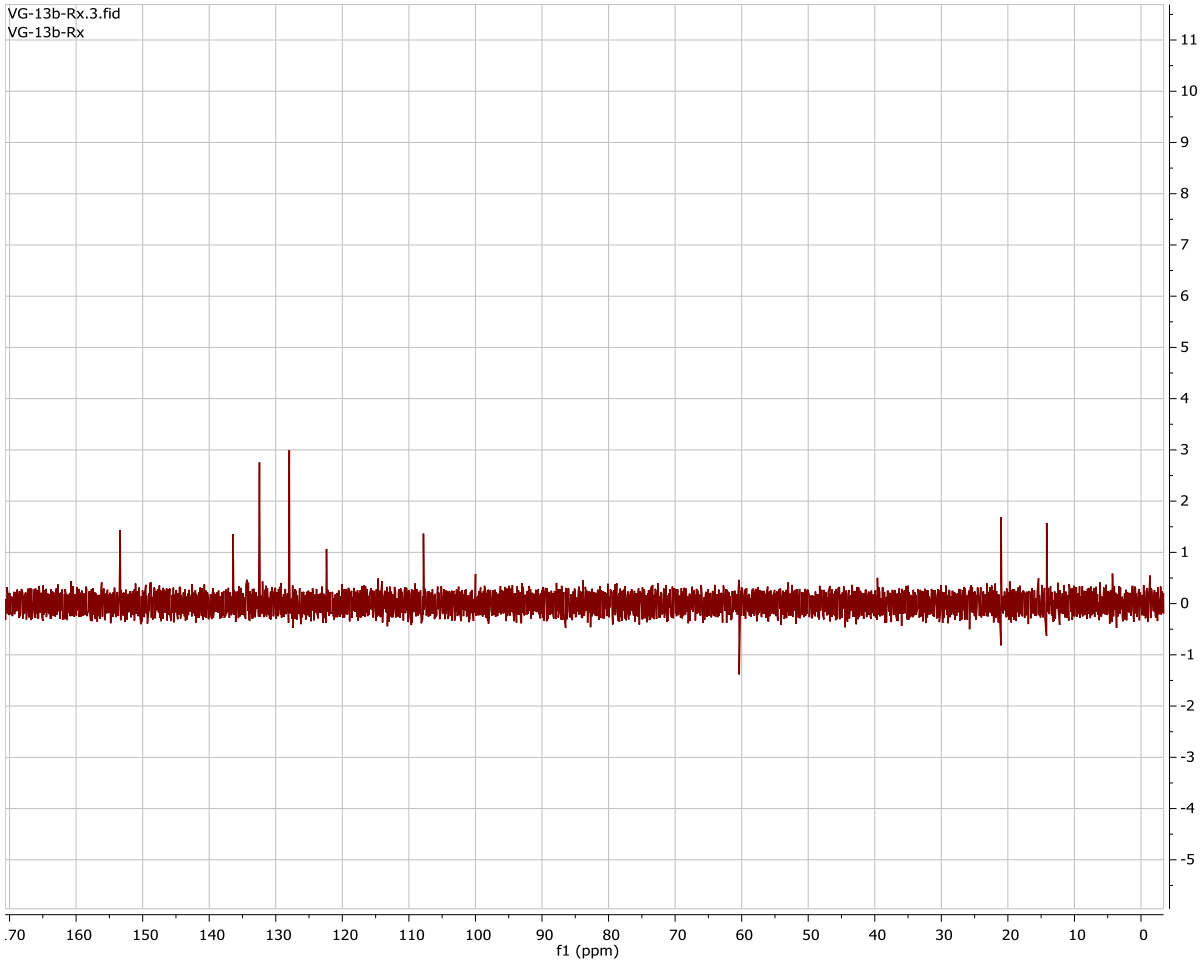

^{1}H-Spectrum of Compound 14c

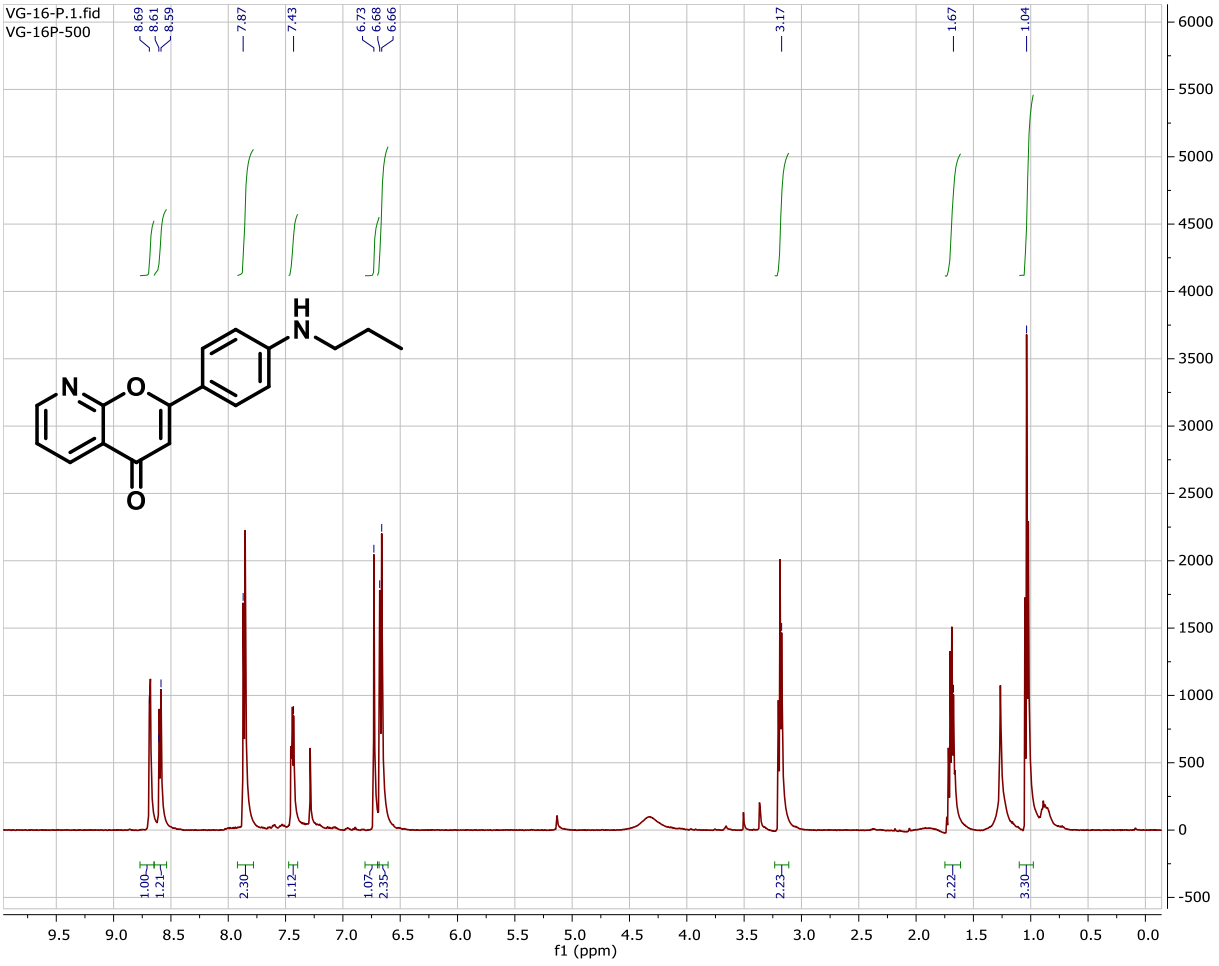

^{13}C-Spectrum of Compound 14c

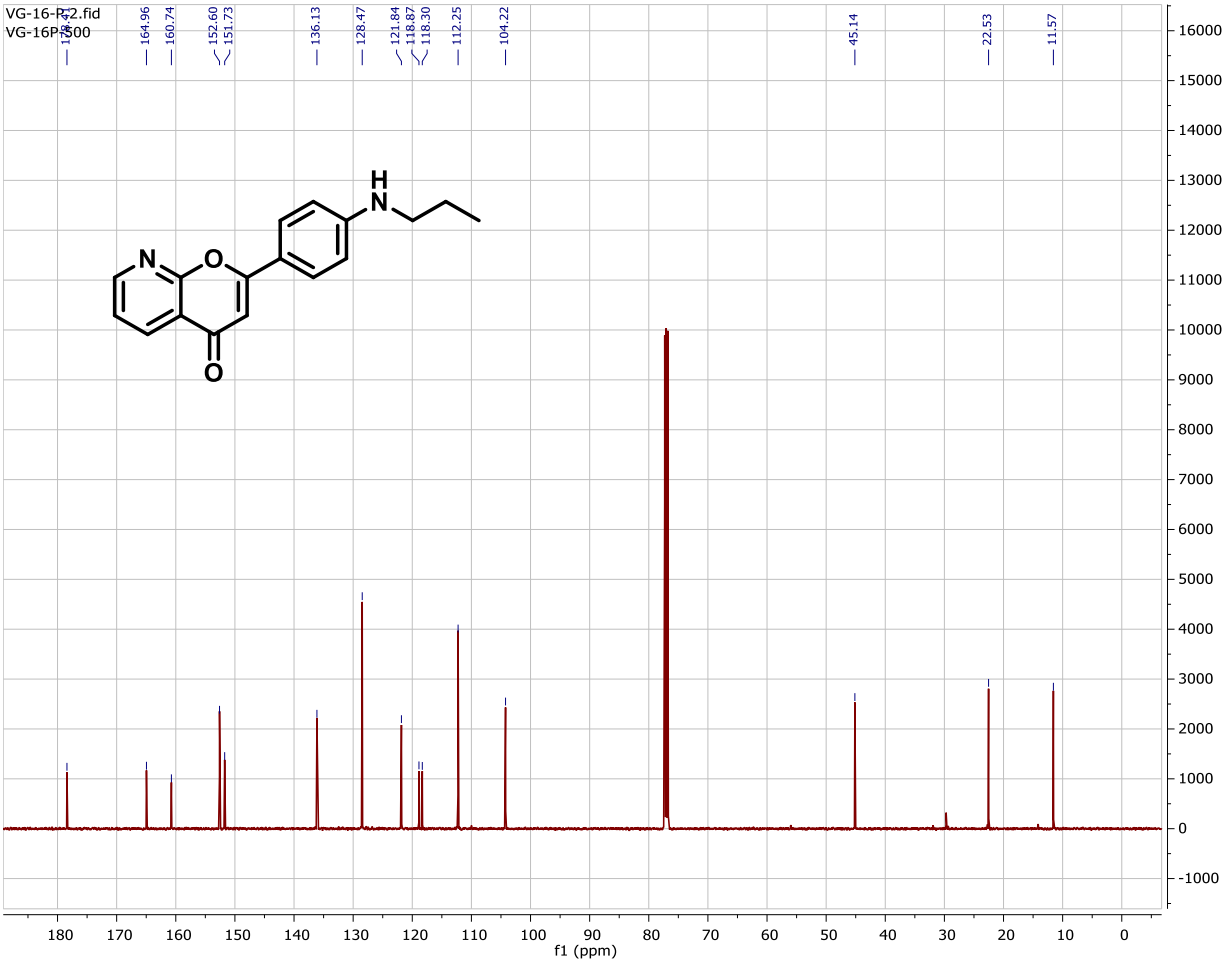

DEPT-135 Spectrum of Compound 14c

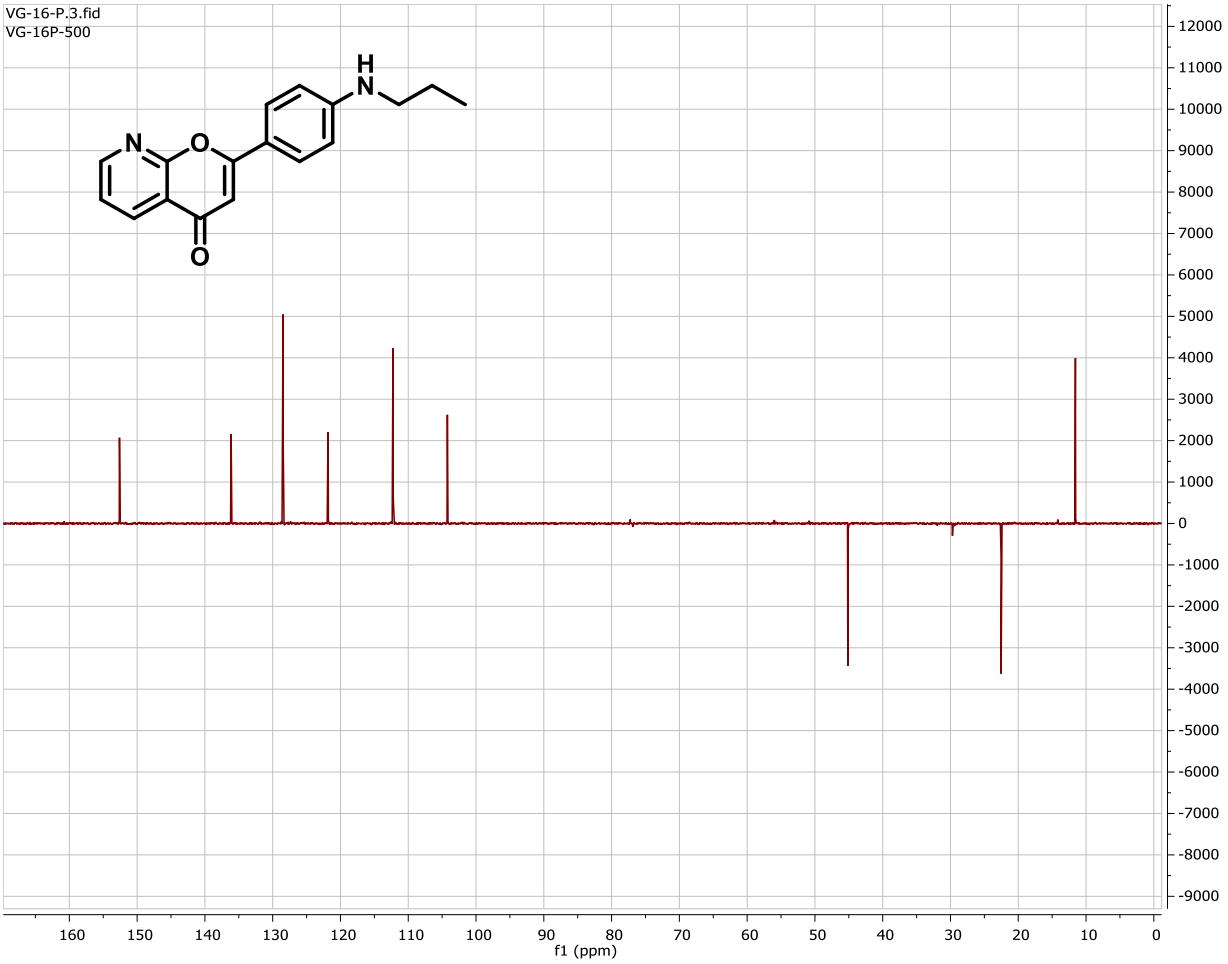

HSQC Spectrum of Compound 14c

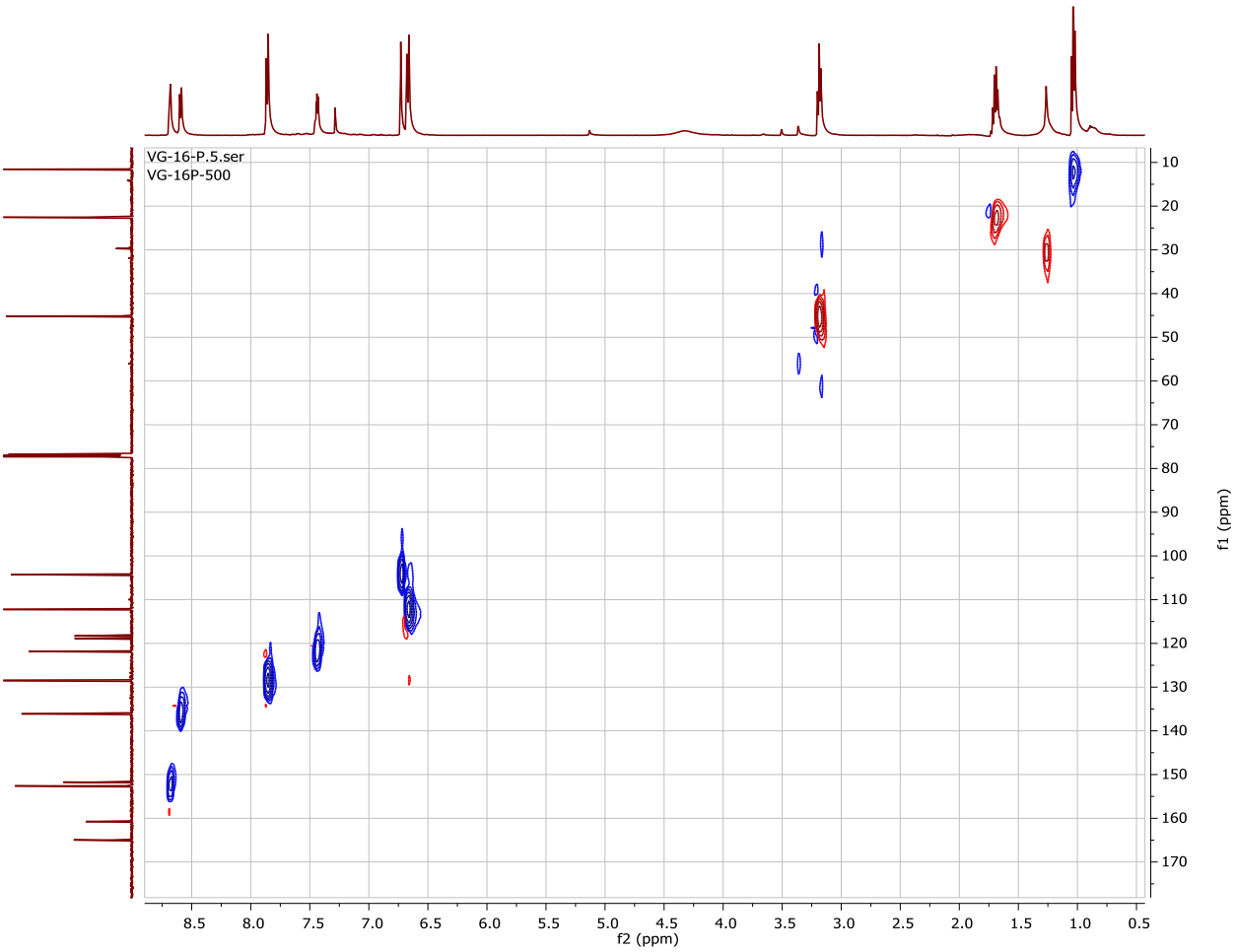

HMBC Spectrum of Compound 14c

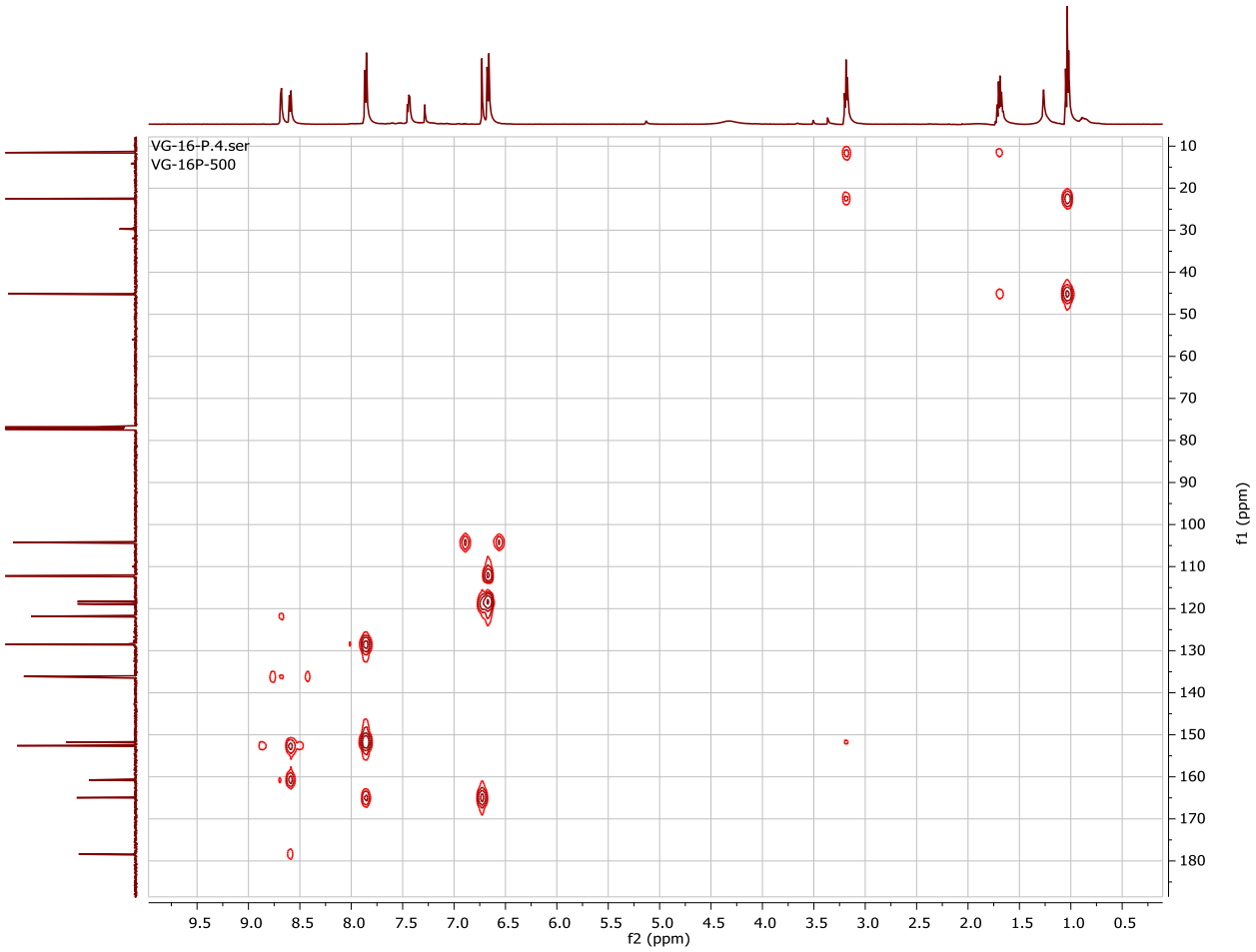

^{1}H-Spectrum of Compound 15c

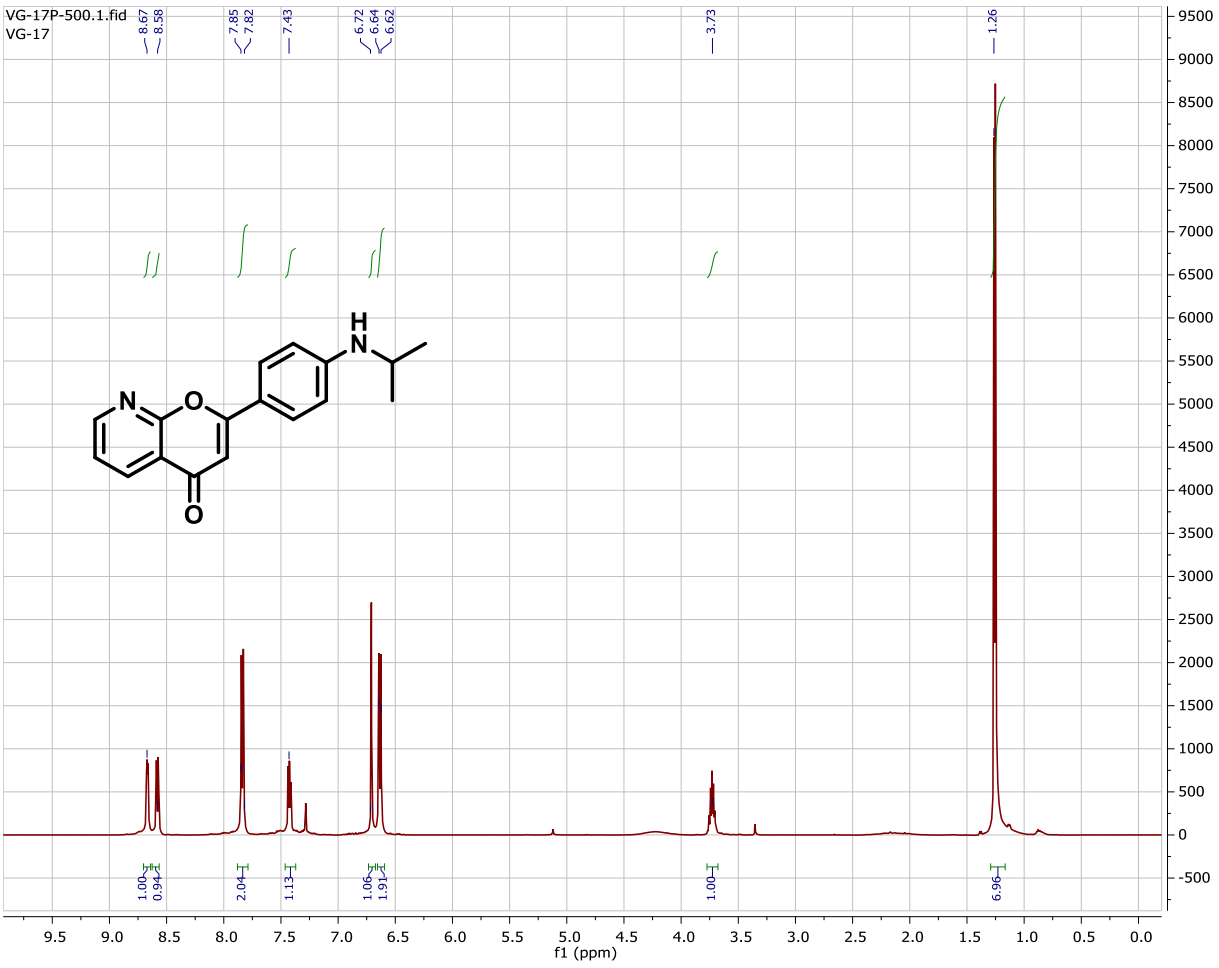

^{13}C-Spectrum of Compound 15c

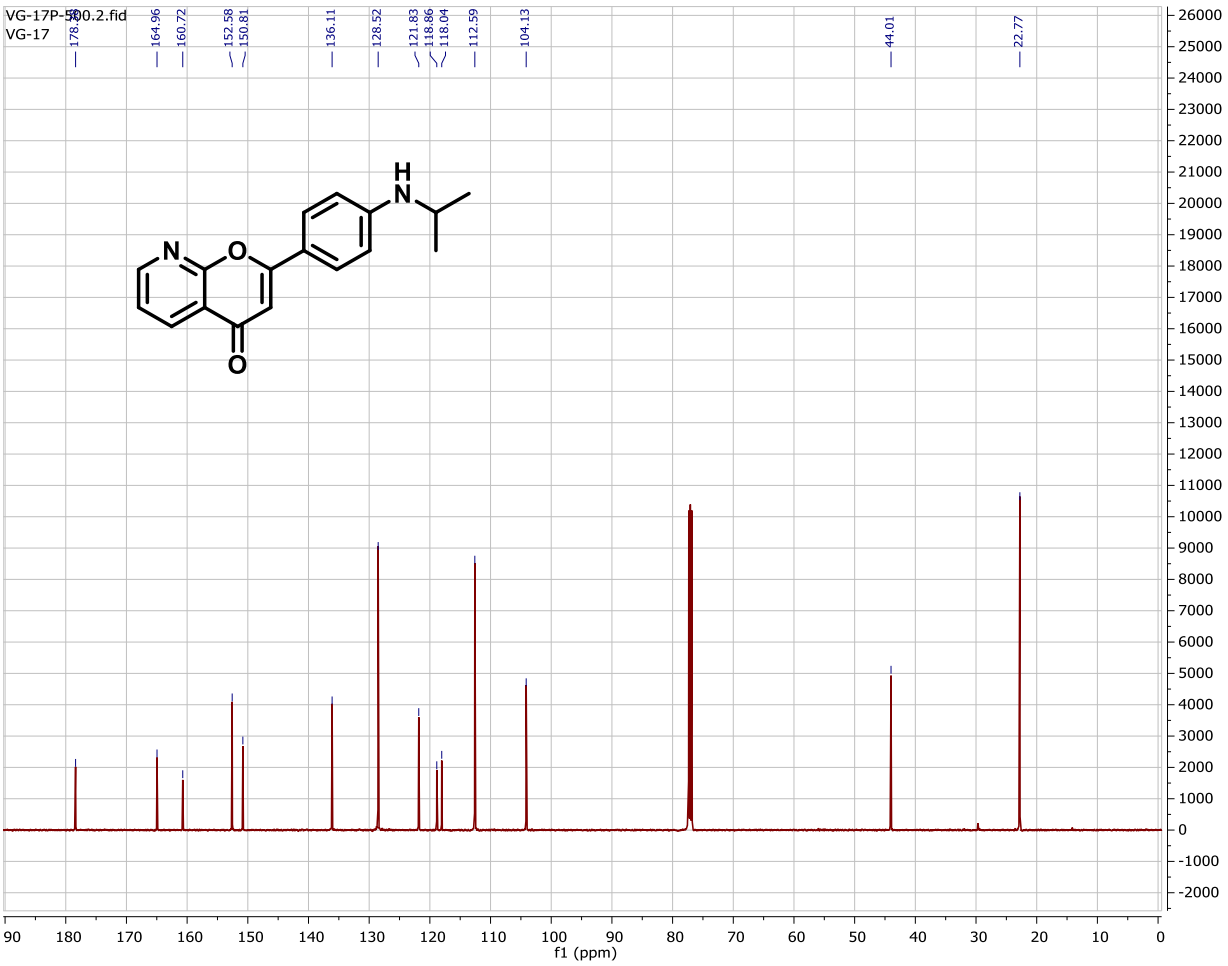

DEPT-135 Spectrum of Compound 15c

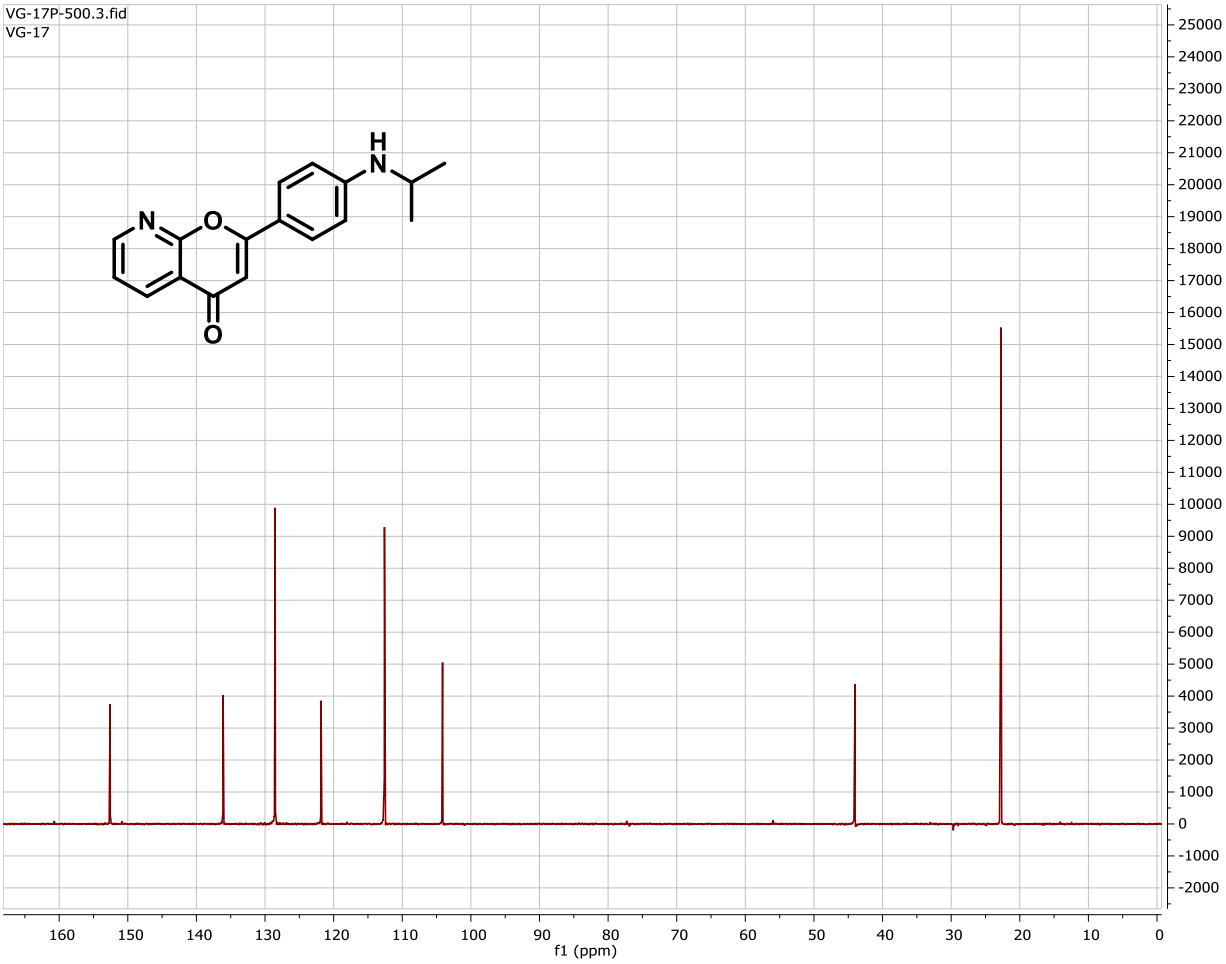

HSQC Spectrum of Compound 15c

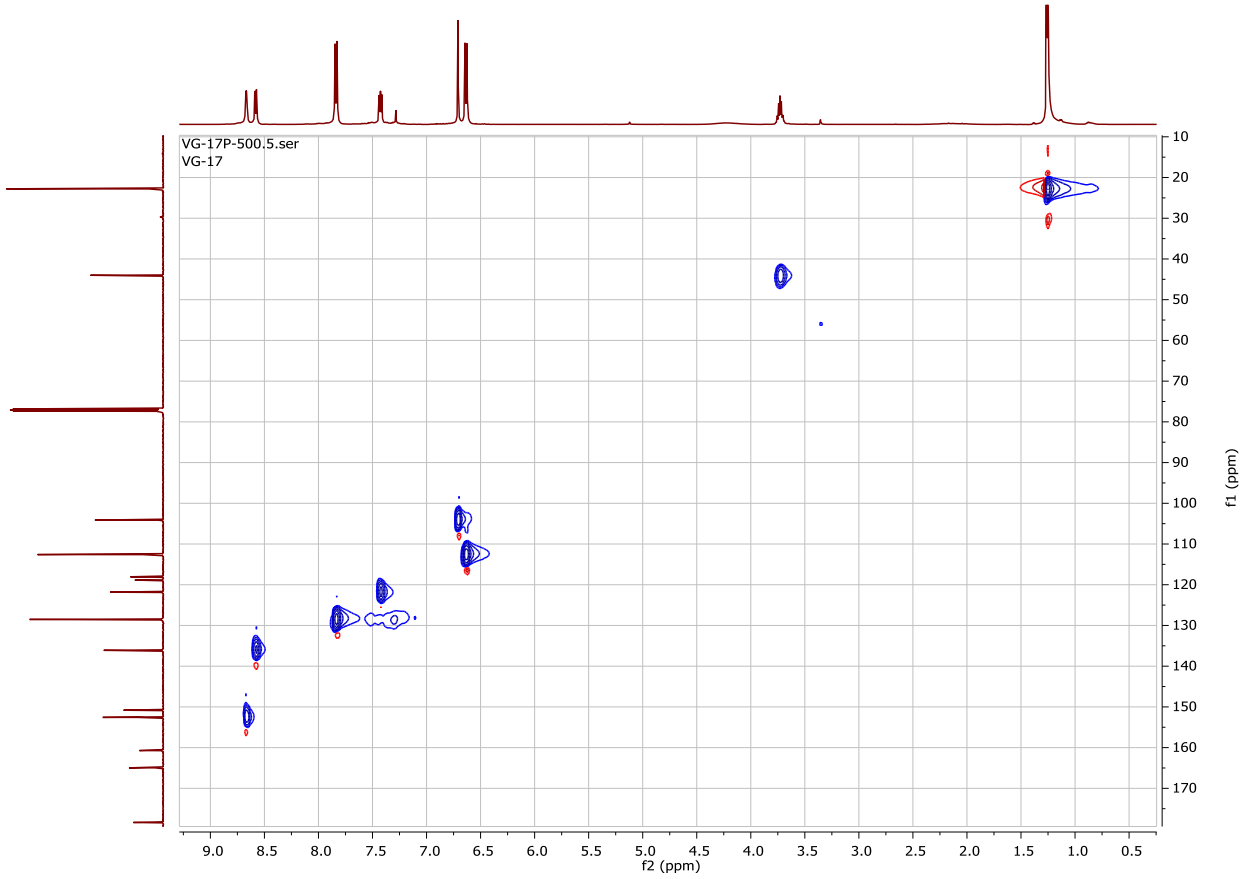

HMBC Spectrum of Compound 15c

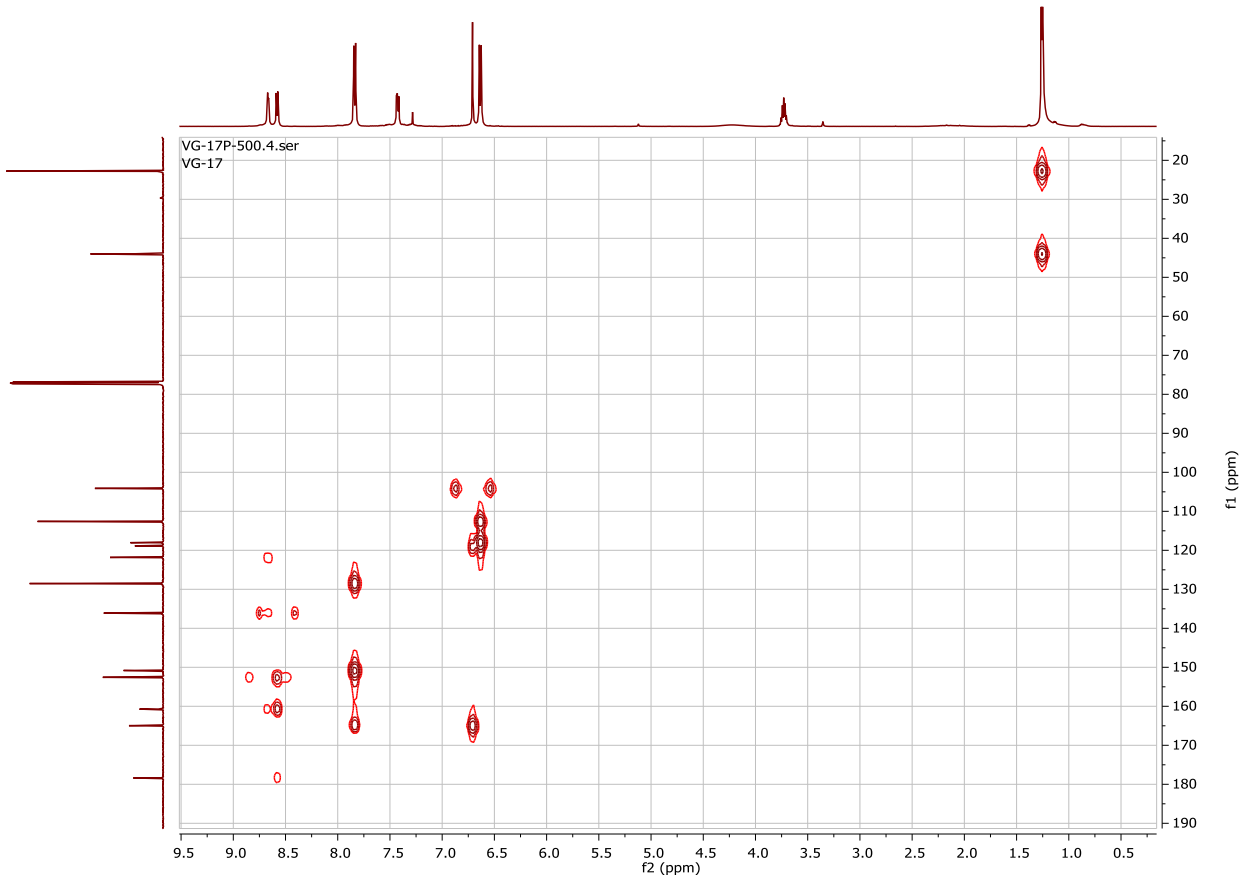

APPENDIX B.

IR SPECTRAL DATA

IR Spectrum of Caleanolene-A

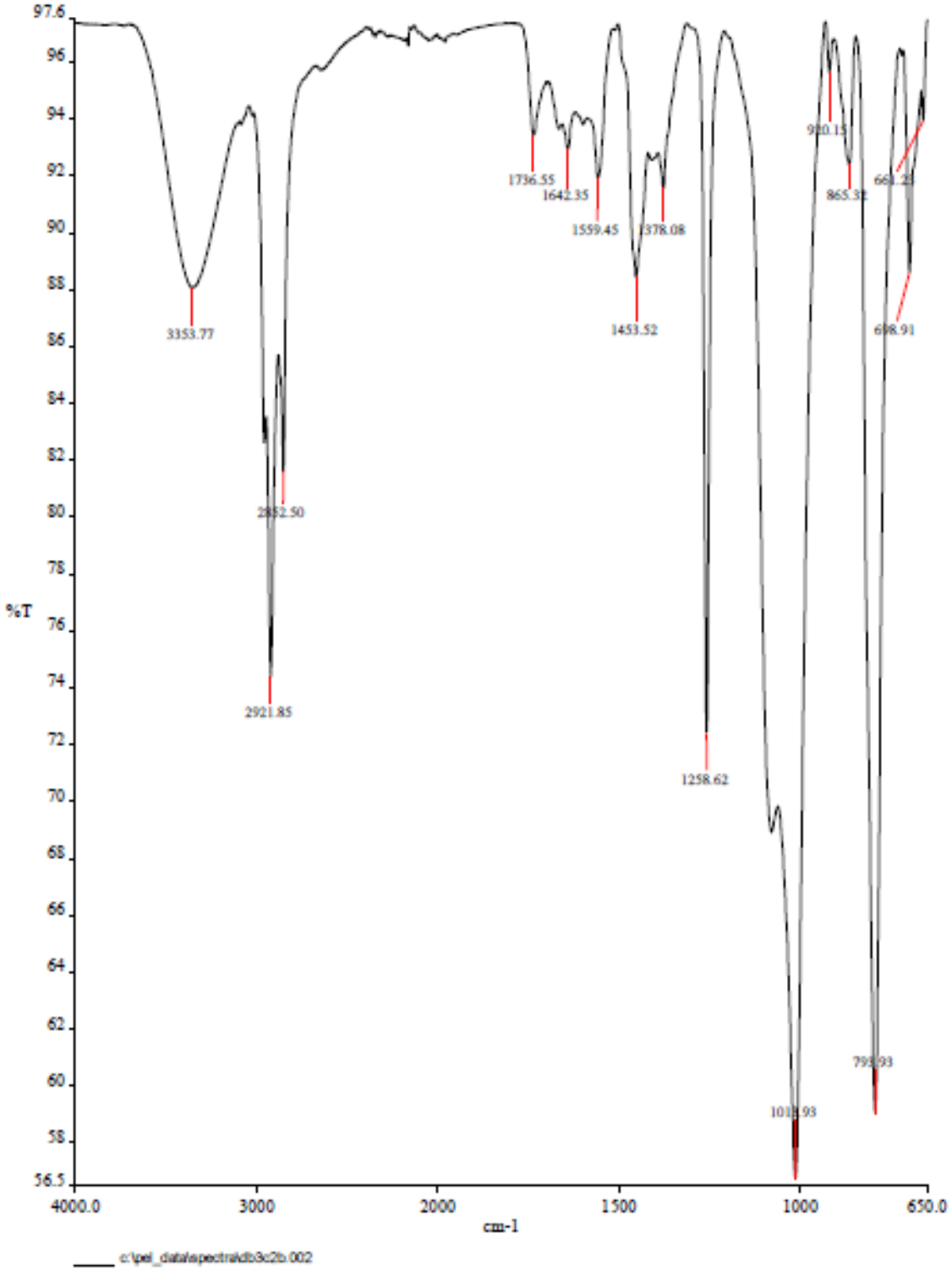

IR Spectrum of Caleanolene-B

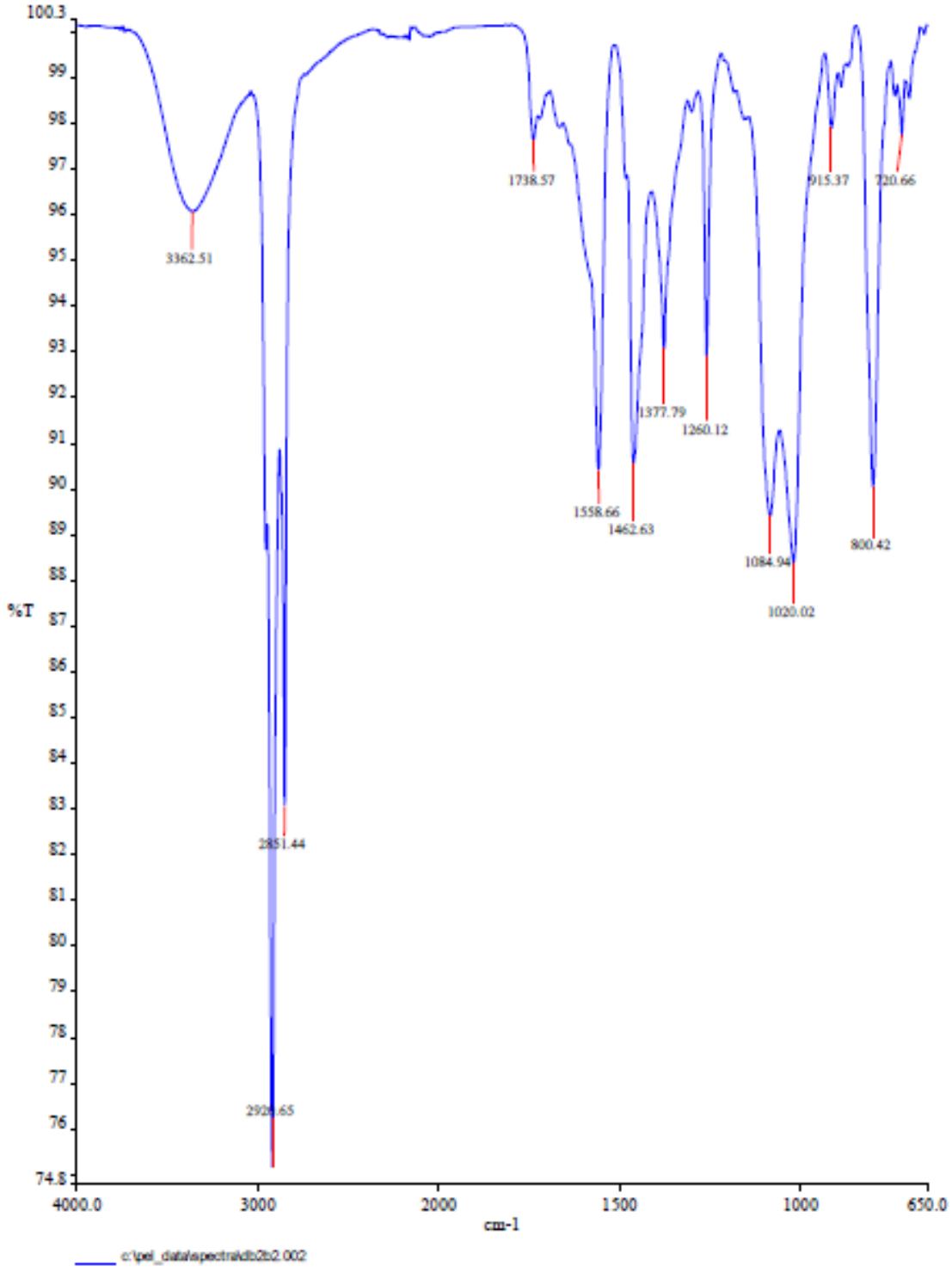

IR Spectrum of Caleanolene-C

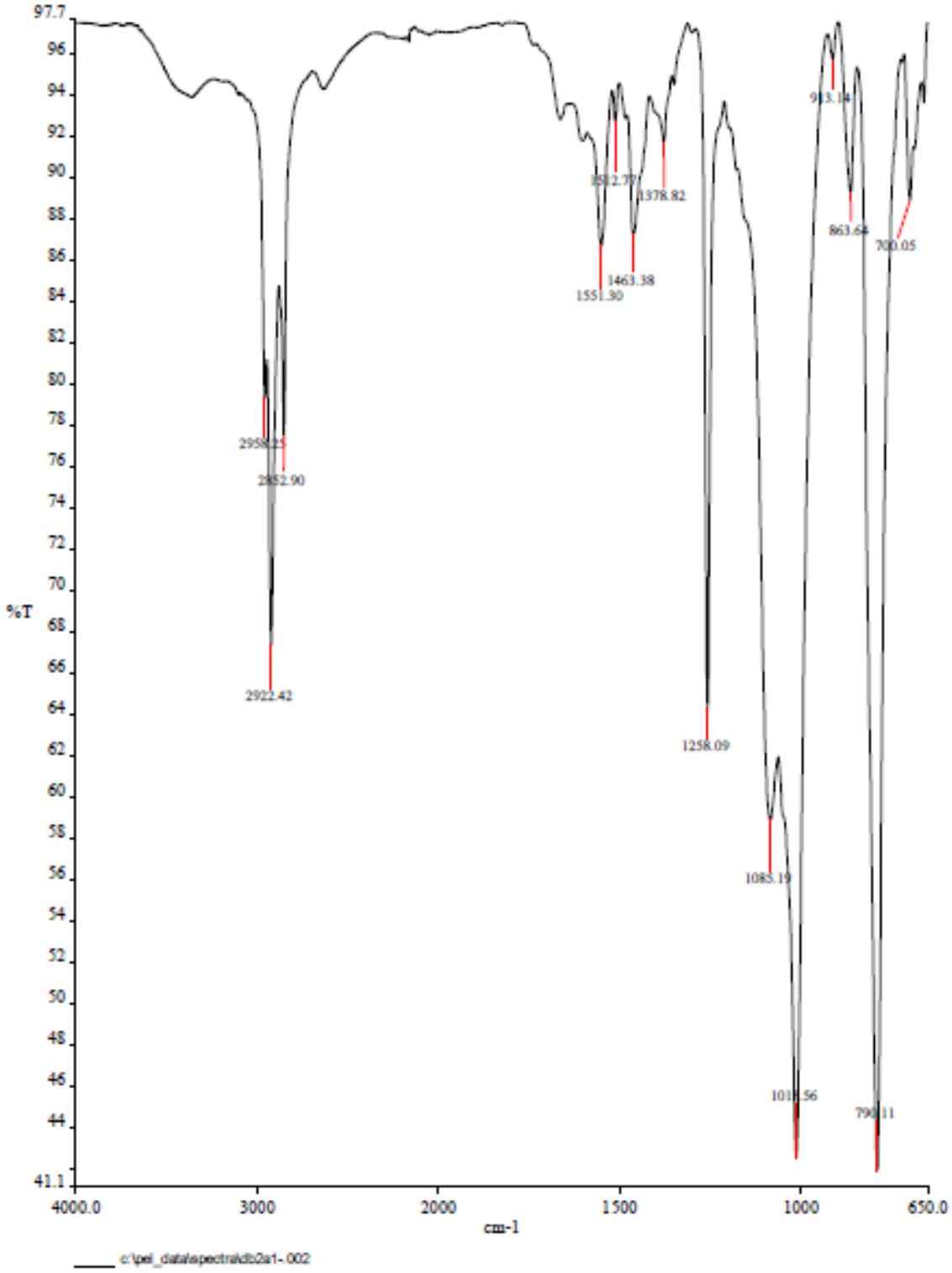

APPENDIX C.

THERMOSPRAY LC/MS SPECTRAL DATA

HRESIMS (+) of Acacetin

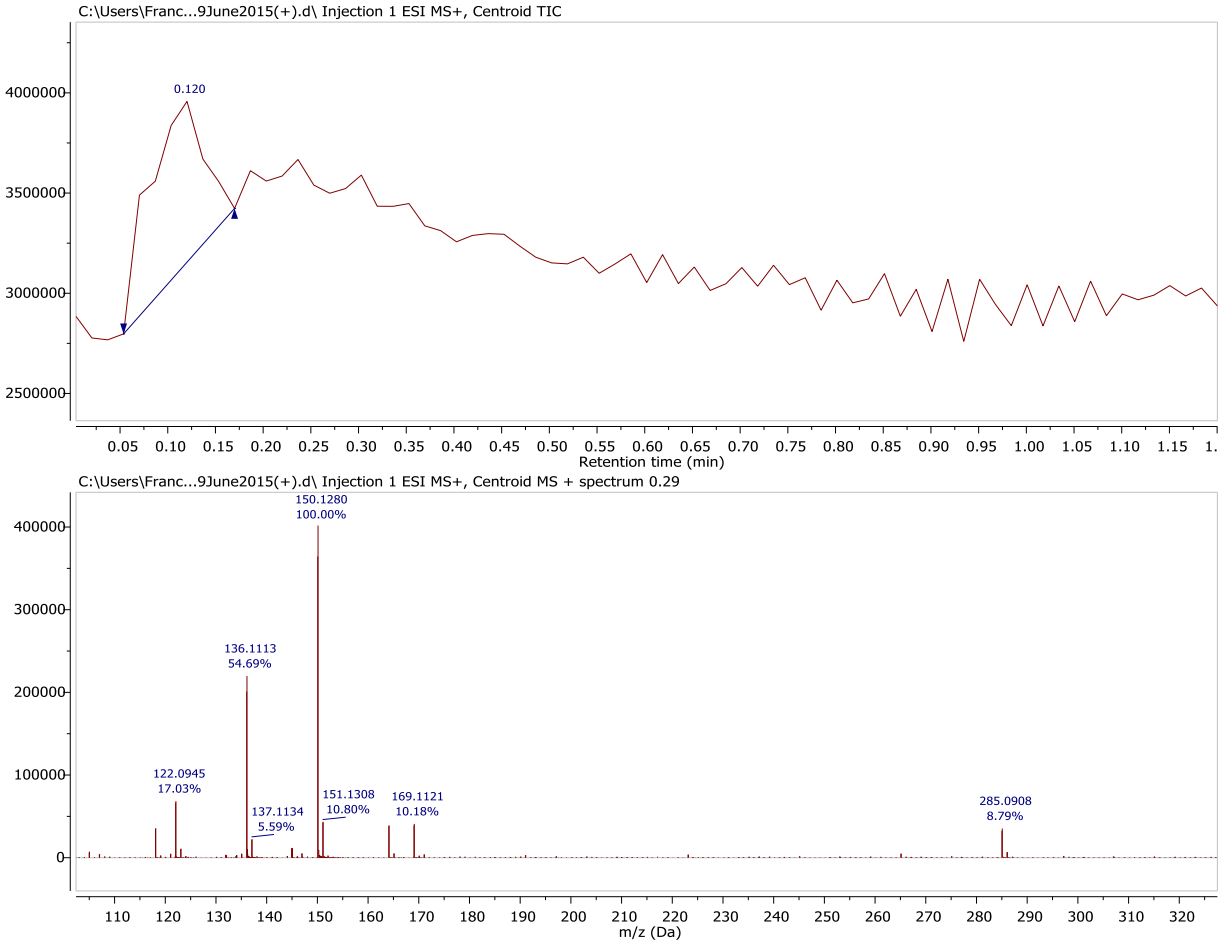

HRESIMS (+) of Caleanolene-A

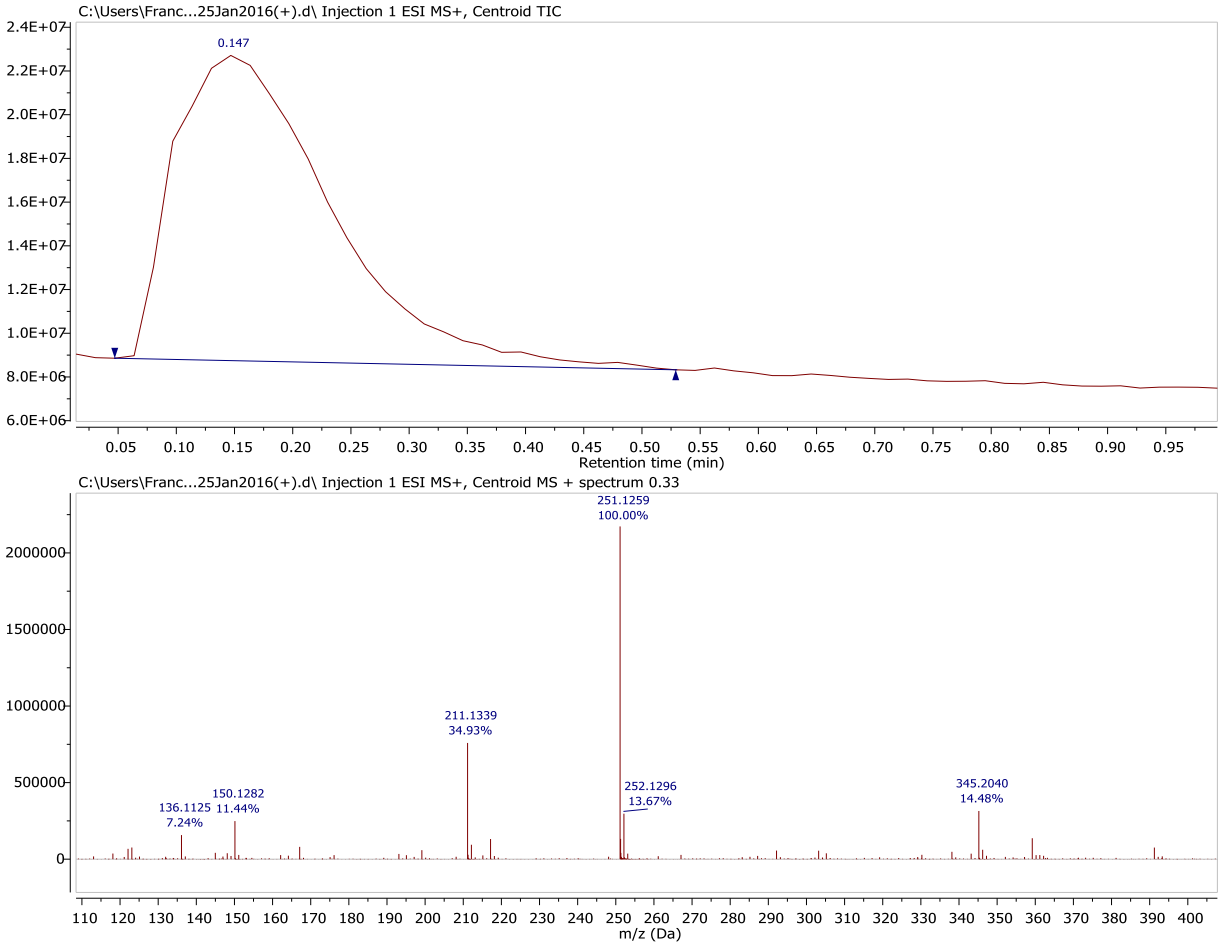

HRESIMS (+) of Caleanolene-B

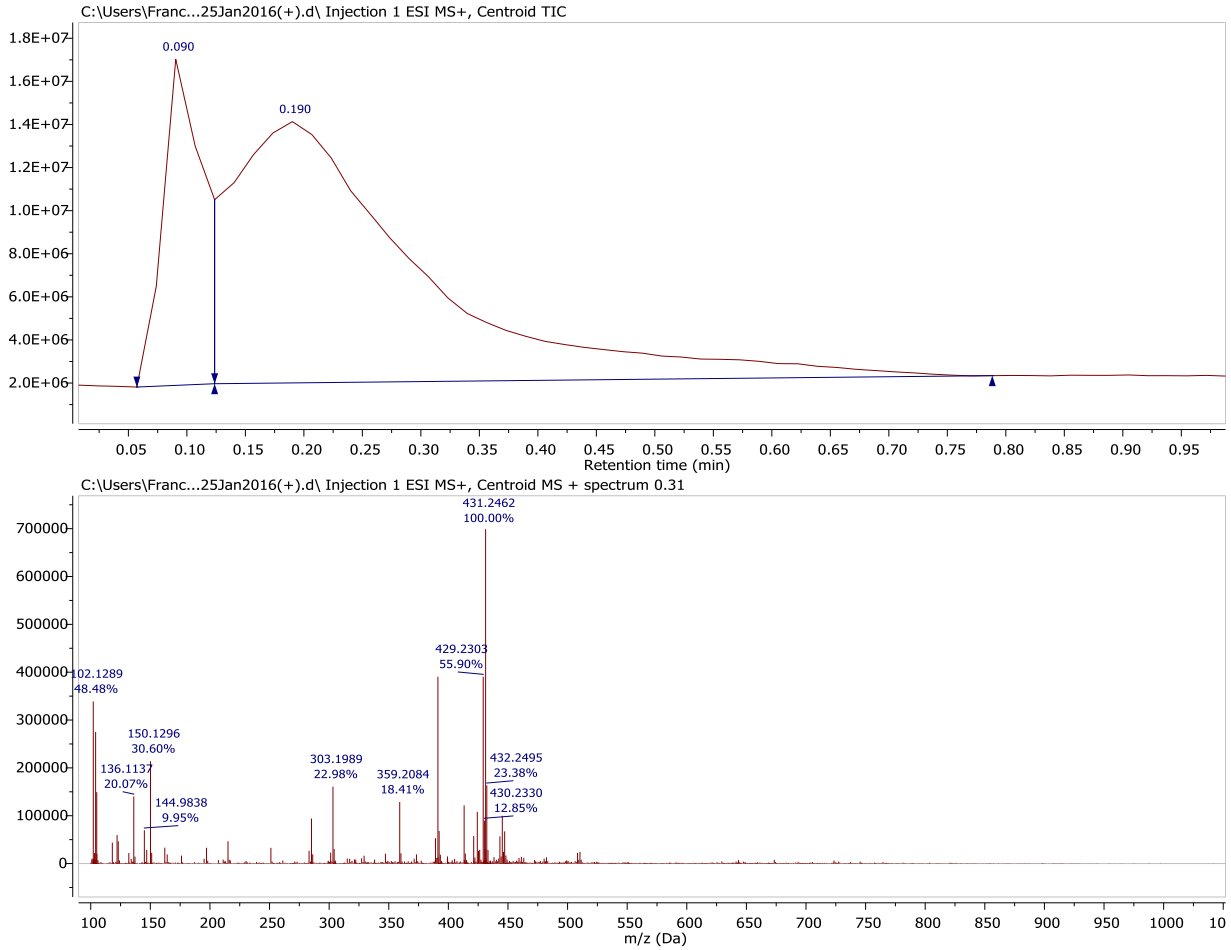

HRESIMS (+) of Caleanolene-C

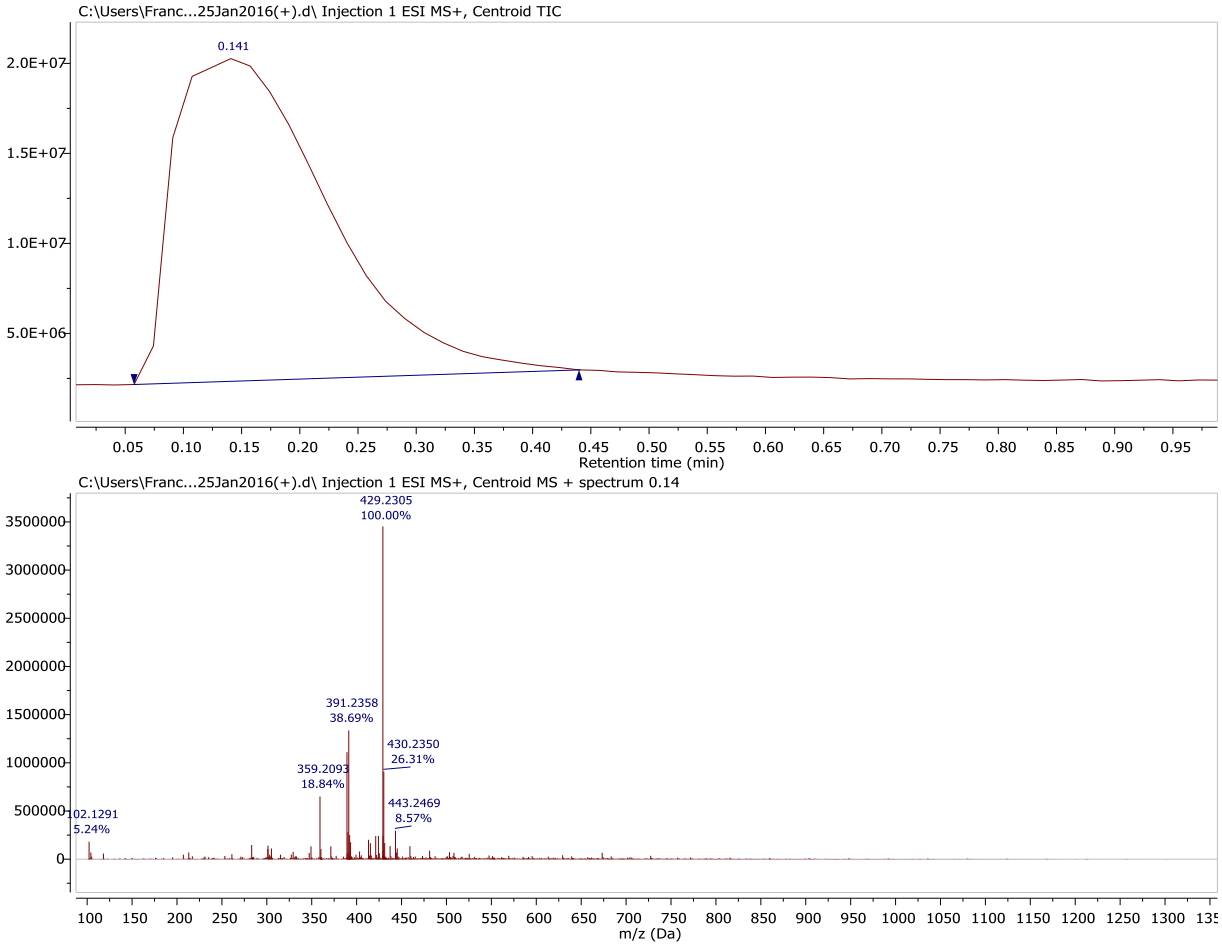

HRESIMS (-) of 2,3-Epoxyjuanislamin

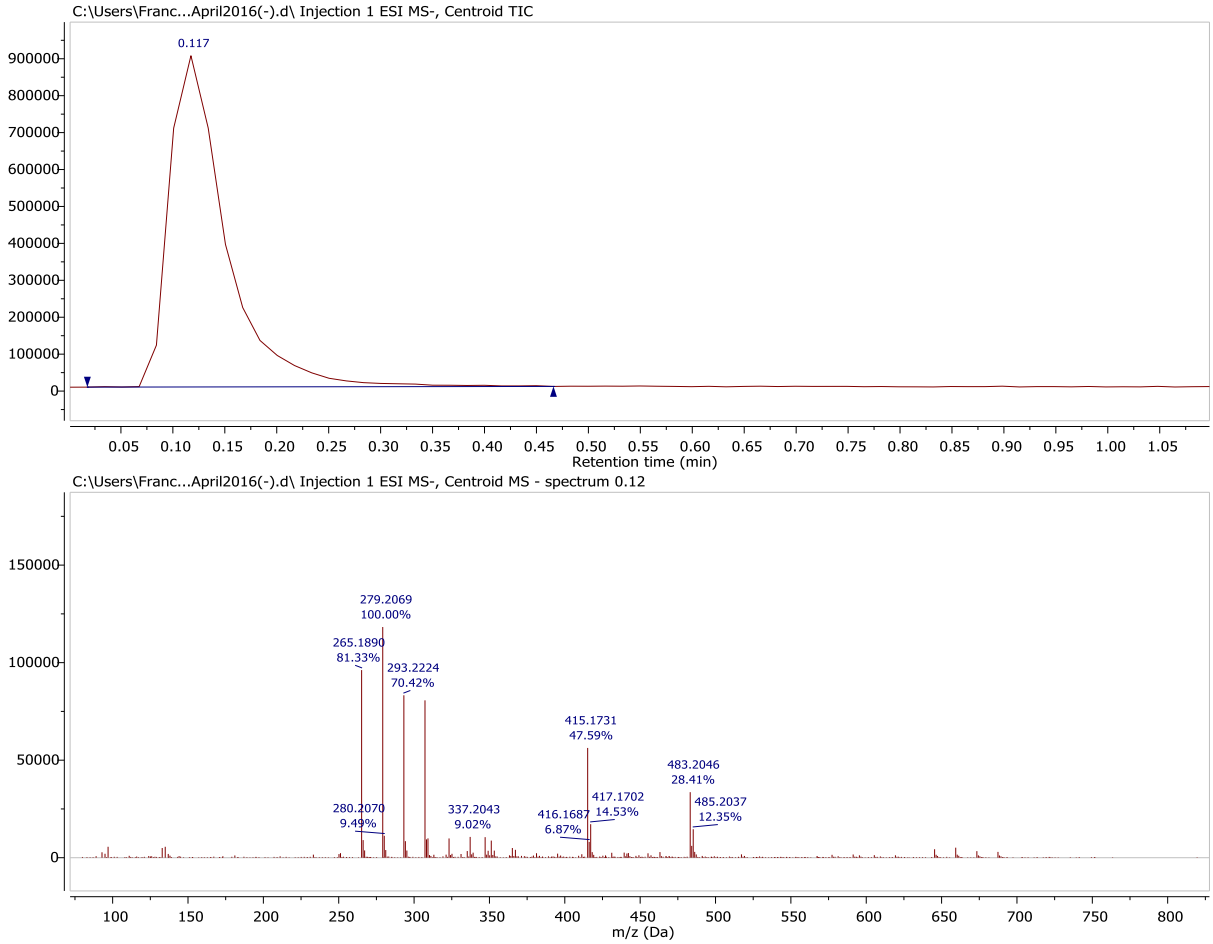

HRESIMS (-) of Calealactone-B

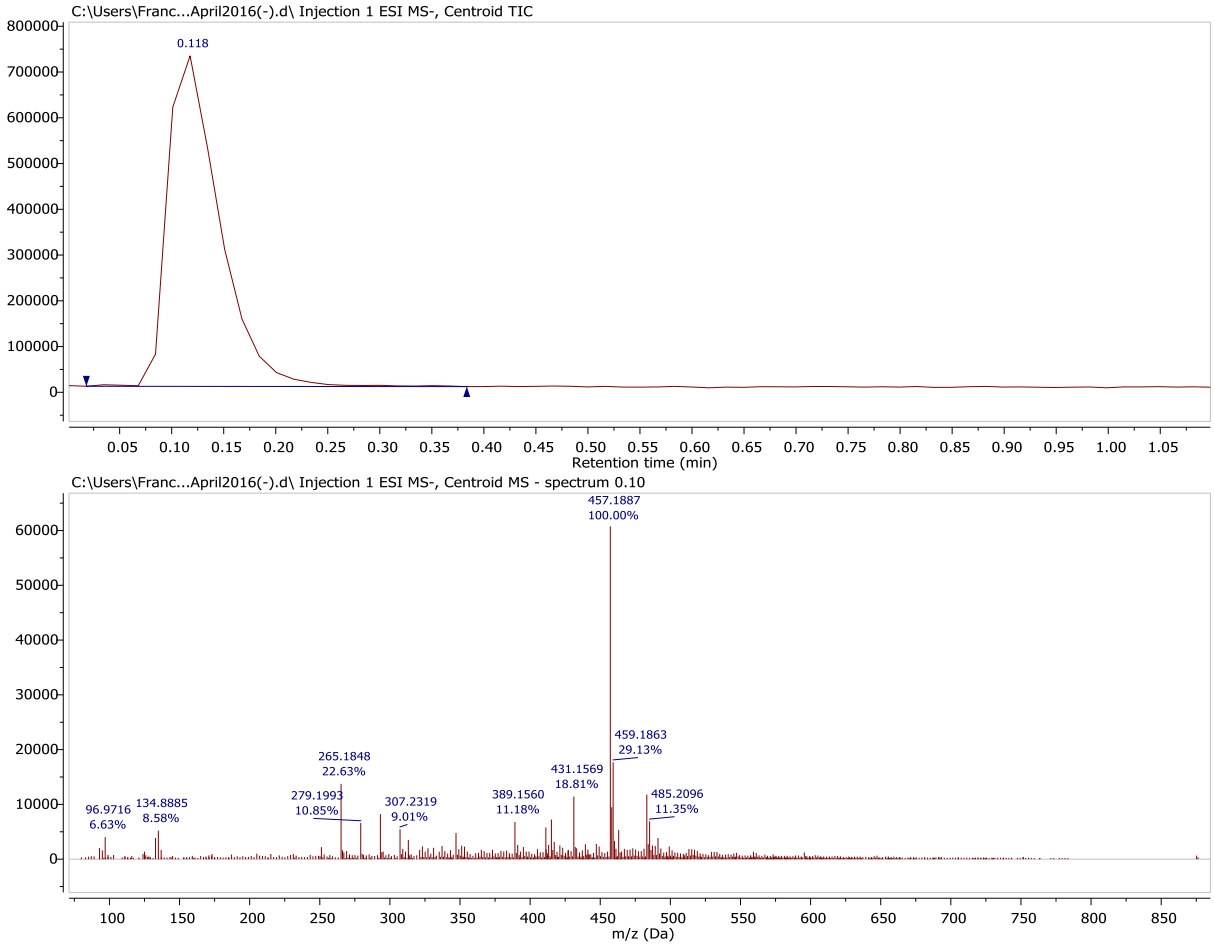

HRESIMS (+) of Calein-C

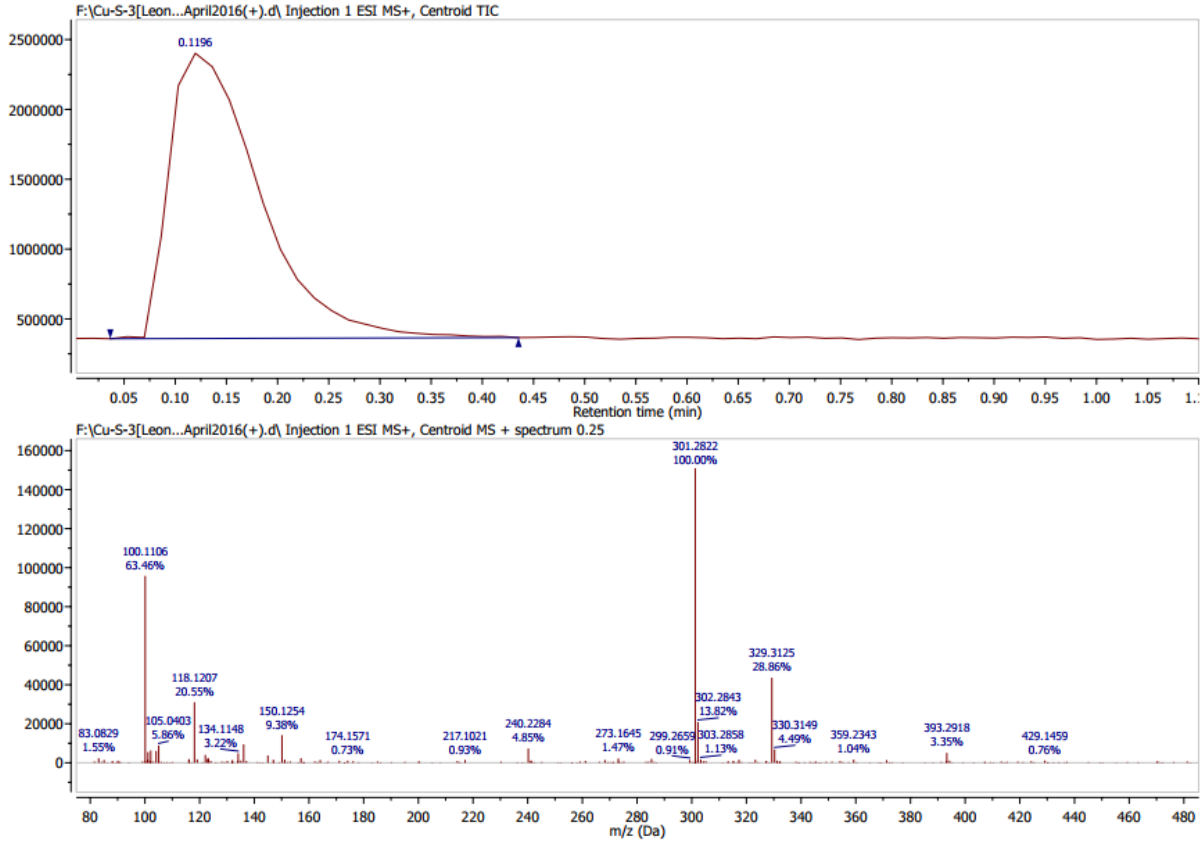

Scanning Mass Spectra of Compound 1a

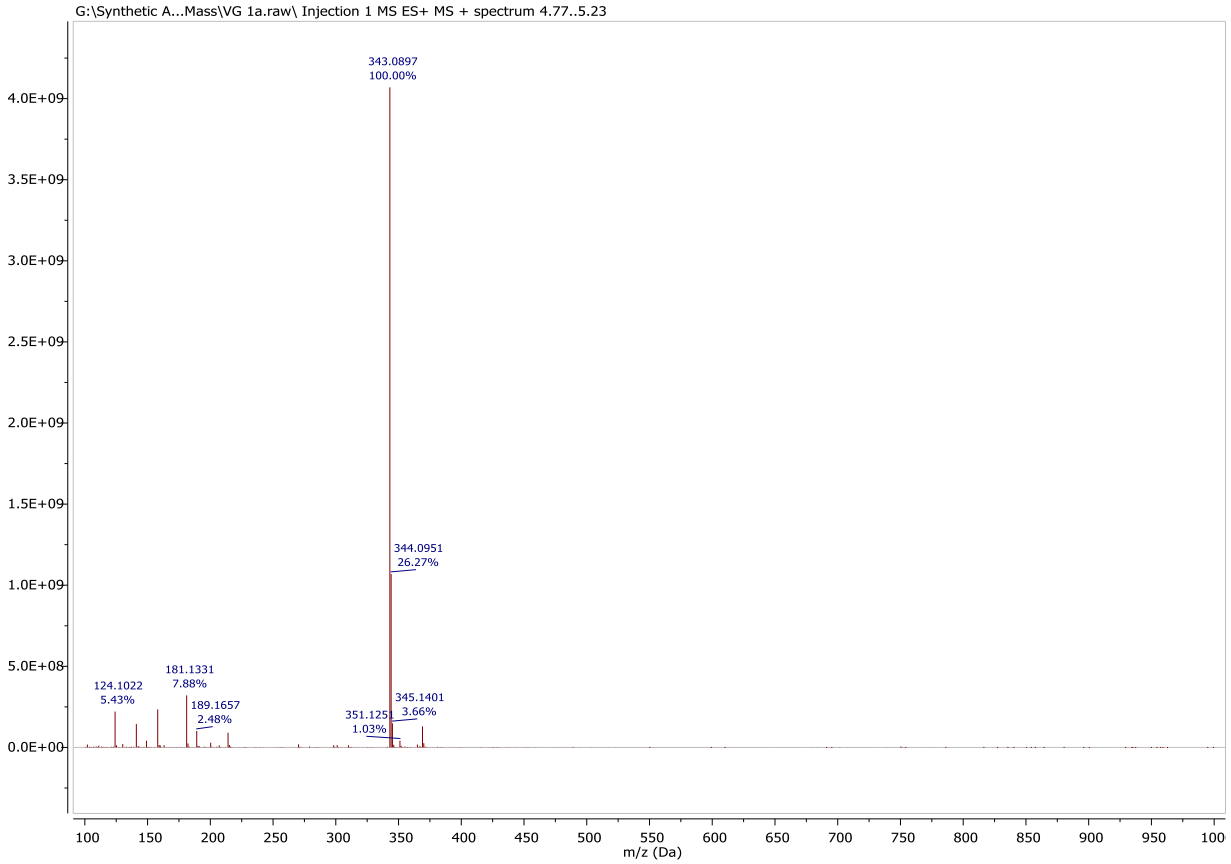

Scanning Mass Spectra of Compound 1b

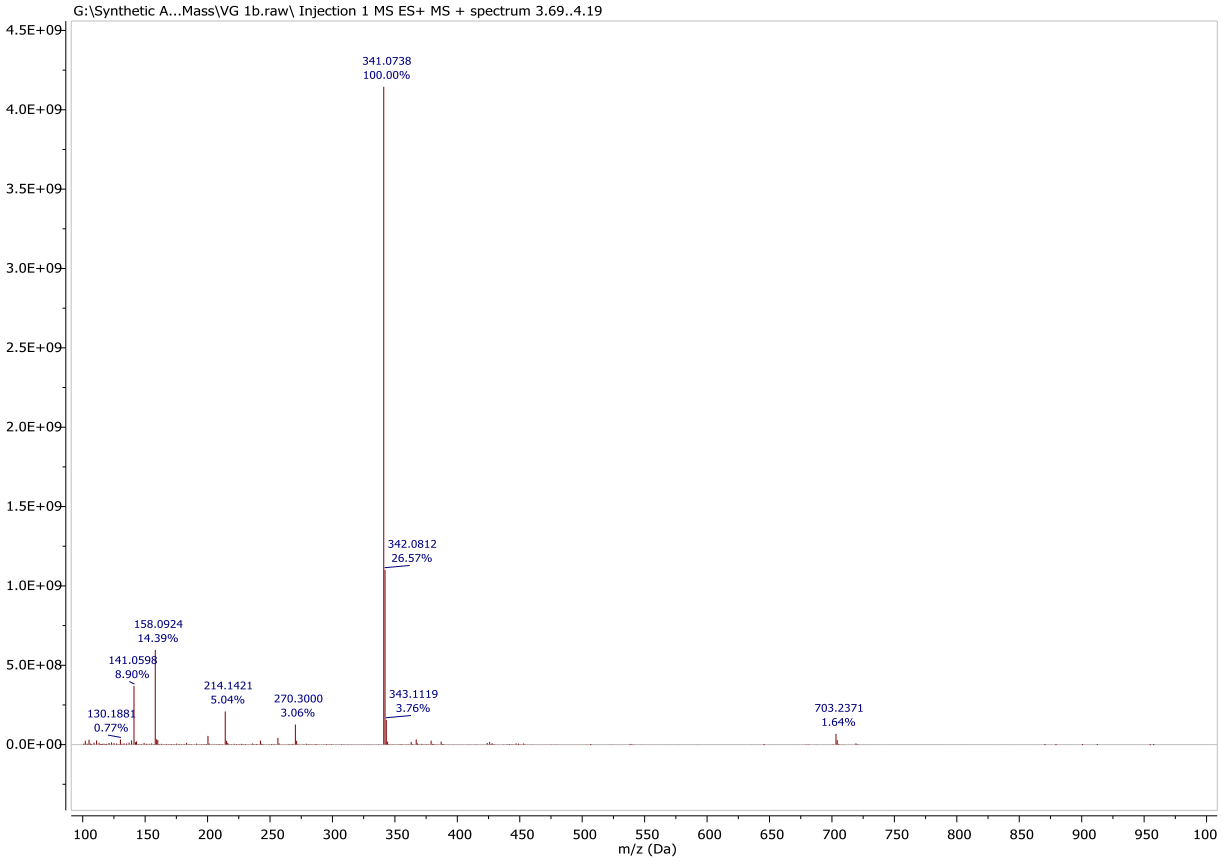

Scanning Mass Spectra of Compound 1c

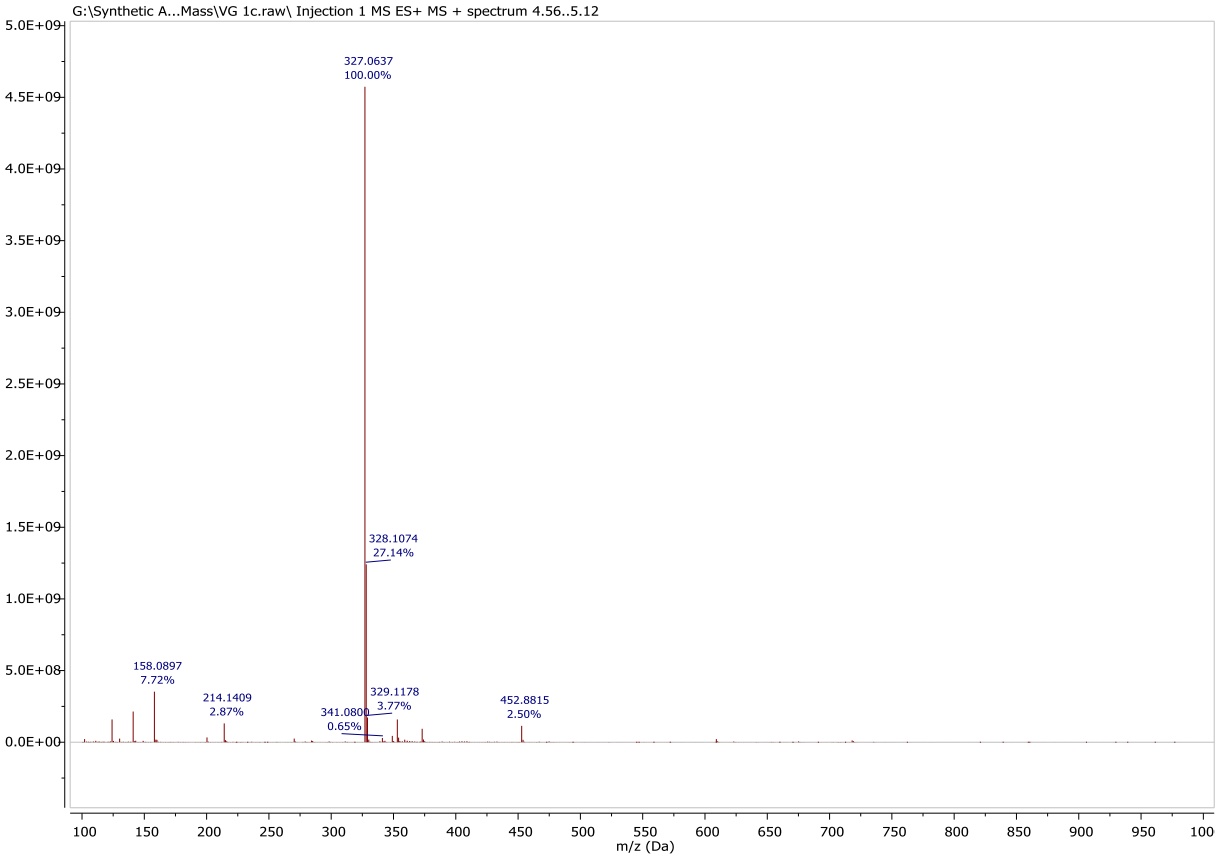

Scanning Mass Spectra of Compound 2a

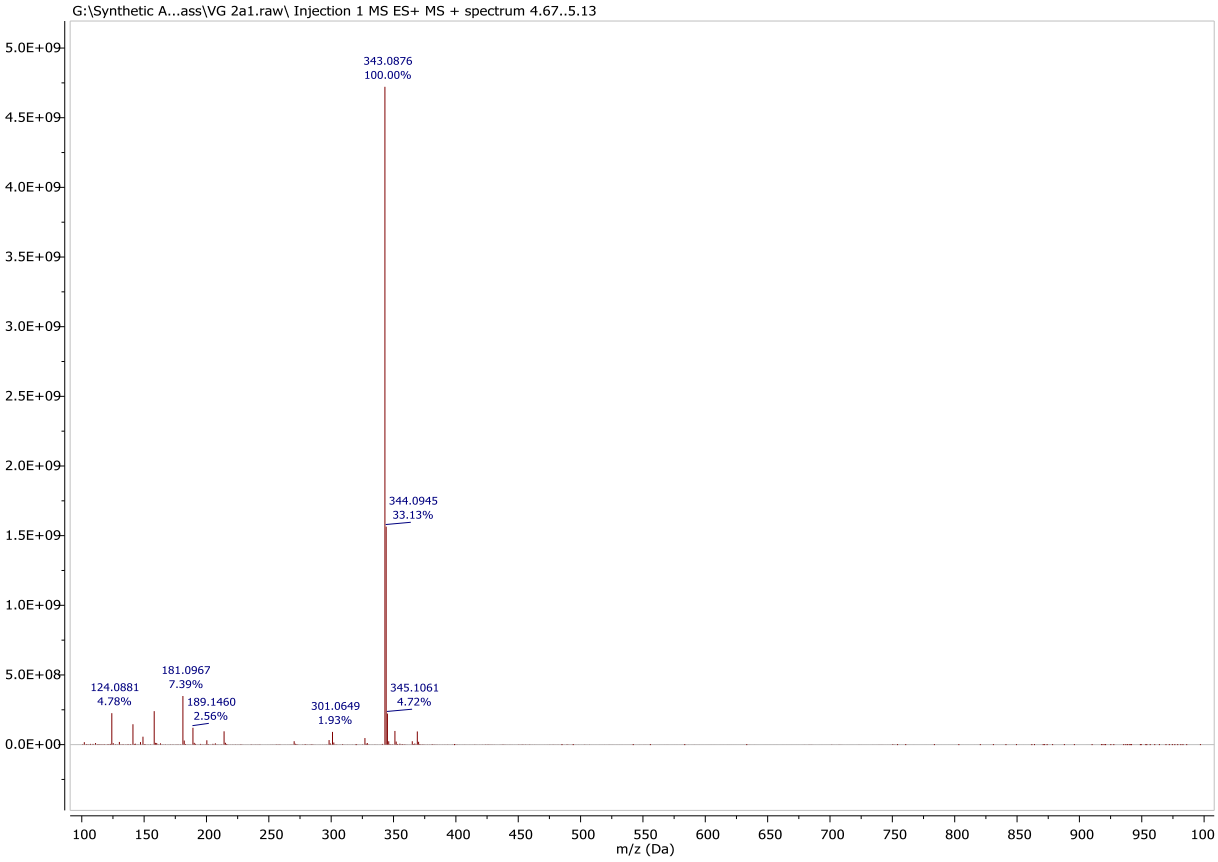

Scanning Mass Spectra of Compound 2b

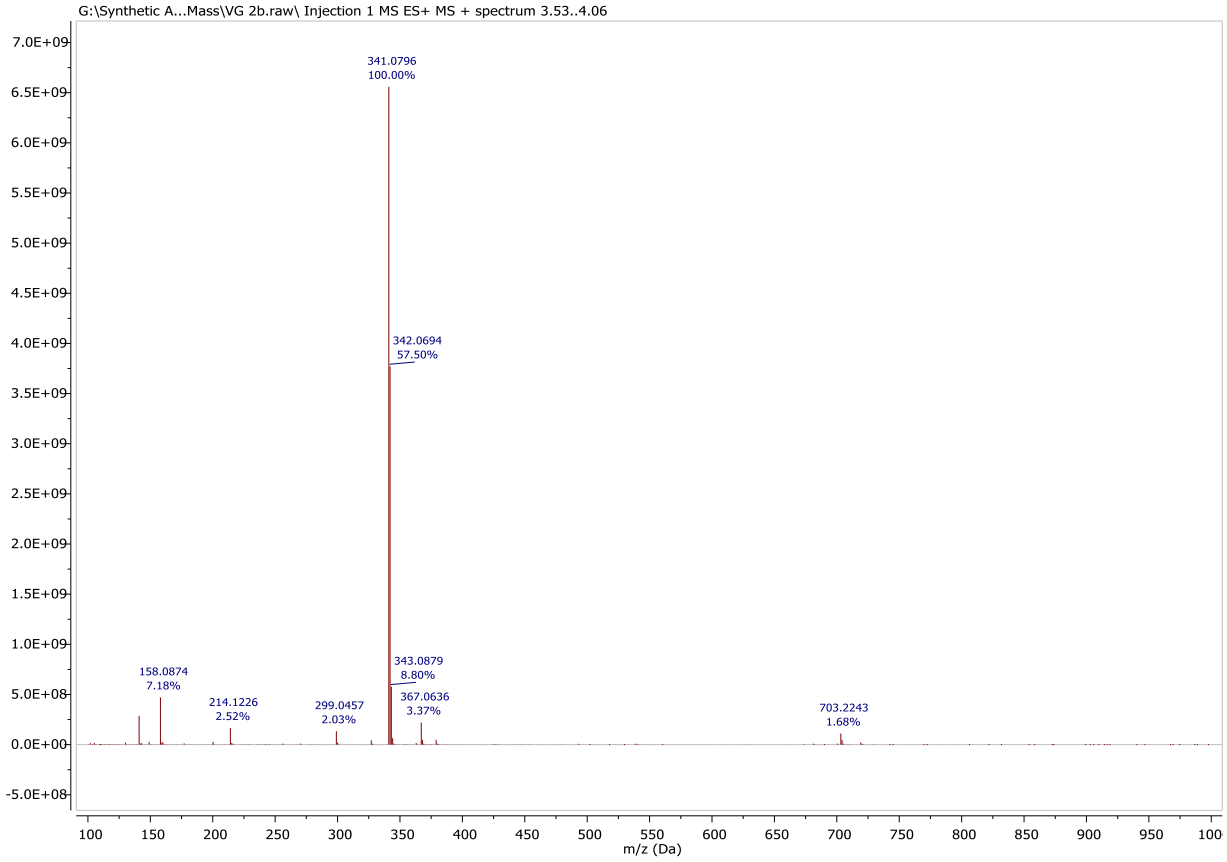

Scanning Mass Spectra of Compound 2c

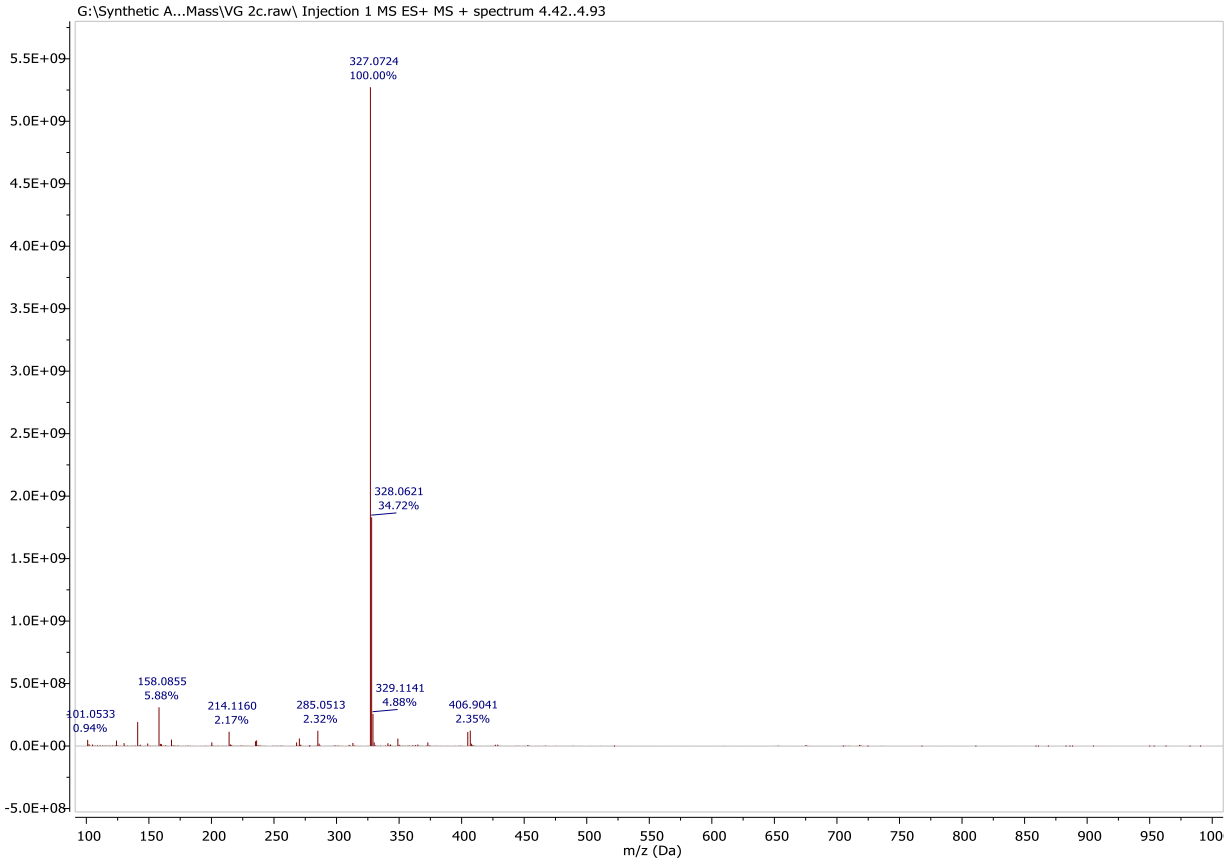

Scanning Mass Spectra of Compound 3a

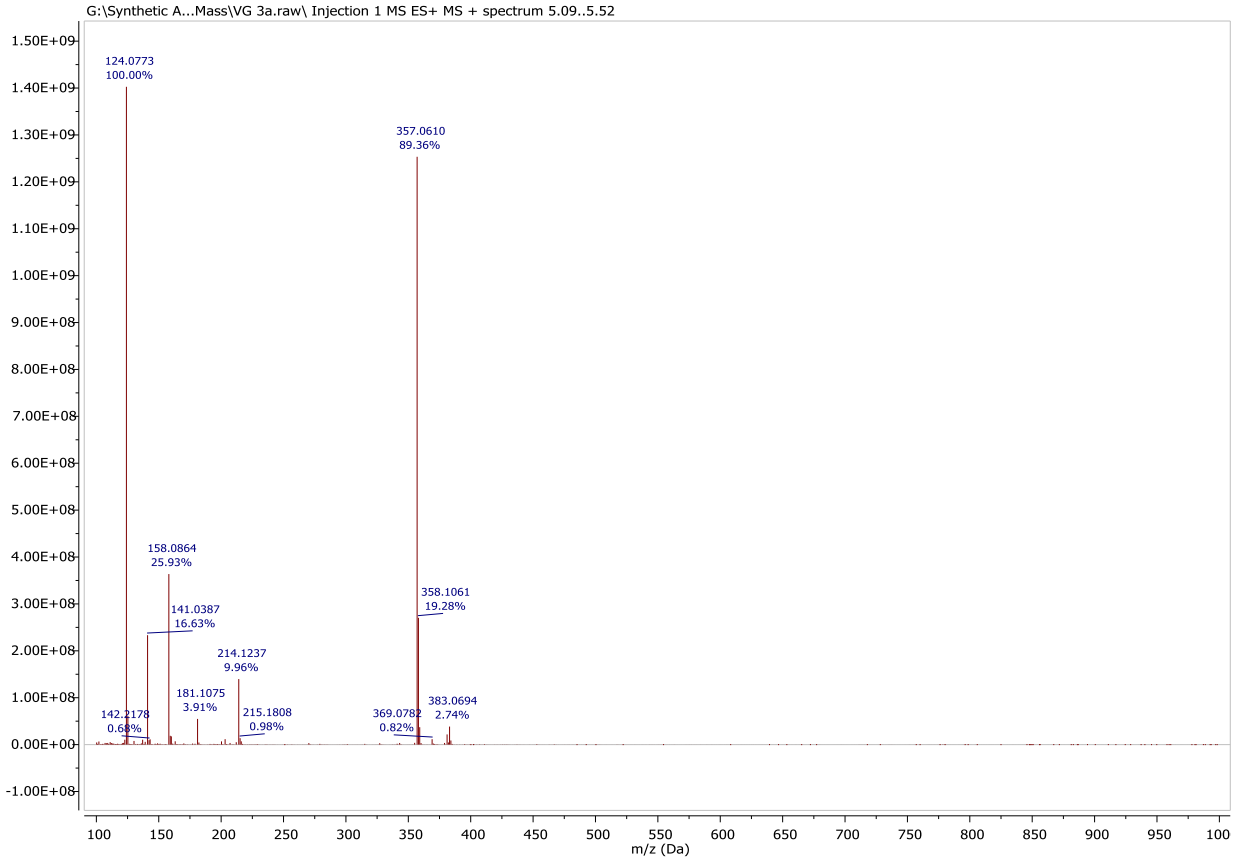

Scanning Mass Spectra of Compound 3b

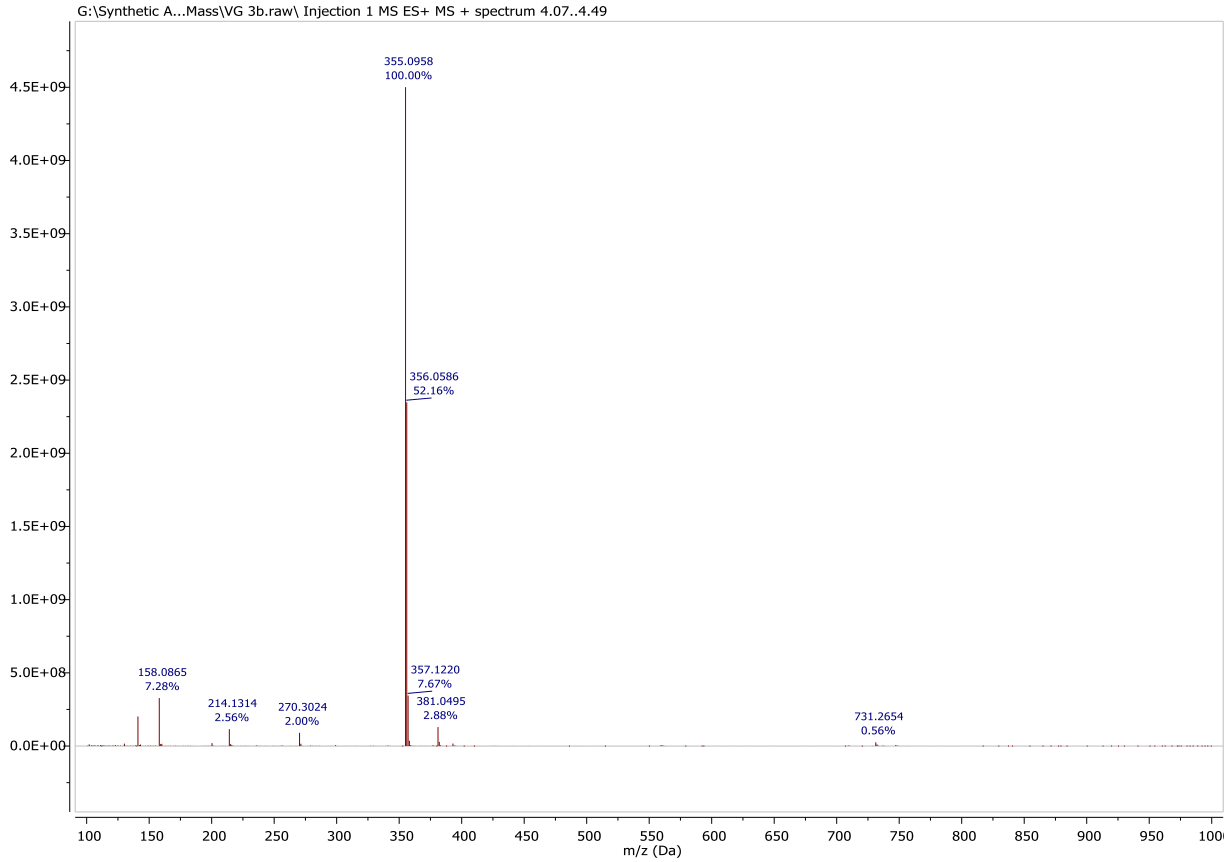

Scanning Mass Spectra of Compound 3c

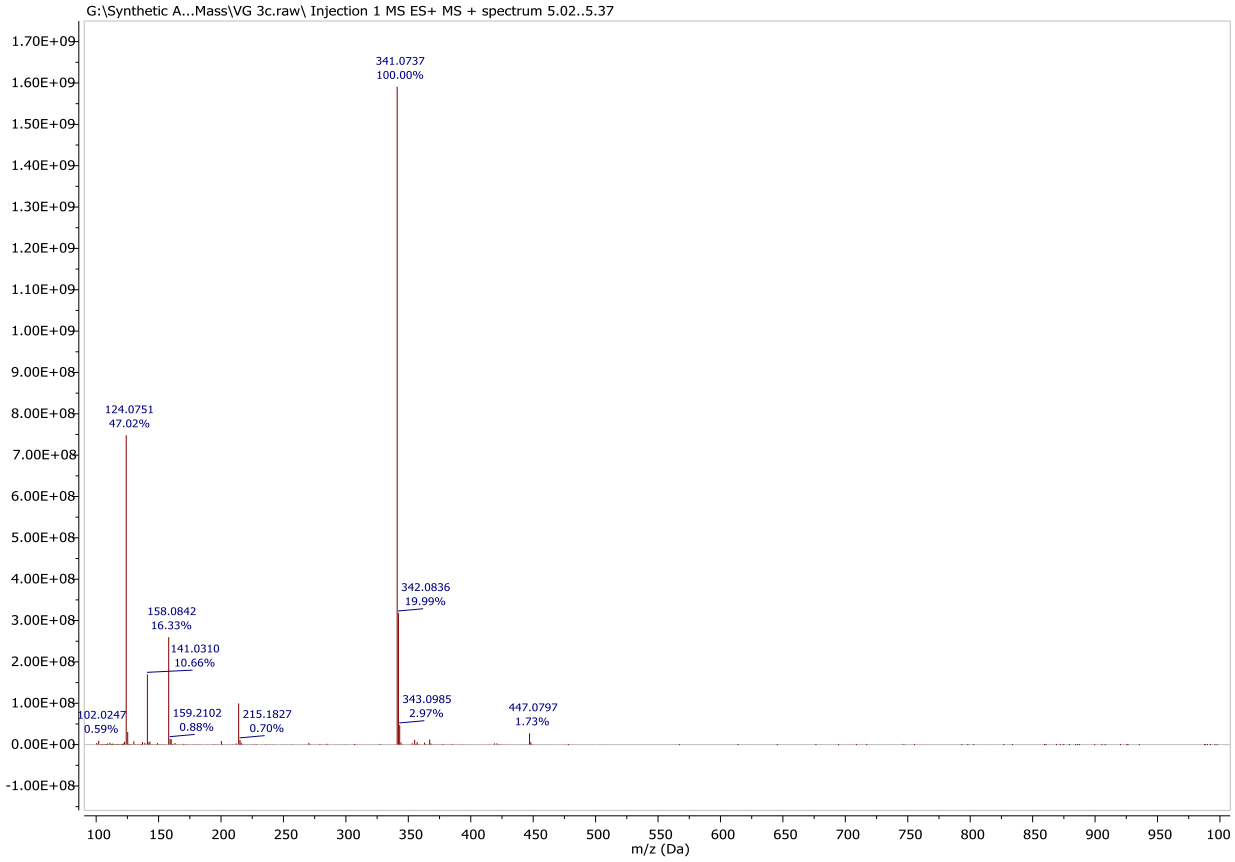

Scanning Mass Spectra of Compound 4a

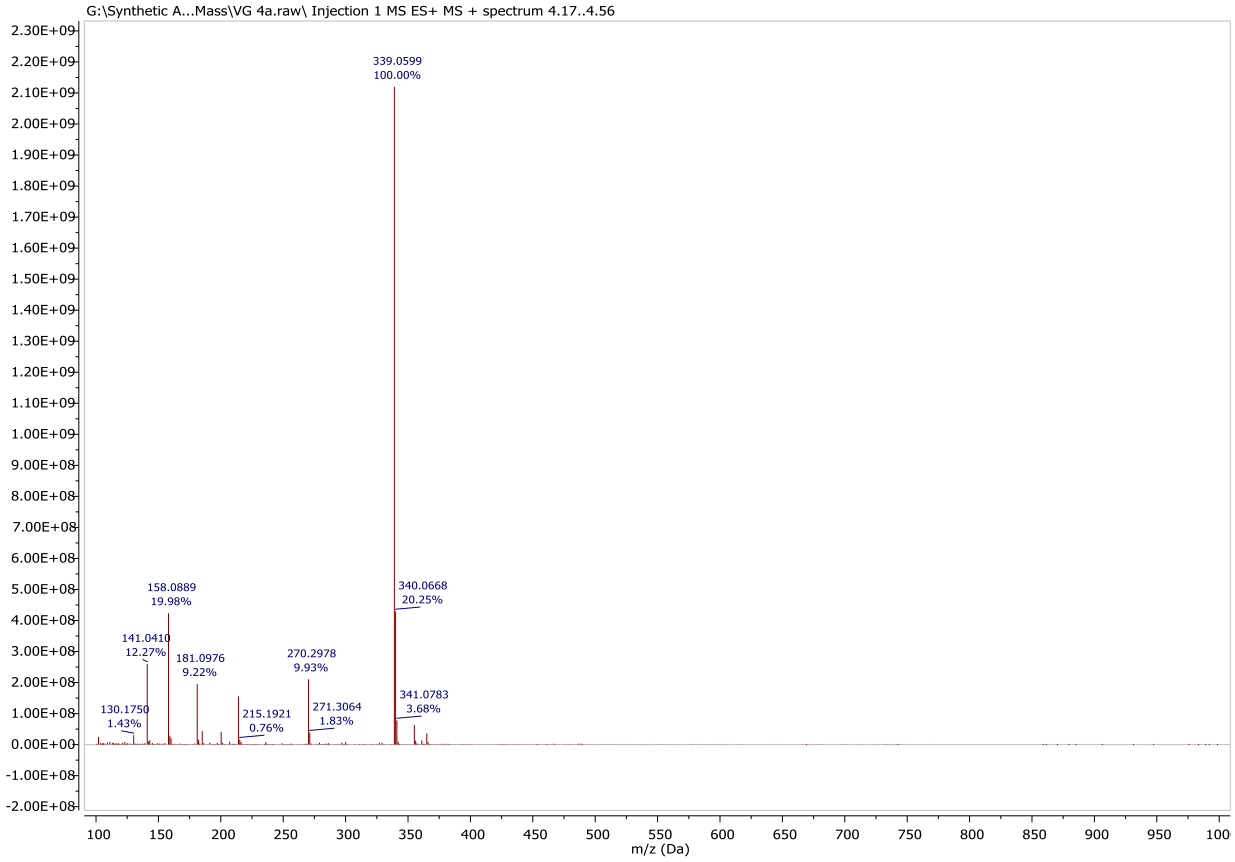

Scanning Mass Spectra of Compound 4b

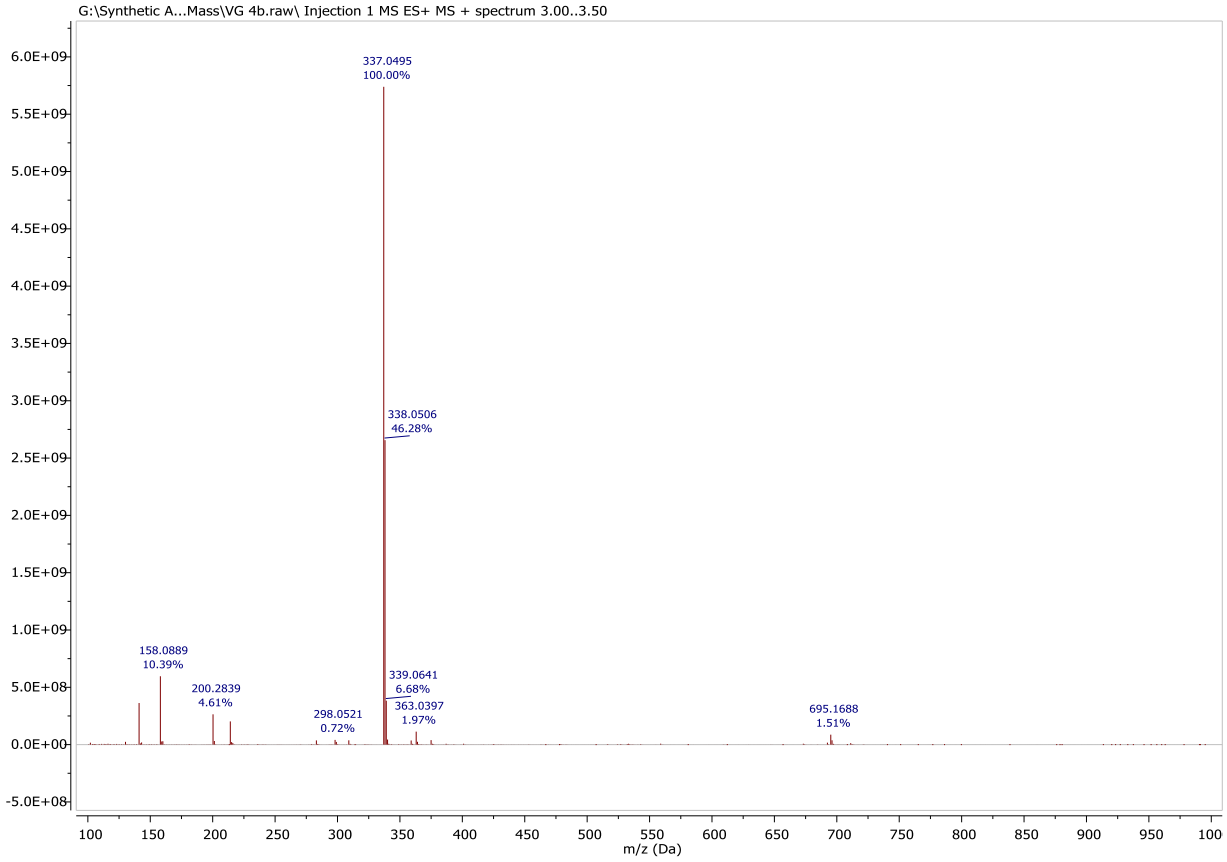

Scanning Mass Spectra of Compound 4c

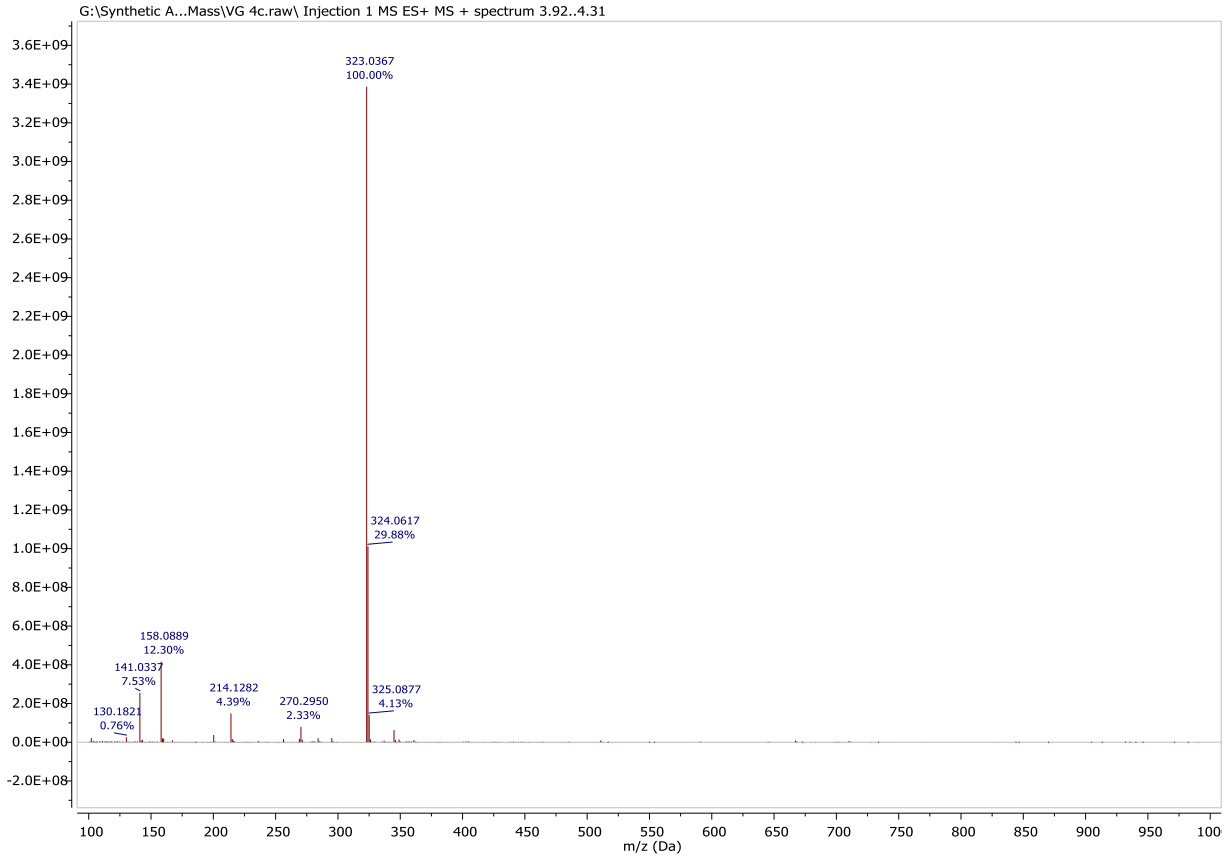

Scanning Mass Spectra of Compound 5a

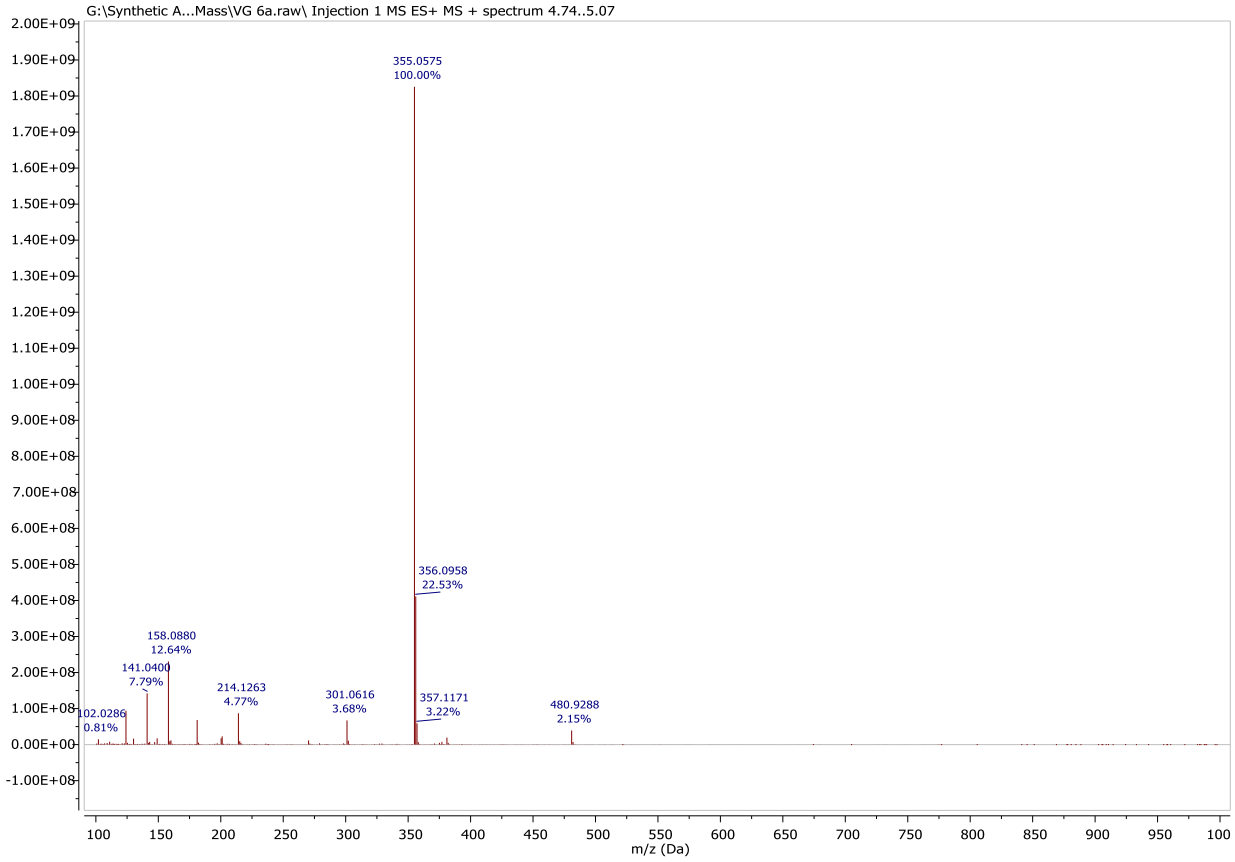

Scanning Mass Spectra of Compound 5b

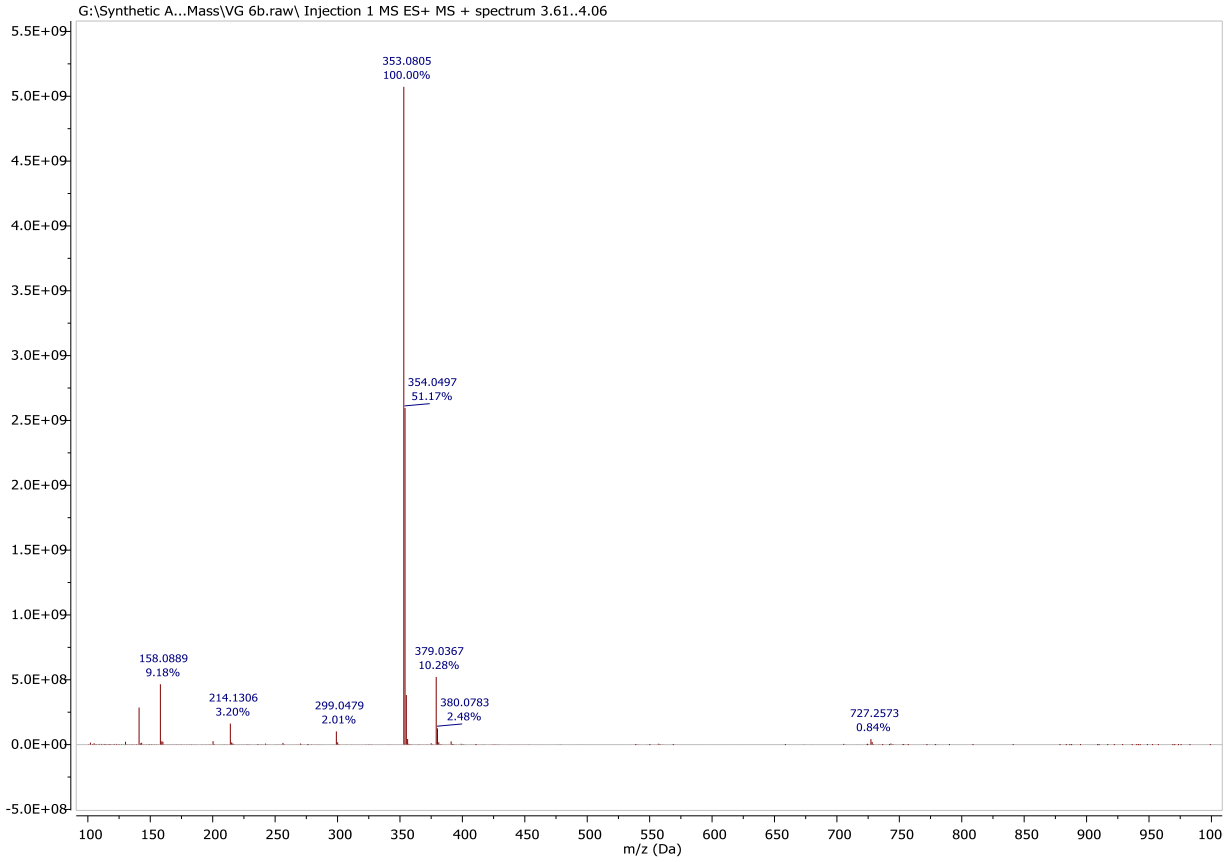

Scanning Mass Spectra of Compound 6a

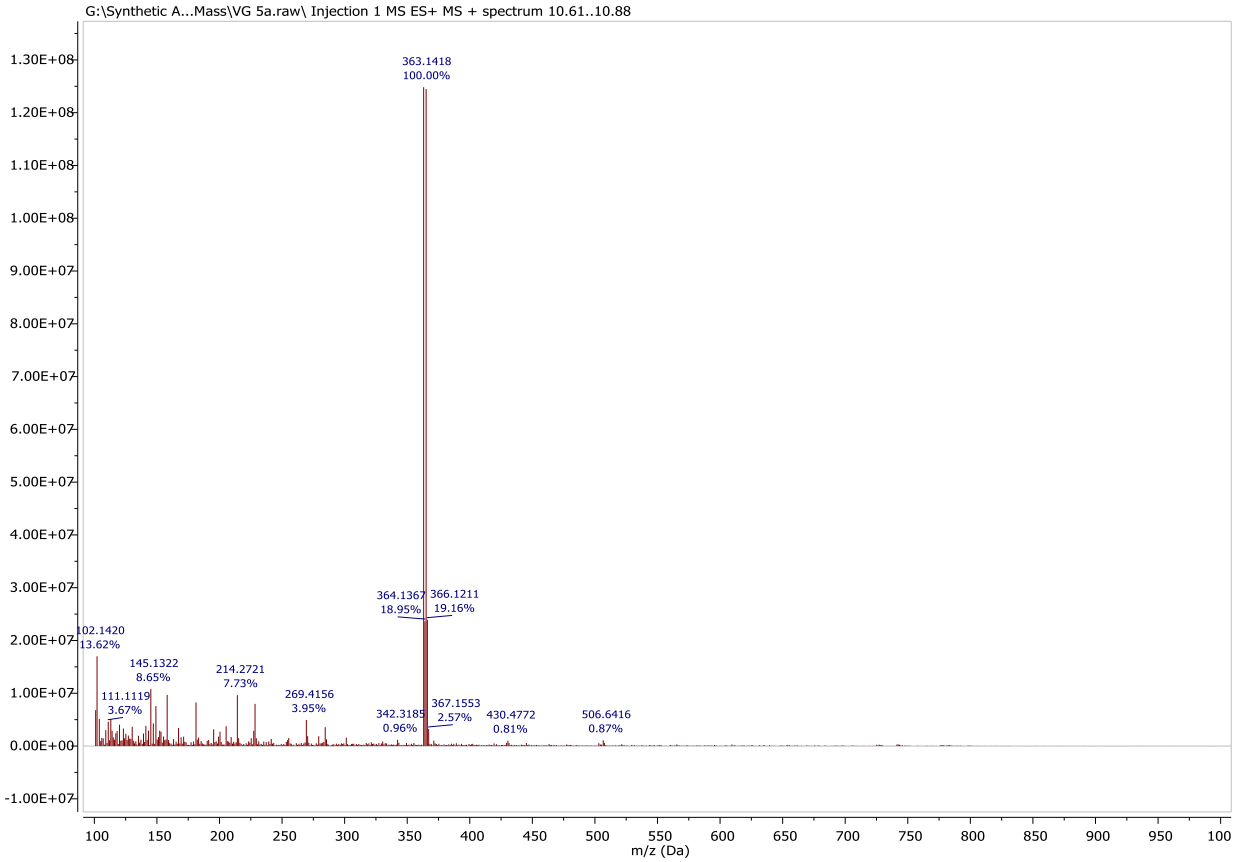

Scanning Mass Spectra of Compound 6b

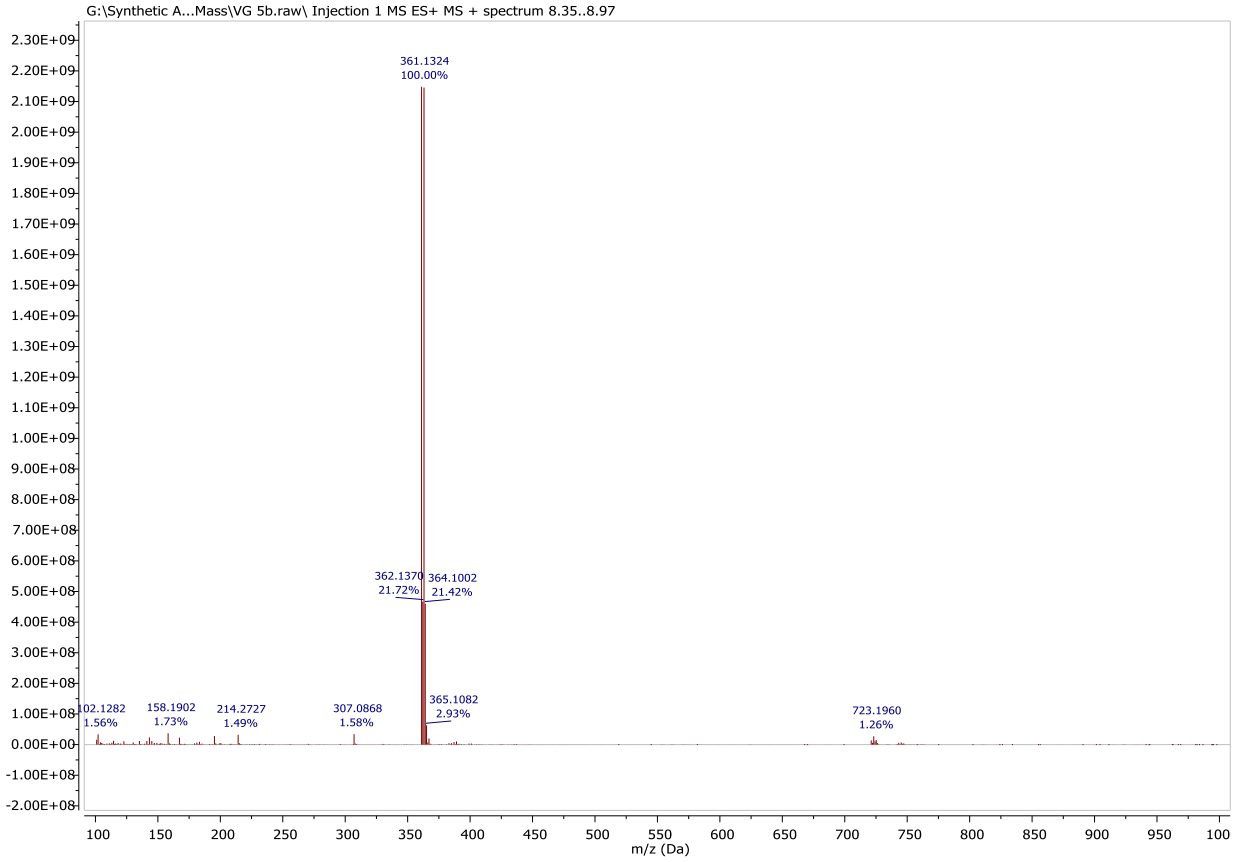

Scanning Mass Spectra of Compound 6c

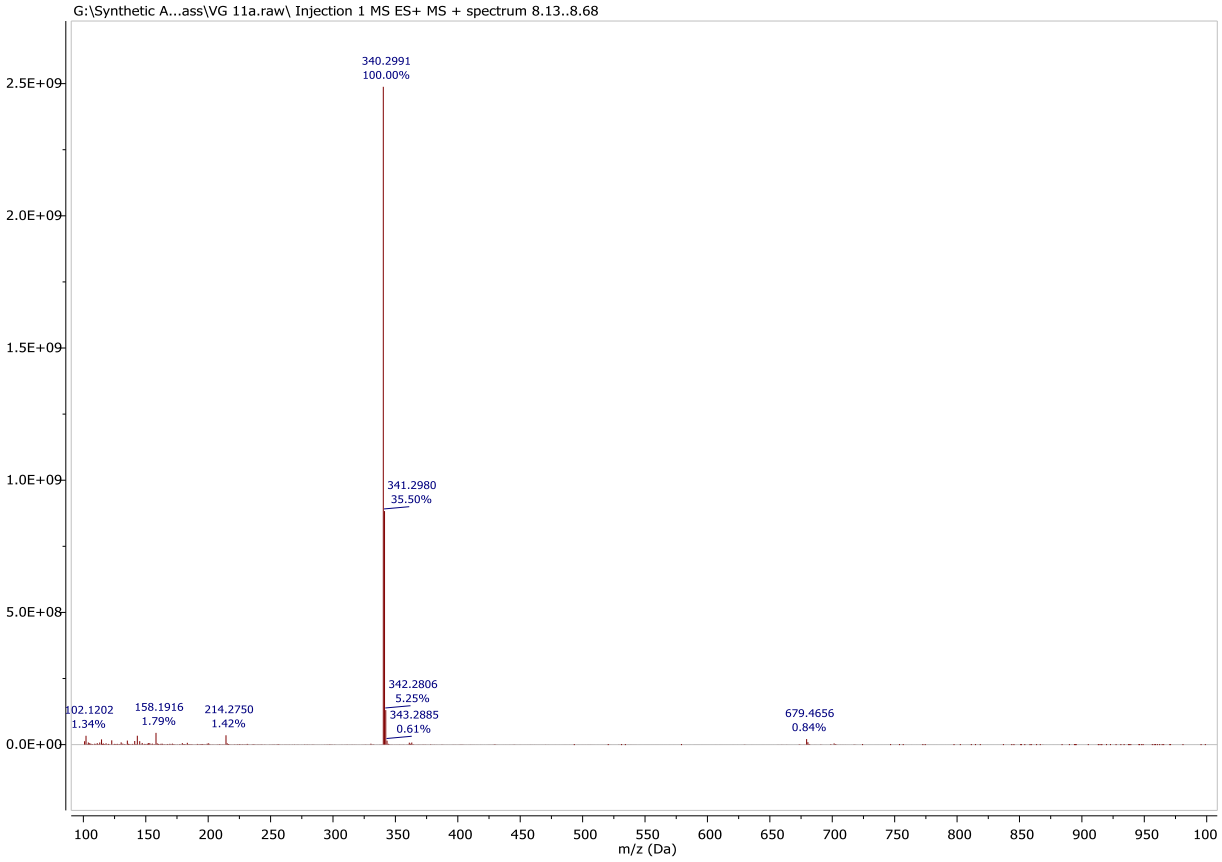

Scanning Mass Spectra of Compound 6d

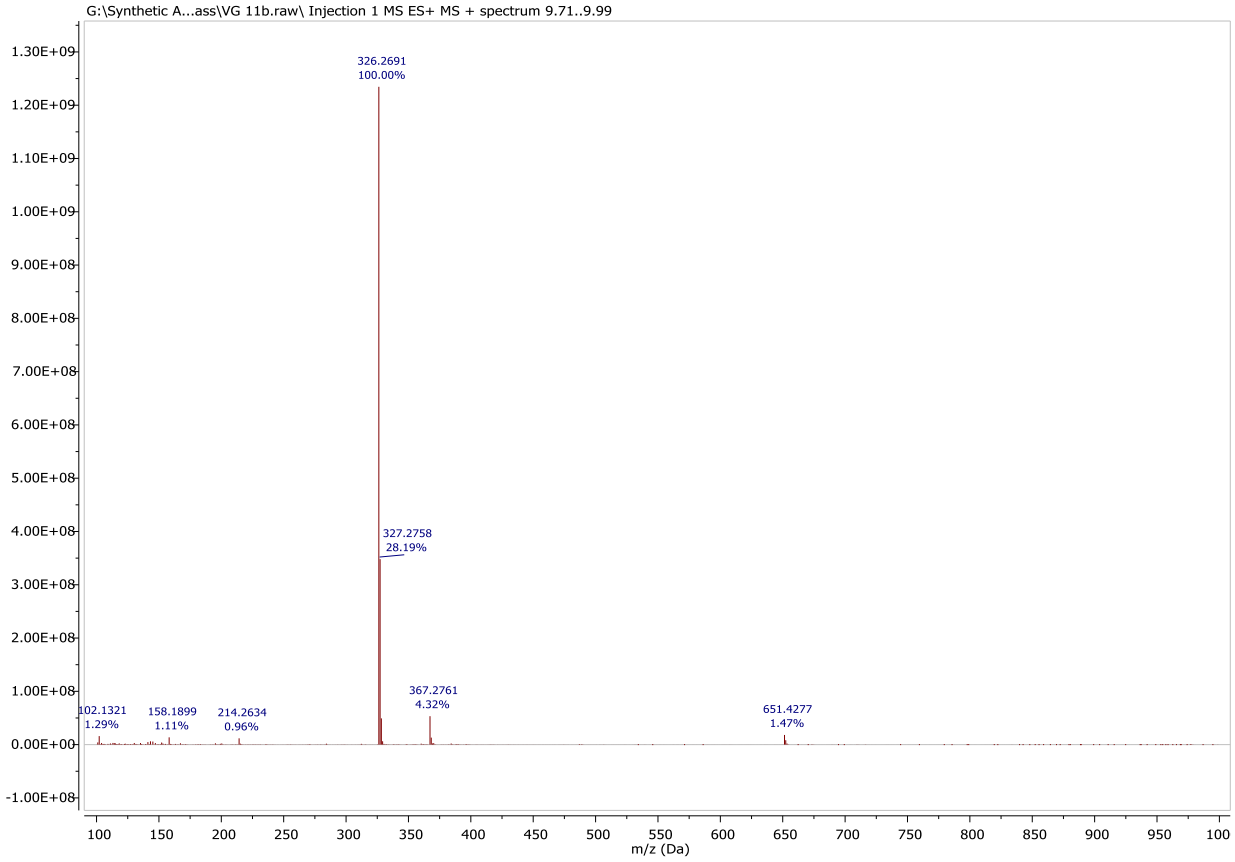

Scanning Mass Spectra of Compound 7c

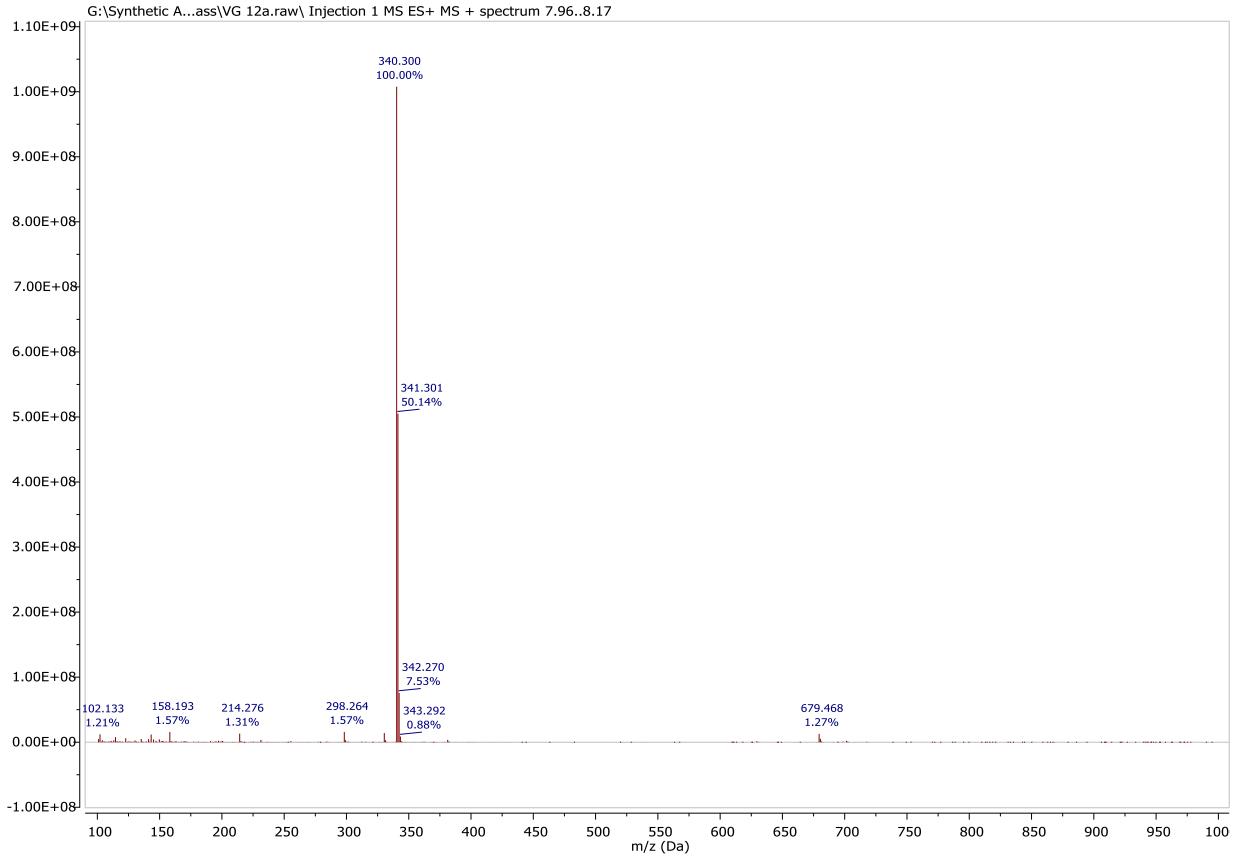

Scanning Mass Spectra of Compound 7d

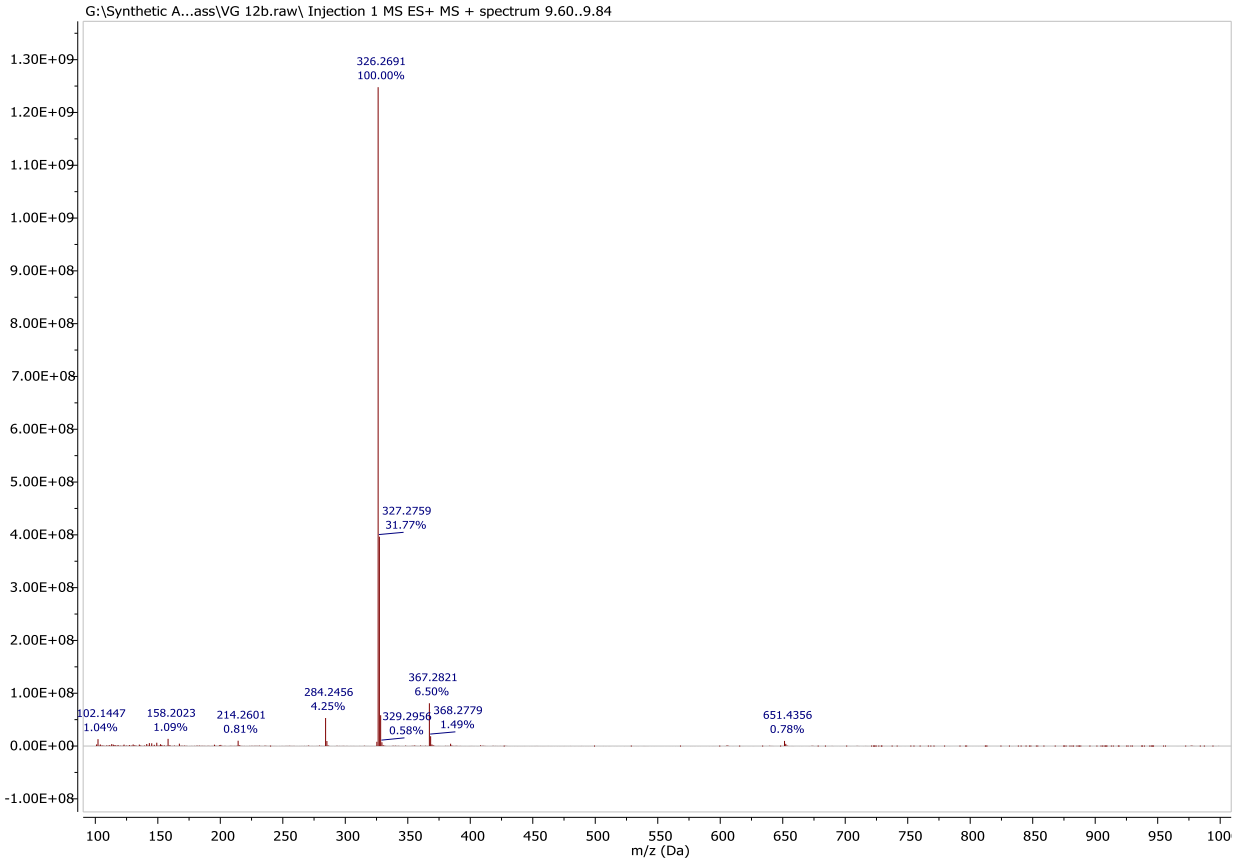

Scanning Mass Spectra of Compound 9c

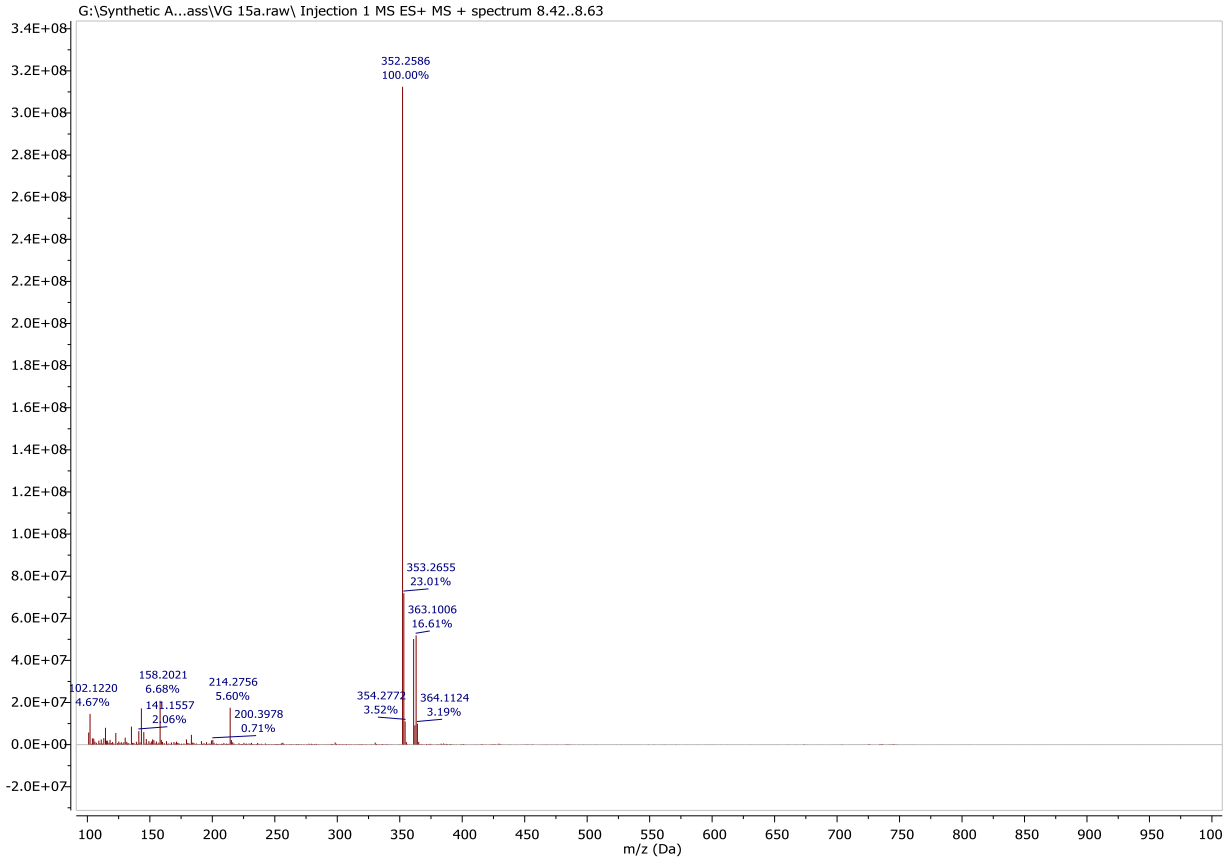

Scanning Mass Spectra of Compound 9d

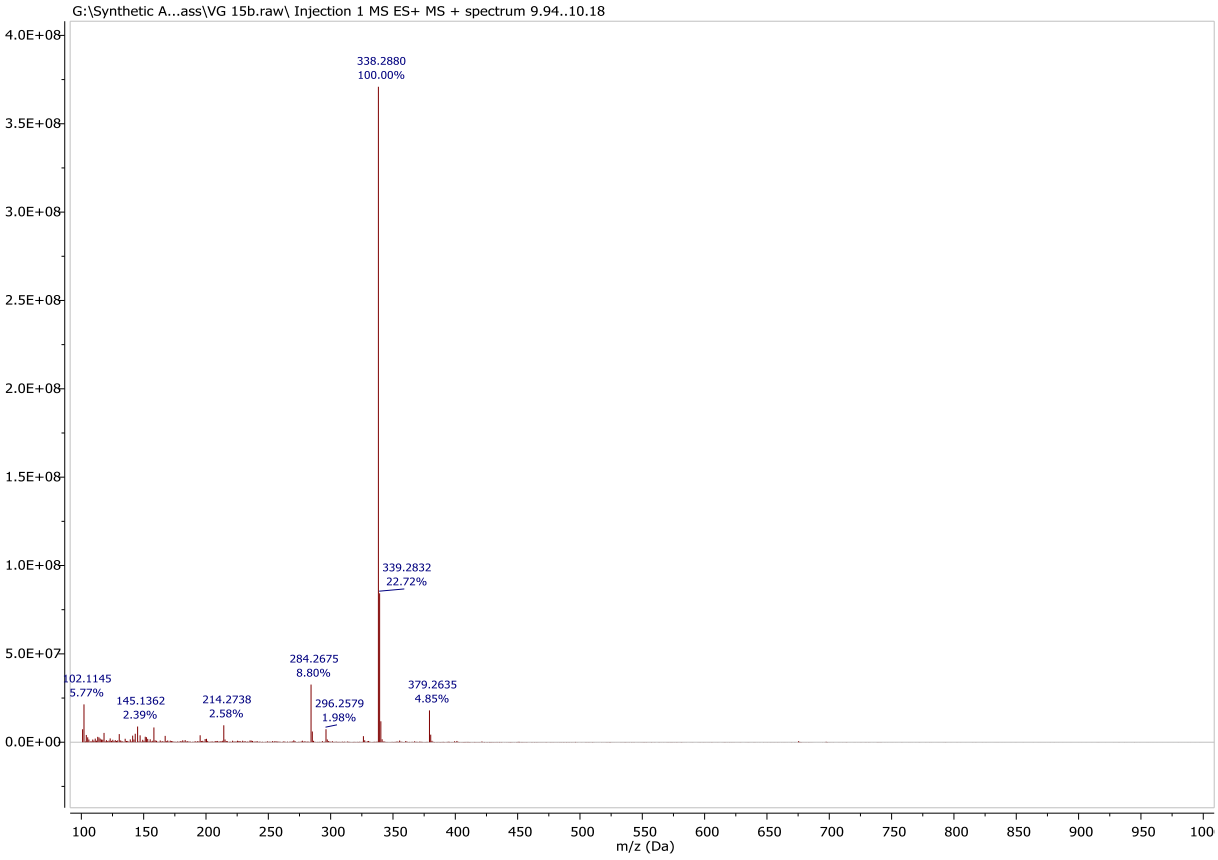

Scanning Mass Spectra of Compound 10a

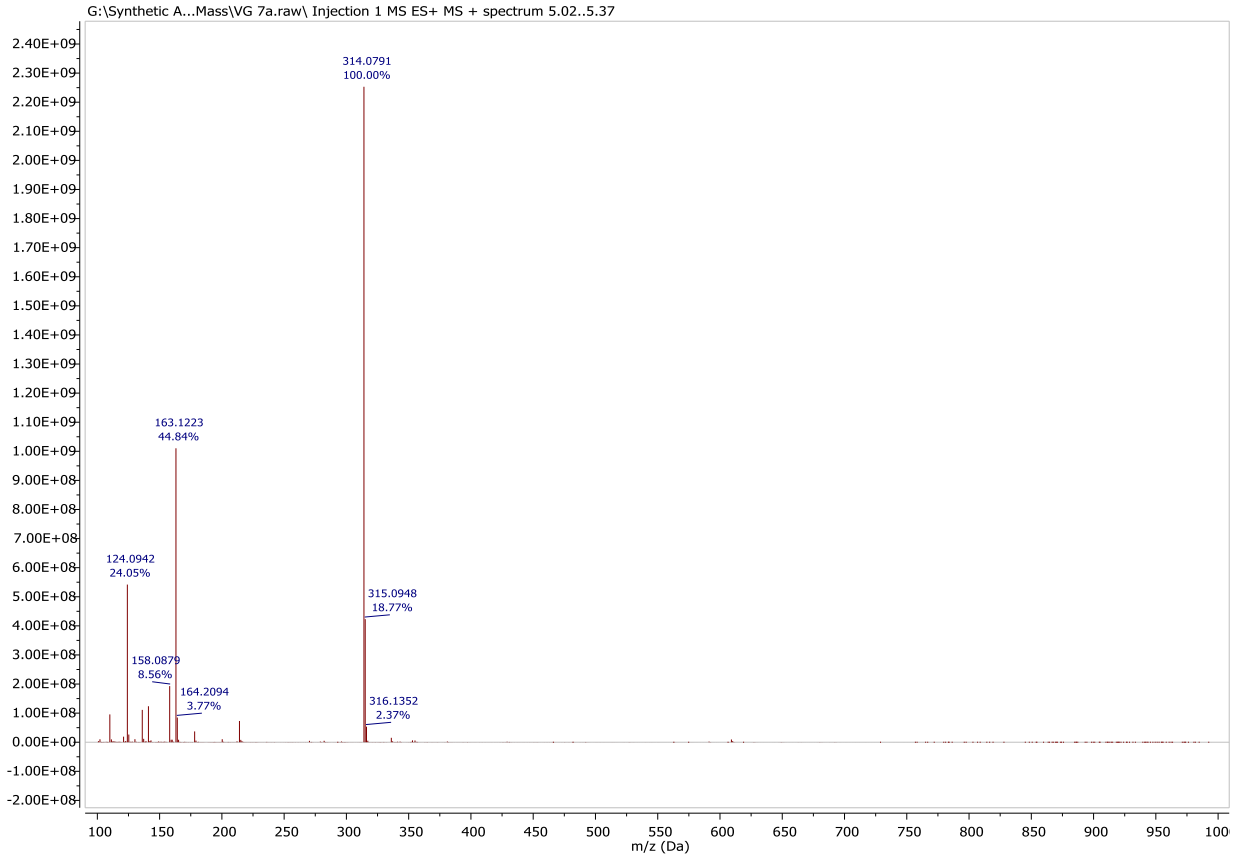

Scanning Mass Spectra of Compound 10b

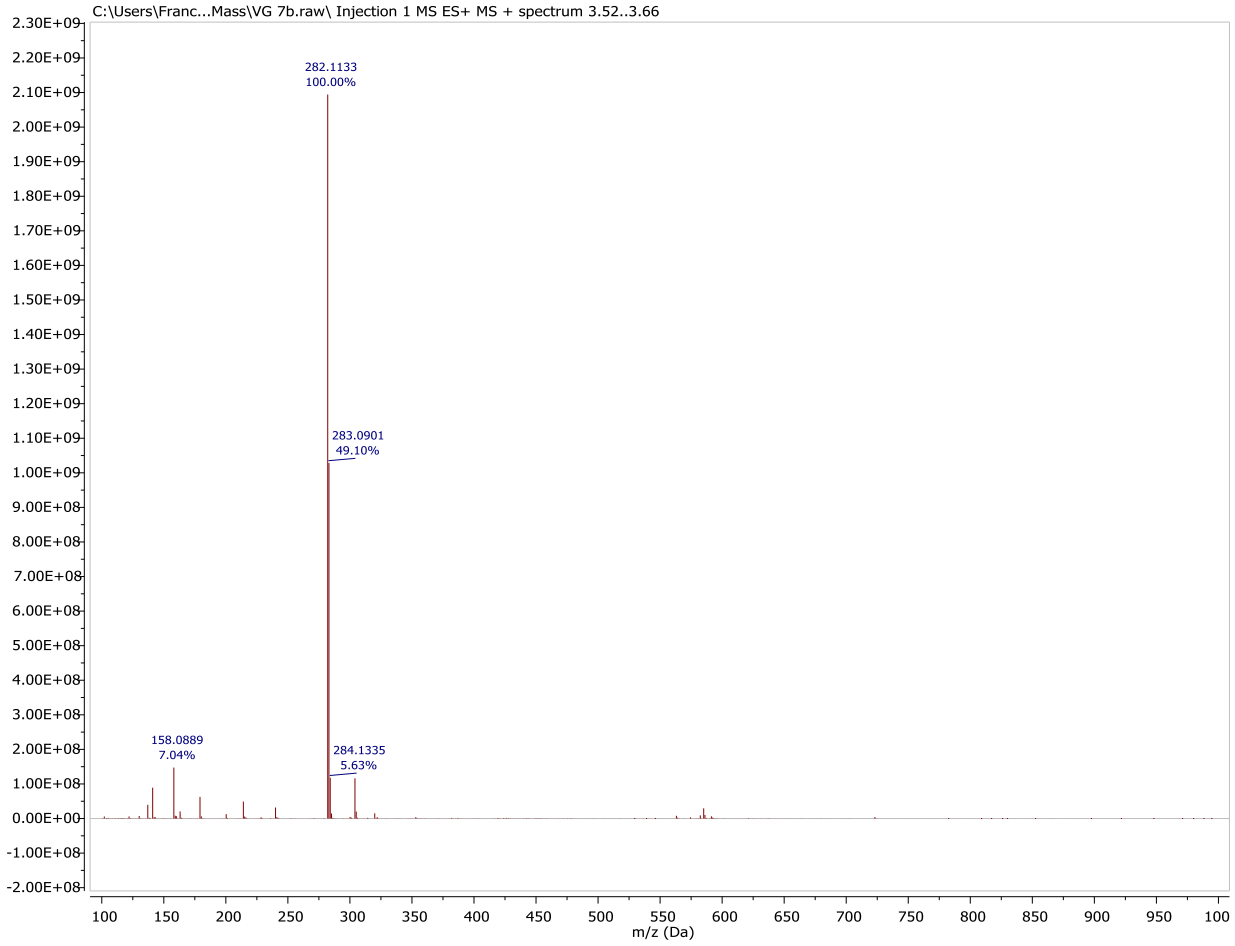

Scanning Mass Spectra of Compound 11a

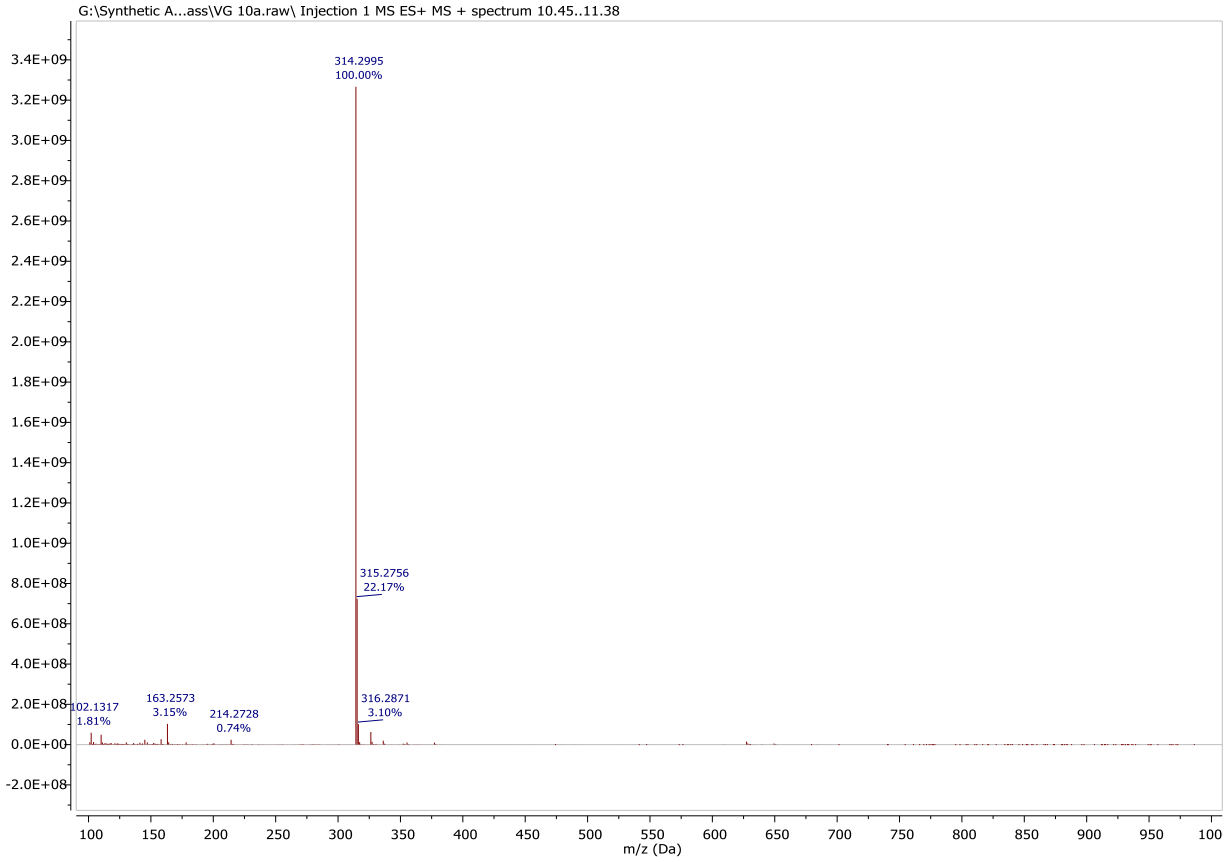

Scanning Mass Spectra of Compound 11b

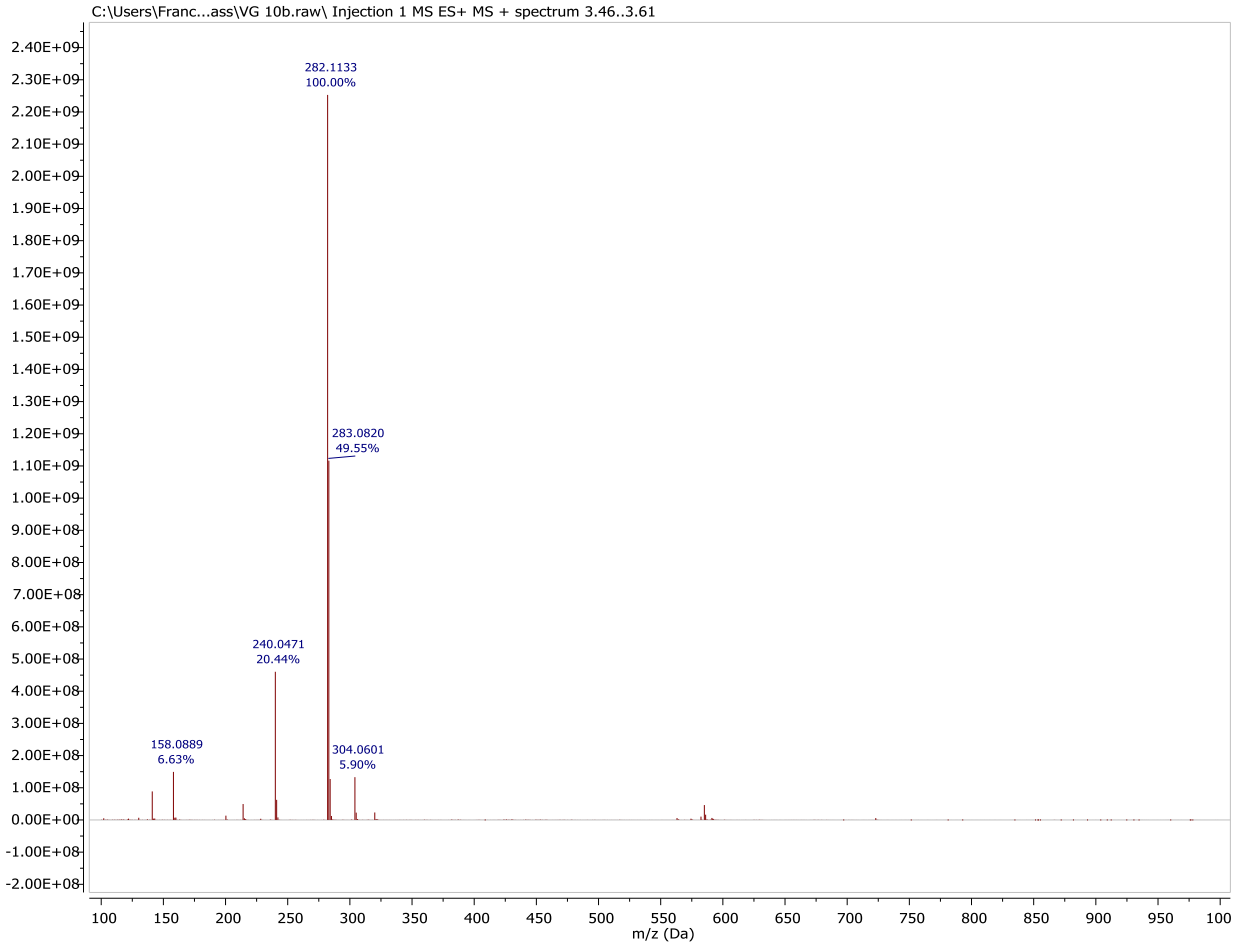

Scanning Mass Spectra of Compound 12a

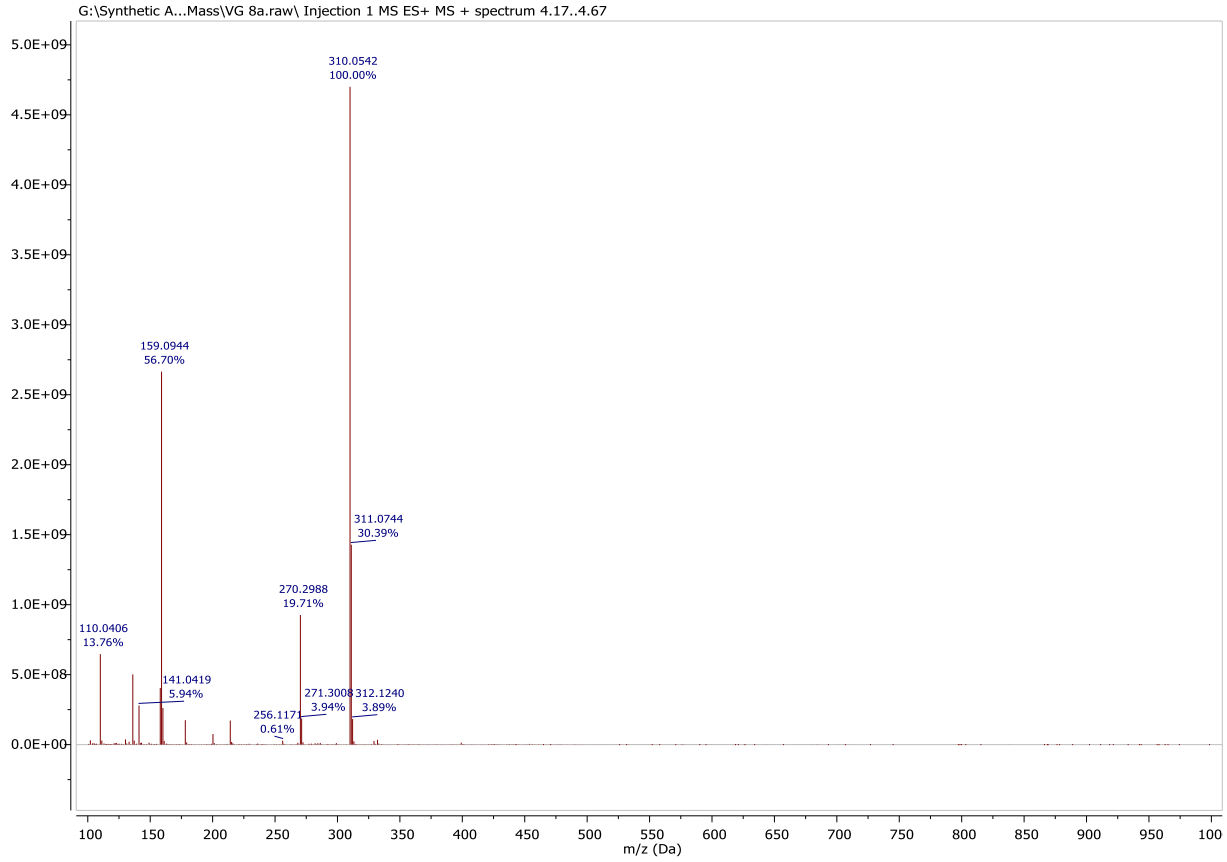

Scanning Mass Spectra of Compound VIII

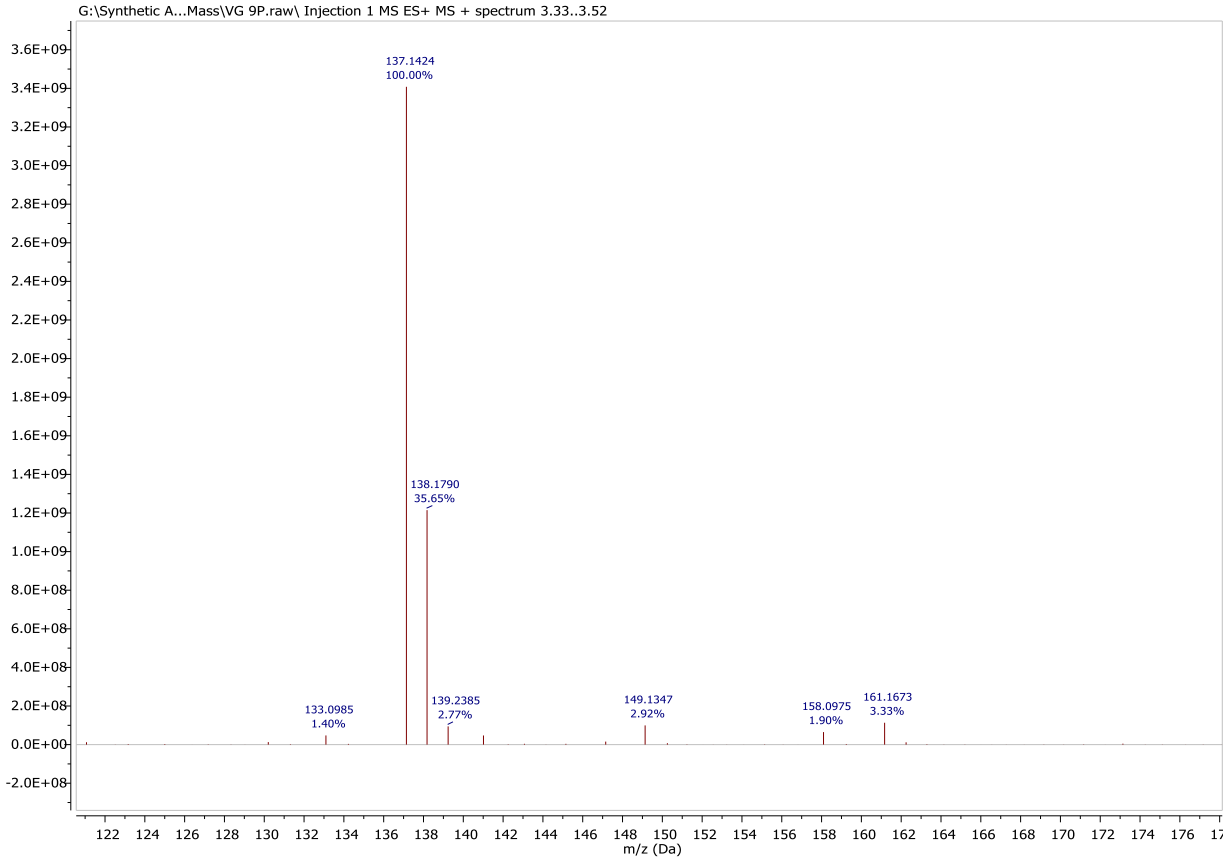

Scanning Mass Spectra of Compound 13a

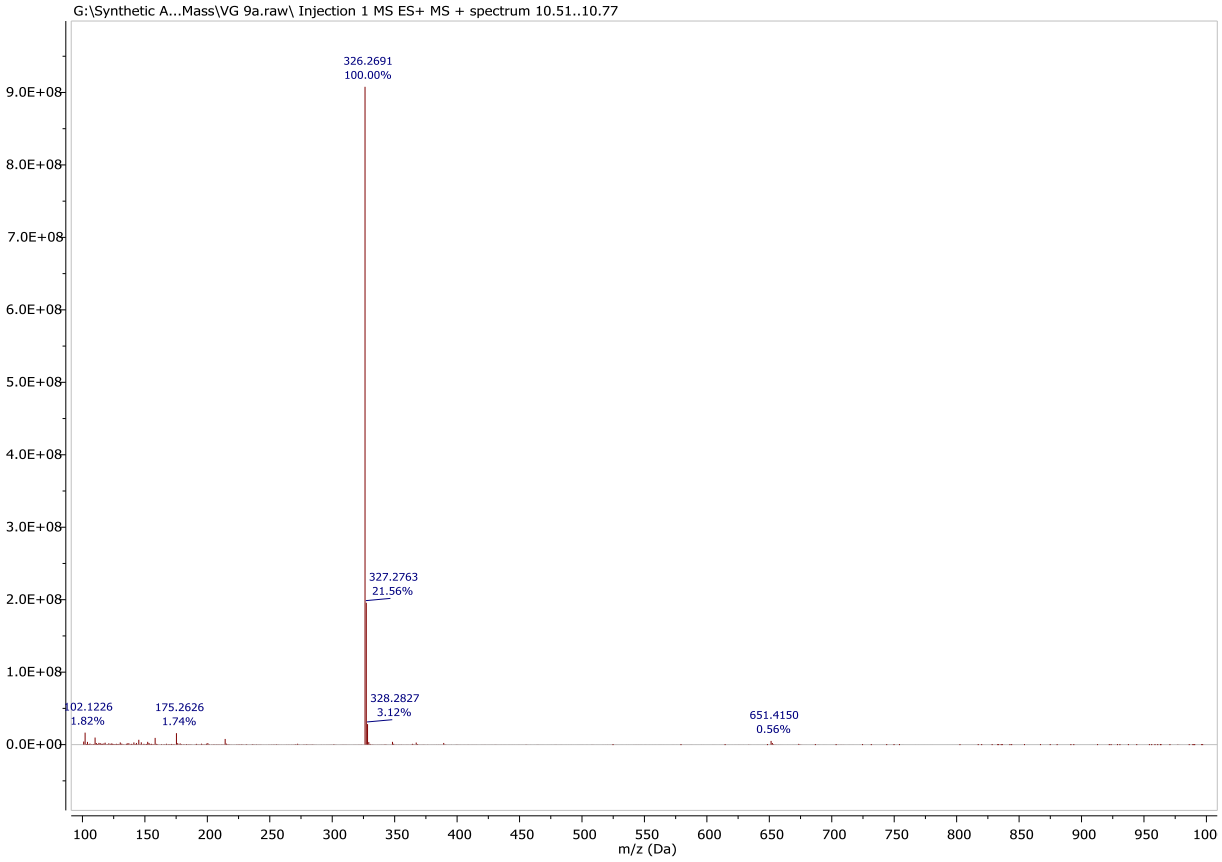

Scanning Mass Spectra of Compound 13b

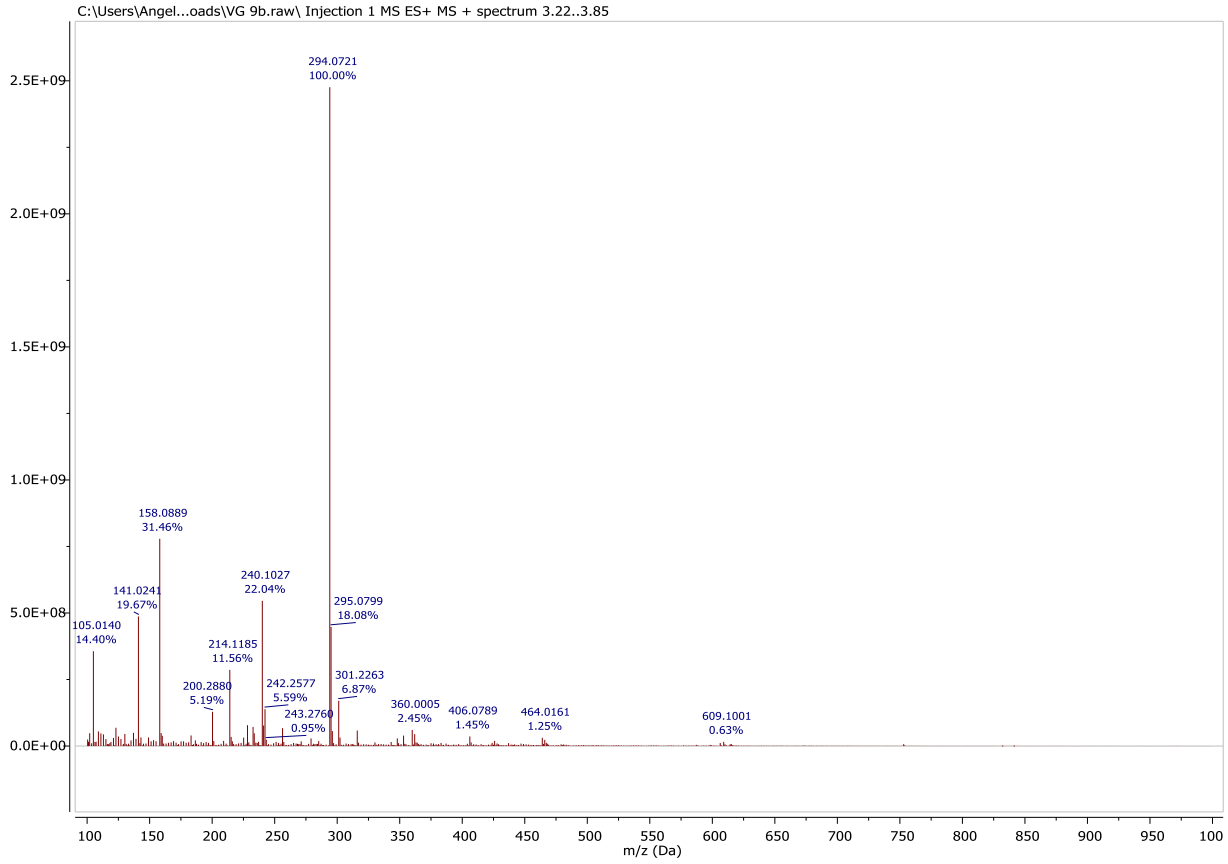

Scanning Mass Spectra of Compound 14a

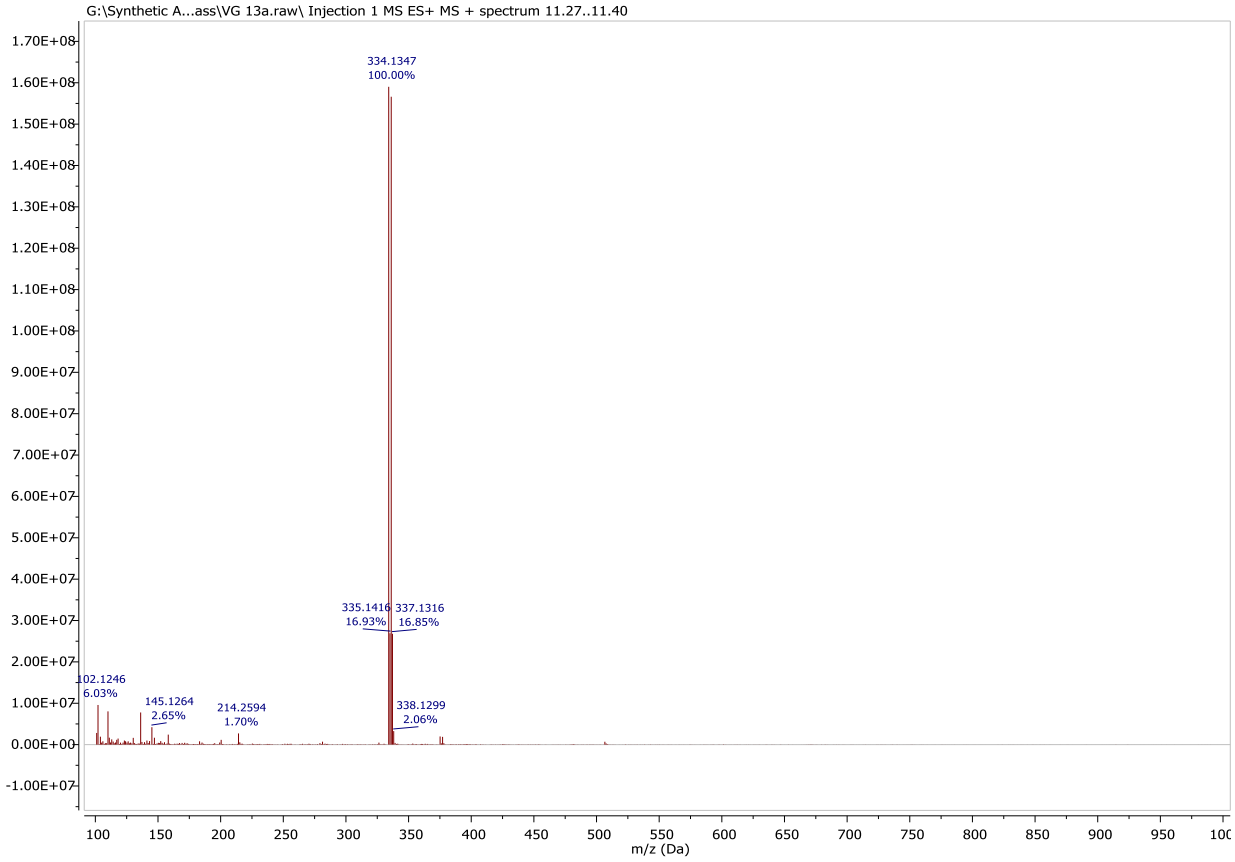

Scanning Mass Spectra of Compound 14b

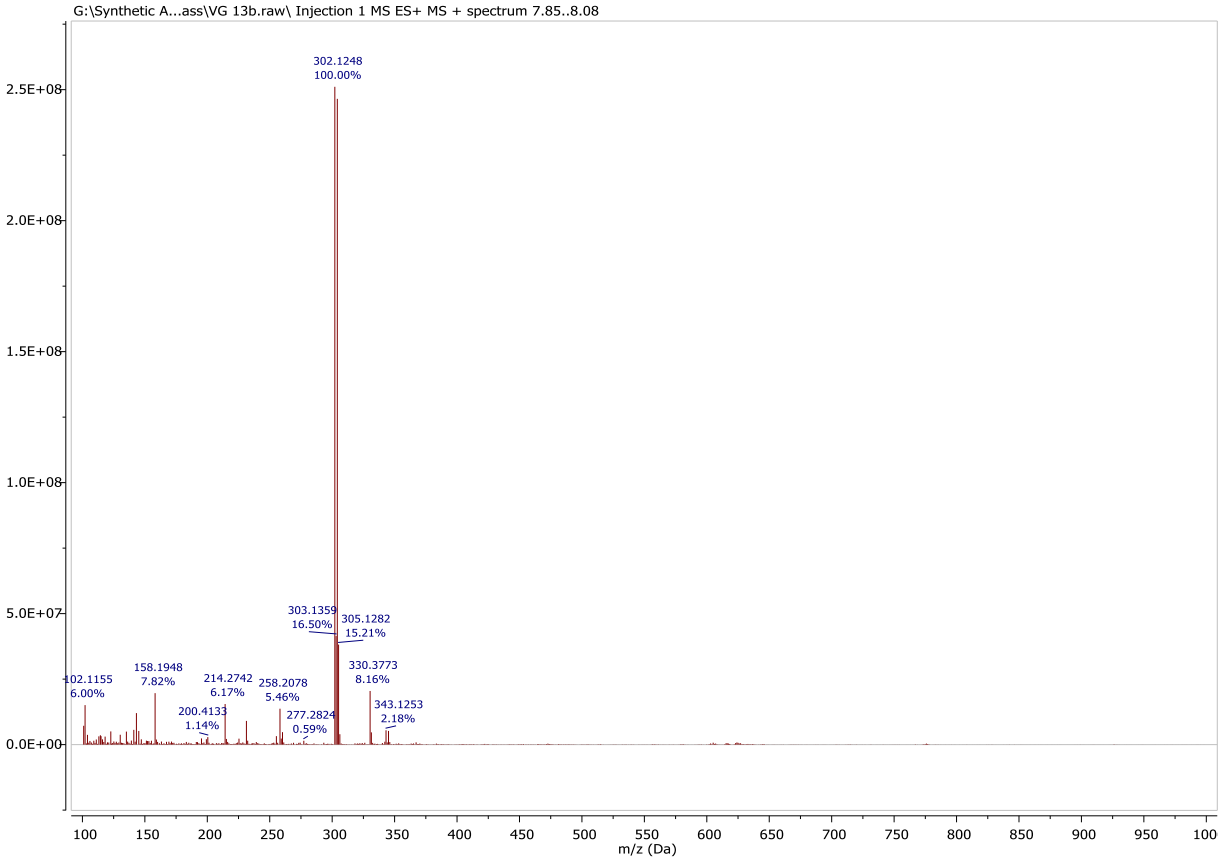

Scanning Mass Spectra of Compound 14c

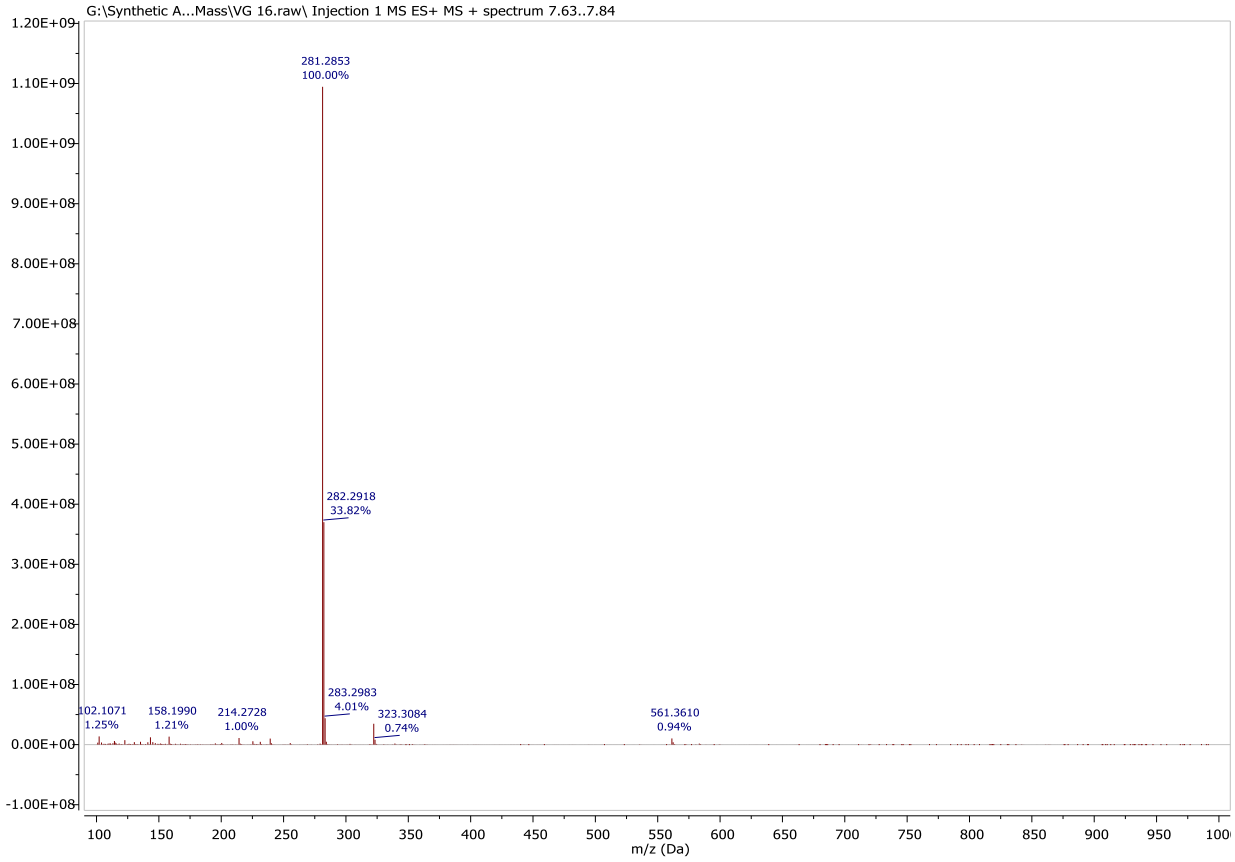

Scanning Mass Spectra of Compound 15c

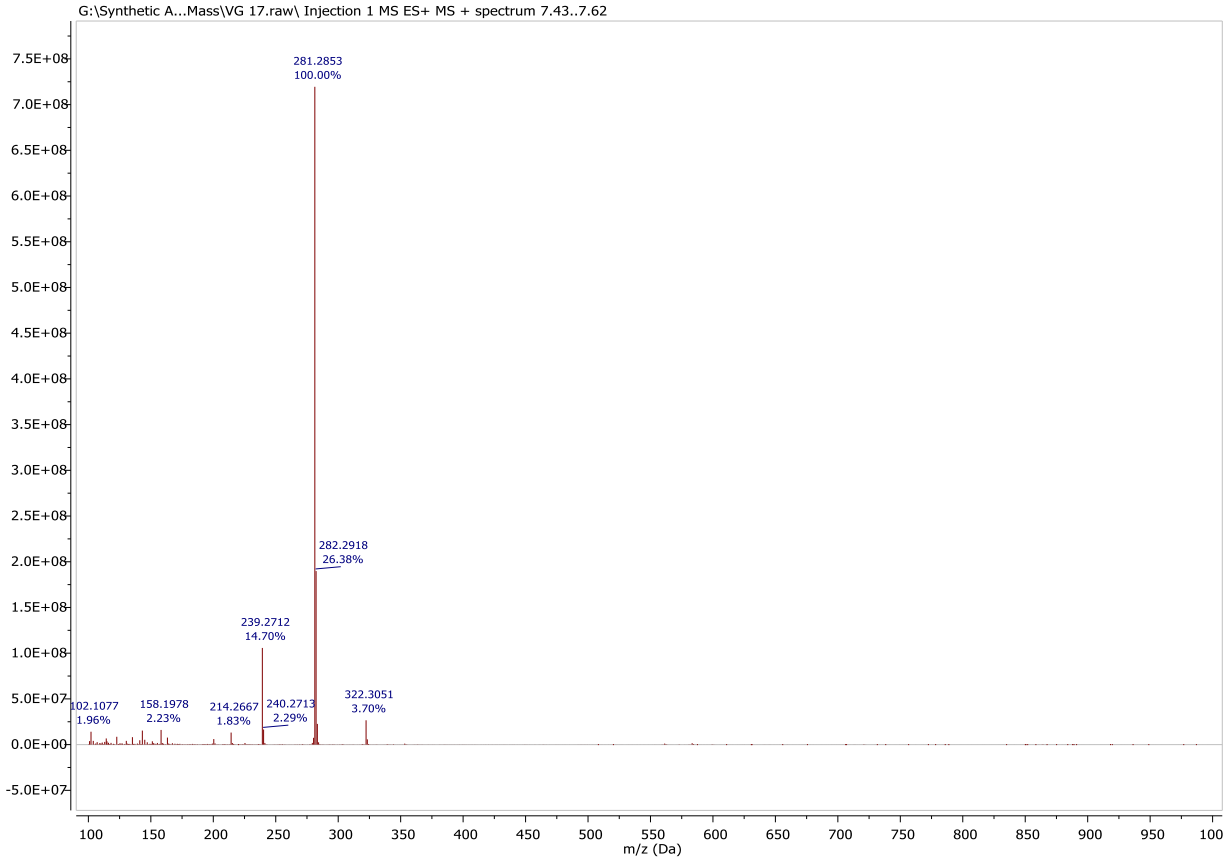

APPENDIX D.

HPLC ANALYSIS FOR PURITY

All the synthesized analogs were purified using the following parameters:

Injection Volume: 10.00 µL

Run Time: 15.00 min

Acquisition Method Set: Isocratic 20% H_2O_80% MeOH

Wavelength: PDA 254.0 nm

HPLC Analysis of Compound 1a

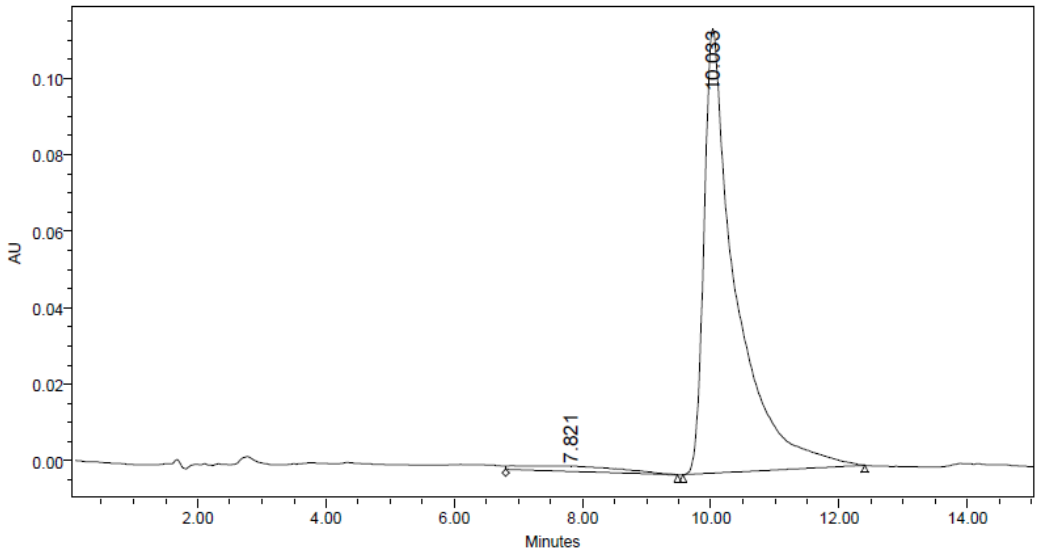

	RT	Area	% Area	Height
1	7.821	152721	3.67	1365
2	10.033	4006531	96.33	116178

HPLC Analysis of Compound 1b

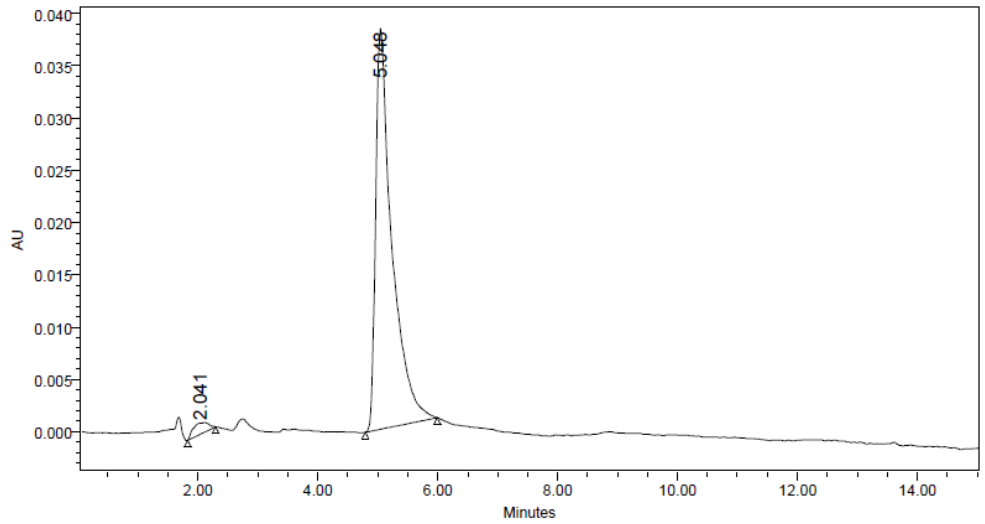

	RT	Area	% Area	Height
1	2.041	19203	2.59	1078
2	5.048	722712	97.41	38387

HPLC Analysis of Compound 1c

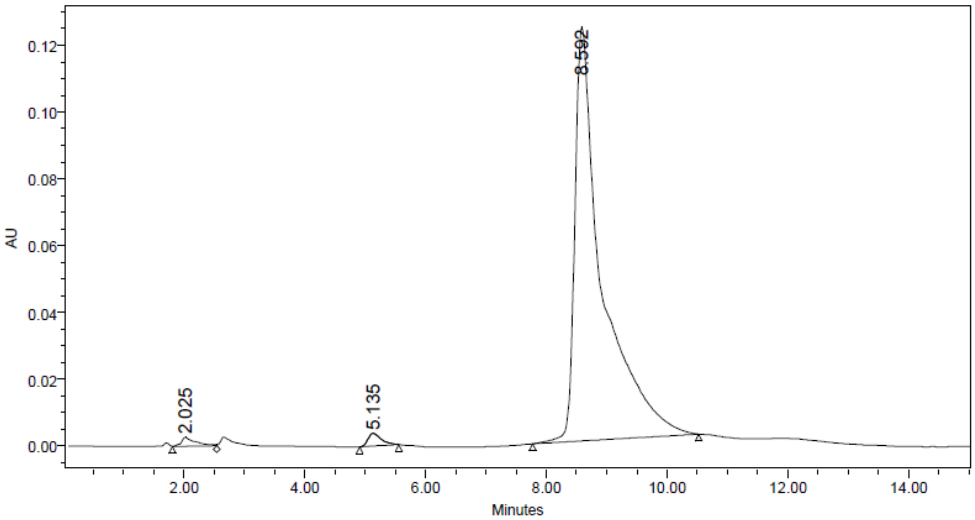

	RT	Area	% Area	Height
1	2.025	44612	1.11	2653
2	5.135	58004	1.45	3804
3	8.592	3898897	97.44	123939

HPLC Analysis of Compound 2a

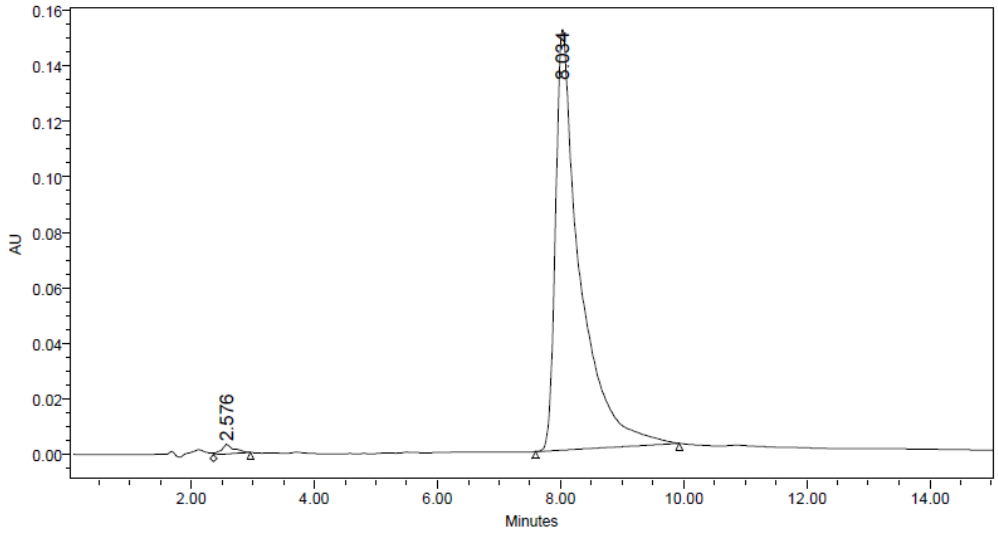

	RT	Area	% Area	Height
1	2.576	49026	1.16	3352
2	8.034	4191738	98.84	151660

HPLC Analysis of Compound 2b

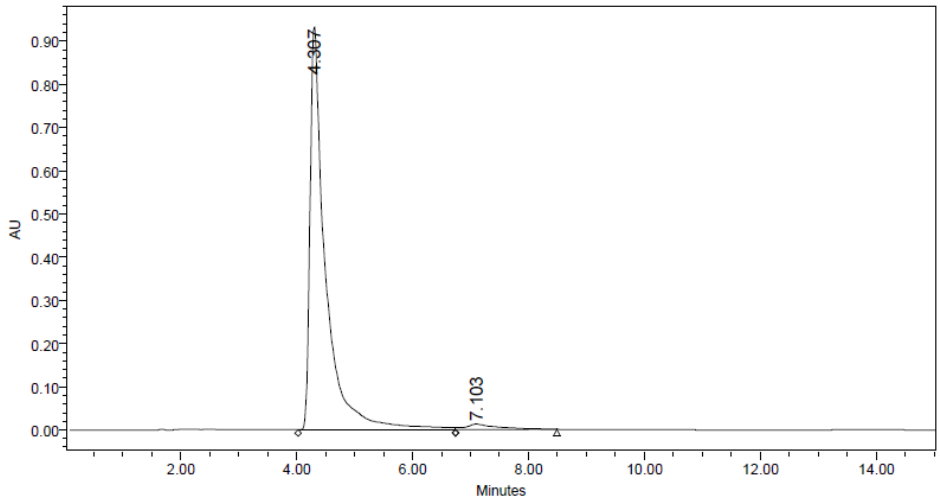

	RT	Area	% Area	Height
1	4.307	17252559	97.24	933300
2	7.103	489332	2.76	12562

HPLC Analysis of Compound 2c

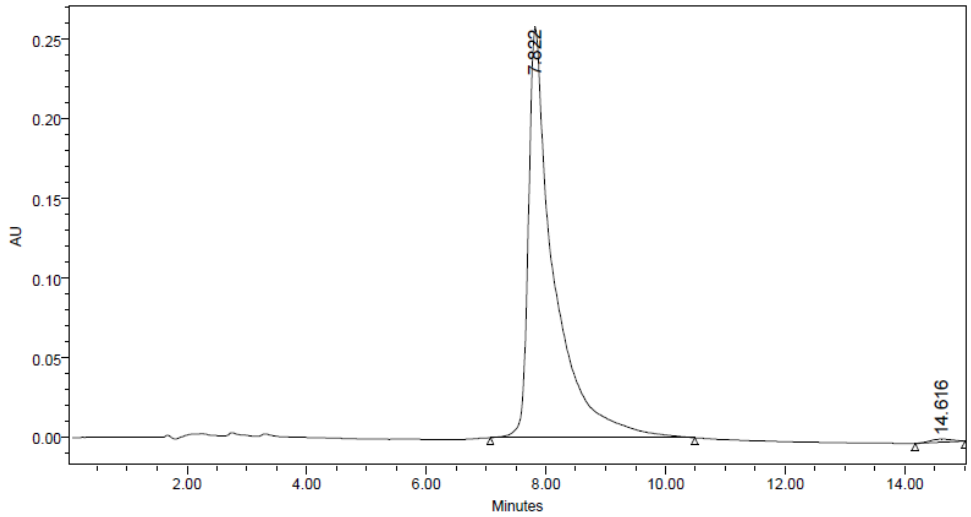

	RT	Area	% Area	Height
1	7.822	7574755	99.33	257925
2	14.616	51202	0.67	1993

HPLC Analysis of Compound 3a

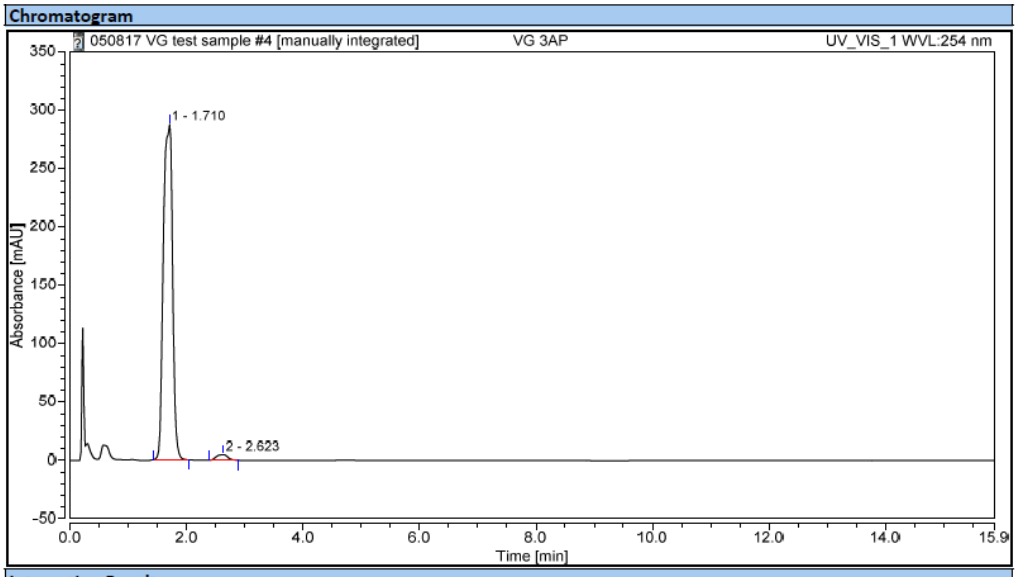

Integration Results

No.	Peak Name	Retention Time min	Area mAU*min	Height mAU	Relative Area %	Relative Height %	Amount
1		1.710	52.405	287.423	97.98	98.33	n.a.
2		2.623	1.081	4.885	2.02	1.67	n.a.
n.a.	Component 2	n.a.	n.a.	n.a.	n.a.	n.a.	n.a.
n.a.	Component 1	n.a.	n.a.	n.a.	n.a.	n.a.	n.a.
Total:			**53.486**	**292.307**	**100.00**	**100.00**	

HPLC Analysis of Compound 3b

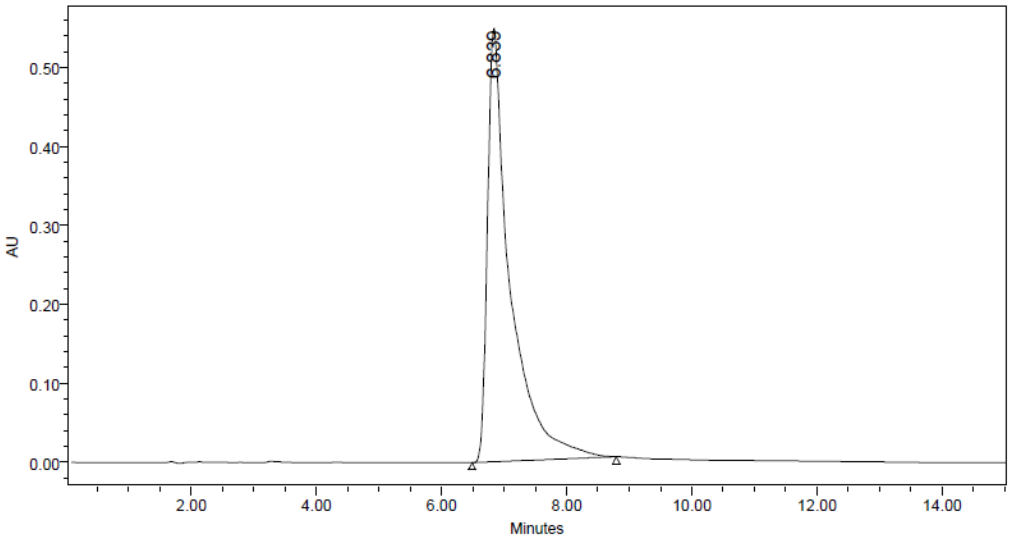

	RT	Area	% Area	Height
1	6.839	13833819	100.00	549069

HPLC Analysis of Compound 3c

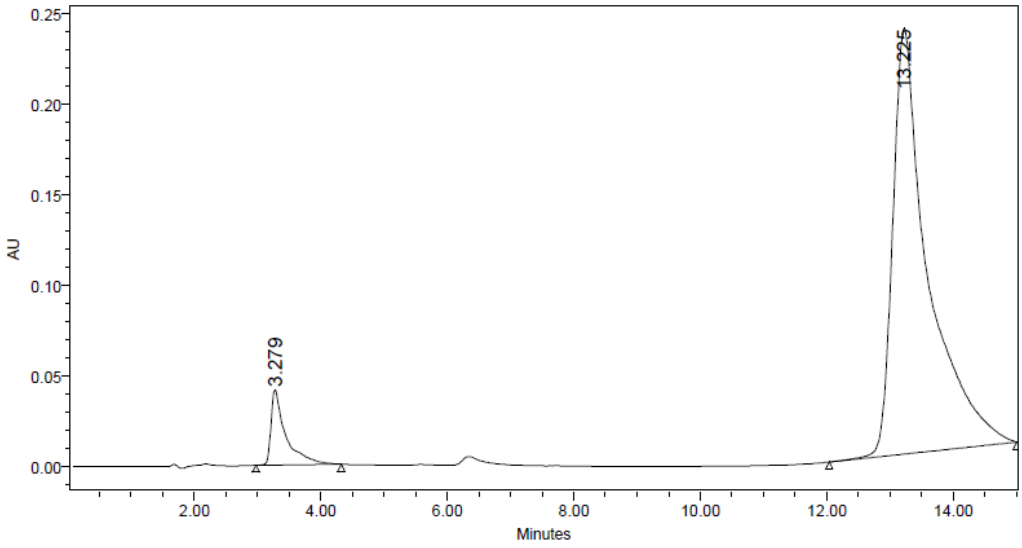

	RT	Area	% Area	Height
1	3.279	668393	6.86	41685
2	13.225	9081009	93.14	235095

HPLC Analysis of Compound 4b

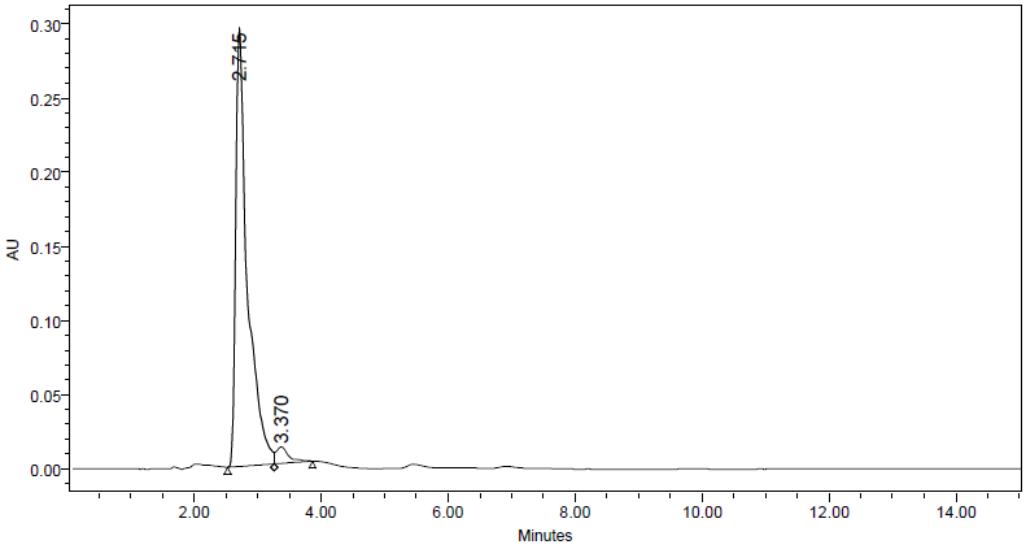

	RT	Area	% Area	Height
1	2.715	3790097	96.10	296156
2	3.370	153671	3.90	11114

HPLC Analysis of Compound 4c

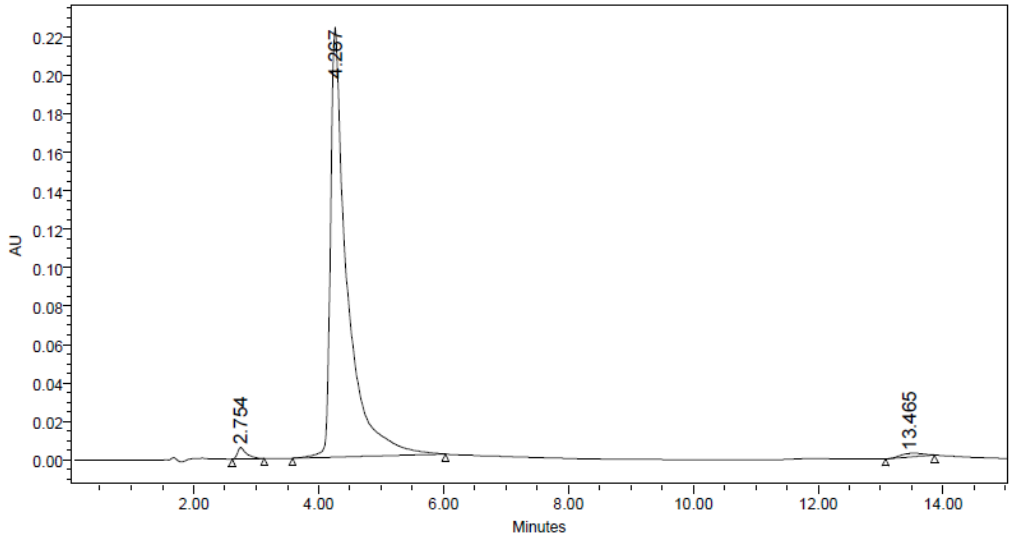

	RT	Area	% Area	Height
1	2.754	59107	1.40	5877
2	4.267	4117522	97.53	223503
3	13.465	45011	1.07	1818

HPLC Analysis of Compound 5a

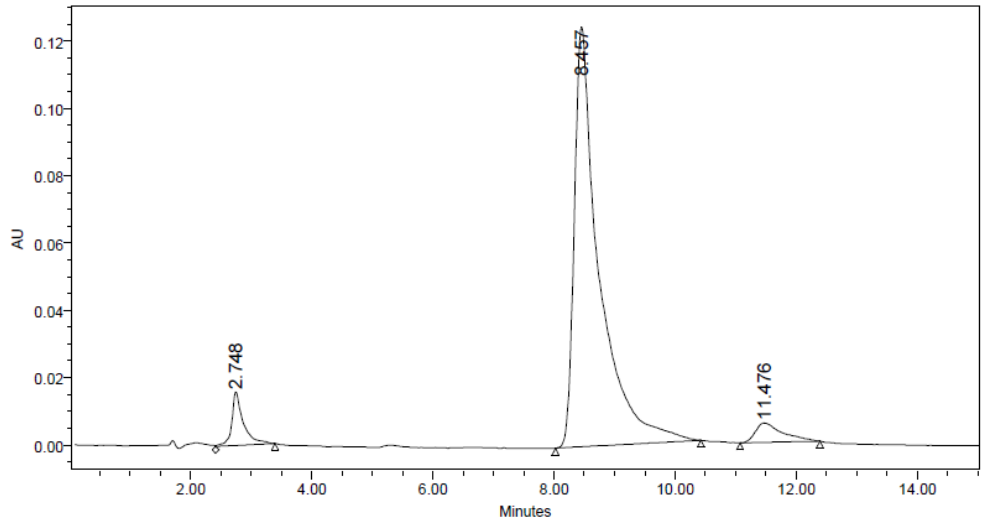

	RT	Area	% Area	Height
1	2.748	209535	5.30	15902
2	8.457	3566791	90.15	124604
3	11.476	180390	4.56	5736

HPLC Analysis of Compound 5b

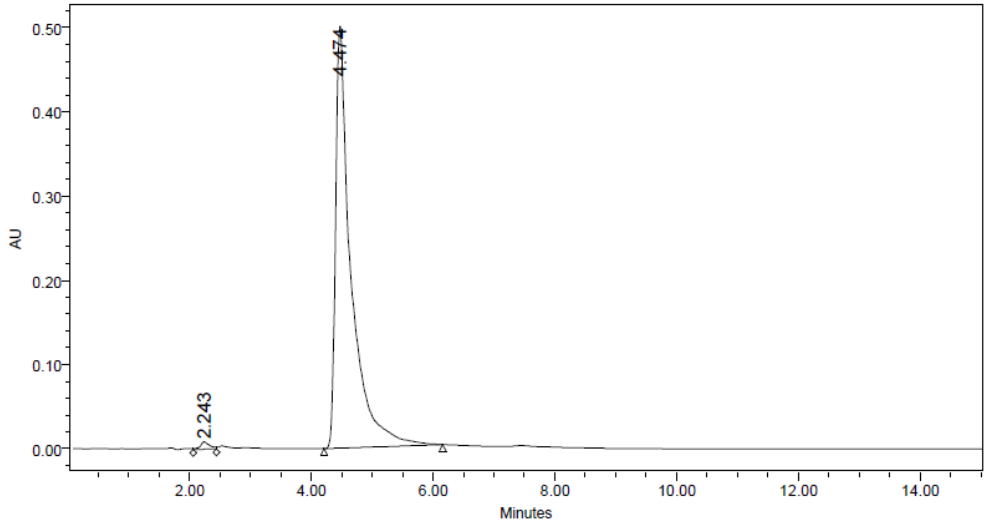

	RT	Area	% Area	Height
1	2.243	93465	1.04	8591
2	4.474	8915956	98.96	501399

HPLC Analysis of Compound 6c

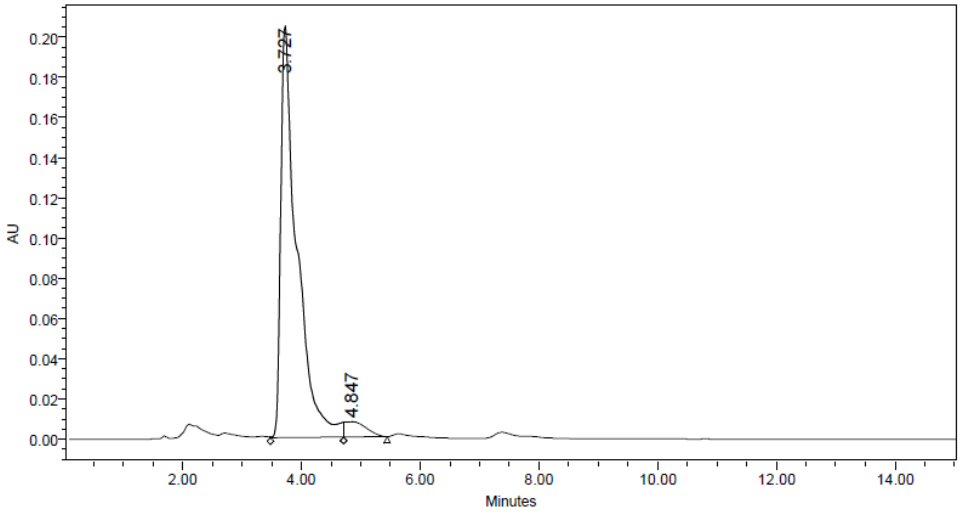

	RT	Area	% Area	Height
1	3.727	3857715	95.27	204912
2	4.847	191419	4.73	7652

HPLC Analysis of Compound 10b

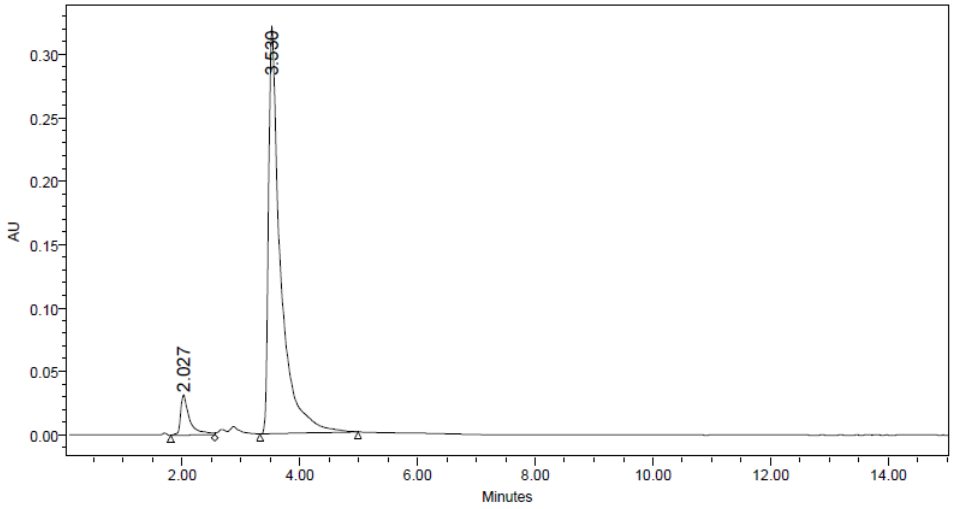

	RT	Area	% Area	Height
1	2.027	339281	6.89	31821
2	3.530	4583946	93.11	322045

HPLC Analysis of Compound 11b

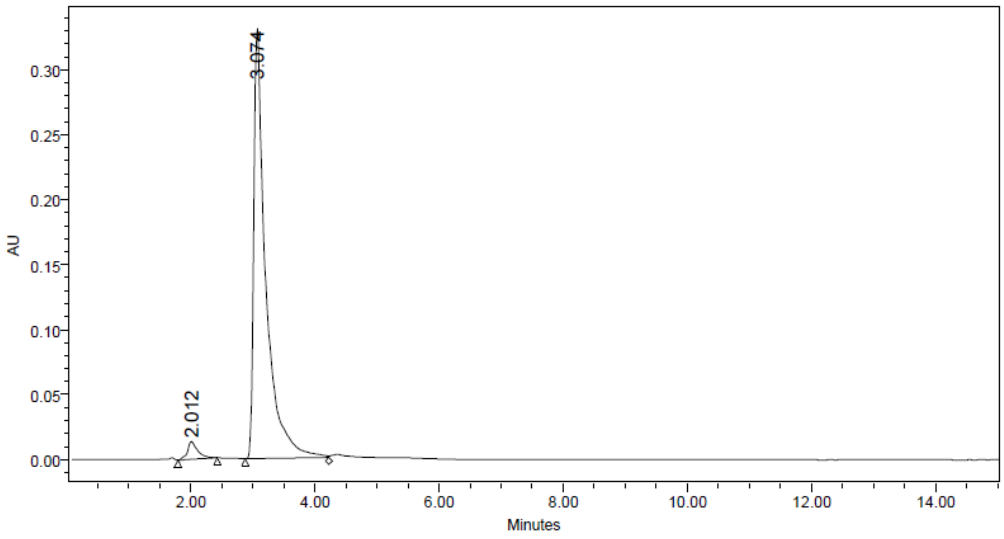

	RT	Area	% Area	Height
1	2.012	157657	3.41	13678
2	3.074	4461111	96.59	331034

HPLC Analysis of Compound VIII

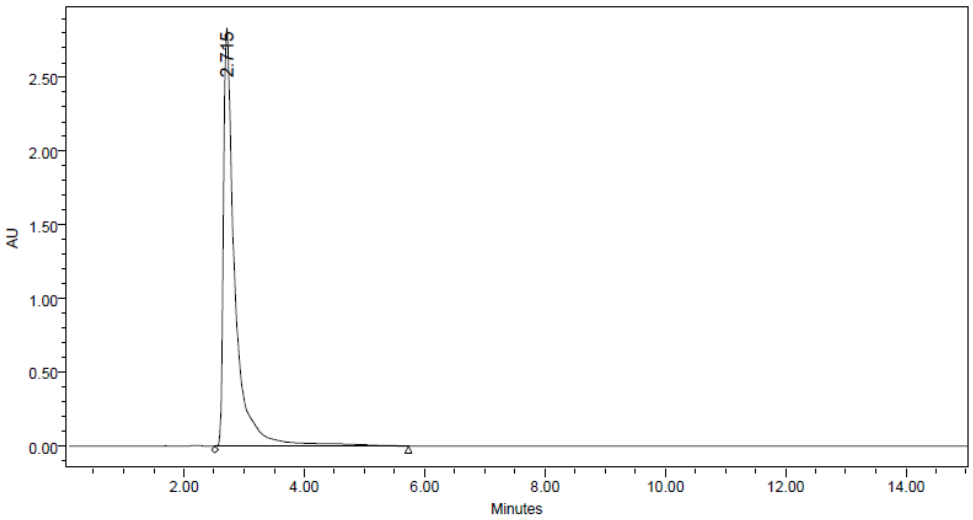

	RT	Area	% Area	Height
1	2.715	37411081	100.00	2837402

HPLC Analysis of Compound 13b

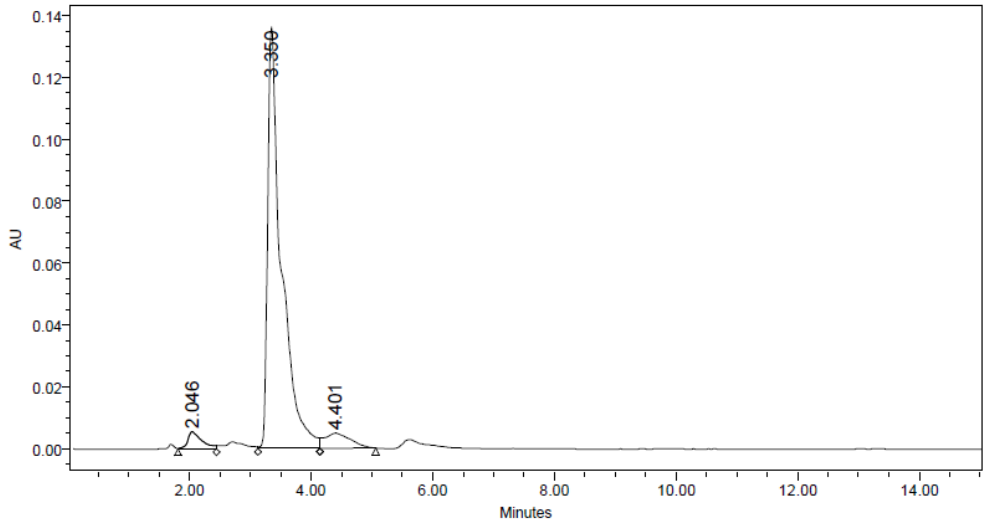

	RT	Area	% Area	Height
1	2.046	88096	3.71	5612
2	3.350	2140445	90.17	136489
3	4.401	145260	6.12	4814

APPENDIX E

COPYRIGHT PERMISSIONS

Figure 1.1.

License Details

This Agreement between Vedanjali Gogineni ("You") and Nature Publishing Group ("Nature Publishing Group") consists of your license details and the terms and conditions provided by Nature Publishing Group and Copyright Clearance Center.

License Number	4167820299191
License date	Aug 14, 2017
Licensed Content Publisher	Nature Publishing Group
Licensed Content Publication	Nature Reviews Drug Discovery
Licensed Content Title	The evolving role of natural products in drug discovery
Licensed Content Author	Frank E. Koehn, Guy T. Carter
Licensed Content Date	Feb 24, 2005
Licensed Content Volume	4
Licensed Content Issue	3
Type of Use	reuse in a dissertation / thesis
Requestor type	academic/educational
Format	electronic
Portion	figures/tables/illustrations
Number of figures/tables/illustrations	1
High-res required	no
Figures	Figure 1. Worldwide pharmaceutical natural-product patents
Author of this NPG article	no
Your reference number	10295516
Title of your thesis / dissertation	Phytochemical Investigation of Psychoactive Medicinal Plants for the Treatment of Neurological Disorders
Expected completion date	Dec 2017
Estimated size (number of pages)	400
Total	**0.00 USD**

Figure 1.4

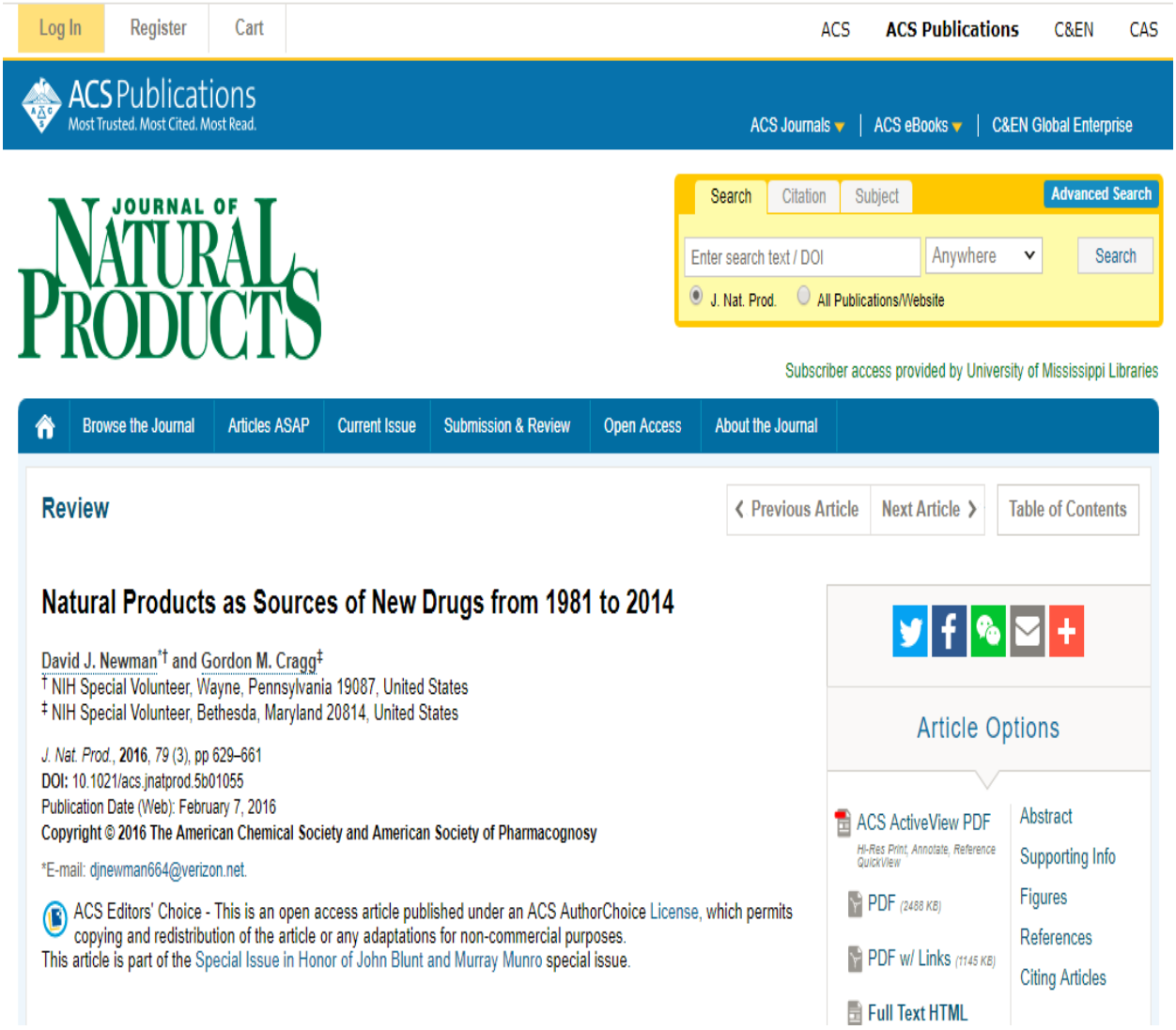
Log In
Register
Cart
ACS
ACS Publications
C&EN
CAS
ACS Publications
Most Trusted. Most Cited. Most Read.
ACS Journals
ACS eBooks
C&EN Global Enterprise
JOURNAL OF NATURAL PRODUCTS
Search
Citation
Subject
Advanced Search
Enter search text / DOI
Anywhere
Search
J. Nat. Prod.
All Publications/Website
Subscriber access provided by University of Mississippi Libraries
Browse the Journal
Articles ASAP
Current Issue
Submission & Review
Open Access
About the Journal
Review
Previous Article
Next Article
Table of Contents
Natural Products as Sources of New Drugs from 1981 to 2014
David J. Newman*† and Gordon M. Cragg‡
† NIH Special Volunteer, Wayne, Pennsylvania 19087, United States
‡ NIH Special Volunteer, Bethesda, Maryland 20814, United States
J. Nat. Prod., 2016, 79 (3), pp 629–661
DOI: 10.1021/acs.jnatprod.5b01055
Publication Date (Web): February 7, 2016
Copyright © 2016 The American Chemical Society and American Society of Pharmacognosy
*E-mail: djnewman664@verizon.net.
ACS Editors' Choice - This is an open access article published under an ACS AuthorChoice License, which permits copying and redistribution of the article or any adaptations for non-commercial purposes.
This article is part of the Special Issue in Honor of John Blunt and Murray Munro special issue.
Article Options
ACS ActiveView PDF
Hi-Res Print, Annotate, Reference QuickView
PDF (2488 KB)
PDF w/ Links (1145 KB)
Full Text HTML
Abstract
Supporting Info
Figures
References
Citing Articles

Figure 1.6

plos.org create account sign in

PLOS ONE | TENTH ANNIVERSARY

Publish About Browse Search

advanced search

OPEN ACCESS PEER-REVIEWED

RESEARCH ARTICLE

The Global Burden of Mental, Neurological and Substance Use Disorders: An Analysis from the Global Burden of Disease Study 2010

381 Save | 125 Citation | 24,854 View | 10 Share

Harvey A. Whiteford, Alize J. Ferrari, Louisa Degenhardt, Valery Feigin, Theo Vos

Published: February 6, 2015 • https://doi.org/10.1371/journal.pone.0116820

The Global Burden of Mental, Neurological and Substance Use Disorders: An Analysis from the Global Burden of ...

Harvey A. Whiteford, Alize J. Ferrari, Louisa Degenhardt, Valery Feigin, Theo Vos

Citation: Whiteford HA, Ferrari AJ, Degenhardt L, Feigin V, Vos T (2015) The Global Burden of Mental, Neurological and Substance Use Disorders: An Analysis from the Global Burden of Disease Study 2010. PLoS ONE10(2): e0116820. https://doi.org/10.1371/journal.pone.0116820

Academic Editor: Gianluigi Forloni, "Mario Negri" Institute for Pharmacological Research, ITALY

Received: August 17, 2014; **Accepted:** December 15, 2014; **Published:** February 6, 2015

Data Availability: All relevant data are within the paper.

Funding: HAW and AJF are supported by the Queensland Centre for Mental Health Research which receives its funding from the Queensland Department of Health. LD is supported by an Australian National Health and Medical Research Council (NHMRC) Principal Research Fellowship (#1041742). The National Drug and Alcohol Research Centre at UNSW Australia is supported by funding from the Australian Government under the Substance Misuse Prevention and Service Improvements Grants Fund and an Australian National Health and Medical Research Council Principal Research Fellowship. TV receives funding from the Bill and Melinda Gates Foundation. The funders had no role in study design, data collection and analysis, decision to publish, or preparation of the manuscript.

Competing interests: The authors have declared that no competing interests exist.

Figures 1.7, 1.8, & 1.9

License Details

This Agreement between University of Mississippi -- Vedanjali Gogineni ("You") and Nature Publishing Group ("Nature Publishing Group") consists of your license details and the terms and conditions provided by Nature Publishing Group and Copyright Clearance Center.

License Number	4200060836415
License date	Oct 01, 2017
Licensed Content Publisher	Nature Publishing Group
Licensed Content Publication	Nature Reviews Neuroscience
Licensed Content Title	Pathogenesis of parkinson's disease: dopamine, vesicles and [alpha]-synuclein
Licensed Content Author	Julie Lotharius and Patrik Brundin
Licensed Content Date	Dec 1, 2002
Licensed Content Volume	3
Licensed Content Issue	12
Type of Use	reuse in a dissertation / thesis
Requestor type	academic/educational
Format	electronic
Portion	figures/tables/illustrations
Number of figures/tables/illustrations	3
High-res required	no
Figures	Figures 1, 2, 3
Author of this NPG article	no
Your reference number	3001195206
Title of your thesis / dissertation	Phytochemical Investigation of Psychoactive Medicinal Plants for the Treatment of Neurological Disorders
Expected completion date	Dec 2017
Estimated size (number of pages)	400
Total	**0.00 USD**

Figure 1.12

License Details

This Agreement between University of Mississippi -- Vedanjali Gogineni ("You") and John Wiley and Sons ("John Wiley and Sons") consists of your license details and the terms and conditions provided by John Wiley and Sons and Copyright Clearance Center.

License Number	4200061422503
License date	Oct 01, 2017
Licensed Content Publisher	John Wiley and Sons
Licensed Content Publication	Journal of Neurochemistry
Licensed Content Title	Current and experimental treatments of Parkinson disease: A guide for neuroscientists
Licensed Content Author	Wolfgang Oertel, Jörg B. Schulz
Licensed Content Date	Aug 30, 2016
Licensed Content Pages	13
Type of Use	Dissertation/Thesis
Requestor type	University/Academic
Format	Electronic
Portion	Figure/table
Number of figures/tables	1
Original Wiley figure/table number(s)	Figure 2
Will you be translating?	No
Order reference number	3001195206
Title of your thesis / dissertation	Phytochemical Investigation of Psychoactive Medicinal Plants for the Treatment of Neurological Disorders
Expected completion date	Dec 2017
Expected size (number of pages)	400
Total	**0.00 USD**

Figure 1.13

License Details

This Agreement between University of Mississippi -- Vedanjali Gogineni ("You") and John Wiley and Sons ("John Wiley and Sons") consists of your license details and the terms and conditions provided by John Wiley and Sons and Copyright Clearance Center.

License Number	4200070173884
License date	Oct 01, 2017
Licensed Content Publisher	John Wiley and Sons
Licensed Content Publication	British Journal of Pharmacology
Licensed Content Title	Monoamine oxidase: isoforms and inhibitors in Parkinson's disease and depressive illness
Licensed Content Author	Moussa B H Youdim, Y S Bakhle
Licensed Content Date	Jan 1, 2006
Licensed Content Pages	1
Type of Use	Dissertation/Thesis
Requestor type	University/Academic
Format	Electronic
Portion	Figure/table
Number of figures/tables	1
Original Wiley figure/table number(s)	Figure 2
Will you be translating?	No
Title of your thesis / dissertation	Phytochemical Investigation of Psychoactive Medicinal Plants for the Treatment of Neurological Disorders
Expected completion date	Dec 2017
Expected size (number of pages)	400
Total	**0.00 USD**

Figure 1.14

Welcome, Vedanjali
Not you?

Log out | Cart (0) | Manage | Feedback | Help
Account

Get Permission / Find Title

Copy order

Confirmation Number: 11673484
Order Date: 10/02/2017

Print this page
Print terms & conditions
Print citation information
(What's this?)

Customer Information

Customer: Vedanjali Gogineni
Account Number: 3001195206
Organization: University of Mississippi
Email: vgoginen@go.olemiss.edu
Phone: +1 (662) 915-2014

This is not an invoice

Order Details

Future medicinal chemistry

Billing Status *N/A*

Order detail ID: 70701501
ISSN: 1756-8919
Publication Type: Journal
Volume:
Issue:
Start page:
Publisher: Future Science

Permission Status: **Granted**
Permission type: Republish or display content
Type of use: Thesis/Dissertation
Order License Id: 4200681286869

View details

Note: This item was invoiced separately through our **RightsLink service.** More info **$ 0.00**

Total order items: 1 **Order Total: $0.00**

Newlands Press Ltd LICENSE
TERMS AND CONDITIONS

Nov 12, 2017

This is a License Agreement between University of Mississippi -- Vedanjali Gogineni ("You") and Newlands Press Ltd ("Newlands Press Ltd") provided by Copyright Clearance Center ("CCC"). The license consists of your order details, the terms and conditions provided by Newlands Press Ltd, and the payment terms and conditions.

License Number	4200681286869
License date	Oct 02, 2017
Licensed content publisher	Newlands Press Ltd
Licensed content title	Future medicinal chemistry
Licensed content date	Jan 1, 2009
Type of Use	Thesis/Dissertation
Requestor type	Academic institution
Format	Electronic
Portion	chart/graph/table/figure
Number of charts/graphs/tables/figures	1
The requesting person/organization is:	University of Mississippi
Title or numeric reference of the portion(s)	Figure 1. Active site architecture of human MAO-A and human MAO-B
Title of the article or chapter the portion is from	Monoamine oxidase A and B substrates: probing the pathway for drug development
Editor of portion(s)	N/A
Author of portion(s)	Chajkowski-Scarry & Rimoldi
Volume of serial or monograph.	6
Issue, if republishing an article from a serial	6
Page range of the portion	698
Publication date of portion	06/04/2014
Rights for	Main product and any product related to main product
Duration of use	Current edition and up to 5 years
Creation of copies for the disabled	no
With minor editing privileges	no
For distribution to	United States
In the following language(s)	Original language of publication
With incidental promotional use	no
The lifetime unit quantity of new product	Up to 499

Title	Phytochemical Investigation of Psychoactive Medicinal Plants for the Treatment of Neurological Disorders
Instructor name	n/a
Institution name	n/a
Expected presentation date	Dec 2017
Expected size	400
Total (may include CCC user fee)	0.00 USD

Figure 1.16

My Orders > Orders > All Orders

Welcome vedanjalig@gmail.com Log out | Help

License Details

This Agreement between University of Mississippi -- Vedanjali Gogineni ("You") and John Wiley and Sons ("John Wiley and Sons") consists of your license details and the terms and conditions provided by John Wiley and Sons and Copyright Clearance Center.

License Number	4187860840706
License date	Sep 14, 2017
Licensed Content Publisher	John Wiley and Sons
Licensed Content Publication	British Journal of Pharmacology
Licensed Content Title	Monoamine oxidase: isoforms and inhibitors Parkinson's disease and depressive illness
Licensed Content Author	Moussa B H Youdim, Y S Bakhle
Licensed Content Date	Jan 1, 2006
Licensed Content Pages	1
Type of Use	Dissertation/Thesis
Requestor type	University/Academic
Format	Electronic
Portion	Figure/table
Number of figures/tables	1
Original Wiley figure/table number(s)	Figure 1
Will you be translating?	No
Title of your thesis / dissertation	Phytochemical Investigation of Psychoactive Medicinal Plants for the Treatment of Neurological Disorders
Expected completion date	Dec 2017
Expected size (number of pages)	400
Total	**0.00 USD**

VITA

VEDANJALI GOGINENI
Department of BioMolecular Sciences, Division of Medicinal Chemistry
The University of Mississippi, Faser 430, Phone: (662) 915-2014
Email: vgoginen@go.olemiss.edu

ACADEMIC TRACK RECORD

2002–2007	Bapatla College of Pharmacy, B.S. (Pharmacy)
2008–2009	Fairleigh Dickinson University, M.S. (Pharmaceutical Chemistry)

PROFESSIONAL EMPLOYMENT

08/13–01/15	Graduate Research Assistant, Department of Medicinal Chemistry, School of Pharmacy, University of Mississippi, University, MS
02/15–05/15	Graduate Teaching Assistant, Department of BioMolecular Sciences, Division of Medicinal Chemistry, School of Pharmacy, University of Mississippi, University, MS
08/15–12/15	Graduate Teaching Assistant, Department of BioMolecular Sciences, Division of Pharmacology, School of Pharmacy, University of Mississippi, University, MS
01/16–12/17	Graduate Research Assistant, Department of Medicinal Chemistry, School of Pharmacy, University of Mississippi, University, MS

TEACHING EXPERIENCE

- Guest lecture for Herbal Supplements and Alternative Therapy PHCG 329 (PY1) University of Mississippi, Oxford, MS 38655, USA : February 25, 2016
- Guest lecture for Herbal Supplements and Alternative Therapy PHCG 329 (PY1) University of Mississippi, Oxford, MS 38655, USA : February 23, 2016
- Teaching Assistant (TA) for Herbal Supplements and Alternative Therapy PHCG 329 (PY1), University of Mississippi, Oxford, MS 38655, USA : Spring 2015–2016
- Guest lecture for Oceans and Human Health, PHCG320 (PY2) University of Mississippi, Oxford, MS 38655, USA : September 21, 2015
- Guest lecture for Oceans and Human Health, PHCG320 (PY2) University of Mississippi, Oxford, MS 38655, USA : September 16, 2015

- Teaching Assistant (TA) for Biochemical Foundations of Therapeutics Section [PHCL 343], University of Mississippi, University, MS 38677, USA : Fall 2015–2016

- Teaching Assistant (TA) for Advanced Medicinal Chemistry II, Section 1 [MEDC 417], University of Mississippi, University, MS 38677, USA : Spring 2014–2015

- Guest lecture for Oceans and Human Health, PHCG320 (PY2) University of Mississippi, Oxford, MS 38655, USA : September 10, 2013

- Guest lecture for Oceans and Human Health, PHCG320 (PY2), University of Mississippi, Oxford, MS 38655, USA : September 5, 2012

HONORS AND AWARDS

- Nobles-Sam Award in Medicinal Chemistry, 2017–18
- Fall Dissertation Fellowship from the University of Mississippi, 2017–18
- Outstanding Service Award for Gamma Beta Phi (GBP), 2016–17
- 2016 American Association of Pharmaceutical Sciences (AAPS) Graduate Student Research Award in Drug Discovery and Development Interface
- Winner of Graduate Student Award in the Chemistry Research Category at the 2016 Sigma Xi Student Research Conference
- 2016 American Chemical Society (ACS) Women Chemists Committee Travel Award sponsored by Eli Lilly & Company
- Outstanding Member of Gamma Beta Phi (GBP), 2015–16
- Graduate Student Council (GSC) Research Grant Award, 2015–16
- Outstanding Member of Gamma Beta Phi (GBP), 2014–15
- Graduate Student Council (GSC) Research Grant Award, 2014–15
- 2013–2014 NIH Natural Products Neuroscience Assistantship Award

INTERNAL FUNDING

- **Phytochemical Analysis of *Banisteriopsis caapi* for Opioid-Binding Affinity**. Center for Research Excellence in Natural Products Neuroscience (CORE-NPN). The National Institutes of Health – National Center for Research Resource (NIH-NCRR) as one of its Centers of Biomedical Research Excellence (COBRE). 2014
  Vedanjali Gogineni – Principal Investigator
  Amount Awarded: $9,000

- **Opioid Binding Affinity for Ayahuasca Constituents**. Graduate Student Council (GSC) Research Grant Proposal. The Office of Research and Sponsored Programs (ORSP) and the Graduate School of University of Mississippi. 2014
  Vedanjali Gogineni – Principal Investigator
  Amount Awarded: $1,000
- **Human Monoamine Oxidase (MAO) Inhibitory Constituents of *Calea urticifolia***. Graduate Student Council (GSC) Research Grant Proposal. The Office of Research and Sponsored Programs (ORSP) and the Graduate School of University of Mississippi. 2015
  Vedanjali Gogineni – Principal Investigator
  Amount Awarded: $1,000

PROFESSIONAL AFFILIATIONS

- American Chemical Society (ACS)
- American Society of Pharmacognosy (ASP)
- American Association of Pharmaceutical Sciences (AAPS)
- Rho Chi
- Gamma Beta Phi (GBP)
- Sigma Xi
- Graduate Women in Science (GWIS)
- Golden Key International Honor Society (GKIHS)

PEER REVIEWED PUBLICATIONS

1. Role of Marine Natural Products in the Genesis of Antiviral Agents. **Vedanjali Gogineni**, Raymond F. Schinazi, and Mark T. Hamann. *Chemical Reviews*, **2015**, *115* (18), pp 9655–9706. **DOI:** 10.1021/cr4006318. Epub: 2015 Aug 28. PMID: 26317854

2. Isolation of Acacetin from *Calea urticifolia* with Inhibitory Properties against Human MAO-A and –B. Narayan D Chaurasiya, **Vedanjali Gogineni**, Francisco León, Marvin J Nuñez, Khaled M. Elokely, Michael L. Klein, Larry A. Walker, Stephen J. Cutler, and Babu L. Tekwani. *Journal of Natural Products*, **2016**, *79* (10), pp 2538–2544. **DOI:** 10.1021/acs.jnatprod.6b00440. Epub: 2016 Oct 18.

3. Marine Natural Product Peptides with Therapeutic Potential: Chemistry, Biosynthesis, and Pharmacology. **Vedanjali Gogineni** and Mark T. Hamann. *Biochimica et Biophysica Acta - General Subjects*, **2018**, *1862* (1), pp 81–196. **DOI:** 10.1016/j.bbagen.2017.08.014

BOOK

1. Therapeutics of Infectious Diseases: **Vedanjali Gogineni** and Dr. Mark T. Hamann. In the process of writing for "*Springer*" publications

BOOK CHAPTER

1. Phytochemistry of *Mitragyna speciosa*: **Vedanjali Gogineni**, Francisco León, Bonnie A. Avery, Christopher McCurdy and Stephen J. Cutler. In, "Kratom and Related Compounds: Chemistry and Pharmacology of Opioids from a Non-Opium Source" Edited by Robert B. Raffa. Chapter 6. Taylor and Francis Group, Boca Raton, **2014**.

EDITORIAL BOARD

Journal of Research in Pharmaceutics and Drug Development

REVIEWER FOR

- Medicinal Chemistry Research (MCR)
- Modern Applications in Pharmacy & Pharmacology (MAPP)

ABSTRACT PUBLICATIONS

1. Isolation of Acacetin from *Calea urticifolia* as a Potent Inhibitor of Human Monoamine Oxidase-A and –B. Narayan D. Chaurasiya, **Vedanjali Gogineni**, Francisco León, Marvin J Nuñez, Stephen J. Cutler, Larry A. Walker, and Babu L. Tekwani: *Planta Medica*, **2015**, *81*(11), PV4 [DOI: 10.1055/s-0035-1556428]
2. Cannabinoid and Opioid Radioligand Displacement by Secondary Metabolites from *Banisteriopsis caapi*. **Vedanjali Gogineni**, John C. Fitzpatrick, Francisco León and Stephen J. Cutler: *14th Annual Oxford International Conference on the Science of Botanicals* (ICSB). *Planta Medica* 10:80, PD123, **2014** [DOI: 10.1055/s-0034-1382544]

ORAL PRESENTATIONS

1. Design and synthesis of monoamine oxidase-B inhibitors. **Vedanjali Gogineni**, Francisco León, Narayan D. Chaurasiya, Babu L. Tekwani, Manal Nael, Stephen J. Cutler, and Christopher R. McCurdy. Presented at the 44th Annual MALTO Medicinal Chemistry & Pharmacognosy Meeting-in-Miniature, University of Louisiana, School of Pharmacy, Monroe, LA. May 21–23, 2017

2. Secondary Metabolites Isolated from *Calea urticifolia***. Vedanjali Gogineni**, Francisco León, Marvin J Nuñez, and Stephen J. Cutler. Presented at the 43rd Annual MALTO Medicinal Chemistry & Pharmacognosy Meeting-in-Miniature, University of Houston, College of Pharmacy, Houston, TX. May 22–24, 2016

3. Interactions of Acacetin on MAO Isoenzymes**. Vedanjali Gogineni,** Narayan D. Chaurasiya, Khaled M. Elokely, Francisco León, Marvin J. Nuñez, Michael L. Klein, Larry A. Walker, Babu L. Tekwani, and Stephen J. Cutler. Presented at the 6th GSC Annual Research Symposium, University of Mississippi, University, MS. April 15, 2016

4. Computational Studies on Acacetin, a MAO Inhibitor from *Calea urticifolia*. **Vedanjali Gogineni,** Narayan D. Chaurasiya, Khaled M. Elokely, Francisco León, Marvin J. Nuñez, Michael L. Klein, Larry A. Walker, Babu L. Tekwani, and Stephen J. Cutler. Presented at the 2nd Annual Research Showcase by the Neuroscience Minor, University of Mississippi, University, MS. April 1, 2016

5. Identification and Evaluation of Potent Inhibitor of Human Monoamine Oxidase B from *Calea urticifolia*. **Vedanjali Gogineni**, Narayan D Chaurasiya, Francisco León, Marvin J Nuñez, Larry A Walker, Babu L Tekwani and Stephen J. Cutler. Presented at the 42nd Annual MALTO Medicinal Chemistry & Pharmacognosy Meeting-in-Miniature, University of Mississippi, University, MS. May 17–19, 2015

6. *Mitragyna speciosa*: Isolation & Pharmacological Evaluation of the Indole Alkaloids – **Vedanjali Gogineni**, J. Francisco León, Lisa Wilson, Bonnie A. Avery, Christopher R. McCurdy, Stephen J. Cutler. Presented at the 40th Annual MALTO Medicinal Chemistry – Pharmacognosy Meeting-in-Miniature, Department of Pharmaceutical Sciences, College of Pharmacy, University of Arkansas for Medicinal Sciences, Little Rock, AR. May 19–21, 2013.

POSTER PRESENTATIONS

1. Absolute Configuration and Therapeutic Potential of Novel and Known Sesquiterpenoids Isolated from *Calea urticifolia*. **Vedanjali Gogineni,** Francisco León, Manal Nael, Tracy Brooks, Stephen J. Cutler and Christopher R. McCurdy. Presented at the 17th Annual Oxford International Conference on the Science of Botanicals, Oxford Convention Center, Oxford, MS. April 03–06, 2017.

2. Design of New Opioid Modulators using Structure- and Ligand-Based Virtual Screening. Manal Nael, **Vedanjali Gogineni**, and Khaled M. Elokely. Presented at the Drug Discovery Workshop, National Research Center, Cairo, Egypt. December 05, 2016.

3. Phytochemical Studies on *Juanislama*, an El Salvadorian Medicinal Plant. **Vedanjali Gogineni,** Francisco León, Marvin J. Nuñez, Narayan D. Chaurasiya, Babu L. Tekwani, Khaled M. Elokely, Michael L. Klein, and Stephen J. Cutler. Presented at the American Association of Pharmaceutical Sciences Annual Meeting and Exposition, Colorado Convention Center, Denver, CO. November 13–17, 2016.

4. Isolation and Structural Elucidation of the Secondary Metabolites from *Calea urticifolia*. **Vedanjali Gogineni,** Francisco León, Marvin J. Nuñez, Narayan D. Chaurasiya, Babu L. Tekwani, Khaled M. Elokely, Michael L. Klein, and Stephen J. Cutler. Presented at the Sigma Xi Research Symposium, Hyatt Regency, Atlanta, GA. November 11–13, 2016.

5. Phytochemical Investigation of Novel Sesquiterpenes of *Calea urticifolia*. **Vedanjali Gogineni,** Francisco León, Marvin J. Nuñez, and Stephen J. Cutler. Presented at the 20th Annual Poster Session, National Center for Natural Products Research (NCNPR), Centennial Auditorium, University, MS. October 7, 2016.

6. New Bisabolenes Isolated from *Calea urticifolia*. **Vedanjali Gogineni,** Francisco León, Khaled M. Elokely, Marvin J. Nuñez, Michael L. Klein, and Stephen J. Cutler. Presented at the 252nd American Chemical Society National Meeting, Pennsylvania Convention Center, PA. August 21–25, 2016.

7. Optimization of Proteome Sample Preparation Procedures for Characterization of Biotherapeutics. **Vedanjali Gogineni,** Pegah Jalili, and Kevin Ray. Presented at Millipore Sigma, St. Louis, MO. August 5, 2016.

8. Computational Studies on Acacetin, a MAO Inhibitor from *Calea urticifolia*. **Vedanjali Gogineni,** Narayan D. Chaurasiya, Khaled M. Elokely, Francisco León, Marvin J. Nuñez, Michael L. Klein, Larry A. Walker, Babu L. Tekwani, and Stephen J. Cutler. Presented at the 2nd Annual Research Showcase by the Neuroscience Minor, University of Mississippi, University, MS. April 1, 2016.

9. Isolation of Acacetin from *Calea urticifolia* as a Potent Inhibitor of Human Monoamine Oxidase-A and B. Narayan D. Chaurasiya, **Vedanjali Gogineni**, Francisco León, Marvin J. Nuñez, Stephen J. Cutler, Larry A. Walker and Babu L. Tekwani. Presented at the American Society of Pharmacognosy Annual Meeting, Copper Mountain Resort and Conference Center, Copper Mountain, CO. July 25–29, 2015

10. Opioid Binding Affinity for Ayahuasca Constituents. **Vedanjali Gogineni**, John C. Fitzpatrick, Sara Pettaway, Francisco León and Stephen J. Cutler. Presented at the COBRE Natural Products Neuroscience Assistantship Research, University of Mississippi, University, MS. May 27, 2015

11. Opioid Binding Affinity for Ayahuasca Constituents. **Vedanjali Gogineni**, John C. Fitzpatrick, Sara Pettaway, Francisco León and Stephen J. Cutler. Presented at the 5th Annual Graduate Student Council Research Forum, University of Mississippi, University, MS. April 28, 2015

12. Cannabinoid and Opioid Radioligand Displacement by Secondary Metabolites from *Banisteriopsis caapi*. **Vedanjali Gogineni**, John C. Fitzpatrick, Francisco León and Stephen J. Cutler. Presented at the American Society of Pharmacognosy, Oxford Convention Center, Oxford, MS. August 2–6, 2014

13. Radioligand Displacement of *Ayahuasca* Leaves Towards Opioid and Cannabinoid Receptors. **Vedanjali Gogineni**, John C. Fitzpatrick, Francisco León and Stephen J. Cutler. Presented at the 41st Annual MALTO Medicinal Chemistry – Pharmacognosy Meeting-in-Miniature, University of Tennessee Health Science Center, Memphis, TN. May 18–20, 2014

PROFESSIONAL SKILLS

- Hands-on experience with isolation, bioassay-guided fractionation, semi-synthesis, and total synthesis
- Hands-on experience in peptide mapping including processing samples with multiple enzymes [trypsin, chymotrypsin] prior to LC/MS/MS analysis. Reporting post-acquisition protein and peptide identification data, compiling the summed data from enzymes to maximize the sequence-coverage observed in the proteins
- Hands-on experience in performing opioid and cannabinoid assays
- Hands-on experience with QE, Xevo GS-2 QTof, ESI-mass spectroscopy, and MALDI-TOF
- Experience in chromatographic techniques including paper chromatography, thin layer chromatography (TLC), low-(LPLC), medium-(MPLC), high performance liquid chromatography (HPLC-analytical, semi-preparative, and preparative), and Ultra-high performance liquid chromatography (UPLC) utilizing various stationary phases: gel chromatography (functional and Sephadex LH-20) cellulose, silica, and reverse phase chromatography (HPLC : C18) and chiral columns.
- Structure elucidation of compounds including analytical, spectroscopic, and spectrometric methods: HPLC-mass spectroscopy (HPLC-ESIMS), gas chromatography-mass spectroscopy (GC-MS), FAB-mass, ESI-mass, MALDI-TOF mass, IR, optical rotation, and NMR (^{1}H-, ^{13}C –NMR, DEPT, COSY, NOESY, HMBC, HSQC, TOCSY and ROESY)
- Expertise in handling Bruker NMRs: 400 MHz, 500 MHz, and 600 MHz